Laboratory Corrosion Tests and Standards

Haynes/Baboian, *editors*



ASTM STP 866

LABORATORY CORROSION TESTS AND STANDARDS

A symposium by
ASTM Committee G-1 on
Corrosion of Metals
Bal Harbour, FL, 14–16 Nov. 1983

ASTM SPECIAL TECHNICAL PUBLICATION 866
Gardner S. Haynes and Robert Baboian,
Texas Instruments, Incorporated,
editors

ASTM Publication Code Number (PCN)
04-866000-27



1916 Race Street, Philadelphia, PA 19103

Library of Congress Cataloging in Publication Data

Laboratory corrosion tests and standards.

(ASTM special technical publication; 866)
Proceedings of the Symposium on Laboratory Corrosion Tests and Standards.
Includes bibliographies and index.
"ASTM Publication code number (PCN) 04-866000-27."
1. Corrosion and anti-corrosives—Testing—Congresses. 2. Corrosion and anti-corrosives—Testing—Standards—Congresses. 1. Haynes, Gardner S. II. Baboian, Robert. III. Symposium on Laboratory Corrosion Tests and Standards (1983: Bal Harbour, FL) IV. American Society for Testing and Materials. V. Series.
TA462.L15 1985 620.1,'1223 85-7375
ISBN 0-8031-0443-X

Copyright© by AMERICAN SOCIETY FOR TESTING AND MATERIALS 1985
Library of Congress Catalog Card Number: 85-7375

NOTE

The Society is not responsible, as a body,
for the statements and opinions
advanced in this publication.



William Henry Ailor, Jr.

15 July 1917 to 9 November 1983

Dedication

This volume, recording the activities of the International Symposium on Laboratory Corrosion Tests and Standards and serving as a permanent record of contributions to the field of laboratory corrosion testing, is hereby dedicated as a living memorial to our professional colleague and personal friend, Bill Ailor, who passed away on 9 November 1983.

Bill received his Bachelor of Science degree in history from the University of Tampa in 1939 and his Bachelor of Chemical Engineering from North Carolina State University in 1948.

A Lieutenant Commander in the U.S. Naval Reserve from 1942 to 1946 and from 1952 to 1953, Bill joined the Atlantic Coast Line Railroad as a chemist in 1948. In 1953, he became a research engineer in diesel engineering for North Carolina State University. He was an adjunct math instructor for Virginia Commonwealth University from 1959 to 1979, and joined Reynolds Metals Company in 1954 as a research engineer. He retired in 1982.

The author of 45 papers and editor of four books, Bill concentrated his career in atmospheric, marine, and deep sea corrosion, corrosion testing, engine coolant testing, and diesel engineering.

Bill served as Chairman of Committee G-1 on Corrosion of Metals from 1966 to 1972 and was active in committee

task groups and subcommittees for many years including chairing the ASTM Advisory Committee on Exposure Testing Facilities. In addition to his many other honors, he received the ASTM Award of Merit in 1970.

Bill will truly be missed, by his many friends and colleagues in Committee G-1. His many contributions to the Committee, however, provide a legacy that will serve its membership for years to come.

Foreword

The symposium on Laboratory Corrosion Tests and Standards was presented at Bal Harbour, FL, 14–16 Nov. 1983. The symposium was sponsored by ASTM Committee G-1 on Corrosion of Metals. Gardner S. Haynes and Robert Baboian of Texas Instruments, Incorporated presided as chairmen of the symposium and are editors of this publication.

Related ASTM Publications

Atmospheric Corrosion of Metals, STP 767 (1982), 04-767000-27

Electrochemical Corrosion Testing, STP 727 (1981), 04-727000-27

Corrosion of Reinforcing Steel in Concrete, STP 713 (1980), 04-713000-27

Stress Corrosion Cracking—The Slow Strain-Rate Technique, STP 665 (1979), 04-665000-27

Intergranular Corrosion of Stainless Alloys, STP 656 (1978), 04-656000-27

A Note of Appreciation to Reviewers

The quality of the papers that appear in this publication reflects not only the obvious efforts of the authors but also the unheralded, though essential, work of the reviewers. On behalf of ASTM we acknowledge with appreciation their dedication to high professional standards and their sacrifice of time and effort.

ASTM Committee on Publications

ASTM Editorial Staff

Susan L. Gebremedhin
Janet R. Schroeder
Kathleen A. Greene
Bill Benzing

Contents

Introduction 1

DESIGN AND INTERPRETATION OF LABORATORY TESTS

An Engineering View of Laboratory Corrosion Tests— 5
RICHARD S. TRESEDER

Developing an Accelerated Test: Problems and Pitfalls— 14
SARA J. KETCHAM, AND EDWARD J. JANKOWSKY
Discussion 22

Microcomputer Data Aquisition for Corrosion Research— 24
DAVID G. TIPTON
Discussion 34

Corrosion Test Loop—TE-LIN YAU AND R. TERRENCE WEBSTER 36

An Accelerated Simulated Can Corrosion Test for Tinplate— 48
MALCOLM E. WARWICK AND WILLIAM B. HAMPSHIRE
Discussion 64

Laboratory Electrochemical Test Methods—OLIVER W. SIEBERT 65
Discussion 89

A Method to Avoid Crevice Corrosion in Electrochemical Determination of Pitting Potentials—TERO HAKKARAINEN 91
Discussion 106

Current Versus Voltage Hysteresis: Effect on Electrometric Monitoring of Corrosion—STANLEY T. HIROZAWA 108

Electromechanical Impedance Tests for Protective Coatings— 122
FLORIAN MANSFLED AND MARTIN W. KENDIG
Discussion 142

Applications of Electrochemical Techniques in Screening Metallic-Coated Steels for Atmospheric Use—NEAL S. BERKE AND JOHN J. FRIEL 143
Discussion 158

Development of a Fluorescent Ultraviolet and Condensation Apparatus with a Light Energy Control System—SHIGERU SUGA 159

LABORATORY TESTS FOR SPECIFIC ENVIRONMENTS

Corrosion Testing in Potable Waters—KATE NIELSEN 169
Discussion 182

Corrosion of Mild Steel in Distilled Water and Chloride Solutions: Development of a Test Method—PETER E. FRANCIS AND ANTONY D. MERCER 184
Discussion 195

A Comparison of Actual and Estimated Long-Term Corrosion Rates of Mild Steel in Seawater—FREDERIC D. BOGAR AND MILLER H. PETERSON 197
Discussion 205

Once Through Versus Recirculated Seawater Testing for Calcareous Deposit Polarization of Cathodically Protected Steel—TRACY L. NYE, SAMUEL W. SMITH, AND WILLIAM H. HARTT 207

A Corrosiveness Test for Fibrous Insulations—STEPHEN V. CRUME 215

Electrochemical Methods for Evaluating Corrosion Inhibitors in Strong Acid Systems—SHELDON W. DEAN, ROBERT A. WOODROOF, AND JAMES NICHOLS 228
Discussion 245

Laboratory Corrosion Testing of Metals and Alloys in Environments Containing Hydrogen Sulfide—ROBERT D. MACK, S. MARK WILHELM, AND BEVERLEE G. STEINBERG 246

Development of an Environmental Wear Corrosion Test for Coinage Materials—ROBERT BABOIAN AND GARDNER S. HAYNES 260

Laboratory Tests for Corrosion of Steel in Concrete— 275
PHILIP A. ROOSKOPF AND R. CRAIG VIRNELSON

Corrosion Induced Deformation Behavior of Brick Masonry Wall Panels—STEPHEN A. DIAL, RAMON L. CARRASQUILLO, AND JOHN E. BREEN 285

TESTS FOR CORROSION TYPE

Recent Developments in Test Methods for Investigating Crevice Corrosion—ROBERT M. KAIN AND THAD S. LEE 299
Discussion 322

Crevice and Pitting Corrosion Tests for Stainless Steels: A Comparison of Short-Term Tests with Longer Exposures—M. HUBBELL, C. PRICE, AND R. HEIDERSBACH 324

A Technique for Characterizing Crevice Corrosion Under Hydrothermal Conditions—HIMASHU JAIN, TAE-MOON AHN, AND PETER SOO 337
Discussion 356

Jet-in-Slit Test for Studying Erosion-Corrosion— 358
MASANOBU MATSUMURA, YOSHINORI OKA, SATOFUMI OKUMOTO, AND HIROYUKI FURUYA
Discussion 371

MTI Corrosion Tests for Iron- and Nickel-Base Corrosion Resistant Alloys—RICHARD S. TRESEDER AND EDWARD A. KACHIK 373

Evaluating the Suitability of the NACE Standard Test, TM-01-77, for Testing 13% Chromium Martensitic Stainless Steels for Sulfide Stress Cracking Resistance— 400
TIMOTHY D. WHITEHEAD AND CALVIN H. BALOUN

Slow Strain Rate Testing in High-Purity Water at Controlled Electrode Potentials—BO ROSBORG AND ANDERS ROSENGREN 415
Discussion 427

The Effect of Strain Rate on the Stress Corrosion Cracking of Steels for Prestressing Concrete—V. SÁNCHEZ GÁLVEZ, LUIS CABALLERO, AND MANUEL ELICES 428

An Improved Intergranular Corrosion Test for HASTELLOY® Alloy C-276—PAUL E. MANNING 437

Surface Preparation Requirements for ASTM A 262— JOHN M. SCHLUTER AND JOSEPH A. CHIVINSKY 455

APPENDIX OF SELECTED ASTM STANDARDS

A 262-85	**Practices for Detecting Susceptibility to Intergranular Attack in Austenitic Stainless Steels**	469
B 117-85	**Method of Salt Spray (Fog) Testing**	496
G 1-81	**Practice for Preparing, Cleaning, and Evaluating Corrosion Test Specimens**	505
G 5-82$^{\epsilon 1}$	**Practice for Standard Reference Method for Making Potentiostatic Anodic Polarization Measurements**	511
G 15-85a	**Definitions of Terms Relating to Corrosion and Corrosion Testing**	522
G 28-85	**Methods of Detecting Susceptibility to Intergranular Attack in Wrought Nickel-Rich, Chromium-Bearing Alloys**	527
G 31-72 (1985)$^{\epsilon 1}$	**Practice for Laboratory Immersion Corrosion Testing of Metals**	534
G 34-79	**Test Method for Exfoliation Corrosion Susceptibility 2XXX and 7XXX Series Aluminum Alloys (EXCO Test)**	545
G 46-76 (1980)	**Recommended Practice for Examination and Evaluation of Pitting Corrosion**	552

G 48-76 (1980)$^{\epsilon 1}$	**Test Methods for Pitting and Crevice Corrosion Resistance of Stainless Steels and Related Alloys by the Use of Ferric Chloride Solution**	562
G 61-78	**Practice for conducting Cyclic Potentiodynamic Polarization Measurements for Localized Corrosion**	566
G 71-81	**Practice for Conducting and Evaluating Galvanic Corrosion Tests in Electrolytes**	572
G 85-85	**Practice for Modified Salt Sprat (Fog) Testing**	578
G 87-84	**Practice for Conducting Moist SO_2 Tests**	584

SUMMARY

Summary 591

Index 597

Introduction

The corrosion resistance of a product or material is evaluated by service history, field testing, or laboratory corrosion testing. The most reliable predictor of performance is, of course, service experience followed closely by field testing since they are based upon the actual environment. When service history is lacking and time or budget constraints prohibit field testing, laboratory corrosion tests are used to predict corrosion performance. They are particularly useful for quality control, specification, materials selection, and materials development.

Laboratory corrosion tests fall into the following categories: immersion tests, simulated atmosphere tests, electrochemical tests, and environmentally aggressive tests. All of these are accelerated tests by design and therefore must be used carefully. The problems associated with laboratory corrosion tests include inappropriate test selection or evaluation, and incorrect or misleading results. The need for standardization of laboratory testing procedures and for determining the applicability of the results is obvious. Therefore, ASTM Committee G-1 on Corrosion of Metals, through Subcommittee G01.05 on Laboratory Corrosion Tests, sponsored the International Symposium on Laboratory Corrosion Tests and Standards from which the papers from the basis of this STP. The intent of this symposium was to provide a forum for discussion of existing standardized tests as well as the design and interpretation of new tests. It was truly international in scope with authors from eight countries.

The topics discussed in the STP include (1) the design and interpretation of laboratory tests, (2) laboratory tests for specific environments, and (3) laboratory tests for specific types of corrosion. An Appendix containing the standards most often referred to in the papers is included in the STP.

The papers on design and interpretation of laboratory tests deal with the engineering aspects of development of relevant tests as well as the newest electrochemical laboratory tests. New accelerated tests for salt-sulfur dioxide environments, high-temperature acidic environments, crevice corrosion, corrosion of cans, and atmospheric corrosion are described. Electrochemical techniques that are addressed include AC impedance, linear polarization, potentiodynamic polarization, current versus voltage hysteresis, and computer data acquisition. The papers on tests for specific environments address laboratory tests for potable waters, seawater, hydrogen sulfide environments, steel in concrete, inhibitors, and coinage environments. Results from these tests are correlated with field tests

Copyright© 1985 by ASTM International www.astm.org

and service performance. The topics of papers on tests for specific types of corrosion include crevice corrosion, erosion corrosion, stress corrosion cracking, and intergranular corrosion.

The information in this STP is useful for experienced as well as new investigators involved with conducting, specifying, or evaluating laboratory corrosion tests. It defines the state of the art in laboratory corrosion testing, describes limitations of accelerated tests, provides significant information on relevance of existing tests as well as information useful for the development of new tests, and includes the standards most often used for laboratory corrosion testing.

Gardner S. Haynes and
Robert Baboian
Texas Instruments, Incorporated
Attleboro, MA 02703, symposium cochairmen and coeditors

Design and Interpretation of Laboratory Tests

Richard S. Treseder[1]

An Engineering View of Laboratory Corrosion Tests

REFERENCE: Treseder, R. S., **"An Engineering View of Laboratory Corrosion Tests,"** *Laboratory Corrosion Tests and Standards, ASTM STP 866*, G. S. Haynes and R. Baboian, Eds., American Society for Testing and Materials, Philadelphia, 1985, pp. 5–13.

ABSTRACT: Many laboratory tests designed to assist in engineering decisions regarding materials selection have not received the desired user acceptance. Possible explanations for this situation are discussed with examples taken from test methods for evaluating stress corrosion cracking of alloys and crevice corrosion susceptibility of stainless steels in chloride systems. Suggested means of improving tests include: (1) improved definition of the limits of the corrosion system for which the test is designed, (2) use of the rank ordering concept in evaluating materials, (3) selecting rank ordering factors that are mechanistically sound and that have engineering significance, (4) correlating laboratory data with field experience to establish acceptable/unacceptable criteria for alloys for specific environments, and (5) standardizing test details so that comparable results can be obtained by different laboratories.

KEY WORDS: corrosion tests, stress corrosion, concentration cell corrosion, materials selection

This paper is concerned with the problem of engineer-user acceptance of laboratory corrosion tests designed for alloy evaluation. That this problem exists is indicated by the contrast between the large number of such tests that have been proposed in recent years and the relatively few that have achieved the acceptance indicated by group usage. The problem is most pronounced with laboratory tests for evaluation of stress corrosion cracking resistance and for evaluation of resistance to crevice corrosion. Possible causes for this situation are explored, and suggestions are made for approaches that could assist in a more rapid acceptance of laboratory corrosion tests of this type. Corrosion tests for evaluating corrosion control measures (for example, corrosion inhibition) are within the scope of this paper, but will be handled as a special case.

Certain categories of laboratory corrosion tests are outside the scope of this paper. These include corrosion tests designed to provide an answer to a specific corrosion problem involving a specific environment, corrosion tests aimed at developing understanding of corrosion mechanisms, and corrosion tests designed as quality assurance tests.

[1] Consulting corrosion engineer, 6272 Girvin Drive, Oakland, CA 94611.

Copyright© 1985 by ASTM International www.astm.org

Nature of the Problem

Alloy selection generally involves a go, no-go interpretation of corrosion data rather than a quantitative evaluation. An alloy is either acceptable or unacceptable depending on established design criteria, which involve first cost, service life, maintenance costs, cost of failure, and safety aspects. However, it is essential to know how close an alloy is to the acceptable/unacceptable limit in order to compare alloys of differing costs and to permit comparison of the failure risks for different alloys. This thinking leads to the rank ordering concept, which can be expressed qualitatively in terms such as definitely susceptible, probably susceptible, possibly resistant, probably resistant, or definitely resistant.

Within a given corrosion system the engineer-user expects to find, by definition, the relation shown in Fig. 1 between severity of the environment and alloy susceptibility to corrosion.

The engineer-user would like to have rank ordering data that would allow statements such as "Alloys in Category 3 or lower can be used with minimum probability of failure if the environmental factors are in Category C or lower; if an extra margin of safety is required, alloys in Category 2 or lower should be used."

Development of the ideal test requires considerable research and engineering effort. Research aspects involve defining the limits of the corrosion system, defining the dominant corrosion factors, and developing the corrosion test procedure. The engineering aspect involves collecting field experience data and correlating it with laboratory corrosion test data to permit establishment of acceptability criteria, such as the above, "Severity C = Susceptibility 3" criterion.

In the following sections of this paper various aspects of the problem will be discussed, with emphasis on those features of laboratory corrosion tests, which in the writer's opinion, have a major influence on user acceptance.

Defining the Corrosion System

It is obvious that for any laboratory corrosion test method designed for alloy evaluation, the limits of the corrosion system to which it can be applied must be defined. In practice this turns out to be an evolutionary process involving input from both laboratory research and field experience.

The problem of defining the limits of a corrosion system can be described by examples. For many years the stress corrosion cracking of austenitic stainless steels in chloride solutions was considered to be one system, and the magnesium chloride test was the way to evaluate the stress corrosion cracking resistance of alloys. Experience has shown that there are several systems instead of one. Currently there are three major systems of interest, each of which requires a separate test for alloy evaluation:

(1) acidic chloride solutions,
(2) neutral chloride solutions, oxygen present, and
(3) chloride solutions containing hydrogen sulfide.

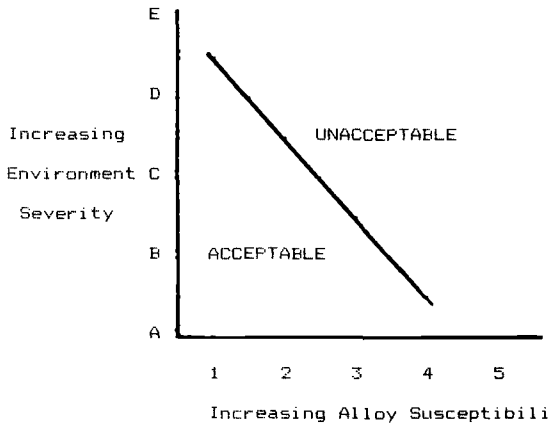


FIG. 1—*Relationship between severity of the environment and alloy susceptibility to corrosion.*

Work is in progress to define the limits of each system and to develop test methods. Environmental factors to be considered in setting the system limits include acidity, halide concentration, hydrogen sulfide concentration, oxygen concentration, and temperature. Alloy composition limits must be set. For example, is one test applicable to nonaustenitic stainless steels and nickel base alloys as well as austenitic stainless steels? Another question to be resolved is whether sensitized alloys are to be included in the system, or whether a separate system is required for them.

A second example describes the evolution from one corrosion system to four systems within one set of environmental conditions. This occurred with the environmental cracking of metallic materials in sour gas service. At first, the system was thought to consist only of sulfide stress cracking of carbon and low alloy steels, and that one laboratory corrosion test would serve to evaluate materials for this service. Subsequently, field experience showed that there are at least three other systems. It was then necessary to devise additional tests for materials evaluation. These systems are

(1) hydrogen induced cracking (sometimes known as stepwise cracking) of low-strength steels,

(2) embrittlement of certain high-strength nickel alloys by hydrogen generated from galvanic coupling to steel, and

(3) stress corrosion cracking of austenitic stainless steel and related alloys.

During development of the test method, it is essential to confirm that the method has duplicated the dominant corrosion factors of the corrosion system being studied. This is done by comparing the corrosion effects obtained in the laboratory with those experienced in the field. For example, measured corrosion rates should certainly compare within a reasonable factor (two or three) and the response to changes in major corrosion factors (for example, temperature) should parallel field experience.

Rank Ordering Factors

In the development of laboratory corrosion tests for alloy evaluation it is necessary to determine the dominant corrosion factors (for example, alloy condition, temperature, solution composition, and concentration). Preferred practice is to design the test so that it will represent a severe condition for the corrosion system involved, thus reducing the time for effects to be observed. One of the dominant factors is then chosen to be the rank ordering factor. Study of alloy response as this factor is varied provides a means for comparing the corrosion resistance of different alloys. This factor can be one imposed by the test designer such as temperature, stress, or concentration; or it can be a factor that results from the test conditions alone. The latter would include such factors as time to failure, corrosion rate, and pitting frequency. Selection of the rank ordering factor is important because of the influence it has on engineer-user acceptance of a laboratory corrosion test.

Table 1 is a partial listing of factors that have been used for evaluating the susceptibility of alloys to stress corrosion cracking. Table 2 is a similar listing for the susceptibility of stainless steels to crevice corrosion in chloride systems. The large number of rank ordering factors in these listings plus additional complications that arise from variations in specimen design and test solution composition have led to a confusing situation. A more critical approach to rank ordering would be one way of improving user acceptance of laboratory test results.

It is reasonable to assume that the preferred rank ordering factors are those that are mechanistically sound and that have engineering significance. The mechanistically sound aspect refers to the mechanism of the corrosion reaction involved. Engineering significance indicates that the rank ordering factor has some relation to a possible engineering design factor. However, too direct a relation might prove undesirable. Because a laboratory test cannot duplicate all

TABLE 1—*Factors that have been used for evaluating the stress corrosion cracking susceptibility of alloys.*

Factors
Time to failure under constant load conditions
Time to failure under constant strain conditions
Threshold stress for failure[a]
Threshold stress for failure/yield strength[a]
Threshold strain for failure[a]
Threshold stress intensity[a]
Strain for 50% probability of failure[a]
Crack growth rate
Time to failure (slow strain rate test)
Loss of ductility (slow strain rate test)
Fracture appearance (slow strain rate test)
Work to failure (slow strain rate test)
Critical strain rate

[a]Fixed time period (for example, 1000 h).

TABLE 2—*Factors that have been used to evaluate the crevice corrosion susceptibilities of stainless steels in chloride systems.*

Factors
Critical temperature—pitting, multiple crevice assembly (MCA)
Critical temperature—critical current at 600-mV SCE[a]
Critical temperature—400-mV SCE pitting potential
Critical pitting potential
Critical protection potential
Critical chloride concentration
Probability of crevice corrosion initiation, MCA
Probability of crevice corrosion propagation, MCA
Depth of penetration
Time for crevice corrosion initiation
Critical crevice solution composition

[a]SCE is saturated calomel electrode.

the complexities of actual service conditions, laboratory results can be misleading if interpreted literally.

In the following paragraphs a number of possible rank ordering factors are discussed with examples used to illustrate the above points.

1. *Corrosion Damage*—This factor includes such items as corrosion rate, pit depth, and percentage of area attacked. Generally it is not a satisfactory rank ordering factor since the values that have engineering significance are usually so low that there is not enough range in values to permit rank ordering a wide variety of materials. For example, if weight loss corrosion is the factor, corrosion rates above about 0.2 mm/year may not have engineering significance since they are unacceptable, and values below 0.01 mm/year may be technically insignificant. Corrosion damage is most useful in evaluating materials in field tests, in laboratory tests aimed at predicting service life for a specific application, and in quality assurance tests.

2. *Time to Failure*—This factor has been used extensively in stress corrosion tests, but it lacks engineering significance since failures within a practical test duration (for example, 30 days) occur in times too short to be acceptable in practice.

3. *Critical Temperature*—Determination of the temperature at which a predetermined level of corrosion damage has occurred is a common way of rank ordering corrosion resistance of alloys. In many systems it is mechanistically sound since increasing temperature results in a fairly regular increase in corrosivity. It is acceptable from an engineering standpoint since temperature is often a controllable design variable. Temperature is the rank ordering factor selected for the weight loss corrosion tests for iron- and nickel-base corrosion resistant alloys developed by the Materials Technology Institute of the Chemical Process Industries (MTI) [*1*]. Temperature may be an acceptable rank ordering factor for crevice corrosion of stainless steels in certain oxidizing acidic chloride systems. However, in a complex system, such as seawater, there are some doubts

about the mechanistic soundness of temperature as a rank ordering factor. These arise from results of field crevice corrosion tests with stainless steels in which there was a decreased tendency for crevice corrosion on increasing the temperature from 30 to 50°C [2]. The critical temperature concept for crevice corrosion in seawater service has an added disadvantage in that it might mislead a user into believing that temperature could be used as a design factor to control crevice corrosion.

4. *Critical Potential*—Determination of a critical pitting potential is questionable from a mechanistic viewpoint for evaluating resistance to crevice corrosion. Additional problems of test reproducibility and the question of engineering significance have limited its use as a rank ordering factor.

5. *Crevice Geometry*—The use of some aspect of crevice geometry, such as crevice gap, crevice depth, or surface finish, is being explored as a possible rank ordering factor in crevice corrosion [3]. This idea has appeal from both the mechanistic and the engineering significance points of view. It offers the prospect of simulating variables, such as joint design and surface cleanliness, which in practice influence the severity of exposure.

6. *Critical Concentration*—For those systems where concentration of a specific component of the system is a major corrosion factor, the use of concentration as a rank ordering factor is attractive from both the mechanistic and engineering significance points of view. For example, pH has been used as a rank ordering factor for crevice corrosion of titanium alloys in chloride systems.

7. *Critical Stress (Strain)*—Critical stress or strain is often used as a rank ordering factor for stress corrosion cracking systems. Either threshold stress for failure or the stress for 50% probability of failure has been used. This approach has been used successfully in both constant load and constant strain tests for evaluating the resistance of steels to sulfide stress cracking. From both the mechanistic and the engineering significance viewpoints this rank ordering factor is generally considered acceptable.

8. *Critical Stress Intensity*—From a mechanistic point of view the fracture mechanics approach to stress corrosion cracking testing has some attractive features. The rank order factor can be stress intensity, crack velocity, or the complete curve of stress intensity versus crack velocity. The latter provides more mechanistic information but is difficult to use as a rank ordering tool. Objections to the fracture mechanics method of rank ordering alloys in their resistance to stress corrosion cracking arise mainly from the experimental complications caused by specimen complexity and size limitations. These complications make it difficult (and costly) to apply such tests to some materials.

Environment Rank Ordering

Within any general corrosion system there will be wide ranges of severity as related to a specific corrosion effect such as crevice corrosion or stress corrosion cracking. In the case of seawater this could result from such factors as temper-

ature, acidity, salinity, oxygen content, solids contaminants, soluble contaminants, velocity, and the time distribution of these factors. Since in most cases a less severe corrosive environment would permit use of a less resistant (and possibly less costly) alloy, there is an obvious need for a means of evaluating the severity of environments with a rank ordering scheme similar to that discussed for alloys. It would be preferable to use the same basic test method. This has been done in the case of sulfide stress cracking. Values of hydrogen sulfide concentration and temperature have been defined where there is a significant change in severity of the environment as measured by changes in susceptibility to cracking of standard alloys [*4*].

In evaluating the above rank ordering variables for possible use as environment rank ordering factors, it is seen that some of them have the potential of being easily converted. These include critical stress, critical stress intensity, and crevice geometry. Those rank ordering factors that are environmental factors would have obvious limitations. Corrosion damage can be used effectively in rank ordering environments. For example, constant strain rate stress corrosion tests have been used for this purpose in liquid ammonia systems, with reduction of area as the rank ordering factor to evaluate the effect of contaminants in liquid ammonia on the stress corrosion cracking of steel [*5*]

Field Experience Correlation

The rank ordering concept requires that a value of the rank ordering factor be established that defines the border between nonacceptable and acceptable materials. Such a value can be determined only by a correlation of laboratory test data with field experience data, which includes failures as well as successes. Since many of the service cases reported will not have complete operating information or details of the materials used and their metallurgical histories, it will be desirable to establish some cross-links in data by conducting laboratory tests with samples of the failed items, or with solutions that duplicate some unusual environmental factor. An example of how this was done in the case of sulfide stress cracking is shown in Tables 3 and 4. In this example, "critical

TABLE 3—*Correlation of field sulfide corrosion cracking experience with typical laboratory test data that allowed establishment of the acceptability criterion of Sc > 10* [4].

Field Experience		
Type of Steel	Failure Frequency	Sc[a] (typical)
API Grade J-55	nil	11 to 17
API Grade C-75	nil	10 to 17
API Grade N-80	moderate	5 to 14
API Grades P-105, P-110	high	3 to 10

[a]Sc is defined as the "critical stress: (ksi × 0.1), calculated from deflection of a beam specimen (three-point loading), which corresponds to a 50% probability of failure in a standardized hydrogen sulfide solution as calculated from results obtained at varying beam deflections.

TABLE 4—*Laboratory corrosion test data for specimens from sulfide corrosion cracking field failures that confirmed acceptability criterion of Sc > 10* [4].

Laboratory Tests With Specimens From Field Failures	
Failed Item	*Sc*[a]
API Grade N-80 tubing[b]	9.5
API Grade N-80 casing	6.4
API Grade N-80 casing	6.7
API Grade N-80 tubing	5.5
AISI 4340 tubing hanger[b]	2.2
Cast steel valve body	7.5

[a]*Sc* is defined as the "critical stress" (ksi × 0.1), calculated from deflection of a beam specimen (three-point loading), which corresponds to a 50% probability of failure in a standardized hydrogen sulfide solution as calculated from results obtained at varying beam deflections.

[b]API is the American Petroleum Institute and AISI is the American Iron and Steel Institute.

stress" *Sc* for 50% probability of failure in a standard laboratory test was the rank ordering factor for materials considered for use in sour gas environments. Accumulated field experience with various materials was used to set an *Sc* acceptability limit. The validity of this *Sc* limit was confirmed by showing that specimens cut from actual field failures had *Sc* values below the acceptability limit.

The lack of an acceptability limit for the rank ordering factor can delay engineering acceptance of a proposed laboratory corrosion test. A cooperative industry effort is usually required to obtain the necessary field experience information.

Evaluation of Inhibitors

In the foregoing discussion emphasis was on laboratory tests for evaluation of alloys. The same general ideas apply to tests for evaluation of corrosion control measures such as inhibition. An additional rank ordering factor is available to compare the effectiveness of different inhibitors. This factor is the critical inhibitor concentration required to achieve some arbitrary percentage reduction in corrosion rate.

Some laboratory tests for inhibitor evaluation have had only limited user acceptance because the test conditions fail to simulate the field corrosion system. For example, many of the tests used to evaluate oil field inhibitors are in reality evaluating only the film forming nature of the inhibitors. The corrosion conditions selected for these tests do not include some of the dominant field corrosion factors such as velocity, scale, and phase effects. This is evidenced by the low corrosion rates obtained in the laboratory control tests. Therefore, users generally rely on field tests for evaluation of inhibitors screened by the laboratory test.

Standardization

Lack of standardized methods is another factor responsible for delay in user acceptance of laboratory corrosion tests intended for alloy evaluation. There is a need for more alloy evaluation test methods to be written with sufficient specification of details to permit different laboratories to use the methods and obtain results that can be compared. In the past a number of alloy evaluation methods issued by industry groups, such as ASTM and the National Association of Corrosion Engineers (NACE), have been written as recommended practices, with many significant test details left to the discretion of the user. This approach results in published data that cannot be evaluated properly by the user since the data from different sources are not comparable.

Conclusions

The following suggestions can be made for improving the rate of user acceptance of laboratory corrosion tests aimed at the evaluation of the relative corrosion resistance of alloys.

1. Define the limits of the corrosion system represented by the corrosion test.
2. Use the rank ordering concept for evaluating materials, and select as the rank ordering factor one that is mechanistically sound for the corrosion system involved and that has engineering significance.
3. If possible, design the test so that it can also be used for evaluating the relative severity of different corrosive environments within the corrosion system involved.
4. Collect sufficient field experience data so that a correlation between laboratory results and field experience can be made, which will permit establishment of criteria for acceptable/unacceptable alloys for a specified level of environment severity.
5. More alloy evaluation test methods should be written as standard tests rather than as recommended practices.

References

[1] Treseder, R. S., *Guideline Information on Newer Wrought Iron- and Nickel-Base Corrosion Resistant Alloys*, MTI Manual No. 3, Materials Technology Institute of the Chemical Process Industries, Inc., Columbus, OH, 1980.

[2] Kain, R. M., "Crevice Corrosion Resistance of Austenitic Stainless Steels in Ambient and Elevated Temperature Seawater," Paper 230, *CORROSION/79*, National Association of Corrosion Engineers, Houston, TX, 1979.

[3] Lee, T. S. and Kain, R. M., "Factors Influencing Crevice Corrosion Behavior of Stainless Steels in Seawater," Paper 69, *CORROSION/83*, National Association of Corrosion Engineers, Houston, TX, 1983.

[4] Treseder, R. S. and Swanson, T. M., *Corrosion*, Vol. 24, No. 2, Feb. 1968, p. 31.

[5] Deegan, D. C. and Wilde, B. E., *Corrosion*, Vol. 29, No. 8, Aug. 1978, p. 310.

Sara J. Ketcham[1] *and Edward J. Jankowsky*[1]

Developing an Accelerated Test: Problems and Pitfalls

REFERENCE: Ketcham, S. J. and Jankowsky, E. J., **"Developing an Accelerated Test: Problems and Pitfalls,"** *Laboratory Corrosion Tests and Standards, ASTM STP 866*, G. S. Haynes and R. Baboian, Eds., American Society for Testing and Materials, Philadelphia, 1985, pp. 14–23.

ABSTRACT: Naval aircraft spend considerable time on the decks of aircraft carriers exposed to sea spray and sulfur-bearing stack gases. A series of exposure tests of various aircraft materials and coatings have been conducted on operational carriers for over five years. There were two objectives for this work: (1) to find out how the materials behaved in the hostile carrier environment and (2) to develop a laboratory test to simulate that environment. The first objective is being successfully met. The second objective is more difficult to achieve.

To date, experiments have included use of a salt fog chamber with periodic introduction of sulfur dioxide gas. Various cyclic conditions have been studied, such as spraying salt fog, introducing sulfur dioxide gas followed by a soak period at high humidity. This cycle reproduces in two weeks the exfoliation attack on susceptible aluminum alloys that occur on a carrier in about eight months. However on cadmium plated steel, which undergoes little or no attack on the carrier, this cycle causes considerable attack on the coating. Since an accelerated test is also desired for materials, such as paints, corrosion preventive compounds, sealants, and other organics used on naval aircraft, finding one accelerated test that will reproduce carrier results on such a wide variety of materials presents a formidable task.

KEY WORDS: accelerated tests, corrosion tests, corrosion environments, salt-sulfur-dioxide environments

The lack of correlation between laboratory salt spray tests and outdoor exposure tests has been known for years. This became especially apparent to the air arm of the Navy when high-strength aluminum alloys began to be used for aircraft skins. Exposure to neutral salt fog pitted these alloys, but did not cause them to exfoliate the way they do during exposure on an aircraft carrier or a seacoast corrosion rack. It was obvious that a better laboratory test was needed to simulate service conditions.

Some clues as to what the service conditions on an aircraft carrier actually were emerged as the result of a study by an aircraft manufacturer.[2] Measurements of pH were made on the soot obtained from surfaces of aircraft parked on the

[1] Head of Materials Protection Branch (now retired) and chemist, respectively, Aircraft and Crew Systems Technology Directorate, Naval Air Development Center, Warminster, PA 18974.

[2] Douglas Aircraft Co., Long Beach, CA 1967, private communication.

Copyright© 1985 by ASTM International www.astm.org

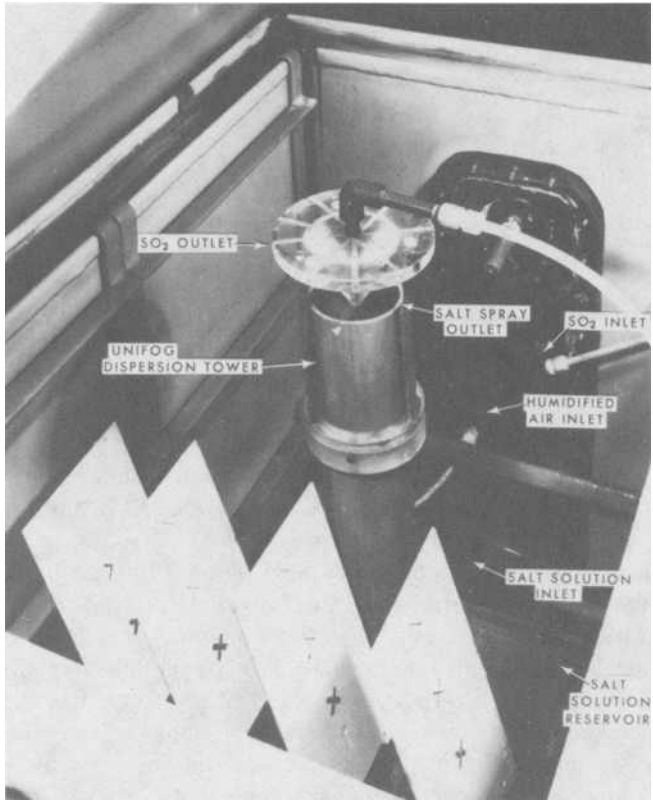


FIG. 1.—*Interior view of cabinet used for NaCl-SO_2 test.*

flight decks of four different carriers. Values of 2.4 to 4.0 were obtained. The presence of sulfate ion was also detected. The manufacturer concluded that the environment of the carrier combined salt spray with weak sulfuric acid. The source of the sulfur was assumed to be the gases emitted from the carrier stacks.

Following these disclosures it was reasoned that adding sulfur dioxide to the salt fog would bring the test environment closer to actual conditions on an aircraft carrier. Three different systems were tried for introducing sulfur dioxide. First, exhaust gases from a small engine burning sulfur-containing fuel were fed into the cabinet. This was awkward and gave inconsistent results. Adding sulfuric or sulfurous acid directly to the salt solution also produced only fair results. The method that produced exfoliation most similar to that obtained in service was direct addition of sulfur dioxide to the salt fog chamber (Fig. 1). This test was standardized and refined.

Laboratory Test Procedures

Final test conditions are presented in Table 1. One of the most important parameters is the amount of sulfur dioxide gas to be introduced. An effort was

TABLE 1—*Sodium chloride-sulfur dioxide test.*[a]

Parameters	Values
OPERATING CONDITIONS	
Salt solution	5% NaCl
Bubble tower temperature	46°C (115°F)
Cabinet temperature	35°C (95°F)
SO_2 gas injection	1/6-hr cycle
SO_2 gas flow of box	35 $cm^3/min/m^3$ (1.0 $cm^3/min/ft^3$)
CONDITIONS IN COLLECTION BOTTLE	
Collection rate	1 to 2 mL/h
pH	2.5 to 3.2

[a]All other aspects of the test according to ASTM Salt Spray (Fog Testing) (B 117).

made to find out how much sulfur dioxide might be present on the flight deck of a carrier so the test would be as realistic as possible.

Navy ships use a fuel that has a maximum allowable sulfur content of 1%. Actual sulfur content apparently varies according to the source of the fuel, some having 0.3 to 0.4% sulfur and some having 0.7 to 0.8% sulfur.

Discussions were held with the Naval Ship Systems Engineering Station on more quantitatively characterizing the carrier environment.[3] It is possible, knowing the sulfur content of the fuel, the amount consumed, and the percentage of excess air in which it is burned, to calculate the parts per million (ppm) of sulfur dioxide that will be discharged at the stack, that is, "static discharge." The level of operation of the boilers controls fuel consumption, and this will vary with time. Maximum effluent is generated when planes are warming up for takeoff since the level of boiler operation is highest at that time.

Assuming a fuel with a sulfur content of 0.7 to 0.8%, being burned in 100% excess air, a volume concentration of 330 ppm can be present at static discharge. With a sulfur content of 0.3 to 0.4% burned in 100% excess air, the volume concentration would be half of that value.

The amount of sulfur dioxide that will reach the planes parked on the flight deck depends on air currents, ship speed, and weather conditions. These can vary from hour to hour. Obviously, this amount will be considerably less than that at static discharge.

In an effort to determine the relationship between the amount of sulfur dioxide at static discharge and that in the laboratory simulated carrier environment, calculations were made to convert the amount of sulfur dioxide being introduced into a 0.85-m^3 (30-ft^3) cabinet into ppm [*1*]. The concentration of sulfur dioxide was determined to be 70 ppm at the end of 1 min and should increase at the rate of 70 ppm/min. However, the 70 ppm/min is not cumulative because of two important factors. First, much of the gas introduced into the cabinet flows out through the exhaust system. And second, some of the sulfur dioxide is

[3] Boyle, J. and Gorin, N., Naval Ship Systems Engineering Station, Philadelphia, PA, Aug. 1977, private communication.

dissolved in the salt spray. Lacking more quantitative data, it appears reasonable to assume that the concentration of sulfur dioxide in the chamber is at least in the same range as that on an aircraft carrier. The flow rate of 35 ± 7 $cm^3/min/m^3$ (1.0 ± 0.2 $cm^3/min/ft^3$) of box is therefore considered realistic.

The use of 5% synthetic sea salt in place of 5% sodium chloride was studied several years ago. Limited correlative studies between the two cabinets have indicated that the synthetic sea salt/sulfur dioxide was less severe for unpainted aluminum alloys and more severe for cadmium plated steel than the sodium chloride/sulfur dioxide. Aluminum alloys protected by MIL-P-23377 primer and MIL-C-83286 topcoat showed no differences. It was decided that the synthetic sea salt offered no particular advantage so the majority of environmental tests conducted to date on metals, alloys, coatings, and finishes have been in the sodium chloride-sulfur dioxide fog. This method has been used for some years now to evaluate corrosion resistance of a variety of materials, processes, and hardware projected for use in an aircraft carrier environment.

Aircraft Carrier Tests

About four years ago, arrangements were made to place corrosion racks on the flight decks of aircraft carriers. The racks are made of steels that have been cadmium plated, chromated, and painted. They are attached to radar towers from 1.8 to 3.7 m (6 to 12 ft) from the flight decks (the height is slightly different on each carrier) (Fig. 2). Specimens are attached to the rack while the carrier is in the United States, just before deployment, and taken off when the carrier returns after exposure to the normal seven to eleven month deployment. To date, specimens have been exposed on aircraft carriers in the Indian, the Mediterranean, and the Pacific Oceans. Aluminum alloys with various heat treatments, paint systems, avionics materials, composites, and various types of inorganic coatings have been tested. A corrosion monitor that measures corrosivity of the environment was also installed on several carriers [*2*].

This has provided a unique opportunity to compare results in the real environment with those in the accelerated laboratory tests.

Tests on the first carrier were with aluminum alloys that had been used in an ASTM/Aluminum Association interlaboratory testing program. These alloys had been exposed to a number of natural environments and accelerated laboratory tests so a direct comparison could be made. Results of these tests have been published elsewhere [*3*]. Figure 3 summarizes the results that showed the carrier environment to be more severe than seacoast or industrial environments.

The first carrier was deployed to the Mediterranean and conventionally powered so sulfur dioxide was present. The second carrier was nuclear powered and originally deployed to the Mediterranean. This should have provided the opportunity to determine how important a role sulfur dioxide played. Unfortunately after four months in the Mediterranean the ship was sent to the Indian Ocean where it stayed for six months. The corrosion that occurred was even more severe



FIG. 2—*Aircraft carrier exposure tests. Arrow pinpoints rack location.*

than that on the first conventionally powered carrier. Tests on four additional carriers have been made, all of which were conventionally powered and spent most of their time during deployment in the Indian Ocean. It has therefore not been possible to compare a carrier with and without sulfur dioxide in the same theater of operation.

The theater of operation definitely plays a role. Cruising the Mediterranean, Pacific, and Atlantic Oceans provides a more severe environment than seacoast locations, but these areas are mild compared to the Indian Ocean. Reports from the Indian Ocean indicate that during the months of May through August there is a continuous monsoon flow producing extremely high humidity. The weather has been described as unchanging: low overcast, winds 5 to 10 m/s (10 to 20 knots), seas 3.0 to 3.7 m (10 to 20 ft), temperature 27 to 32°C (80 to 90°F), relative humidity 70 to 80% rising to 95 to 100% at night with a continuous salt/sand mist in the air. Corrosion problems are being reported on systems and hardware that previously presented no problems.

Although there has been no opportunity to compare carriers with and without sulfur dioxide, there has been an opportunity to compare results of carrier exposure and the sodium chloride-sulfur dioxide tests on a variety of materials. Generally correlation was good. A major discrepancy is the behavior of cadmium plated steel. Cadmium plated parts (0.013 mm or 0.0005 in.) held up well on the carrier, but not in the sodium chloride-sulfur dioxide test.

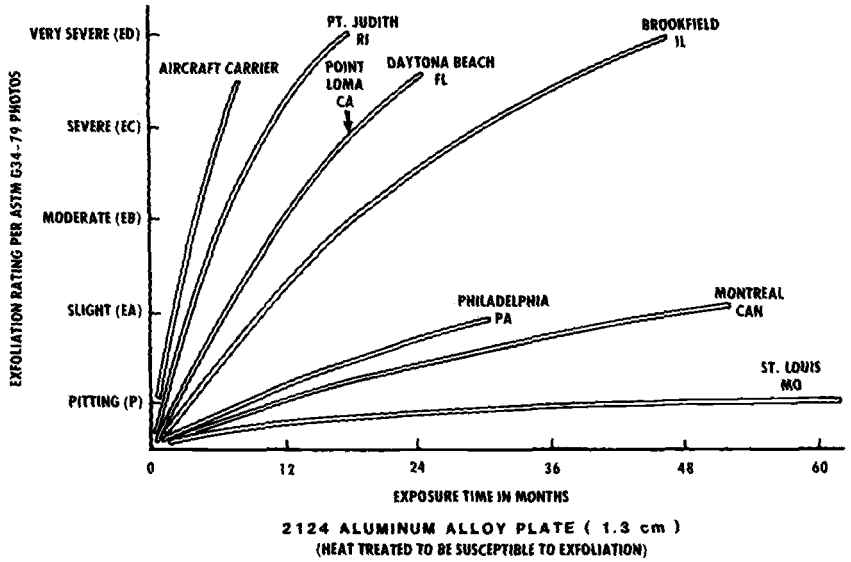


FIG. 3—*Comparison of corrosivity of seacoast and industrial environments with that of an aircraft carrier.*

Initially this created some concern so some modifications to the test were tried. Experiments were conducted with cyclic testing to see the effect of alternate wetting and drying. The cycle shown in Table 2 was selected for further investigation. For aluminum alloys, this test procedure gave results very similar to those obtained on a carrier. However, when cadmium plated steel was tested under the same conditions, the cadmium was completely gone in about four days, and the steel was badly rusted.

A comparative study of the sodium chloride-sulfur dioxide test versus ASTM Testing Acidified Synthetic Sea Water (Fog) (G 43) was then conducted. ASTM G 43 is an acidified salt spray test that is frequently used as an exfoliation test for aluminum alloys. The results of this study were then compared with results of exposure tests on the carriers.

TABLE 2—*Cyclic sodium chloride-sulfur dioxide test.*

Parameters	Hours
Salt spray (5% NaCl)	½
SO_2 gas	½
Soak (no salt spray or gas)	2
Salt spray[a]	4
SO_2[a]	4

[a]Per day.

TABLE 3—*Comparative salt spray results on aluminum alloys susceptible to exfoliation (ASTM Test Method for Exfoliation Corrosion Susceptibility in 2XXX and 7XXX Series Aluminum Alloys [EXCO Test] [G 34] Ratings).*

Test Method	7075-T6[a]	2124-T351[a]
	ORIGINAL NaCl-SO_2	
2 weeks	EC	EB
4 weeks	ED	EC
	CYCLIC NaCl-SO_2	
2 weeks	EC	EC
4 weeks	>ED	ED
	ASTM G 43	
2 weeks	ED	EA
4 weeks	ED	EB
	CARRIER	
8 months	ED	ED

[a]EA = slight exofoliation. EB = moderate exfoliation. EC = severe exfoliation. ED = very severe exfoliation.

Results on two aluminum alloys heat treated to be susceptible to exfoliation are presented in Table 3. The cyclic sodium chloride-sulfur dioxide test correlated very well with the carrier results. Results on 17-4 precipitation hardening stainless steel with two surface conditions and a chromium plate are shown in Table 4. Again the cyclic sodium chloride-sulfur dioxide test reproduced the carrier results very closely.

Several other coatings were also tested, aluminum alloy panels chromated and painted with the MIL-P-23377 epoxy primer and the MIL-C-83286 polyurethane topcoat, then scribed with an X down to the basis metal: 1010 steel with 0.013 mm (0.0005 in.) of cadmium plate and cadmium plated steel fasteners installed in 7075-T6 aluminum. Results for these specimens are shown in Table 5.

In all three tests, the epoxy/polyurethane painted panels showed no sign of attack on the paint or at the scribe mark (two weeks). An additional two weeks exposure resulted in blistering of the paint that did not occur on the carrier. All three tests were too severe for the cadmium plated steel. Results on the cadmium plated steel fasteners installed in aluminum were closer to those on the carrier.

TABLE 4—*Comparative salt spray results on 17-4 PH stainless steel.*

Test Method[a]	As Received	Grit Blasted	Chromium Plated
		CYCLIC NaCl-SO_2	
2 weeks	no corrosion	slight rust	few small pits
4 weeks	20% rust	50% rust	slight pitting with incipient rust
		ASTM G 43	
2 weeks	no corrosion	no corrosion	no corrosion
4 weeks	no corrosion	few pits	no corrosion
		CARRIER	
11 months	light rusting	moderate rusting	few rust spots

[a]Original NaCl-SO_2 test omitted because of insufficient number of specimens.

TABLE 5—*Comparative salt spray results on organic and electrodeposited coatings.*

Test Method	Epoxy/Polyurethane Paint System	Cadmium Plated Steel	Cadmium Plated Fasteners Installed in Aluminum
		ORIGINAL NaCl-SO_2	
2 weeks	OK	100 % rust	no rust yellow stains
4 weeks	blistered	...	rust
		CYCLIC NaCl-SO_2	
2 weeks	OK	100% rust	no rust yellow stains
4 weeks	blistered	...	rust
		ASTM G 43	
2 weeks	OK	100% rust	slight rust
4 weeks	blistered	...	rust
		CARRIER	
11 months	OK	general white corrosion with light rust stains	slight rust

A summary table is presented in Table 6. Overall the cyclic sodium chloride-sulfur dioxide test gave the best correlation with the carrier. None were satisfactory for cadmium plated steel for periods of four days or more. A one or two day exposure would be all the cadmium can tolerate without excessive unrealistic attack. The test does however provide much useful information on the majority of aircraft materials.

Exposure tests on aircraft carriers of materials projected for use on naval aircraft will be continued. To initially screen materials in the laboratory for such use, the cyclic sodium chloride-sulfur dioxide test will be used since in general its results correlate very well with those of carrier exposure.

Summary

Accelerated laboratory tests can be a valuable tool for screening materials for use in a corrosive environment. However, for the results of such tests to have any real validity, there must be evidence that a correlation exists with results in the actual environment of interest. The only way to obtain such correlation is by conducting exposure tests in the natural environment. Before attempting to simulate the natural environment, that environment should be characterized as to pH, ions present, temperature, and so forth. A monitor to assess corrosivity, or at least determine times of wetness and dryness, would be

TABLE 6—*Summary of correlation with carrier exposure.*

Material	Best Test Method, Time of Exposure
Al Alloys	cyclic NaCl/SO_2, 4 weeks
17-4 PH Steel	cyclic NaCl/SO_2, 3 weeks
Cadmium plated steel	None
Epoxy/polyurethane paint system	all, 2 weeks
Cd plated fasteners installed in Aluminum	all, 2 weeks

useful. When an environment keeps changing as it does on an aircraft carrier, depending on its theater of operation and the time of year, the test should be designed to simulate the most severe condition. It is therefore important to be aware that such variations exist.

Even if a test is designed based on the considerations just outlined, it is possible that the test will not reproduce the actual corrosion behavior for all materials. Cadmium plated steel was an example of this in the test development program described in this paper. This can be one of the pitfalls, expecting too much of one test. It has been concluded that it is not realistic to expect one accelerated test to be applicable across the board for all materials.

References

[1] Dean, J. A., Ed., *Lange's Handbook of Chemistry*, 11th ed., McGraw-Hill, New York, 1973, pp. 10–146.

[2] Agarwala, V. S., "A Probe for Monitoring Corrosion in Marine Environments," in *Atmospheric Corrosion*, W. H. Ailor, Ed., Wiley, New York, 1982, pp. 183–192.

[3] Ketcham, S. J. and Jankowsky, E. J., "How Aluminum Alloys Fare in Shipboard Exposure Tests," *Metal Progress*, March 1981, pp. 38–44.

DISCUSSION

L. Floyd[1] (*written discussion*)—The automotive industry finds they need a dry period in the corrosion cycle (among the components). Did your testing arrive at a similar requirement?

S. J. Ketcham (*author's response*)—We did find that, for most materials, cyclic salt spray sulfur dioxide gave better correlation with carrier exposure than continuous salt spray with sulfur dioxide added. However, we have never looked at the specimens during the period when the salt spray was off to see if they dried completely.

R. Baboian[2] (*written discussion*)—The average pH of "?" in the northeastern United States is 4 with readings as low as 2.2 (60% mostly sulfuric acid). Also about 10 million tons of road salts per year are used on our highways for deicing purposes. Do you feel that the salt-sulfur dioxide test you have developed has applicability for testing in the severe automobile environment in the northeastern United States?

S. J. Ketcham (*author's response*)—Yes, the salt-sulfur dioxide test would certainly be worth trying with automotive alloys to determine whether or not it is suitable.

[1] Glidda Division, Sem Corp., P.O. Box 8826, Stragville, OH 44136.

[2] Texas Instruments, Inc., M/S 10-13, Attleboro, MA 02703.

J. J. Friell[3] (*written discussion*)—How much of a role is played by sulfur-laden particulates coming out of the carrier's stack when blowing soot off boiler tubes?

S. J. Ketcham (*author's response*)—We do not know the answer to this question, but it is our feeling that the particulate matter from blowing out the stacks plays a much smaller part than the sulfur dioxide from normal burning of the fuel.

N. S. Berke[4] (*written discussion*)—Did you test galvanically coupled metals? Was the correlation to aircraft carrier environments as good as that for the aluminum and steel specimens?

S. J. Ketcham (*author's response*)—Galvanically coupled metals were not tested. We plan to expose some couples in our next series of tests.

[3] Bethlehem Steel Corp., Homer Research Labs., Bethlehem, PA 18016.
[4] W. R. Grace, CPD-Research, 62 Whittemore Ave., Cambridge, MA 02140.

David G. Tipton[1]

Microcomputer Data Acquisition for Corrosion Research

REFERENCE: Tipton, D. G., **"Microcomputer Data Acquisition for Corrosion Research,"** *Laboratory Corrosion Tests and Standards, ASTM STP 866*, G. S. Haynes and R. Baboian, Eds., American Society for Testing and Materials, Philadelphia, 1985, pp. 24–35.

ABSTRACT: Computer data acquisition in the corrosion laboratory is described. These techniques can provide higher resolution and be less labor intensive, faster, and more interactive than conventional data recording. Typical system design, component description and specification, interfacing, signal processing, and software considerations are presented. Several examples of computer data acquisition systems (DAS) in corrosion research applications are given.

KEY WORDS: computers, data acquisition, corrosion, interfaces, software (computers), hardware

A major task in corrosion research involves the acquisition of electrical data, usually voltages, during the course of an experiment. Traditionally, strip chart and *x-y* voltage recorders have been used for acquiring data over relatively long times (for example, longer than 1 s). Oscilloscopes have been used similarly for shorter times (for example, 1 ms). With the advent of digital circuitry and the widespread use of microcomputers in the laboratory, new extremely powerful techniques are now available for data acquisition, numerical processing, data management, and data communication.

With their low cost, high performance, and ease of use, microcomputers are becoming widespread in the laboratory as test instruments. The modern microcomputer can be easily interfaced with experimental apparatus to provide automated monitoring of data signals or control of test input signals or both. A number of analog-to-digital (A/D) converters and digital-to-analog (D/A) converters are available to provide the communications hardware for interfacing. An additional advantage is the economic benefit of minimizing human labor costs involved in data collection, collation, computation, and storage.

Microcomputer data acquisition has been used successfully in a wide variety of laboratory corrosion tests. These range in complexity from corrosion potential

[1]Engineer, Westinghouse Electric Corp., Oceanic Division, P.O. Box 1488, Annapolis, MD 21404.

Copyright© 1985 by ASTM International www.astm.org

measurements to AC impedance frequency analysis. Simple acquisition and recording of signals, such as corrosion potential, galvanic current, thermocouple voltage, or other transducer output, with time uses the computer data acquisition system as an automated electronic data storage strip chart. Used in potentiodynamic polarization tests, the computer can serve as an electronic storage *x-y* recorder with full graphic plotting of the auto scaled data during the test. In AC impedance electrochemical testing, the computer can serve as a controller to operate the function generator, acquire the potential and current wave form data, carry out the complex mathematical analysis of the data, and graphically and numerically present the results.

All these applications use low cost, readily available, "user-friendly" microcomputers, A/D and D/A converters, and relatively simple computer programs. The present article describes computer applications for a wide variety of typical laboratory corrosion testing requirements. Hardware specifications, computer program design, and examples of computer data output are presented.

Equipment

A/D Converters

Real world data signals from most corrosion experiments are usually continuously variable voltages or currents. Analog to digital (A/D) converters are devices that convert analog voltages or currents to numerical binary signals for computer input [*1*].

Twelve-bit A/D converters (1 part in 4096 resolution) are generally considered of medium performance with respect to acquisition speed. A typical maximum speed is 20 000 samples/s. Eight-bit A/D converters (1 part in 256 resolution) may be capable of very high speeds, for example, up to 100 000 000 samples/s. A/D converters are available with up to 16-bits resolution (1 part in 65 536), but with correspondingly lower maximum speeds (1000 samples/s).

One other option in the selection of an A/D converter is a multiplexer. A multiplexer is a discrete device under digital control to allow one A/D converter to become a multichannel device. Multiplexed A/D converters are readily available for 16-channel operation with a small penalty in maximum speed for multiplexer operation.

Real Time Clocks

Most microcomputers are not configured with a clock for automatic input of time keeping, or "real time." A real time clock is required for timing of data acquisition intervals and to allow management of acquired data as voltage-time data pairs. Real time clocks are readily available with resolution of milliseconds, which can time events for a year or more in duration. Although a relatively complex programming problem, many microcomputers can support interrupt signals that can be sent from a real time clock to interrupt another running

computer program. This scheme can allow the computer to perform data acquisition routines at precise timing intervals while simultaneously performing other computation chores.

D/A Converters

For feedback control of processes, function generating, or other requirements for a variable output voltage under computer control, digital to analog (D/A) converters are available. D/A converters are the functional and operational inverse of an A/D converter. A 12-bit D/A converter with a 0- to 1-V range can output variable voltages in 0.0002-V increments.

Binary I/O

The most basic architecture of a digital computer can be used in simple binary input/output (I/O). Since information in a computer is stored at this level as binary digits of on or off, these digits can be converted via an interface to off-on output control by relays. Binary input, or computer reading of the status of switches, can be obtained by a binary interface in an inverse mode to the output.

Microcomputer

The central system component is the microcomputer. Virtually any computer is a feasible controller for data acquisition. However, some microcomputers are more useful for this task than others. An ideal microcomputer should have a large number of peripheral equipment available, including magnetic storage devices, printers, and plotters. A number of microcomputers are available with 8-bit microprocessors, 64-K bytes of random access memory, magnetic data storage devices, and high level computer languages, such as BASIC, for ease in programming. Among the microcomputers that have been used for laboratory data acquisition are APPLE II, COMMODORE, IBC PC, TRS-80, and Hewlett-Packard 9825.

Mass Storage

An important peripheral device for a microcomputer data acquisition system is a magnetic mass storage device for permanent, nonvolatile (not dependent on continuous electrical power) data storage. Mass storage devices usually use magnetic media such as tape, flexible (floppy) disks, or hard disks. Magnetic tape is by far the least expensive and lowest performance; hard disks are the most expensive and highest performance; and floppy disks are intermediate in both.

Printers and Plotters

Line printers are very useful for permanent hardcopy output of acquired data and other information. Data are often used as the raw tabular printout of voltages

measured. It is often possible, however, to obtain quality printout of engineering units, statistics, and other computations from the raw voltage values. Thus, a report-ready table of experimental results is available directly from the DAS.

Digital plotters are available for all microcomputers that allow translation of numerical data to graphical plots in a report-ready format. Digital plotters allow final presentation of data acquired and analyzed by computer such that no manual manipulation of data is required.

Interfacing

The most important specification for any of the computer equipment and peripheral accessories described is the compatibility of the equipment with the microcomputer in question. All computers have unique logical and communications architecture that requires an interface to translate or facilitate communications between the device and the microcomputer or both. If left to the user unfamiliar with computer architecture and digital circuit design, fabrication and installation of these interface firmware are, at best, formidable tasks. Several interface conventions are in widespread use to solve this problem.

It should be pointed out that compatible interfacing assures only that communication is possible between the computer and the peripheral device; software must be written and correctly used for successful operation of an A/D converter or other device. Quality, "user-friendly" equipment should include software documentation and sample programs, preferably supplied as computer programs stored on floppy disk, for ease in software development.

Signal Processing

Like any data recorder, the maximum resolution of an A/D converter is possible only if the voltage to be measured reasonably matches the input range of the A/D converter. For example, a 12-bit A/D converter with a 0 to 10 V range has a resolution of $\pm$ 0.0024 V. This is excellent precision for a high-level input (>1 V) but poor for the low-level outputs (for example, <100 mV) typical of many transducers. Signal conditioners are available for many A/D converters to allow preamplification of low-level signals with user-selectable input voltage ranges.

In addition to simple preamplification, modern digital and analog circuitry allows signal conditioning of specialized transducers, such as thermocouples, resistance temperature detectors (RTD) for very sensitive temperature measurement, and bridge amplifier signal conditioners, based on the Wheatstone bridge, to allow input from strain gages, load cells, pressure transducers, linear variable differential transformer (LVDT), and so forth.

Data Acquisition System

A microcomputer based data acquisition system (DAS) is composed of the above equipment selected for the capabilities specific to the data acquisition task.

Figure 1 shows a schematic diagram of a general purpose microcomputer DAS. A DAS may be selected and built "a la carte" as with accumulated A/D converters and other peripherals interfaceable to existing microcomputers. For example, TecMar offers multichannel A/D converters with thermocouple preamps, D/A converters, and timers/counters directly interfaced to APPLE II, COMMODORE, AIM, KIM, TRS-80, and IBM-PC microcomputers. Interactive Structures has A/D converters with temperature, light, sound, and humidity sensors for APPLE II microcomputers. M. C. Miller Company has a microprocessor controlled A/D converter with a general purpose RS-232C serial interface compatible with most computers.

Interactive Microware, Cyborg, and Optim Electronics offer complete DAS packages compatible with APPLE II microcomputers with A/D conversion, D/A conversion, on-off binary control, on-off binary sensing, and variable amplification for many channels including software and presentation graphics to printers and plotters. Hewlett-Packard and Data Translation offer stand-alone DAS complete with computer. For the first time user, the complete system approach can be extremely flexible, can produce high performance results, and is relatively easy to use.

Software Considerations

One fact not to be overlooked in microcomputer DAS is the requirement of computer programs for any useful tasks to be performed. Software support for A/D converters and other peripherals should be a primary consideration in equipment selection. Interfacing compatibility alone is useless until a computer

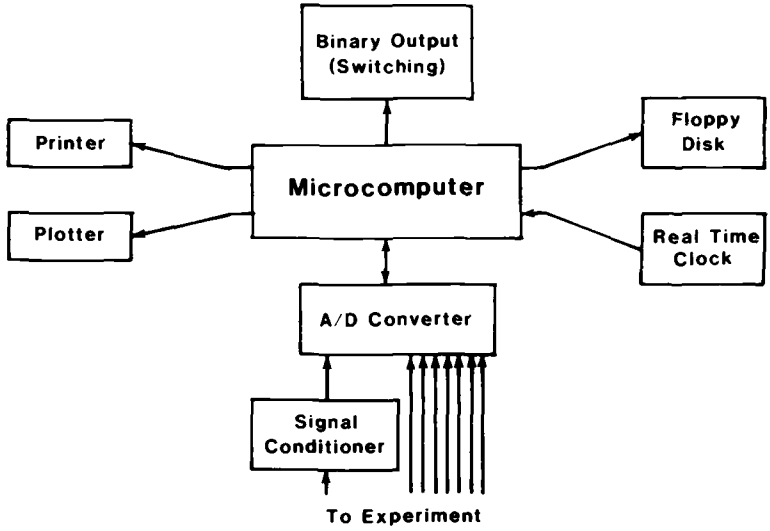


FIG. 1—*Functional diagram of a microcomputer controlled data acquisition system showing key components.*

program is available. Adequate software support can consist of written documentation or sample computer programs or both that illustrate all aspects of control, input, and output from the device. These illustrations of use of A/D converters, for example, can then be used as functional subroutines in user written software.

Some DAS hardware, such as the Issacs DAS by Cyborg for the APPLE II microcomputer, employ a special modification of the computer language (BASIC). These modifications allow special commands to be implemented for ease in programming. The special commands establish software selectable options for DAS hardware operation, start and stop DAS operations, pass data into computer memory, and display data graphically on the monitor screen. DAS language implementations allow microcomputer programmers with average skill, but no DAS experience, to immediately begin microcomputer data acquisition. From another viewpoint, the laboratory instrumentation technologist with no experience in microcomputer programming often finds computer DAS an effective and practical problematic approach to learn microcomputer programming.

Many A/D converters, such as those by TecMar and Interactive Structures, allow access and operation by the microcomputer using machine language instead of the typical high-level programming languages, such as BASIC or FORTRAN. Programming in machine language is extremely tedious, but programs run as much as 100 times faster. The A/D converters mentioned above are capable of sampling rates faster than the BASIC language on the APPLE II. For very high performance data acquisition, short subroutines can be written to perform some number of A/D measurements, write the results directly to a contiguous block of memory locations, and transfer control back to the calling program written in BASIC. Thus the bulk of the programming chore is accommodated by the easily programmed BASIC language while the very high performance DAS task uses machine language at high speed.

Perhaps the most powerful attribute of computer data acquisition is the availability of mathematical computations to be performed on the raw voltage values. Such computations can range from simple engineering units conversion, to statistical analysis, to complex interactive computations involving several channels. Not only are mathematical computations available, but also mathematical logic operations. Computer DAS software, using IF . . . THEN logic, can control, effect changes, or initiate alarm or limit routines. Data can be integrated, differentiated, summed, and so forth as it is being generated, or in "real time," since the data already reside in the computer and, generally, the data acquisition procedures require very little devoted time from the computer.

Corrosion Laboratory Applications

Potential Measurement

Potential measurement is functionally a very simple use of microcomputer DAS. A real time clock is used to time the acquisition interval, and an A/D

converter performs the measurements. An electrometer (a very high impedance voltmeter) is typically used for electrochemical potentiometry to avoid polarizing the reference electrode. A/D converters are typically fairly high in impedance ($\sim 1 \times 10^8\ \Omega$), but more importantly they are connected to the specimen/reference electrode only for the duration of the A/C conversion, typically about 1-μs, avoiding the experimental problem of reference electrode polarization. For critical applications requiring higher impedance, simple buffer amplifier circuits can provide impedance as high as $1 \times 10^{12}\ \Omega$ [2]. The software establishes the time interval of data acquisition, starts an A/D conversion, retrieves the value, retrieves the time, and stores the voltage-time data pairs. Figure 2 shows an example of corrosion potential versus time for a freely corroding specimen of nickel-aluminum bronze in natural seawater. This example illustrates several advantages of computer data acquisition as compared to conventional data recording by strip chart voltage recorder. First, this specimen was but 1 of over 100 whose potential was being monitored concurrently. Also, large quantities of data were collected, over 500 data pairs per specimen. Digital plotting the data then allowed compression of the time axis to show 120 days of data while still retaining the resolution of frequent measurements.

Current Measurement

Current measurement by computer DAS is analogous to potential measurement. For galvanic current measurement, a 1-Ω shunt resistor can be used for many engineering tests where the additional resistance (to the solution and in-

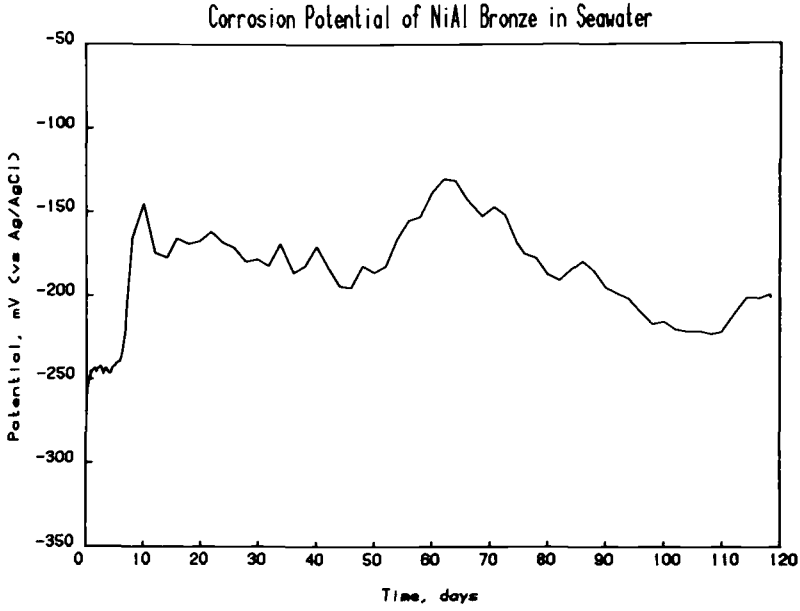


FIG. 2—*Typical digital plotter presentation of potential versus time data from computer DAS.*

terface resistance) represents little error. For more exacting demands, a zero resistance ammeter (ZRA) is required as a signal conditioner. ZRAs are available from electrochemical instrumentation suppliers, or may be fabricated by the user [*3*]. For potentiostatic experiments, a ZRA is not required and the current to voltage conversion of the potentiostat or a potential drop measurement across a shunt resistor in series with the counter electrode will provide an accurate measure of current.

Potentiodynamic Polarization

Potentiodynamic polarization curves generated by computer DAS require current and potential measurements by two channels of A/D conversion. Figure 3 shows apparatus for computer data acquisition from a research potentiostat. A multichannel A/D converter is used to monitor the potential and current outputs from the potentiostat. The computer graphics capabilities are utilized to draw in real time the polarization curve, correctly scaled as shown on the monitor screen. After completion of the experiment, the curves may be replayed on the screen. For hardcopy output in a report ready format, the data recorded on a floppy disk may be used as input to a separate graphics routine for a digital plotter interfaced to the computer. Figure 4 shows a typical polarization curve from the digital plotter. The current-potential data pairs are acquired in this example every 4 mV during the potential ramp. An anodic scan is taken by one experiment and a cathodic scan by another experiment on another electrode. The two data sets may be recalled and plotted together for the complete polarization curve as shown. The recall and replotting features allow simultaneous plotting of any number of curves and convenient rescaling of curves with no loss in the numerical accuracy of the data.

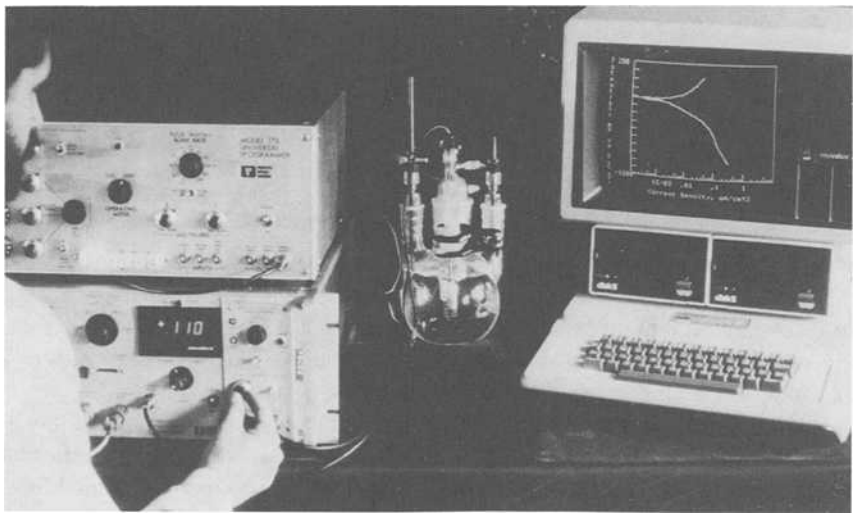


FIG. 3—*Apparatus for computer data acquisition of potentiodynamic polarization data.*

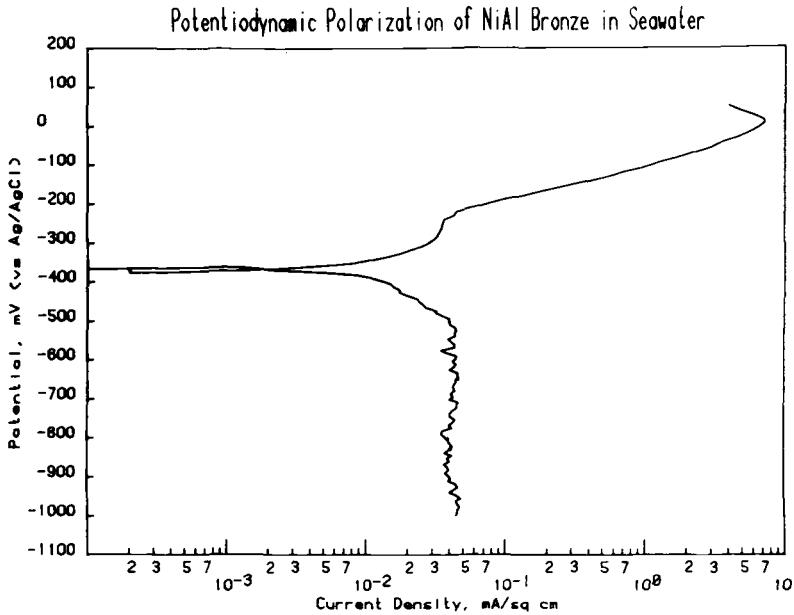


FIG. 4—*Typical digital plotter presentation of potentiodynamic polarization curve from computer DAS.*

Research potentiostats are now available with a built-in microprocessor dedicated to data acquisition, a D/A converter used to generate the reference voltage for the potentiostat (in lieu of a function generator or programmer), an A/D converter for data acquisition, a real time clock for interval timing, and an interface for communication to and from a computer, all the ingredients for a DAS, but dedicated to the input and output instrumentation requirements for a research potentiostat. Here, computer DAS offers the advantage of high resolution, graphics, data recording, and easy data recall.

Current Distribution

Figure 5 shows a schematic of a simulation of galvanic corrosion between a tube and tubesheet in a seawater cooled heat exchanger. Zero resistance ammeters were used as signal conditioners for 10 channels of galvanic current measurements between the tubesheet and segments of the tube. The computations were made as indicated to determine the profile of current density down the tube from the tubesheet. Figure 6 shows a current distribution obtained after 120-days exposure to flowing seawater.

In this example, data recording would be difficult and tedious by conventional means. Ten channels of data were simultaneously recorded with incremental currents computed from cumulative raw data and current density computed from currents. Computer DAS allows the data to be accumulated as a three-dimensional

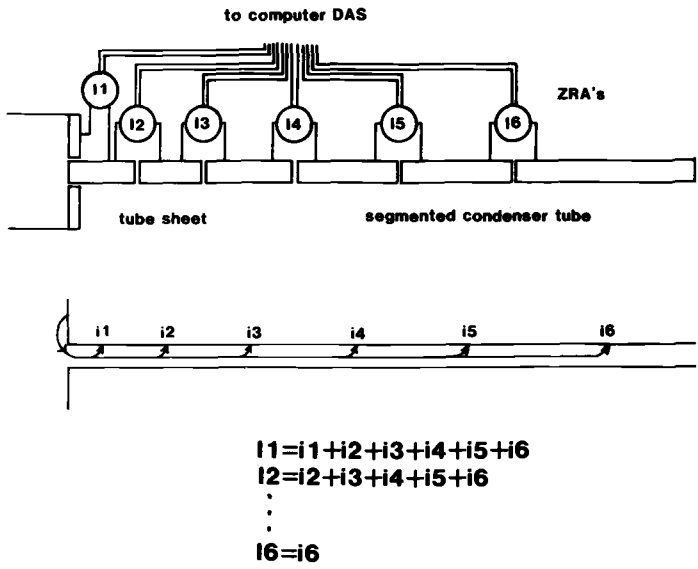


FIG. 5—*Schematic diagram of segmented tube for determination of galvanic current distribution between tube and tubesheet in a heat exchanger.*

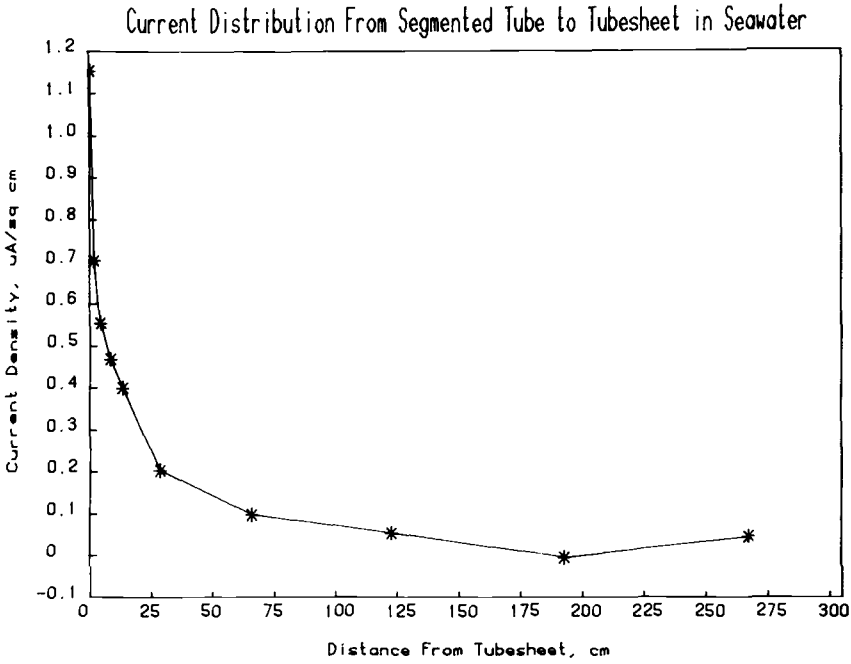


FIG. 6—*Digital plotter presentation of galvanic current distribution in a simulated seawater cooled heat exchanger tube.*

array of current density, distance and time, of which these data in Fig. 6 are but one data set at one time.

Fatigue Crack Growth

A microcomputer DAS has also been used to allow automated, unattended fatigue crack growth testing [*4*]. Here, an A/D converter reads 200 load-displacement data pairs during a single fatigue load cycle. Crack length is computed from load-displacement slope, geometry, and elastic compliance equations. The test method uses the high performance characteristics of computer data acquisition in the data acquisition speed, resolution, and the ability to perform very complex computations very quickly in real time. The system software also contains validity criteria with respect to appropriate ASTM Test Method for Constant-Load-Amplitude Fatigue Crack Growth Rates Above 10^{-8} m/Cycle (E 647) and ASTM Test Method for Plane-Strain Fracture Toughness of Metallic Materials (E 399).

Summary

Microcomputers, already useful in the laboratory for data processing and management, are extremely valuable as controllers for data acquisition systems. The equipment is low cost, but effective software is required for any successful use. Computer DAS can provide higher resolution and be less labor intensive, faster, and more interactive than conventional data recording. Mathematical operations, computer graphics, and multichannel data management are features contributed by the computer that have no parallel in more traditional methods. The corrosion research laboratory can benefit from computer DAS techniques in all but the simplest, nonrepetitive, short-term test.

References

[*1*] "Microcomputer Analog I/O Systems," Data Translation, Inc., 4 Strathmore Road, Natick, ME.

[*2*] Smith, J. I., *Modern Operational Circuit Design*, Wiley-Interscience, New York, 1971.

[*3*] Von Fraunhofer, J. A. and Banks, C. H., *Potentiostat and Its Applications*, Butterworths, London, 1972.

[*4*] Tipton, D. G., *Environment-Sensitive Fracture: Evaluation and Comparison of Test Methods, STP 821*, American Society for Testing and Materials, Philadelphia, 1984, pp. 484–496.

DISCUSSION

Thomas J. Timme[1] *(written discussion)*—In the world of corrosion, we deal with readings at the millivolt and microamp levels. Therefore, any noise present in a system can have a significant impact on the digitized signal read by the

[1]Monsanto Co., 800 N. Lindbergh, W4A, St. Louis, MO 63167.

microcomputer. Have you seen this problem and if so what have you done to overcome this interfacing problem?

D. G. Tipton (author's response)—Certainly noise can be a major problem in any DAS. The computer itself uses digital signals of up to 10 V changing at greater than 1-MHz frequencies. Many A/D converters have an "analog ground" connection, separate from the electrical chassis ground, to which the manufacturer recommends connections of shielded input data cables. Also, A/D conversion physically outside the computer (then connection to the computer only by digital communication lines) seems to improve computer-generated noise. Furthermore, signal conditioning to a high-level signal at the transducer when long data cables are required will improve signal to noise ratio.

Martin Kendig[2] *(written discussion)*—Corrosion monitoring of a large number of materials simultaneously can require a large dynamic range for a current sensor. Can the system that you described auto range, or at least adjust the channel gains?

Computer collection of corrosion data provides an important service in that it allows for easy standardization of test procedures, for example, electrode pretreatment. This is an important point for the particular meeting.

D. G. Tipton (author's response)—As mentioned, most A/D converters are at least user selectable with jumpers, switches, and so forth to different input ranges. Many are also software-selectable by computer commands to different input ranges, which would allow computer controlled auto ranging. One other useful technique is to use simultaneous measurement by more than one A/D converter set to different input ranges, then utilizing the measurement from the optimum range.

[2]Rockwell International Science, Thousand Oaks, Thousand Oaks, CA.

Te-Lin Yau[1] *and R. Terrence Webster*[1]

Corrosion Test Loop

REFERENCE: Yau, T-L. and Webster, R. T., **"Corrosion Test Loop,"** *Laboratory Corrosion Tests and Standards, ASTM STP 866*, G. S. Haynes and R. Baboian, Eds., American Society for Testing and Materials, Philadelphia, 1985, pp. 36–47.

ABSTRACT: In order to study the corrosion of zirconium under heat-transfer conditions, a corrosion test loop has been set up at Teledyne Wah Chang Albany. The major components of this test loop are a 37.85-L (10-gal) tank, a zirconium centrifugal pump, a heat-transfer heater, a vertical single-tube heat exchanger, and monitors for temperature, pressure, and flow speed at critical areas. Specimens were 0.9-m (3-ft) long tubes and wires, which were and were not subjected to a heat flux, respectively.

Tests of zirconium versus 50% sulfuric acid were conducted. Test results indicate that the effect of heat flux on zirconium in 50% sulfuric acid at about 160°C (330°F) is negligible. However, acid concentration may change in the process because of vaporization, imperfect sealing, condensation, and so forth. When the acid becomes too strong, zirconium will be susceptible to localized corrosion.

KEY WORDS: zirconium, corrosion, sulfuric acid, heat transfer, heat flux, corrosion test loop, localized corrosion, vaporization, condensing, industrial applications

Fisher and Whitney [*1*] have found that the corrosion rate of heat-transfer metal is determined by the wall temperature. This was confirmed by Zarubin et al [*2*] for iron in concentrated sulfuric acid. However, the assumption, by Fisher and Whitney [*1*], that in the presence of heat flux the wall temperature always influences the corrosion rate in the same way as does the temperature in an isothermal system, could be oversimplified or incorrect for many other systems. The mechanism by which heat-transfer affects the corrosion process is very complicated and is in need of further study. The factors that affect corrosion under heat-transfer include heat flux, wall temperature, solution velocity, solution temperature, pressure, vapor phase, and so forth [*3*]. A suitable test method to study corrosion under heat-transfer conditions is one that could control all of the above factors.

Zirconium heat exchangers are being used in many chemical processes because of their excellent corrosion resistant and heat-transfer properties. For example, zirconium heat exchangers have been used in urea fertilizer manufacturing for over 25 years and they show no signs of corrosion [*4*]. Apparently, the heat-

[1] Corrosion group head and principal metallurgical engineer, respectively, Metallurgical Research and Development, Teledyne Wah Chang Albany, Albany, OR 97321.

Copyright© 1985 by ASTM International www.astm.org

transfer performance of these heat exchangers has been consistent during this period of time. However, laboratory testing results show that zirconium may or may not corrode differently under the influence of heat-transfer compared with the control specimen as indicated in Table 1 [5].

In order to have a better understanding of the corrosion of zirconium in various media under heat-transfer conditions, a corrosion test loop has been set up and operated at Teledyne Wah Chang Albany, Albany, OR. The object of this paper is to describe this test loop that is designed for the purpose of simulating plant conditions as closely as possible. Information generated using this test loop can provide an indication as to the performance of zirconium under service conditions. The test results of zirconium versus sulfuric acid solutions will also be reported.

Corrosion Test Loop

The flow diagram of the corrosion test loop is shown in Fig. 1. In essence, this test loop consists of two recirculating pressurized circuits: the main experimental loop and the heat-transfer oil loop.

The test solution, after preparation in a suitable apparatus, is stored in the glass-lined tank with temperature and pressure indicators and a safety relief valve. The test solution is circulated through the single-tube heat exchanger by the zirconium centrifugal pump at a flow speed controlled by the bypass valve and measured by the flow meter. By controlling the flow speed and temperature, it is possible to have a single-phase flow (liquid) or a two-phase flow (liquid and vapor) through the tube. Both the temperatures and the pressures are monitored at the inlet and the outlet of the single tube of the heat exchanger. This tube is the experimental specimen under the influence of heat flux. A wire specimen can also be installed within the tube. The wire specimen is not subjected to the influence of heat flux. Therefore, comparative data can be obtained from this test loop. Finally, it should be noted that the components in the main loop are joined using polytetrafluoroethylene (PTFE) lined piping.

The oil loop provides the heat source for the test solution. The oil is heated to a chosen temperature using the heat-transfer heater. Then, the hot oil is used to heat the test solution to the testing temperature. Moreover, by adjusting the globe valves, the temperature difference between the inlet and the outlet of the heat exchanger can be maintained at a desired value.

Experimental Procedure

Commercially pure zirconium, which meets the Unified Numbering System (UNS) R60702 (Zr 702) standards, was used in this study. Tube specimens 0.9 m (3 ft) long, with a 12.7 mm (0.5 in.) outer diameter (OD) and 0.89 mm (0.025-in.) wall were prepared for corrosion tests. Heat treated tubes were vacuum annealed at 760°C (1400°F) for 30 min. A wire specimen 0.9 m (3 ft.) long

TABLE 1—*Corrosion of zirconium under heat-transfer conditions* [5].

Environment		Specimen		Control Specimen Corrosion Rate, mm/year (mil/year)
Corrodent	Temperature, °C (°F)	Temperature, °C (°F)	Corrosion Rate, mm/year (mil/year)	
Copper plating liquor containing H_2SO_4 and $CuCl_2$	65 (149)	135 (275)	56 (2240)	0.013 (0.5)
5%, 10%, 20% H_2SO_4	boiling	150 (302)	<0.025 (<1)	<0.025 (<1)

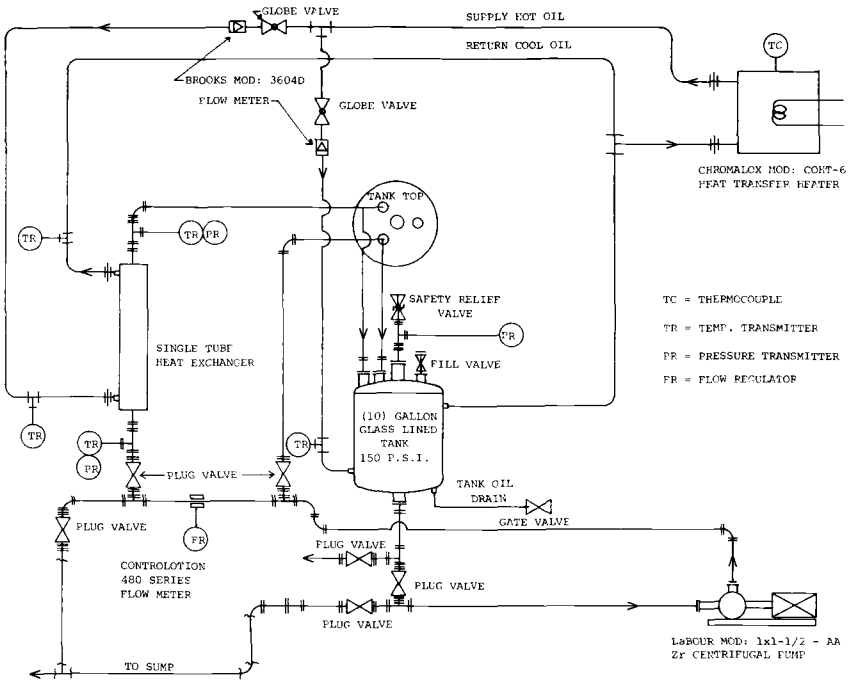


FIG. 1—*Flow diagram of the corrosion test loop.*

with a 2.03 mm (0.08 in.) diameter was placed inside the tube in some tests. As the wire specimen was not subjected to a heat flux, comparative data were obtained. All specimens were tested in the as-supplied condition without any surface conditioning other than cleaning.

Fifty percent sulfuric acid, which was prepared from reagent grade sulfuric acid and distilled water, was used in this study. Thirty litres of 50% sulfuric acid was prepared for each run. The acid storage vessel was pre-pressurized with nitrogen gas to make the acid less vulnerable to concentration change. When the acid was heated to the testing temperature, the pump was activated and plug valves were opened. It was estimated that, in order to have single-phase flow through the test tube at a temperature of approximately 166°C (330°F), the acid flow speed should be 2.1 m/s (7 ft/s).

Results

Results of three test runs of Zr 702 using 50% sulfuric acid are given in Table 2. All specimens, tube or wire, exhibited low corrosion rates, based on weight loss measurements, after seven-days exposure to the flowing acid. The wall thickness or wire diameter did not show measurable changes either. However, all specimens were covered with tarnished film.

In test run A, the tank was not pre-pressurized with nitrogen gas. The tested

TABLE 2—*Corrosion of Zr 702 under heat-transfer or isothermal conditions for seven days.*[a]

Test Run	Specimen	Solution, % H_2SO_4	Pressure of N_2 at 11°C, psi (mm Hg)	Working Pressure in Tank, psi (mm Hg)	Temperature, °F (°C)		Average Corrosion Rate, mm/year (mil/year)
					In Acid/Oil	Out Acid/Oil	
A	as-welded tube	50	N/A	41 (2120)	330/389 (166/198)	333/381 (167/194)	0.025 (1.0)
B	as-welded tube	50	25 (1293)	72 (3723)	318/382 (159/194)	320/374 (160/190)	<0.025 (<1)
B	wire	50	25 (1293)	72 (3723)	318/382 (159/194)	320/374 (160/190)	<0.025 (<1)
C	heat-treated tube	50	25 (1293)	52 (2689)	328/396 (164/202)	330/388 (166/198)	<0.025 (<1)
C	wire	50	25 (1293)	52 (2689)	328/396 (164/202)	330/388 (166/198)	<0.025 (<1)

[a]1 psi = 6.8948 kPa. N/A is not applicable.

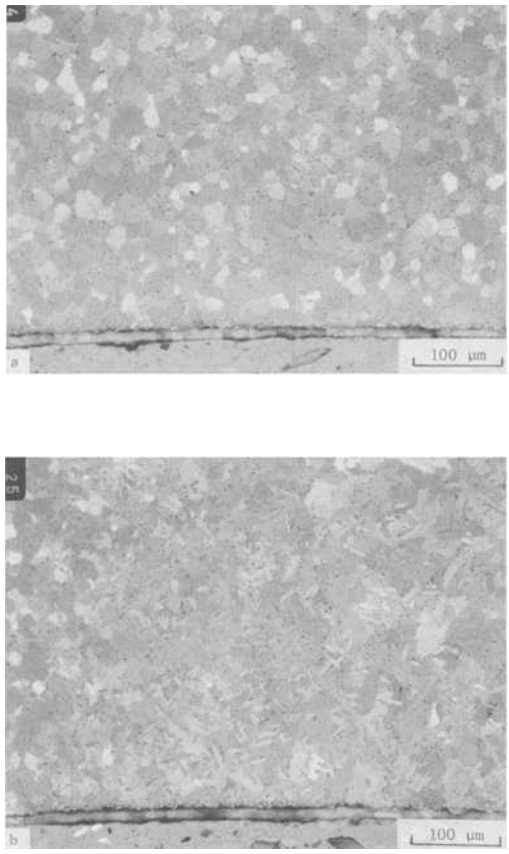


FIG. 2—*The metallographs of the middle section of the tube in test run A:* (a) *base metal and* (b) *weld metal.*

tube showed a color change from gray at the bottom to dark black at the top. Microscopic examinations showed that the middle section of the tube suffered some minor localized corrosion. Both the base metal and the weld metal had about the same degree of attack as shown in Fig. 2. The top and the bottom sections of the tube did not show any sign of localized corrosion as shown in Fig. 3. Nevertheless, there was a difference between the film thickness of the top section and the bottom section as indicated in Fig. 3.

It was suspected that the minor localized corrosion in test run A was primarily caused by the change in acid concentration rather than the heat flux. Therefore, in test runs B and C, the tank was pre-pressurized with 172-kPa (25-psi) nitrogen gas while the prepared 50% sulfuric acid was still hot (approximately 71°C). Microscopic examinations of the tested as-welded tube, heat-treated tube, and wires indicated that there was no sign of localized corrosion. A respresentative micrograph is given in Fig. 4. It should be noted that the pressure measurements

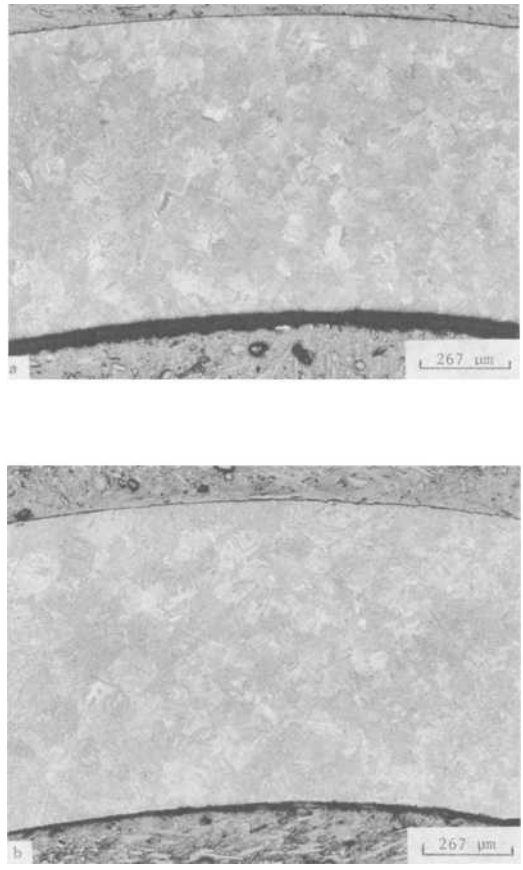


FIG. 3—*The metallographs of the tube in test run A:* (a) *weld metal from the top section and* (b) *weld metal from the bottom section.*

as shown in Table 2 were inconsistent, which was attributed to the imperfect sealing of the system.

Discussion

The effect of heat flux on Zircaloy corrosion in pressurized water has been reported by several investigators [*6–9*]. It appears that increased corrosion (oxidation) under heat-transfer conditions can occur at heat fluxes exceeding 1 580 000 W/m^2 (500 000 Btu/ft^2 h). For example, a change in heat flux from 1 580 000 to 1 890 000 W/m^2 (500 000 to 600 000 Btu/ft^2 h) in the temperature range 304 to 360°C (580 to 680°F) will result in a 5% reduction in life as compared with the predicted time under isothermal conditions [*6*]. It is not expected that such high heat fluxes are involved in chemical processes. Therefore, heat flux

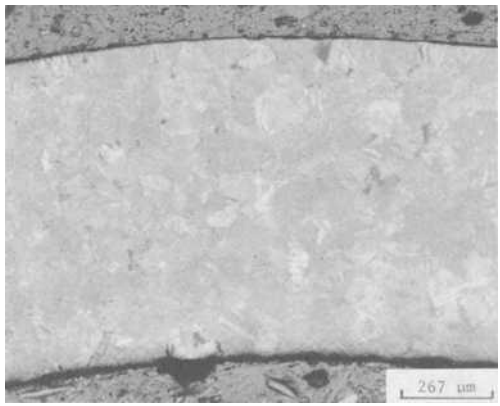


FIG. 4—*The metallograph of weld metal from the top section of the tube in test run B.*

could only play a minor role in the corrosion of zirconium in many chemical applications. However, heat flux could become an important factor when zirconium is not compatible with the medium as indicated in Table 1.

Test results of this study as given in Table 2 show that the effect of heat flux on zirconium corrosion in 50% sulfuric acid at approximately 166°C (330°F) is negligible. Therefore, the significance of the minor localized corrosion found in the middle section of the tube in test run A shall be addressed. Some properties of sulfuric acid, which are given in Figs. 5 through 7, are needed for the discussion.

Figure 5 gives the compositon of vapors in equilibrium with boiling sulfuric acid solutions at 760-mm mercury. Figure 5 indicates that in ≤65% sulfuric acid the vapor phase is almost entirely water vapor. However, it is not expected that the vaporization of sulfuric acid would cause a significant concentration change in a closed system. For example, in test run A, it requires

$$n_{H_2O} = PV/RT = (41/14.7 \text{ atm})(7.85 \text{ L})/(0.08205)(440)$$
$$= 0.6 \text{ moles } H_2O$$

to yield 283-kPa (41 psi) (2120-mm mercury). However, when a system is not perfectly sealed, water in sulfuric acid will continue to vaporize to make up the lost water vapor. (There were some minor leaks in the corrosion test loop.) Therefore, the acid concentration change could become significant.

The boiling points of pressurized sulfuric acid are shown in Fig. 6. Line A in Fig. 6 indicates that boiling 50% sulfuric acid at 166°C (330°F) should have 414-kPa (60-psi) (3103-mm mercury) vapor pressure. The 283-kPa (41-psi) (2120-mm mercury) reading in test run A implied that the acid concentration could have concentrated in 58% as shown by Line B in Fig. 6. Since the wall tem-

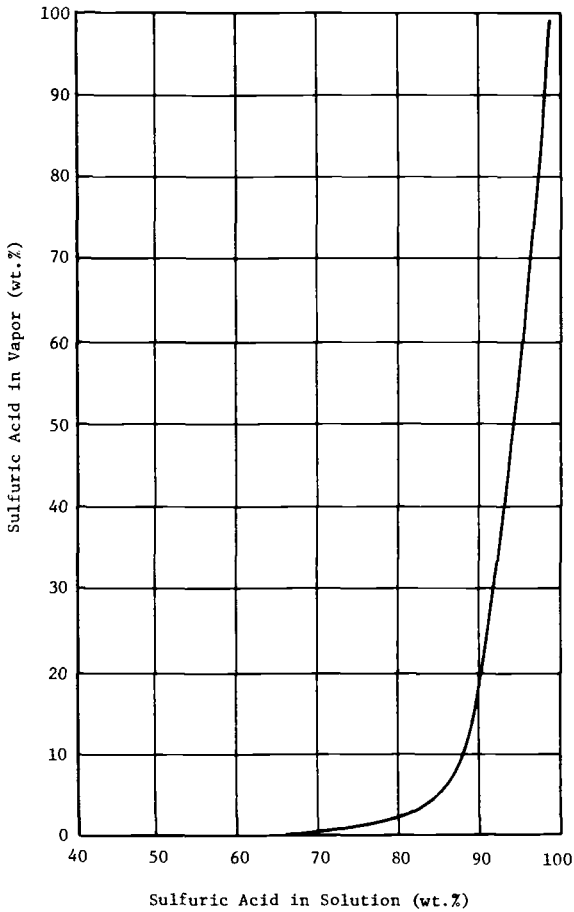


FIG. 5—*Composition of vapors in equilibrium with boiling sulfuric acid solutions at 760-mm mercury* [10].

perature was higher than the acid temperature, the actual acid concentration could have been greater than 58%. The change of acid concentration in test run B or C was expected to be less severe than test run A.

Another question is why the minor localized corrosion only occurred at the middle section of the tube in test run A. The likely cause is the vaporization occurring within the heat-exchanger tube. (Pressure indicators were added later to monitor the vaporization possibilities of future tests.) Therefore, the acid could have further concentrated at the middle section and caused the localized corrosion. Pre-pressurizing the system with nitrogen as done in test runs B and C probably prevented the occurrence of vaporization within the heat-exchanger tube and, consequently, the localized corrosion. The vapor phase of sulfuric acid is not expected to be corrosive to zirconium. The vapor phase of sulfuric acid could become corrosive when it condenses. Sulfuric acid concentration in con-

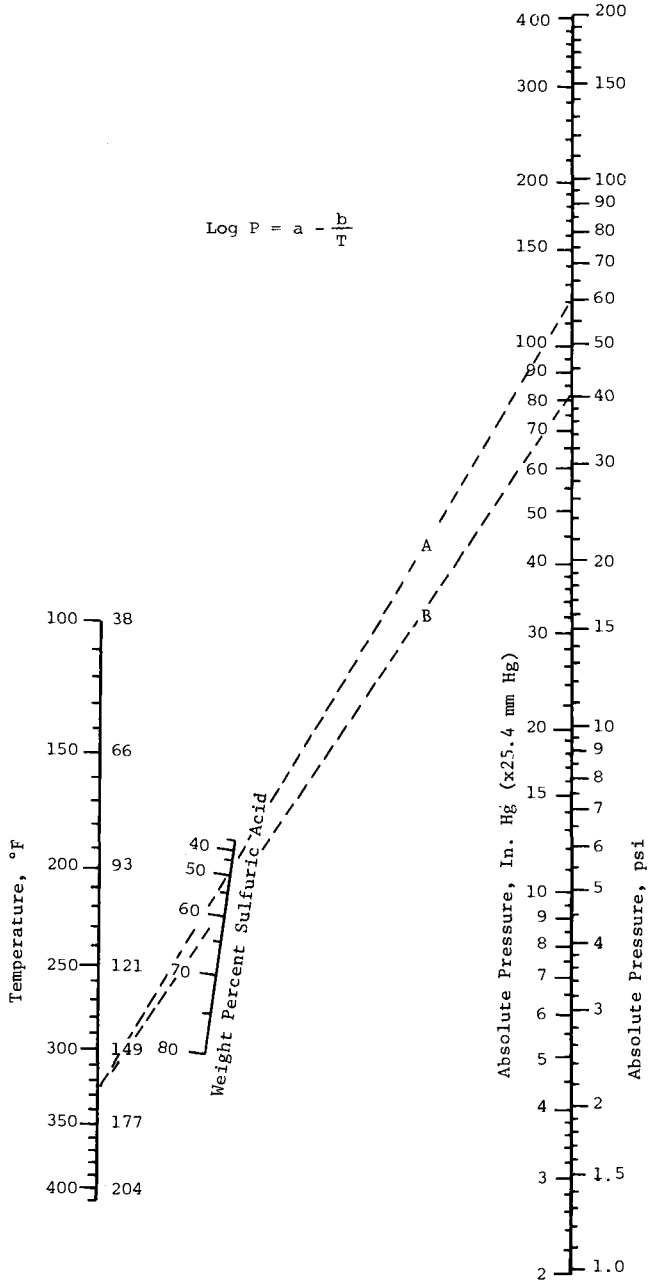


FIG. 6—*Boiling temperatures of sulfuric acid* [11].

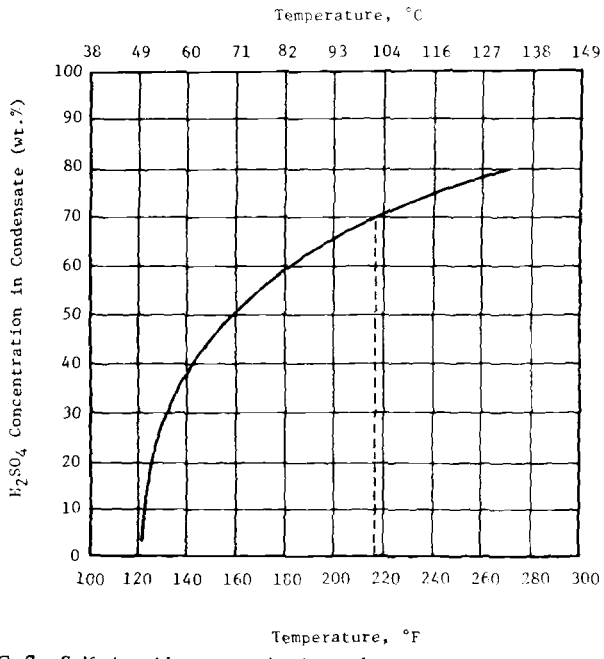


FIG. 7—*Sulfuric acid concentration in condensate versus temperature* [12].

densate does not depend on the percent of sulfuric acid in vapor but depends on temperature as shown in Fig. 7. As indicated in Fig. 7, sulfuric acid concentration in condensate is 70% at 102°C (215°F). Therefore, it is recommended that the condensation of sulfuric acid vapor at temperatures above 102°C (215°F) should be prevented for zirconium equipment. We do not believe that sulfuric acid could have vaporized and then condensed immediately in test run A.

Conclusions

Testing results of zirconium in 50% sulfuric acid under dynamic conditions indicate that heat flux does not play an important role on zirconium corrosion. However, zirconium could become susceptible to localized corrosion, if acid concentration changes significantly because of vaporization, imperfect sealing of a system, and so forth.

References

[1] Fisher, A. D. and Whitney, F. L. Jr., *Corrosion*, Vol. 15, May 1959, p. 257t.
[2] Zarubin, P. I., Poluboyartseva, L. A., and Novokovskii, V. M., *Zashchita Metallov*, Vol. 1, No. 3, 1965 p. 297.
[3] Thompson, N. and Payer, J., Final Report on Corrosion Under Heat-Transfer Conditions: Phase 1, State-of-the-Art Survey to Materials Technology Institute, 18 Nov. 1982.
[4] *Zirconium Outlook*, Vol. 1, No. 1, Teledyne Wah Chang Albany, Albany, OR, 1980.

[5] Green, M. L., *British Corrosion Journal,* Vol. 2, No. 4, 1967, p. 153.
[6] Dyce, I. H., *Nuclear Engineering,* July, 1964, p. 253.
[7] Thomas, K. C. and Allio, R. J., *Transactions of the American Society of Metals,* Vol. 58, 1965, p. 658.
[8] Johnson, C. R., Koch, D. W. and Campbell, T. M., *American Nuclear Society Transactions,* Vol. 9, 1966, p. 31.
[9] Rubright, M. M. and Koch, D. W., Paper Presented at 25th Annual National Assoiation of Corrosion Engineers Meeting, Houston, TX, Preprint 78, 1969.
[10] Fasullo, O. T., *Sulfuric Acid,* McGraw-Hill, New York, 1965, p. 290.
[11] *Chemical Processing,* Aug. 1960.
[12] Haffner, R. F. and Ebner, A. M., "Material Behavior in the Ducts and Chimneys of the Pleasants Power Station," presented at a seminar on Solving Corrosion Problems in Air Pollution Control Equipment sponsored by APCA, IGCI and NACE, 11-13 Aug. 1981.

Malcolm E. Warwick[1] *and William B. Hampshire*[2]

An Accelerated Simulated Can Corrosion Test for Tinplate

REFERENCE: Warwick, M. E. and Hampshire, W. B., **"An Accelerated Simulated Can Corrosion Test for Tinplate,"** *Laboratory Corrosion Tests and Standards, ASTM STP 866*, G. S. Haynes and R. Baboian, Eds., American Society for Testing and Materials, Philadelphia, 1985, pp. 48–64.

ABSTRACT: The internal corrosion of tinplate and lacquered tinplate containers is extremely complex and is a function of many interacting parameters. Electrochemical tests give an insight to the main reaction pathways controlling such corrosion but are not widely applicable to real situations. Industry is forced to rely on expensive and time-consuming pack tests when contemplating changes in either the design of the container or the characteristics of the product packed.

This paper describes an accelerated test that takes the form of a simulated can, which has been developed and used at the International Tin Research Institute over the last decade. The results of investigations into particular aspects of tinplate corrosion using this test are described and related to industrial experience with real containers. Providing care is taken in the interpretation of results, it is felt that the accelerated test provides a reliable way of reducing the need for pack testing.

KEY WORDS: corrosion tests, accelerated tests, tin coatings, cans, canning, solders, lacquers

Tinplate is a family of products that finds a very wide range of applications as container materials. This is in part because of the compatability of tin-coated steel, with or without organic lacquers, to a wide range of food and nonfood products [*1*]. In practice, there is no easy way to test the compatability of particular tinplate specifications with new or modified products, and pack testing must be carried out before marketing can be undertaken. Even with elevated temperature storage, pack tests are time consuming and expensive, involving a large number of specimens and extensive facilities for can filling, processing, and handling.

Fundamental electrochemical measurements have proved to be disappointingly uninformative concerning can shelf-life prediction although they have contributed much to the basic understanding of the corrosion pathways inside both plain

[1]Head of metallurgy and tinplate division, International Tin Research Institute, Fraser Rd., Perivale, Greenford, Middlesex UB6 7AQ, United Kingdom.

[2]Assistant Manager, Tin Research Institute, Inc., 1353 Perry St., Columbus, OH 43201.

Copyright© 1985 by ASTM International www.astm.org

tinplate cans [*2–5*] and lacquered containers [*6–12*]. Experience has shown that characteristic responses to particular electrochemical measurements may be correlated reasonably well with certain types of corrosion, and where sufficient comparative data are available, pack testing may be reduced to an assessment of only those systems that would probably prove to be acceptable. This approach is used at the International Tin Research Institute (ITRI), but in order to transfer findings in the laboratory to commercial practice, it was necessary to develop an accelerated corrosion test that indicates the probable outcome of full-scale pack tests. This paper describes the test currently in use at the institute and those areas of application where a good correlation with canning experience has been obtained.

Principles of Tinplate Can Corrosion

Before describing the accelerated simulated can corrosion (ASCC) test, it is necessary to consider briefly the factors that are relevant to the corrosion of tinplate cans. This is an extremely complex subject that has been summarized well by Britton [*1*] who quotes important references on the subject. In most situations, tin is anodic towards iron inside a hermetically sealed container, and its corrosion rate is affected by the relative exposed areas of the two metals and the nature of the corroding medium. The tin coating thickness and the presence of lacquers on the surface of the tinplate are the principal factors controlling the relative exposed areas of tin and steel in a can, and of course they are chosen to match the properties of the foodstuff. Foods and drinks are usually slightly acidic and, in the presence of oxygen, cause the dissolution of tin. Thus cans are sealed with a minimum headspace volume, and the hot preparation of many food products before packing ensures that much of the dissolved oxygen that they contain has been removed. Once the residual oxygen inside a can has been consumed by the dissolution of tin, other cathode depolarizers in the product may promote further corrosion. In addition to a number of unidentified natural food chemicals, nitrate ions, sulfur compounds, and some crop spray residues are known to affect corrosion rates.

Tin corrosion in most food media in the absence of cathode depolarizers is very slow since the metal has a high overpotential for the evolution of hydrogen. Where steel is exposed beneath the tin coating, at pores or sites of damage, it will act as an effective cathode and accelerate tin corrosion, although under normal conditions, attack is still very slow.

Situations do arise inside cans where the polarity of the tin/steel couple is reversed, and since these could lead to perforation of the container, it is clearly valuable to be able to predict their occurrence [*1*]. The availability of tin for corrosion is important in such situations, and the exhaustion of tin at discontinuities in a lacquer coating or the passivation of tin by sulfur compounds are both thought to be relevant effects.

Principles of the ASCC Test

It will be evident from the foregoing that there are several ways to accelerate the corrosion reactions that take place inside a tinplate container. The ratio of the areas of tin and steel exposed in the test could be altered so as to increase the tendency for one to corrode at the expense of the other. This is not of direct value when the specification of the tinplate is being assessed. There are, however, occasions when altering the area ratios of constituents of a can is valuable. For example, in studying soldered cans, disproportionately large areas of solder may be exposed to exaggerate corrosion of that alloy. The same principle may be applied to the testing of a welded can seam. By increasing the areas of the seam in relation to the area of the body of the can, the chance of localized corrosion occurring may be increased. It is also advantageous when studying lacquered tinplate to scratch deliberately the organic film. This simulates random can-making damage in a reproducible way, and the increased ratio between damaged to undamaged areas accelerates corrosion in some cases.

The second obvious way of accelerating corrosion reactions in a can is to increase the aggressivity of the product being packed, but clearly this has disadvantages if it is the properties of the foodstuff that are being assessed. When the "quality" of the tinplate or general principles of corrosion are being investigated, this approach has proved to be very useful. However, rather than select an aggressive foodstuff, an alternative approach is to increase the sum total of available cathode depolarizers in the product. This is most easily done by making more oxygen available inside the container.

Finally, the storage temperature of a tinplate container may be increased to accelerate diffusion and corrosion reactions, since under normal conditions none of the reacting species are capable of escaping from the can. For most products, there is a period of thermal treatment after the cans are sealed during which the contents are sterilized. Following this, storage is at "ambient" temperature, and it is common practice for pack tests to be carried out with storage temperatures higher than those normally found.

As with all accelerated corrosion tests, there is the inherent danger that reaction pathways will be disturbed and erroneous conclusions will be drawn from the results. It is therefore important that the test described in this paper is applied in a form suitable for the work being carried out. Even then, the results obtained cannot be used as a substitute for industrial pack tests, and their real value lies in being able to plan such trials in a more cost-effective manner.

Experimental Procedure

The ASCC test makes use of specimens of tinplate hermetically sealed into glass tubes in such a way that the composition of the electrolyte and the headspace gas in contact with the specimen can be controlled. The tinplate specimens are coated on the back and cut edges with a self-curing silastomer (Dow-Corning RTV silicone) to prevent contact with the corrosive medium. This silastomer

has demonstrated good adhesion with tin, steel, and can lacquers, and it withstands the high temperatures involved during sterilizing treatments.

The most reliable way to ensure that the glass tubes used in the test are hermetically sealed is to fuse them closed in a gas torch flame. It is therefore normal practice to prepare a tube, sealed at one end, put the tinplate specimen inside, and then neck-in the other end. It is then easy to fill the tube with electrolyte and headspace gas using the apparatus shown in Fig. 1 before finally fusing the tube closed at the necked-in region. This also ensures that the total sealed volume of the glass tube is reasonably reproducible, and this in turn produces adequate control over the amount of oxygen available inside the tube. The effect of fusing the tube is to cause the gases inside to become slightly hot so that the interior pressure after sealing is approximately 80% of the atmospheric pressure.

The sealed tubes may be heated in an autoclave to simulate the normal processing conditions for real cans before they are stored in a thermostatically controlled cabinet. A storage temperature of 30°C has been found suitable in all applications of the test at ITRI and, while the processing conditions may be chosen to correspond to those used for different products, 20 min at 115°C has proved to be adequate.

The dimensions of the test system are essentially arbitrary, although in some applications it is preferable to keep the tinplate specimen area to electrolyte volume ratio the same as that found in the real can being simulated. There are also obvious advantages in reducing the amount of material required for the ASCC test providing sufficient electrolyte is available for analysis after the test [*13*]. Typical specifications for the ASCC test used at ITRI are given in Table 1, but these values should not be regarded as essential requirements.

The electrolyte used in the ASCC test depends of course on the purpose of the test. Real foods, beverages, or packaged chemicals may all be used providing

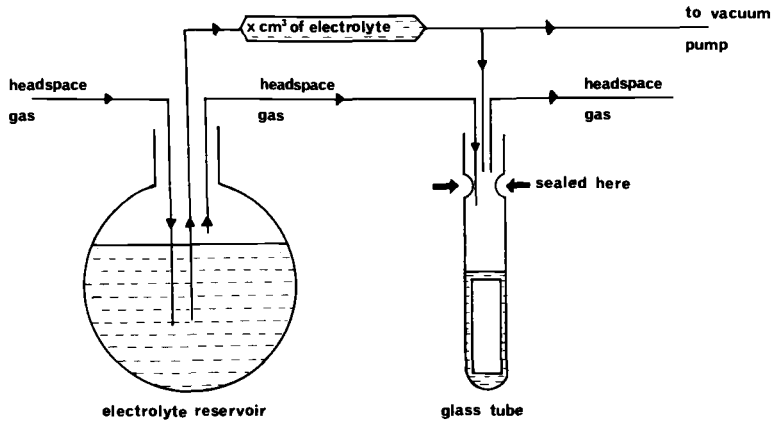


FIG. 1—*Schematic representation of the apparatus used to seal specimens for the accelerated simulated can corrosion test in a controlled environment.*

TABLE 1—*Typical cell specifications for the ASCC test.*

Parameter	Value
Glass specification	
internal diameter	1.9 cm
wall thickness	1 mm
approximate length	15 cm
approximate volume	40 cm^3
Tinplate specimen	
length	5.5 cm
width	1.5 cm
Approximate headspace volume	20 cm^3
Solution volume	20 cm^3

they can be introduced successfully into the cell. The test is therefore most convenient when testing liquids or suspensions of comparatively fine material. Fruit or vegetable products may be macerated to provide a homogeneous test medium. In such cases, it may be more convenient to fill the test cell by alternative means and to follow this by very thorough flushing of the headspace region of the glass tube.

The studies carried out at ITRI with the ASCC test have generally been intended to elucidate basic corrosion data rather than information linked to specific food products. It has therefore been normal to make use of wholly synthetic solutions that simulate classes of particular products. Most often these are based on the simple carboxylic acid solutions used widely in electrochemical studies on tinplate.

If the headspace gas used in the ASCC test was to be made oxygen free, then the test cell should resemble a normal can. The corrosion reactions would occur at rates comparable with those found in real containers, and there is some indication from limited work at ITRI that this is the case. Furthermore, it is apparent that real foods in the ASCC test stimulate more corrosion than carboxylic acid solutions under oxygen-free conditions. This confirms the role of naturally occurring cathode depolarizers in foods in accelerating attack of tinplate. There is, however, little merit in using the ASCC test cell in its nonaccelerated form, since the same results could be achieved more reliably in the same time scale with real cans. Early experiments were therefore undertaken to establish how much artificial cathode depolarizer, in the form of oxygen, should be added to the test cell. It has been found that a mixture of 3% oxygen in argon provides sufficient acceleration of corrosion, typical of that promoted by cathode depolarizers normally present in canned foods, without causing undue distortion of the relative importance of the reactions involved. This is illustrated by the results contained in Tables 2 and 3, which show analytical data for sample tubes processed at 115°C for 20 min, then stored at 30°C for 30 days. In obtaining these results, the tinplate test pieces were modified by the addition of rivets of 2% tin/98% lead solder in electrical contact with the steel base of the specimen. The area ratio between solder and tinplate (1:100) was far higher than might

TABLE 2—*Effect of oxygen concentration in ASCC test of unlacquered tinplate.*[a]

Headspace Oxygen Concentration, %	Metal Concentration, ppm		
	Tin	Iron	Lead
0	10 (2.2)	2 (0.4)	0.1
3	81 (6)	25 (5)	0.5 (0.1)
21	92 (8)	~850	0.6 (0.5)

[a]Effect of headspace oxygen concentration on the dissolution of metals from a 2% tin/98% lead and unlacquered tinplate (2.8 gm^2) couple immersed in 0.05*M* citric acid solution brought to pH of 3 with sodium hydroxide solution. The sealed tubes had been heated to 115°C for 20 min then stored at 30°C for 30 days. The results are expressed as mean (standard deviation) in ppm.

occur in real cans in order to accelerate attack of the solder, but despite this it can be seen that very little lead dissolved in the electrolytes.

Table 2, showing the results for an accelerated test on simulated plain tinplate cans at different headspace gas oxygen concentrations, contains data that correlate well with the known reaction pathways occurring inside real cans. Under the test conditions, complete detinning of the specimens would have contributed approximately 100 ppm of tin to the solution, and it can be seen that this amount has virtually all dissolved before significant amounts of iron dissolve. Even with a headspace gas of air, the dissolution of lead from the solder is very small and iron corrosion is favored after the exhaustion of the available tin.

The results in Table 3 for an accelerated test on simulated lacquered cans show the same trend as those in Table 2. Under these test conditions, more tin could have dissolved but was prevented from doing so by the lacquer coating. For the same reason, iron dissolution is relatively restricted and lead dissolution is more pronounced although it is still limited, except under the conditions of an air headspace gas. This general pattern of corrosion is very similar to that occurring in real cans, and the differences between unlacquered and lacquered containers, a relatively increased tendency to iron and lead dissolution of the latter, are well illustrated in comparison of Tables 2 and 3. It is also important to note that these trends were detected using only four replicate specimens because of the ease of analysis of the test solutions and the acceleration of corrosion achieved by the presence of oxygen in the test cells.

TABLE 3—*Effect of oxygen concentration in ASCC tests of lacquered tinplate.*[a]

Headspace Oxygen Concentration, %	Metal Concentration, ppm		
	Tin	Iron	Lead
0	6 (2.5)	3 (1.0)	0.6 (0.1)
3	30 (3)	29 (6)	1.6 (0.6)
21	65 (19)	99 (14)	290 (61)

[a]The test conditions are exactly the same as in Table 2 except that lacquered tinplate (2.8 g/m^2) was used.

Results and Discussion

The ASCC test has been widely used at the laboratories of ITRI, and the results of studies of the fundamental corrosion reactions of tinplate have been published [*2–5*]. In this paper, areas of research directly linked to more practical canning experience will be used to illustrate the value of the test. For simplicity, the results of several studies are considered separately.

Corrosion of Solder

The can-making and canning industries throughout the world are currently investing heavily in new can-making technologies. Part of the incentive for the investment is to eliminate the soldered three-piece can from the marketplace in response to concern expressed about the use of lead in such cans. In the period between making the decision to eliminate solder and achieving complete conversion to other technologies there was a need for a study of the basic parameters controlling solder corrosion in cans. In that study [*14–16*], extensive use was made of the ASCC test and many of the data generated correlated well with opinions previously expressed on the basis of subjective observations and experiences within the canning industry.

In a large-scale test in which 200 replicate specimens were prepared, the distribution of results of measurements of the dissolution of tin, iron, and lead

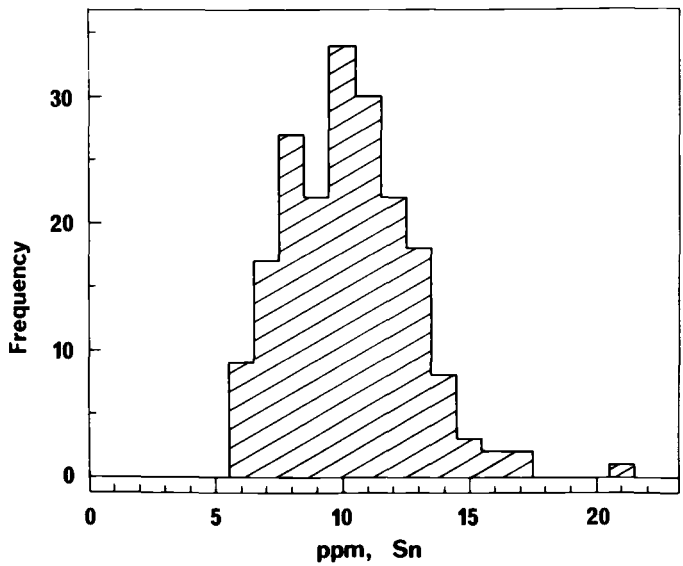


FIG. 2—*Distribution of results of the analysis for tin in solution for an ASCC test using 200 replicate specimens. The tinplate (5.6 g/m² was lacquered and electrically coupled to a pellet of 2% tin/98% lead solder. The test solution was 0.05M citric acid brought to pH of 3 with sodium hydroxide solution under a headspace gas of nitrogen, and the specimens were processed at 115°C for 20 min then stored at 30°C for 30 days.*

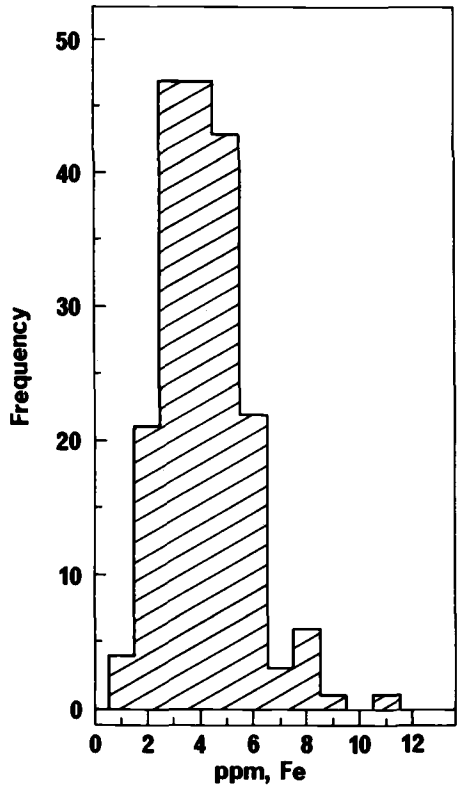


FIG. 3—*Distribution of results of the analysis for iron from the same specimens shown in Fig. 2.*

was established. As with real cans, the results for tin and iron dissolution shown in Figs. 2 and 3 followed a normal distribution so that data handling was relatively easy. Mean and standard deviations of replicate results were compared using Student's test, and as noted above, acceleration of corrosion produced significant differences in the results of tests carried out under different conditions with as few as four replicate specimens.

The results for lead dissolution did not follow this pattern and recent evidence[3] suggests that once again, the ASCC test reproduces effects found with real cans. Figure 4 shows that the results for lead dissolution follow a distinctly skew distribution, and replotting the data in Fig. 5 suggests that it is best described as lognormal. Thus, strictly speaking, mean and standard deviations should be derived from the logarithms of the values for lead dissolution and tests for significant difference applied to the data in this form. A further consequence is

[3]Hall, M. N. and Jewel, K., Campden Food Preservation Research Association, Chipping Campden, England; and Hollaender, J., Institute for Food Industry, Munich, West Germany, private communications.

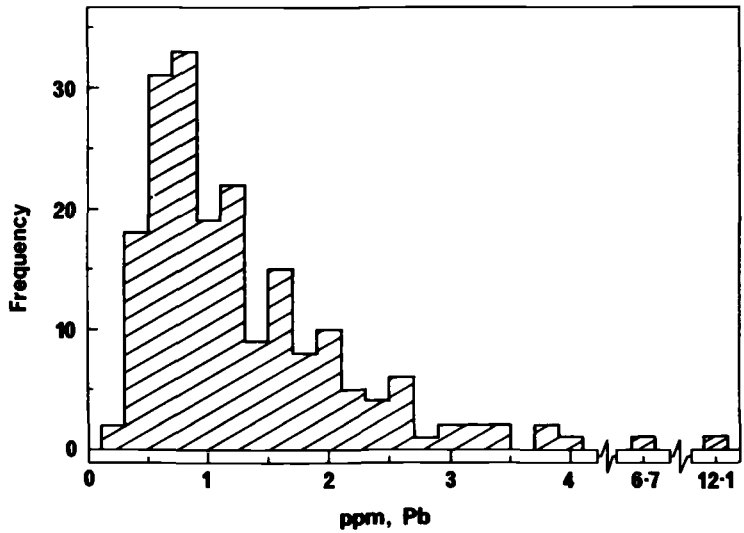


FIG. 4—*Distribution of results of the analysis for lead from the same specimens shown in Fig. 2.*

that results for lead dissolution should be expressed as a mean value plus or minus a standard deviation, not plus or minus the error. In practice we have found that acceleration of corrosion produces results that show the same dependence of lead corrosion on various parameters whether the data are assumed to follow a normal or skew distribution, but in real cans, such subtleties of interpretation are important.

A number of factors were studied in connection with solder corrosion using

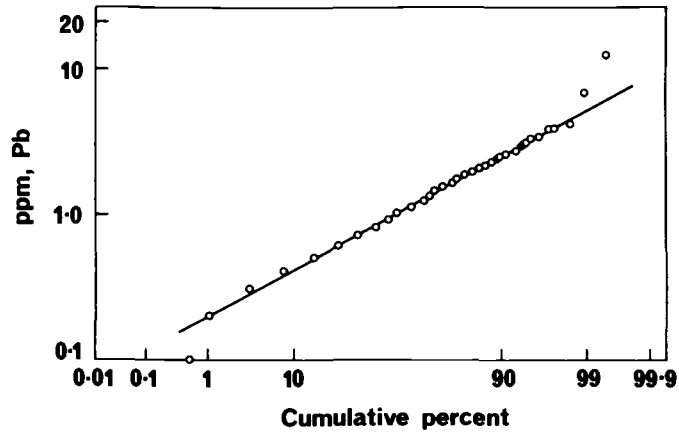


FIG. 5—*Data from Fig. 4 presented as a log-log plot. The linearity of the data in this form is a good indication that the distribution of results may be described as log-normal.*

the ASCC test, and the results are illustrated here with just two examples. The probable mechanisms by which lead corrosion is inhibited in real cans are illustrated by close examination of the results in Table 4. It can be seen that exposure of tin in a can galvanically protects solder against corrosion so that unlacquered cans are generally safer in this respect than lacquered ones. At the same time, electrical coupling is not essential and the dissolution of tin also depletes the available cathode depolarizers thus restricting the corrosion of lead, which like tin has a high overpotential for hydrogen evolution and thus a low rate of self corrosion in the absence of depolarizers. Finally there is also a clear indication that lead, which does dissolve into the electrolyte, may be removed during storage, presumably by plating out onto the corroding tinplate.

The importance of the solder alloy composition in controlling lead dissolution is well illustrated by the results of the ASCC test shown in Fig. 6. Further work demonstrated that this is due in part to the preferential corrosion of the tin-rich phase in solders containing more than a few percent of lead. It should be noted that observations such as these are supported by practical experience [*17*], and this reinforces the claim that this accelerated test has some value to industry.

Tin Powder in Lacquer

During the course of a study aimed at combining the advantages of lacquered and unlacquered cans by the incorporation of tin powder in the lacquer film, use was made of the ASCC test to establish the validity of a mathematical analysis of the problem [*18,19*].

The aim of the project was to obtain the controlled release of tin to preserve the organoleptic properties of a range of products that benefit from the reducing action of dissolved tin, which are sensitive to the presence of iron in solution. This followed earlier work [*20*] which gave variable results when submitted to testing in several commercial organizations throughout the world.

Mathematical analysis suggested that tin powder particle size was crucial to the correct functioning of the new lacquer system with optimum results being achieved where the radius of the powder particles was equal to the thickness of

TABLE 4—*Effect of storage conditions on lead dissolution from tinplate.*

Tinplate Surface Coating	State of Bi-metal Contact	Lead in Solution, ppm		
		Processed at 115°C for 20 min	Stored for 30 days at 30°C	Processed then Stored
Unlacquered	coupled	0.1 (0)	0.1	0.1
	uncoupled	2.2 (1.1)	0.1	0.15 (0.1)
Lacquered	coupled	1.5 (1.2)	0.15 (0.08)	0.55 (0.1)
	uncoupled	3.3 (0.9)	0.55 (0.1)	0.5 (0.2)

[a]The effect of storage conditions on lead dissolution from tinplate (2.8 g/m^2 or 5.6 g/m^2 lacquered) and 2% tin/98% lead solder combinations immersed in 0.05*M* citric acid solution brought to pH of 3 with sodium hydroxide solution and sealed under a headspace of nitrogen.

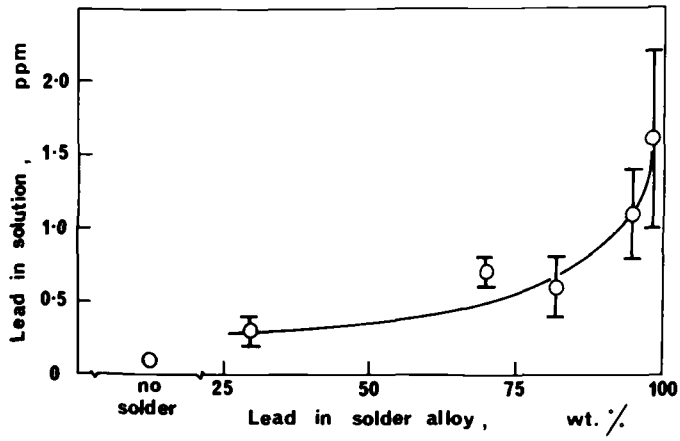


FIG. 6—*The effect of solder alloy composition on the dissolution of lead in the ASCC test, shown as a mean of four replicates with error bars plus or minus standard deviation, for a solder and lacquered tinplate (5.6 g/m² couple immersed in 0.05M citric acid solution brought to pH of 3 by the addition of sodium hydroxide solution under a headspace of 3% oxygen in argon. The sealed tubes had been heated to 115°C for 20 min then stored at 30°C for 30 days.*

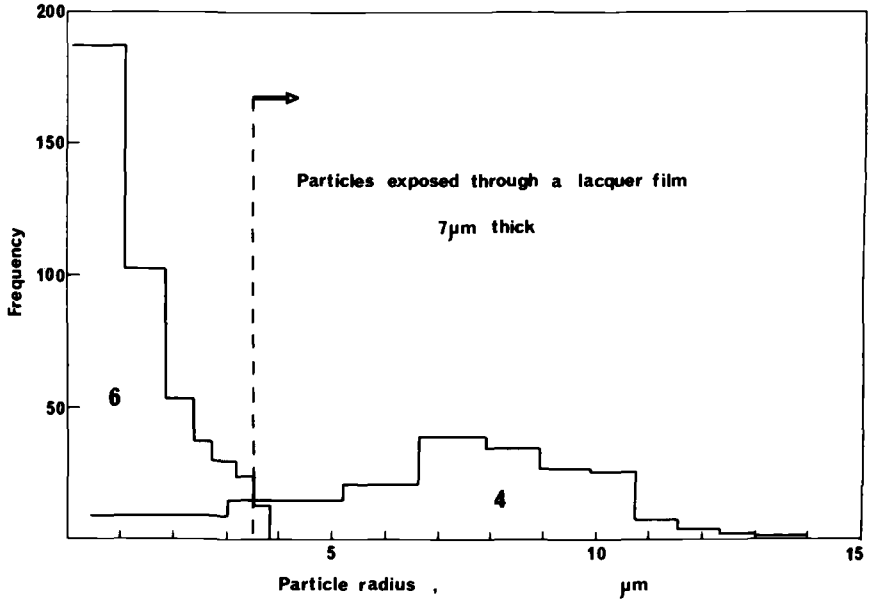


FIG. 7—*Particle size distributions of two specimens (4 and 6) of tin powder showing which material should be exposed through a lacquer film 7 μm thick on the assumption that the spherical particles all sink in the lacquer.*

TABLE 5—*Dissolution of tin and iron from scratched tinplate.*[a]

Tin Surface Coating	Area of Tin Exposed, mm^2	Metal Dissolution, ppm	
		Tin	Iron
Unlacquered	825	47.0 (9.2)	<0.1
Lacquered + tin powder 4	50	27.2 (2.4)	<0.1
Lacquered + tin powder 6	~0	4.1 (0.2)	4.2 (1.0)
Lacquered	0	3.6 (0.5)	4.0 (2.0)

[a]The dissolution of tin and iron from scratched tinplate (5.6 g/m^2) specimens with various coatings in the ASCC test. The electrolyte was 0.05*M* citric acid brought to pH of 3 oxygen in argon. Specimens were stored at 30°C for 30 days.

the lacquer film. Figure 7 shows particle size distributions for tin powders called 4 and 6, and it is clear that 4 meets the criteria for effective tin release while 6 does not. The ASCC test quickly showed (Table 5) that this was indeed the case. The results show that the controlled release of tin was achieved for a specimen coated with a lacquer containing tin powder 4, and that this specimen also behaved like an unlacquered test-piece in that iron dissolution was inhibited. By contrast, the specimen coated with lacquer containing tin powder 6 behaved just like a conventionally lacquered test-piece in all respects.

On the basis of these and other results, commercial test packs were carried out in a number of centers, and the results from one program will be referred to here. A full report of the study has been made elsewhere [*21*], but the real value of the results for the purposes of this paper is illustrated in Figs. 8 and 9. These show that in two real pack tests, plain cans, lacquered cans, and containers

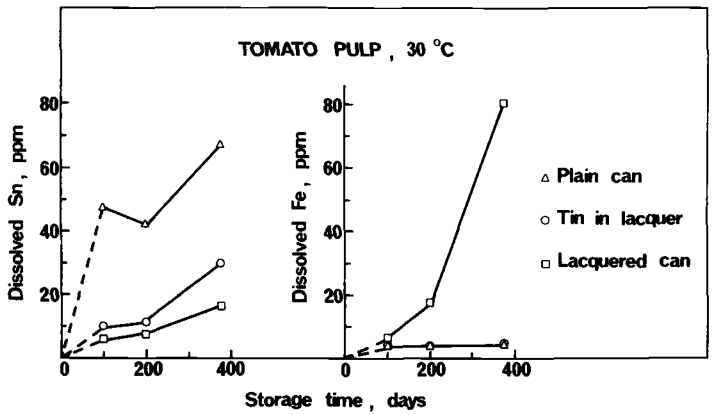


FIG. 8—*Results of a pack test using real cans (300 by 405) made from plain tinplate (11.2 g/m^2), lacquered tinplate (2.8 g/m^2), and tinplate (2.8 g/m^2) lacquered with tin powder distributed in the lacquer at a rate of approximately 2 g/m^2.*

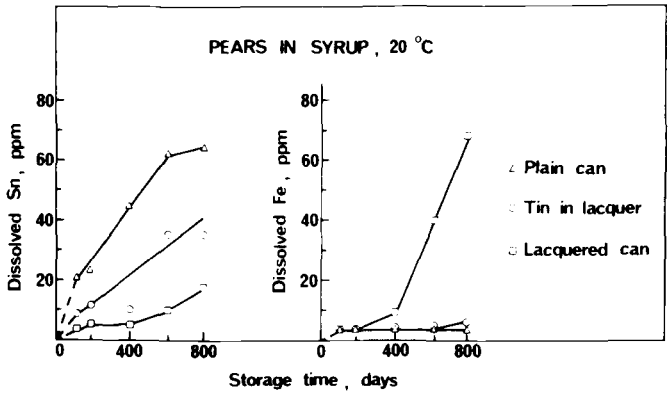


FIG. 9—*Results of a second pack test using the same materials shown in Fig. 8 but with a different product and storage temperature.*

carrying internal lacquers pigmented with tin powder behaved in the way predicted by the ASCC test. Of equal value was the observation that the appearance of the specimens used in the ASCC test was similar to the appearance of the internal surfaces of the real cans. There was evidence of lacquer undermining corrosion in the ASCC test, and this appeared in real cans. The extent of lacquer detachment was however food product related, and for tomato puree and pears in syrup it was not extensive. Most aggressive foods have however caused an unacceptable level of deterioration in the appearance of test cans although the tin pigmented lacquers offered superior characteristics to systems not loaded with tin.

Lacquer Undermining

The surface of tinplate is treated during its production to develop chemical characteristics that are desirable from the point of view of can making and can corrosion. Typically the surface of tin is covered with a thin film of mixed oxides of tin and chromium, probably with some metallic chromium, during cathodic polarization in a solution of dichromate ions. The exact composition of the film is the center of much debate [*22–24*] although studies using the techniques of X-ray photoemission spectroscopy (XPS) and auger electron spectroscopy (AES) claim to have resolved the matter [*25–29*]. The performance of tinplate is in many respects related to the composition of this "passivation" film including the phenomenon of lacquer undermining.

When lacquered tinplate is used to make containers, the relative areas of tin and steel exposed to the product are drastically altered in comparison with unlacquered tinplate. In addition, the lacquers commonly used are permeable toward several ions and oxygen so that even a perfectly continuous lacquer film can take part in electrochemical reactions.

It is not therefore surprising that the chemical constitution of the lacquer/tin interface can affect both the nature of the chemical reactions occurring there and their subsequent effect on the bond between the lacquer and the tin. A study

concerned with the effect of tinplate passivation film composition on lacquer undermining was undertaken, and an electrochemical test was developed to predict material performance with respect to this type of failure. An inverse relationship between the ratio of electrochemically oxidizable chromium to alkali-soluble chromium in the passivation film and the extent of lacquer undermining during the electrochemical test was demonstrated [*30,31*].

This was further shown with the aid of the ASCC test, again using a headspace gas of 3% oxygen in argon to promote rapid attack. In this case, undermining was further promoted by introducing a scratch to the lacquered tinplate surface with the aid of a ball-point scriber under a predetermined load. A subjective assessment of the extent of undermining could then be periodically made without removing the specimens from test. Table 6 shows the results of such an analysis, and a correlation between the electrochemical test and the ASCC test is evident. This does not of course mean that the ASCC test simulates real can performance, but indirect evidence for this has come from reports that the electrochemical test or variants of it have proved to be useful predictors of undermining in commercial containers. In our own laboratory, cans received for examination of undermining corrosion problems have shown excessive attack during electrochemical testing compared with controls that did not suffer from lacquer detachment.

The whole subject of lacquer undermining has recently received renewed interest as a result of developments in can-making technology. New tinplate materials are being developed that have exceptionally thin tin coatings, and clearly this will have an impact on the corrosion reactions inside cans made with such materials. In consequence, the ASCC test was used to determine how lacquered, low coating weight tinplate might behave in food media. Tinplate produced in the laboratory was used for the study, and it was deliberately left without a passivation treatment to eliminate the effects referred to above since it is not certain how the relative exposure of tin and iron on tinplate affects the passivation process. The results of the test may be summarized in Fig. 10, which

TABLE 6—*Lacquer undermining comparison of results.*

Electrochemical Test, cm^2 of lacquer removed	Accelerated Simulated Can Corrosion Test, degree of undermining
0.16	none
0.30	
0.30	
0.70	slight
0.70	moderate
0.75	
0.80	
0.96	
0.96	severe

[a]Specimens of normal lacquered commercial tinplate were examined by an electrochemical test and the ASCC test to assess the variation in the extent of undermining. The different levels of performance resulted from the presence of different passivation films on the tinplate specimens [*30,31*].

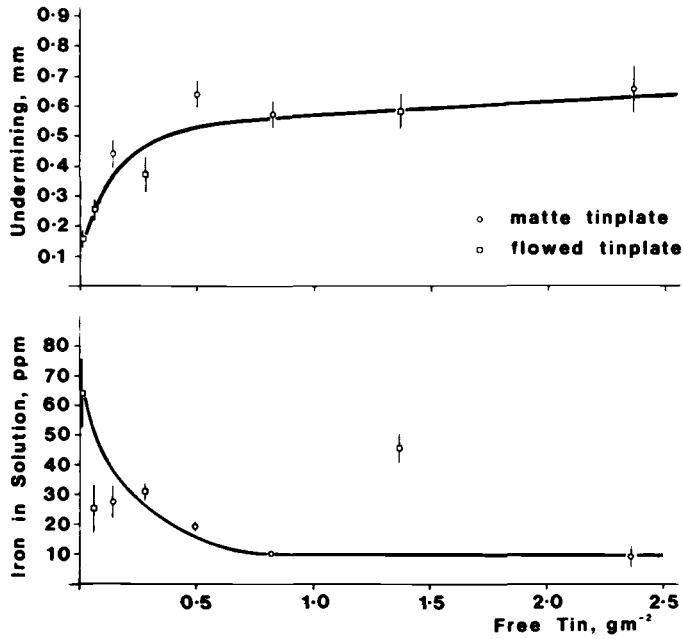


FIG. 10—*The effect of the amount of residual, unalloyed, tin on the surface of tinplate on the lacquer undermining corrosion and iron dissolution for deliberately scratched specimens in the ASCC test. The electrolyte was 0.05*M *citric acid brought to pH of 3 by the addition of sodium hydroxide solution. The headspace gas was 3% oxygen in argon and the glass tubes were stored for 40 days at 30°C.*

shows both the extent of undermining visible at scratches in the lacquer coating on the tinplate and the dissolution of iron into the test medium. There is clearly an interrelationship between undermining attack, promoting tin dissolution, and attack of the steel substrate leading eventually to pitting and possibly perforation. The data have been presented to relate both effects to the thickness of the "free tin" coating on the tinplate specimens. Some of the test material was lacquered in the as-plated condition while the coating was reflowed by resistance heating for other specimens. This operation, together with thermal treatment during the curing of the lacquer film, induces the alloying of some of the tin coating with the steel substrate. It is clear from our work that it is the unalloyed tin that moderates the undermining corrosion reactions and that 0.5 to 1.0 g/m^2 are required to control iron dissolution in this particular test system.

In a parallel study using commercially produced tinplate carrying a normal passivation treatment, the ASCC test produced similar results to those described for laboratory tinplate. However, more significantly, the commercial material was also used to make can ends for containers used in test packs of grapefruit juice and a cola product. The results in Fig. 11 show that the dependence of lacquer undermining corrosion resistance on free tin coating thickness was the same as that predicted in the ASCC test. It is probable that there is an effect of the composition of the food product on the amount of free tin required in the

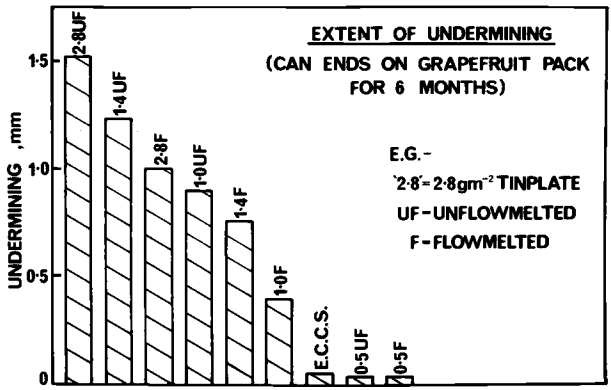


FIG. 11—*The extent of undermining on scratched lacquered can ends (330 by 207) made from commercial quality tinplate of different tin coating thicknesses. The cans containing grapefruit juice were stored for 6 months at 30°C. The specimen marked* E.C.C.S. *is a nontinplate steel packaging material, which together with* 0.5F *and* 0.5UF *showed high levels of iron dissolution into the product.*

tinplate coating to inhibit excessive corrosion of the steel but so far extensive work has not been carried out with the ASCC test to see if it can be used in such a study. Preliminary work has however demonstrated different levels of iron corrosion for citrate buffer solutions at pH values of 3 and 4.

Conclusions

The limitations of the ASCC test as a predictor of metal container performance should not be minimized. It is important that it is applied to a particular problem with due regard to the factors likely to be controlling the corrosion reactions taking place. At the International Tin Research Institute, the ASCC test has been most widely used to elucidate the mechanisms of general corrosion phenomena, but the results contained in this paper do show that it can be valuable as a sorting test for full-scale pack tests. Three widely different aspects of corrosion have been considered here, and the qualitative predictions of the ASCC test have been reproduced in studies with real cans.

It is to be hoped that other laboratories can make use of the ASCC test so that its strengths and limitations can be more fully appreciated.

Acknowledgments

The efforts of the staff of the Tinplate Section and Analytical Chemistry Section at the International Tin Research Institute in producing the data quoted in this paper are gratefully acknowledged as is the permission of the International Tin Research Council to present these results.

References

[1] Britton, S. C., "Tin Versus Corrosion," International Tin Research Institute, Publication 510, London, England, 1975.

[2] Sherlock, J. C. and Britton, S. C., *British Corrosion Journal,* Vol. 7, 1972, p. 180.

[3] Sherlock, J. C., Hancox, J. H., and Britton, S. C., *British Corrosion Journal*, Vol. 7, 1972, pp. 222 and 227.
[4] Sherlock, J. C. and Britton, S. C., *British Corrosion Journal*, Vol. 8, 1973, p. 210.
[5] Sherlock, J. C., *British Corrosion Journal*, Vol. 10, 1975, p. 144.
[6] Koehler, E. L., *Werkstoffe und Korrosion*, Vol. 21, 1970, p. 554.
[7] Collanteur, H. A. P., *Comm. International Symposium*, Vol. 1, Liege, 1971, p. 82.
[8] Maercks, O., *Verpackungs-Rundschau*, Vol. 24, No. 12, 1973, p. 1561.
[9] Maercks, O., *Verpackungs-Rundschau*, Vol. 25, No. 11, 1974, p. 83.
[10] Maercks, O., *Verpackungs-Rundschau*, Vol. 28, No. 6, 1977, p. 45.
[11] Maercks, O., *Verpackungs-Rundschau*, Vol. 29, No. 4, 1978, p. 25.
[12] Kleniewski, A., *British Corrosion Journal*, Vol. 10, 1975, p. 91.
[13] Sherlock, J. C., *Corrosion Science*, Vol. 14, 1974, p. 401.
[14] Warwick, M. E., *Proceedings of the 2nd International Tinplate Conference*, London, England, 1980, p. 337.
[15] Warwick, M. E. and Müller, B. F., *Verpackungs-Rundschau*, Vol. 31, 1980, p. 1.
[16] Bearfield, D. B., Greenwood, E. A., Warwick, M. E., *British Corrosion Journal*, Vol. 18, 1983, pp. 47 and 51.
[17] Mazzone, R., *Proceedings of the 2nd International Tinplate Conference*, London, England, 1980, p. 388.
[18] Warwick, M. E., *Proceedings of the 1st International Tinplate Conference*, London, England, 1976, p. 343.
[19] Warwick, M. E., *British Corrosion Journal*, Vol. 12, 1977, p. 247.
[20] Biston, R. and Guerrier, J., *Bulletin Inacol*, Vol. 24, 1973, p. 88.
[21] Barbieri, G., Rosso, S., Milanese, G., and Warwick, M. E., *Industria Conserve*, Vol. 57, 1982, p. 151.
[22] Britton, S. C., *British Corrosion Journal*, Vol. 10, 1975, p. 85; Sherlock, J. C., Vol. 9, 1974, p. 96; and Vol. 1, 1965, p. 91.
[23] Aubrun, P. J. and Fousse, D. H., *2nd International Tinplate Conference*, London, England, 1980, p. 263.
[24] Azzeri, N. and Splendorini, L., *Imballagio*, Vol. 292, 1980, pp. 65–79, 81, 107.
[25] Coad, J., Mott, B., Harden, G., and Walpole, J., *British Corrosion Journal*, Vol. 11, 1976, p. 219.
[26] Leroy, V., Servais, J. P., Habraken, L., Renard, L., and Lempereur, J., *Proceedings of the 1st International Tinplate Conference*, London, England, 1976, p. 399.
[27] Renard, L. and Leroy, V., *British Corrosion Journal*, Vol. 14, 1969, p. 126.
[28] Maeda, S., Asai, T., and Sawairi, T., *Proceedings of the 2nd International Tinplate Conference*, London, England, 1980, p. 286.
[29] Johannessen, J. S., Grande, A. P., and Notevarp, T., *Proceedings of the 2nd International Tinplate Conference*, 1980, London, England, p. 274.
[30] Sherlock, J. C. *Proceedings of the 1st International Tinplate Conference*, London, England, 1976, p. 322.
[31] Sherlock, J. C., *Verpackungs-Rundschau*, Vol. 6, 1977, p. 810.

DISCUSSION

Kate Nielsen[1] *(written discussion)*—Did the mentioned lead dissolution from a lacquered tin plated surface originate from pinholes in the lacquer?

M. E. Warwick (author's closure)—No, to provide control of the variables, the tinplate was lacquered first. The rivets of lead-tin solder were then attached to the specimens.

[1]Korrosionscentralen, Park Allee 345, Glostrup, Denmark.

Oliver W. Siebert[1]

Laboratory Electrochemical Test Methods

REFERENCE: Siebert, O. W., **"Laboratory Electrochemical Test Methods,"** *Laboratory Corrosion Tests and Standards, ASTM STP 866,* G. S. Haynes and R. Baboian, Eds., American Society for Testing and Materials, Philadelphia, 1985, pp. 65–90.

ABSTRACT: Corrosion is an electrochemical reaction of a metal and its environment. The aim of this paper is to provide an understanding of some of the electrochemical processes that result in corrosion and to provide a reference compendium of the present state of the art laboratory test methods used to evaluate these reactions. An analysis of the mechanism of electrochemical corrosion needs to try to identify anodic and cathodic corrosion partial processes, establish the thermodynamic possibility of these processes (the tendency to corrode), and determine the kinetics of these processes (the rate of corrosion). A study of the thermodynamic relationship of the solution pH to the system potential indicates the corrosion product ions or precipitates with the lowest free energy. When corrosion occurs, the current that flows between individual small anodes and cathodes on the metal surface causes the electrode potential of the system to change. While this current cannot be measured, it can be evaluated indirectly on a metal specimen with an inert electrode and an external electrical circuit. Kinetic polarization is described as the extent of the change in potential of an electrode from its equilibrium potential caused by a net current flow to or from the electrode, galvanic or impressed. This review covers the several laboratory electrochemical test methods used to identify and evaluate these metallic corrosion reactions.

KEY WORDS: corrosion, electrical resistance, electrochemical corrosion, impedance, velocity, immersion corrosion testing, controlled potential, Tafel extrapolation, linear polarization, potentiodynamic polarization, kinetic polarization, corrosion behavior diagram, pitting corrosion, crevice corrosion, thermodynamic EMF-pH diagrams, Poubaix diagrams, slow strain rate

The primary purpose of materials selection is to provide the optimum equipment for a process application in terms of materials of construction, design, and corrosion control measures. Optimum here means that which comprises the best combination of cost, life, safety, and reliability.

The selection of materials to be used in design dictates a basic understanding of the behavior of materials and the principles that govern such behavior. If proper design of suitable materials of construction is incorporated, the equipment should deteriorate at a uniform and anticipated gradual rate, which will allow

[1]Senior fellow, Monsanto Company, Corporate Engineering Department, 800 North Lindbergh Blvd., St. Louis, MO 63167.

Copyright© 1985 by ASTM International www.astm.org

scheduled maintenance or replacement at regular intervals. If localized forms of corrosion are characteristic of the combination of materials and environment, the materials engineer should still be able to predict the probable life of equipment, or devise an appropriate inspection schedule to preclude unexpected failures. The concepts of predictive, or at least preventive, maintenance are minimum requirements to proper materials selection. This approach to maintenance is certainly intended to minimize the possibility of unscheduled production shutdowns because of corrosion failures, with their attendant possible financial losses, hazard to personnel and equipment, and resultant environmental pollution.

Chemical processes may involve a complex variety of both inorganic and organic chemicals. Hard and fast rules for selecting the appropriate materials of construction can be given when the composition is known and constant, free of unsuspected contaminates, when the relevant parameters of temperature, pressure, velocity, and concentration are defined, and when the mechanical and environmental degradation of the material is uniform, that is, free of localized attack. For example, it is relatively simple to select the materials of construction for a regimen of equipment for the storage and handling of cold, concentrated sulfuric acid. On the other hand, the choice of suitable materials for producing phosphoric acid by the digestion of phosphate rock with sulfuric acid is much more difficult because of the diversity in kind and concentration of contaminants, the temperatures of the reactions and strength of sulfuric and phosphoric acid used or formed. Probably the best way to approach the study of materials selection is to categorize the types of major chemicals that might be encountered, describe their inherent characteristics, and generalize about the corrosion characteristics of the prominent materials of construction in such environments [*1,2*].

The background information that materials selection is based on is derived from a number of sources. In many cases, information as to the corrosion resistance of a material in a specific environment is not available and must be derived experimentally. It is to this need that the primary remarks of this paper are addressed.

Unfortunately, there is no standard or preferred way to evaluate an alloy in an environment. While the chemistry of the operating plant environment can sometimes be duplicated in the laboratory, factors of velocity, hot and cold wall effects, crevice, chemical reaction of the fluid during the test, stress levels of the equipment, contamination with products of corrosion, trace impurities, dissolved gases, and so forth also have a controlling effect on the quality of the answer. Then, too, the progress of the corrosion reaction itself varies with time. Notwithstanding, immersion testing remains the most widely used method for making materials of construction selections [*3*].

Immersion Test

The National Association of Corrosion Engineers (NACE) Standard Laboratory Corrosion Testing of Metals for the Process Industries (TM-01-69) and ASTM Recommended Practice for Laboratory Immersion Corrosion Testing of

Metals (G 31) are the general guides for immersion testing. Small pieces of the candidate metal are exposed to the medium, and the loss of mass of the metal is measured for a given period of time. Immersion testing remains the best method to eliminate from further consideration those materials that obviously cannot be used. This technique is frequently the quickest and most satisfactory method of making a preliminary selection of the best candidate materials.

Probably the most serious disadvantage of this method of corrosion study is the assumed average-time weight loss. The corrosion rate could be high initially and then decrease with time (it could fall to zero). In other cases the rate of corrosion might increase very gradually with time or it could cycle or be some combination of these things.

Electrical Resistance

The measurement of corrosion by electrical resistance is possible by considering the change in resistance of a thin metallic wire or strip sensing element (probe) as its cross section decreases from a loss of metal. Since small changes in resistance are encountered as corrosion progresses, changes in temperature can cause enough change in the wire resistance to complicate the results. Commercial equipment, such as the Corrosometer®, have a protected reference section of the specimen in the modified electrical Wheatstone bridge (Kelvin) circuit to compensate for these temperature changes. Since changes in the resistance ratio of the probe are not linear with loss of section thickness, compensation for this variable must be included in the circuit. In operation, the specimen probe is exposed to the environment and instrument readings are periodically recorded. The corrosion rate is the loss of metal averaged between any two readings.

The corrosion rate can be studied by this method over very short periods of time, but not instantaneously. The environment does not have to be an electrolyte. Studies can be made in corrosive gas exposures.

The main disadvantage of the technique is that local corrosion (pitting, crevice corrosion, galvanic, stress corrosion cracking, fatigue, and so forth) will probably not be progressively identified. If the corrosion product has an electrical conductivity approaching that of the lost metal, little or no corrosion will be indicated. The same problem will result from the formation of conducting deposits on the specimen.

EMF versus pH (Pourbaix) Diagrams

Potential (EMF) versus pH equilibrium (Pourbaix) diagrams derived from physical property data about the metal and its environment provide a basis for the expression of a great amount of thermodynamic data about the corrosion reaction [*4*]. These relatively simple diagrams graphically represent the thermodynamics of corrosion in terms of electromotive force, that is, an indication of oxidizing power and pH, or acidity. As an aid in corrosion prediction, their usefulness lies in providing direction for establishing a corrosion study program.

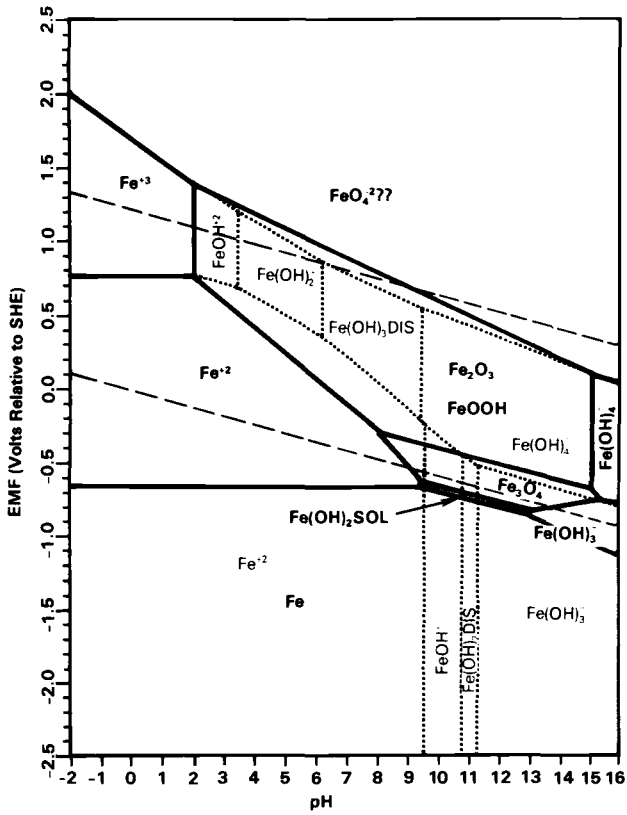


FIG. 1—*EMF-pH diagram for an iron-water system at 25°C. All ions are at an activity of* 10^{-6}.

Figure 1 is a typical Pourbaix diagram. Generally, the diagrams show regions of immunity (the metal), passivity (the surface film), and corrosion (metallic ions). While of considerable qualitative usefulness, these diagrams have important limitations. Since they are calculated from thermodynamic properties, they represent equilibrium conditions and do not provide kinetic information. Thus, while they show conditions where corrosion will not occur, they do not necessarily indicate under what conditions corrosion will occur. To determine the quantitative value of corrosion, kinetic rate measurement would still be required. Pourbaix diagrams were developed for the study of pure metals. Since few engineering structures are made of pure metals, it is important to extend this technique to include information on the passive behavior of alloys of engineering interest. Values of the open circuit corrosion potential (OCP) or a controlled potential occur, if a steady site potential can be used in conjunction with the solution pH and these diagrams to show what component is stable in the system defined by a given pH and potential. Theoretical diagrams so developed estimate the corrosion product in various regions. The use of computers to construct

diagrams for alloy systems provides an opportunity to mathematically overcome many of the limitations inherent in the theoretical pure metal system [*5–7*].

Recently, a potentio-kinetic electrochemical hysteresis method of diagram construction has led to consideration of three-dimensional Pourbaix diagrams for alloy systems useful in alloy development, evaluation of the influence of crevices, prediction of the tendency for dealloying, and the inclusion of kinetic data on the diagram is useful in predicting corrosion rather than just the absence of damage. These proposed diagrams are kinetic, not thermodynamic, expressions. The two should not be confused as being the same reaction, as they are not.

Tafel Extrapolation

Corrosion is an electrochemical reaction of a metal and its environment. When corrosion occurs, the current that flows between individual small anodes and cathodes on the metal surface causes the electrode potential for the system to change. While this current cannot be measured, it can be evaluated indirectly on a metal specimen with an inert electrode and an external electrical circuit. Polarization is described as the extent of the change in potential of an electrode from its equilibrium potential caused by a net current flow to or from the electrode, galvanic or impressed (Fig. 2).

Electrochemical techniques have been used for years to study fundamental phenomenological corrosion reactions of metals in corrosive environments. Unfortunately, the learning curve in the reduction of these electrochemical theories

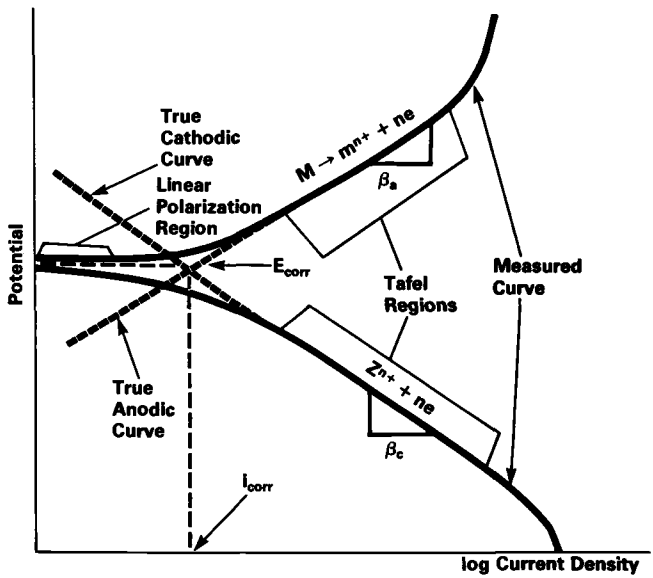


FIG. 2—*Tafel extrapolation and linear polarization curves.*

to practice has been painfully slow. However, a recent survey has shown that many organizations in the Chemical Process Industries are now adding electrochemical methods to their materials selection techniques. Laboratory electrochemical tests of metal/environment systems are being used to show the degree of compatibility and describe the limitations of those relationships. The general methods being used include electrical resistance, Tafel extrapolation, linear polarization, and potentiodynamic polarization, both slow and rapid-scan. Depending upon the study technique used, it has also been possible to indicate the tendency of a given system to suffer local pitting or crevice attack or both. These same tools have been the basis of design protection of less noble structural metals [*3*].

To study the anode reaction of a specimen in an environment, sufficient current is applied to change the freely corroding potential of the metal in a more electropositive direction with respect to the inert electrode (acting as a cathode). The opposite of this so-called anodic polarization is cathodic polarization. Polarization can be studied equally well by varying the potential and measuring the resultant changes in the current. Both of the theoretical (true) polarization curves are straight lines when plotted on semilog axis. The corrosion current can be measured from the intersection of the corrosion potential and either the anodic or cathodic curve. The corrosion rate of the system is a function of that corrosion current. Experimentally derived curves are not fully linear because of the interference from the reactions between the anodes and cathodes in the region close to the corrosion potential. IR losses often obscure the Tafel behavior. Away from the corrosion potential the measured curves match the theoretical (true) curves. The matching region of the measured curves is called the Tafel region, and their (Tafel) slopes are constant. Corrosion rates can be calculated from the intersection of the corrosion potential and the extrapolation of the Tafel region. The main advantage of the technique is that it is quick; curves can be generated in about an hour [*2,3*].

The technique is of limited value where more than one cathodic reduction reaction occurs. In most cases it is difficult to identify a sufficient linear segment to the Tafel region, to extrapolate accurately. Since currents in the Tafel region are one to two orders of magnitude larger on the log scale than the corrosion current, relatively large currents are required to change the potentials from what they are at the corrosion potential. The environment must be a conductive solution. The Tafel technique does not indicate local attack, only an average, uniform corrosion rate.

The primary use of this laboratory technique today is as a quick check to determine the order of magnitude of a corrosion reaction. Sometimes the calculated rate from an immersion test does not "look" correct when compared to the visual appearance of the metal coupon. While the specific corrosion rate number determined by Tafel extrapolation is seldom accurate, the method remains a good confirmation tool [*2,8*].

Linear Polarization

Some of the limitations of the Tafel extrapolation method can be overcome by using the linear-polarization technique to determine the corrosion rate. A relationship exists between the slope of the polarization curves E/I (with units of resistance, linear polarization is sometimes termed "polarization resistance") and instantaneous corrosion rates of a freely corroding alloy. The polarization resistance is determined by measuring the amount of applied current needed to change the corrosion potential of the freely corroding specimen by about 10-mV deviations. The slope of the curves thus generated is directly related to the corrosion rate by Faraday's law. Several instruments are available that are used in linear polarization work. The main advantage is that each reading on the instrument can be translated directly into a corrosion rate [*9,10*].

As with all electrochemical studies, the environment must be electrically conductive. The corrosion rate is directly dependent on the Tafel slope. The Tafel slope varies quite widely with the particular corroding system and generally with the metal under test. As with the Tafel extrapolation technique, the Tafel slope generally used is an assumed, more or less average value. Again, as with the Tafel technique, the method is not sensitive to local corrosion [*8,11–14*].

Potentiodynamic Polarization

Not all metals and alloys react in a consistent manner in contact with corrosive fluids. One of the common intermediate reactions of a metal (surface) is with oxygen, and those reactions are variable and complex. Oxygen can sometimes function as an electron acceptor, that is, oxygen can act as an oxidizing agent, and remove the "protective" film of hydrogen from the cathodic area, cathodic depolarization. The activation energy of the oxygen/hydrogen reaction is very large. This reaction does not normally occur at room temperature at any measureable rate. In other cases, oxygen can form protective oxide films. The long-term stability of these oxides also varies; some are soluble in the environment, others form more stable and inert or passive films [*15*].

Because corrosion is an electrochemical process, it is possible to evaluate the overall reaction by the use of an external electrical circuit called a potentiostat [*16*]. When corrosion occurs, a potential difference exists between the metal and its ions in solution. It is possible to electrically control this potential; changes in potential cause changes in current (corrosion). Oxidation is a reaction with a loss of electrons (anodic—the reacting electrode is the anode); reduction is a reaction with a gain of electrons (cathodic—the reacting electrode is the cathode). Rather than allowing the electrons being evolved from the corrosion reaction to combine with hydrogen, by internal circuitry, these electrons can be removed, sent through a potentiostat, then causing a cathodic (or anodic) reaction to occur at a platinum counter electrode. This is always true for the external polarization method; it is not unique for a potentiostat.

The potentiostat has a three electrode system, a reference electrode, generally a saturated calomel electrode (SCE), a platinum counter, or auxiliary, electrode through which current flows to complete the circuit, and a working electrode that is a sample of interest (Fig. 3). The potentiostat is an instrument that will allow control of the potential, either holding constant at a given potential, stepping from potential to potential, or changing the potential anodically or cathodically at some linear rate [*16*].

In the study of the anode/cathode polarization behavior of a metal/environment system, the potentiostat will provide a plot of the relationship of current changes resulting from changes in potential most often presented as a plot of log current density versus potential, or Evans diagram. A typical active-passive metal anodic polarization curve is seen in Fig. 4, generally showing the regions of active corrosion and passivity, and a transpassive region.

Scan Rates

Sweeping a range of potentials in the anodic (more electropositive) direction of a potentiodynamic polarization curve at a high scan rate of about 60 V/h (high by the perspective of the corrosion engineer, slow by the reference of a physical chemist) is to indicate regions where intense anodic activity is likely. Secondly, for otherwise identical conditions, sweeping at a relatively slow rate

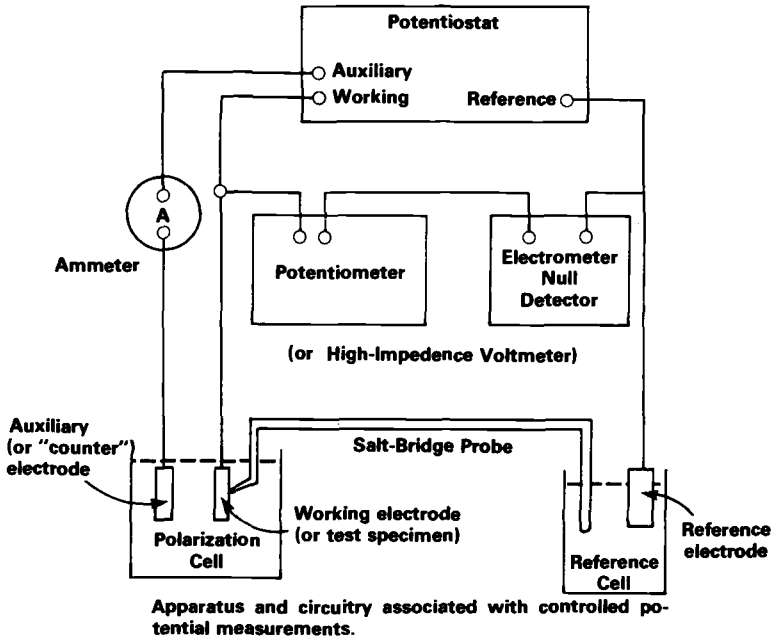


FIG. 3—*The potentiostat-apparatus and circuitry associated with controlled potential measurements of polarization curves.*

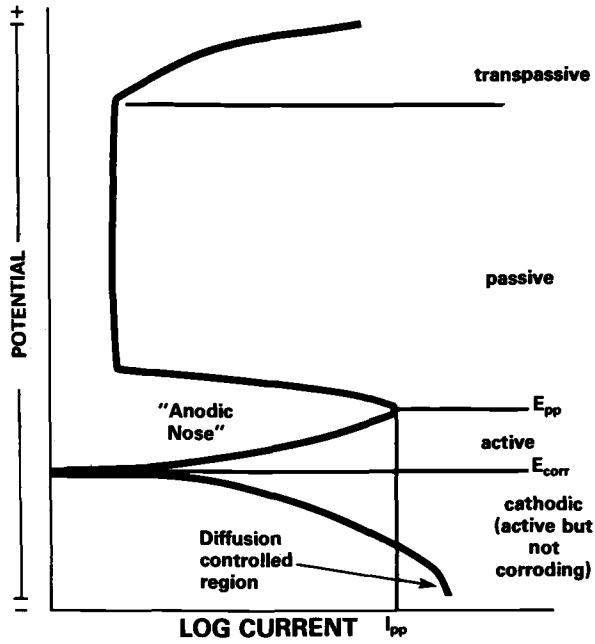


FIG. 4—*Typical electrochemical polarization curve for an active-passive alloy (with cathodic trace) showing active, passive, and transpassive regions and other important features. (Note:* E_{pp} = *primary passive potential and* E_{corr} = *freely corroding potential.)*

of potential change of about 1 V/h will indicate regions wherein relative inactivity is likely. The rapid sweep of the potential range has the object of minimizing film formation, so that the currents observed relate to relatively film-free or thin-film conditions. The object of the slow sweep rate experiment is to allow time for filming to occur [*17*]. A zero-scan rate provides the opportunity for maximum stability of the metal surface, but at high electropositive potentials, the environment could be affected or changed. A rapid-scan rate compromises the steady state nature of the metal surface but better maintains the stability of the environment. Whenever possible, corrosion tests should be conducted using as many of the techniques available, potentiodynamic polarization at various scan rates, crevice, stress, velocity, and so forth. An evaluation of these several results, on a holistic basis, can greatly reduce or temper their individual limitations [*18,19*].

Slow-Scan Technique

In ASTM Polarization Practice for Standard Reference Method for Making Potentiostatic and Potentiodynamic Anodic Polarization Measurements (G 5), all oxygen in the test solution is purged with hydrogen for a minimum of ½ h before introducing the specimen. The test material is then allowed to reach a steady state of equilibrium (open circuit corrosion potential, E_{corr}) with the test medium

before the potential scan is conducted. Starting the evaluation of a basically passive alloy (that is already) in its "stable" condition precludes any detailed study of how the metal reaches that protected state (the normal intersection of the theoretical anodic and cathodic curves is recorded as a zero applied current on the ASTM potentiostatic potential versus applied diagram). These intersections between the anodic and cathodic polarization curves are the condition where the total oxidation rate equals the total reduction rate (ASTM Recommended Practice for Conventions Applicable to Electrochemical Measurements in Corrosion Testing [G 3]) [*20–22*].

Three general reaction types compare the activation-control reduction processes. In Fig. 5, in Case I, the single reversible corrosion potential (anode-cathode intersection) is in the active region. A wide range of corrosion rates is possible. In Case II, the cathodic curve intersects the anodic curve at three potentials, one active and two passive. If the middle active-passive intersection is not stable, the lower and upper intersections indicate the possibility of very high corrosion rates. In Case III, corrosion is in the stable, passive region, and the alloys generally passivate spontaneously and exhibit low corrosion rates. Most investigators report that the ASTM method is effective for studying Case I systems. An alloy-medium system exhibiting Case II and III conditions generally cannot be evaluated by this conventional ASTM method [*15,18,19, 23–37*].

The potentiodynamic polarization electrochemical technique can be used to study and interpret corrosion phenomena. It may also furnish useful information on film breakdown or repair [*15,33–37*].

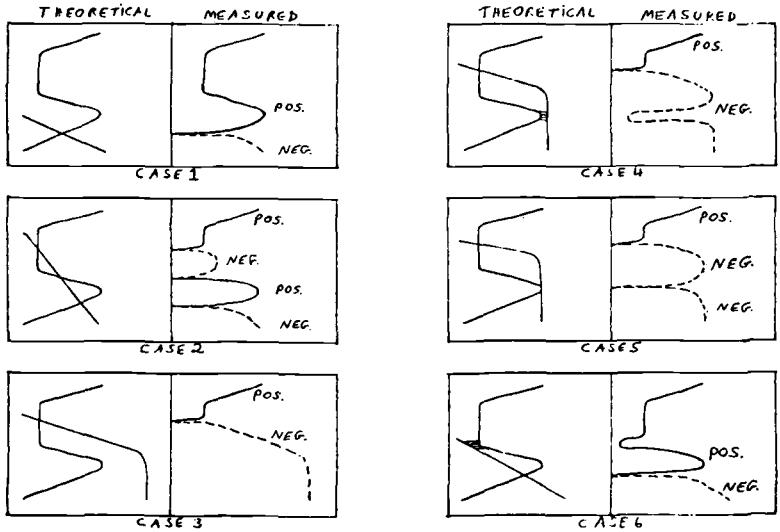


FIG. 5—*Six possible types of behavior for an active-passive alloy in a corrosive environment.*

Rapid-Scan Corrosion Behavior Diagram

Basically, all the same equipment used in the conductance of an ASTM G 5 slow-scan polarization study is used for rapid-scan/CBDs (that is, a standard test cell, potentiostat, voltmeters, log converters, *X-Y* recorders, and electronic potential scanning devices). The differences are in technique; the slow-scan is run at a potential sweep rate of about 0.6 V/h, the rapid-scan/CBDs at about 50 V/h [*38–40*].

In the conductance of rapid-scan/CBDs, the test specimen is mechanically and chemically cleaned immediately before immersion in the test cell. Without any further delay, a cathodic polarization scan is made at a sweep rate of about 50 V/h (compared to the 0.6 V/h for the ASTM method). This rapid cathodic charging (hydrogen evolution) further cleans the specimen of oxygen so that the subsequent anodic polarization enables a full study of how the corrosion reaction progresses as the potential is changed potentiodynamically in the more noble (positive) direction without the interference of any preexisting passive or corrosion product film or scale. The test is run open to the atmosphere without any purge gas, and the rapid scan rate permits completion of the anodic curve before oxygen is replenished. This cathodic cleaning further activates the specimen and allows it to follow the pattern of its corrosion reaction(s) before it has an opportunity to spontaneously passivate or return to equilibrium with its environment [*19,41–42*].[2]

Different from the slow-scan technique, which is generally limited to Case I alloy-medium systems, the rapid-scan technique allows full anodic polarization study of alloys showing all Case I, II, and III behavior. In Case I, the single reversible corrosion potential (the anode-cathode intersection) is in the active region. A wide range of corrosion rates is possible. In Case II, the cathodic curve intersects the anodic curve at three potentials, one in the active region and two in the passive. Since the middle active-passive intersection is not stable, the intersections indicate the possibility of very high corrosion rates depending on the environment or even slight changes to the exposure/environment system. In Case III, the curves intersect in the most stable, passive region; the alloys generally passivate spontaneously and exhibit low corrosion rates. Case II exhibits the most corrosion, is difficult to study, and presents the most risk for materials of construction selection. Anything that can change the oxygen solubility of the oxidizing agent can alter the corrosion reaction. Seemingly identical environmental conditions from one day to another, from one laboratory or plant to another, and so forth, can give rise to widely differing results. Those desiring a more detailed review of the subject are directed to the works of Pourbaix, Edeleanu, and other works referred to in their publications [*4,20–22*].

The conductance of a CBD is generally as follows: At a rapid scan rate of about 50 V/h, the clean specimen is cathodically charged (polarized) starting at an electronegative position (with respect to SCE) that will produce a current

[2]Morris, P. E., Siebert, O. W., and Stoecker, J. G., unpublished research.

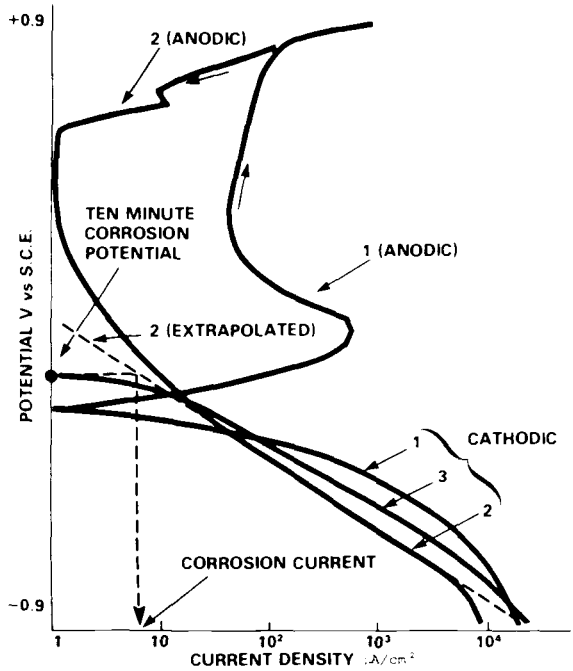


FIG. 6—*Corrosion behavior diagram.*

density of 10^4 μA/cm^2 (nickel, chromium, and iron alloys in aggressive environments) and proceed in a noble (positive) direction. After completing the cathodic curve, proceed anodically until the current density reaches 10^3 μA/cm^2. The scan direction is reversed and potentials/currents recorded back to the starting point. The potentiostat is then shut off. The freely corroding potential (FCP), also referred to as the open circuit potential (OCP), is recorded after 10 min (or when it is stable, that is, the potential value remains constant). A third cathodic polarization curve is then generated by scanning from the corrosion potential in the negative direction to i_{start}, again at a scan rate of 50 V/h. As noted earlier, this diagram can be produced in about 15 min [*38*] (Fig. 6).

The CBD diagram can provide various kinds of information about the performance of an alloy-medium system. The technique can be used for a direct calculation of the corrosion rate as well as for indicating the conditions of passivity and tendency of the metal to suffer local pitting and crevice attack.

Corrosion Rate by CBD

Somewhat similar to the Tafel extrapolation method, the corrosion rate is found by intersecting the extrapolation of the linear portion of the second cathodic curve with the equilibrium stable corrosion potential. The intersection corrosion

current is converted to a corrosion rate (Mils penetration per year [mpy]) by use of a conversion factor (based upon Faraday's law, the electrochemical equivalent of the metal, its valence and gram atomic weight). For 13 alloys, the conversion factor ranges from 0.42 for nickel to 0.67 for Hastelloy B or C. For a quick determination, 0.5 is used in all of our studies. Generally, the accuracy of the corrosion rate calculation is dependent upon the degree of linearity of the second cathodic curve; when it is less than ½ decade long, it becomes more difficult to extrapolate accurately. Obviously, the longer the better [*22,43*].

Expected Order of Magnitude of Corrosion by CBD

The third cathodic curve will generally fall between the first two, or the first and third will coincide and fall positive to the second curve. These two curve configurations are only valid relationships for the projection of accurate corrosion rates. When, however, the second or third curve falls positive to the other two curves, a very high corrosion rate may be indicated. Another possibility is that the second or third curve in this positive position is not controlling corrosion because of surface films, and so forth [*19,38*].

Spontaneous Passivation

The anodic nose of the first curve describes the primary passive potential E_{pp} and critical anodic current density (the transition from active to passive corrosion). If the initial active/passive transition is 10^3 $\mu A/cm^2$ or less, the alloy will spontaneously passivate in the presence of oxygen or any strong oxidizing agent [*31*].

Anodic Protection

On the reverse anodic scan there will be a low current region (LCR) in the passive range. The passive potential range of the LCR is generally much narrower than the passive region seen on a forward slow-scan. In anodic protection (AP) work the mid-point of the LCR potential is the preferred design range. This factor was verified for sulfuric acid (H_2SO_4) in our laboratory and field studies [*44,45*].

Pitting and Crevice Corrosion

The general literature for predicting pitting tendency with the slow-scan reviews the use of the reverse scan (if a hysteresis loop develops that comes back to the repassivation potential below the FCP (E_{corr}), the alloy will pit at crevices, when the value of the repassivation potential identified by the return of the hysteresis loop is above the FCP (E_{corr}), the pits will tend to grow) [*26*]. These rules of thumb have been expanded for rapid-scan. (1) If E_{corr} is equal to or greater than the pitting potential E_{pit}, both pitting and crevice type attack are likely to occur on the specimen in an immersion test. (2) If E_{corr} is less than E_{pit}, pitting

type attack of the specimen is unlikely in an immersion test. (3) If the repassivation potential E_{repass} is greater than E_{corr}, crevice type attack is possible in an immersion test. (4) If E_{corr} is equal to or larger than E_{repass}, crevice type attack is probably in an immersion test. (5) If no E_{pit} can be determined, but cathodic Curves 1 and 2 cross at E_x forming a hysteresis loop, crevice type attack during the rapid-scan is indicated. (6) If E_x is equal to or greater than E_{pit}, pitting type attack will be predominant during the rapid-scan test. (7) If E_{pit} is equal to or greater than E_x plus 100 mV, crevice type attack is indicated during the rapid-scan test. (8) If the plot of Curve 1 continues from E_{pit} with a large increase in current density versus a small increase in voltage, the test specimen will suffer vigorous local attack during the rapid-scan test. (9) If the Curve 1, positive with respect to the value of E_{pit}, plots with a small increase in current density per large increase in voltage, the test specimen in the rapid-scan test will suffer only mild local attack (ASTM G 31) [*19,39,42,43*].

Scan Rates: Advantages Versus Disadvantages

As to the question of disadvantages of using the rapid-scan/CBD, we believe it is more of a case of looking to the limitations of the various benefits. In many of the places where these limitations to the use of the CBD show themselves, where the limitation provides information, for example, the corrosion rate will be too high, and so forth. Only in the case of interpretation of unstable active-passive conditions do we see the results of the rapid scan as a possible weakness of the technique (but it is not handled any better by other techniques). When the FCP is noble (positive) to the E_{pp}, the alloy is passive; when the FCP is active (negative) to the E_{pp}, the alloy will corrode in the active state; and when the FCP is only slightly more noble (positive) than the E_{pp}, the alloy could show active/passive tendencies. When the FCP oscillates and will not stabilize, the potential should be plotted against time. The alloy will probably not be resistant without AP but in these latter two cases, the CBD does not tell for sure.

Logic Sequence Diagram

In order to expedite the interpretation of the 50.0-V/h anodic polarization data, three logic sequence diagrams (LSD) were constructed (Figs. 7 through 9). These diagrams can be linked to each other to provide a more complete analysis of behavior if necessary. These LSDs contain "benchmark" values that have been derived from conducting more than 10 000 potentiodynamic experiments at scan rates of either 50.0 or 60.0 V/h [*19*].

Crevice Corrosion Prediction

The most common type of localized corrosion is the occluded mode crevice corrosion. Pitting can, in effect, be considered a self-formed crevice. A crevice must be wide enough to permit liquid entry, but sufficiently narrow to maintain a stagnant zone. It is nearly impossible to build equipment without mechanical

crevices; on a microlevel, scratches can be a sufficient crevice to initiate or propagate corrosion in some metal-environment systems. The conditions in a crevice can, with time, become a different and much more aggressive environment than those on a nearby, clean, open surface. Crevices may also be created by factors foreign to the original system design such as deposits, corrosion products, and so forth. In many studies, it is important to know or to be able

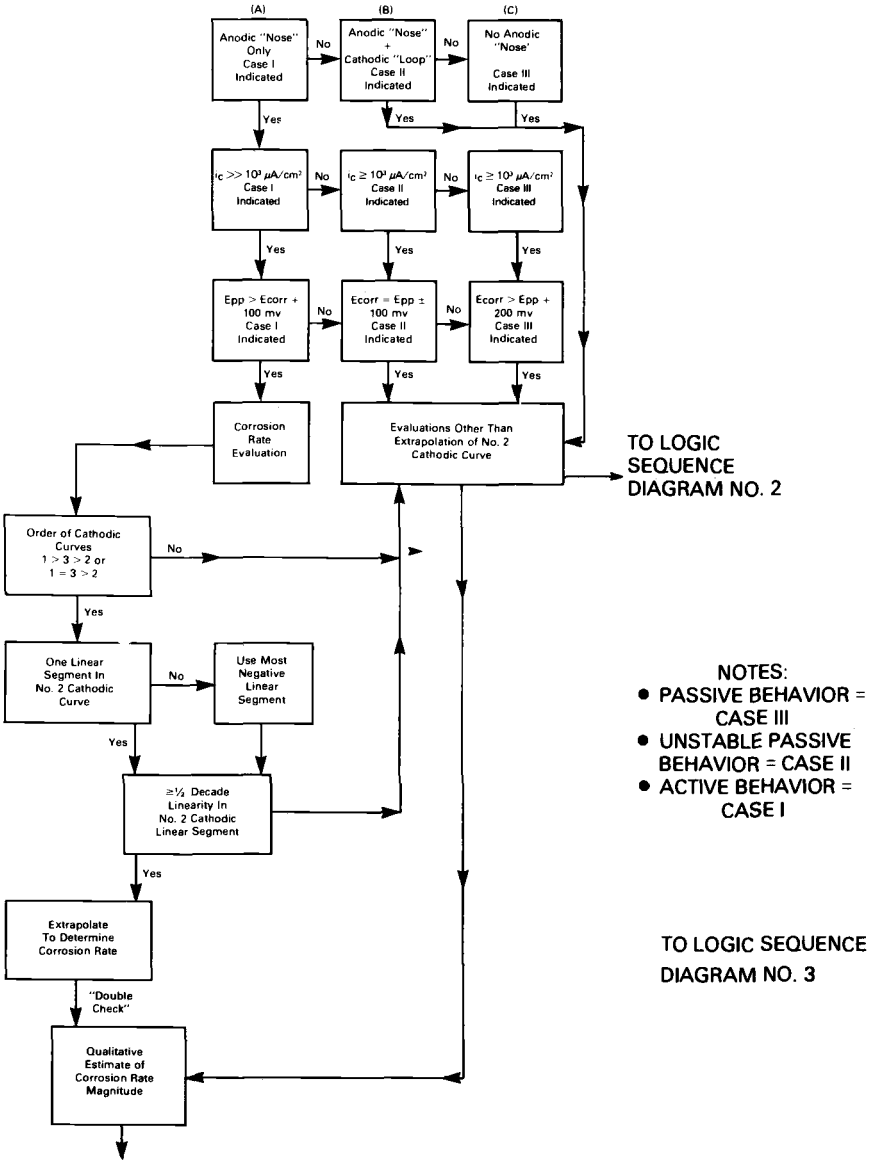


FIG. 7—*Logic sequence Diagram 1 used to determine behavior type (Case I, II, and III) and corrosion rate from a CBD.*

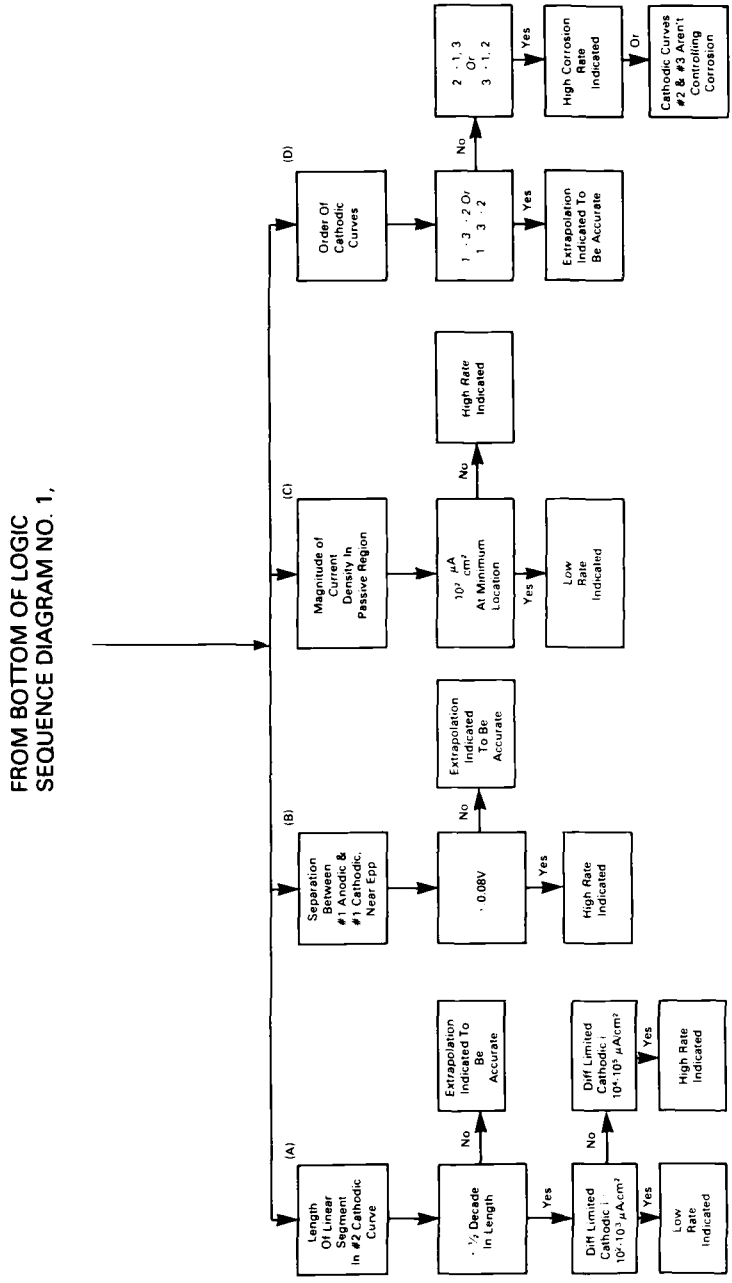


FIG. 8—*Logic sequence Diagram 2 used to evaluate localized corrosion resistance from a CBD.*

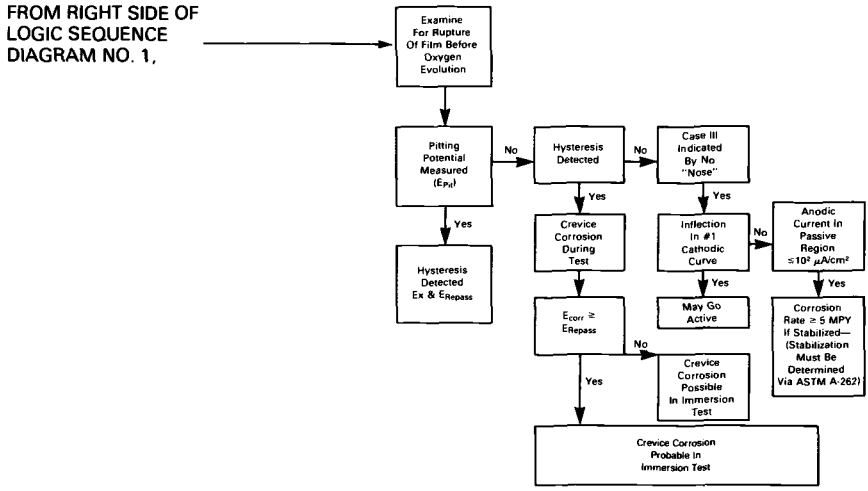


FIG. 9—*Logic sequence Diagram 3 used to qualitatively evaluate the degree of corrosion for systems that cannot be evaluated by extrapolation of the cathodic polarization Curve 2 from a CBD.*

to evaluate the crevice corrosion sensitivity of a metal to a specific environment and to be able to monitor a system for predictive maintenance.

Historically, the immersion test technique involved the use of a crevice created by two metal test specimens clamped together or a metal specimen in contact with an inert plastic or ceramic. More recently, the Materials Technology Institute (MTI) funded a study that resulted in an electrochemical cell to monitor crevice corrosion. It consists of a prepared crevice containing an anode that is connected through a zero resistance ammeter to a freely exposed cathode. A string bridge provides a solution path that is attached externally to the cell. The electrochemical cell is shown in Fig. 10. A continuous, semi-quantitative, real-time indication of crevice corrosion is provided by the magnitude of the current flowing between an anode and a cathode, and a qualitative signal is provided by shifts in electrode potential. Both the cell current and electrode potential produced by the test correlate well with the initiation and propagation of crevice corrosion. During development of the MTI test technique, results were compared with crevice corrosion produced by a grooved TFE plastic disk sandwich-type crevice cell. In nearly every instance, corrosion damage on the anode was similar in severity to that produced by the sandwich-type cell [*46,47*].

Velocity

For corrosion to occur, an environment must be brought into contact with the metal surface and the metal atoms or ions must be allowed to be transported away. Therefore, the rate of transport of the environment with respect to a metal surface is a major factor in the corrosion system. Changes in velocity may increase or decrease attack depending on its effect on the corrosion mechanism

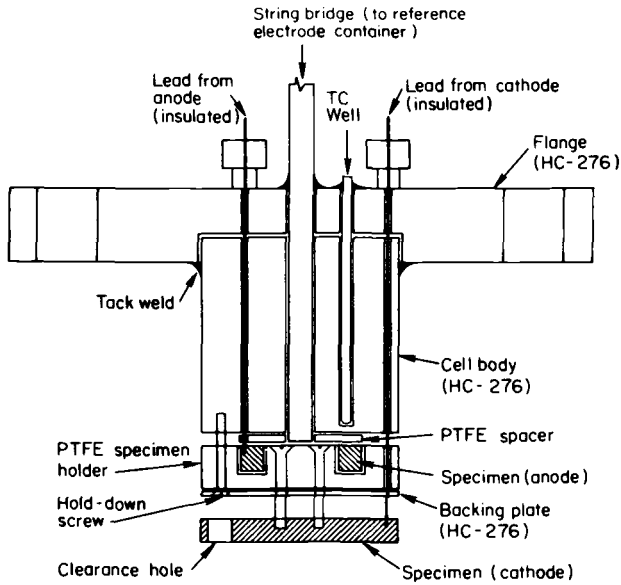


FIG. 10—*Schematic diagram of the electrochemical cell used for crevice corrosion testing. Not shown are three hold-down screws, gas inlet tube, and external thermocouple tube.*

involved. A varying quantity of dissolved gas may be brought in contact with the metal, or velocity changes may alter diffusion or transfer of ions by changing the thickness of the boundary layer at the surface. The boundary layer, which is not stagnant, moves except where it touches the surface. Many metals depend upon the development of a protective surface for their corrosion resistance. This may consist of an oxide film, a corrosion product, an adsorbed film of gas, or other surface phenomena. The removal of these surfaces by effect of the fluid velocity exposes fresh metal, and as a result, the corrosion reaction may proceed at an increasing rate. In these systems, corrosion might be minimal until a so-called critical velocity is attained where the protective surface is damaged or removed and the velocity is too high for a stable film to reform. Above this critical velocity, the corrosion may increase rapidly [*48*].

The NACE Landrum Wheel velocity test is typical of several mechanical-action immersion test methods to evaluate the effects of corrosion. Unfortunately, these laboratory simulation techniques did not consider the fluid mechanics of the environment or metal interface and service experience very seldom supported the test predictions [*49*]. A rotating cylinder within a cylinder electrode test system has been developed that operates under a defined hydrodynamics relationship (Figs. 11 and 12). The assumption is that if the rotating electrode operates at a shear stress comparable to that in plant geometry, the mechanism in the plant geometry may be modeled in the laboratory. Once the mechanism is de-

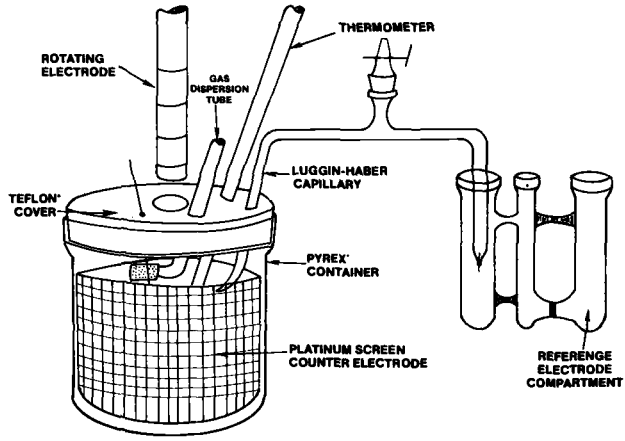


FIG. 11—*Rotating cylinder electrode apparatus.*

fined, the appropriate relationship between fluid flow rate and corrosion rate in the plant equipment as defined by the mechanism can be used to predict the expected corrosion rate. If fluid velocity does affect the corrosion rate, the degree of mass transfer control, if that is the controlling mechanism (as opposed to activation control), can be estimated. Conventional potentiodynamic polarization scans are conducted as described above. In other cases, the corrosion potential can be monitored at a constant velocity until steady state is attained. While the value of the final corrosion potential is virtually independent of velocity, the time to reach steady state may be dependent on velocity. The mass transfer control of the corrosion potential can be proportional to the velocity raised to its appropriate exponent. The rate of breakdown of a passive film is velocity sensitive.

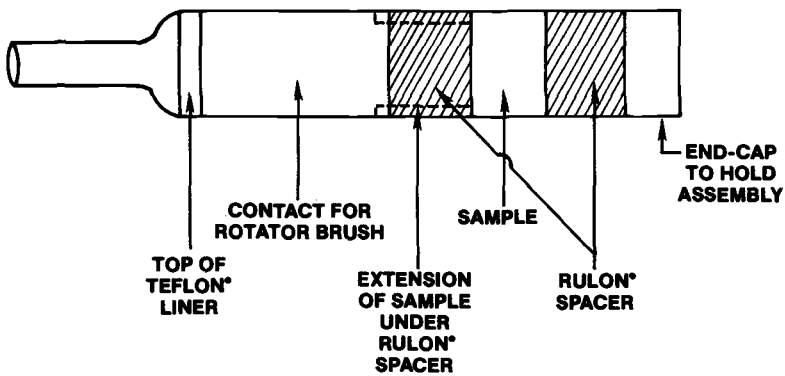


FIG. 12—*Inner rotating cylinder used in laboratory apparatus of Fig. 7.*

Environmental Cracking

The problem of environmental cracking of metals and their alloys is very important. Of all the failure mechanism tests, the test for stress corrosion cracking (SCC) is the most illusive. Stress corrosion is the acceleration of the rate of corrosion damage by static stress. SCC, the limiting case, is the spontaneous cracking that may result from combined effects of stress and corrosion. It is important to differentiate clearly between stress corrosion cracking and stress accelerated corrosion. Stress corrosion cracking is considered to be limited to cases in which no significant corrosion damage occurs in the absence of a corrosive environment; the material exhibits normal mechanical behavior under the influence of stress; before the development of a stress corrosion crack, there is little deterioration of strength and ductility. Stress corrosion cracking is the case of the interaction between chemical reaction and mechanical forces that results in structural failure (that otherwise would not occur). SCC is a type of brittle fracture of a normally ductile material by the interaction between specific environments and mechanical forces, for example, tensile stress [*50–52*]. Stress corrosion cracking is an incompletely understood corrosion phenomenon. Much research activity (aimed mostly at mechanisms) plus practical experience have allowed crude empirical guidelines, but these contain a large element of uncertainty. No single chemical, structural, or electrochemical test method has been found to respond with enough (consistent) reproducibility to known crack-causing environmental/stressed metal systems to justify a high confidence level.

As was cited in the case of immersion testing, most SCC test work is accomplished using mechanical, nonelectrochemical methods. It has been estimated that 90% of all SCC testing is handled by one of the following methods: (1) constant strain, (2) constant load, or (3) precracked specimens. In the constant strain method, the specimen is stretched or bent to a fixed position at the start of the test. The most common shape of the specimens used for constant strain testing is the U-bend, hairpin, or horseshoe type. A bolt is placed through holes in the legs of the specimen, and it is loaded by tightening a nut on the bolt. In some cases, the stress may be reduced during the test as a result of creep. In the constant load test the specimen is supported horizontally at each end and is loaded vertically downward at one or two points and has maximum stress over a substantial length or area of the specimen. The load applied is a predetermined, fixed dead weight. Specimens used in either of these tests may be precracked to assign a stress level or a desired location for fracture to occur or both as is used in fracture mechanics studies. These tensile stressed specimens are then exposed in situ to the environment of study.

Slow Strain Rate Test

In its present state of development, the results from slow strain-rate tests (SSRT) with electrochemical monitoring are not always completely definitive; but, for a short-term test, they do provide considerable useful SCC information.

Work in our laboratory shows that the SSRT with electrochemical monitoring and the U-bend tests are essentially equivalent in sensitivity in finding SCC. The SSRT is more versatile and faster, providing both mechanical and electrochemical feedback during testing [*3,14,41*].

The SSRT is a test technique where a tension specimen is slowly loaded in a test frame to failure under prescribed test conditions. The normal test extension rates are from 2.54×10^{-7} to 2.54×10^{-10} m/s (10^{-5} to 10^{-8} in./s). Failure times usually occur in one to ten days. The failure mode will be either SCC or tensile overload sometimes accelerated by corrosion. An advantage behind the SSRT, compared to constant strain tests, is that the protective surface film is thought to be ruptured mechanically during the test, thus giving SCC an opportunity to progress. To aid in the selection of the value of the potential at which the metal is most sensitive to SCC that can be applied to accelerate SSRT, potentiodynamic polarization scans are conducted as described above. It is common for the potential to be monitored during the conduct of the SSRT. The strain rates that generate SCC in various metals are reported in the literature [*3,14,17,41,53*]. There are several disadvantages to the SSRT. First, indications of failure are not generally observed until the tension specimen is plastically stressed, sometimes significantly, above the yield strength of the metal. Such high stressed conditions can be an order of magnitude higher than the intended operating stress conditions. Second, crack initiation must occur fairly rapidly to have sufficient crack growth that can be detected using the SSRT. The occurrence of SCC in metals requiring long initiation times may go undetected [*15,34,35*].

Modulus Measurements

A relatively new SCC test technique is the use of changes of modulus as a measure of the damping capacity of a metal. It is known that a sample of a given test material containing cracks will have a lower effective modulus than does a sample of identical material free of cracks. The technique provides a rapid and reliable evaluation of the susceptability of a sample material to SCC in a specific environment. The so-called internal friction test concept can also be used to detect and probe nucleation and progress of cracking, and the mechanisms controlling it.

The Young's modulus of the specimen is determined by accurately measuring its resonant frequency while driving it in a standing longitudinal wave configuration. A Marx composite piezoelectric oscillator is used to drive the specimen at a resonant frequency. The specimen is designed to permit measurements while undergoing applied stress and while exposed to an environmental test solution. The specimens are three half wavelengths long; the gripping nodes and solution cup are silver-soldered on at displacement nodes, so they do not interfere with the standing wave (Fig. 13). As discussed in SSRT above, potentiodynamic polarization scans are conducted to determine the potential that can be applied to accelerate the test procedure. Again, the potential can be monitored during a

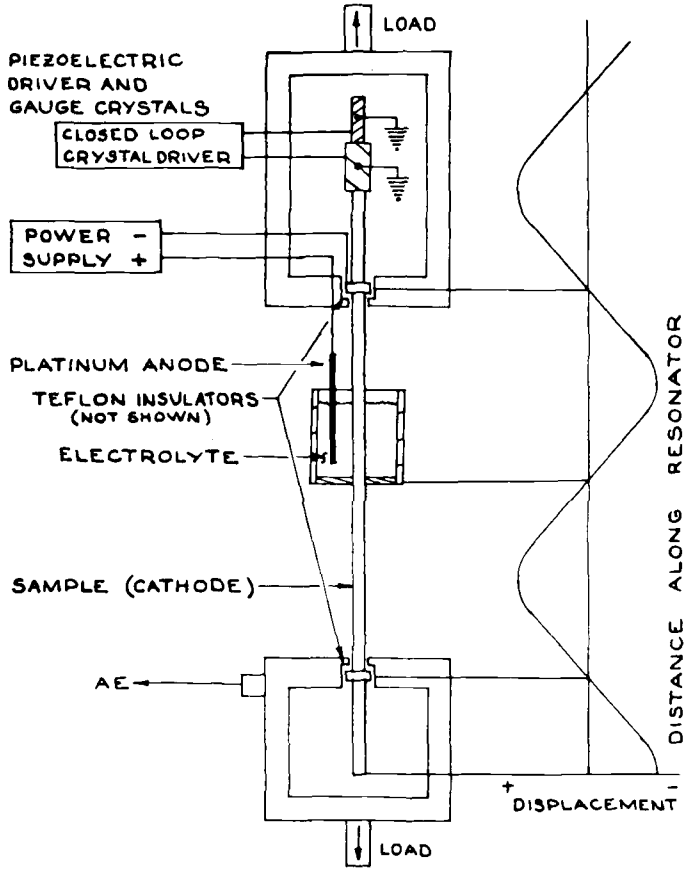


FIG. 13—*Equipment for measuring internal friction (modulus) changes during in situ tensile exposure of a metal in a corrosive environment.*

retest as is the acoustic emission (AE) as an indicator of nucleation and progress of cracking [*54*].

Conjunctive Use of Slow- and Rapid-Scan Polarization

The use of the methods discussed above requires a knowledge of the likely potential range for SCC to occur. Potentiodynamic polarization curves can be used to predict those SCC sensitive potential ranges. The technique involves conducting both slow- and rapid-scan sweeps in the anodic direction of a range of potentials. Comparison of the two curves will indicate any ranges of potential within which high anodic activity in the film-free condition reduces to insignificant activity when the time requirements for film formation are met. This should indicate the range of potentials within which SCC is likely. Most of the SCC theories presently in vogue predict these domains of behavior to be between the primary passive potential and the onset of passivity. This technique shortens the search for that SCC potential [*17,53*].

Separated Anode-Cathode

Realizing, as noted above, that localized corrosion is usually active to the surrounding metal surface, a stress specimen with a limited area exposed to the test solution (the anode) is electrically connected to an unstressed specimen (the cathode). A potentiostat, used as a zero resistance ammeter, is placed between the specimens for monitoring the galvanic current. It is possible to approximately correlate the galvanic current I_g and potential to crack initiation and propagation, and eventually catastrophic failure. By this arrangement, the galvanic current I_g is independent of the cathode area. In other words, the potential of the anode follows the corrosion potential of the cathode during the test. The SSRT apparatus discussed above may be used for tensile loading [*55,56*].

AC Impedance

Electrode surfaces in electrolytes generally possess a surface charge that is balanced by an ion accumulation in the adjacent solution thus making the system electrically neutral. The first component is a double layer created by a charge difference between the electrode surface and the adjacent molecular layer in the fluid. Electrode surfaces may behave at any given frequency as a network of resistive and capacitive elements from which an electrical impedance may be measured and analyzed. The application of an impressed alternating current on a metal specimen can generate information on the state of the surface of the specimen. The corrosion behavior of the surface of an electrode is related to the way in which that surface responds to this electrochemical circuit. The AC impedance technique involves the application of a small sinusoidal voltage across this circuit. The frequency of that alternating signal is varied. The voltage and current response of the system are measured.

The so-called white-noise analysis by the Fast Fourier transform technique (FFT) is another viable method. The entire spectrum can be derived from one signal. The impedance components thus generated are plotted on either a Nyquist (real versus imaginary) or Bode (log real versus log frequency plus log phase angle versus log frequency) plot. These data are analyzed by computer; they can be used to determine the polarization resistance and thus the corrosion rate if Tafel slopes are known. It is also thought that the technique can be used to monitor corrosion by examining the real resistance at high and low frequency and by assuming the difference is the polarization resistance. This can be done in low and high conductivity environments. Systems prone to suffer localized corrosion have been proposed to be analyzed by A/C impedance and should aid in determining the optimum scan rate for potentiodynamic scans [*8,57–62*].

The use of impedance electrochemical techniques to study corrosion mechanisms and to determine corrosion rates is an emerging technology. Electrode impedance measurements have not been widely used largely because of the sophisticated electrical equipment required to make these measurements. Recent advantages in microelectronics/computers has moved this technique almost overnight from being an academic experimental investigation of the concept itself to

one of shelf-item commercial hardware and computer software, available to industrial corrosion laboratories.

References

[1] Dillon, C. P., draft proposal, National Association of Corrosion Engineers, Education Course 3, National Association of Corrosion Engineers, Houston, TX, 1972.

[2] Diegle, R. B., "Application of Polarization Techniques in Corrosion Studies," National Association of Corrosion Engineers North Central Region, Conference, Cincinatti, 26 Oct. 1976.

[3] Siebert, O. W., Paper 66, 153 Meeting, The Electrochemical Society, Seattle, WA, 23 May 1978.

[4] Pourbaix, M., *Thermodynamics of Dilute Aqueous Solutions*. Arnold, London, 1949.

[5] Silverman, D. C., *Corrosion*, Vol. 37, No. 9, 1981, p. 546.

[6] Silverman, D. C., *Corrosion*, Vol. 38, No. 8, 1982, p. 453.

[7] Silverman, D. C., *Corrosion*, Vol. 38, No. 10, 1982, p. 541.

[8] Dean, S. W., France, W. D., and Ketcham, S. J., *Handbook on Corrosion Testing and Evaluation*, Wiley, New York, 1971, pp. 171–215.

[9] Liening, E. L. *CORROSION/76*, Paper 38, National Association of Corrosion Engineers, Houston, TX, March 1976.

[10] Liening, E. L., *CORROSION/79*, Paper 246, National Association of Corrosion Engineers, Houston, TX, 1979.

[11] Wilde, B. E., *Corrosion*, Vol. 28, No. 8, 1972, p. 283.

[12] Siebert, O. W., "A Phologiston Theory of Corrosion," Monsanto Report 729:1828–732, No. 1, St. Louis, MO, Oct. 1956, pp. 1–2.

[13] Dearnalay, G., *Corrosion*, Vol. 34, No. 1, 1978, pp. 20–29.

[14] Siebert, O. W., "The Alchemist Looks at Corrosion, AIChE Symposium 77, St. Louis, MO, 29 March 1977.

[15] Hackerman, N., "Sorption, Oxidation and Passivity," Passivity Symposium, National Association of Corrosion Engineers, Houston, TX, April 1962.

[16] Hickling, A., *Transactions of the Faraday Society*, Vol. 38, No. 1 1942, pp. 27–33.

[17] Parkins, R. N., *Corrosion Science*, Vol. 20, No. 2, 1980, pp. 147–166.

[18] Stoecker, J. G., Morris, P. E., and Siebert, O. W., *CORROSION/80*, Paper 76, National Association of Corrosion Engineers, Houston, TX, March 1980.

[19] Siebert, O. W., Stoecker, J. G., and Morris, P. E., *Materials Performance*, Vol. 22, No. 11, 1983, pp. 13–22.

[20] Edeleanu, C., *Metallurgica*, Vol. 50, No. 2, 1954, pp. 113–116.

[21] Edeleanu, C., *Nature*, Vol. 173, No. 4407, 1954, p. 739.

[22] Edeleanu, C. and Gibson, J. G., *Chemistry and Industry*, Vol. 9, No. 3, March 1961, pp. 301–308.

[23] Stern, M., *Journal of the Electrochemical Society*, Vol. 104, No. 56, 1957, pp. 559–563.

[24] Phelps, E. H., *Corrosion*, Vol. 18, No. 6, 1962, pp. 239t–246t.

[25] Greene, N. D., *Corrosion*, Vol. 18, No. 4, 1962, pp. 136t–142t.

[26] Martin, R. L., *Materials Performance*, Vol. 18, No. 3, March 1979, pp. 41–50.

[27] Bockris, J. O. M., "Overpotential, A Lacuna in Scientific Knowledge," *Journal of Chemical Education*, Vol. 48, No. 6, June 1971, pp. 352–358.

[28] Whitney, W. R., "The Corrosion of Iran," *Journal of the American Chemical Society*, Vol. 25, No. 4, 1903, pp. 394–406.

[29] Dean, S. W., National Association of Corrosion Engineers Conference, *CORROSION/76*, National Association of Corrosion Engineers, Houston, TX, March 1976, pp. 1–16.

[30] Stern, M., *Journal of the Electrochemical Society*, Vol. 104, Sept. 1957, pp. 559–563.

[31] Flade, F., *Zeitschrift Fuer Physikalisch Chemie*, Vol. 76, No. 5, May 1911, pp. 513–518.

[32] Weil, K. G., *Elektrochem*, Vol. 59, No. 7, 1955, pp. 711–715.

[33] International Kolloquiumuber die Passiviat der Metalle, *Zeitschift Fur Elecktrochemic Beriche Der Bunsenqesellschaft Fur Physikalische Chemie*, Vol. 62, No. 6/7, 1958, pp. 619–830.

[34] Evans, U. R., "Protective Films in Passivity," Passivity Symposium, National Association of Corrosion Engineers, Houston, TX, April 1962.

[35] Uhlig, H. H., "The Adsorption Theory of Passivity and the Flade Potential," Passivity Symposium, National Association of Corrosion Engineers, Houston, TX, April 1962.

[36] Greene, N. D., "Corrosion," National Association of Corrosion Engineers, Houston, TX, April, 1962, pp. 136t–142t.
[37] Kim, C. D. and Wilde, B. E., *Corrosion Science,* Vol. 10, No. 10, Oct. 1970, pp. 735–744.
[38] Morris, P. E. and Scarberry, R. C., *Corrosion,* Vol. 28, No. 12, 1972, p. 44.
[39] Morris, P. E. and Kain, R. M., *Chemical Engineering Progress,* Vol. 73, No. 6, 1977, p. 103.
[40] Scarberry, R. C., Hibner, E. L., and Crum, J. R., *CORROSION/79,* Paper 245, National Association of Corrosion Engineers, Houston, TX.
[41] Siebert, O. W., Golden Gate Metals and Welding Conference, San Francisco, CA, 23 January, 1981.
[42] Kain, R. M. and Morris, P. E., *CORROSION/76,* Paper 146, National Association of Corrosion Engineers, Houston, TX, March 1976.
[43] Morris, P. E., "Use of Rapid-Scan Potentiodynamic Techniques to Evaluate Pitting and Crevice Corrosion Resistance of Iron-Chromium-Nickel Alloys," *Galvanic and Pitting Corrosion—Field and Laboratory Studies, STP 576,* American Society for Testing and Materials, 1976, pp. 261–275.
[44] Palmer, J. D., *Canadian Chemical Processing,* Vol. 60, No. 8, 1976, pp. 35–39.
[45] Siebert, O. W., Materials Protection, Vol. 20, No. 2, 1981, pp. 38–43.
[46] Breeze, G. A. and Diegle, R. B., Materials Technology Institute, MTI Technical Report 3, "Electrochemical Monitoring of Occluded Cell Corrosion," March 1981.
[47] Diegle, R. B., *Materials Performance,* Vol. 21, No. 3, 1982, pp. 43–50.
[48] Streicher, M. A., *Materials Performance,* Vol. 22, No. 5, 1983, pp. 37–50.
[49] Siebert, O. W. and Engman, W. C., *Corrosion,* Vol. 20, No. 10, 1964, p. 0–24.
[50] Wille, M. G., Design Engineering Conference, American Society for Mechanical Engineers Paper 83-DE-14, 1982, pp. 1–5.
[51] Copson, H. R., *Corrosion,* Vol. 16, No. 2, 1960, pp. 86t–92t.
[52] Gabe, D. R., *Journal of Applied Electrochemistry,* Vol. 4, No. 1, 1974, pp. 91–108.
[53] Congleton, J., Parkins, R. N., and Shoji, T., *CORROSION/83,* Paper 126, National Association of Corrosion Engineers, Houston, TX, April 1983.
[54] Carpenter, S. H. and Siebert, O. W., *Corrosion,* Vol. 39, No. 3, 1983, pp. 103–107.
[55] Suzuki, T., Yamabe, M., and Kitamura, Y., *Corrosion,* Vol. 29, No. 2, 1973, pp. 70–74.
[56] Tong, H. S. and Swartz, D. J., *Journal of the Electrochemical Society,* Vol. 127, No. 1, 1980, pp. 31–36.
[57] Macdonald, D. D., *Journal of the Electrochemical Society,* Vol. 125, No. 9, 1978, pp. 1443–1449.
[58] Macdonald, D. D., *Journal of the Electrochemical Society,* Vol. 125, No. 12, 1978, pp. 2062–2064.
[59] Macdonald, D. D., *Journal of the Electrochemical Society,* Vol. 125, No. 12, 1978, pp. 1977–1981.
[60] Lorenz, W. J. and Mansfeld, F., *Corrosion Science,* Vol. 21, No. 9, 1981, p. 647.
[61] Mansfeld, F. and Kendig, M. W., *Corrosion,* Vol. 37, No. 9, 1981, pp. 545–546.
[62] Mansfeld, F. and Kendig, M. W., *CORROSION/83,* Paper 255, National Association of Corrosion Engineers, Houston, TX, April 1983.

DISCUSSION

M. Kendig[1] *(written discussion)*—Why does the potentiodynamic forward and reverse scan predict the optimum position for anodic protection in the example that you gave?

O. W. Siebert (author's response)—First off, I refer to the text of authors (Ref

[1]Rockwell International Science Center, Thousand Oaks, CA.
[2]W. R. Grace, CPD, 62 Whittemore Ave., Cambridge, MA 02140.

45) as well as similar information in Refs 39 and 42 and in "Anodic Protection of Mild Steel in Nitric Acid," by Sastry and Rao. *Corrosion*, Vol. 39, No. 2, Feb. 1983, pp. 55–60.

Considerable empirical data have been obtained by observation to support the reverse-scan low current region (LCR) as the optimum position for anodic protection. While little or no valid first-principle explanation is available to support the artificially induced conditions experienced during potentiodynamic polarization, regardless of scan rate, I have some thoughts. During the fast forward scan, the hydrogen that was generated maintained the cathodically cleaned metal surface before oxides could form any appreciable film. At the time of the rapid reverse scan, copious amounts of oxygen and metal ions, the raw materials for a passive film (if a passive film is possible), are available in the repassivation region. In conjunction with these raw materials, the repassivation potential in the region of the double layer, gives what amounts to be the optimum conditions of passivation. If both the forward and reverse scans are conducted too slowly, most of the components needed for passivation have been depleted; you are looking at an oxide in-place. This observation seems to support the conclusion of Staehle when he noted that passive films most likely would cause the excess oxygen and metal ions to thermodynamically form in the region of the double layer with the application of cathodic currents.

N. S. Berke (written discussion)—Do potentiostatic measurements at different potentials support the smaller anodic protection region determined by your rapid scan technique for H_2SO_4 solns?

O. W. Siebert (author's response)—Yes. The data in the text and on Table 2 and on Figs. 3 and 4 of author's Ref *45* as well as similar information in Refs *39* and *42*.

Tero Hakkarainen[1]

A Method to Avoid Crevice Corrosion in Electrochemical Determination of Pitting Potentials

REFERENCE: Hakkarainen, T., **"A Method to Avoid Crevice Corrosion in Electrochemical Determination of Pitting Potentials,"** *Laboratory Corrosion Tests and Standards, ASTM STP 866*, G. S. Haynes and R. Baboian, Eds., American Society for Testing and Materials, Philadelphia, 1985, pp. 91–107.

ABSTRACT: A test arrangement is described, where the electrolyte is brought into contact with the test surface along a multilayered textile tape. This method brings several advantages when compared to the common specimen holders, where part of the specimen surface is masked off by some insulating material. In the absence of crevices, there is no crevice corrosion. No special pretreatment of the test surface is required. Thus, various surface conditions can be tested, including as-received surfaces. The test surface need not be planar. Specimens like bars or weld beads can easily be tested. The desired surface can be selected for the test. The spatial orientation of the test surface can be chosen deliberately. The shape and size of the specimen can vary greatly, which makes the specimen preparation in most cases extremely easy.

The possible uses of the method are demonstrated by room temperature testing of stainless steel sheets and welds in sodium chloride solutions, as well as testing of prestressing steel wire in a saturated calcium hydroxide solution with various concentrations of sodium chloride. Both pit nucleation and repassivation potentials are determined using potentiokinetic techniques. The effects of some experimental variables are studied and discussed.

KEY WORDS: corrosion, pitting, electrochemistry, anodic polarization, corrosion tests, stainless steels, concentration cell corrosion

The pitting susceptibility of metals and alloys is often determined by measuring the critical pitting potentials, that is, the pit nucleation potential or the pit repassivation potential or both [*1–5*]. This approach is especially widely used in the case of stainless steels. In making the electrochemical measurements, however, the interference of crevice corrosion is often a major problem. Crevices are formed, when part of the specimen surface is masked off by some insulating material.

To avoid crevices, specimen mountings are sometimes used, where all immersed surfaces of the specimen are exposed to the electrolyte [*6–8*]. This may however lead to other undesired effects. First, the exposed surfaces necessarily

[1] Research professor, Technical Research Centre of Finland (VTT), Metallurgy Laboratory, SF-02150 Espoo 15, Finland 0-4561.

Copyright© 1985 by ASTM International www.astm.org

include transverse sections that may be more susceptible to pitting than the sheet, tube, or bar surface [6]. The latter, in fact, should usually be the only object of the study. Second, in some of these methods the orientation of the exposed surfaces is restricted to exclude upward surfaces [7,8].

If the results of electrochemical pitting potential measurements are to be used to determine the behavior of a material or a component with a given surface treatment in a given environment, the preparation of the test surface becomes important. The pretreatment may have a strong effect on the pit nucleation potential [6]. In the commonly used specimen mountings, factors like modifications of surface composition caused by, for example, pickling or welding are difficult, if not impossible, to take into account.

The use of laboratory pitting potential measurements to predict the behavior of a given component in a specific environment poses certain requirements for the test method. Undesired crevice corrosion has to be eliminated, there must be a possibility of testing as-received surfaces, and only such surfaces must be exposed that will be exposed in practical applications. In this paper a test arrangement is described that satisfies these requirements.

Test Arrangement

Principle

In the test arrangement the electrolyte is brought into contact with the specimen surface with the aid of a textile tape (Fig. 1). The electrolyte is made to flow slowly from one beaker to another along a multilayered textile tape ("narrow fabric," 100% cotton). A section of the wet tape is pressed against the specimen surface. Only the area wetted by the tape is exposed to the electrolyte. No artificial masking of other parts of the specimen is needed. The test area is covered by a counter electrode of equal size on the opposite side of the tapes.

An electrolytic connection is made along another textile tape to the reference

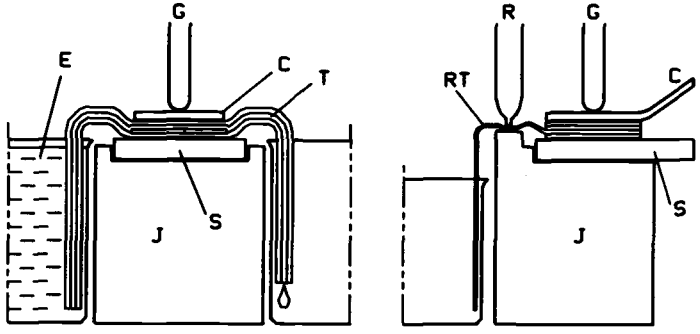


FIG. 1—*Principle of tape test arrangement. Two mutually perpendicular sections.* S *is specimen,* T *is multiple textile tape,* RT *is tape to reference electrode,* R *is reference electrode,* C *is counter electrode,* G *is glass rod,* E *is electrolyte, and* J *is jig.*

electrode, the tip of which can simply be pressed against the tape. One end of this tape lies between the flow-tape layers close to the specimen surface. To avoid concentration of electrolyte by evaporation and possible flow of solution from the reference electrode to the specimen surface, the electrolyte is made to flow along this tape down to another beaker.

The electrolyte level in the full beaker has to be kept lower than the test surface, otherwise a growing pool of electrolyte may form on the specimen surface. By adjusting the levels of the electrolyte and the free end of the tape, the flow rate of the electrolyte can be controlled to some extent. In the experiments of this paper, a triple tape was used. The flow rate of the electrolyte was of the order of 0.1 mm/s.

Modifications

Planar Surfaces—The most straightforward application of the method is the testing of sheet or other planar surfaces. The size of the test area may easily be varied by varying the width of the tape. Guide supports for the tape and specimen may be used to facilitate the placing of the tape onto the surface (Figs. 1 and 2). Surfaces facing downwards can be tested as easily as those facing upwards. In the former case the specimen is pressed against the tape from above.

Nonplanar Surfaces—The counter electrode, for example, a stainless steel strip, can easily be shaped to match nonplanar specimen surfaces, such as bars or weld beads. In the case of the cylindrical outer surfaces of small diameter tubes or rods, the counter electrode may be shaped to hold the tape on the specimen surface (Fig. 3).

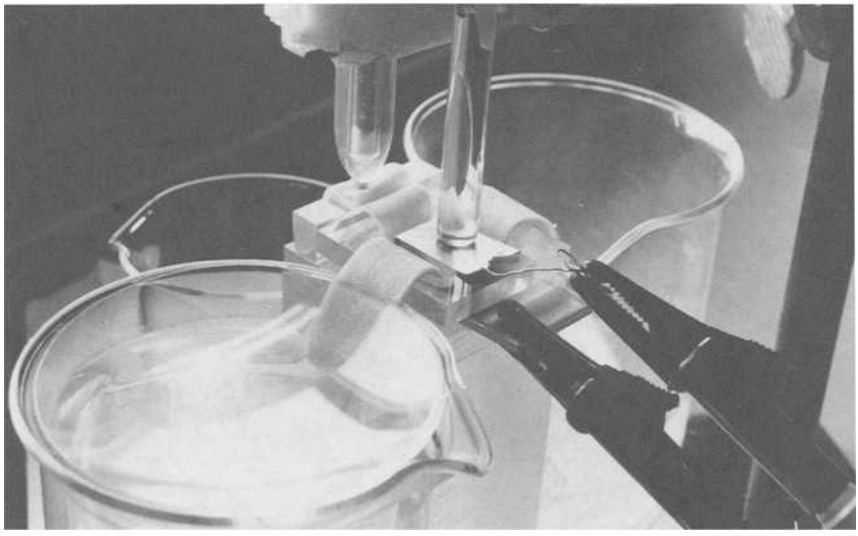


FIG. 2—*View of tape test arrangement for testing pieces of plate.*

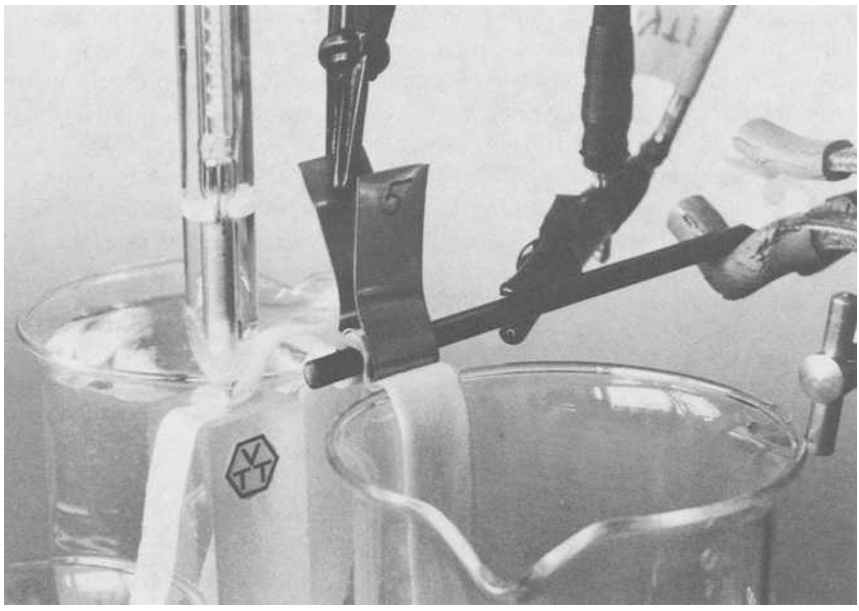


FIG. 3—*View of tape test arrangement for testing of small diameter rods.*

Transverse Sections—Transverse sections with small dimensions, for example, cross sections of plates, can also be tested by simply pressing the desired surface against the tape. If the test area extends to the edge of the surface, possible preferential attack there has to be checked by examining the specimen after the test.

Experiments and Results

The effects of various factors were studied mainly on an austenitic stainless steel sheet. Some experiments were also made on weld joints of a ferritic stainless steel as well as on a prestressing steel wire to be used in concrete.

Stainless Steel Plates

Test Material—The experiments were made using a 2-mm-thick sheet of type AISI 304 (Unified Numbering System [UNI] S30403) stainless steel. The chemical composition of this steel is shown in Table 1.

TABLE 1—*Chemical composition of the stainless steel plates used, % by weight.*

C	Si	Mn	S	P	Cr	Ni	Mo	Cu	Co	Iron
0.04	0.54	2.0	0.016	0.033	18.5	9.7	0.10	0.30	0.05	balance

The surface treatment of the as-received sheet was finish 2B (cold rolled, annealed, pickled, and lightly rolled on polished rolls). When testing as-received surfaces, the specimens were only degreased.

Measuring Procedures—Cyclic potentiokinetic tests were used in the experiments. The potential was swept either continuously or in 1-mV steps from the open circuit potential towards more noble values until a certain value of external current was reached, usually 1 mA. Here the potential scan direction was reversed. The experiment was stopped when the external current decreased below 1 μA. To prevent excessive growth of the current close to the potential of scan reversal, a two to ten times higher scan rate was usually applied as long as the current exceeded the "reversal value."

Another procedure was to stop the potential scan at fixed potentials for fixed periods in order to give the experiments a semipotentiostatic nature.

The electrolytes were primarily 0.1 or 0.5*M* sodium chloride solutions. At least a few millilitres of electrolyte were allowed to flow through the tape to the empty beaker before the experiments were started. All tests were made at room temperature. No attempts were made to exclude air from the solutions. The test area was 1.5 by 1.5 cm.

Before the use in pitting tests, the tapes were immersed for several hours in boiling distilled water in order to remove any soluble impurities. After the tests, solid corrosion products were dissolved from the tapes by prolonged immersion into oxalic acid or hydrochloric acid, and the tapes were carefully rinsed.

Distribution and Type of Attack—Pits were found to form randomly over the whole test surface with no preference to the border lines of the exposed area. After a single test with potential scan reversal at 1 mA, the number of pits was typically five to ten in all environments. Both an increased current value at potential scan reversal and multiple tests on the same surface led to an increased number of pits (Fig. 4). The form of attack was sharply defined pits. On surfaces

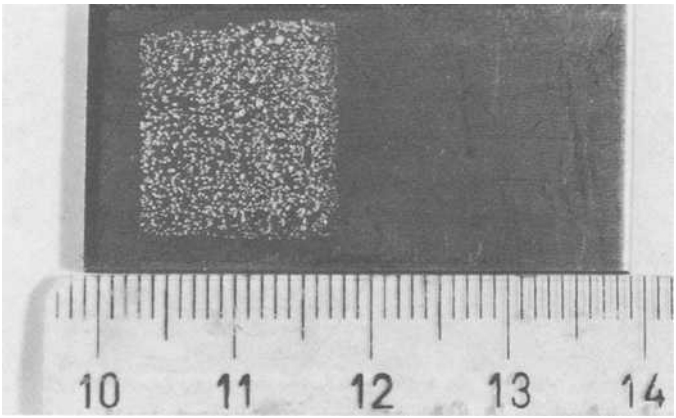


FIG. 4—*Distribution of pits after multiple testing of a type AISI 304 stainless steel plate. The surface was facing downwards during the tests.*

facing upwards, the pits tended to be "closed," that is, with only small openings to the free surface. On surfaces facing downwards, "open" pits predominated, that is, the diameter of the pit opening at the surface was about the same as the pit diameter.

Reproducibility—The reproducibility of the test results was studied both by making multiple tests on the same specimen and by repeating the tests on new specimens. In the former case, the tape was not removed from the test surface between the tests. In multiple tests on the same surface, almost identical results were usually obtained (Fig. 5). In similar tests on several specimens, the scatter of both pit nucleation and pit repassivation potentials was generally less than 50 mV.

Potential Scan Rates—To study the effects of potential scan rates, experiments were made at rates ranging from 0.02 to 2 mV/s (1.2 to 120 mV/min) in the pit nucleation and repassivation regions. Typical results are shown in Fig. 6. The differences in pit nucleation potentials were generally within the scatter of individual test results, with perhaps a slight tendency to higher potentials at higher scan rates. The slope of current increase versus potential increase was generally higher at lower scan rates. The pit repassivation potential of upward surfaces was shifted towards lower values when the potential scan rate was decreased.

In the experiments, where the potential scan was stopped for 10 to 20 min at 50-mV intervals, both the pit nucleation and pit repassivation potentials were essentially the same as in the experiments with a continuous potential scan.

Pretreatment of Test Surface—The effects of three different surface treatments on the test results are shown in Fig. 7. In the case of ground or pickled surfaces, the open circuit potential was initially several hundreds of millivolts lower than that of as-received surfaces. If the test was started not too long after the exposure

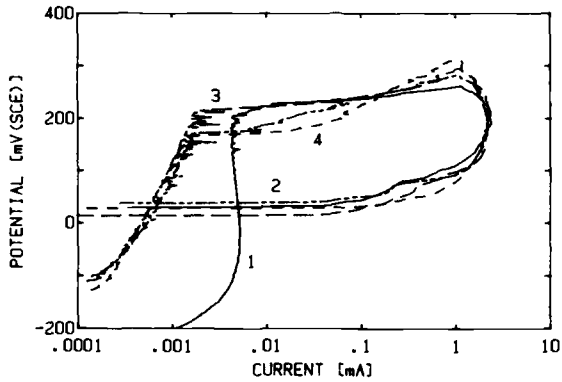


FIG. 5—*Results of four successive tests on the same specimen surface using the tape method. Type AISI 304 stainless steel, 0.5M sodium chloride. Scan rate 0.5 mV/s below and 1 mV/s above 1mA. Upward surface, wet ground to 600 grit. Periods at open circuit potential between the tests were about 25 min. Figures indicate the number of test.*

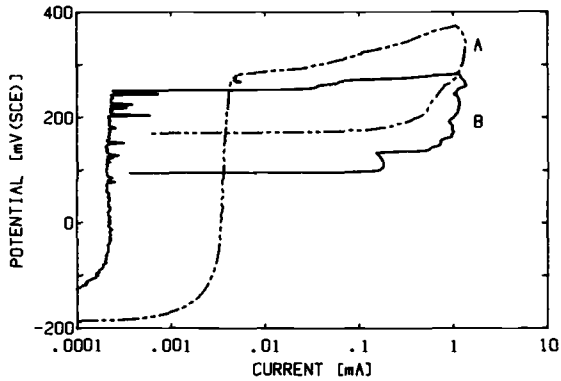


FIG. 6—*Example of the effect of scan rate on the pitting potentials of AISI 304 stainless steel plate in 0.1*M *sodium chloride solution. Upward surfaces, wet ground to 600 grit.* A: *scan rate 0.5 mV/s below and 1 mV/s above 1 mA.* B: *scan rate 0.02 mV/s below and 0.2 mV/s above 1 mA.*

of the surface to the electrolyte and if the potential scan rate was not too low, the current levels before pit initiation were substantially higher than those of as-received or passivated surfaces. Prolonged immersion before starting the test resulted in both higher open circuit potentials and lower prepitting currents. A low current was also observed at very low scan rates (Fig. 6). On surfaces passivated in nitric acid after grinding, pit nucleation potentials of 500 to 600 mV versus saturated calomel electrode (SCE) were observed in 0.1*M* sodium chloride.

Orientation of Test Surface—The pit nucleation potential values measured on surfaces facing downwards were equal to those measured on surfaces facing upwards. At high scan rates, 0.5 mV/s or more, the repassivation potentials were about equal in the two cases. At lowering scan rates, however, the repas-

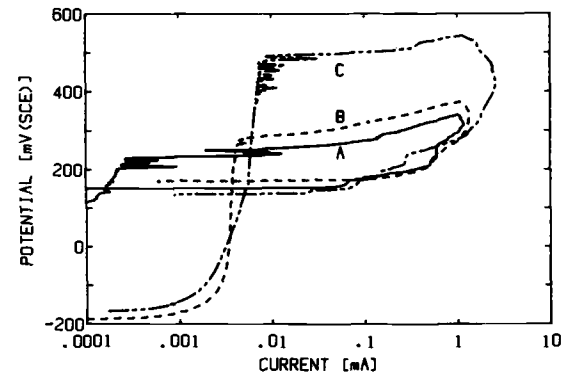


FIG. 7—*Examples of the effect of surface pretreatment on pitting potentials of AISI 304 steel in 0.1*M *sodium chloride solution. Upward surfaces, scan rate 0.5 mV/s below and 1 mV/s above 1 mA.* A: *as-received surface.* B: *surface wet ground to 600 grit.* C: *pickled in hydrochloric acid after grinding.*

sivation potential on downward surfaces was shifted towards higher values and the hysteresis loop became narrower. For surfaces facing upwards, the opposite behavior was observed.

Electrolyte Levels—The sensitivity of test results to variations in electrolyte flow rates in the tape was investigated by adjusting the electrolyte levels in the two beakers to various heights with respect to the test surface. By doing this, the flow rate of the electrolyte in the tape at the specimen surface was varied in the range of 0.03 to 0.5 mm/s. These variations in the flow rate had no effect on the results.

If the electrolyte flow was completely stopped by raising the free ends of the tapes above the electrolyte level in the full beaker, the current in the pit growth range was rapidly increased to values over one order of magnitude higher than those in a flowing electrolyte. Nevertheless, the potential values of pit nucleation and repassivation were not changed.

Apart from the above experiments, the most elevated part of the tape was usually about 2 cm above and the free end of the tape about 7 cm below the electrolyte level in the full beaker. This resulted in an electrolyte flow rate of about 0.1 mm/s at the specimen surface.

Electrolyte Composition—The dependence of both pit nucleation and pit repassivation potentials were investigated in the range of 0.005 to 2*M* sodium chloride (Fig. 8).

To find out whether significant changes in the composition or pH of the bulk solution at the specimen surface occur during the tests, cation contents and pH values were determined from the tape layer in contact with the test surface after interrupted pitting tests in 0.5*M* sodium chloride. The cation content measurements were made by atomic absorption spectroscopy from a solution obtained by immersing the tape section (1.5 by 1.5 cm) in 10 mL of 0.5*M* hydrochloric acid for 1 h. In the pH measurements the tape section was pressed against a pH indicator paper.

After 30-min constant potential polarization in the passive region (+110 mV [SCE], very low external current, no pitting) the pH value and the sodium content in the solution in the tape were the same as those in the original solution (6.8 and 0.5*M*, respectively). Insignificant values only were obtained for the iron ($8 \times 10^{-5}M$), chromium ($2 \times 10^{-5}M$), and nickel ($3 \times 10^{-5}M$) contents.

When an "ordinary" test (for example, see Fig. 5) was interrupted in its final stage (current 0.5 mA) and the tape section was immediately removed for analysis, the following cation contents in the tape solution were obtained: sodium 0.5*M*, iron $7.5 \times 10^{-4}M$, chromium $2 \times 10^{-4}M$, and nickel $3 \times 10^{-4}M$. The pH indicator paper showed no change in the pH value as compared with the original solution. On the other hand, at the edge of the counter electrode a pH value of about 12 was measured.

After a long period with an exceptionally high current (3 to 3.5 mA for 20 min), the following cation contents were obtained for the tape solution: sodium 0.42*M*, iron $25 \times 10^{-3}M$, chromium $7 \times 10^{-3}M$, and nickel $3.5 \times 10^{-3}M$.

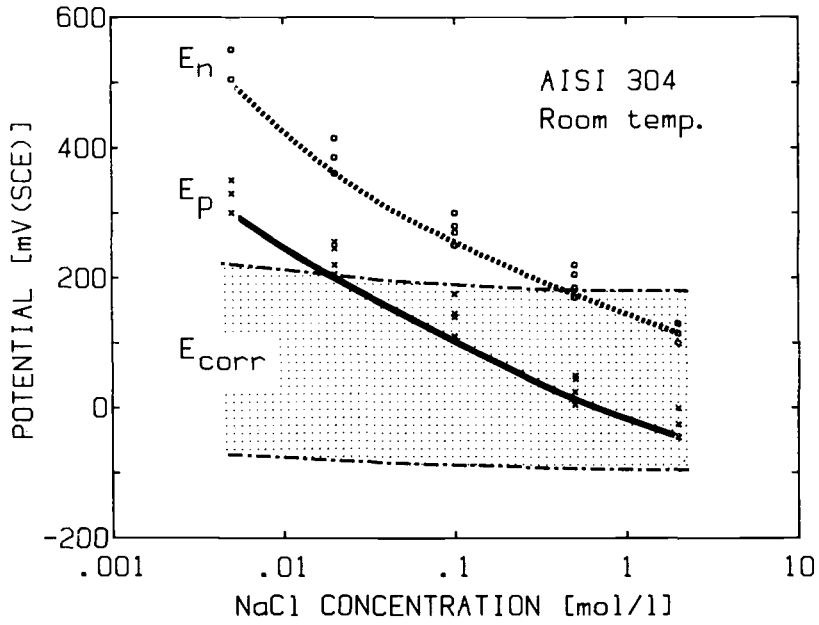


FIG. 8—*The dependence of critical potentials of pitting on the concentration of sodium chloride solution, as determined by the tape method. Type AISI 304 stainless steel, as-received surfaces, scan rate 0.5 mV/s below and 1mV/s above 1 mA.* E_n*: pit nucleation potential.* E_p*: pit repassivation potential.* E_{corr}*: open circuit potential region.*

After a similar test at somewhat lower current (1.5 mA for 20 min), the pH indicator paper showed no major overall change in pH, but locally values around 4 were observed at areas that had been close to the largest pits. Again, pH values of about 12 were measured at the counter electrode.

Discoloration caused by corrosion products was generally observed after the test in the intermediate tape layers between the working and counter electrodes, but not in the tape layers that had been in contact with the electrode surfaces during the test. During long tests, this discoloration was gradually spread to the surface layers of the tape, away from the test specimen in the electrolyte flow direction.

Comparison to Other Specimen Holders—For comparison, some experiments were made by using immersed test specimens and two different "conventional" specimen holders. In one of these, the sheet specimen was mounted in synthetic resin, the surface to be exposed was wet ground, and its border lines were masked off with a chemically resistant lacquer. The other one was a polytetrafluoroethylene (PTFE) holder, where the test area was bordered by a circular PTFE gasket pressed tightly against the sheet surface.

In these experiments, the apparent pit nucleation potentials varied from ones close to those obtained with the tape method to values considerably lower (Figs. 9 and 10). The "repassivation potentials" were invariably much lower than those

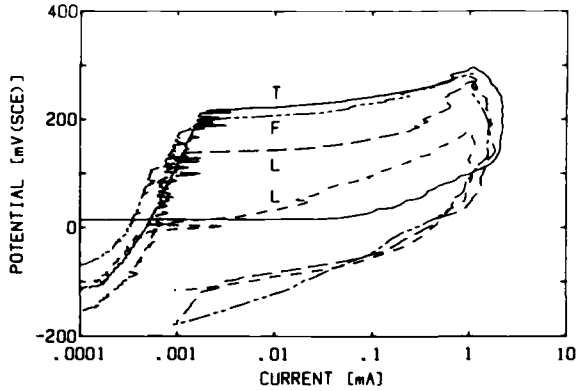


FIG. 9—*Examples of test results with various specimen holders. Type AISI 304 stainless steel, 0.5M sodium chloride, surfaces wet ground to 600 grit. Scan rate 0.5 mV/s below and 1 mV/min above 1 mA.* T: *tape method.* L: *immersed specimen test area bordered by lacquer.* F: *immersed specimen test area bordered by a PTFE gasket pressed against the surface.*

obtained with the tape method. Also no sharp repassivation at a specific potential was observed, but the current decreased gradually with lowering potential.

In all cases, the main attack occurred at the border lines of the test area, partly under the lacquer or the PTFE ring. At the border lines, deep attack typical of pitting was observed, but the attacked regions extended to the crevice as shallow ones, typical of crevice corrosion.

Stainless Steel Welds

The applicability of the tape test method to testing of the pitting susceptibility of as-welded joints was studied by experiments on a welded 18/2-type low-interstitial ferritic stainless steel.

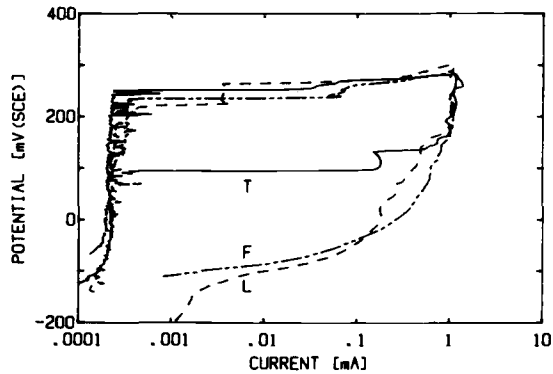


FIG. 10—*Examples of slow scan test results with various specimen holders. Type AISI 304 stainless steel, 0.1M sodium chloride surfaces wet ground to 600 grit. Scan rate 0.02 mV/s below and 0.2 mV/s above 1 mA.* T: *tape method.* L: *immersed specimen, test area bordered by lacquer.* F: *immersed specimen, test area bordered by a PTFE gasket pressed against the surface.*

TABLE 2—*Chemical composition of the stainless steel welds used, % by weight.*

C	Si	Mn	S	P	Cr	Ni	Mo	V	Ti	Iron
0.02	0.21	0.38	0.007	0.025	18.5	0.20	2.1	0.1	0.35	balance

Test Material—The chemical composition of the 2-mm-thick steel sheet used is shown in Table 2.

The specimen had been welded in hot arc conditions using a root support of copper and a shield gas of argon + 2% carbon dioxide. The filler wire was high alloy austenitic stainless steel (chromium 22%, nickel 15%, and molybdenum 3%.

In the electrochemical tests, the specimen surface was in the as-welded state. The only cleaning operations made were rinsing with water and alcohol. As a result of welding, both the weld bead and the heat affected zone had been slightly oxidized.

Tests—In the tests on the weld joint, the area exposed was about 1.5 by 1.5 cm and extended from the centerline of the weld bead to the base material unaffected by welding. Test results are shown in Fig. 11. Other experiments on welds of the same kind [*9*] have shown that at potential scan rates that are too high, the effect of pitting may initially be fully masked by some other transient oxidation process.

After the two successive anodic polarization experiments on the weld joint, pits typical of stainless steel were observed mainly in the weld bead close to the fusion line. Small hemispherical pits and partial brightening of the surface were observed in the heat affected zone in areas, which obviously had been covered by an oxide layer during the test.

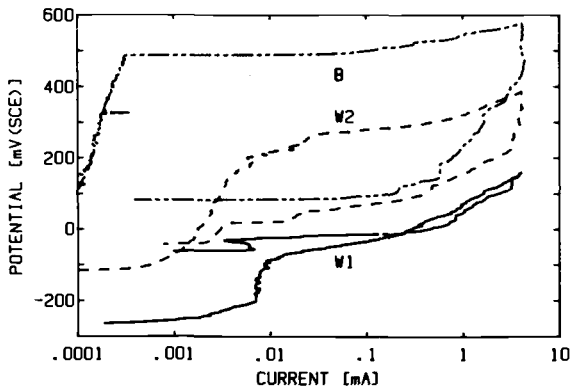


FIG. 11—*Cyclic anodic polarization curves for the base metal and the weld joint of a 18/2-type ferritic stainless steel in 0.5*M *sodium chloride.* B: *base metal, scan rate 0.2 mV/s below and 1 mV/s above 4 mA.* W1: *weld joint, scan rate 0.02 mV/s below and 0.5 mV/s above 4 mA.* W2: *test on the same area as W1, without removing the tape, scan rate 0.2 mV/s below and 1 mV/s above 1 mA.*

TABLE 3—*Chemical composition of the prestressing steel used, % by weight.*

C	Si	Mn	S	P	Cr	Ni	Mo	Cu	Al	As	Iron
0.75	0.30	0.74	0.024	0.020	0.02	0.05	0.01	0.05	0.06	0.06	balance

Prestressing Steel

Localized corrosion caused by chloride ions in an environment simulating that of steels embedded in concrete was studied by experiments in saturated calcium hydroxide solutions with various contents of sodium chloride.

Test Material—The test material was a prestressing wire of 5 mm diameter. The chemical composition of the steel used is shown in Table 3.

The wire was in the as-received state. The surface was only degreased with alcohol before testing.

Tests—The experiments were made using the test arrangement shown in Fig. 3. Examples of the results are shown in Fig. 12. The type of attack differed from that in the experiments on stainless steels described above. The areas attacked in the solutions containing chloride were again sharply defined, but they were fully open to the surface and had a very small depth to diameter ratio.

Discussion

Features of Tape Test Method

Types of Attack—One might suppose that in pitting conditions of stainless steel the attack under the tape would be a form of crevice corrosion, similar to that under deposits, rather than proper pitting. There is however an important difference between these two cases. In the tape arrangement, the electrolyte

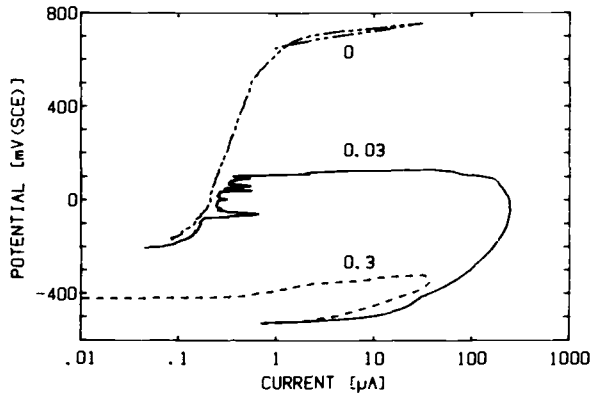


FIG. 12—*Cyclic anodic polarization curves of prestressing steel wire in a saturated calcium hydroxide solution with various contents of sodium chloride. The molarity of solution with respect to sodium chloride is given by the figures at the curves.*

flows along the specimen surface, thus preventing any macroscopic accumulation of ions on the unattacked surface. Sharply defined "proper" pits is also the form of attack that is observed after testing clean surfaces. Also, the rapid final decrease of the current, as is observed in the tests on surfaces with no deposits (Figs. 5 through 7), is typical of pitting but not of crevice corrosion (Figs. 9 and 10).

If there is on the surface a solid layer, such as an oxide, crevice corrosion may of course occur in addition to or instead of pitting.

In the case of prestressing steel, both the form of attack and the repassivation behavior differed from those of stainless steel. The attack, although it was on relatively small, well defined areas, was not in the form of deep pits, but extended more along the surface. Also, the repassivation was not such a sudden process as in pitting of stainless steel (Figs. 5, 6, and 12). These differences are however considered to be a consequence of differences in the corrosion process, rather than a result of the test method.

In the highly alkaline test environment of the prestressing steel wire, solid corrosion products of iron hydroxides may be expected to be immediately deposited on the area attacked. With a true crevice thus formed, the corrosion behavior is also expected to show the features of crevice corrosion.

Bulk Electrolyte—The electrolyte volume at a time in the tape on the test surface is very small. Corrosion processes, both on the anode and on the cathode, may thus be expected to be able to change the properties of the effective bulk electrolyte. On the other hand, the flow of the solution brings continuously fresh electrolyte to the "cell."

In the experiments described above, the electrolyte volume between the anode and the cathode was about 0.5 mL. The flow rate corresponded to a complete renewal of the electrolyte in about 2 min. During this time, a total corrosion current of 1 mA on the surface should be able to increase the ferrous ion content of the solution to about 1.5×10^{-3} mol/L. The measurements reported above indeed showed cation concentrations of this order of magnitude, but no major changes in the pH at the test surface. It is thus concluded that the electrochemical conditions at the specimen surface have not been significantly changed because of the restricted volume of electrolyte.

As the solubilities of the oxides and hydroxides of iron and other major constituents of stainless steels are very small, precipitation of solid corrosion products is expected. This is also observed, not at the specimen surface, however, but at the intermediate tape layers. The flow of electrolyte transports these corrosion products slowly away from the test area. In this process, the contents of soluble constituents in the electrolyte are not significantly changed.

Rapid general corrosion of the surface may of course lead to an accumulation of corrosion products close to the test surface and thus alter the electrochemical conditions.

Advantages of the Method—In the tape test method, crevice corrosion is avoided, unless the corrosion process itself produces the crevices, as seems to

have been the case in the experiments on the prestressing wire. The absence of crevice corrosion in electrochemical tests makes it possible to use very slow scan rates and to determine the repassivation potentials of pits by the cyclic anodic polarization procedure.

In addition to the elimination of crevice corrosion the test method offers several further advantages. No special pretreatment of the test surface is required. This enables one to test various surface conditions, including as-received surfaces or ones where the surface composition of the product has been modified by a manufacturing process, for example, welding.

The test surface need not be planar. Specimens like weld beads and rods can easily be tested. From a given product, the desired surface can be selected for testing. This may be important because in wrought products the transverse surfaces often have inferior pitting resistance. In practical applications such transverse surfaces of plates or tubes are rarely exposed to the environment.

The spatial orientation of the test surface can be chosen deliberately. Tests on surfaces facing upwards may be particularly important because these are the ones where pitting damage is most commonly encountered in practice.

The shape and size of the specimen may vary considerably. This makes the specimen preparation in most cases extremely easy.

Restrictions of the Method—If the solution is to be deaerated, special arrangements are needed. Deaeration is however necessary in exceptional cases only. In specimens of reasonable size, the total of cathodic currents caused by oxygen reduction at the pitting potentials is usually negligible compared to the total of anodic currents needed for pit formation and growth. Also, deaerated solutions may not be common in practical pitting conditions.

A more important restriction may be encountered, if tests are to be made at elevated temperatures. Evaporation of water at the border lines of the test area tends to increase the concentration of the solution there and may lead to a preferential attack in these areas.

Because the amount of electrolyte at the test surface is small, very intense anodic and cathodic reactions may lead to changes in the bulk electrolyte, as seen by the specimen. This may restrict the applicability of the test arrangement to studies of general corrosion.

Only very slow flow rates may be achieved in the tape. Thus, effects of significant flow rates cannot be investigated.

Effects of Test Variables

Potential Scan Rates—The pit nucleation potential on "clean" stainless steel surfaces seems to be fairly insensitive to the potential scan rate in potentiokinetic tests (Fig. 6). The main effect of the scan rate is that the increase of current in current versus potential presentation becomes steeper at lower scan rates. This is easily understood because the initial growth of pits and the increase of the anodic current requires time. If the changes of current are plotted against time, a similar behavior will be observed irrespective of the scan rate.

The apparent dependence of the pit repassivation potential on the scan rate may be due to differences in pit sizes rather than a direct consequence of different scan rates. In tests with lower scan rates the pits grow larger. Larger pits, in upward surfaces, are likely to repassivate at lower potentials, because transport of metal ions out of the pit becomes slower with increasing pit depths. When the repassivation potentials measured from different specimens are to be compared, the pit sizes, that is, the pit growth times, should be equal.

In tests on specimens with surface oxides, very low scan rates seem to be necessary. Transient oxidation processes may otherwise give rise to unrealistically low apparent pit nucleation potentials. In this case, higher pit nucleation potentials are obtained with lower scan rates.

Surface Condition—The preparation of the specimen surface may have a very strong effect on the value of pit nucleation potentials. Whether the surface is in an active or passive state seems not as such to be of great importance. In Fig. 7 the surface of the Specimen A has been passive and those of Specimens B and C have been active at the start of the test. The value of the pit nucleation potential is probably determined by the availability and nature of favorable nucleation sites, not by the general properties of the passive layer. On immersion in the electrolyte, a proper passive layer is gradually formed on initially active stainless steel surfaces in solutions containing chloride ions, as demonstrated by the polarization curves in Figs. 5 and 6.

Oxide layers on the specimen surface, either preexisting as on the weld joints, or formed during the test as on the prestressing wire, may change the character of the attack towards crevice corrosion.

Surface Orientation—It is generally agreed, that the solution inside growing pits in stainless steels is concentrated in metal chlorides [*10,11*]. Such solutions have a higher density (up to 1.5 g/cm^3 [*12*]) than the common bulk solutions. On downward surfaces, the pit solution tends to flow out of the pits, thus causing repassivation. This effect seems to be insignificant at small pit sizes, when the dissolution rate is high [*12*], but becomes more important when the pits grow larger. In tests at low scan rates, higher repassivation potentials were indeed observed on surfaces facing downwards than on those facing upwards. Even a vertical test surface may not be representative of the pit growth on a horizontal surface facing upwards.

Conclusions

Compared to the common test arrangements, where a rigid specimen holder is immersed in the electrolyte, the tape test method offers several advantages in the electrochemical determination of pit nucleation and repassivation potentials. It also allows great flexibility in the specimen preparation and may thus facilitate greatly the test procedure. Because as-received and nonplanar test surfaces may be studied, the tape test method may be used for the prediction of the performance of a given component in a given environment.

References

[1] Janik-Czachor, M., *Werkstoffe u. Korrosion*, Vol. 31, No. 8, Aug. 1980, pp. 606–610.
[2] Wilde, B. E., *Localized Corrosion*, National Association of Corrosion Engineers, Houston, 1974, pp. 342–350.
[3] Manning, P. E., *Corrosion*, Vol. 39, No. 3, March 1983, pp. 98–102.
[4] Herbsleb, G. and Schwenk, W., *Werkstoffe u. Korrosion*, Vol. 26, No. 1, Jan. 1975, pp. 5–18.
[5] Man, H. C. and Gabe, D. R., *Corrosion Science*, Vol. 21, No. 4, 1981, pp. 323–326.
[6] Manning, P. E., Duquette, D. J., and Savage, W. F., *Corrosion*, Vol. 35, No. 4, April 1979, pp. 151–157.
[7] Bernhardsson, S., Mellström, R., and Brox, B., *8th International Congress on Metallic Corrosion—Proceedings*, Deutsche Gesellschaft fuer Chemisches Apparatewesen, Frankfurt/Main, West Germany, 1981, pp. 1418–1423.
[8] Levlin, E., *9th Scandinavian Corrosion Congress—Proceedings*, Korrosionscentralen ATV, Glostrup, Denmark, 1983, pp. 31–42.
[9] Hakkarainen, T., *Third Scandinavian Symposium in Materials Science—Proceedings*, University of Oulu, Oulu, Finland, 1983, pp. 159–164.
[10] Suzuki, T., Yamabe, M., and Kitamura, Y., *Corrosion*, Vol. 29, No. 1, Jan. 1983, pp. 18–22.
[11] Mankowski, J. and Szklarska-Smialowska, Z., *Corrosion Science*, Vol. 15, No. 8, Sept. 1975, pp. 493–501.
[12] Hakkarainen, T., *8th International Congress on Metallic Corrosion—Proceedings*, Deutsche Gesellschaft fuer Chemisches Apparatewesen, Frankfurt/Main, West Germany, 1981, pp. 157–162.

DISCUSSION

Naim S. Istephanous[1] (*written discussion*)—What percentage of specimens tested for determining their tendency towards pitting attack, using the standard ASTM specimen holder, exhibited crevice corrosion around the circumference of the sealing ring?

T. Hakkarainen (*authors' response*)—As the materials tested were in sheet form (2 mm) or were to be tested in as-received surface condition (prestressing wire), the standard ASTM specimen holder could not be used. On testing the type AISI 304 stainless steel using PTFE or lacquer masking, about half of the specimens showed pit nucleation potentials similar to those obtained with the tape method. In all cases, however, crevice attack was observed when inspecting the specimen, and the repassivation behavior was typical of crevice corrosion.

Neal S. Burke[2] (*written discussion*)—Can you explain why E_p values varied with scan rate? Most observers think E_p is a function of chlorine and alloy. Could cathodic reactions be significantly different enough to cause differences? That is, $j_{measured} = j_{anodic} - 1\ j_{cathode}$.

[1] Energy Technology—Division of Medtronic, 6700 Shingle Parkway, Brooklyn Center, MN 55430.
[2] W. R. Grace, 62 Whittemore Ave., Cambridge, MA 02140.

T. Hakkarainen (author's response)—Lower scan rates in the cyclic experiments imply longer times for pit growth and larger pits at the repassivation stage. The shape of large pits is often no more hemispherical but shows features of "pits growing inside the pits." Thus, their repassivation behavior is expected to shift towards that of crevice corrosion. Also, the dilution of the pit solution through diffusion becomes more slow as the pit depth increases. This is especially true in upward surfaces, where the more dense solution tends to remain at the pit bottom. The intensity of the cathodic reactions during the pit growth in the tests is negligible compared to that of the anodic reactions.

Stanley T. Hirozawa[1]

Current Versus Voltage Hysteresis: Effect on Electrometric Monitoring of Corrosion

REFERENCE: Hirozawa, S. T., **"Current Versus Voltage Hysteresis: Effect on Electrometric Monitoring of Corrosion,"** *Laboratory Corrosion Tests and Standards, ASTM STP 866*, G. S. Haynes and R. Baboian, Eds., American Society for Testing and Materials, Philadelphia, 1985, pp. 108–121.

ABSTRACT: Potential-controlled polarization methods can cause large positive shifts of the breakdown potential because of induction effect. The latter gives rise to current hysteresis, which leads to large unpredictable charge densities, which leads to poor accuracy and precision in determining the protection potential E_{prot}. Galvanostaircase polarization (GSCP) prevents induction effect and current hysteresis; however, it is subject to voltage hysteresis, which could make the determination of E_{prot} difficult if not impossible. Fortunately, voltage hysteresis can be avoided easily by staying at low current levels and charge densities.

Hysteresis caused by slow electrode kinetics can give erroneous results in the cyclic potentiodynamic polarization resistance measurement. A potentiostaircase polarization method was used to eliminate hysteresis. A graphic averaging technique was developed to determine the polarization resistance of a system where the corrosion potential E_{corr} and the corrosion rate were changing rapidly.

KEY WORDS: corrosion, hysteresis, polarization, current hysteresis, voltage hysteresis, corrosion monitoring, galvanostaircase polarization, potentiostaircase polarization, linear polarization, polarization resistance

There are two regions in a polarization curve with practical utility. The polarization resistance of the region ±20 mV around the corrosion potential E_{corr} is useful for the determination of instantaneous corrosion rates [*1*], while the critical potentials determined around the transpassive or breakdown region have been found to correlate with localized corrosion [*2,3*]. Hysteresis in both regions can lead to erroneous results.

The breakdown region in potential-controlled polarization curves of metals that show a high tendency to passivate, for example, aluminum, are very prone to current hysteresis [*4,5*]. Hysteresis in potential-controlled tests is henceforth referred to as current hysteresis since the measured current is the factor expe-

[1]Senior research associate, BASF Wyandotte Corporation, 1419 Biddle Ave., Wyandotte, MI 48192.

Copyright© 1985 by ASTM International www.astm.org

riencing hysteresis. Similarly, hysteresis during current-controlled testing is hereafter referred to as voltage hysteresis. The buildup of charge across the dielectric (passive layer) during the induction period, which is the cause of current hysteresis, shifts the apparent breakdown potential E_b in the noble direction. Current hysteresis makes it difficult to obtain an accurate and precise E_{prot}. The values of E_b and E_{prot} are affected by scan rate and the total coulombs per centimetre squared passed per test. In a potential-controlled polarization test, there is absolutely no control over the total charge used because of the current hysteresis. Current-controlled polarization, particularly the galvanostaircase method, eliminates the induction period, and the total charge passed during a test can be programmed exactly. While current hysteresis is not possible in a current-controlled method, voltage hysteresis can occur under certain conditions; when it does occur, it can make it difficult if not impossible to determine E_{prot}. Examples of voltage hysteresis and ways to avoid it are covered in this paper.

The potentiodynamic polarization resistance measurement is also very prone to hysteresis. In a dynamic procedure, the kinetics of the electrode process is not evident; therefore, one is never certain whether the points in the curve are at steady state. A potentiostaircase polarization resistance method was used to overcome the shortcoming of the potentiodynamic method. A graphical averaging technique was developed to make it possible to determine the instantaneous corrosion rate of a system in which both the corrosion rate and E_{corr} are changing rapidly.

Experimental Procedure

Apparatus

A current staircase generator was described earlier [*4*]. It consists of a Princeton Applied Research Company (PARC) potentiostat/galvanostat (Model 173) with the log current converter module (Model 376), two universal programmers (Model 175), a programmable timer (Kearsarge Model 831), and an *X-Y* recorder. The timer and one of the programmers were used to generate a voltage staircase, which was applied in two ways. First it was applied directly to the electrode specimen to yield potentiostaircase polarization resistance (PSC-PR) diagrams, which consisted of a regular succession of current transients. Second, the voltage staircase was fed to the signal input of the potentiostat/galvanostat, and under the I CONTROL mode, the resulting current staircase signal was applied to the specimen. The recording of voltage transients in response to the current staircase signal gave the galvanostaircase polarization (GSCP) curves.

The polarization cell was a 500-mL flat-bottom pyrex vessel (Metrohm Model A765-500) with a cell cover (Metrohm Model EA874) with tapered openings to accept a flat specimen holder (PARC Model K0105), two graphite counter electrodes (Ultra Carbon, Ultra F Purity, U-50-7, 7312207) and a salt bridge with a porous VYCOR junction (PARC Model G0095). A saturated calomel electrode (PARC Model K0077) was placed in the tapered opening of the salt bridge. The

area of the specimen exposed to the electrolyte was exactly 1 cm^2; therefore, all currents reported here are equivalent to current density.

Preparation of Specimens

The copper and brass specimens were prepared by abrading with pumice, degreasing in boiling toluene, rinsing with methanol, air-drying, and storing in a desiccator. Aluminum was simply degreased.

Results and Discussion

Current Hysteresis

Cyclic potentiodynamic polarization is used most often to study the localized corrosion of metals. The hysteresis loop obtained in the polarization curve has been related to crevice corrosion [*3*], the larger the area of the loop or the larger the difference between E_b (sometimes called the pitting potential E_{pit}) and E_{prot}, the greater is the tendency for crevice corrosion. Unfortunately, E_b or E_{pit} is shifted significantly by scan rate and prior history of the metal [*6*] while E_{prot} is affected in a semilogarithmic manner by the charge density [*3*].

The effect of induction time on current hysteresis can be demonstrated most effectively by comparing quasi-stationary potentiostatic polarization (QSP) curves [*7*] with GSCP curves of aluminum immersed in 0.08 *M* sodium benzoate in 3000-ppm sodium chloride for ½ and 16 h. Figure 1 shows the QSP curves by Rudd and Scully [*7*] and the corresponding GSCP curves [*4,5*] are overlaid after appropriate scale adjustment. Both QSP curves show large current hysteresis loops, while in the case for GSCP, the ½-h curve gave identical E_b and E_{prot} and the 16-h curve showed only a slight separation of E_b and E_{prot}. The E_b obtained by QSP is far more noble than the E_b obtained by GSCP. In the QSP curves, the authors tried to keep the current to a minimum by reversing the step direction on the very next step after the first indication of breakthrough. The maximum current in the 16-h QSP curve is about 15 times higher than that in the ½-h curve, and the charge density was 15.2 C/cm^2 compared to 0.8 for the ½-h curve. It is apparent that in a potential-controlled polarization method the charge density cannot be predetermined because of the uncontrollable current hysteresis. In both of the GSCP curves, the charge density is preprogrammed precisely at 0.086 C/cm^2.

The difference between the QSP and GSCP methods observed in the preceding paragraph is due to the fundamental differences between the methods. In voltage-controlled polarization, one applies a voltage across a dielectric layer (passive layer) and passively waits for the breakthrough at the most vulnerable points. When breakthrough does occur, the current keeps on rising because the voltage or driving force, which is much higher than required for the breakthrough, cannot be brought down immediately because the rate of drop has been preprogrammed. In a current-controlled method, such as GSCP, the breakthrough is initiated actively and immediately with whatever voltage that is required, but as soon as breakthrough is achieved, the voltage drops rapidly to a level just sufficient to

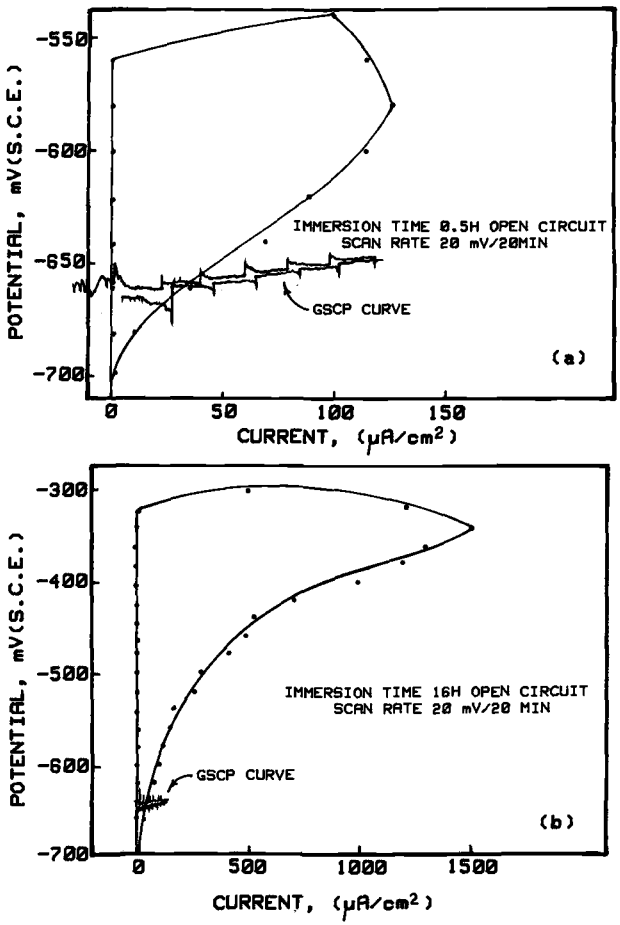


FIG. 1—*Potential/current density curves of aluminum obtained in 0.08* M *benzoate solutions after* (a) *0.5-h pre-exposure and* (b) *16-h pre-exposure. Different values of* E_{pit} (E_b) *were attained as a result of different times of exposure. (Courtesy of W. J. Rudd and J. S. Scully and the Pergamon Press.) GSCP curves of the identical systems are overlaid on the respective curves. 20* $\mu A/cm^2$*: 2-min steps. 0 to 120* $\mu A/cm^2$.

maintain the programmed current level. This active nature of GSCP eliminates the inductive effect thus avoiding the noble bias in E_b.

Voltage Hysteresis

Figure 2 shows the GSCP curve for a well-inhibited coolant. The up step and down step curves form what appears to be a typical current hysteresis loop observed in a PDP curve. Under current-control, it is not possible to have current hysteresis; however, voltage hysteresis is possible. In voltage hysteresis, voltage would lag the current and if it did occur in Fig. 2, the voltage would keep on rising when the current direction was reversed and the curve would have looped upward instead of downward.

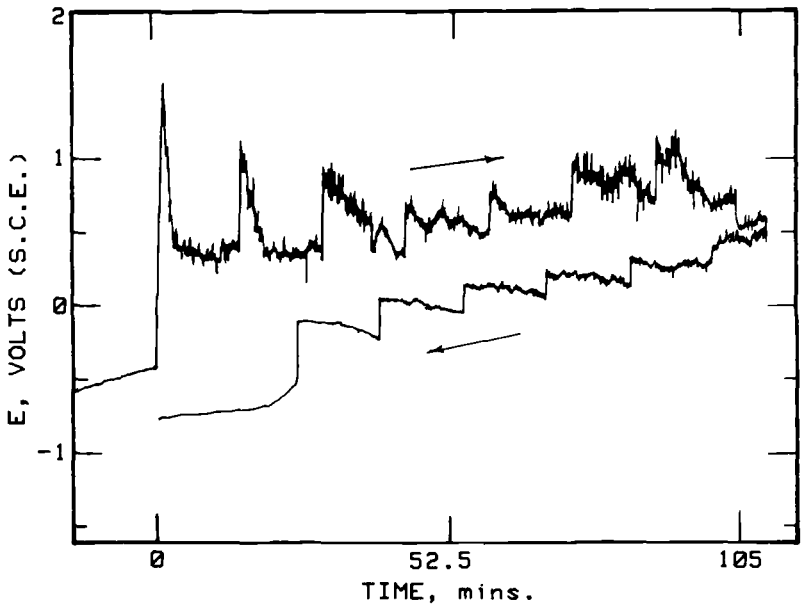


FIG. 2—*GSCP curve of 3003 aluminum in a well-inhibited coolant. 40 μA/cm²: 15-min steps. 0 to 280 μA/cm².*

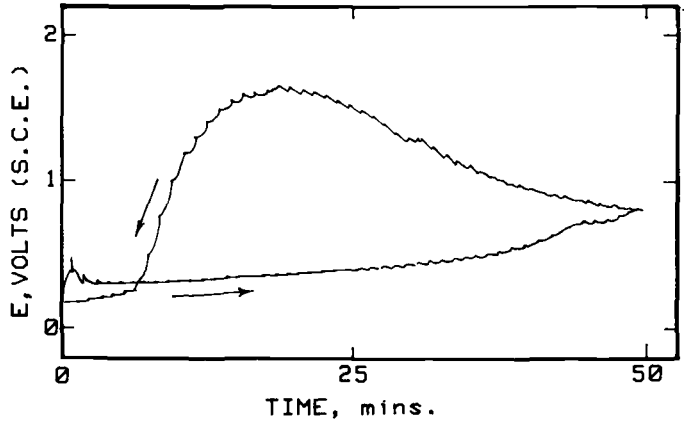


FIG. 3—*GSCP curve of copper in 25% ethylene glycol containing 0.5% sodium nitrate, 1% borax, and 0.5% sodium benzotriazole. 20 μA/cm²: 1-min steps. 0 to 1 mA/cm².*

Figure 3 shows a voltage hysteresis loop in the GSCP curve of copper in the presence of benzotriazole. Note that the curve recovers just in time and ends in the normal position to yield E_{prot} upon extrapolation. Earlier it was noted that current hysteresis gives rise to uncontrollable excessive charge densities which affect E_{prot}. In contrast, voltage hysteresis does not affect the charge density. However, excessive voltage hysteresis could make the extrapolation for E_{prot} less accurate (Fig. 4) or virtually impossible (Fig. 5). In practice, voltage hysteresis can be avoided very easily by avoiding high current and high charge densities. The charge density is usually kept at around 0.5 C/cm^2 or preferably around 0.2 C/cm^2.

Hysteresis During Measurement of Polarization Resistance

Any electrochemical method using the sweep technique (voltage or current ramp) has a disadvantage in that the kinetics of the electrode process is not evident. If the scan rate is too fast relative to the electrode kinetics, one would anticipate hysteresis. Figure 6 shows the cyclic potentiodynamic polarization curve around the corrosion potential E_{corr} of brass in 3000-ppm sodium chloride using a scan rate of 0.2 mV/s. The polarization is started at the open circuit E_{corr} in the cathodic direction. Note that the curve bottomed out giving an apparent E_{corr} slightly more negative than the open circuit E_{corr}. The third segment gives a cathodic E_{corr} (at current minimum obtained approaching from the cathodic

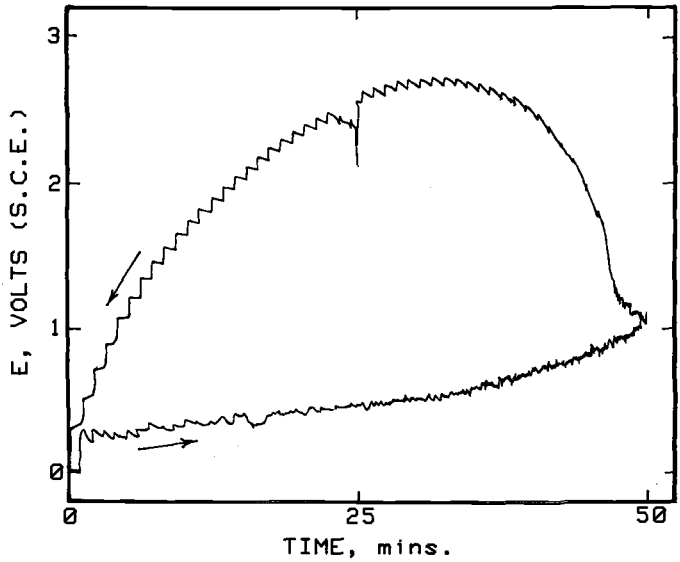


FIG. 4—*GSCP curve of brass in 25% glycol containing 0.5% sodium nitrate, 1% borax, and 1% disodium phosphate. 20 μA/cm^2: 1-min steps. 0 to 1 mA/cm^2.*

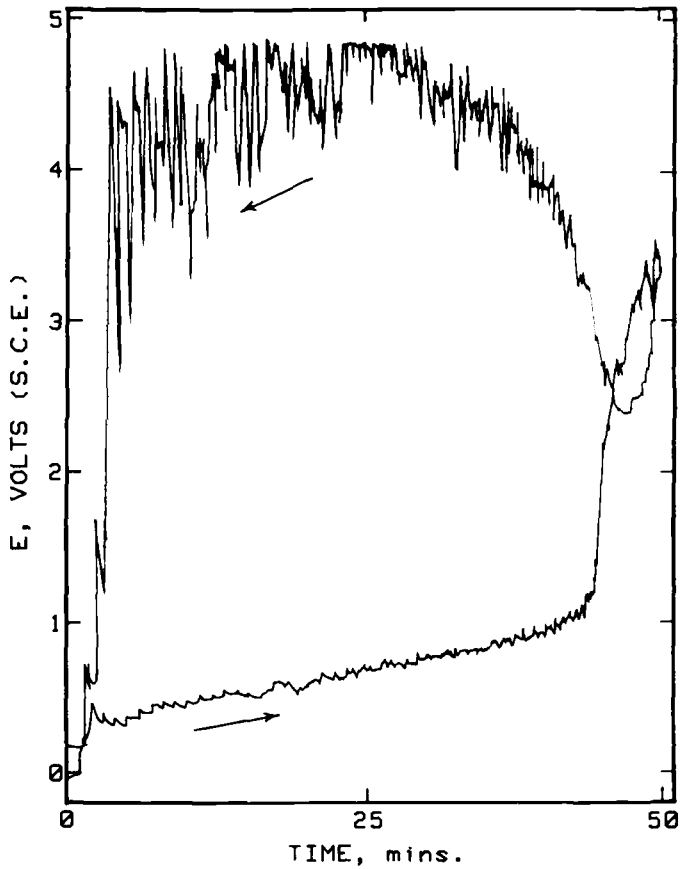


FIG. 5—*GSCP curve of copper in 25% ethylene glycol containing 0.5% sodium nitrate, 1% borax, and 0.5% sodium mercaptobenzothiazole. 20 μA/cm²; 1-min steps. 0 to 1 mA/cm².*

side) that is about 20 mV more negative than the open circuit E_{corr} while Segment 5 returning from the anodic side gives an anodic E_{corr} (at current minimum obtained approaching from the anodic side), which virtually coincides with the open circuit E_{corr}. The second cathodic E_{corr} given by Segment 7 is shifted further in the negative direction.

Figure 7 shows a curve recorded under the same conditions as above except that the current (instead of log current) is plotted as a function of potential. Again it is noted that the cathodic E_{corr} (where Segment 2 crosses zero current) is shifted in the negative direction relative to the open circuit E_{corr} while the anodic E_{corr} (where Segment 3 crosses zero current) agrees fairly well with the open circuit E_{corr}.

Unlike dynamic signals, staircase signals produce response transients with

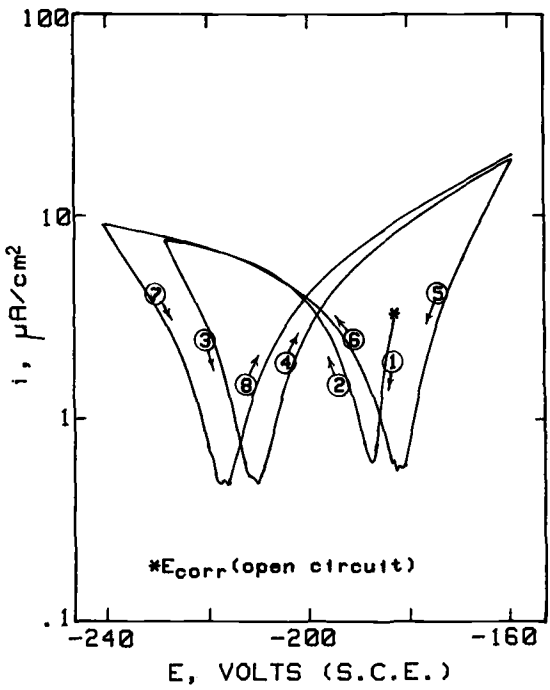


FIG. 6—*Cyclic potentiodynamic polarization resistance curve for brass in aqueous 3000-ppm sodium chloride, 0.2 mV/s. The polarization was started at* E_{corr} *and the segments are numbered sequentially. Arrows indicate scan direction.*

kinetic information [*4*]. We have noted in the previous sections that the GSCP method overcame both induction and hysteresis effects in the determination of E_b and E_{prot}. Since the polarization resistance measurement does not involve breaking through the passive layer, and therefore, no induction time is involved, such drastic measure as GSCP is not necessary. Moreover, under potentiostatic mode, the current approaches steady state rather rapidly in the vicinity of E_{corr}. Therefore, the PSC-PR method was used to obtain the polarization resistance R_p. Curve *a* in Fig. 8 shows a PSC-PR curve obtained under the same conditions as Figs. 6 and 7 including the same scan rate. It is obvious that the current did not have enough time to reach steady state. In the PSC-PR method, the scan rate can be changed by changing the step interval, the step height, or both. In Curve *b* of Fig. 8 the scan rate was reduced by changing the step height from 2 to 0.8 mV, keeping the step interval the same at 10 s; this yielded an effective scan rate of 0.08 mV/s. The current appears to be much closer to steady state, and the R_p obtained from the slope increased by 10%; hence the calculated corrosion rate was 10% lower.

It appeared that kinetic effects could lead to some hysteresis that could lead

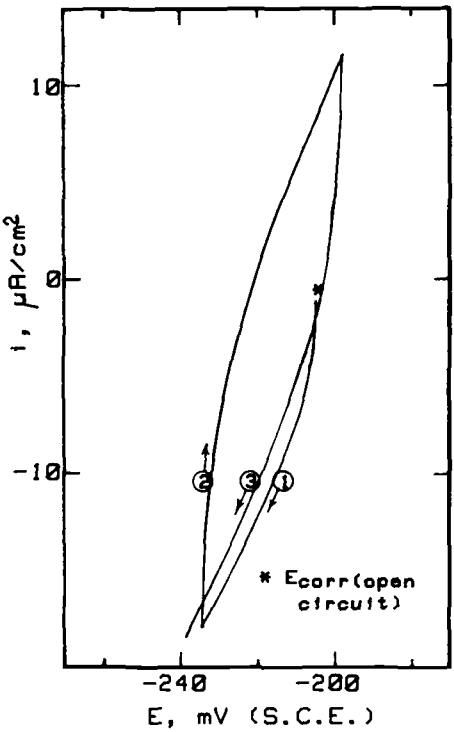


FIG. 7—*Cyclic potentiodynamic polarization resistance curve for brass in aqueous 3000-ppm sodium chloride, 0.2 mV/s. Polarization was started at* E_{corr} *and the segments are numbered sequentially. Arrows indicate scan direction.*

to the type of cyclic potentiodynamic polarization curves shown in Figs. 6 and 7. However, the separation of the open circuit E_{corr} and cathodic E_{corr} seemed excessive. If hysteresis was the cause of the separation, the anodic and cathodic E_{corr} should occur symmetrically about the open circuit E_{corr}. Instead the anodic E_{corr} coincided with the open circuit E_{corr}. Also if hysteresis was the cause of the separation of the anodic and cathodic E_{corr}, decreasing the scan rate should cause the anodic and cathodic curves in Fig. 6 to approach coincidence while the anodic and cathodic segments in Fig. 7 should approach a straight line. Surprisingly, the exact opposite was found to be true, that is, the separation of the cathodic and anodic E_{corr} became wider, the slower the scan rate. This phenomenon can be explained in the following manner. When the curve goes cathodic relative to an anodic E_{corr}, the oxide layer and other passive compounds can be reduced thereby making the metal more sucseptible to corrosion (upon reverting to open circuit conditions), and the apparent E_{corr} is shifted in the negative direction. When the applied potential is in the anodic region, that is, positive with respect to a cathodic E_{corr}, the oxide and other passive compound are being reformed. Since the condition of the passive layer is approaching the condition

existing under the open circuit condition, the anodic E_{corr} agrees quite well with the open circuit E_{corr}.

Because of the cathodic shift of the apparent E_{corr} by cathodic polarization, it seems preferable to run the polarization resistance measurement starting at the open circuit E_{corr} and to minimize the extent of excursions into the anodic and particularly into the cathodic regions. This is practiced in our routine PSC-PR tests where the excursions are limited to 10 mV in each direction.

There is a commercial instrument that is dedicated to running PSC-PR curves. Starting at the origin, it takes five steps in one direction (select anodic or cathodic). Fifty seconds is allowed in the open circuit condition to allow the open circuit E_{corr} to stabilize. Then five steps are taken in the other direction. We have noted that if the initial direction is cathodic, the stabilized E_{corr} obtained in 50 s coincides with the original E_{corr} if the system is aged or well inhibited or both, but a cathodic shift in the E_{corr} is observed if the medium is noninhibiting. The latter observation corroborates our curves in Figs. 6 and 7, which were obtained in 3000-ppm sodium chloride, which does not inhibit brass corrosion.

There are certain conditions that cause excessive noise. It is a common practice

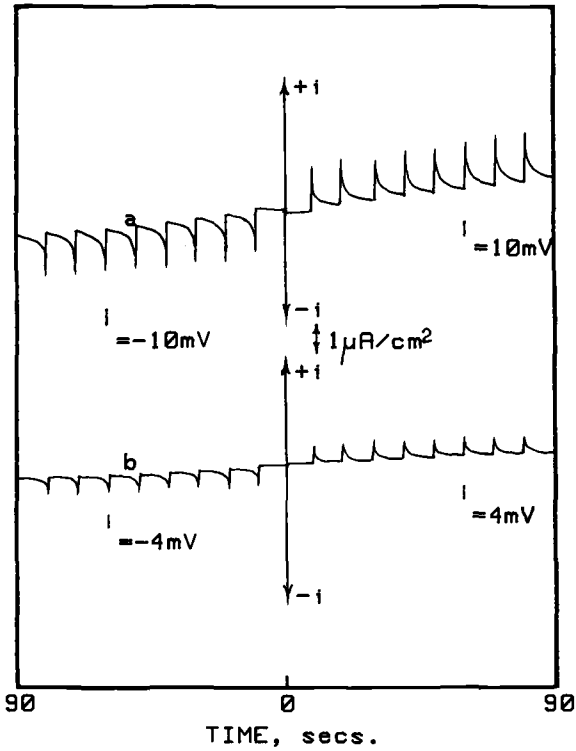


FIG. 8—*PSC-PR curves for brass in aqueous 3000-ppm sodium chloride at two step sizes:* (a) *2 mV: 10 s and* (b) *0.8 mV: 10 s.*

to filter out such noise. Filtering has been found to reduce the slope as much as 2.7 times and often distorts the current transients so that the kinetic information is lost (Fig. 9). We found it preferable to live with the noise and draw the best possible line to determine R_p.

Graphic Averaging of Polarization Resistance

When a metal is immersed in an electrolyte, the corrosion rate is quite rapid at first but the rate usually slows down with time. The change in the corrosion rate is particularly rapid in the initial 1 to 2 h. Concurrently there is a rather rapid change in E_{corr}. It is extremely difficult to determine the instantaneous corrosion rate under such a rapidly changing condition. A graphic averaging technique using the PSC-PR method was used to obtain data in this unstable region.

Figure 10 shows the PSC-PR curve of brass in the presence of metavanadate ions after 24-h immersion. The rather flat response before the first step in both the cathodic and anodic direction indicates that the corrosion rate and E_{corr} have

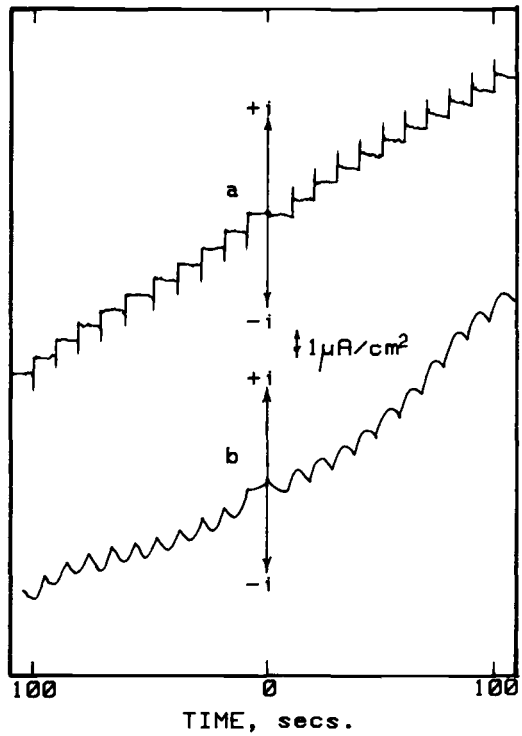


FIG. 9—*PSC-PR curves for 319 aluminum in aqueous 3000-ppm sodium chloride showing effect of filtering:* (a) *without filtering and* (b) *filtered at 10 ms. Specimen temperature 133°C (275°F). Cell under 6.8-kg (15-lb) pressure.*

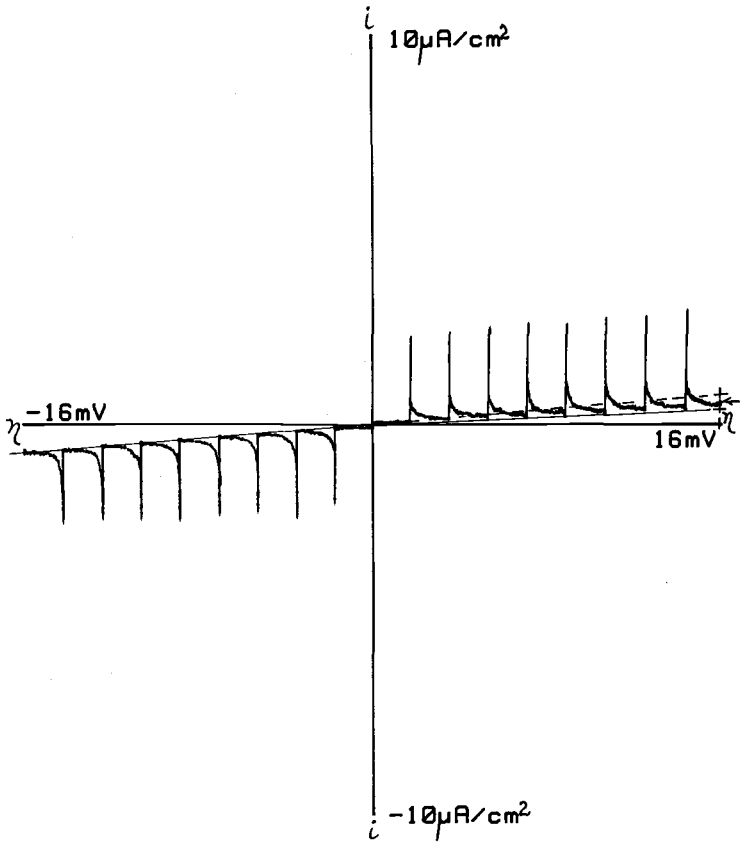


FIG. 10—*PSC-PR curve for copper in 25% ethylene glycol containing 0.5% sodium nitrate, 1% borax, and 1% sodium metavanadate after 24-h pre-immersion at 82°C (180°F). 2 mV: 10-s steps. Graphic averaging.*

stabilized. The first step in the graphic averaging is to draw a line parallel to the steady state currents at the end of each step in the anodic quadrant and passing through the origin. Draw a straight line similarly in the cathodic quadrant and extend it into the anodic quadrant as shown by the broken line. A line half way between the two lines will give the average slope, which is equivalent to $1/R_p$. In practice the average current is read after the fifth step and divided by 10 to obtain $1/R_p$. R_p was used in the Stern Geary equation to calculate the instantaneous corrosion rate. Graphic averaging is not too significant after 24-h immersion because the corrosion rate is quite low. At 2-h immersion time, graphic averaging is quite helpful as shown by Fig. 11. At first glance it appears that the current transients have not attained steady state. However, it is noted that the transients attain a constant slope before the first steps; these slopes reflect the decrease of corrosion rate with change of E_{corr} and show up in each step. The current transient at each voltage step reaches a constant slope, which is

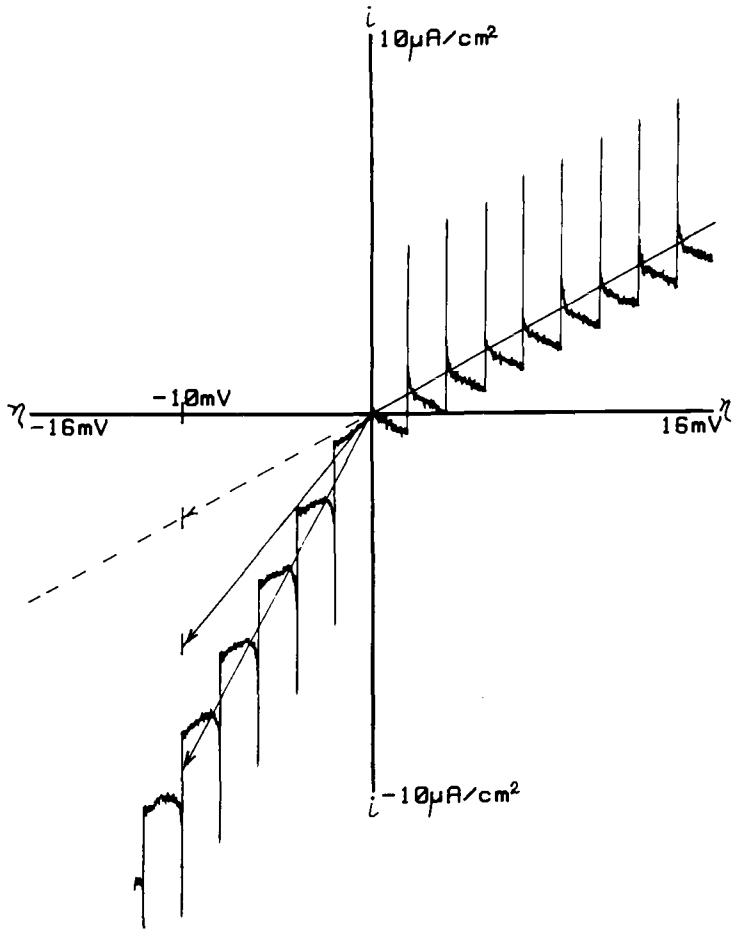


FIG. 11—*Same as Fig. 10 but with only 2-h pre-immersion.*

about equivalent to the background slope; therefore, the current transients are believed to be at steady state even though the transients are not flat. The graphic averaging is carried out in a similar manner as in Fig. 10, but it is carried out (arbitrarily) in the cathodic quadrant. In the case of very rapidly changing corrosion rate, the anodic slope has been observed to acquire a negative sign, that is, moved into the lower right quadrant. Slope averaging is still possible by extrapolating to the upper left quadrant.

Conclusions

The induction effect observed in potential-controlled polarization has deleterious effects on corrosion monitoring: it can cause a large positive bias in E_b and it is the cause of current hysteresis, which makes charge density unpre-

dictable, which in turn causes poor accuracy and precision in the determination of E_{prot}. GSCP eliminates the induction effect and current hysteresis; however it is subject to voltage hysteresis, but fortunately, it is easily avoided.

Linear polarization resistance measurements are also prone to errors because of current hysteresis. Such errors can be eliminated or at least minimized by using the potentiostaircase polarization resistance method. A graphic averaging technique was used to determine R_p when E_{corr} and the corrosion rate were changing rapidly. The cathodic shift of E_{corr} could affect the determination of the cathodic Tafel slope and the polarization resistance.

Acknowledgments

The author wishes to thank Dan Coker for assistance in the laboratory work and discussion on the interpretation of the results and Drs. John Conville and Louis C. Pizzini for their support and encouragement.

References

[1] Stern, M. and Geary, A. L., *Journal of the Electrochemical Society*, Vol. 105, 1958, p. 638.
[2] Smialowska, S. and Czachor, M., *Localized Corrosion, NACE-3*, R. W. Staehle, B. F. Brown, J. Kruger, A. Agrawal, Eds., National Association of Corrosion Engineers, Houston, TX, 1974, p. 353.
[3] Wilde, B. E., *Localized Corrosion*, NACE-3, National Association of Corrosion Engineers, Houston, TX, 1974, p. 343.
[4] Hirozawa, S. T., "Galvanostaircase Polarization: a Powerful Technique for the Study of Localized Corrosion," *Journal of the Electrochemical Society*, Vol. 130, 1983, p. 1718.
[5] Hirozawa, S. T., "Study of the Mechanism for the Inhibition of Localized Corrosion of Aluminum by Galvanostaircase Polarization," presented at International Conference on Corrosion Inhibition, National Association of Corrosion Engineers, Research Committee, May 1983.
[6] Hirozawa, S. T., *CORROSION/82*, Paper 263, National Association of Corrosion Engineers, Houston, TX, 1982.
[7] Rudd, W. J. and Scully, J. C., *Corrosion Science*, Vol. 20, 1980, p. 611.

Florian Mansfeld[1] *and Martin W. Kendig*[1]

Electrochemical Impedance Tests for Protective Coatings

REFERENCE: Mansfeld, F. and Kendig, M. W., **"Electrochemical Impedance Tests for Protective Coatings,"** *Laboratory Corrosion Tests and Standards, ASTM STP 866*, G. S. Haynes and R. Baboian, Eds., American Society for Testing and Materials, Philadelphia, 1985, pp. 122–142.

ABSTRACT: The experimental approach for carrying out electrochemical impedance measurements for coated metals is described. Models for the impedance behavior have been developed for different coating systems, and methods for the analysis of experimental impedance diagrams in terms of coating and interface properties and their changes during exposure to corrosive environments are discussed. The systems studied include polybutadiene coatings on bare and conversion coated steel and aluminum alloys, commercial chromate conversion coatings on aluminum alloys and sulfuric acid, or chromic acid anodized aluminum alloys. For the anodized aluminum alloys, suggestions for development of a quality control test are given.

KEY WORDS: corrosion tests, conversion coatings, polymers, electrochemical impedance tests, polymer coatings, anodized aluminum, computerized analysis

The development of electrochemical impedance techniques has made it possible to design electrochemical laboratory tests for applications where traditional DC techniques could not be used such as organic coatings and low conductivity media. The only electrochemical measurements carried out routinely for polymer coated steel were determinations of the open-circuit potential and occasion capacitance measurements at a fixed frequency. In a review article of 1973, Wolstenholm [*1*] concluded, "It is disappointing to note that the results of electrochemical tests so far have not been very informative." This pessimistic view is not justified anymore as can be seen from the increasing amount of papers dealing with evaluation of coated metals with impedance techniques. A review of earlier work has been given by Szauer [*2*]; more recent work was reviewed by Mansfeld et al [*3*].

Broad frequency determination of the electrochemical impedance is particularly well suited for the study of polymer coated steel since it distinguishes between the many phenomena that contribute to the rate of charge transfer across

[1]Manager and member of technical staff, respectively, Rockwell International Science Center, 1049 Camino Dos Rios, Thousand Oaks, CA 91360.

Copyright© 1985 by ASTM International www.astm.org

a polymer coated metal. DC techniques give well defined resistances only for sufficiently slow application of a test potential. The DC resistance may include contributions from the resistance of defects and the polarization of the interface that cannot be separated. On the other hand, fixed frequency AC measurements will not provide sufficient information necessary for separating the ionic transport through the film from the film capacitance.

The authors have evaluated polybutadiene coatings on bare or conversion coated steel and aluminum alloys, commercial conversion coatings on aluminum alloys, and anodized aluminum alloys with impedance measurements over a wide frequency range in laboratory tests. The background for electrochemical impedance measurement methods and experimental data analysis has been given earlier [*3–7*].

Experimental Approach

The impedance measurements are carried out as discussed earlier [*4,5*] using a Solatron Model 1174 transfer function analyzer and a Princeton Applied Research (PAR) potentiostat 173 with the Model 179 coulometer plug-in. The data are stored and displayed for analysis using a Hewlett Packard (HP) 9825 desktop computer and the HP 9872 plotter. Measurements are usually carried out between 10^6 Hz and 2×10^{-2} Hz, but phase shift problems limit the useful upper frequencies to $\leq 1.5 \times 10^5$ Hz, depending on the system studied. The lower frequency limit was chosen based on reasonable time limitations for a given test. Recent improvements in the experimental procedure make it possible to carry out measurements to 5×10^{-4} Hz in the same time period [*8*].

The polybutadiene coatings are applied by spin coating followed by a curing resulting in a coating thickness of 8 ± 2 μm. Zinc phosphate coatings were applied according to standard procedures. Commercial (Alodine) chromate conversion coatings were applied to the Aluminum alloys 2024, 6061, and 7075. Anodic coatings were produced from chromic acid and sulfuric acid solutions with proper sealing according to MIL-A-8625C. The coated specimens are exposed to aerated 0.5 *N* sodium chloride (exposed area 20 cm^2) and measurements are carried out at the corrosion potential E_{corr} as a function of time.

Analysis of Impedance Data

After each experiment the AC impedance data are displayed as Bode plots [*3–5*] (log $|Z|$ versus log ω and θ versus log ω, where $|Z|$ is the absolute value of the impedance, θ the phase angle, and ω the angular frequency, rad/s). The advantage of this procedure is that the data for all measured frequencies are shown and that a wide range of impedance values can be displayed. The frequency dependence of the phase angle indicates whether one or more time constants occur and can be used to determine the values of the parameters in the equivalent circuit such as the model in Fig. 1. Complex plane plots have also been used, and where Warburg impedance type phenomena seem to occur, Randles plots

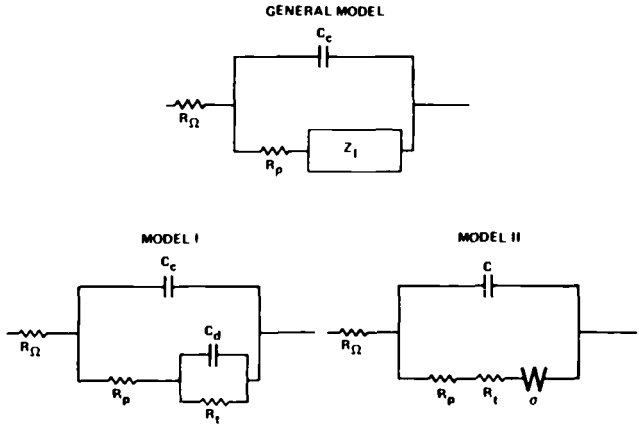


FIG. 1—*Equivalent circuits for impedance of coated steel and aluminum alloys.*

were analyzed. All these procedures are available on the computer programs developed by the authors [*3–7*].

In general, the equivalent circuit for a polymer coated metal consists of the solution resistance R_Ω of the test electrolyte, the capacitance C_c of the intact coating layer, the pore resistance R_p caused by penetration of electrolyte, and a general impedance Z_I, which characterizes the reactions at the metal interface (Fig. 1). For many systems, Z_I can be characterized by a transfer resistance R_t in parallel with a double layer capacitance C_d (Model I) or by R_t in series with a Warburg or pseudo-Warburg [*9*] impedance W (Model II). R_t corresponds to the corrosion reaction at the metal/coating interface. The generalized Warburg

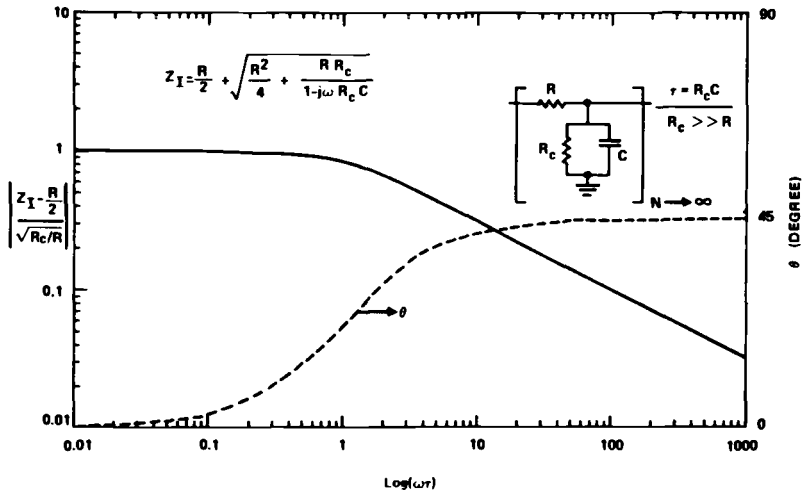


FIG. 2—*A plot of the transmission line model for* Z_I *in reduced units.*

impedance may be expressed as $W = k(j\omega)^{\alpha}$. In the case that $\alpha = -0.5$, W behaves as a true diffusion impedance, where $k = \sigma/\sqrt{2}$, σ being the Warburg coefficient. The general case where $-1 < \alpha < 0$ may result from tangential penetration of electrolyte at the coating/metal interface or by heterogeneous penetration of an electrolyte [*9*], which gives rise to a distribution of time constants. Both cases result in a transmission line analog for the electrical response (Fig. 2). With the assumption that each equivalent unit cell of the transmission line includes an ohmic resistance R representing a path parallel to the metal/coating interface and a corresponding corrosion resistance R_c, the total impedance exhibits $\omega^{-1/2}$ or pseudo-Warburg behavior at high frequencies, and the depolarization of the corrosion reaction R_c provides a DC limit equal to $\sqrt{R_c R}$ (Fig. 2). Figure 2 shows a normalized Bode plot for the case $R_c \gg R$ and a very large number N of unit cells. Under ideal polarizability of the interface ($R_c \rightarrow \infty$), the impedance gives $\omega^{-1/2}$ behavior at all frequencies and in the case that R_c is replaced by a Warburg impedance, $\omega^{-1/4}$ frequency dependence can result.

Results and Discussion

Coated Steel

For steel the effects of different surface pretreatment on the corrosion resistance of the polybutadiene coating metal were evaluated [*6,10*]. These surface pretreatment procedures are listed in Table 1. Some of these procedures were used as discussed in Federal Specification TT-C-490B; other pretreatment processes were selected in an attempt to produce a wide variety of surface structures for the study of the effects of surface properties on coating adhesion and corrosion protection [*11*].

Examples for the changes of the impedance during exposure to 0.5 N sodium chloride are given for coated steel in Figs. 3 through 5. For a surface that was degreased and then treated using the alkaline derusting procedure (Table 1), deviation from capacitive behavior occurs only for frequencies below 1 Hz (Fig. 3). This deviation does not change very much with time; the coating capacitance

TABLE 1—*Surface pretreatment procedures for steel.*

Pretreatment	Procedure
Decreased (d)	trichloroethylene, 15 min, TT-C-489, Method II
Polished (p)	wet polish, 600-grit SiC
p + d	Polished and degreased
d + hot alkaline cleaning	5 min, 100°C, TT-C-490, Method III
d + alkaline derusting	10 min, 50°C, TT-C-490, Method V, Type III
p + d + inh · HCl	5 min, RT, 42 v/o HCl + 5.8-g/L 2-butyne-1,4-diol
d + anodic etch (AE)	2 min, RT, 30 v/o H_2SO_4, 0.1 A/cm^2
d + concentrated HNO_3	30 min, RT

[a]RT is room temperature and v/o is volume percent.

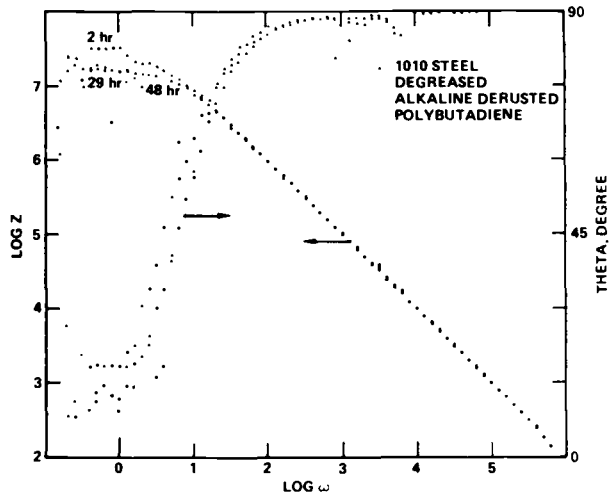


FIG. 3—*Bode plots for coated steel* (d *and alkaline derusting*).

stays constant at about 0.01 μF indicating that the film thickness (about 6 μm) does not change during exposure.

While the coating on the surface that was cleaned by alkaline derusting stayed very protective, relatively rapid deterioration of the protective properties of the coating occurred for the treatment of concentrated nitric acid (Fig. 4). Already after 2-h exposure, pronounced changes from that of an intact coating can be observed. After 19- and 45-h exposure, the impedance (Fig. 4) and the phase angle have changed drastically and two semicircular arcs are observed in the complex impedance plot. Using a curve-fitting procedure for determination of

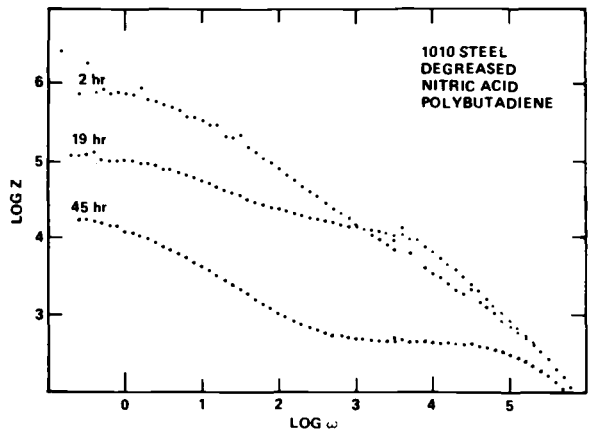


FIG. 4—*Bode plots for coated steel* (d *and concentrated nitric acid*).

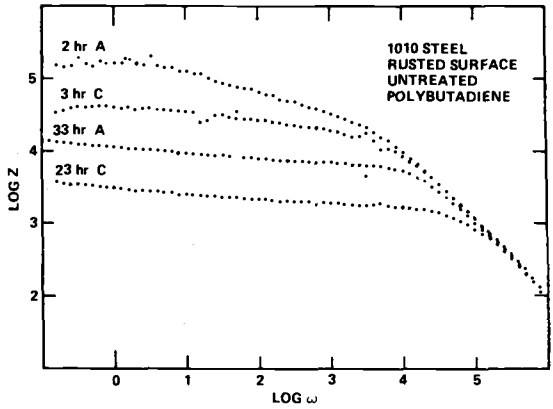


FIG. 5—*Bode plots for coated steel (initial rust spot not removed).*

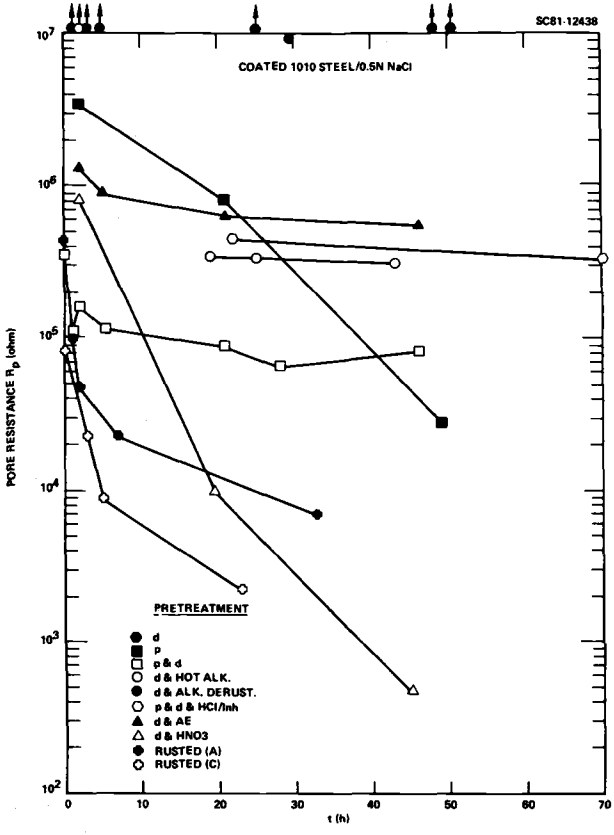


FIG. 6—*Time dependence of pore resistance* R_p *for coated steel with different surface pretreatment procedures.*

semicircles in the complex impedance plot [7], R_p and R_t were calculated as $R_p = 2.56 \times 10^5\ \Omega \cdot cm^2$ and $R_t = 2.44 \times 10^6\ \Omega \cdot cm^2$ for 19-h exposure and $R_p = 7.90 \times 10^3\ \Omega \cdot cm^2$ and $R_t = 4.26 \times 10^5\ \Omega \cdot cm^2$ after 45 h. In both cases the low-frequency semicircular arc had its center below the Z' axis. After 45 h, the coating has become thinner or has an increased effective dielectric constant caused by water uptake [*12*] as indicated by the increase of the capacitance from 0.6 to 0.85 nF/cm^2. A number of rust spots were observed after the 48-h test. This pretreatment gave by far the poorest results.

While most surface pretreatment procedures (with the exception of nitric acid passivation) resulted in very little degradation of the coating properties as shown by the impedance measurements, relatively rapid changes in the impedance occurred for surfaces from which rust particles were not removed before application of the coating. Figure 5 shows examples for surfaces with a small amount (A) and a large amount of rust particles (C). After 7-h exposure for the first case, R_p was about $4.6 \times 10^5\ \Omega \cdot cm^2$ while after 5-h R_p was about $1.8 \times 10^5\ \Omega \cdot cm^2$ for the second case. Complex impedance plots showed a semicircle at high frequencies corresponding to the time constant related to R_p and C_c. The lower frequency impedance behavior determined by Z_l could not be accurately resolved into individual components. These results show that AC impedance measurements can detect in a very short time the harmful effects of surface contamination on the protective properties of an organic coating.

The impedance data for a coated steel seem to follow Model I shown in Fig. 1. Since in most cases very little corrosion occurred in the 48-h exposure period, R_t remained very high and could not be determined at the present low-frequency limit of 20 mHz. The pore-resistance R_p has been determined from the experimental Bode plots for the surface pretreatments in Table 1. Figure 6 shows the time dependence of R_p for exposure of the coated steel of different pretreatment to 0.5 *N* sodium chloride. For the alkaline derusting pretreatment, and the specimen that was only degreased, the impedance at $\omega = 1$ rad/s (0.16 Hz) exceeded $10^7\ \Omega$ ($2 \times 10^8\ \Omega \cdot cm^2$) at all times. The impedance for the specimen with the hot alkaline treatment initially exceeded $10^7\ \Omega$, but then dropped to lower values with increasing exposure time and stayed below the values for the anodic etch and the acid pickling treatments. For the polished surface and for the surface passivation in concentrated nitric acid, R_p decreased faster than for the other surface treatments. The surface from which rust was not removed before coating exhibited the lowest initial and final R_p values (with the exception of the nitric acid treatment).

The data in Fig. 6 can be used to rank the effect of surface pretreatments on corrosion protection by the polybutadiene coating. This ranking in order of decreasing resistance to environmental effects based on the values of R_p at 48 h is the following: degreased $\simeq$ alkaline derusting $\gg$ anodic etch $\simeq$ inhibited/HCl $\simeq$ hot alkaline $>$ polished + degreased $\simeq$ polished $\gg$ low rust $\simeq$ high rust $\simeq$ concentrated HNO_3. This ranking results in four groups

of surface pretreatments, which give rise to different resistance to corrosion attack.

The tests summarized in Fig. 6 have been repeated over longer time periods with visual observation of the extent of corrosion (CORR) and delamination (DEL) according to ASTM Evaluating Degree of Rusting on Painted Steel Surfaces (D 610). Figure 7 shows the variation of R_p with time in the first seven days of the exposure test for films formed on steel with different surface pretreatments as compared to R_p determined for a free film measured in a Hittorf cell. The thickness of the free film was comparable to the thickness of the coating on steel, as determined from normalized capacitance data. The values of R_p for the different surface pretreatments and the free film extrapolate back to nearly the same R_p^o, the value of R_p at zero time. However, R_p's for the coatings on the metal substrate decrease with time, while R_p for the free film remains virtually unchanged. R_p for coatings on the metal substrates decrease by different amounts in the first seven days, depending on the surface pretreatment. The polished and

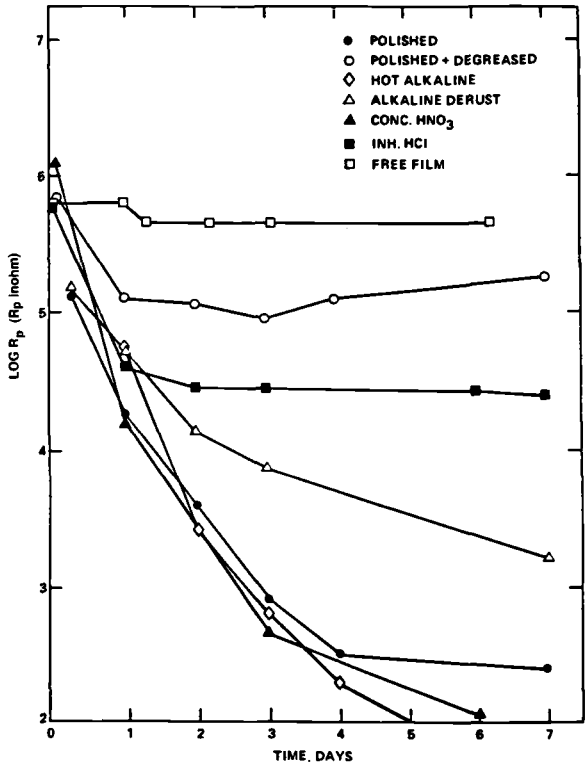


FIG. 7—*Time dependence of the pore resistance* R_p *of a free film (polybutadiene) and of the same coating on steel with different pretreatments.*

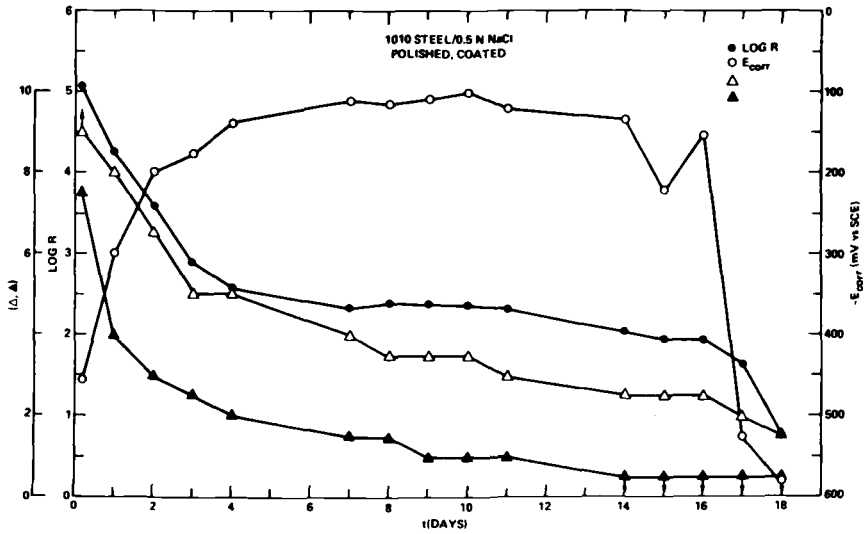


FIG. 8—*Time dependence of DEL. CORR.* E_{CORR} *and* R_p *for a polybutadiene coated 1010 steel that was polished before coating.*

degreased specimen showed only an order of magnitude decrease, but R_p for the specimens that were polished or treated in concentrated nitric acid, or in the hot alkaline solution before coating, decreased to a much greater extent upon prolonged exposure. For the specimen with the hot alkaline treatment (Table 1), R_p decreased by more than a factor of 10^4 after seven days. The importance of the substrate in accelerating the decrease in R_p can be attributed to the tensile stress produced in the film caused by the growth of corrosion products at the initial microscopic defects. Clearly the mechanical properties as well as mass transport behavior of polymers have comparable importance for corrosion protection.

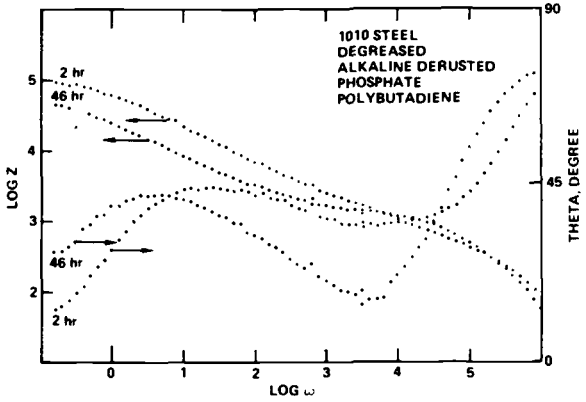


FIG. 9—*Bode plots for phosphated and coated steel* (d *and alkaline derusting*).

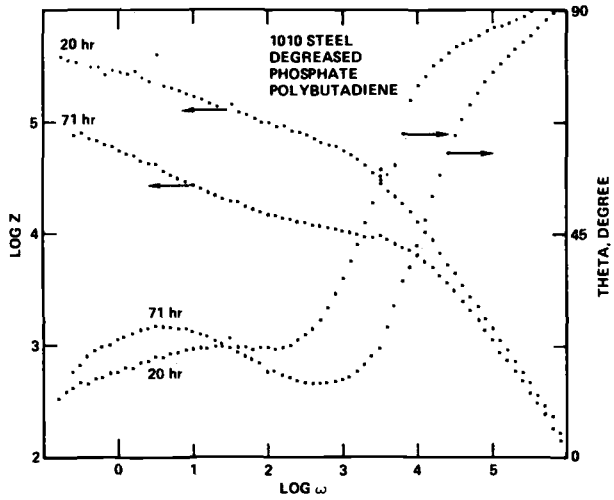


FIG. 10—*Bode plots for phosphated and coated steel* (d).

As can be seen for the example in Fig. 8, R_p decreases as both CORR and DEL increase. E_{CORR} increases for the first few days because of the development of cathodic areas and establishment of galvanic couples. After reaching a plateau value, it drops sharply to E_{CORR} for bare steel as the majority of the surface becomes active. DEL and CORR show trends similar to R_p. A more detailed discussion of these results given elsewhere [*10*] has shown that the value of R_p in the plateau region correlates with the lifetime of the polymer coated steel.

Phosphated and Coated Steel

Zinc phosphate coatings were applied on 1010 steel surfaces that had been cleaned according to the procedures in Table 1. A characteristic difference of the impedance spectra for phosphated and coated steel with different surface pretreatments can be seen at longer exposure times when a Warburg-type impedance occurs with either slope of $-\frac{1}{2}$ or $-\frac{1}{4}$ in the Bode plot and a corresponding $\delta = 45°$ or 22.5° [*3*]. The former case is illustrated in Fig. 9 for the alkaline derusting treatment, and the latter case, which could correspond to semi-infinite diffusion in pores, can be seen in Fig. 10 for the degreased specimen. A slope of $-\frac{1}{4}$ was observed only for this specimen and the polished specimen.

Aluminum Alloys

Comparison of Surface Pretreatment Procedures for Bare Surfaces

Figure 11 shows impedance plots for Aluminum 7075 with three different pretreatments (degreased, STAB [surface treatment for aluminum bonding], conversion coating Alodine 600) and with the polymer coating without special

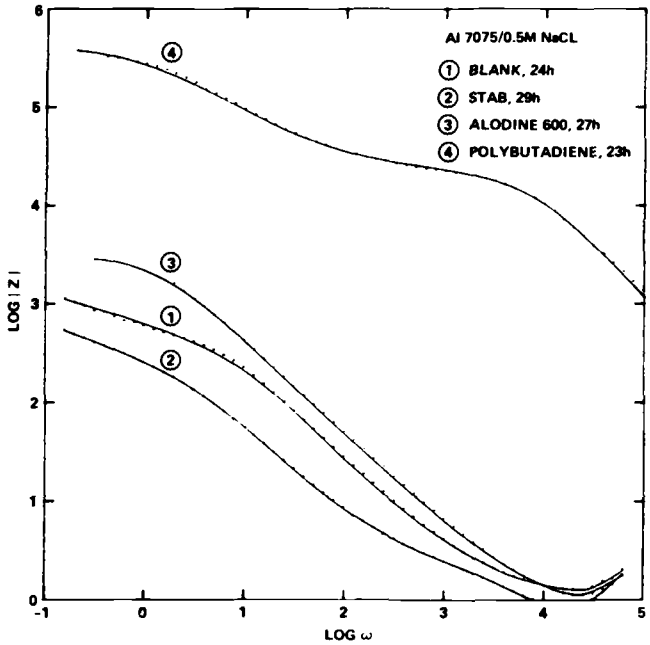


FIG. 11—*Bode plots for Aluminum 7075 for three different surface pretreatments and for a coated specimen.*

surface treatment (degreased only). The STAB treatment [*13*] consists of degreasing in acetone for 10 min, followed by immersion in 60-g/L sodium hydroxide for a time that depends on alloy composition (10 min for Aluminum 2024-T3, 30 min for Aluminum 6061-T6 and 60 min for Aluminum 7075-T6). The general shape of the impedance plots is the same as for the uncoated alloys. The conversion coating increased the corrosion resistance somewhat as can be seen by the higher low-frequency limit, while the STAB treated surface was less corrosion resistant. Similar trends have been observed for Aluminum 2024 and 6061. The coated Aluminum 7075 showed much greater corrosion resistance after similar exposure times (Fig. 11) as will be discussed in the following.

Coated Aluminum Alloys

Degreased and Coated Alloys—For all three aluminum alloys that were degreased and coated a deviation from capacitive behavior, which indicates porosity of the coating, was observed after very short immersion times, as shown in Fig. 12 for Aluminum 7075. The pore resistance R_p decreases with time. It is not entirely clear whether the impedance at lower frequencies follows Model I or II (Fig. 1). At longer times a third time constant seems to appear at about 60 kHz, the origin of which is not known at present.

The capacitance of the coating C_c was determined to be 0.38 nF/cm^2, which

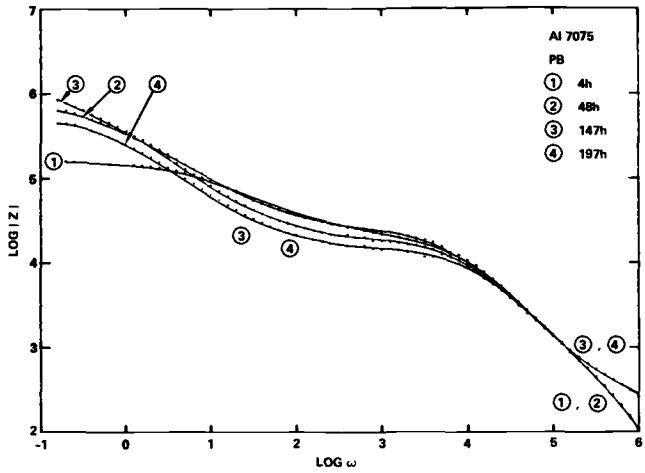


FIG. 12—*Bode plots for coated Aluminum 7075 as a function of immersion time in 0.5* N *sodium chloride.*

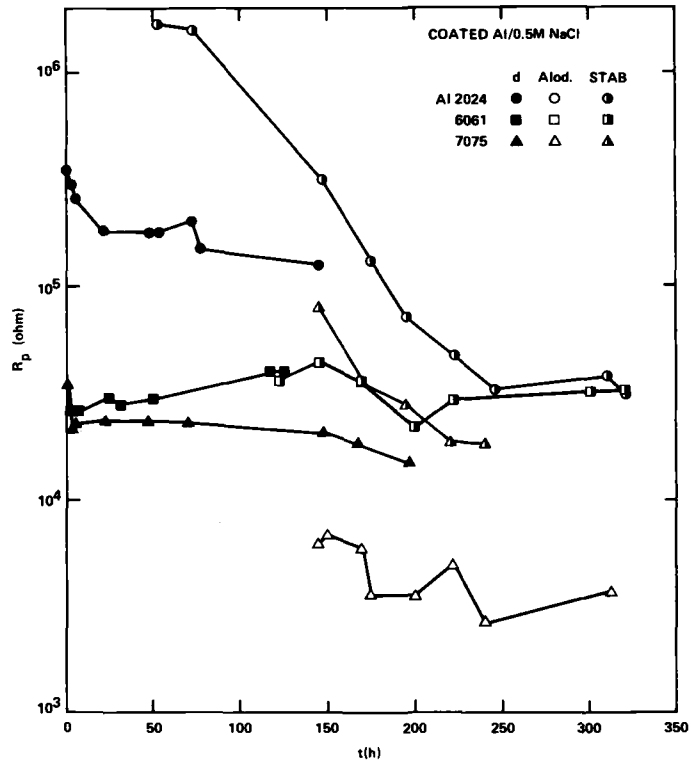


FIG. 13—*Time dependence of pore resistance* R_p *for three coated aluminum alloys with different surface pretreatments.*

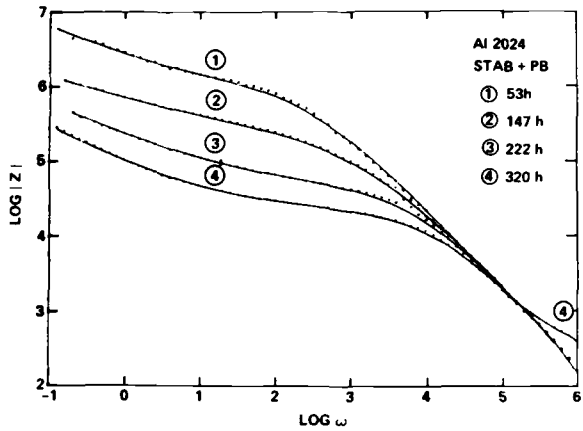


FIG. 14—*Bode plots for coated Aluminum 2024 with STAB pretreatment as a function of exposure time to 0.5* N *sodium chloride.*

corresponds to a coating thickness of about 8 μm for a dielectric constant $\epsilon = 3.5$ and did not change during the 197-h test period. A comparison of pore resistance R_p values is given for the three alloys in Fig. 13 as a function of exposure period. Coated Aluminum 2024 has R_p values that are about a factor of ten higher than those for Aluminum 6061 and 7075. For Aluminum 6061 a small increase of R_p occurs during exposure, while for the other two alloys a gradual decrease occurs.

STAB and Coated Alloys—For the Aluminum alloys that had been first subjected to STAB and then polymer coated the impedance was higher than for the corresponding alloys that were only coated. For Aluminum 2024 shown in Fig. 14, it was possible to determine the pore resistance R_p for times exceeding 53 h. These values are shown in Fig. 13, where a sharp decrease of R_p with time is indicated. A similar effect is found for Aluminum 7075. At comparable times R_p is higher for the STAB treated surface. For Aluminum 6061, corrosion resistance is very good and R_p could not be determined for the present exposure times. From the capacitance $C_c = 0.32$ nF/cm^2, which was independent of time, a coating thickness of 10 μm was estimated.

For the STAB and coated alloys a frequency dependence of the impedance between $-1/2$ or $-1/4$ was found at lower frequencies after longer exposure times. The phase angle reflects this behavior with a maximum of less than 45° at lower frequencies. A third maximum at very high frequencies is found at longer exposure times.

Alodine Treated and Coated Alloys—For Aluminum 2024 and 6061, which were first treated with the commercial conversion coating and then polymer coated γ, the corrosion resistance was so good that strictly capacitive behavior was observed for Aluminum 2024 up to 675 h and for Aluminum 6061 up to

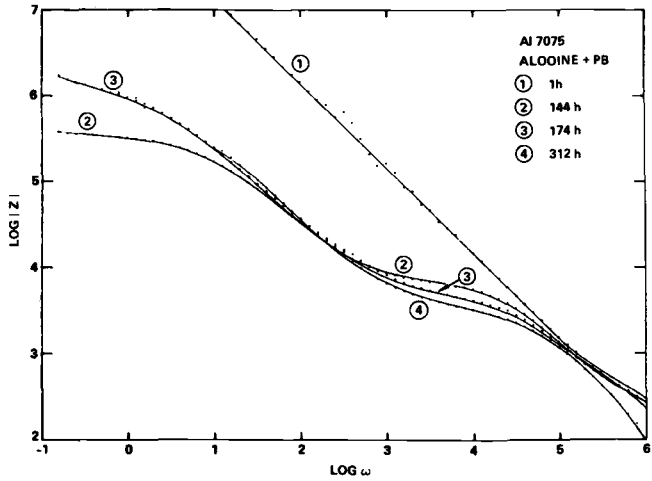


FIG. 15—*Bode plots for coated Aluminum 7075 with conversion coating pretreatment as a function of exposure time to 0.5* N *sodium chloride.*

440 h, after which time small deviations occurred. For Aluminum 7075, deviations from capacitive behavior occurred after 55 h with $R_p > 1 \times 10^7\ \Omega \cdot \text{cm}^2$. Figure 15 illustrates the behavior for Aluminum 7075 for exposure times up to 312 h. The frequency dependence of the phase angle suggests that Model I applies. After 144 h the pore resistance R_p dropped to values that are lower than those for the coated alloy without surface treatment.

Anodized Aluminum Alloys

Figure 16 gives Bode plots for chromic acid anodized (CAA) Aluminum 6061, while Fig. 17 shows the results for sulfuric acid anodized (SAA) Aluminum 6061. The impedance was first measured after 1-h immersion. As can be seen from the frequency dependence of the phase angle, at least two time constants determine the impedance behavior at 1-h exposure. This behavior reflects contributions from the porous oxide layer and the barrier layer below it. After about 500 h, an arrest of the impedance was detected at lower frequencies for CAA Aluminum 6061. After 888 h (Fig. 16), the impedance spectrum changed drastically. Several pits were observed at this time. Very little change of the impedance occurred for SAA Aluminum 6061 during the 1632-h test (Fig. 17). No pits were observed after 1632 h.

Figure 18 gives a comparison of the impedance spectra obtained for SAA and CAA Aluminum 2024. The SAA treatment was followed by sealing in dichromate and the CAA by sealing in hot water. Very little change occurred for SAA Aluminum 2024 during exposure for 300 h; no pits were observed. CAA Aluminum 2024 is apparently less corrosion resistant, and a large number of pits

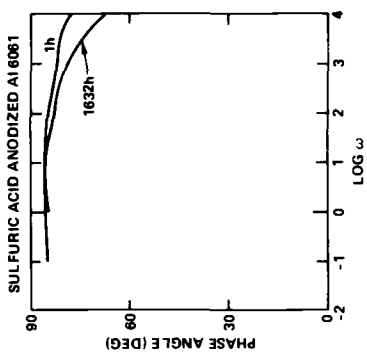


FIG. 17—*Bode plots for SAA Aluminum 6061.*

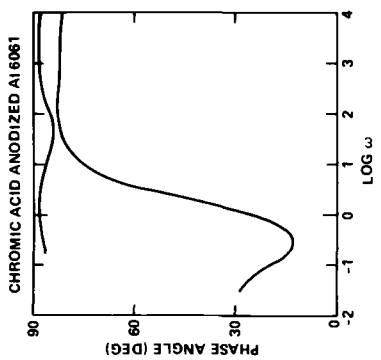


FIG. 16—*Bode plots for CAA Aluminum 6061.*

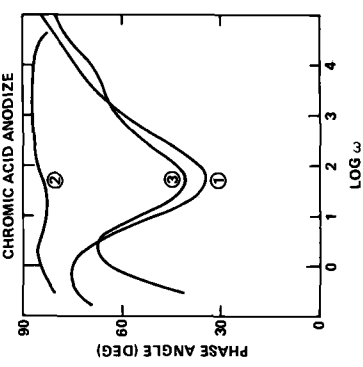


Fig. 19—*Comparison of impedance spectra CAA Aluminum 2024, 6061, and 7075.*

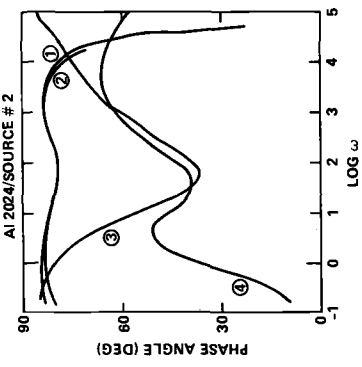


Fig. 18—*Bode plots for CAA (hot water seal) and SAA (dichromated) Aluminum 2024.*

were found at the end of the test. The ohmic behavior at about 10 Hz, which is reflected in a deep minimum of the phase angle, could be related to the porosity of the oxide layer.

A comparison of the impedance spectra for the Aluminum alloys 2024, 6061, and 7075 that were chromic acid anodized is given in Fig. 19. Significant differences occur between the less corrosion resistant CAA Aluminum 2024 and Aluminum 7075, which exhibit a deep minimum in δ, and the much more corrosion resistant CAA Aluminum 6061. These differences might be related to the different degree of sealing for these alloys.

Hoar and Wood [*14*] have proposed an electrical analog for an anodized aluminum alloy surface, which in its refined form contains three resistor capacitor (RC) circuit analogs in series representing the (partially) sealed pores (Figs. 20*a* and *b*). A Bode plot is shown in Fig. 21 for the data of Table 2 in Ref *14* and for two times of sealing. Although the Hoar and Wood model may have conceptually correct features, the experimental data obtained in the present study for two SAA Aluminum 2024 (dichromated sealing) specimens do not agree with this model with regard to the resolution of the time constants and the magnitude and frequency dependence of the impedance modulus $|Z|$. Koda et al [*15*] have determined impedance spectra for aluminum that was anodized in a 2% oxalic acid at 30°C and then sealed by immersion in hot water for different time periods up to 1 h. The equivalent circuit for the sealed surface was considered

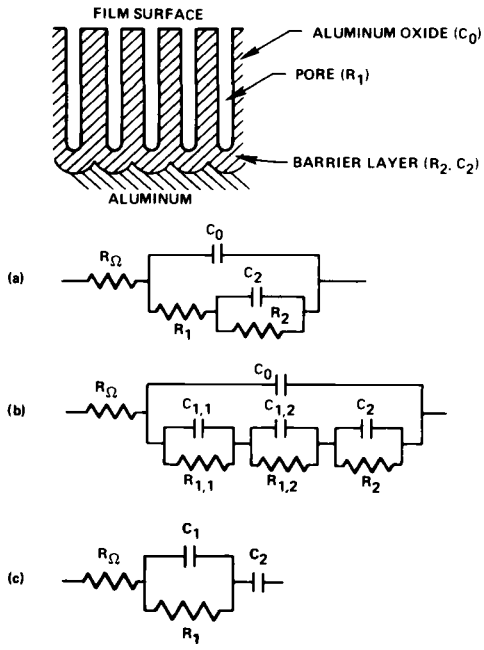


FIG. 20—*Models for impedance of anodized aluminum* [12.13].

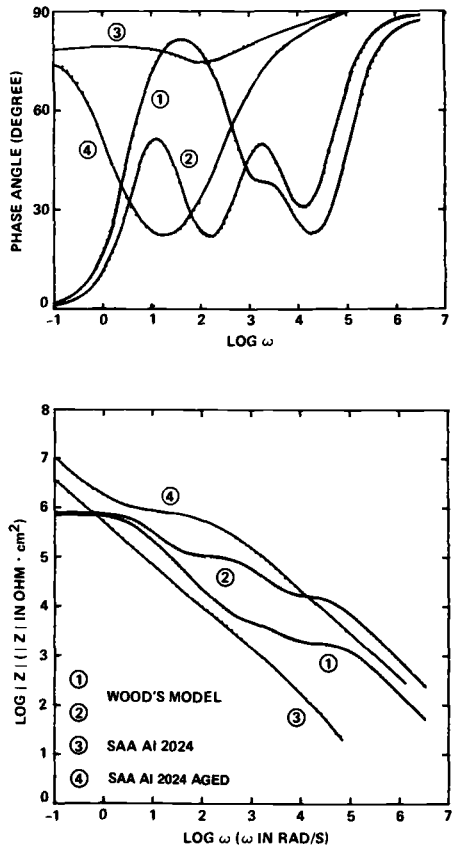


FIG. 21—*Impedance spectra for model and data by Hoar and Wood* [12] *and experimental data for SAA Aluminum 2024.*

to consist of a capacitance and a resistance in parallel, which represent the hydrous oxide film formed in the pores, and a capacitance in series, which represents the barrier layer at the bottom of the pores (Fig. 20*c*). The experimental data for CAA Aluminum 2024 that had the lowest corrosion resistance are in qualitative agreement with Koda's model.

The present analysis has been limited to a qualitative comparison of different procedures and alloys characteristics. Table 2 shows characteristic impedance parameters for 24-h exposure, which could be useful for characterizing anodized surfaces. The impedance at 1 kHz Z_{1K} is the basis of ASTM Measurement of Impedance of Anodic Coatings on Aluminum (B 457). Another parameter listed in Table 2 is the impedance Z_1 at 1 Hz in the capacitive region at low frequencies. It should be related to the properties of the porous layer. The pore resistance R_{po} has been estimated as the impedance at the minimum of the phase angle δ_{min}. Also listed in Table 2 is cot δ_{min}. No obvious correlations of these parameters

TABLE 2—*Impedance parameters for anodized aluminum alloys (24-h exposure to 0.5 N NaCl).*

Alloy	Treatment	Source Number	$Z_{1K'}$, $\Omega \cdot cm^2$	Z_1, $\Omega \cdot cm^2$	R_{po}, $\Omega \cdot cm^2$	cot δ_{min}	COR, pits/h
2024	SAA	1	300	1.70×10^5	5.9×10^3	0.15	0/300
2024	SAA	2	264	1.59×10^5	3.6×10^4	0.12	0/300
2024	SAA	3	200	1.20×10^5	3.6×10^5	0.16	0/300
2024	SAA "aged"	3	2240	1.52×10^5	1.5×10^4	1.08	...
2024	CAA	1	428	2.00×10^5	3.8×10^4	0.13	+ +/170
2024	CAA	1	330	1.87×10^5	1.7×10^4	0.17	0/100
2024	CAA	2	5140	2.89×10^5	1.3×10^5	1.23	+ +/300
6061	SAA	1	356	3.03×10^5	3.0×10^4	0.20	0/1632
6061	CAA	1	760	5.26×10^5	2.1×10^5	0.13	+/888
7075	CAA	2	8340	2.89×10^5	1.2×10^5	1.52	0/100

NOTE: CAA is followed by sealing in dichromate solutions, CCA by sealing in hot water. + = few pits. + + = many pits. 0 = no pits.

seem to exist with the corrosion behavior (COR), which is expressed as the number of pits for a given exposure time.

In the case of anodized aluminum alloys the impedance test as applied here has to be considered more as a quality control test, which shows whether a given specimen has been properly anodized and sealed, than a test that predicts the long-time corrosion behavior of such a specimen. Since the salt spray behavior of properly prepared alloys determined over a 336-h period is well known, the impedance test would be advantageous in that it results in quantitative numbers and can be carried out in only a few hours. Efforts in developing a quality control test and establishing correlations with known corrosion behavior are now being carried out in this laboratory.

The data presented here for anodized aluminum alloys show that a large wealth of information can be obtained from impedance spectra measured over a large frequency range. This is clearly an advantage over the approach of ASTM B 457 where a measurement is made at only one frequency. A revision of this standard or development of a new standard based on the approach discussed here might be a great advantage.

Summary

The results reported in this paper document that it is possible to obtain in laboratory tests that are based on the impedance technique valuable information concerning the corrosion behavior of coated metals. Since a wide frequency range is scanned in these tests, the properties of the coating, the reaction rate at the metal/coating interface, and the changes of these properties caused by interaction with the environment can be determined if the individual time constants are sufficiently separated. As more experience is obtained with the analysis of impedance data obtained for organic coatings, it should be possible to obtain more quantitative information concerning number, size, and distribution of pores and defects in the coating, water uptake, and corrosion rates at the coating/metal interface. Similar progress should be possible for phosphate and chromate conversion coatings and anodized aluminum alloys. For this latter case, a new quantitative test for the degree of sealing of the pores in the oxide is presently being developed.

Acknowledgment

This work has been performed in part under Contract N00014-79-C-0437 with the Office of Naval Research. The authors acknowledge many helpful discussions with Dr. P. Clarkin. The work on anodized aluminum alloys was carried out under the Rockwell International IR&D Program.

References

[*1*] Wolstenholm, J., *Corrosion Science*, Vol. 13, 1973, p. 321.
[*2*] Szauer, T., *Progress in Organic Coatings*, Vol. 10, 1983, p. 171.
[*3*] Mansfeld, F., Kendig, M. W., and Tsai, S., *Corrosion*, Vol. 38, 1982, p. 478.

[4] Mansfeld, F. and Kendig, M. W., "Evaluation of Protective Coating with Impedance Measurements," *Proceedings of the 9th International Conference on Metallic Corrosion*, Toronto, Canada, June 1984.
[5] Mansfeld, F., *Corrosion*, Vol. 37, 1981, p. 301.
[6] Mansfeld, F., Kendig, M. W., and Tsai, S., *Corrosion*, Vol. 38, 1982, p. 570.
[7] Kendig, M. W., Meyer, E., Lindberg, G., and Mansfeld, F., *Corrosion Science*, Vol. 23, 1983, p. 1007.
[8] Kendig, M. W., Allen, A. T., and Mansfeld, F., *Journal of the Electrochemical Society*, Vol. 131, 1984, p. 935.
[9] Scheider, W., *Journal of Physical Chemistry*, Vol. 79, 1975, p. 127.
[10] Kendig, M., Mansfeld, F., and Tsai, S., *Corrosion Science*, Vol. 23, 1983, p. 3178.
[11] Mansfeld, F., Lumsden, J. B., Jeanjaquet, S. L., and Tsai, S., *Proceedings of Corrosion Control by Organic Coatings*, H. Leidheiser, Jr., Ed., National Association of Corrosion Engineers, Houston, TX, 1981, p. 227.
[12] Leidheiser, H., Jr. and Kendig, M. W., *Corrosion*, Vol. 32, 1976, p. 69.
[13] Smith, T., *26th National SAMPE Symposium*, Houston, TX, April 1981, p. 664.
[14] Hoar, T. P. and Wood, G. C., *Electrochima Acta*, Vol. 7, 1962, p. 333.
[15] Koda, M., Takahashi, H., and Nagayama, M., *Extended Abstracts of the 34th Meeting of the International Society on Electrochemistry*, Paper 803, Erlangen, West Germany.

DISCUSSION

R. Baboian[1] (*written discussion*)—Use of impedance electrochemical tests have not gained wide use to date. Only a few select laboratories are capable of using this technique. Do you feel that, in the near future, impedance tests will become widely used in industry?

M. W. Kendig (*author's response*)—Yes, we do. There is a large interest in impedance techniques. Task groups are being set up at present in ASTM (G01.11) and NACE (T-3L) to prepare recommended practices and describe experimental procedure, respectively. The Electrochemical Society has held symposia on this subject in Denver, CO, Oct. 1981 and in New Orleans, LA, Oct. 1984.

H. Jain[2] (*written discussion*)—What are the advantages of using phase angle and $|Z|$ versus ω plots as against $Z'(G)$ and $Z''(G)$ versus ω?

C. Souvino[3] (*written discussion*)—Considering that for the same current density the temperature of the anodizing electrolyte will produce anodized film with different pore size and pore number. Did the actual tests detect the difference?

M. W. Kendig (*author's response*)—We have not studied conditions that are outside of the specifications. However, we plan to investigate this aspect.

[1]Texas Instruments, Attleboro, MA 02703.
[2]Brookhaven National Labs, Building 830, Upton, NY 11973.
[3]Emerson Electric, St. Louis, MO 63136.

Neal S. Berke[1] *and John J. Friel*[2]

Applications of Electrochemical Techniques in Screening Metallic-Coated Steels for Atmospheric Use

REFERENCE: Berke, N. S. and Friel, J. J., **"Applications of Electrochemical Techniques in Screening Metallic-Coated Steels for Atmospheric Use,"** *Laboratory Corrosion Tests and Standards, ASTM STP 866*, G. S. Haynes and R. Baboian, Eds., American Society for Testing and Materials, Philadelphia, 1985, pp. 143–158.

ABSTRACT: Electrochemical tests were conducted on several aluminum-zinc-coated steels whose long-term atmospheric corrosion resistance is known in order to evaluate such tests as a screening technique. Linear polarization resistance measurements were made in aerated 1 *N* sodium chloride and 0.5 *N* sodium sulfate both at pH 4 to rank the different coatings and then compare this ranking with that found in marine and industrial environments. Weight loss was also measured, and the specimens were examined microscopically to verify the corrosion mechanism. Cathodic polarization tests were conducted in deaerated 1 *N* hydrochloric acid and 1 *N* sulfuric acid to examine a system with only one cathodic reaction. The results obtained in the pH 4 chloride and sulfate solutions were in good general agreement with the data from atmospheric exposures. Thus polarization resistance testing in 1 *N* sodium chloride and 0.5 *N* sodium sulfate at pH 4 shows promise as a screening technique for predicting the atmospheric corrosion resistance of metallic-coated steels.

KEY WORDS: galvanic corrosion, atmospheric corrosion, polarization, electrochemical testing, linear polarization, polarization resistance, corrosion potential, Tafel slope, potentiodynamic polarization, metallic-coated steel, galvanized steel

Metallic coatings are extensively used to provide corrosion protection for steel exposed to the atmosphere. For the three principal coated steel sheet products, namely, zinc-coated (galvanized), aluminum-coated, and 55% aluminum-zinc-coated steel, data comparing their corrosion resistance in marine, rural, and industrial environments are available [*1–3*]. Although the long-term corrosion performance of the established commercial products is well known, the corrosion resistance of new products can only be predicted based on results of accelerated laboratory tests.

A large number of laboratory tests have been developed to predict the corrosion resistance of materials in atmospheric exposure. A brief review of several of the

[1]Senior research engineer, W. R. Grace and Co., 62 Whittemore Ave., Cambridge, MA 02140.
[2]Project leader, Bethlehem Steel Corp., Homer Research Labs, Bethlehem, PA 18016.

Copyright© 1985 by ASTM International www.astm.org

tests for coated structural steels was made by Campbell et al [*4*]. Even though these steels had organic coatings, several of the tests such as ASTM Salt Spray (Fog) Testing (B 117) and Deutsches Institut für Normung (DIN) Method of Test in Damp Heat Alternating Atmosphere Containing Sulfur Dioxide (DIN 50018), are used for the evaluation of metallic-coated steels. The authors of the preceding paper [*4*] noted that while the accelerated tests are usually right, there are many cases in which they are misleading. Townsend and Meitzner reported that 4% aluminum-zinc- and 7% aluminum-zinc-coated steel showed superior salt-spray resistance over zinc-coated steel. However, all the coatings performed similarly in industrial, mild marine, and rural environments [*3*]. Nevertheless, accelerated tests do play an important role in the screening of new coatings, and indeed, initial salt-spray tests showed that 55% aluminum-zinc-coated steel would have the best overall corrosion resistance of the aluminum-zinc-coated steels [*2*]. This prediction has been verified after several years of atmospheric exposure [*1,3*].

Because of discrepencies found between salt-spray and atmospheric exposure data, Bethlehem Steel has initiated several studies to develop and rate accelerated corrosion tests for metallic-coated steels. These include a standing water test to simulate water ponds on metal building roofs [*5*] and an evaluation of the Kesternich (sulfur dioxide) cabinet test, which simulates severe industrial environments [*6*]. Corrosion performance of zinc-, aluminum-, and 55% aluminum-zinc-coated steels in the standing water and Kesternich test were in qualitative agreement with observed atmospheric behavior [*5,6*].

The major aim of this work was to determine if a rapid electrochemical procedure could be developed that qualitatively predicts the relative long-term atmospheric corrosion resistance of metallic-coated steel sheet. This technique would provide a useful screening tool for the development of new coatings and for the selection of coatings for various applications.

Whereas our major goal was to develop a screening test, a secondary objective was to examine the corrosion mechanism through electrochemical testing and a study of the corrosion morphology. A close correlation between the corrosion mechanisms in the electrochemical tests and those observed in metallic-coated steels exposed to atmospheric service will add further validity to the choice of the accelerated environment. Furthermore, if the similarity of the corrosion mechanisms holds, then a new technique to examine the corrosion mechanisms in both metallic coatings and multiphase alloys will result.

Experimental Procedure

Materials

Sheet steels coated with zinc, aluminum, 5% aluminum-zinc, 7% aluminum-zinc, and 55% aluminum-zinc were used in the corrosion tests and are described in Table 1. Specimens were 16 mm in diameter and were degreased and acetone wiped. Solutions were made from distilled water and reagent grade sodium

TABLE 1—*Materials tested.*

Material	Average Coating Thickness, μm	Source
55% Al-Zn coated[a]	31	commercial (Bethlehem Steel)
G90 galvanized	26	commercial (Bethlehem Steel)
Al-coated Type 2	45	commercial (Armco Steel)
5% Al-Zn[b]	27	commercial (Nippon Steel)
5% Al-Zn[c]	32	Ziegler trial
7% Al-Zn	27	pilot line (Bethlehem Steel)
DQSK steel sheet	...	commercial (Bethlehem Steel)

[a]Galvalume® sheet steel (trademark of Bethlehem Steel Corporation).
[b]Superzinc® sheet steel (trademark of Nippon Steel).
[c]Galfan® sheet steel (trademark of the International Lead Zinc Research Organization).

sulfate, sodium chloride, sulfuric acid, and hydrochloric acid. The pH was adjusted with sulfuric acid or hydrochloric acid and measured with a Beckman pH meter. The solutions used were aerated 1 *N* sodium chloride and 0.5 *N* sulfuric acid both at pH 4, and deaerated 1 *N* hydrochloric acid and 1 *N* sulfuric acid.

Instrumentation

Electrochemical testing was performed using a microprocessor controlled potentiostat, EG&G Princeton Applied Research (PAR) 350 Corrosion Measurement System, which was described by Peterson and Siegerman [7]. A Tefzel® flat specimen holder with Kalrez® washers was utilized to expose 1.0 cm^2 of specimen surface area to the solution. Specimens were examined carefully after testing to verify that there was no leaking.

The microprocessor controlled corrosion system allowed for automated testing of specimens, but to provide for further data analysis and storage, the RS232 port of the PAR 350 was utilized to transmit data to an International Business Machines, Inc. (IBM) 3032 computer. Scanning electron microscopy (SEM) analysis was performed on an AMRAY 1600.

Tests Performed

Both linear polarization and cathodic polarization methods were used at a scan rate of 0.166 mV/s. The linear polarization tests were performed as a function of time in aerated chloride and sulfate solutions at pH 4. These solutions were chosen to determine if polarization resistance provides an accurate ranking of the performance of standard metallic-coated sheet steels in marine and industrial atmospheres. The scans began at -15 mV and ran to $+10$ mV with respect to the initial corrosion potential E_{corr}. Specimens were in solution for two days, and after mass loss was measured, they were cross sectioned, mounted, and polished in mineral spirits for metallographic observation.

Cathodic polarization was performed in nitrogen-deaerated hydrochloric acid and sulfuric acid to investigate solutions in which the only cathodic reaction is hydrogen ion reduction. The first polarization was performed after 10 min and the second one after 1 h of free corrosion. The initial applied potential was 0 mV, and the final potential was −200 mV with respect to the corrosion potential.

Data Analysis

Polarization test data were analyzed using the PAR 350 programs, which use a least-squares fit to determine the polarization resistance R_P and the cathodic Tafel slope. Further analysis was possible because the data was transferred to the mainframe computer. A regression curve-fitting routine was used to determine R_p for those cases in which the PAR unit could not calculate a value or calculated a value that did not visually appear to correspond to the current versus voltage slope at E_{corr}. Cathodic polarization data were analyzed on the IBM 3032 in a method similar to that used by Greene and Gandhi on microcomputers [*8*].

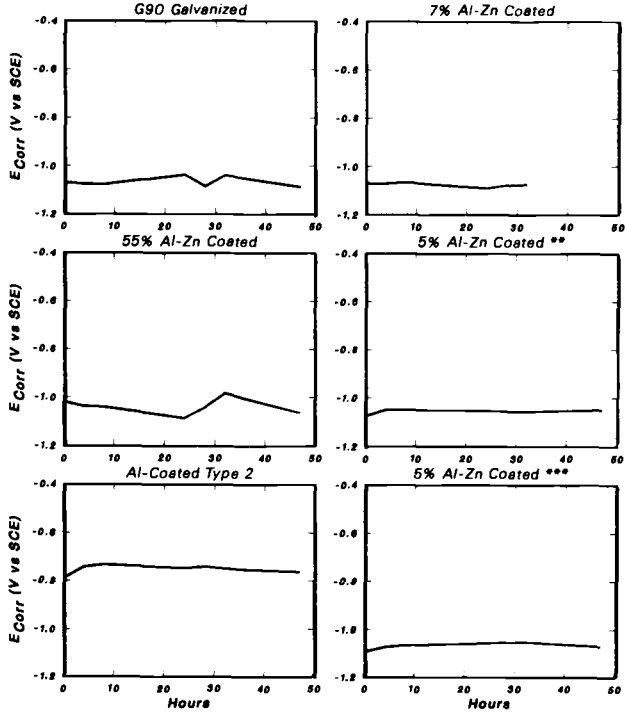


FIG. 1—*Corrosion potentials versus time for metallic-coated steels in aerated 1* N *sodium chloride at pH 4.* ** = *Superzinc and* *** = *Galfan.*

Results and Discussion

1.0 N *Sodium Chloride at pH 4*

Figure 1 shows the corrosion potentials of the metallic-coated steels in 1.0 *N* sodium chloride at pH 4. The lower potentials for the zinc containing coatings indicate that they should offer the best galvanic protection to steel at cut edges or bare spots. However, the aluminum-coated steel Type 2 is also at a potential that should protect steel, which had a potential of -612 mV_{SCE} where SCE is saturated calomel electrode in this solution. Corrosion potentials of coated steel specimens with bare steel edges were also measured, and the results are listed in Table 2. All of these coating/steel couples had potentials that were substantially lower than that of steel, and thus the coatings should be galvanically protective to steel.

The polarization resistance determined as the slope of the potential versus current polarization curve at zero current is inversely proportional to the corrosion current [*9*]. Average initial R_P values determined by using the polarization resistance routine of the PAR 350 are plotted in Fig. 2, and typical curves are shown in Figs. 3 through *5*. The higher R_P values of the aluminum-coated and 55% aluminum-zinc-coated steels indicate that they were corroding at a lower rate than were the zinc-rich coatings. The ratio of R_P values for 55% aluminum-zinc-coated steel to that of G90 galvanized steel varied from about 2 to 6, which is in good agreement with atmospheric corrosion results that showed a 2 to 4 times improvement in durability for 55% aluminum-zinc-coated steels [*1,2*]. The similarity between R_P values of 5% aluminum-zinc- and 7% aluminum-zinc-coated steel with those of galvanized steel is consistent with long-term atmospheric data showing these coatings essentially as durable as galvanized steel in marine environments [*3*].

Figure 6 shows the average mass loss of each coating after two days of corrosion and illustrates the improvement in performance when aluminum is added to the coatings. The five fold greater mass loss of the galvanized coating translates to approximately twice the coating thickness loss over that of the 55%

TABLE 2—*Corrosion potentials of 1.3 by 1.9 cm of coated steels with exposed steel edges after 5 min in 1.0* N *sodium chloride at pH 4.*

Coated Steel	E_{corr}, mV_{SCE}
G90 galvanized	−1044
Al-coated Type 2	−838
55% Al-Zn-coated	−994
5% Al-Zn-coated (Galfan®)	−1044
5% Al-Zn-coated (Superzinc®)	−1044
Bare steel	−612

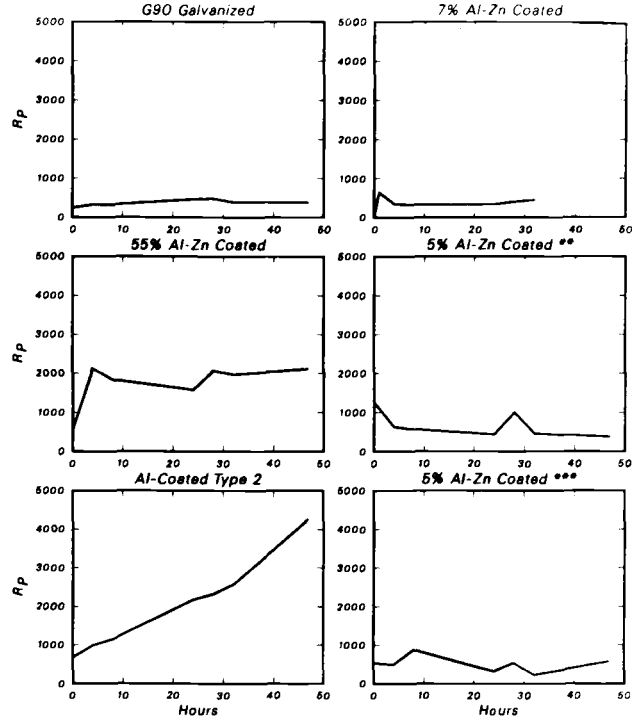


FIG. 2—*Average* R_p *versus time for metallic-coated steels in aerated 1* N *sodium chloride at pH 4.* ** = *Superzinc and* *** = *Galfan.*

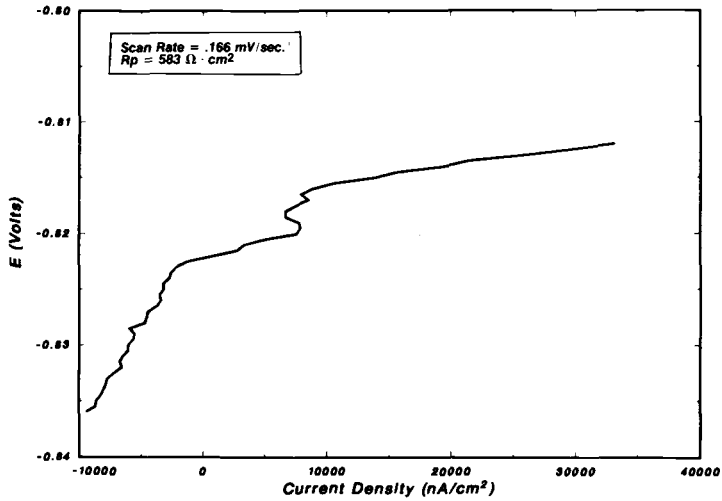


FIG. 3—*Typical linear polarization curve in aerated 1* N *sodium chloride at pH 4. Polarization resistance 55% aluminum-zinc coated.*

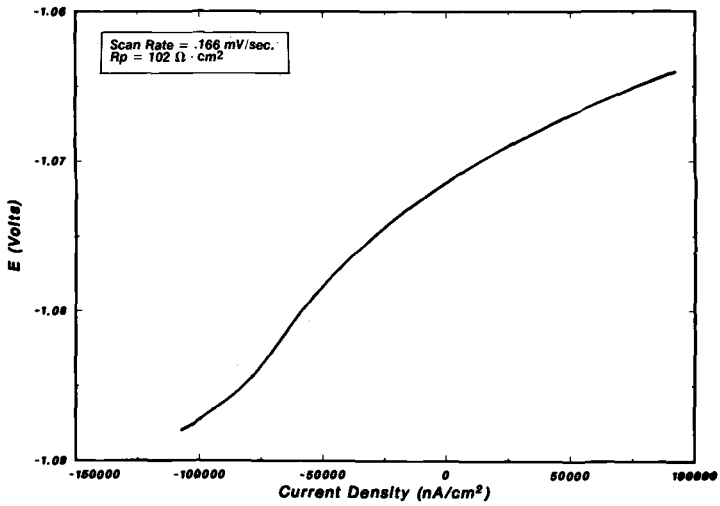


FIG. 4—*Typical linear polarization curve in 1* N *sodium chloride at pH 4. Polarization resistance G90 galvanized.*

aluminum-zinc coating based on density considerations (zinc = 7.14 g/cm^3 and 55% aluminum-zinc = 3.75 g/cm^3) and uniform corrosion in the 55% aluminum-zinc coating. This is in good agreement with reported marine environment studies [*1–3*].

The lower mass losses found for the 7% aluminum-zinc- and both 5% aluminum-zinc coated steels over galvanized steel are consistent with their per-

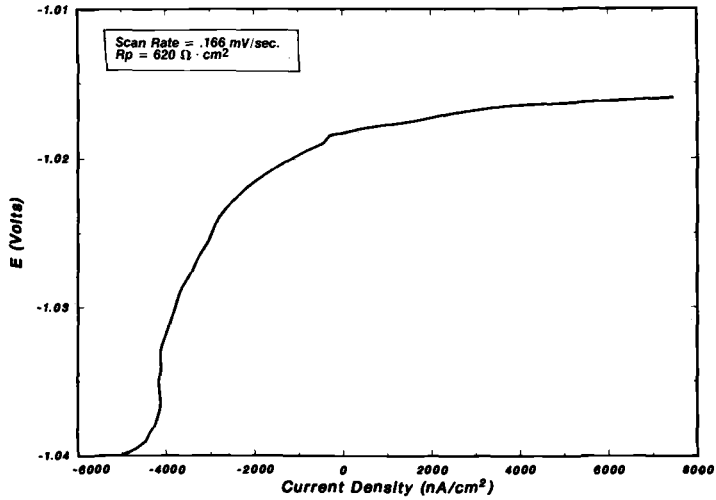


FIG. 5—*Typical linear polarization curve in aerated 1* N *sodium chloride at pH 4. Polarization resistance aluminum-coated Type 2.*

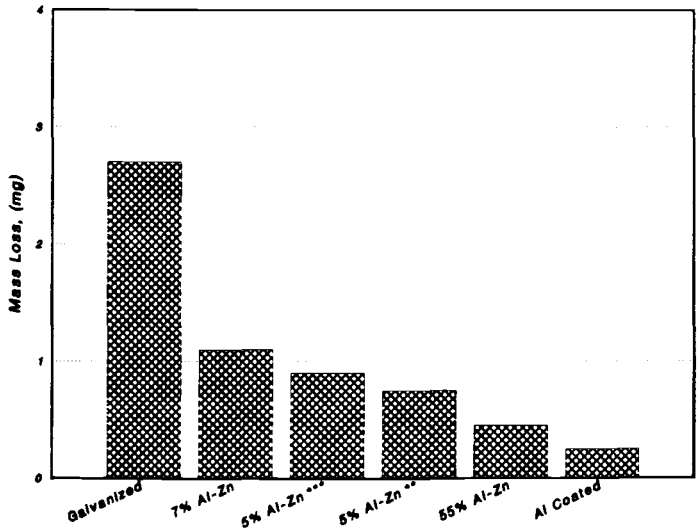


FIG. 6—*Average mass loss of metallic-coated steels in aerated 1* N *sodium chloride at pH 4 after two days.* ** = *Superzinc and* *** = *Galfan.*

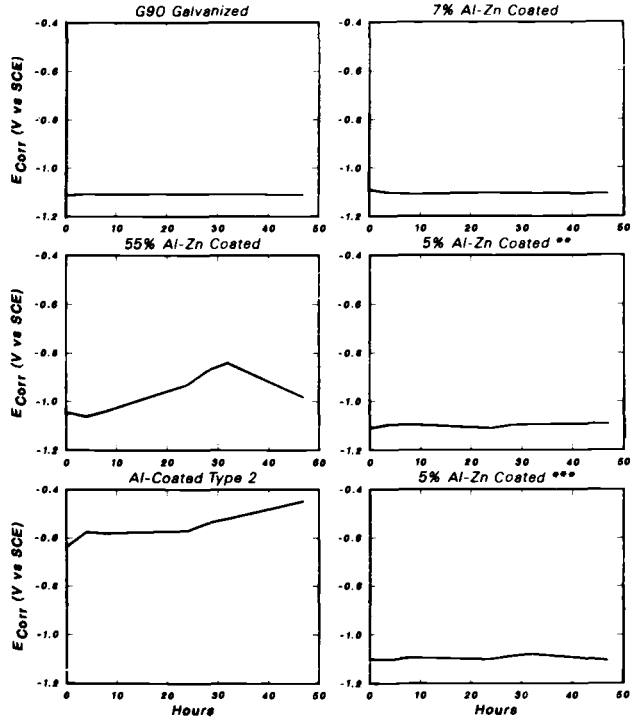


FIG. 7—*Corrosion potentials versus time for metallic-coated steels in aerated 0.5* N *sodium sulfate at pH 4.* ** = *Superzinc and* *** = *Galfan.*

formance in salt-spray tests [2] as well as their atmospheric corrosion resistance under severe marine conditions [3].

0.5 N *Sodium Sulfate at pH 4*

Corrosion potentials are shown as a function of time in Fig. 7. Only the aluminum coating exhibited potentials that are not active compared to steel, and therefore in this solution aluminum coatings would not be expected to offer galvanic protection to the steel substrate. These results agree with those found for metallic-coated steels in industrial environments [1,2,5].

Further evidence for the lack of galvanic protection of the aluminum coating is presented in Table 3. This table shows the potentials measured in this solution for coated steels with bare steel edges. The aluminum-coated steel was the only coated metal tested that does not polarize steel below its corrosion potential. The slightly higher potential of the aluminum-coated Type 2 steel over steel itself is probably due to a difference between the steel substrate in this specimen and the DQSK steel tested, and also to the aluminum-iron phases in the coating.

Aluminum-coated steel had the highest R_P values over time (Fig. 8) corresponding to the lowest corrosion rate. This is in good agreement with the long-term durability of aluminum-coated steels in industrial environments [1,2,10]. The next best performance was found for 55% aluminum-zinc-coated steel. The predominantly zinc coatings were approximately equivalent to each other, and their cumulative corrosion rate was over two times higher than that of the 55% aluminum-zinc-coated steel. This is in good agreement with long-term atmospheric studies that showed the superior durability of 55% aluminum-zinc-coated steel and essentially no difference between 4% aluminum-zinc, 7% aluminum-zinc and galvanized steels in industrial atmospheres [2,3].

Mass loss measurements after two days in solution are shown in Fig. 9. In agreement with atmospheric observations in industrial environments [1–3,5,10], the best durability is found for aluminum-coated steel followed by 55% aluminum-zinc-coated and then by the galvanized and low aluminum containing zinc-coated steels. In contrast with Kesternich test results [6] the 5% aluminum and 7% aluminum-zinc-coated steels are not more durable than galvanized steel, and this finding agrees with the long-term results recently reported by Townsend and Meitzner [3].

TABLE 3—*Corrosion potentials of 1.3 by 1.9 cm coated steels with exposed steel edges after 5 min in 0.5* N *sulfuric acid at pH 4.*

Coated Steel	E_{corr}, mV_{SCE}
G90 galvanized	−1086
Al-coated Type 2	−644
55% Al-Zn-coated	−970
5% Al-Zn-coated (Galfan®)	−1096
5% Al-Zn-coated (Superzinc®)	−1100
Bare steel	−688

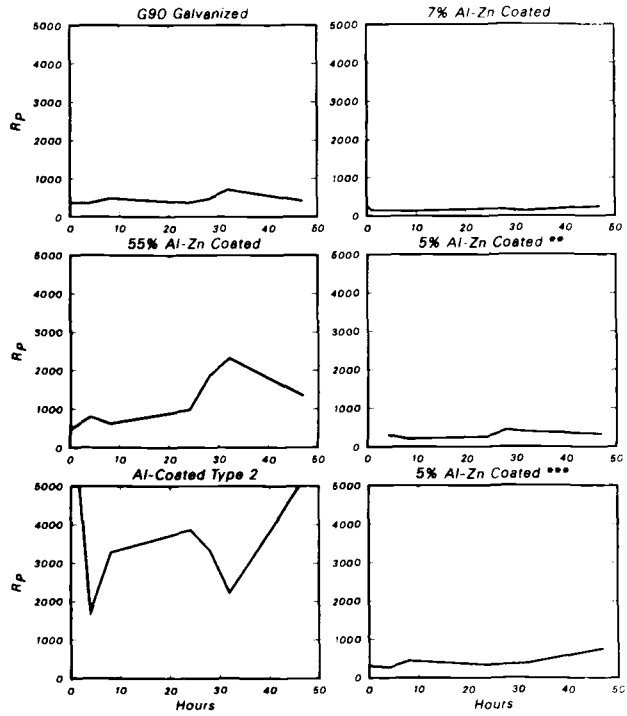


FIG. 8—*Average* R_p *versus time for metallic-coated steels in aerated 0.5* N *sodium sulfate at pH 4.* ** = *Superzinc and* *** = *Galfan.*

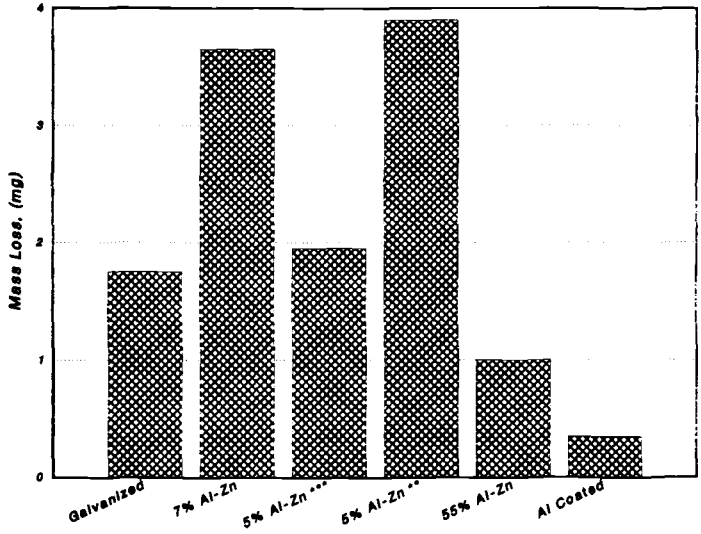


FIG. 9—*Average mass loss of metallic-coated steels in aerated 0.5* N *sodium sulfate at pH 4 after two days.* ** = *Superzinc and* *** = *Galfan.*

Microstructure

The zinc-rich coatings, including those with the 5% aluminum-zinc eutectic, corrode by general corrosion, as does aluminum-coated steel at a much slower rate. Figure 10 shows an example of G90 galvanized steel in cross section in the scanning electron microscope. The photomicrograph on the right shows an uncorroded portion of the specimen, and the one on the left shows an area of the specimen exposed to 0.5 *N* sodium sulfate for two days, during which time the electrochemical measurements were made. Figure 11 shows the microstructure of aluminum-coated steel Type 2 under the same conditions. Less thickness loss is evident in this specimen, consistent with the lower corrosion currents. Figure 12 shows the microstructure of the 55% aluminum-zinc coating also under the same conditions. Again, less thickness loss is evident than in galvanized steel, but in this case the corrosive solution preferentially attacked the zinc-rich areas. Moreover, electron microprobe analysis revealed the presence of zinc corrosion products within the interdendritic former zinc-rich areas. This corrosion mechanism is consistent with the corrosion potential measured for 55% aluminum-zinc-coated steel. A potential of about -1.0 V versus SCE is nearly as cathodic as that of galvanized steel and accounts for the galvanic protection provided by this coating. In sodium chloride solution, the microstructures were similar to those described for sulfate solution.

1 N *Hydrochloric Acid*

Typical cathodic polarization curves after 10 min in deaerated 1 *N* hydrochloric acid are shown in Fig. 13. All of the coated steels were anodic to steel.

Table 4 shows the results of analyzing the data with a curve-fitting algorithm in a method similar to that suggested by Greene and Gandhi [*8*]. The relatively

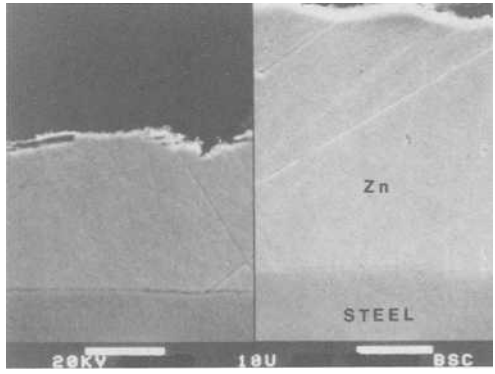


FIG. 10—*Scanning electron photomicrograph of galvanized steel in cross section. Left side shows the microstructure after exposure to 0.5* N *sodium sulfate at pH 4 for two days. Right side shows the microstructure before corrosion. Scale bar = 10*μ*m.*

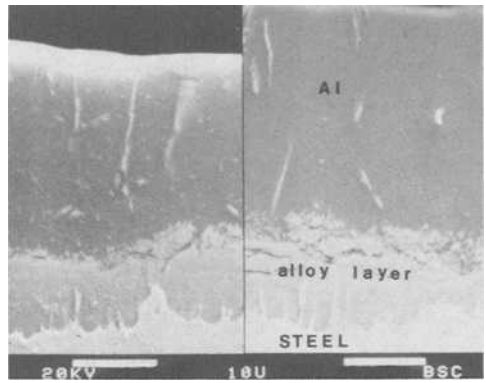


FIG. 11—*Scanning electron photomicrograph of aluminized steel in cross section. Left side shows the microstructure after exposure to 0.5* N *sodium sulfate at pH 4 for two days. Right side shows the microstructure before corrosion. Scale bar = 10* μm.

low anodic Tafel slopes B_a suggest that the coatings would cathodically protect steel. The B_a found for galvanized steel of approximately 25 mV/decade compares favorably with the value of 29.5 mV/decade found by Walker in a more mild 0.1*M* sodium chloride at pH 5.3 [*11*]. Walker also found that at pH 5.9 aluminum-killed steel had a B_a of approximately 69 mV/decade, while in 1 *N* hydrochloric acid we found a B_a of approximately 58 mV/decade.

The calculated corrosion rates I_{corr} and simple extrapolations back to the corrosion potentials given in Table 4 indicated that 55% aluminum-zinc and 5% aluminum-zinc were the most durable followed by aluminum-coated and then galvanized steel. In particular the galvanized steel had a corrosion rate two to three orders of magnitude higher than that of the other materials. These results are not in agreement with long-term data in marine environments [*1–3,10*] and

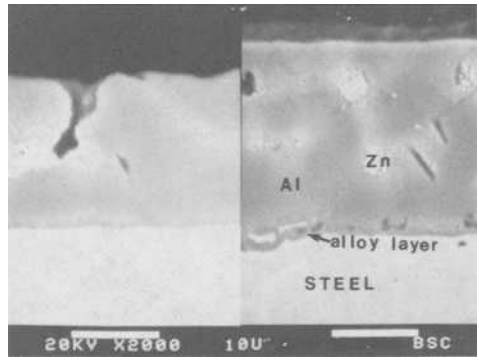


FIG. 12—*Scanning electron photomicrograph of the 55% aluminum-zinc coating in cross section. Left side shows the microstructure after exposure to 0.5* N *sodium sulfate at pH 4 for two days. Right side shows the microstructure before corrosion. Scale bar = 10* μm.

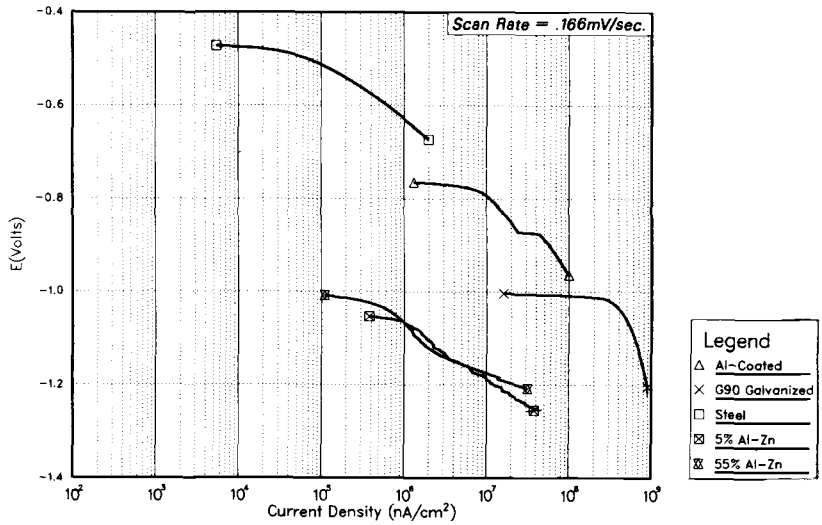


FIG. 13—*Typical cathodic polarization curves in deaerated 1* N *hydrochloric acid.*

thus indicate that deaerated 1 *N* hydrochloric acid is not a good choice of solution for screening tests. Inasmuch as the hydrogen ion reduction reaction is not common on coated steels exposed to marine atmospheres, this lack of agreement is reasonable.

1 N *Sulfuric Acid*

Cathodic polarization curves in deaerated 1 *N* sulfuric acid are shown in Fig. 14 and summarized in Table 5. The aluminum-coated steel had the lowest corrosion rate, followed by 55% aluminum-zinc and 5% aluminum-zinc-coated.

TABLE 4—*Cathodic polarization results in 1* N *hydrochloric acid (after 10 min in solution).*[a]

Specimen	E_{corr}, mV_{SCE}	B_c, mV_{decade}	B_a, mV_{decade}	I_{corr}, $\mu A/cm^2$
Al-coated Type 2	−764	213	26.6	7 797
Al-coated Type 2	−768	160	6.84	8 448
55% Al-Zn-coated	−1008	212	46.8	539
55% Al-Zn-coated	−1004	145	53.1	3 594
G90 galvanized	−1004	378	26.1	353 372
G90 galvanized	−976	232	24.6	445 408
5% Al-Zn (Superzinc®)	−1054	961	4.13	846
5% Al-Zn (Superzinc®)	−1054	107	7.62	836
Steel	−472	111	58.6	490
Steel	−482	131	66.5	277

[a] B_c and B_a are the cathodic and anodic Tafel/constants. E_{corr} and I_{corr} are the corrosion potential and calculated corrosion current calculated from 201 potential/current pairs. Individual replicates are shown.

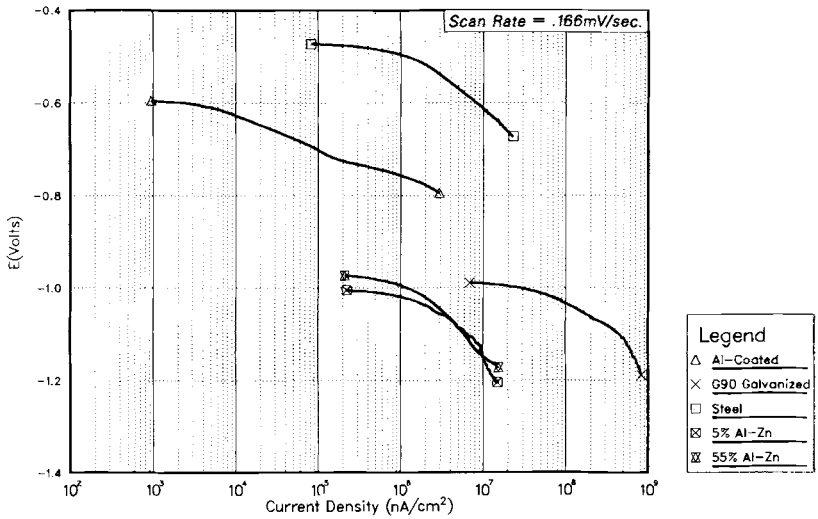


FIG. 14—*Typical cathodic polarization curves in deaerated 1* N *sulfuric acid.*

The G90 galvanized steel had by far the highest corrosion rate. The lower corrosion rate of the 5% aluminum-zinc-coated steel over G90 galvanized steel was not expected based on atmospheric experience [*3*] in industrial environments. This result might be related to the severity of the sulfuric acid and mimics the improved performance of 5% aluminum-zinc-coated steels in the Kesternich cabinet [*6*].

Examination of the calculated B_a values in Table 5 shows that the aluminum coating does not galvanically protect steel since the steel would still be rapidly

TABLE 5—*Cathodic polarization results in sulfuric acid (after 10 min in solution).*[a]

Specimen	E_{corr}, mV_{SCE}	B_c, mV_{decade}	B_a, mV_{decade}	I_{corr}, $\mu A/cm^2$
Al-coated Type 2	−594	73.9	28.0	3.79
Al-coated Type 2	−614	85.0	20.1	6.39
55% Al-Zn-coated	−972	169	57.7	1 118
55% Al-Zn-coated	−970	173	50.1	2 661
55% Al-Zn-coated	−972	176	78.5	3 026
55% Al-Zn-coated	−970	148	57.9	2 701
55% Al-Zn-coated	−970	170	64.5	1 075
55% Al-Zn-coated	−962	191	50.6	1 618
55% Al-Zn-coated	−956	205	59.8	1 680
G90 galvanized	−988	98.3	41.0	353 845
G90 galvanized	−992	124	44.2	208 206
5% Al-Zn (Superzinc®)	−1004	136	49.1	1 319
5% Al-Zn (Superzinc®)	−1008	115	56.8	1 281
Steel	−472	167	108	1 360
Steel	−492	128	37.4	1 376

[a] B_c and B_a are the cathodic and anodic Tafel/constants. E_{corr} and I_{corr} are the corrosion potential and corrosion current calculated from 201 potential/current pairs. Individual replicates are shown.

corroding where the aluminum anode curve intersects the steel cathode curve. For the other coatings tested, the extrapolated anode curves would intersect the steel cathode curve in a region where the steel is not corroding. The above analysis is based on equal areas of bare steel and coated steel. If the coated area to bare area is large, as in the case of scratches, the intersections of the different coating anode curves and steel cathode curve would occur at more active potentials.

The preceding analysis used Tafel slopes derived using an algorithm [*9*] for fitting the applied current, I to the equation, $I = I_{corr} \exp(\Delta E/B_a - \Delta E/B_c)$. Values for iron found by Milam et al [*12*] and Molten and Myers [*13*] were B_a = 40 to 78 mV/decade and B_c = 100 mV/decade, E_{corr} = −509 to −514 mV_{SCE}, and a corrosion current I_{corr} = 90 to 120 $\mu A/cm^2$ in 1 *N* sulfuric acid. The values in Table 5 for steel compare favorably with these values considering the differences between steel and iron and the higher corrosion potential of steel. Thus, Greene and Gandhi's method [*8*] appears promising when single cathode and single anode reactions are occurring.

Conclusions

Comparisons of our electrochemical tests with those from long-term atmospheric tests showed that:

- Corrosion potential measurements in aerated pH 4 chloride and sulfate solutions can be used to rank aluminum-zinc coatings in terms of their galvanic protection of steel.
- Relative corrosion rates determined by polarization resistance and mass loss of the coatings in aerated pH 4 chloride and sulfate solutions are in general agreement with those observed in long-term marine and industrial exposures.
- Corrosion rates in 1 *N* hydrochloric acid and 1 *N* sulfuric acid are exaggerated for the zinc coating.

Therefore, linear polarization testing in aerated pH 4 solutions shows promise as a screening tool for predicting the relative long-term atmospheric corrosion performance of metallic coated steels.

Acknowledgments

The authors wish to acknowledge J. A. Moravek for preparing the specimens and J. F. Hart for carrying out the experiments and the computer data reduction. We also wish to acknowledge J. Tiers for his assistance in transferring the data to the mainframe computer.

References

[*1*] Townsend, H. E. and Zoccola, J. C., *Materials Performance*, Vol. 18, No. 10, Oct. 1979, p. 13.

[*2*] Zoccola, J. C., Townsend, H. E., Borzillo, A. R., and Horton, J. B., "Atmospheric Corrosion

Behavior of Aluminum-Zinc Alloy-Coated Steel," *Atmospheric Factors Affecting the Corrosion of Engineering Metals, STP 646*, American Society for Testing and Materials, Philadelphia, 1978, pp. 165–184.

[3] Townsend, H. E. and Meitzner, C. F., *Materials Performance*, Vol. 22, No. 1, Jan. 1983, p. 54.

[4] Campbell, P. G., Martin, J. W., and McKnight, M. E., "Short-term Evaluation Procedures for Coatings on Structural Steel," NBS Technical Note 1149, National Bureau of Standards, 1981.

[5] Allegra, L., Berke, N. S., and Townsend, H. E., "Resistance of Galvanized, Aluminum-Coated and 55% Al-Zn Coated Steel Sheet to Atmospheric Corrosion Involving Standing Water," *Atmospheric Corrosion*, John Wiley and Sons, Inc., New York, 1982, pp. 595–606.

[6] Berke, N. S. and Townsend, H. E., "Comparison of Kesternich SO_2 Test with Industrial Atmospheric Corrosion Tests of Zinc-, Aluminum- and Al-Zn-Coated Steel Sheet," *Journal of Testing and Evaluation*, Vol. 13, No. 1, Jan. 1985, p. 74.

[7] Peterson, W. M. and Siegerman, H., "A Microprocessor-Based Corrosion Measurement System," *Electrochemical Corrosion Testing, STP 727*, American Society for Testing and Materials, Philadelphia, 1981, pp. 390–406.

[8] Green, N. D. and Gandhi, R. H., *Materials Performance*, Vol. 21, No. 7, July 1982, p. 34.

[9] Stern, M. and Geary, A. J., *Journal of the Electrochemical Society*, Vol. 105, 1958, p. 638.

[10] Lawson, H. H., "Atmospheric Corrosion of Aluminum-Coated Steels," *Atmospheric Corrosion*, W. H. Ailor, Ed., John Wiley and Sonce, Inc., New York, 1982, pp. 575–93.

[11] Walker, G. W., *Corrosion Science*, Vol. 16, 1976, p. 573.

[12] Milam, E. E., Crow, W. B., and Myers, J. R., *Corrosion*, Vol. 33, 1977, p. 240.

[13] Molten, M. M. and Myers, J. R., *Corrosion*, Vol. 24, 1968, p. 197.

DISCUSSION

R. A. Corbett[1] (*written discussion*)—If the corrosion resistance of aluminum and aluminum alloys in chloride solutions is superior to galvanized or zinc coatings, what do you attribute the greater corrosion resistance of 5% aluminum-zinc compared to 7% aluminum-zinc alloys?

N. S. Berke (*author's closure*)—The 5% aluminum-zinc-coated steel was commercially produced versus the 7% aluminum-zinc-coated steel, which was produced on a pilot line. The finer microstructure in the 5% aluminum-zinc coating might be the reason for the better performance. Also since both zinc and aluminum corrode in the chloride solutions, the difference of only 2% aluminum might not have an effect large enough to offset the better coatings produced on commercial hot-dip lines.

[1]E. I. Dupont Co., Engineering Department, Wilmington, DE 19898.

Shigeru Suga[1]

Development of a Fluorescent Ultraviolet and Condensation Apparatus with a Light Energy Control System

REFERENCE: Suga, S., **"Development of a Fluorescent Ultraviolet and Condensation Apparatus with a Light Energy Control System,"** *Laboratory Corrosion Tests and Standards, ASTM STP 866*, G. S. Haynes and R. Baboian, Eds., American Society for Testing and Materials, Philadelphia, 1985, pp. 159–166.

ABSTRACT: In order to improve the reproducibility of the alternate fluorescent ultraviolet (UV) and condensation test specified in ASTM Recommended Practice for Operating Light- and Water-Exposure Apparatus (Fluorescent UV-Condensation Type) for Exposure of Nonmetallic Materials (G 53) the following modifications have been developed for the test apparatus: (1) fluorescent UV lamps are preconditioned and equipped with means to yield a stable radiant output during operational life; (2) all of the eight lamps that have been preconditioned and have similar characteristics in radiant output are installed in the apparatus at the same time; and (3) the lamp spacing and arrangement is modified and the light intensity is automatically controlled. By providing uniform distribution of irradiance with a constant level throughout the test period, these modifications improve the reproducibility of the test, increase acceleration, and facilitate operation.

KEY WORDS: corrosion, irradiance, condensation tests, exposure test

The alternate fluorescent ultraviolet (UV) light- and condensation exposure test specified in ASTM Recommended Practice for Operating Light- and Water-Exposure Apparatus (Fluorescent UV-Condensation Type) for Exposure of Nonmetallic Materials (G 53) is widely used for rapidly evaluating the physical deterioration of paint coatings, such as cracking, checking, and so forth, and is also used as a screening test for the fastness of plastics to light. However, there are papers which report that the reproducibility of the test is poor. Furukawa and his colleagues have demonstrated that the range of exposure hours in a fluorescent UV and condensation apparatus (FUCA) corresponding to an outdoor exposure (at Hiroshima, Japan) was large (Fig. 1), based on initiation of clear cracks on metallic pigmented paint coatings [*1*]. Epps and Pepenich [*2*] have also suggested that there was a large position to position variation in the FUCA

[1]Vice-president, Suga Test Instruments Co., Ltd., 4–14, Shinjuku 5-chome, Shinjuku-ku, Tokyo, Japan.

Copyright© 1985 by ASTM International www.astm.org

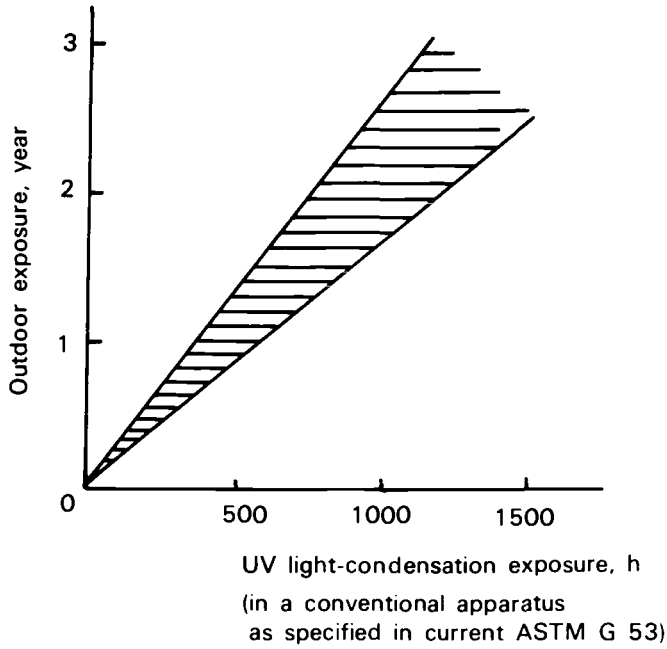


FIG. 1—*Correlation on degradation of metallic pigmented coating.*

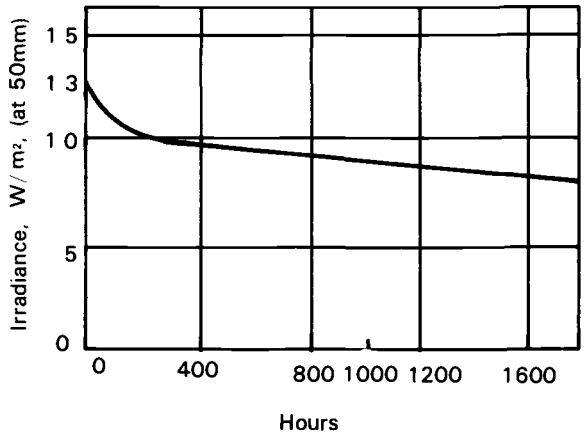


FIG. 2—*Change in irradiance of a single commercial fluorescent UV lamp because of use.*

in their experiment. One of the prime reasons for such a variation is the problem of light energy. The specifications for the apparatus and its operation are described in ASTM G 53. These specifications should be changed to improve reproducibility of the FUCA. This paper describes the problems (limited to the light energy) in the FUCA specified in ASTM G 53 (hereafter referred to as conventional FUCA) and improvements to the FUCA.

Problems with the Conventional FUCA

The fluorescent UV lamp, like all gas charged lamps, has a progressive drop in radiant output with continued use, including a large drop during early use. There is also a difference in the amount of radiant output among lamps. Figure 2 illustrates the decrease of irradiance from a single lamp, as specified in ASTM G 53, showing a reduction to 60% of the initial value after 1600 of use, which was almost identical to that described in ASTM G 53. The position to position variation in irradiance is great. In particular the irradiance at the top and bottom positions is considerably less than that of the middle positions.

In order to minimize these undersirable effects, ASTM G 53 specifies a rotation method for the eight lamps. However the conventional FUCA using this method does not provide uniform distribution of irradiance on a sample as shown in Fig.

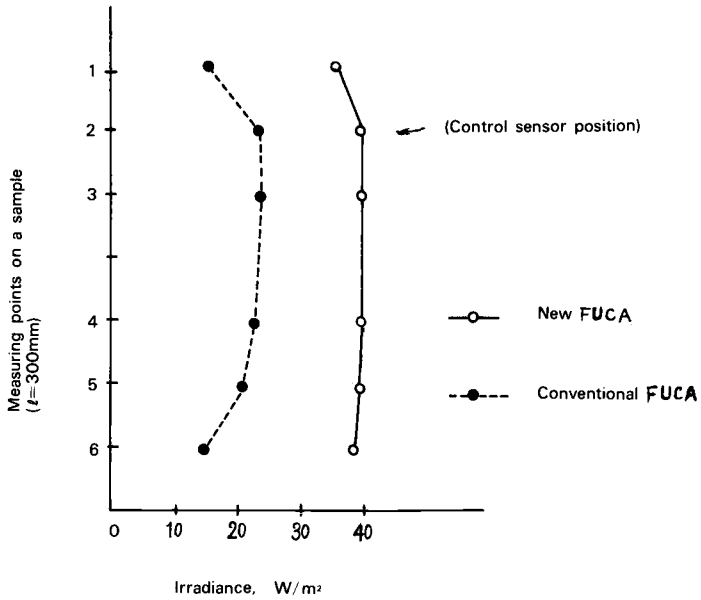


FIG. 3—*Irradiance related to six points on a sample* (l = *300 mm*).

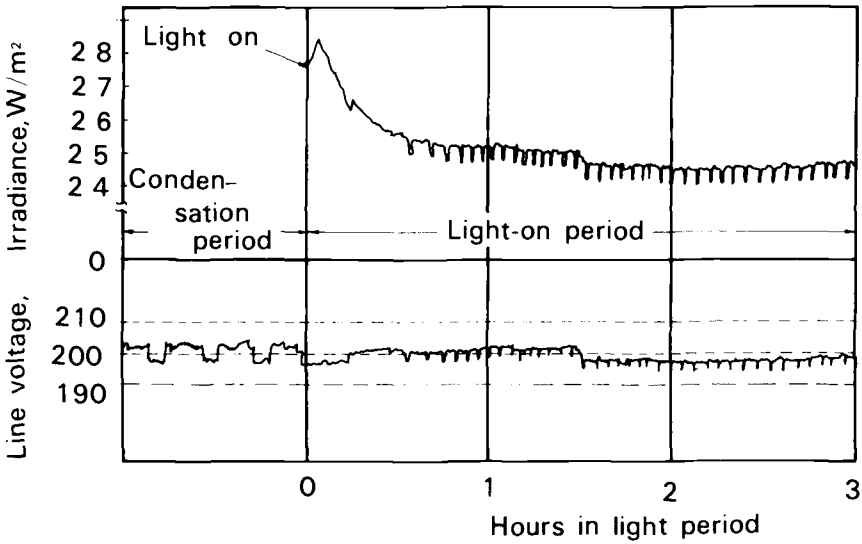


FIG. 4—*Change in irradiance because of change in line voltage in a nonenergy-controlled apparatus.*

3. Furthermore, the irradiance varies when the lamps are turned on just after the exchange from the condensation period to the "light-on" period and also fluctuates because of changes in line voltage and On-Off operation of electric heaters. Figure 4 shows data on the irradiance at a sample plane recorded when all eight lamps are operated as specified in the test method. The measurement of irradiance was conducted with a radiometer whose light receptor consisted of a silicon photocell and filter having response to the wavelength of 270 through 700 nm. The factors mentioned above made it difficult to obtain good reproducibility and repeatability. In order to eliminate these variations, it is necessary to continuously maintain the irradiance at a constant level throughout a test period.

Modifications

Fluorescent UV Lamp

The rapid drop in radiant output of a fluorescent lamp at an early stage of use is caused by the vapor of the electrodes more rapidly accumulating on the inner wall of a fluorescent UV lamp tube at an electric discharge. To avoid this, lamps were preconditioned by placing two pairs of permanent magnets (total four magnets), meaning the two ends of the electrodes, as illustrated in Fig. 5, and aging for 20 h. Magnets with a magnetic flux density of 0.25T are suitable for preconditioning. Two smaller magnets of 0.11T were then placed on both ends of a preconditioned lamp in a similar manner.

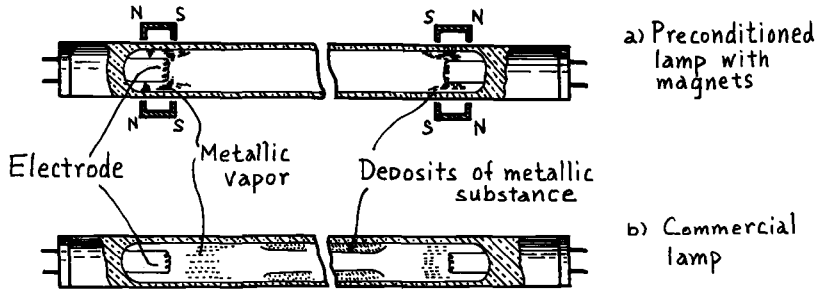


FIG. 5—*Fluorescent UV lamp.*

Preconditioned lamps equipped with magnets showed less drop in radiant output throughout their operational lives. They also yielded a higher radiant output of higher level.

The preconditioned lamps are divided into groups with a similar radiant output performance; eight lamps with similar performance characteristics are then mounted in the new apparatus at the same time, instead of relying on the rotation method.

Lamp Spacing and Arrangement

ASTM G 53 specifies that the lamps shall be placed in two banks of four lamps each to provide uniform distribution of irradiance, that lamp spacing shall be at 70-mm centers, and that the distance between test surface and the nearest surface of the lamp shall be 50 mm, as shown in (Fig. 6).

However, our experiments and other studies showed large variations of irradiance, position to position, in the conventional FUCA specified in the standard. This stationary arrangement of lamps is questionable for ensuring uniform distribution of irradiance; a preferable arrangement might be a rotating rack method.

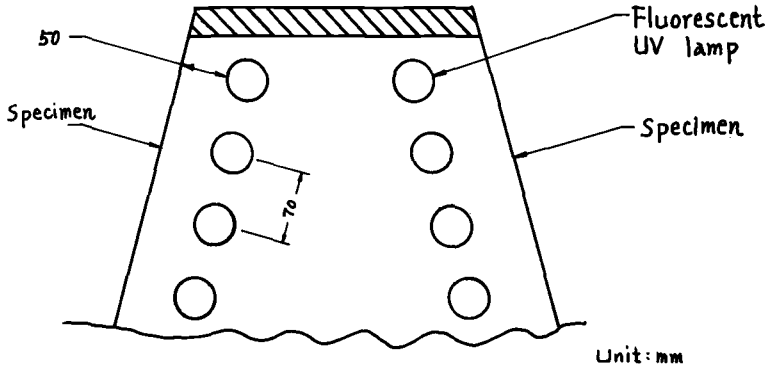


FIG. 6—*FUCA, schematic section (ASTM G 53).*

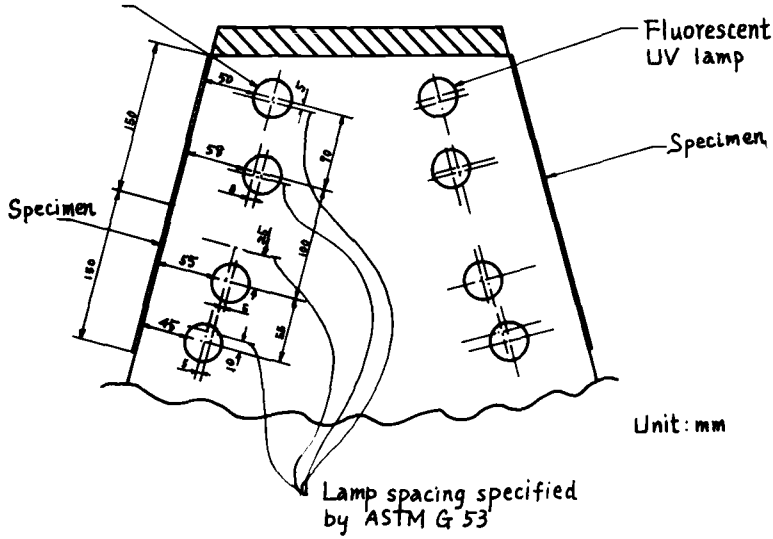


FIG. 7—*New FUCA, schematic section.*

Our study was limited to the stationary arrangement described in ASTM G 53. However, in order to improve the unbalanced irradiance, we mounted the lamps in two banks of four each as specified but modified the spacing between the parallel lamps. The distance between the lamps in either bank and the test surface was also modified so that all the test surfaces were uniformly irradiated, when the eight preconditioned lamps were mounted at the same time. The optimum spacing and arrangement of lamps determined in our studies is shown in Fig. 7. It reduces the position to position variation of irradiance (Fig. 3).

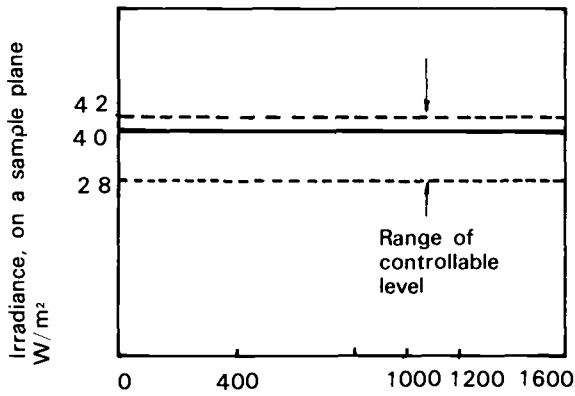


FIG. 8—*Irradiance on a sample in new apparatus when eight lamps are turned on.*

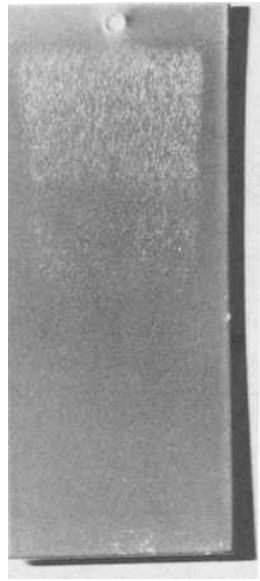


FIG. 9—*Appearance of metallic pigmented paint coatings exposed in conventional FUCA for 400 h.*

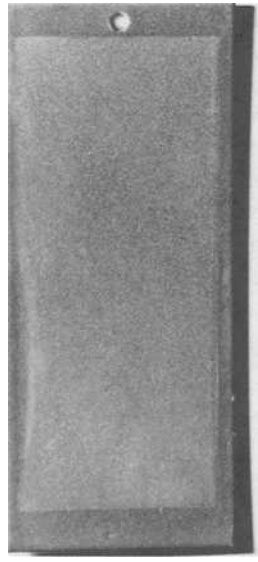


FIG. 10—*Appearance of metallic pigmented paint coatings exposed in new FUCA for 400 h.*

Automatic Control of Irradiance

When the irradiance is measured for control, it should be detected at the plane of the test surface. An automatic system for controlling the irradiance was designed such that the radiation is received by a photo sensor at a sample plane. The input power to the lamp is automatically controlled according to the change in irradiance detected so as to hold a specific level of radiant energy on the sample plane throughout the test period. The irradiance can be set to a desired level within 28 to 42 W/m^2 at the wavelength of 270 to 700 nm, with the level monitored on a digital panel meter or a strip-chart recorder during the test. The level of irradiance to be utilized determines the operational life of the lamps. It can allow 1600 h at 30 W/m^2 or 1000 h at 40 W/m^2. A higher level of irradiance contributes to a more accelerated test. In our experiments, it was confirmed that the spectral energy distribution did not significantly change throughout the operational life.

This automatic control system, together with improved lamp spacing and arrangement, made it possible to maintain a given constant level of irradiance on the samples throughout the test period (Fig. 8). Figures 9 and 10 show the appearance of paint coatings exposed for 400 h in the conventional FUCA and the new apparatus, respectively. The sample exposed in the new apparatus shows that it received uniformly distributed radiation over its whole area.

Conclusion

In order to evaluate test results correctly, one should have a test apparatus that gives repeatable test results without position to position variation. The new FUCA can provide reproducible and repeatable test results, greater acceleration, and easier operation, as summarized below.

1. The automatic control system for irradiance (in W/m^2) and the improved arrangement of lamps minimize the hours to hours and position to position variation in irradiance on sample planes, resulting in improved reproducibility.
2. The modified lamps provide high and stable radiant output throughout their operational life, resulting in acceleration of the test.
3. The level of the irradiance can be varied within specific ranges.
4. Mounting all eight lamps at the same time avoids the replacements that must be conducted every 400 h in a conventional FUCA. These modifications should contribute to the increased reproducibility of the test procedure in ASTM G 53.

References

[1] Furukawa, T., Tanimoto, Y., and Takano, M., "Accelerated Weathering Test of Coating," *Automobile Engineering (Japan)*, Vol. 36, No. 11, 1982, p. 1155.
[2] Epps, H. H. and Perenich, T. A., *Textile Chemist and Colorist*, Vol. 15, No. 6, June 1983, p. 109.

Laboratory Tests for Specific Environments

Kate Nielsen[1]

Corrosion Testing in Potable Water

REFERENCE: Nielsen, K., **"Corrosion Testing in Potable Water,"** *Laboratory Corrosion Tests and Standards, ASTM STP 866,* G. S. Haynes and R. Baboian, Eds., American Society for Testing and Materials, Philadelphia, 1985, pp. 169–183.

ABSTRACT: Corrosion in potable water varies greatly depending upon the water composition. The most important factors are oxygen content, pH value, temporary hardness, chloride, sulfate, and conductivity. To be able to carry out tests of corrosion resistance, thorough knowledge of corrosion processes of the individual metals and alloys in supply water is required. This is important in order to identify the most deleterious combinations of the relevant factors. Testing must take place as a combination of field tests and laboratory tests. Not only methods for testing materials are required in the efforts to prevent corrosion but also methods for testing water types. The actual corrosion also depends on design and performance of the individual parts and the complete pipe system. Where it is not possible to control the corrosion, easy replacement of the pipes must be ensured. An account is given of corrosion and corrosion testing of the commonly used materials galvanized steel, copper, and brass and of soldering metals, also in relation to metal pickup. This paper reviews the use of test methods to control different corrosion types in tap water systems and describes recent developments in this field at the Danish Corrosion Centre.

KEY WORDS: corrosion, tests, potable water, metals, pitting, dezincification, corrosion fatigue, erosion corrosion, field tests, copper, brasses, general corrosion, passive film, metal pickup, metal contamination, water composition, synthetic water, galvanized steel, solder metal, brazing metal

Supply water is a corrosive medium varying greatly from place to place. Individual metals and alloys may have very good corrosion resistance in some waters, and are quite unacceptable in others with corrosion rates up to 3 mm/year [*1–7*] (Deutsches Institut für Normung [DIN] 50930). The purpose of this paper is to illuminate the capabilities and limitations of corrosion testing of metals in the laboratory and to describe corrosion in potable water.

The Influence of Water Composition

Tests and standards are instruments in the control of corrosion. Treatment of the water to some minimum level is usually necessary for corrosion control since it is not otherwise possible to achieve the desirable lifetime of the construction materials (galvanized steel, copper, copper alloys, and so forth) and discoloration of the water may occur. Therefore only water that fulfills the general minimum

[1]Senior research engineer, The Danish Concrete Centre, Park Allí 345, 2600 Gostrup, Denmark.

Copyright© 1985 by ASTM International www.astm.org

requirements set by the authorities [*8*] is of interest when examining the corrosion behavior of metals in potable water.

Even though corrosion control is one of the main reasons for setting requirements for water composition, their fulfillment does not ensure that the water is not corrosive for commonly used construction materials [*1*,*9*]. The minimum requirements prevent a heavy attack of general corrosion for several metals but do not necessarily ensure the formation of passive layers fully resistant against localized corrosion.

Potable water contains oxygen, and the carbonate content is, for many metals, important in the formation of protective layers [*10*]. Furthermore, the water should be calcium carbonate precipitating so that a reasonable minimum requirement for drinking water could be

$$\begin{aligned} \text{pH} &> 7.0 \\ (HCO_3^-) &> 1 \text{ mol/m}^3 \\ (Ca^{++}) &> 0.5 \text{ mol/m}^3 \\ \Delta\text{pH} &= 0 \text{ to } 0.3 \end{aligned}$$

where the saturation index ΔpH is the difference between the observed pH and the pH for the same water in a calcium carbonate to carbon dioxide equilibrium.

While some of the salts in the water are advantageous for the formation of protective layers, for example, phosphates and silicates, others are disruptive. Generally chlorides, sulfates, and nitrates promote corrosion though each in its own special way (DIN 50930 and Refs *1*, *6*, *8*, and *9*). Regard for the formation of protective layers on galvanized steel, has led to DIN 50930 requiring

$$\begin{aligned} &\text{pH} && > 7.5 \\ &(HCO_3^-) && > 2 \text{ mol/m}^3 \\ &[(Cl^-) + \tfrac{1}{2}(SO_4^{--})]/(HCO_3^-) && > 7 \end{aligned}$$

Among the many water composition factors that influence corrosion, the most important are oxygen content, pH value, temporary hardness, chloride, sulfate, total salts, and conductivity.

Apart from these, 10 to 15 factors influence the corrosion process. It is sometimes impossible to determine the responsible factors analytically. An example is the organic compound found in surface waters that acts as an inhibitor for pitting, Type I, in copper [*3*]. The composition of water required for the formation of passive films varies from material to material. For example, sulfate disturbs the formation of passive films on copper but is unimportant for the corrosion of brass, while the chloride/bicarbonate relationship must in this case be kept low [*1*].

Internationally, a very great scientific effort has been put into trying to explain the complicated relationship between the many factors important for corrosion in potable water. The result is that today we are usually able to characterize the water types that are particularly unfavorable for a given metal. There remain, nevertheless, gaps in our knowledge. At the moment, the greatest difficulties are in the understanding of the development of corrosion in water systems receiving a mixture of waters from different sources. Large cities commonly receive water of varying composition, because supplies are based on several water works. The composition of a protective layer in a pipe for supply water will depend on the actual water composition. Thus a change of water type may result in dissolution of some components and in stability of the protective layer. There are several well-known examples of a mixture of two water types, each by itself conducive to the formation of protective films, causing pitting [*9,11*].

Until a few years ago, we were almost only interested in the depth of corrosion so that we could determine how quickly penetration occurred. Today great attention is being paid to the increased metal content in the water caused by corrosion [*12,13*]. Metal pickup is closely related to the solubility of the corrosion products. Generally corroding surfaces give large metal releases, particularly with waters with high dissolution capacities.

It may be assumed that even surfaces which are otherwise passive can release substantial amounts of metal, and that metal pickup from the passive surfaces is normally of considerable importance. On the other hand, a significant amount of metal is not necessarily released from a pipe system where local corrosion has led to rapid penetrations.

Testing Metals in Potable Water

A prerequisite for testing and setting standards for corrosion of metals in potable water is the clear identification of which type of corrosion one wishes to test. Practical experience must be used to identify those combinations of water composition and temperature likely to be most deleterious for the type of corrosion under investigation.

Testing must frequently take place as a combination of field tests and laboratory tests (possibly using electrochemical methods), and only the experienced research worker with thorough knowledge of corrosion processes in practice will be able to develop relevant tests. In some cases the best test will be to distribute test specimens in practical installations. Experience has shown that it can occassionally be difficult to prepare satisfactory synthetic supply water in the laboratory. For instance several laboratories have had difficulties in studying pitting corrosion, Type I, of copper tubes in synthetic supply water, for example, BNF Metals Technology Centre [*14*]. Consequently, an especially corrosive type of water, or perhaps a local water, is sometimes chosen as test medium, but in such cases the method cannot be standardized for use in other places.

Corrosion and Testing of Materials

The corrosion of individual metals in supply water has been described in detail elsewhere and will only be reviewed briefly here. However, an attempt will be made to describe how corrosion is controlled in practice. The role of testing and standardization and recent research results from the Danish Corrosion Centre will be referenced where appropriate.

Galvanized Steel

Galvanized steel is used to a great extent in waters high in calcium-carbonate hardness. However, the content of other salts is often very high too, and numerous cases of pitting corrosion occur in these waters, which are often from mixed sources. It is not yet understood in detail how the water composition influences pitting corrosion.

For many years the satisfactory use of galvanized steel in larger hot water systems in Denmark and some other countries was often associated with so-called electrolytic water treatment. The treatment consists of the implacement of an aluminum anode with impressed current in the hot water tank. Newer research [*15*] proved that the effectiveness of the treatment is due to the action of aluminum compounds as cathodic inhibitors, these being deposited on the pipe surfaces.

In DIN 50930 it is stated that a considerable improvement in combatting certain kinds of corrosion will be achieved if the pipe quality was up to the DIN Standard, Zinküberzüge auf Stahlrohren (DIN 2444). This standard specifies among other things a zinc layer of at least 56 μm, a smooth zinc surface produced by steam blowing and no burrs at the weld.

An attempt was made to elucidate whether a zinc coating with these properties improves the resistance to pitting corrosion [*16*]. One hundred eighty-six pieces of pipes of eight different manufacturers were installed in a test rig, built to resemble a practical installation for cold and hot supply water with automatic tapping (Fig. 1).

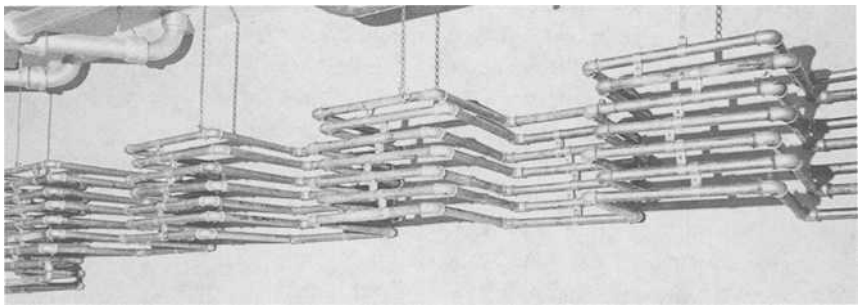


FIG. 1—*Part of the experimental setup for the test in galvanized steel pipes.*

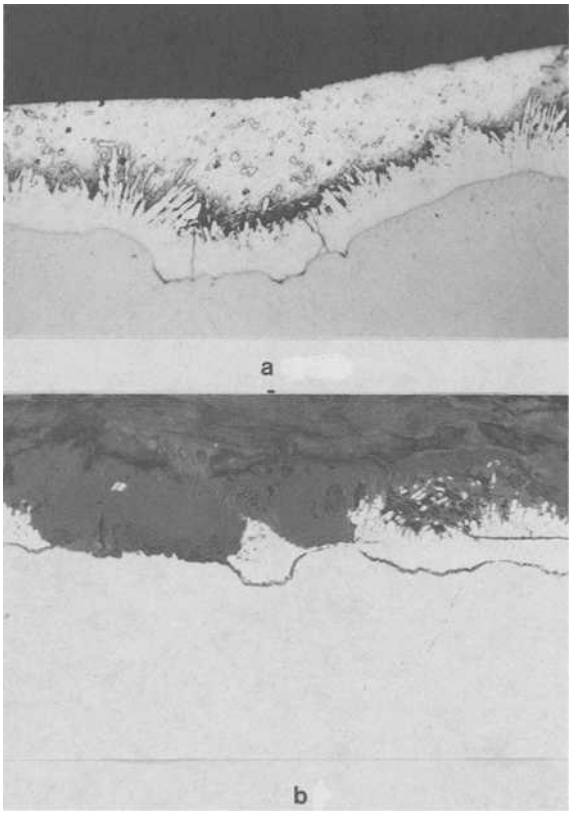


FIG. 2—*Cross section of Pipe A (DIN 2444)* (a) *before and* (b) *after exposure to the hot tap water with pump circulation* ($\sim \times 300$).

Experiments were made throughout a period of 15 months under conditions closely simulating conditions in practice. In these experiments the observed corrosion was, with the exception of one out of eight pipe types, not influenced by the pipe quality. The smoothness of the pipe inner surface and the presence or absence of burrs had no discernible effect on the corrosion. The only pipe quality showing less resistance to pitting corrosion was a pipe with a thin zinc coating (50 μm) and without a layer of pure zinc (Figs. 2 and 3).

Pipes in which hot water circulated continuously showed on the whole more corrosion than pipes with cold water or with hot water without circulation.

Copper

The use of copper is widespread since copper is regarded as a durable material when used in supply water installations. The corrosion of copper is not however entirely under control as was revealed in a new investigation [*17*] of 2000 Danish

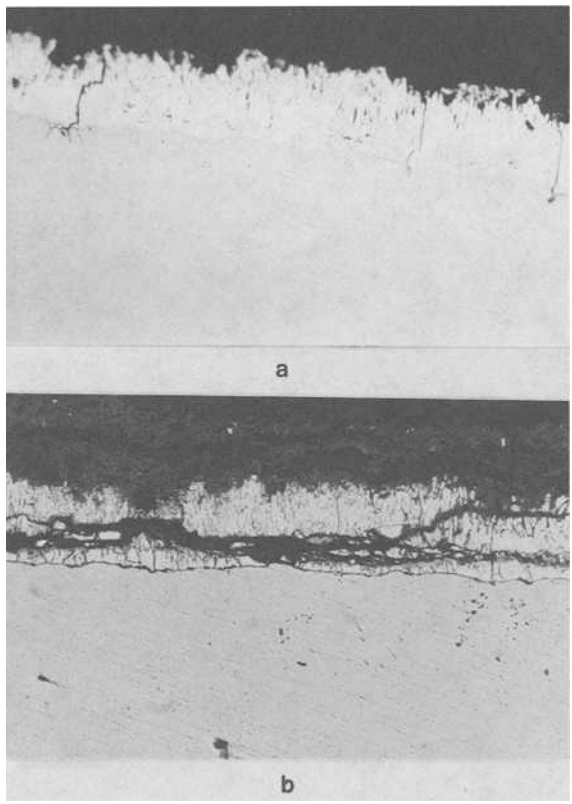


FIG. 3—*Cross section Pipe C* (a) *before and* (b) *after exposure* (~ ×300). *Pipe C was the only pipe with considerably lower corrosion resistance. The zinc coating was thin and was not covered by a pure zinc layer.*

homes struck by water damages. There were 410 cases of leaking copper pipe systems involving the types of damage shown in Table 1.

The exact distribution of types of damage depends on local conditions, and investigations from other countries show other distributions [*5,18*]. The local factors affecting which kinds of corrosion are most prominent relate to geochemical conditions, as well as traditions of craftmanship and building techniques.

Measures to control corrosion fatigue and erosion corrosion are well known [*1,5–7*]. In both cases water composition has little influence while the method of installation determines whether the system will be subject to attack by corrosion. It is therefore, craftsmen and civil engineers who have the task of preventing corrosion by optimal design and installation.

Corrosion fatigue of copper pipes and fittings occurs almost exclusively in association with brazed joints where thermal expansion is prevented by incorrect fixing or inappropriate embedding. Brazing anneals the copper locally and cracks

TABLE 1—*Distribution of causes of failures of copper tubes* [*17*].

Types of Damage	Percent
Corrosion fatigue	25
Pitting corrosion	20
Erosion corrosion	10
Leaky soldered joints	20
Other leaky joints	10
Burst by winter frost	5
Other	10
Total	100

appear in the soft material. The use of soft soldering prevents the appearance of corrosion fatigue cracks in copper. However, if the free thermal expansion is not obtained the soft solders will be destroyed by corrosion fatigue cracks in the soldering material itself (see below).

Erosion corrosion is found only in hot water circulated by pumping. Elaborate test rig investigations in Sweden showed that in steady flow conditions the water velocity should be kept under 1.3 m/s to avoid attack at 50°C [*5*]. Reviewing a number of cases investigated by the Danish Corrosion Centre over the last ten years suggests that the pump effect must be even further reduced to avoid corrosion under practical conditions. Corrosion does not appear when design velocities in the circulation system are held at 0.5 m/s, and elbows are formed in such a manner as to minimize disturbances to the flow pattern.

Pitting is commonly divided into several categories with Type I and II being the most important [*3,4,9,18*]. Reliable data all show that Type II pitting occurs at temperatures above 60°C in waters with a high sulfate/bicarbonate ratio [*5*] and that the frequency of corrosion increases with falling pH. Type II is countered by suitable water treatment, possibly including both alkalization and recarbonization. In most countries, Type II pitting presents only limited problems.

Type I pitting is more widespread in deep well waters and more difficult to control. That Type I chiefly appears in pipes where carbon films remain after production is well known. However, other conditions can suffice to allow the occurrence of pitting (flux remnants, stagnation, thick oxide layers, and so forth). Since a pipe with an ideal surface is considerably more resistance against attack than one with deleterious films, there remains a real need for a test for whether the surface is optimal. Unfortunately, the development of a reliable accelerated test has not yet been successful. Until now, only test rig investigations of at least six months duration, combined with electrochemical measurements, in water that naturally provokes pitting, are really usable.

Lucey [*9*] has successfully worked with determining which parameters in the water composition influence pitting propensity. His somewhat complicated nomograms for Type I pitting show that, in the water types he has studied, the factors affecting pitting propensity are pH, sulfate, chloride, nitrate, sodium, and dis-

solved oxygen. He also succeeded in predicting the pitting propensity in mixed waters (Fig. 4) [9].

Experience from other countries, shows that even more factors than the earlier mentioned are important. Lucey has developed a test [9] that determines the pitting propensity of water without requiring knowledge of the water composition. The test cell has a multiple anode and gives an irregular current when pitting occurs. The test cell has also been tested in Denmark, and preliminary results show good agreement between practical experience and test cell results using water with a different basic composition [19].

Brass

It has been possible to standardize a method for determination of whether dezincification of brass will occur in corrosive water types. Turner [20] showed that dezincification occurs in water with a high chloride/bicarbonate ratio. Conditions of high pH and temperature amplify the effect.

A comparison was made of several test methods including dip tests, electrochemical tests, and a test where the test specimens were exposed four weeks

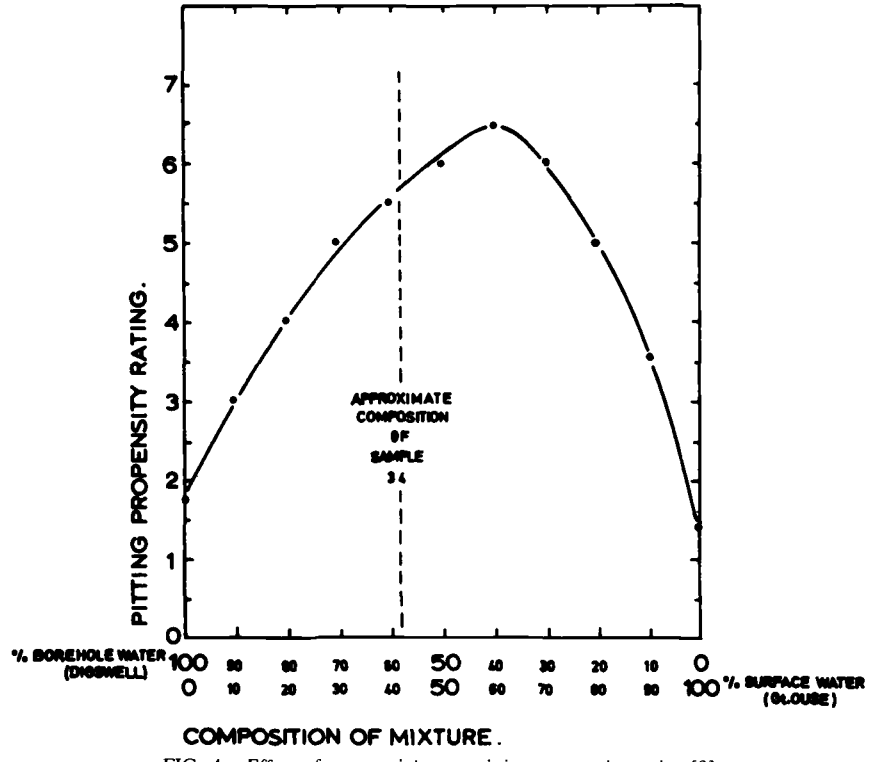


FIG. 4—*Effect of water mixing on pitting propensity rating* [9].

at 90°C to a local corrosive water [*21,22*] (both naturally and synthetically made). The test results were compared with results from a field test in different water types. Several European corrosion laboratories took part in a round-robin test. It was concluded that a modified Swedish method showed the best correlation to practical conditions. The method consisted of dipping a specimen mounted in bakelite in a 1% cupric-chloride solution for 24 h [*23*]. The method has become an International Standards Organization (ISO) Determination of Dezincification Resistance of Brass (ISO 6509), Swedish Standard (SS) Determination of Dezincification Resistance of Brass (SS 117110), and British Standard (BS) Copper and Copper Alloys AMD 3282 (BS 2872).

Demands concerning dezincification have been administrated very differently from country to country. Although Denmark participated in these investigations, it was decided not to set requirements for resistance to dezincification at all as only 6% of the Danish waters were able to cause dezincification. In Sweden an approval system demands that valves and fittings in the pipe system must be manufactured of material resistant to dezincification. In England it is preferred to allow the use of ordinary brass in some water areas while requirements to dezincification resistance are set in others. In these special areas the requirements are stricter than those in Sweden.

Soft Soldering and Brazing Metals

In 1977 the Scandinavian countries decided [*24*] that all solders to be used in drinking water installations should not contain cadmium or lead. The selection of alternative soldering materials was difficult. Knowledge of the durability of individual solders was limited. Endurance of the soldered joint, together with the solderability and strength, is most affected by resistance to creeping, fatigue and corrosion.

It was decided to clarify the role of corrosion in the degradation of soldered and brazed joints. The corrosivity of fluxes was investigated. It was shown that normal soft soldering fluxes, containing ammonium chloride and zinc chloride, are much more corrosive than fluxes used for brazing.

In spite of the necessity of reducing the corrosiveness of fluxes, it is still the most corrosive soft solder fluxes that are used. These are easiest to work with in practice, since they give the best surface wetting.

The resistance of solders to corrosion was investigated by Sørensen and Nielsen [*25*]. Three test rigs of copper pipes joined with nine different solders or brazing alloys were exposed to hot tap water in Copenhagen, Gothenburg, and Oslo for 18 months under normal service conditions. The alloys investigated were the silver brazing alloys L-Ag55Sn, L-Ag34Sn, and L-Ag18Sn, the copper-phosphorus brazing alloys L-Ag15P, L-Ag5P and L-CuP6, and the soft solders L-Sn5Ag and L-SnCu3.

In spite of the large differences in water analyses in the three cities, there were no major differences in the degree of corrosion of the joints. Nearly all the joints

were noticeably corroded but the form varied with the solder or brazing alloy type (Fig. 5). Maximum depth was 3 mm/year of silver brazing alloys, 0.3 mm/year for soft/solders while copper adjacent to the copper-phosphorus alloys was attacked by up to 0.2 mm/year.

The rapid corrosion rate indicates that attention should be paid to the contribution of corrosion to the failure of soldered and brazed joints in tap water. It should be noted that, although the joints were prepared under good workshop conditions, they did contain some cavities.

Jensen and Neilsen [26] examined both leaky and nonleaky soldered joints, which had been in use for many years. Examination of 16 joints showed that corrosion did not continue at the initial high rate.

A metallographic examination of 26 leaky soldered joints from water supply systems (and 15 from heating systems) showed that soft solders had been used in 90% of the leaky joints.

The soft solders included both tin-lead and tin-silver types and the failure of some of them was due to extremely bad workmanship. But most of the soldered

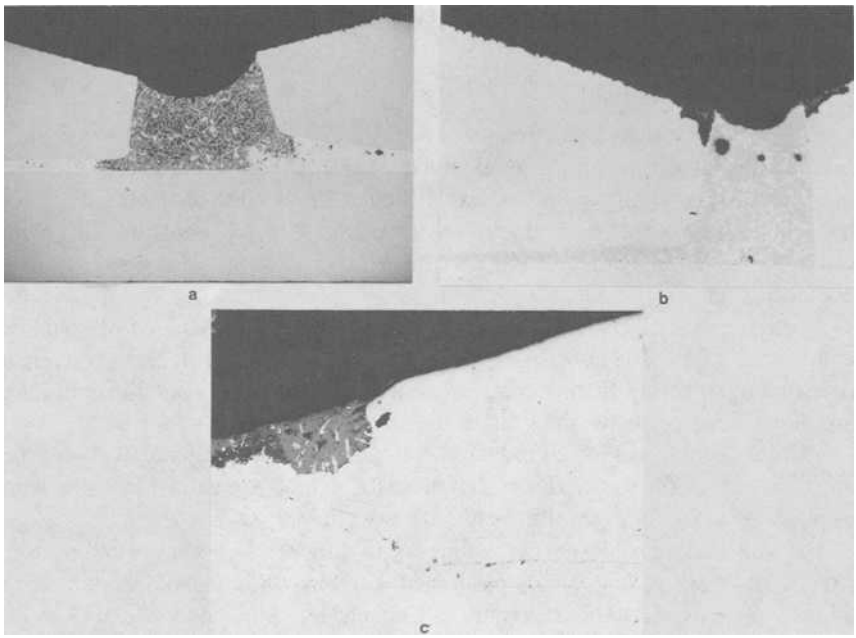


FIG. 5—(a) *Silver brazing alloy, L-Ag55Sn (D2) (~ ×30). Exposed to hot tap water in Copenhagen for 18 months. The unattacked filler metal has small cavities.* (b) *Copper-phosphorus brazing alloy, L-Ag5p (D6) (~ ×60). No corrosion of the filler metal after exposure in Copenhagen for 18 months, but corrosion of the copper adjacent to the filler metal can be seen. The self-fluxing brazing alloy has wetted the copper surface, which is now slightly attacked by general corrosion.* (c) *Tin-silver soft solder, SnAg5 (S19), Gothenburg (~ ×60). General corrosion of filler metal. Metallic tin-silver grains are left in the corrosion products.*

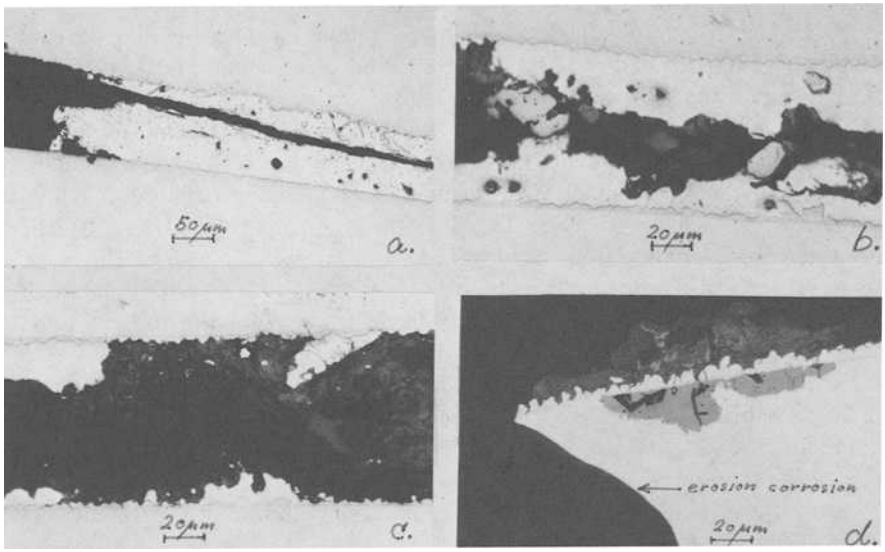


FIG. 6—(a) *Corrosion fatigue crack in tin-silver soft solder.* (b) *Along the crack the filler metal quickly corrodes when water is seeping through the crack in the gap.* (c) *The corrosion of the filler metal continues until only the intermetallic compounds* Cu_6Sn_5 *and* CU_3Sn *remain.* (d) *The copper underneath the intermetallic compounds corrodes. Erosion corrosion can occur because of high water velocities in the narrow gap of a leaky joint.*

joints were degraded by corrosion fatigue although the gap was satisfactorily filled since more than 60% of the area was covered by filler metal. Crack formation is secondarily influenced by creeping, but the importance of the effect is unknown. Thermal movements had influenced the joints mechanically and caused corrosion fatigue where the pipe system had been fastened inappropriately (Fig. 6). Most failures were seen in soldered hot water pipes without pump circulation especially on pipes molded in concrete.

The described problem with soft soldered joints can not be solved by brazing. Brazed pipe systems will be subject to corrosion fatigue in copper fittings and pipes instead.

Metal Pickup

Traces of metals are dissolved when potable water is transported in pipe systems. Some of these metals are toxic at sufficiently high concentrations. Measurements have shown [*12*] that construction materials, including solder and brazing metals, can contaminate the water to an undesirable extent.

Pickup from the materials galvanized steel, brass and gunmetal has been investigated in parallel experiments involving both laboratory tests and field tests in three different waters. Also the lead pickup from gunmetal and brass has been examined in the laboratory with the use of different compositions of synthetic

supply water. The results from the two investigations have been used to develop a modified test method [*13*] for the evaluation of cadmium and lead pickup levels from fittings in potable water systems.

The modified test involves preparing the specimen fitting by removing grease and by flushing water through for 1 h. The specimen is then filled with synthetic supply water made from distilled water by adding sodium chloride, sodium sulfate, and calcium carbonate. The water is aerated and the pH is 7.0. The synthetic water is allowed to stand for 24 h in the specimen fitting. The water is replaced each day for ten days and the metal content analyzed on the ninth and tenth day. The method is primarily intended for pickup of cadmium and lead but can be useful for other metals.

The most important change compared to the earlier test is that the test water is more stable (pH 7 instead of 6.6) and that the test period is increased from three to ten days at which point metal pickup is more stable. The test method has been proposed as a Nord test method.

In new installations the pickup of lead and cadmium is kept sufficiently low by adopting the following rules:

1. Plumbers are not allowed to use lead-containing soft solder or cadmium-containing brazing metal for joining copper tubes.
2. All fittings, tap valves, and other equipment to be installed in future have to be approved, the approval to include a test for cadmium and lead pickup.

General Conclusions

The great efforts that, over the past decades, have gone into the study of the corrosion of potable water systems, have resulted in a thorough understanding of at least some of the involved mechanisms. This understanding has formed the basis for developing tests for a number of situations involving different materials and water types.

There remain, however, great difficulties to be overcome before we will be able to apply relevant, standardized tests to cover all normally arising situations and it is very probable that we will have to conclude that in certain situations, we will not be able to develop and apply such tests.

References

[*1*] Campbell, H. S., "Corrosion, Water Composition and Water Treatment," *Water Treatment and Examination*, Vol. 20, 1971, pp. 11–34.

[*2*] Schwenk, W., "Galvanized Steel and Stainless Steel Tubing for Domestic Water Distribution—Parameters of Internal Corrosion and Protective Measures," *Centre Belge d'Etude et de Documentation des Eaux*, No. 396, Nov. 1976, pp. 382–389.

[*3*] Lucey, V. F., "Pitting Corrosion of Copper—a Review," *International Symposium on Cor-*

rosion of Copper and Copper Alloys in Building, Japan Copper Development Association, Tokyo, 1982, pp. 1–16.

[4] Lyman, W. S., Cohen, A., and Meyers, J. R., "Causes and Prevention of Pitting Corrosion in Copper Plumbing Systems in the USA," *International Symposium on Corrosion of Copper and Copper Alloys in Building,* Japan Copper Development Association, Tokyo, 1982, supplement.

[5] Mattsson, E., "Corrosion of Copper in Fresh Waters," *Corrosion Australia,* Vol. 6, No. 6, Dec. 1981, pp. 4–9.

[6] Nielsen, K., "Vandsammensaetningens betydning for korrosion i brugsvandsanlaeg," *Vandterknik,* Aug. 1969, pp. 1–11.

[7] Nielsen, K. and Yding, F., "Korrosion i brugsvandsanlay," The Danish Corrosion Centre, Korrosionstenknik 3, Glostrup, Denmark, July 1979.

[8] "Quality of Water Intended for Human Consumption," 80/778/EEC, Directive of the Council of the European Communities, July 1980.

[9] Lucey, V. F., "Assessment of Type I Pitting Corrosion Characteristics of Potable Waters," *International Symposium on Corrosion of Copper and Copper Alloys in Building,* Japan Copper Development Association, Tokyo, 1982, pp. 86–103.

[10] Nissing, W., Friehe, W., and Schwenk, W., *Werkstoffe und Korrosion,* Vol. 33, 1982, pp. 346–395.

[11] Linder M. and Lindman, E. K., "Investigation of Pitting Corrosion, Type II in Copper Pipes," *9th Scandinavian Corrosion Congress,* The Danish Corrosion Centre, Glostrup, Denmark, 1983.

[12] Nielsen, K., "Dissolution of Materials from Service Pipes and House Installations and Its Sanitary Aspects," *11th Congress of the International Water Supply Association,* Subject 3, Amsterdam, Netherlands, 1976, pp. M23–M28.

[13] Nielsen, K., "Control of Metal Contaminants in Drinking Water in Denmark," *AQUA,* No. 4, 1983, pp. 173–182.

[14] Bell, W. A. and Campbell, H. S., "Stability of Neutral Waters and Synthetic Solutions," *Chemistry and Industry,* 1965, pp. 303.

[15] Petersen, M. B., "Electrolytic Water Treatment," Confidential Report on Industrial Research Education Programme, EF 72, Copenhagen, Denmark, 1983, to be published in 1986.

[16] Nielsen, K. and Yding, F., "Influence of Pipe Quality on Corrosion of Galvanized Steel Pipes for Domestic Water Supply," *Werkstoffe und Korrosion,* No. 34, 1983, pp. 542–556.

[17] Nielsen, K., "Corrosion of Materials by Supply Water," *9th Scandinavian Corrosion Congress,* The Danish Corrosion Centre, Glostrup, Denmark, 1983.

[18] von Frankque, O., "Pitting Corrosion of Copper Tubes in Cold Water—Situation and Experiences in the Federal Republic of Germany," *International Symposium on Corrosion of Copper and Copper Alloys in Building,* Japan Copper Development Association, Tokyo, 1982, pp. 135–145.

[19] Rosen, L., "Type I pitting i drikkevandsinstallationer af kobber," Student Project, DIA-K, Lyngby, Denmark.

[20] Turner, M. E. D., *Proceedings of the Society of Water Treatment Examinations,* Vol. 10, 1961, p. 162.

[21] Nielsen, K. and Rislund, E., "Comparative Study of Dezincification Tests," *British Corrosion Journal,* Vol. 8, May 1973, pp. 106–117.

[22] Nielsen, K. and Rislund, E., "Dezincification Test of Brass Fittings for Domestic Water Service by the Potentiostatic Test Method," Report C 3391, The Danish Corrosion Centre, Glostrup, Denmark, April 1976.

[23] Linder, M. and Mattsson, E., "Prövningsmetod for avzinkningshardighet hos armaturmässing," *Byggforskningen,* Report R8:1975, Stockholm, Sweden, 1975

[24] "Provisional Approval Requirements and Testing Conditions for Soldering Materials in Water Supply Systems," VA 1.20/DK 010E, Boligministeriets godkendelsesudvalg for vand- og afløbsmateriel, Hørsholm, Denmark, Oct. 1977.

[25] Sørensen, O. B. and Nielsen, K., "Corrosion of Soldered and Brazed Joints in Supply Water," *Brazing and Soldering,* No. 5, Fall 1983, pp. 32–36

[26] Jensen, T. and Nielsen, K., "Failures on Soldered and Brazed Joints of Copper Pipes for Domestic Water," The Danish Corrosion Centre, Report 83/03d, Glostrup, Denmark, 1982.

DISCUSSION

A. C. Headon[1] (*written discussion*)—In your presentation, you mentioned that driven aluminum anodes are used in water heaters to control the corrosion of the galvanized distribution piping. Could you please elaborate on this method?

K. Nielsen (*author's response*)—Aluminum anodes of 99.7% purity are placed in black steel hot water tanks. The size of the anodes depends on the size of the tank, and the impressed current is controlled by the amount of water used. Cathodic protection of the tank is achieved under the dissolution of aluminum. The water becomes supersaturated with aluminum hydroxide on leaving the tank with a content of about 0.2-mg aluminum/L at a pH of 7.5. The aluminum hydroxides will deposit at the cathodic sites of the pipe inner surfaces. The protective layers that consist of corrosion products, calcium carbonate, and aluminum-hydroxide has been proved [*1*] to be very beneficial to prevent pitting corrosion of galvanized pipes in hot tap water.

A. C. Headon[1] (*written discussion*)—Are immersion elements used in Denmark to heat the water in the water heaters? If so, are the immersion elements susceptible to corrosion and scaling? What material are the immersion elements made of and at what watts density do they operate?

K. Nielsen (*author's response*)—Immersion elements are not generally used for heating water in Denmark. Except to some extent for smaller tanks. These are usually enameled or plastlined steel tanks with isolated immersion elements. Tin or nickel-plated copper and stainless steel, 316 L, are used. Localized corrosion does occur in waters corrosive to these metals (high sulfate/low pH waters with respect to copper and high chloride waters with respect to stainless steel), but as shorter lifetimes are generally accepted (2–5 years) complaints are not frequent. Scaling does occur with deposited calcium carbonate increasing the corrosion because of elevated surface temperatures. The immersion heaters operate at 2 to 10 W/cm^2. Low watt density and more resistant materials (Incoloy 825) are recommended for longer lifetimes in corrosive waters. Indirect heat with a heat-transfer surface of enameled steel or ceramics is also used.

Bernd Isecke[2] (*written discussion*)—Did you find any relation between the carbon content of copper tubes and the corrosion rate, for example, a special level?

K. Nielsen (*author's response*)—The presence of a carbon film leads to the development of pits in copper tubes in certain waters. No relationship has been found between measured carbon content and corrosion rates. An interEuropean

[1]Ontario Hydro Research Division, 800 Kipling Ave., Toronto, Ontario, Canada M8Z 5S4.
[2]Bundesanstalt Für Material-Prüfung, 100 Berlin 12, West Germany.

Copyright© 1985 by ASTM International www.astm.org

study [2] has shown that there is no simple threshold carbon content below which susceptibility to corrosion is eliminated. Future work should concentrate on the development of an electrochemical method for determining pitting susceptibility of surface finish of copper tubes.

References

[1] Lrise, C.-L., *Korrosion in Kalt und Warm Wasser Systemen der Hausinstallation*, Deutsche Gesellschaft für Metalkunde e.V., Adenaueralle 21, 6370 Oberusel 1, West Germany, 1984, pp. 145–169.

[2] Lucey, V. F. and Watts, G. A., *An Investigation of Methods to Determine Carbon in the Bores of Copper Tubes*, BNF Metals Technology Centre, Confidential Report S332-3, June 1976.

Peter E. Francis[1] *and Antony D. Mercer*[1]

Corrosion of a Mild Steel in Distilled Water and Chloride Solutions: Development of a Test Method

REFERENCE: Francis, P. E. and Mercer, A. D., **"Corrosion of a Mild Steel in Distilled Water and Chloride Solutions: Development of a Test Method,"** *Laboratory Corrosion Tests and Standards, ASTM STP 866*, G. S. Haynes and R. Baboian, Eds., American Society for Testing and Materials, Philadelphia, 1985, pp. 184–196.

ABSTRACT: Mild steel is the most common structural material and is used in a wide range of environments. However, there are few systematic data on the effects of operating parameters on corrosion behavior in immersed conditions. To obtain such data, a suitable test method is required in which parameters affecting the corrosion process are carefully controlled.

Dissolution of borosilicate glass vessels in water at temperatures above 60°C was shown to lower significantly the corrosion rate of steel in distilled water. The method of aerating the solution was also important. A new test apparatus is described in which the above problems have been overcome and other parameters are capable of more precise control.

Some data obtained with the new test cell are given to validate the design. The data demonstrate the effect of dissolved oxygen on the corrosion of steel in distilled and chloride-containing water at temperatures up to 90°C.

KEY WORDS: corrosion, tests, glass, temperature, oxygen, chlorides, distilled water, mild steel, polytetraflouroethylene

In any valid test method it is essential that all parameters affecting the corrosion process are recognized and controlled. This requirement is not easily achieved since so many factors in the metal/environment situation are difficult to quantify. Parameters, such as solution composition, dissolved oxygen content, and solution movement at the surface of the metal, can vary significantly during a test while apparently conforming to their initial values. These variations can affect not only the reproducibility of the results but also give misleading information concerning the effects of individual parameters on the corrosion process.

The work described in this paper is concerned with the development of a test method for investigating the effect of various parameters on the corrosion of metals in aqueous solutions. Particular attention has been given to the effect of

[1]Principal scientific officers, Division of Materials Applications, National Physical Laboratory, Teddington, Middlesex, England.

Copyright© 1985 by ASTM International www.astm.org

temperatures in the range 25 to 90°C on the corrosion of mild steel in distilled water and chloride solutions.

An earlier procedure used a conventional testing system consisting of borosilicate glass tubes fitted with water-cooled condensers. The action of hot water on the glass vessels used in these tests resulted in some dissolution of the glass, which provided sufficient concentrations of silicon-containing compounds to cause partial inhibition of the corrosion process. Corrosion behavior was also affected by the physical method used to aerate the water; corrosion rates were higher when the supply of air was introduced below rather than above the surface of the water.

A new test apparatus has been designed and commissioned in which the above problems have been overcome and other parameters are capable of more precise control than hitherto. Some results are described from this new technique in which the effect of various parameters, notably temperature, chloride, and dissolved oxygen concentration, on the corrosion/time behavior of mild steel have been described.

Initial Corrosion Tests In Glass and Quartz Vessels

The work described in this section is summarized from earlier published results [*1,2*] and is included here to demonstrate the need for the improved procedure described later.

Experimental Procedure

Test vessels were 200- by 38-mm glass or quartz tubes supported in thermostated water baths and fitted with water-cooled condensers (Fig. 1). Air from the laboratory supply was washed by passage through two baths of distilled water and then passed via a narrow-bore polytetrafluoroethylene (ptfe) tube down through the condenser to either above or below the surface of water used for the tests (Positions A or B in Fig. 1). The latter position resulted in a slow agitation of the water produced by one bubble of air per second. Vessels and condensers were of ordinary borosilicate glass, that is, as obtained from usual laboratory supplies, or of transparent quartz.

Specimens of a low carbon mild steel, 30 by 25 by 1.6 mm, were cut from sheet material that had received an industrial satin finish. Each specimen was abraded with emery paper (Grade 1G), degreased, weighed, and stored in a desiccator for at least 24 h before the start of the test. During the test, the specimens rested at an angle of about 45° at the bottom of the tube. At the end of the test, corrosion products were removed by cathodic cleaning at a current density of 2000 Am^{-2} for 3 min in 5% sulfuric acid solution containing 0.05% quinoline [*3*]. The specimens were then reweighed to determine mass loss during the test. Usually one such treatment was sufficient to remove all corrosion products, subsequent treatments leading to no further mass loss of the specimen [*4*]. Each test was carried out in duplicate.

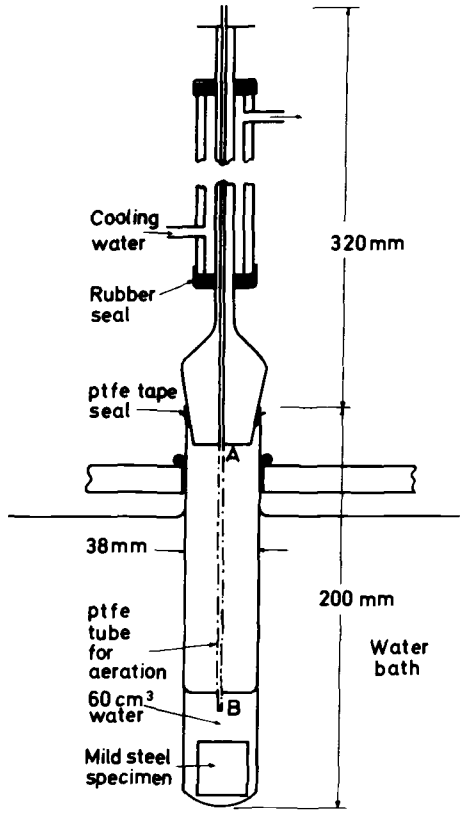


FIG. 1—*Apparatus for studying effect of temperature on corrosion of mild steel in distilled water: for aeration over water, air inlet tube terminates at A and for aeration through water, air inlet tube terminates at B.*

Triply distilled water was used in all tests. Water from a single distillation of the mains supply was distilled with addition of permanganate to remove organic matter and then with potassium hydrogen sulfate to destroy residual traces of ammonia. The final distillate in equilibrium with the air had a pH in the range 5.5 to 5.6 and a specific conductivity of 0.84 $\mu S\ cm^{-1}$.

Each vessel contained 60 cm^3 of water, which was raised to the required temperature over a period of 24 h. Specimens were then inserted and the temperature maintained at the required value $\pm 1.0°C$ without interruption throughout the test periods of 28 and 100 days. All tests were conducted in both glass and quartz vessels.

The procedure was repeated in the absence of steel specimens. Measurement of pH, dissolved oxygen, and silicon content of the water were conducted on the water from all tubes at the beginning and end of the tests. Dissolved oxygen contents were determined by the Winkler method modified for use with small

(<10 cm^3) sample volumes [5]. Silicon was determined spectrophotometrically as those forms of silicon that react with ammonium molybdate. Silicon analyses were made only on water samples from the tests without steel specimens so as to avoid loss of silicon by adsorption on corrosion products.

Results

A number of tests were conducted to compare the effects of aeration over (air inlet tube terminating at A in Fig. 1) and through (B in Fig. 1) the water on (1) the concentration of dissolved oxygen during the tests and (2) the mass loss of the specimens. Results from tests at 40 and 70°C in quartz vessels are shown in Figs. 2 and 3. When no metal specimens were present the concentration of dissolved oxygen remained at the saturation level for that temperature throughout the test (broken lines in Figs. 2 and 3). However, in the presence of corroding metal the concentration of oxygen could be maintained at the saturation value

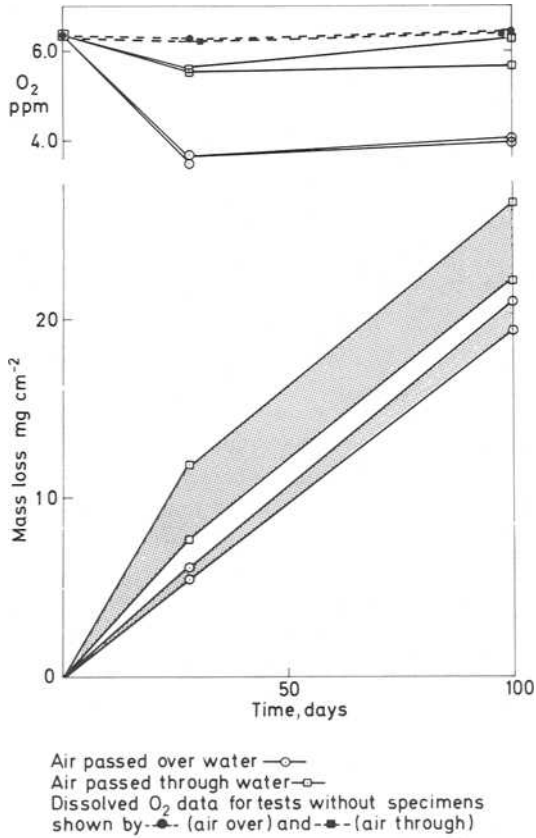


FIG. 2—*Corrosion tests at 40°C in distilled water in quartz vessels: abraded mild steel specimens.*

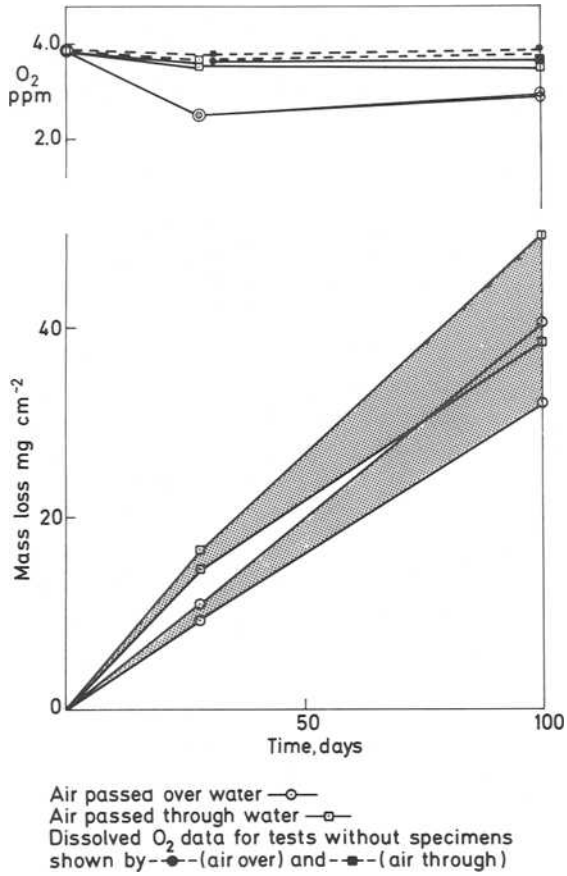


FIG. 3—*Corrosion tests at 70°C in distilled water: abraded mild steel specimens.*

only when air was passed through the solution. Clearly, passage of air above the water did not result in a sufficiently rapid exchange of oxygen across the water/air interface to replace the oxygen consumed in the corrosion process. In the latter case corrosion rates were lower than when the oxygen concentration was maintained at the initial value during the first 28 days of the test period. Consequently, only corrosion rate measurements from experiments where air was passed through the solution are discussed below.

A direct comparison was made at five different temperatures of the corrosion/time behavior of mild steel in distilled water held in glass and in quartz vessels. At 40 and 60°C corrosion developed in a similar manner in both types of vessel, that is, initially as localized areas of attack leading to thick rust layers covering the specimen surfaces. Above 60°C, the corrosion developed more slowly across the surface of specimens in glass tubes compared with those in quartz tubes. At

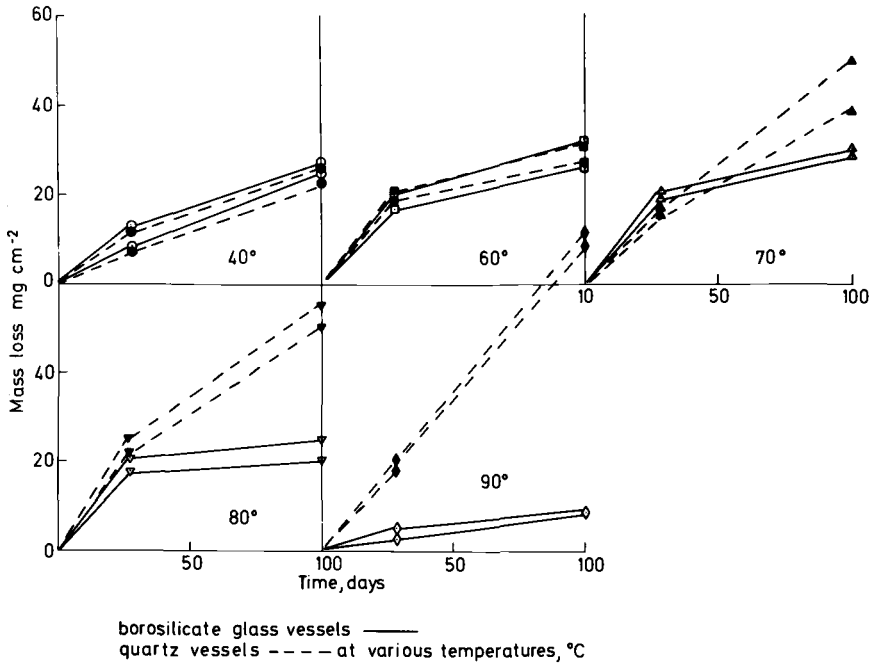


FIG. 4—*Mass loss/time plots for mild steel in distilled water.*

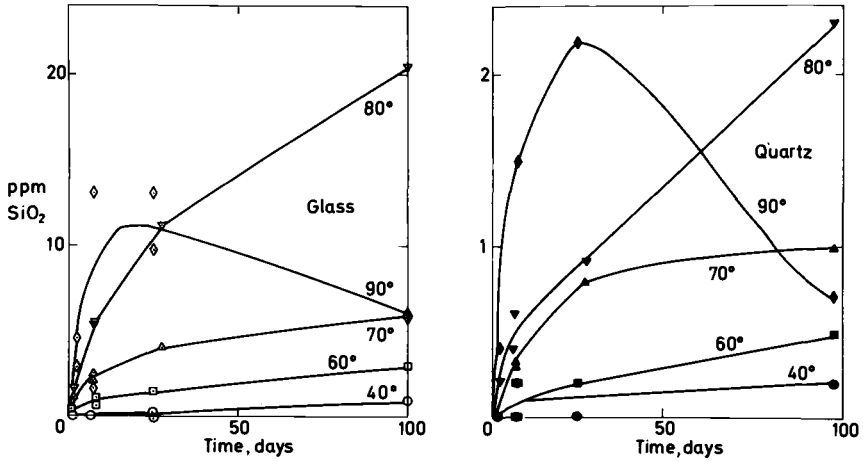


FIG. 5—*Silicon content (as SiO_2) of distilled water in glass and quartz vessels (no metal specimens present) as affected by time and temperature (note difference in vertical scales).*

the end of the tests, specimens from quartz tubes were corroded over their entire surface, whereas specimens from glass tubes retained increasing unattacked areas with increasing temperature.

Figure 4 shows the mass-loss/time curves for mild steel specimens from these tests. At 40 and 60°C the mass loss was little affected by the nature of the test vessel. At 70°C there was an attenuation of corrosion in glass vessels that was more marked at 80°C and most pronounced at 90°C.

A high concentration of silicon-containing compounds built up in distilled water contained in glass vessels when compared with quartz vessels (Fig. 5). There is a clear inference that these compounds in the water are responsible for the reduction in corrosion rates in hot water in glass vessels, although it cannot be ruled out that boron-containing species from the borosilicate glass may be partly or wholly responsible for the observed effects. Boron analysis was not made in this work chiefly because of the limited volumes of water available after other chemical tests had been completed.

These results led us to question the reliability of conventional laboratory test apparatus in glass. It was obvious that the method of aeration was important and that glass should be avoided. Better control of solution movement at the metal surface was also desirable.

New Test Apparatus

Polytetrafluoroethylene (ptfe) was chosen for the construction of the test cell. This material is readily available and easily workable. Furthermore, analysis of solutions contained in ptfe vessels has revealed no significant contamination at operating temperatures up to 200°C [*6*]. An improved method for controlling oxygen concentration has been introduced on the new test apparatus, and the control of diffusion processes at the metal surface has been improved by rotation of the specimen in the test solution at 1 Hz. This rotation velocity was an arbitrary choice with the only requirement being the need to have a uniform movement of the specimen without excessive turbulence or vortex effects. However, later work [*7*] has shown that this rotation speed would be more than adequate to ensure that diffusion-controlled corrosion processes would be controlled by forced convection under all experimental conditions.

Description of the Test Cell

The test solution was contained in a ptfe cylindrical vessel (length 265 mm, diameter 104 mm) closed at both ends by threaded ptfe plugs (Fig. 6). To ensure a leak-tight seal the lower plug was machined oversize and fitted by expanding the lower end of the cylindrical vessel in boiling water. The upper ptfe plug was drilled to accept a specimen holder, gas inlet tube, and an air condenser. An unused drilling, closed by a ptfe stopper, was used to monitor, replenish, and adjust the level of the test solution in the vessel, to insert a probe to check the

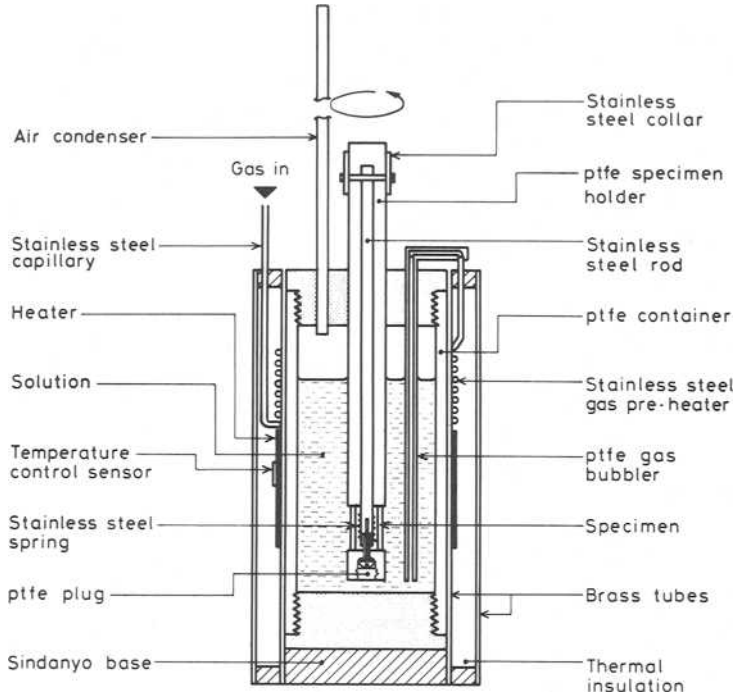


FIG. 6—*Test cell for corrosion studies.*

temperature, or to position a reference electrode during corrosion potential measurements.

The ptfe test cell was surrounded by an electrically heated jacket, and the temperature was controlled by a thermistor in close contact with the brass inner wall of the jacket.

The oxygen concentration of the test solution was controlled by continually purging the test solution at a rate of approximately 1 $cm^3 s^{-1}$ with gas mixtures. By varying the oxygen content of the gas mixture the concentration in the test solution could be maintained at values of <0.01 ppm with a purge gas of 100% nitrogen to a fivefold increase over the aerated value when the purge gas was 100% oxygen. The concentration of oxygen was checked by measurement of the oxygen diffusion current under each condition. To ensure that the temperature of the test solution was not unduly disturbed at the point of entry of the purge gas, the gas was preheated in a stainless steel tube wound round the hot inner brass tube of the heating jacket. Before use, the gases were cleaned and saturated with water by bubbling through a wash bottle fitted with a fine glass sinter and containing distilled water. The purge gases were vented from the ptfe vessel via an air condenser, which was a ptfe tube of external length 330 mm with an outside diameter of 13 mm and wall thickness of 0.6 mm. This arrangement

allowed very little loss of water vapor from the apparatus, and with the test solution at 90°C, water losses from the apparatus were less than 0.5 cm^3 per day. These losses were replaced by occasional additions of distilled water to maintain a constant level of test solution in the vessel as measured by an electronic depth probe inserted through the the unused drilling in the top end-plug.

A hollow cylindrical specimen (length 15 mm, outside diameter 40 mm) was mounted on a rod-type ptfe holder and tightly clamped by a stainless steel rod that ran internally through the specimen holder and a stainless steel bolt that was sealed from the test solution by a ptfe plug. This mounting procedure avoided a crevice at each end of the specimen and prevented access of test solution to the internal surface of the specimen.

The specimen holder was carefully machined so that it was a close fit through the top end-plug but could be freely rotated when attached to a flexible drive shaft rotating at 1 Hz.

Electrical contact with the specimen was achieved through a stainless steel spring mounted on the stainless steel clamp-rod that was bolted to a stainless steel ring at the external end of the specimen holder. Potential measurements were performed by introducing a reference electrode through the unused drilling in the top end-plug and contacting the specimen via the stainless steel ring of the specimen holder by means of a spring-loaded carbon brush.

Test Procedures

At least 24 h before use a mild steel test specimen, previously machined to the required dimensions, was given the required surface finish (for example, machined, etched, shot-blasted, or abraded), degreased, weighed, and stored in a desiccator.

The test solution was prepared from analytical quality reagents, and triply-distilled water which was prepared as outlined above. The test cell containing 700 cm^3 of solution was fitted with a dummy specimen (ptfe) rotated at 1 Hz and heated to the required temperature with the purge gas flowing. At least 24 h were allowed for the solution to attain the correct oxygen concentration and temperature before the dummy specimen was replaced by a steel specimen to start the test.

During the test period, the temperature and level of the test solution were checked daily. Corrosion potentials were measured, and samples of the test solution taken for analysis as required. At the end of the test the general features of the corrosion behavior were noted and the specimen was cathodically cleaned as above [*3*], dried, and reweighed.

Results

Some typical baseline data that have been produced by this test method are described below. The results are for specimens abraded with Grade 1G emery. The facility for accurate control of oxygen concentration has allowed data to be

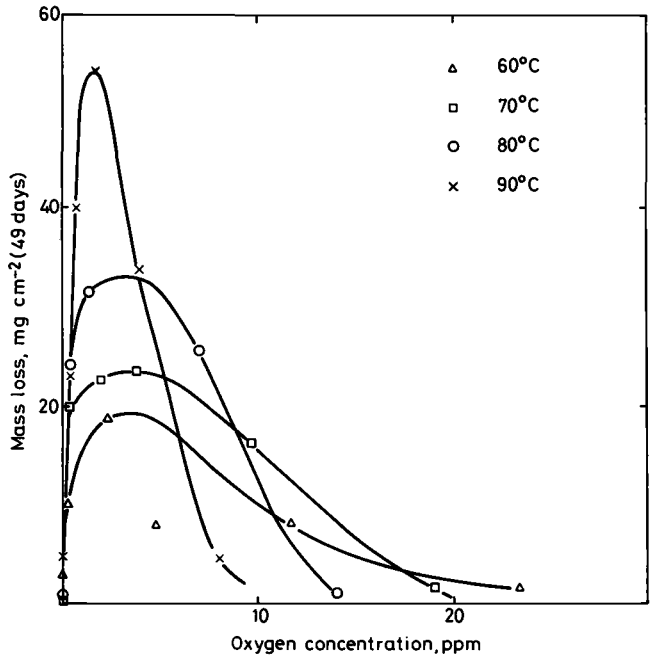


FIG. 7—*Mass loss of mild steel specimens in distilled water at varying temperature and oxygen concentration.*

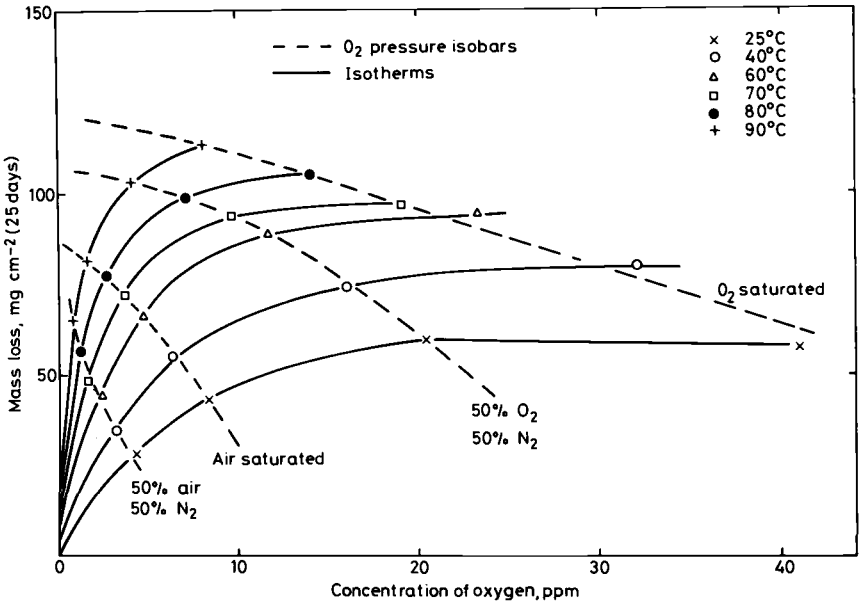


FIG. 8—*Mass loss of mild steel specimens in sodium chloride solution (35 ppm chloride) at varying temperature and oxygen concentration.*

obtained on the corrosion behavior of steel in distilled water at 60, 70, 80, and 90°C over a range of oxygen concentrations between deaerated (<0.01 ppm) and oxygen saturation at each temperature. The purge gas was either oxygen or air, alone or mixed with 50% nitrogen. Air was also mixed with larger quantities of nitrogen to produce an oxygen concentration of 0.4 ppm at each temperature. Deaeration was performed with nitrogen of high purity. Thus, tests were performed at oxygen concentrations up to about 23 ppm at 60°C, but only 8 ppm at 90°C because of the decreased solubility of oxygen in water with increasing temperature.

The results (Fig. 7) demonstrate the importance of good control of oxygen concentration if meaningful baseline data are to be accumulated. In deaerated distilled water the corrosion rate was very low at all test temperatures. With increasing oxygen concentration the mass loss increased more rapidly at the higher temperatures. At a critical oxygen concentration, which decreased as the temperature increased, the corrosion rate reached a maximum value, and thereafter oxygen caused partial passivation of the specimen. The passivation effect was more marked as the temperature increased. The passivating effect of oxygen on steel is now well known at boiler water temperatures and the use of high-purity water dosed with oxygen is increasingly used in power generating plants for corrosion control [*8*,*9*]. At the higher boiler water temperature, passivation can occur at lower concentrations of oxygen of around 0.1 ppm.

However, the marked passivating effect of oxygen is readily destroyed by the

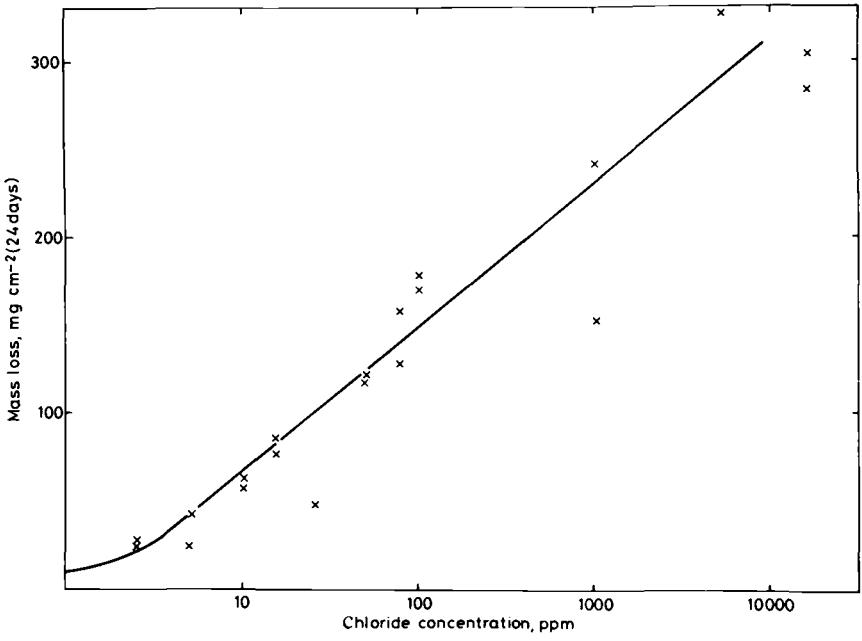


FIG. 9—*Mass loss of mild steel specimens in oxygenated sodium chloride solutions at 90°C.*

addition of chloride ions. Baseline date on the interrelation between temperature and oxygen concentration in a solution of 35 ppm chloride are displayed in Fig. 8. The mass loss of the specimen during a 25-day exposure period increased with increasing temperature and oxygen concentration.

The aggressive nature of the chloride ion is confirmed in the data shown in Fig. 9, which demonstrates the linear relationship between mass loss and the logarithm of chloride ion concentration over a wide range of concentrations. It is noteworthy that if corrosion rates of steel are determined with static solutions the corrosion rate is independent of chloride ion concentration, as is widely accepted. It appears that the corrosion process is under cathodic control in stagnant solutions, but under anodic control in experiments where an adequate supply of oxygen to the surface of the metal is ensured.

Summary

Experiments in distilled water at elevated temperatures have indicated that the reliability of conventional laboratory tests carried out in glass apparatus is doubtful in this medium, and that good control of dissolved oxygen is essential.

A standard test cell has been developed to overcome these problems. Preliminary baseline data have been presented to demonstrate the validity of the design. Data on the passivating influence of oxygen with increasing temperature in distilled water and the aggressive nature of chloride ions have been presented.

References

[1] Butler, G. and Mercer, A. D., *Nature*, Vol. 256, No. 5520, Aug. 1975, p. 719.
[2] Mercer, A. D. and Brook, G. M., *La Tribune du CEBEDEAU*, Vol. 31, No. 417–418, Aug.–Sept. 1978, 0. 299.
[3] Champion, F. A., *Corrosion Testing Procedures*, 2nd ed., Chapman and Hall, London, 1964, p. 189.
[4] Mercer, A. D. and Brook, G. M., *British Corrosion Journal*, Vol. 12, No. 2, 1977, p. 122.
[5] Mercer, A. D. and Warren, G. M., National Physical Laboratory Report No. DMA 257, Teddington, 1976.
[6] Butler, G., Francis, P. E., and McKie, A. S., *Corrosion Science*, Vol. 9, No. 10, 1969, p. 715.
[7] Francis, P. E. and Dolphin, A. S., National Physical Laboratory Report No. DMA(A)38, Teddington, 1982.
[8] Vreeland, D. C., Gaul, G. G., and Pearl, W. L., *Corrosion*, Vol. 17, No. 6, 1961, p. 95.
[9] Tyzack, C. and Berry, R., Conference on Water Chemistry of Nuclear Reactor Systems, British Nuclear Energy Society, Bournemouth, England, Oct. 1977.

DISCUSSION

H. Jain[1] *(written discussion)*—Could you please elaborate on the mechanism by which the tests in pyrex glassware show lower corrosion than in quartz?

P. E. Francis (author's closure)—The results of X-ray powder analyses of

[1]Brookhaven National Lab, Building 830, Upton, NY 11973.

corrosion products removed from the steel specimens indicated the presence of silicates or zeolitic compounds in those products from tests in glass vessels, with the proportion of these compounds in the total (various forms of iron oxides and so forth) product increasing with test temperature. Such compounds were effectively absent in corrosion products from tests in quartz vessels. Furthermore, silicates are known to be effective at quite low concentrations as inhibitors of the corrosion of steel in water whereas borates have not been reported to be effective at similar concentrations. These additional observations lend further support to the conclusion that silicon species are responsible for the low rates of corrosion of steel in hot water in glass vessels.

Frederic D. Bogar[1] *and Miller H. Peterson*[2]

A Comparison of Actual and Estimated Long-Term Corrosion Rates of Mild Steel in Seawater

REFERENCE: Bogar, F. D. and Peterson, M. H., "**A Comparison of Actual and Estimated Long-Term Corrosion Rates of Mild Steel in Seawater,**" *Laboratory Corrosion Tests and Standards, ASTM STP 866*, G. S. Haynes and R. Baboian, Eds., American Society for Testing and Materials, Philadelphia, 1985, pp. 197–206.

ABSTRACT: The linear polarization resistance method of predicting corrosion behavior was compared directly with weight loss measurements on freely corroding specimens. The estimated weight loss was obtained by calculation from the corrosion current and the polarization resistance. The anodic Tafel constant βa was determined from potentiodynamic curves for mild steel in flowing, oxygen containing, natural seawater. The cathodic Tafel constant βc was calculated by substitution of the corrosion current, the anodic Tafel constant, and the polarization resistance into the Stern-Geary relationship. In subsequent experiments, $\beta a = 0.066$ *V*/decade and $\beta c = 0.077$ *V*/decade were used in all calculations. Although an initial agreement between estimated and actual corrosion rates existed for periods of up to 60 days, long-term studies began to produce "anomalous" data in about 120 days. It was observed empirically that the polarization resistance was semi-logarithmically related to the scan rate over three orders of magnitude from 0.001 to 1 mV/s.

KEY WORDS: corrosion, steels, seawater, corrosion rates, polarization resistance, mild steel, Tafel constants, scan rates, evaluation

A number of techniques have been proposed for the estimation of corrosion rates of metals and alloys [*1–6*]. Many of the electrochemical methods are based on linear polarization techniques and, in recent years, a considerable effort has been made to improve accuracy both by novel polarization schemes and by modifications to the analysis of the data [*7,8*]. Several of these techniques lay claim to the determination of the "true" linear polarization curves required for better agreement with weight loss data [*9,10*]. Commercial instruments based on electrochemical methods are readily available and are reported to give satisfactory results, primarily for quality control applications. The validity of such methods in predicting corrosion rates is not well established.

Since the linear polarization resistance (LPR) technique has been widely used,

[1]Research chemist, Naval Research Laboratory, P.O. Box 1739, Key West, FL 33040.
[2]Supervisory research chemist, Naval Research Laboratory, Code 6316, Washington, DC 20375.

Copyright© 1985 by ASTM International www.astm.org

ASTM Subcommittee G01.11 on Electrochemical Measurements in Corrosion Testing established a task group whose work led to the development of the ASTM Practice for Conducting Potentiodynamic Polarization Resistance Measurements (G 59). This procedure provides a standard method for conducting such tests; however, ASTM Practice G 59 must be modified to be used in the investigation of corrosion rates in environments other than those specified by the procedure. Data obtained in the specified oxygen-free sulfuric acid may not be directly relatable to corrosion occurring under other conditions. In this study data obtained from the modified LPR method in quiescent, oxygen containing, natural seawater were evaluated by comparison with long-term weight loss data obtained under identical conditions.

Experimental Procedure

All of the corrosion data reported herein were obtained in flowing fresh natural seawater at the Naval Research Laboratory's (NRL) Marine Corrosion Research Laboratory in Key West, FL. The seawater was strained through a ceramic intake to remove grass and seaweed and distributed to the bench-top laboratory cells via a polyvinylchloride piping system and a Saran® lined pump. The seawater flowed through the cells in a single pass mode providing the specimens with an environment of clean electrolyte not contaminated with the products of the corrosion process. Ambient temperatures ranged from 15 to 31°C, the dissolved oxygen levels from 5.6 to 8.5 mg/dm^3, the salinity (obtained from resistivity data) from 36.58 to 39.02 ppt, and the pH from 8.04 to 8.12.

Samples of mild steel were obtained from several sheets of material; the samples were selected at random from each sheet. Specimens, 7.6 by 10.2 by 0.32 cm, were prepared from these samples. All specimens were degreased with acetone, air dried, polished with 600-grit silicon carbide paper, washed in hot tap water, polished with 600-grit pumice to a clean water break, rinsed with distilled water, and air dried. Electrical connections of insulated 12-gage solid copper wire were soldered to those specimens requiring electrical contacts. The soldered area was covered with epoxy resin. At the conclusion of the tests, the epoxy was removed to check for crevice corrosion under the epoxy. No crevice corrosion was found. The remaining specimens were suspended by glass S-hooks through a 5-mm hole in the top-center of the specimens.

Urethane cells, 20 by 36 by 7 cm, were constructed with a baffle to entrap any light oil films and to prevent a direct flow of seawater across the specimens. The seawater entered the body of the cells from the bottom of the oil trap, and the level was maintained by overflow outlets. The flow was such that the entire volume of the cell was changed once every 30 min. At this flow rate the seawater can be regarded as quiescent. No attempt was made to deaerate the seawater for either the weight loss or the electrochemical tests.

All electrochemical measurements were performed using a commercially avail-

able microcomputer-assisted potentiostat. Initially, the instrumentation and experimental technique were verified according to the method presented in ASTM Practice G 59.

In the seawater tests, the reference electrode was a commercial saturated calomel electrode (SCE) with a glass Lugin capillary bridge. The counter electrodes were either platinum, platinum-10% rhodium, or carbon rods. Initially, the tip of the capillary probe of the reference electrodes was placed within 2 mm of the specimen surface. Later it was found that the potentials measured were independent of the reference electrode position within the cell.

The anodic Tafel constant βa was determined from the slope of the anodic potentiodynamic curve from the open circuit potential to +250 mV versus SCE. The Tafel region was linear for the anodic curve. However, a valid cathodic Tafel constant could not be obtained because the shape of the curve under these conditions is controlled by concentration polarization. It was recognized by Stern [*11*] that βc approaches minus infinity as a limiting condition to yield the equation

$$I_{corr} = (\beta_a/2.303)\, R_p \tag{1}$$

In many practical cases this condition is not met and Prazak [*12*] found it necessary to modify the relationship to the form

$$I_{corr} = (\beta_a/2.303)\, R_p^{\,n} \tag{2}$$

where n is an empirical fitting constant.

At the end of the 28-day preliminary experiment it was found that the corrosion rates calculated from Eq 1 were not in good agreement with those calculated from the weight losses. Stern [*11*] had demonstrated that linear behavior near the open circuit potential would be found experimentally even where the cathodic current was not constant and advocated empirical determination of the fitting constants.

To establish an empirical value for the cathodic Tafel constant βc the corrosion current I_R was estimated by extrapolation of the anodic current density to the open circuit corrosion potential using the same data from which the anodic Tafel constant α_a had been determined as described by Dean [*13*]. Then, as suggested by Stern and Geary [*14*], the cathodic Tafel slope α_c was calculated from the known or estimated values of I_R, β_a, and the mean value of R_p from the 28-day data set. This is in effect equivalent to assuming that the corrosion current calculated from the anodic polarization curve and the open circuit corrosion potential is valid.

The reproducibility of the linear polarization resistance method was estimated by measuring R_p, waiting 15 min, and then repeating the process a minimum of five times. Also, the effect of scan rate on polarization resistance was measured with an additional series of specimens using scan rates from 0.001 to 1 mV/s.

TABLE 1—*Anodic Tafel constants for mild steel in low velocity natural seawater at 24°C.*[a]

βa = 0.0658	s = 0.0035 V/decade
0.065	0.064
0.065	0.065
0.061	0.065
0.066	0.069
0.073	...

Experimental Results

Nine mild steel coupons were immersed in seawater for ten days during which the corrosion potentials reached a steady state equilibrium. The anodic Tafel constant was then determined on each specimen using a scan rate of 0.1 mV/s. The arithmetic mean of βa was 0.0658 V/decade with a standard deviation of 3.5 mV/decade (Table 1).

The corrosion current I_{corr} was obtained graphically from the anodic Tafel curve. The corrosion current was measured as the current obtained by extending the linear region of the anodic curve to the corrosion potential E_{corr}. These data are reported in Table 2. The average value of the corrosion current density for the nine measurements at 24°C is 5.16×10^{-6} A/cm^2 with a standard deviation of 0.46×10^{-6} A/cm^2.

The polarization resistance of each of the above specimens was measured just before the determination of βa. The value of the cathodic Tafel constant was calculated from the Stern-Geary relationship and the above data. These results also are presented in Table 2. The average value of βc was 0.0768 V/decade, and one standard deviation was 0.0226 V/decade. In all subsequent calculations, 0.066 and 0.077 V/decade were used for βa and βc, respectively. The reproducibility of the linear polarization resistance measurements was demonstrated when the same specimen was used to determine R_p at 15-min intervals. In a

TABLE 2—*Estimation of the corrosion current and the apparent cathodic Tafel constant for mild steel in low velocity natural seawater at 24°C.*

I_{corr}, A/cm^2	βc, V/decade[a]
5.44×10^{-6}	0.062
5.27×10^{-6}	0.063
5.47×10^{-6}	0.083
4.45×10^{-6}	0.065
5.73×10^{-6}	0.098
5.30×10^{-6}	0.079
4.42×10^{-6}	0.074
4.95×10^{-6}	0.069
5.40×10^{-6}	0.094
6.20×10^{-6}	0.082

[a] βc = 0.077 and s = 0.013 V/decade.

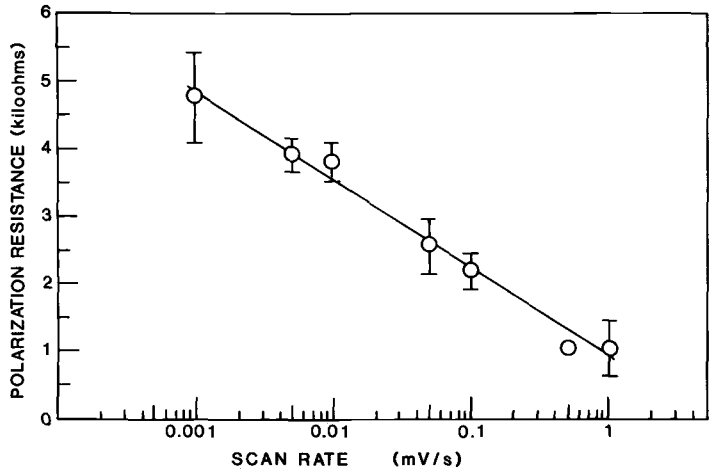


FIG. 1—*The effect of scan rate on the linear polarization resistance of mild steel in low velocity, natural seawater at 25°C.*

typical series, R_p had values of 3660, 3924, 3933, 3911, and 3956 Ω. An average value of R_p of 3877 Ω and a standard deviation of 12 Ω was obtained for the above series.

The effect of scan rate on linear polarization resistance was studied on the same specimen over a period of 39 days. The specimen was allowed to corrode for 48 h before the first test was conducted, previous measurements having shown that the corrosion potential reached a steady state value in less than this time. Since the LPR technique involved excursions of only 5 mV on either side of the freely corroding potential, the specimen was considered to have been unperturbed by the test. The data are on a semilogarithmic scale in Fig. 1.

TABLE 3—*Estimated and actual weight losses for mild steel in low velocity natural seawater after 28-day immersion.*

Actual Weight Loss, g[a]	Estimated Weight Loss from R_p, g[b]
0.58	0.57
0.52	0.57
0.50	0.62
0.58	0.57
0.51	0.50
0.56	0.57
0.51	0.57
0.58	0.56
0.60	0.57
0.57	0.53

[a]Mean = 0.55 and s = 0.037.
[b]Mean = 0.56 and s = 0.031.

TABLE 4—*Estimated and actual weight losses for mild steel in low velocity natural seawater after 305-day exposure.*[a]

Actual Weight Loss, g	Estimated Weight Loss, g
4.62	12.25
5.87	35.87
4.22	10.06
4.97	33.30
5.63	48.60
5.06	45.14
5.34	16.23
5.82	50.70
5.78	52.63
5.85	57.50
5.46	52.77
6.00	68.01
6.03	75.17
5.15	43.01
5.70	61.28
5.06	43.91

[a]Mean weight loss of controls = 5.410 g and s = 0.525 g.

In the long-term corrosion experiments, weight loss was estimated from R_p and the Stern-Geary equation daily for the first three days. Thereafter, weight loss was estimated every other day. At the end of the study, the estimated weight losses were summed and compared with the actual weight losses measured on an analytical balance. The data for the 28-day study are presented in Table 3.

The results of the 305-day study (Table 4) are summarized in Fig. 2 in which

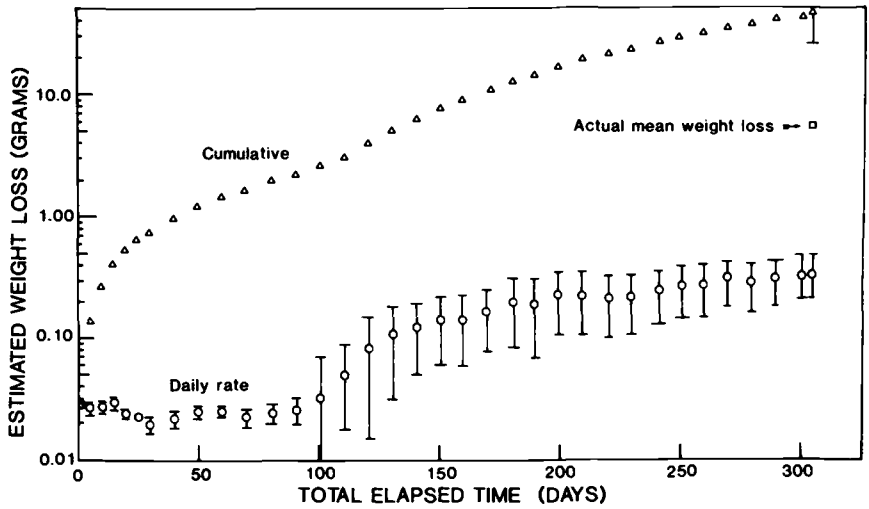


FIG. 2—*Total mean weight loss of mild steel in low velocity natural seawater calculated from* R_p. *The triangle represents the actual mean weight loss.*

the mean cumulative weight loss calculated from R_p with limits defined by plus or minus the standard deviation is plotted on a semilogarithmic scale versus time in days. For the first 120 days of exposure, the total weight loss was nearly linear as a function of time (Fig. 2). After 90 to 120 days, the weight loss appears to be an exponential function of time. After 225 days, the exponential relationship begins to break down. As shown on Fig. 1 the scatter between specimens increased markedly with time. In this Fig. 2, which is the mean data for eleven single specimens, the data agree with the previous 28-day experiment and with the data obtained by others [*15*].

Discussion

From the data of Fig. 2, it was apparent that three regimes were operating during the 305-day exposure test. In the early phase where weight loss was essentially a linear function of time, the specimens appeared free of fouling and marine growth. In the second and third phases of this study, the specimens were covered with a profuse mixture of fouling and corrosion products. It has been observed that at Key West a coating of microfouling attaches to most specimens within two weeks of immersion. Macrofouling, including grasses and bryzoa, forms after three months immersion. In the first phase when little fouling or buildup of corrosion scale had occurred, the specimens corroded freely. However, in the second phase fouling and loosely attached plates of corrosion products had begun to be evident. This phase was exponential in accord with the growth of the fouling. In the third phase, the marine growth and scale apparently reached a steady state balance and the weight loss no longer increased exponentially.

The weight loss curve was a measure of the electrochemical reactions occurring under the fouling and scale. In fact, when the specimens were cleaned and weighed the actual weight losses were less than 5×10^{-3} cm/year. The modified LPR electrochemical method had predicted a corrosion rate two to twelve times higher than the experimentally determined rates. The method failed in the presence of crevices and concentration cell corrosion as well as other forms of localized corrosion where the measured currents were not representative of total surface area exposed. The scatter increased with exposure time because of the unequal growth of marine organisms and scale from specimen to specimen.

Mansfeld [*16*] and Mansfeld and Kendig [*11*] have stated the need to measure the ohmic losses caused by solution conductivity and surface films by independent methods other than by potentiodynamic techniques when the conductivity of the media is low or for systems with high corrosion rates when R_p has the same order of magnitude as R_Ω. It is an error of this sort that is believed to have caused the high corrosion rates observed at 305-days exposure, which surface films of corrosion products and biofouling increased the ohmic resistance of the potentiodynamically observed R_p.

The effect of scanning rates on polarization resistance calculated from potentiodynamic polarization curves on American Iron and Steel Institute (AISI) 1005

(Unified Numbering System [UNS] G10050) low carbon steel in 4% sodium chloride solutions by Wolynec and Escalante [*10*] agree with the data presented here in Fig. 1. In both cases, it was not possible to extrapolate to an infinitely slow scanning rate to obtain a limiting value of the corrosion rate nor to establish a minimum sweep rate below which there was no further effect.

Conclusions

This study has demonstrated some of the limitations of linear polarization resistance measurements in predicting long-term corrosion rates in natural seawater.

1. The apparent weight loss curve for specimens of mild steel calculated from LPR techniques exhibits three distinct regions.
2. In the absence of fouling and loosely attached scale, the LPR method accurately predicts the corrosion rate of mild steel in quiescent seawater.
3. In the presence of fouling or heavy corrosion product films, the LPR technique did not accurately predict the corrosion rate of mild steel in quiescent seawater, the apparent value was from two to twelve times higher than the actual value.
4. Field tests based upon the LPR method, which predict significant differences in corrosion rates from minor changes in R_p data, are open to question because of the wide scatter in the data, and increasingly so with exposure time.
5. A limiting value of R_p was not attainable by extrapolation to infinitely slow scanning rates.

Acknowledgments

The authors wish to acknowledge the technical assistance of C. F. Ramirez and C. W. Billow.

References

[*1*] Baboian, R. and Haynes, G. S., in *Corrosion in Natural Environments, STP 558*, American Society for Testing and Materials, Philadelphia, 1974, pp. 171–184.
[*2*] Baboian, R. and Haynes, G. S., in *Electrochemical Corrosion Testing, STP 727*, American Society for Testing and Materials, Philadelphia, 1981, pp. 274–282.
[*3*] LaQue, F. L., *Marine Corrosion*, Wiley, New York, p. 45.
[*4*] Mansfeld, F., in *Electrochemical Techniques for Corrosion*, R. Baboian, Ed., National Association of Corrosion Engineers, Houston, TX, 1977, p. 18.
[*5*] Uhlig, H. H., *Corrosion and Corrosion Control*, Wiley, New York, 1967, p. 36.
[*6*] Wranglen, G., *An Introduction to Corrosion and Protection of Metals*, Butler and Tanner Ltd., London, 1972, p. 212.
[*7*] Gill, J. S., Callow, L. M., and Scantlebury, J. D., *Corrosion*, Vol. 39, No. 2, Feb. 1983, p. 61.
[*8*] Barnett, S. and Donaldson, M., *Corrosion*, Vol. 39, No. 1, Jan. 1983, p. 33.
[*9*] Macdonald, D. C., *Journal of the Electrochemical Society*, Vol. 125, No. 9, Sept. 1978, p. 1443.
[*10*] Wolynec, S. and Escalante, E., *Corrosion*, Vol. 36, No. 7, July 1980, p. 327.

[11] Stern, M., *Corrosion*, Vol. 14, No. 9, Sept. 1958, p. 440t.
[12] Prazek, M. and Barton, K., *Corrosion Science*, Vol 7, No. 3, March 1967, p. 159.
[13] Dean, S. W., Jr., *Electrochemical Techniques for Corrosion*, National Association of Corrosion Engineers, Houston, TX, 1977, p. 53.
[14] Stern, M. and Geary, A. L., *Journal of the Electrochemical Society*, Vol. 104, No. 1, Jan. 1957, p. 56.
[15] Fink, F. W. and Boyd, W. K., "The Corrosion of Metals in Marine Environments," DMIC Report 245, Defense Metals Information Center, Battelle Memorial Institute, Columbus, OH, 1970, p. 9.
[16] Mansfeld, F., *Corrosion*, Vol. 32, No. 4, April 1976, p. 143.
[17] Mansfeld, F. and Kendig, M., *Corrosion*, Vol. 37, No. 9, Sept. 1981, p. 545.

DISCUSSION

M. W. Kendig[1] *(written discussion)*—I would like to point out that the disagreement between corrosion rates calculated from R_p and those calculated from weight loss data arises from the fact that the R_p's have been incorrectly determined using nonsteady state current versus potential curves. This is clearly the case for some of the data presented here since the observed R_p varies inversely with scan rate. A detailed discussion of the need for a sufficiently slow scan rate for determining R_p has been presented elsewhere [*1*]. In addition, since the cathodic reaction is controlled by O_2 diffusion, the following equation holds

$$R_p = b_a/2.3031 = B/I$$

Thus, the author's calculation of B is in error and will also contribute to an underestimation of R_p.

F. D. Bogar and M. H. Peterson (authors' response)—Dr. Kendig has apparently misread the abscissa on our Fig. 1. The observed R_p did not vary inversely with the scan rate, but inversely with the logarithm of the scan rate. Indeed, it was our intent to show that even at the lowest scan rate at which we could obtain reproducible data (0.001 mV/s) there was no indication that a limiting value had been reached and that further reduction in the scan rate would have no further effect on R_p. This lack of a limiting scan rate was a major factor in concluding that there was no unique limiting R_p value for mild steel in seawater, and that B in Dr. Kendig's equation must in fact be established by empirical or semiempirical methods for each system and experimental variation.

T. S. Lee[2] *(written discussion)*—The authors apparently attribute the lack of agreement between the actual and estimated corrosion rates to the presence of fouling in the natural seawater tests. They infer this renders the electrochemical

[1]Rockwell International Science Center, 1049 Camino do Rios, Thousand Oaks, CA 91360.
[2]LaQue Center for Corrosion Technology, Inc., P.O. Box 656, Wrightsville Beach, NC 28480.

linear polarization method to be inaccurate. However, their Tafel slope constants appear to have been determined at only one time early in the test period. These values were then assumed to remain constant in all subsequent calculations of linear polarization corrosion rate. To obtain "absolute" values of corrosion rate, these Tafel constants should have been adjusted to account for effects of film formation with exposure time. With provision of more samples to obtain this data, a better correlation between the mass loss and electrochemical derived corrosion rates would likely have been obtained.

F. D. Bogar and M. H. Peterson (authors' response)—While marine fouling certainly contributed to the lack of success in predicting corrosion rates in the longer term experiment, the junior author, at least, considers that the effects of heavy plates of rust on the specimen surface and periodic disruption of the corrosion film were also major contributing factors.

It seems unlikely that there were major changes in the Tafel constants as the corrosion rates established by weight loss for the 28- and 305-day experiment were almost identical. It is more likely that the electrolytic and surface film resistance (Ref *15* in paper) increased because of biofouling and to the formation of large plates of semi-attached corrosion products. The point made by Mansfeld and Kendig (Ref *4* of paper) that R_p^{obs} will always differ from the true R_p and that independent measurement of this value should be made in low conductivity media or with systems of high corrosion rates is well taken and in retrospect the authors would have been well advised to attempt to determine this factor separately.

Reference

[*1*] Mansfeld, F. and Kendig, M., "Concerning the Choice of Scan Rate in Polarization Measurements," *Corrosion*, Vol. 37, No. 9, Sept. 1981, pp. 545–546.

Tracy L. Nye,[1] *Samuel W. Smith,*[1] *and William H. Hartt*[1]

Once Through Versus Recirculated Seawater Testing for Calcareous Deposit Polarization of Cathodically Protected Steel

REFERENCE: Nye, T. L., Smith, S. W., and Hartt, W. H., **"Once Through Versus Recirculated Seawater Testing for Calcareous Deposit Polarization of Cathodically Protected Steel,"** *Laboratory Corrosion Tests and Standards, ASTM STP 866*, G. S. Haynes and R. Baboian, Eds., American Society for Testing and Materials, Philadelphia, 1985, pp. 207–214.

ABSTRACT: In seawater, cathodic protection systems for steel structures rely on the formation of a calcareous film to help polarize the surface and thereby reduce the current required to maintain the potential in the protection range. These models require experimental determination of the polarization behavior for the cathodically protected steel. The experiments have been carried out in a variety of electrolytes including artificial seawater, recirculated seawater, and once through fresh seawater. While the latter is obviously the preferred method, there are few research facilities capable of extensive testing in fresh flow-through seawater. This results in the use of the less preferred recirculated natural and artificial seawater procedures.

This paper presents the results of an investigation contrasting data obtained in a series of otherwise identical once-through and recirculating seawater experiments in which the current decay rates of cathodically protected steels were determined. The experiments were run in fresh Atlantic Ocean seawater at the Center for Marine Materials Laboratory at Florida Atlantic University and ASTM Specification for Substitute Ocean Water (D 1141) artificial seawater. Both once-through and recirculating experiments were run concurrently. Possible explanations for the observed polarization rate differences include the effect of dissolved organic carbons and ion depletion.

KEY WORDS: corrosion, cathodic protection, seawater, calcareous deposits, polarization rates, artificial seawater

Cathodic protection is one of the most important tools available for control of corrosion in submerged applications. The current density required to protect steel surfaces in seawater is greatly reduced by the formation of a calcareous film. Recently there have been several attempts to model this effect [*1,2*]. These

[1]Research assistant, assistant professor, and professor, respectively, Department of Ocean Engineering, Florida Atlantic University, 500 NW 20th St., Boca Raton, FL 33431.

Copyright© 1985 by ASTM International www.astm.org

films form because a cathodic current in an aqueous solution, such as seawater, produces an increased pH resulting from the production of hydroxyl ions or the consumption of protons or both. The dominant cathodic half reaction is oxygen reduction or

$$O_2 + 2H_2O + 4e^- \rightarrow 4OH^-$$

Since the pH of seawater is controlled by the carbonate system, the above reaction shifts the carbonate balance according to

$$OH^- + HCO_3^- \longrightarrow CO_3^= + H_2O$$

$$Ca^{++} + CO_{3\ excess}^{=} \longrightarrow CaCO_{3ppt}$$

As can be seen the hydroxyl ions produced tend to be consumed by the precipitation of calcium carbonate. At even higher pH values (by about 10) magnesium hydroxide also precipitates [*3*].

The actual kinetics of this process are complicated [*3*]. Calcium carbonate commonly exists in two crystal structures, calcite and aragonite. Calcite is the equilibrium phase; however, both its nucleation and growth are inhibited by the presence of magnesium ions. For the case of aragonite only the nucleation process is inhibited, while growth is not. Aragonite then tends to be the dominate phase precipitated from seawater and, therefore, the calcium carbonate phase present in the film. There is evidence that marine organics may play an important role in the precipitation of aragonite in seawater [*4*].

While recirculated natural seawater and even artificial seawater have been used for testing and research pertaining to behavior of materials in the marine environment for many applications, it is not clear that these electrolytes permit realistic simulation of normal seawater exposure. Factors inherent to these environments that could cause modified material response from one situation to the next include differences in organic content and minor element and carbonate chemistry.

The purpose of the present paper is to report the results of experiments involving exposure of cathodically polarized low carbon steel in several aqueous environments, including flowing once-through natural seawater, and to point out differences in material behavior that appear to be sensitive to environmental variations.

Experimental Procedure

The experimental apparatus consisted of a pair of concentric Plexiglass® cylinders that served as an inner testing chamber and an outer constant temperature bath. This is illustrated schematically in Fig. 1. Teflon® coated steel rods were employed to position the specimen and to provide an electrical connection. A platinum coated niobium mesh surrounding the specimen served as the counter

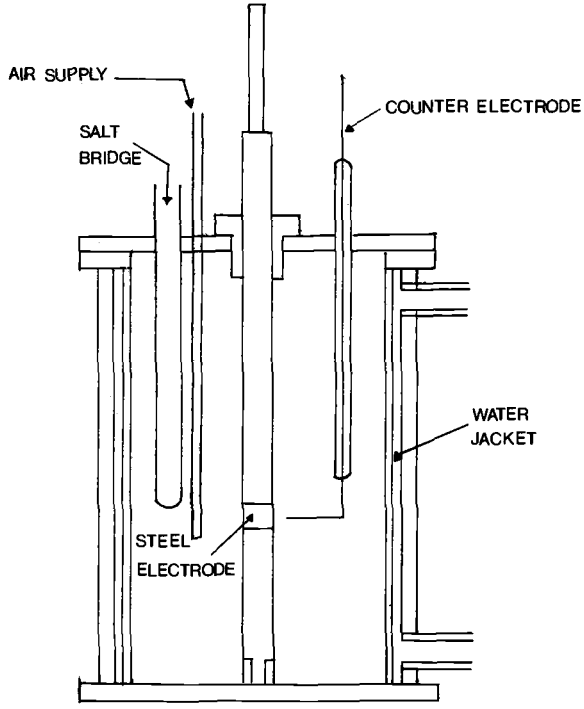


FIG. 1—*Schematic illustration of the experimental apparatus.*

electrode. To keep the electrolyte saturated with atmospheric oxygen and carbon dioxide, the solutions were aerated with air of 100% humidity via a silicon air stone. Seawater for all experiments was that available at the Center for Marine Materials Laboratory located on the ocean front in Boca Raton, FL. Sand filtered water is delivered to this facility via an all plastic pump and piping system. Properties for the water for an annual cycle have been reported [5]. Flow rate through the test cells was 1 L/min in all cases. Experiments involving recirculating electrolyte employed 2.6 L of solution in conjunction with a parastaltic pump. All comparative tests were run simultaneously with the effluent of the once-through test chamber being used to control the temperature of the recirculated test chamber. In this way the temperatures of the two chambers were always the same. Although the temperatures were the same in each test chamber during comparative runs, the ambient water temperature varied from 20 to 26°C during the year.

Specimen Preparation

Specimens 25.4 mm long were prepared from commercial 12.7 mm-diameter mild steel rod by abrading with coarse grade polishing paper followed by 400-grit aluminum oxide paper. Subsequently they were sequentially rinsed with

acetone and alcohol and then mounted on Teflon coated steel rods. Rubber gaskets were used to prevent water leakage into crevices at each specimen end. The specimens were used immediately so that there was no degradation in the surface finish.

Prepared specimens were placed in the testing chamber at a potential of −1.00V saturated calomel electrode (SCE) applied by a locally fabricated potentiostat. Potential and current were monitored and recorded for about 48 h using an Esterline Angus Model PD2064 data acquisition system. After each experiment, the apparatus was cleaned and specimens reprepared as described above. Each experiment was repeated at least three times to assure reproducible results.

Results

Initial control experiments involved specimens cut from mild steel rods selected at random from the existing stock in the laboratory. This was done to determine if the minor variations in the compositions of the rods would significantly affect the results. Unfortunately, they did. Figure 2 shows typical current decay curves for this set of experiments performed in once-through natural seawater. As the calcareous deposit formed on the steel surface the current decayed. These curves show some differences in the rate of current decay, especially during the first 15 to 30 h when the deposit is initially forming. Once the current densities had stabilized better agreement was obtained. When spec-

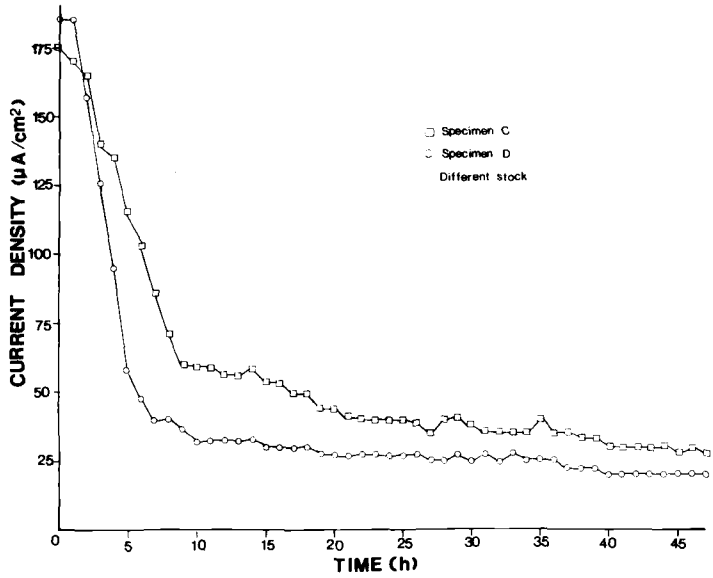


FIG. 2—*Typical current decay curves for experiments performed in once-through natural seawater.*

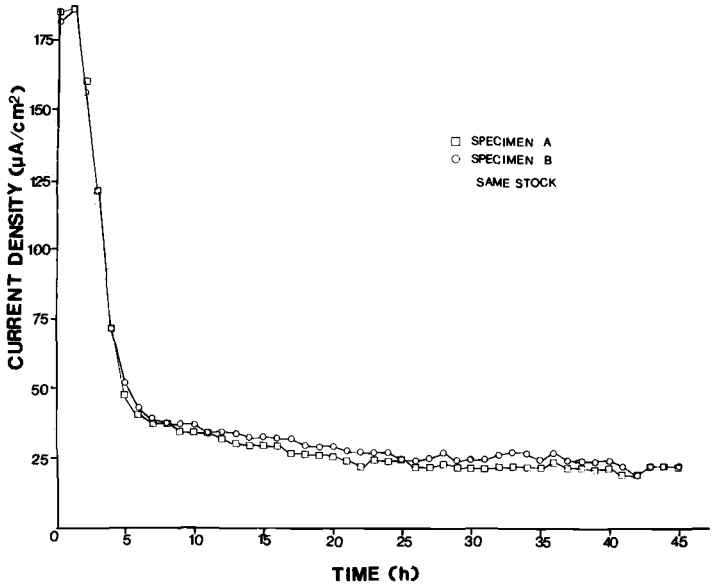


FIG. 3—*Typical set of results for specimens cut from the same mild steel bar.*

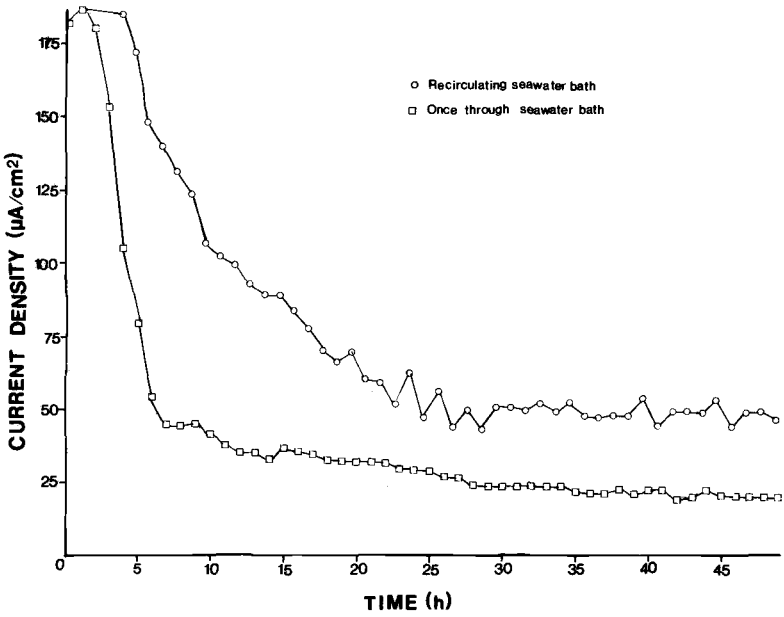


FIG. 4—*Typical results contrasting once-through and recirculating systems.*

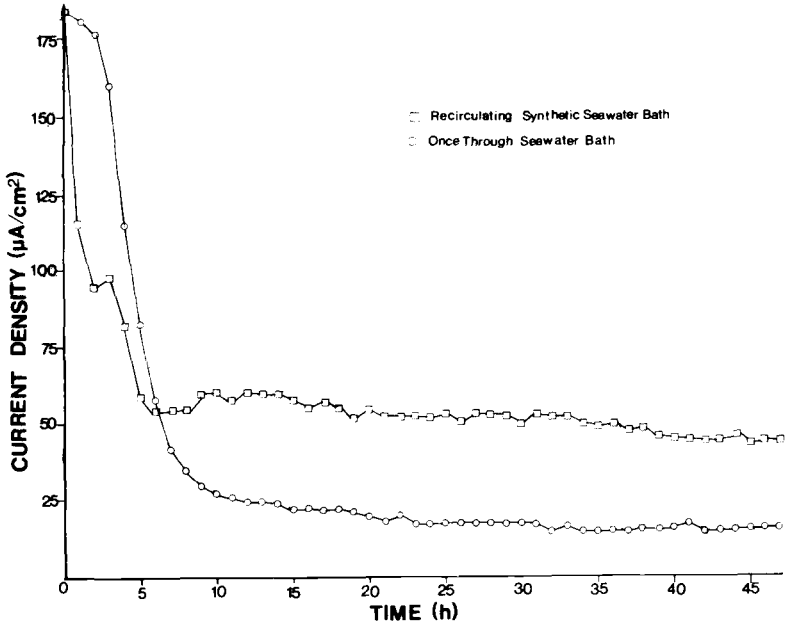


FIG. 5—*Typical results form a comparative run of once-through seawater and artificial seawater.*

imens cut from the same mild steel bar were used, nearly identical current densities were obtained. A typical set of results can be seen in Fig. 3. Note the current dropped from 180 to 25 $\mu A/cm^2$, an 86% drop. This is in agreement with the results of Culberson et al.[2]

Current densities observed for specimens placed in the recirculating seawater bath differed substantially from those observed for once-through seawater. Typical results contrasting once-through and recirculating systems are shown in Fig. 4. Also, results were less reproducible and the steady state current value was much greater than that of the once-through experiments.

Figure 5 illustrates typical results from a comparative run of once-through seawater and artificial seawater. As can be seen the artificial seawater resulted in a higher current density than the once-through system. Although calcareous deposits were observed to form on the steel in the artificial seawater, they did not appear to be as thick as those formed in once-through natural seawater. In spite of being aerated there were problems maintaining the pH of the artificial seawater when the specimen was cathodically protected.

Discussion

The fact that mild steel specimens machined from different bars gave significantly different results during the initial period of film formation was unexpected. This was apparently because of differences in the kinetic activity of the steel

[2]Culberson, C. H. et al, unpublished research.

surfaces. What caused these differences is unknown at the present time, however, an energy dispersive X-ray analysis with an ORTEC EEDS II quantitative unit revealed no chemical differences in the steels. This technique could not determine the carbon content of the steel, but it is difficult to rationalize how small variations in the carbon present could significantly affect the results. Additional experiments are required to better rationalize this observation. The present experiments indicate, however, a need for obtaining specimens from the same material stock. To this regard all specimens were cut from a single mild steel rod.

The observation that recirculated natural and artificial seawater yielded film formation rates that differed from once-through seawater can probably be traced to differences in the organic character of the water or depletion of constituent ions. While care was taken that the area of the specimen was small compared to the volume of the seawater (volume to area of about 270 cm^2/cm^3), there still was a depletion of calcium and perhaps some minor elements during precipitation. Measurements with an Orion calcium specific electrode indicated that there was a 10 to 20 ppm depletion in calcium. Subsequent experiments using larger volumes of recirculated seawater did not show significantly different results indicating that calcium depletion was not the problem. In light of the results of Chave [*4*], it is believed that the organic character of seawater is likely important to the development of the calcareous film. The organics are both very surface active and can change the activity of ions in solution. They may also affect the kinetics if the precipitation reactions. For these reasons organics are suspect as a cause of the differences observed.

Conclusions

For the present set of experiments and experimental conditions where mild steel was cathodically polarized to -1.00-V SCE the following conclusions may be reached:

1. Calcareous deposit formation on mild steel, in conjunction with oxygen concentration polarization, resulted in a reduction of cathodic current density from 180 to 25 $\mu A/cm^2$, an 86% reduction during the 48- to 50-h test period for tests performed in natural, once-through seawater at ambient temperature.
2. The current density decay was reproducible within experimental error for specimens prepared from the same steel rod, but variations on the order of 17% occurred when specimens were prepared from different rods. Attempts to correlate this effect with steel chemistry were unsuccessful.
3. The rate of current density decay and the steady state current density achieved after 48 h were different for natural, once-through seawater as opposed to either recirculated natural or artificial seawater. The films formed in the once-through seawater experiments polarized the cathodic reactions more effectively than those formed in artificial seawater or recirculated natural seawater. This implies that the films formed in the field should reduce the current requirements more than would be predicted by experiments performed in these electrolytes.

Acknowledgments

This work was supported by a National Sea Grant. The test apparatus was designed by C. H. Culberson of the University of Delaware.

References

[1] Vennett, R. M., *Materials Performance*, Vol. 18, No. 11, Nov. 1979, pp. 26–33.
[2] Fu, J. W., *Corrosion*, Vol. 38, No. 5, May 1982, pp. 295–296.
[3] Hartt, W. H., Culberson, C. H., and Smith, S. W., *Corrosion '83*, Paper 59, April 1983.
[4] Chave, K. E., and Suess, E., *Limnology and Oceanography*, Vol. 15, 1970, p. 633.
[5] Hartt, W. H., *Offshore Technology Conference*, Paper 3962, May 1981.

Stephen V. Crume[1]

A Corrosiveness Test for Fibrous Insulations

REFERENCE: Crume, S. V., **"A Corrosiveness Test for Fibrous Insulations,"** *Laboratory Corrosion Tests and Standards, ASTM STP 866*, G. S. Haynes and R. Baboian, Eds., American Society for Testing and Materials, Philadelphia, 1985, pp. 215–227.

ABSTRACT: This paper describes the original development work for an insulation corrosiveness test that is used to test a variety of blanket, loose fill, and rigid fibrous insulations. The test, which provides a relative comparison of insulation corrosiveness with that of an inert control material at elevated temperature and humidity conditions, is reliable and reproducible when properly performed. The test is useful as a product development tool to qualify new insulation products and product formulation changes. The test consists of placing insulation and specially cleaned cotton controls against metal coupons and exposing them to 49° C (120° F) and 95% relative humidity conditions. After exposure, the coupons are ranked in order of corrosiveness by a panel of judges. A nonparametric statistical method is used to identify insulations that are more corrosive than the inert control material. Condition of the metal surfaces, cleanliness of the inert cotton control material, and uniform contact of the insulation against the metal surfaces were three areas identified as critical in conducting the corrosion test.

KEY WORDS: corrosion, insulation, steels, insulation corrosiveness, steel coupon corrosion

This paper describes the development of a test method, C-02A [*1*], used at Owens Corning Fiberglas for evaluating the corrosiveness of fiberglass insulations and other insulation products. The test simulates a typical end use by placing the insulation against metal coupons, and exposing them to accelerated temperature and humidity conditions. Judgements of an insulations corrosiveness are made by comparisons with the similar coupons tested with an inert control material. The test is applicable to blanket, loose fill, and rigid insulations.

Versions of this test method have been adopted by the Society of Automotive Engineers (SAE) [*2*] and have been incorporated into Federal Specifications HH-I-1030B [*3*] and HH-I-521F [*4*]. A version of this test has also been adopted as part of the ASTM Specification for Mineral Fiber Blanket Thermal Insulation for Wood Frame and Light Construction Buildings (C 665) and has been proposed

[1] Advanced Scientist, Research and Development Services, Owens Corning Fiberglas Corporation, Technical Center, Granville, OH 43023.

Copyright© 1985 by ASTM International www.astm.org

for the ASTM Specification for Mineral Fiber Loose Fill Thermal Insulation (C 764).

Although the test has been adapted for several different metals, this paper will cover the original development work that was done only for steel.

Previous Corrosion Testing at Owens Corning

Corrosion testing of insulations at Owens Corning several years ago was done with reuseable 3-mm (1/8-in.) thick steel coupons that were lap polished to a mirror finish. Insulations were secured loosely against one surface of the coupon with tape. The specimens were examined after exposure to elevated temperature and humidity and compared to a blank control. Very little or no corrosion was normally observed, and results were not reproducible.

The corrosion test from Federal Specification HH-I-558B for Industrial Mineral Fiber Insulation [5] was later used. This specification replaced the reuseable coupons with 0.5-mm (0.020-in.) thick, 25- by 100-mm (1- by 4-in.) steel plates. Insulation was placed on each side of the steel coupons and held in place with string or tape. Sterile cotton was introduced as an inert control material. Specimens were conditioned at 49°C (120°F) and 95% relative humidity (RH) for 96 h and examined for corrosion. Passing the test required that an insulation corroded the metal no worse than the cotton control. This test had most of the reproducibility problems of the previous one. Random amounts of corrosion usually developed on the insulation coupons, and very little or none was observed with the cotton control. At this point it was obvious that new test procedures were needed.

New Test Development

A study was undertaken to identify the variables associated with placing insulation against metal surfaces, develop a new control material, and develop a better, more reproducible test.

Metal

The specification for the steel used in HH-I-558B was considered satisfactory and left unchanged: 0.5-mm (0.02-in.) thick, quarter hard, low carbon, cold rolled strip steel, Bright Number 2 finish, straightened, flattened and cut to size. The source used for this steel is the Precision Steel Corporation of Chicago, IL.

One of the variables we wished to minimize was condition of the metal surface. As received the steel surfaces were coated with oils of unknown composition and variable in origin. Some lots of steel had particularly stubborn surface coatings. Difficulty in cleaning the surfaces also appeared to increase with time of storage.

Solvent degreasing was found to be ineffective in cleaning the steel surfaces.

Detergent washes were more effective than solvents but still did not leave the metal surfaces free of water breaks.

Other surface preparation techniques were tried. These included abrading the surfaces with different grit papers. Abrasion was found to obscure the corrosion patterns and to reduce the overall amount of corrosion. This added a new source of variability and resulted in cold working of the surfaces. Pickling the steel in dilute hydrochloric acid dulled the surfaces and caused increased corrosion apparently caused by chloride residue left after rinsing.

The cleaning system found to work best consisted of a short vapor degreasing in perchlorethylene followed by a hot caustic bath (10% potassium hydroxide solution) and a final rinse in distilled water. Inorganic residue left on the steel surfaces after degreasing must be manually wiped off as it will not be removed in the hot caustic bath.

Inert Control

After establishing the metal cleaning procedures, problems with the cotton control material were found. The cotton when placed against the cleaned steel coupons protected the steel from corrosion during the tests. An oily type residue was found on the coupon surfaces that had been exposed to the cotton. Our analytical laboratory indicated that cottonseed oil was present on the sterile cotton.

Acetone and methylene chloride were considered for removal of the cottonseed oil. Acetone was selected because of the toxicity of methylene chloride and the possibility for chloride contamination. The cottonseed oil proved to be difficult to remove completely requiring the use of a cycling batch extractor.

Thorough cleaning of the cotton was found to be critical to the success of the corrosion test. Incomplete cleaning results in nonuniform, nonreproducible, reduced amounts of corrosion on the cotton control coupons. Rolls of sterile cotton from different batches were found to vary in the amount of oil contaminants. Some batches of cotton contained oil that was more difficult to remove than others, apparently because of partial polymerization of the oil.

The outside surface of the sterile cotton as unrolled is more uniform than the inside surface. This outside surface of the cotton is placed against the metal control coupons during the test to provide more uniform and reproducible corrosion patterns.

Other materials, such as polyester batting, were also investigated as possible inert controls but were rejected for various reasons: nonreproducibility, uniformity problems, corrosion properties, availability, and so forth. However, one material, unbonded, unlubricated glass wool was found to perform satisfactorily as an inert control. Washed sterile cotton was chosen over the glass wool as a control material because most of our experience was with cotton and because we wanted to compare fiberglass products with a nonfiberglass control. The SAE

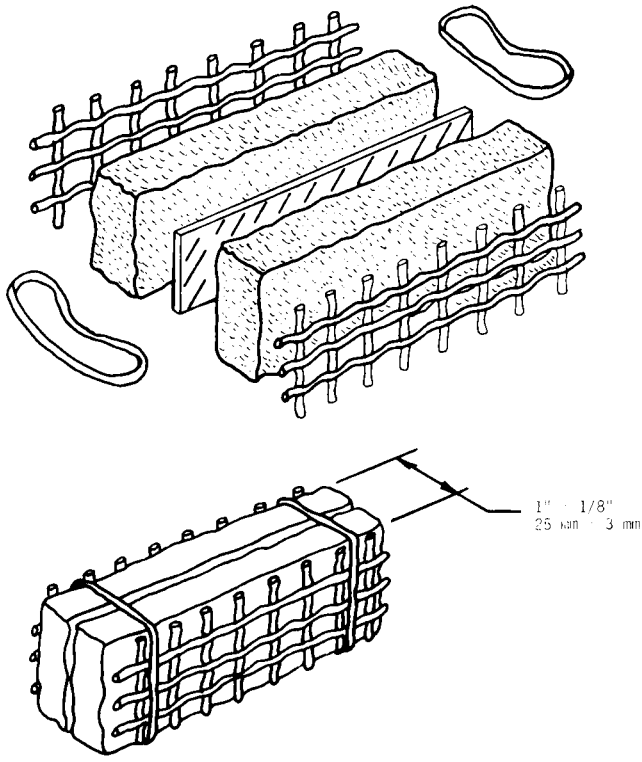


FIG. 1—*Assembly of corrosiveness test piece.*

in their version of this test, Corrosion Test for Insulation Materials (J 1389), has allowed the option of either using washed cotton or unbonded, unlubricated glass wool as the control material.

Specimen Mounting

One of the parameters recognized early in this study was the importance of having uniform contact between the metal and insulation. Instead of taping the insulation to the metal at each end, the concept of applying uniform pressure to the insulation by the use of open grid wire cloth was introduced. The test assembly became a metal coupon sandwiched between two pieces of insulation backed by the woven wire cloth and held together by a rubber band at each end. Uniform pressure is maintained throughout the test by the rubber bands at constant extension. Figure 1 shows the test piece assembly.

Equipment

Most of the equipment needed to perform the corrosion tests is available off the shelf or can easily be constructed.

Cotton Extraction Apparatus

The experimental setup used to clean the cotton is shown schematically in Fig. 2. It consists of a side chamber extractor available from the A. H. Thomas Company, a heating mantle, and a custom designed heating controller. Vacuum grease contamination was avoided in the extractor by using polytetrafluoroethylene (PTFE) sleeves. Because of the high flammability of acetone, the extractor must be set up in a properly operating fume hood for safety.

The heating controller circuit schematic is given in Fig. 3. The controller has two functions: the first is to control the boiling rate of the acetone; the second is to shut the power off should the acetone in the reservoir boil dry.

The heart of the controller is a West Instruments thermocouple controller, which is connected to a copper-constantan thermocouple foil attached to the acetone reservoir using a thermally conducting paste as shown in Fig. 4. An autotransformer is used to control current to the heating mantle. When the temperature exceeds the set point, the thermocouple controller activates a normally closed relay to shut power off to the heating mantle.

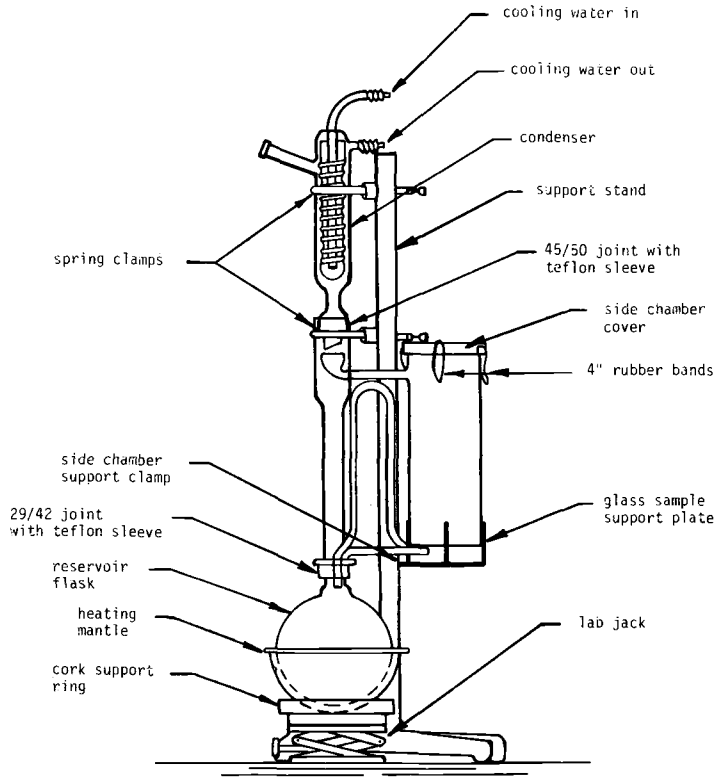


FIG. 2—*Side chamber extractor for cleaning sterile cotton.*

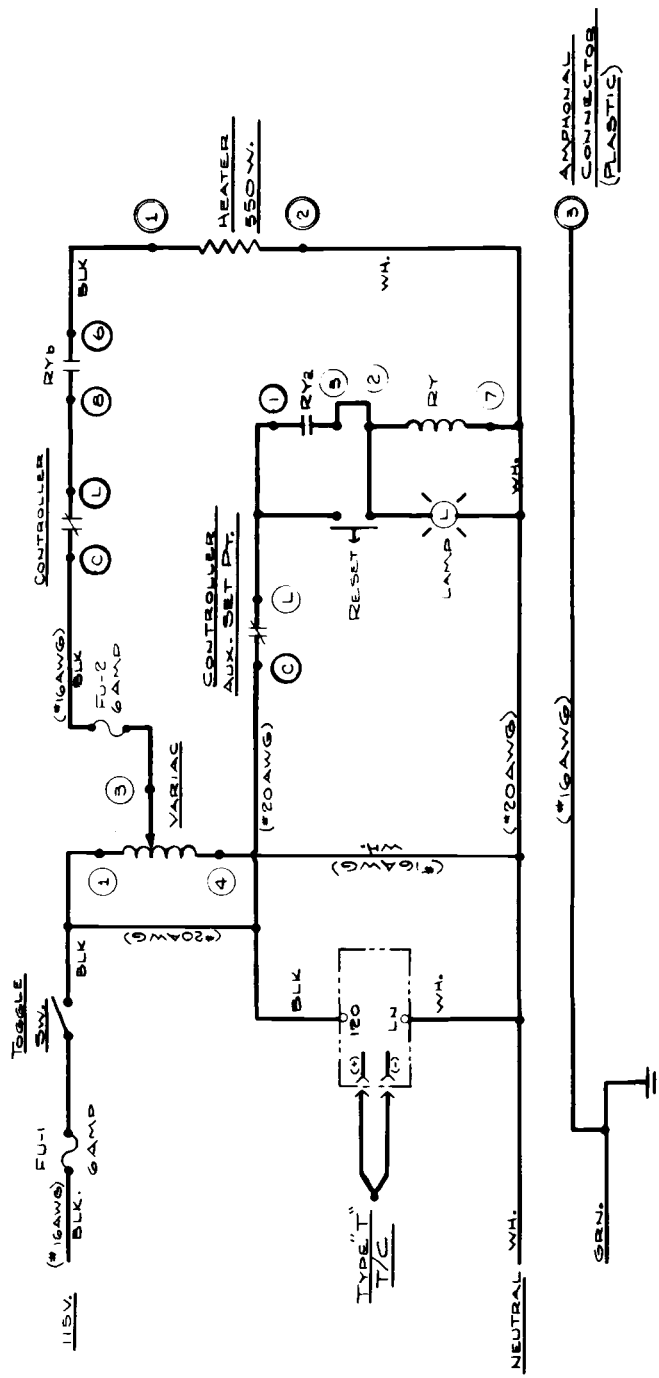


FIG. 3—*Temperature controller for side chamber extractor wiring scheme.*

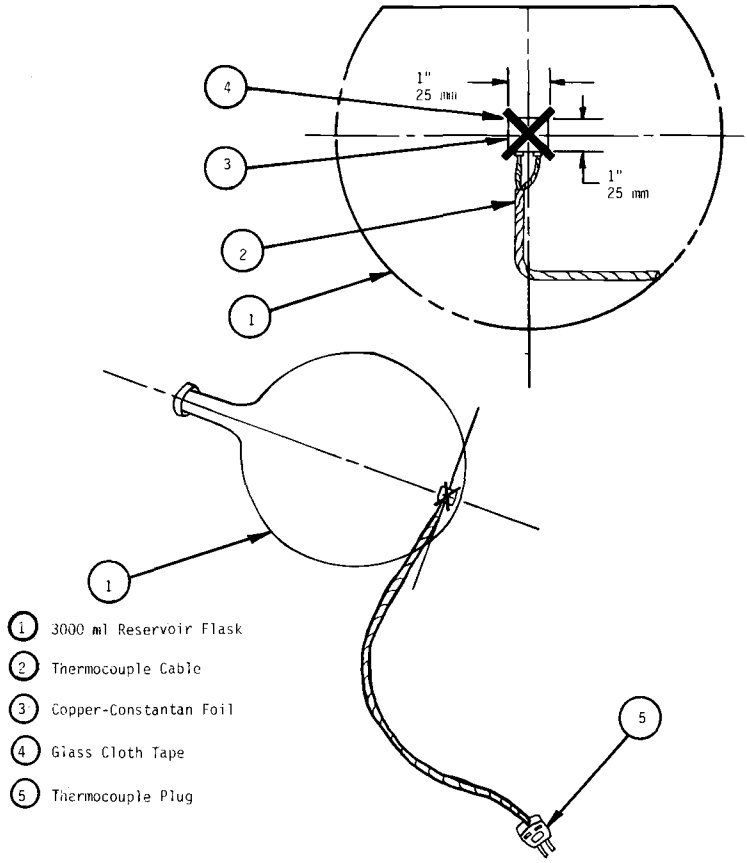


Fig. 4—*Reservoir flask with thermocouple attachment.*

The extractor is operated by placing acetone and boiling chips in the reservoir, turning water on to the condensor, and activating the heating controller. A piece of sterile cotton, approximately 125 by 350 mm (5 by 14 in.) is rolled loosely and placed in the side chamber. The cotton is rolled so that the original outside surface is on the exterior of this small roll. The outside surface is the one that is placed against the metal during the test. Using a larger piece of cotton or stacking the cotton will greatly reduce the cleaning efficiency of the process. The cleaning process is enhanced by manually squeezing the acetone from the cotton at the end of the first or second extraction cycle using solvent resistant gloves.

After a minimum of 48-h extraction time, the cleaned cotton is removed from the extractor and dried at low heat in a vacuum oven.

Humidity Cabinet

A clean, well maintained humidity cabinet regulated at 49 ± 2°C (120 ± 3°F) and 95 ± 3% RH is required for the conditioning of the test coupons. Contaminants in a humidity cabinet may affect results of the corrosion test. A circulating air water bath type humidity cabinet is recommended.

Proper operation of the humidity cabinet is absolutely essential for reproducibility and uniformity of corrosion test results. Improper operation can result in condensation on the test coupons, which occurs in a random and unpredictable manner. The humidity cabinet should be allowed to equilibrate to near ambient conditions before placing corrosion specimens into the cabinet. At ambient, the cabinet should be closed and the dry bulb temperature should be allowed to stabilize to 49°C (120°F). After stabilizing, the wet bulb control is turned on. This procedure can be used for both cold starts and for starting a new test while a test is still in progress.

Degreaser

An industrial degreaser with perchloroethylene solvent is used to preclean the steel coupons at Owens Corning. The coupons are separated in a rack and placed in descending solvent vapors for no more than 5 min. The degreaser should be kept reasonably clean and free of harmful contaminants.

Materials

The following materials are needed for performing the corrosion test:

(1) a supply of washed sterile cotton cleaned by extraction,

(2) a supply of 25 by 100-mm (1- by 4-in.) steel test coupons specified as cold rolled low carbon strip steel, bright Number 2 finish, Number 3 temper, quarter hard,

(3) supply of insulation to be tested,

(4) supply of woven wire screen cut into 100- by 38-mm (4- by 1.5 in.) pieces, American Iron and Steel Institute Type 304 (Unified Numbering System [UNS] S30400) stainless steel with 1.6-mm (0.063-in.) wire and 11-mm (7/16-in.) open grid or similar,

(5) Number 12 rubber bands, a 10% solution of potassium hydroxide, distilled water, laboratory wipes, and stainless steel bent wire hooks.

Test Procedure

Metal Preparation

The steel coupons are precleaned in a vapor degreaser to remove the oily film from the surfaces. After degreasing, the coupons are individually wiped with laboratory wipers to remove any remaining inorganic residue. Next the metal is

cleaned in a hot caustic solution (10% potassium hydroxide) until free of water breaks, several minutes may be required depending on surface conditions. The coupons are then thoroughly rinsed in distilled water and dried with laboratory wipes. Contamination and contact of the cleaned metal plates with bare hands must be avoided. The test coupons should be used immediately, before corrosion develops on the surfaces.

Specimen Preparation

A cleaned steel coupon is individually sandwiched between two pieces of insulation measuring 38 by 115 mm (1½ by 4½ in.) The insulation is held uniformly against each side of the test coupon with wire cloth and two, Number 12 rubber bands. The compressed thickness of each piece of insulation should be approximately 12.7 mm (1/2 in.). Figure 1 illustrates assembly of the test piece. The cotton control test piece is assembled in an identical manner. This procedure can be used with both blanket and rigid insulations.

A similar procedure is used for preparing loose fill insulation specimens using the specimen preparation fixture shown in Fig. 5. Cheesecloth is used to bundle

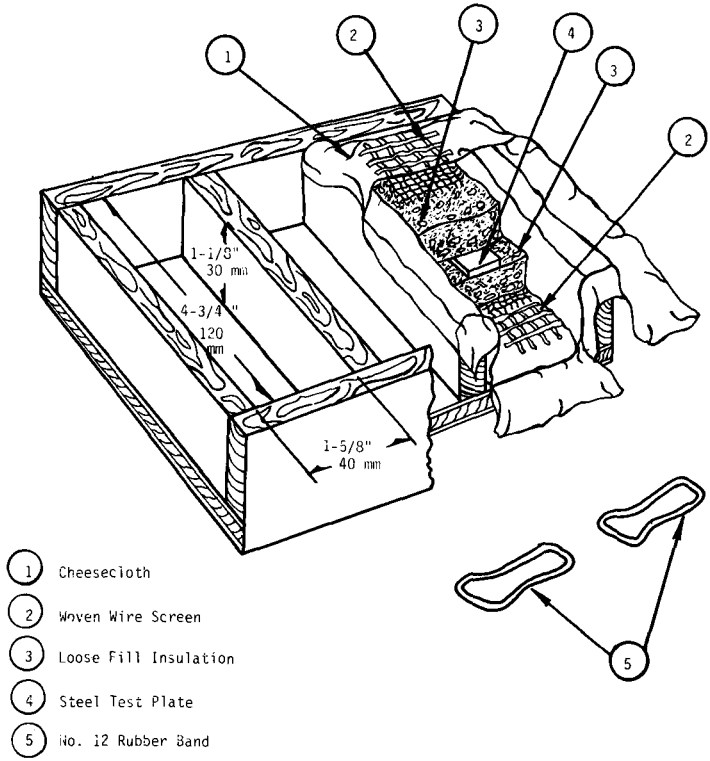


FIG. 5—*Loose fill insulation test specimen preparation.*

the insulation around the test coupon with the woven wire cloth and rubber bands providing uniform compression of the insulation against the metal.

There are five test specimens made for each insulation to be tested and also five specimens for the cotton control.

Specimen Exposure

The steel coupon test specimens are suspended vertically at 49 ± 2°C (120 ± 3°F) and 95 ± 3% RH for 96 h in a humidity cabinet free of contaminants. Proper operation of the humidity cabinet is essential to avoid condensation on the test coupons.

Specimen Evaluation and Corrosion Rating

Initial Examination—After the prescribed exposure period, the test specimens and cotton control specimens are removed from the cabinet and the insulation and cotton are carefully removed from the test plates. Severely corroded specimens may require further cleaning before examination.

The test coupons are then examined carefully and the following characteristics noted if observed:

(1) uniformity of corrosion pattern and variability between specimens of the same group,

(2) presence of surface blush (a uniform area of discoloration over all or part of the plate),

(3) relative severity of pitting, and

(4) type of rust: ordinary red rust, yellow rust (hydrated ferric oxide), black oxide, scaling, and so forth.

Corrosion Rating and Ranking of Test Coupons—Two methods of rating the corroded coupons have been used at Owens Corning. The first method is a subjective comparison between the insulation coupons and the cotton control coupons. The second method ranks the test coupons in numerical order and uses nonparametric statistics for a pass-fail criterion. In both methods a panel of judges is advised to pay more attention to the severity of the corrosion than the uniformity or lack of uniformity in the corrosion patterns. Also surface blush is not weighted strongly.

Subjective Comparison—A panel of knowledgeable observers is asked to rate the test versus control coupon sets according to the following numerical system:

±0 no significant difference,
±1 very slight difference,
±2 slight difference,
±3 moderate difference,
±4 pronounced difference, and
±5 very pronounced difference.

A plus rating indicates that the insulation is better than the control, and a negative rating is given if the insulation test coupons are more corroded than the controls. An insulation must be no worse than the cotton controls to pass the test. This was the original method of evaluating the corrosion coupons and is not currently in general use. Its main value would be in rating test coupons where the type of corrosion is significantly different than that of the controls.

Ranking—The second method of rating the corrosion is a ranking system using nonparametric statistical methods. This procedure is summarized in the following steps:

1. The ten metal test coupons (five test, five control) are ranked in order from the least severe to the most severe corrosion by a panel of judges. The judges should be unaware of the identity of the coupons.
2. The arithmetic sums of all the judges' rankings for each plate are then calculated. Ties in rankings are assigned the arithmetic mean of their rankings.
3. The coupons are then re-ranked from 1 to 10 with the lowest total assigned 1 and the highest total assigned 10.
4. This new ranking is summed for the control coupons only. If this sum is equal to or greater than 21, then there is no statistical difference between the control and test plates, and the insulation has passed. A sum of less than 21 means that the controls are significantly better than the insulation, and the insulation has failed.

This method will identify which are significantly worse than the control with a statistical confidence of $\alpha = 0.10$. This means that there is at most a 10% chance of an insulation being incorrectly failed. This method of ranking cannot make any estimates of the probability of an insulation, which is more corrosive than the control being incorrectly passed.

The ranking procedure is the one in current use at Owens Corning. This method is less subjective than our original rating procedure and provides a clearly defined statistical criterion for pass-fail.

Testing Results

Some typical examples of corroded steel coupons are given in Fig. 6. Shown are coupons for the cotton controls and test coupons of a fiberglass insulation. Figure 7 illustrates coupons from a particularly corrosive material before the corrosion deposits were removed. Several large holes were found in this set of coupons after electrolytic cleaning.

Round-robin testing of this test method, Owens Corning C-02A, was performed by the ASTM Task Force C16.32 on Corrosion in 1979 with six laboratories participating. A total of eight insulations plus a control were tested during the round robin. Weight loss evaluation after cleaning per ASTM Recommended Practice for Preparing, Cleaning, and Evaluating Corrosion Test Methods (G 1, Section 4) was also performed. The weight loss measurements

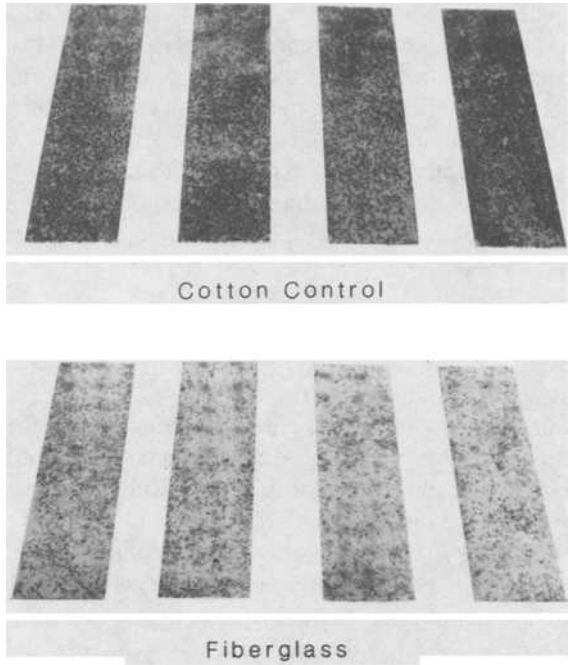


FIG. 6—*Typical examples of corroded steel coupons.*

were generally in qualitative agreement with the numerical ratings assigned using the visual subjective comparisons.

In the area of product development, certain dyes, some cellular plastic formulations, and an occasional binder are rejected because of problems in passing the corrosion test.

A wide range of corrosiveness behavior has been observed in this test. Cor-

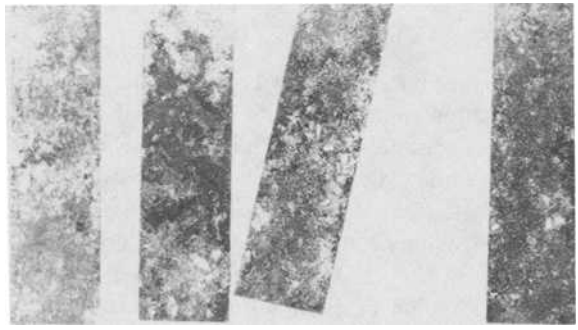


FIG. 7—*Coupons from a particularly corrosive material before the corrosion deposits were removed.*

rosion on the 0.5-mm (0.020-in.) thick steel coupons ranges from virtually no corrosion to corrosion with a 15% weight loss after cleaning and several large holes, all occurring in the four-day span of the test.

Discussion

The principal mechanism of corrosion modelled with this test is contact or crevice corrosion that occurs where the fibers lie along the metal surface. To the extent that insulations are judged worse than the controls, an underlying assumption is that additional corrosion mechanisms are occurring or that contact corrosion is enhanced.

This corrosion test will provide consistent and reproducible results if carefully performed and proper attention is paid to the condition of the metal surfaces and cotton controls. Other advantages of this test are that it is a short-term accelerated test and provides a relative measure of corrosiveness by comparison with a control.

The principal limitation of this test is that it is subjective, requiring a visual ranking of the corrosion coupons. However, the nonparametric statistical criterion for pass-fail removes some of the subjectivity inherent in this test. A situation could arise if the types of corrosion between the test coupons and the controls are significantly different. This could require some expertise of the judges in determining whether or not the test corrosion is detrimental, that is, better, worse, or no worse than the control corrosion.

This situation is rarely encountered with the steel coupons. However, with some of the other metals used with this test, such as aluminum, the test corrosion is generally less severe, more difficult to see, and may be of a different type than the control. In such cases the subjective comparison method of rating corrosion might be preferable to ranking.

Acknowledgments

Credit is due W. S. Miller and G. A. Brower of the Product Testing Laboratory, Owens Corning Fiberglas Technical Center, for their contributions to the test method. E. L. Leeka also of Product Testing Laboratory designed the heating controller.

References

[1] Insulation Corrosiveness Test, C-02A, Owens Corning Fiberglas Technical Center, Granville, OH, Jan. 1977.

[2] Society of Automotive Engineers, Corrosion Test for Insulation Materials, Publication Number J1389, May 1982.

[3] *Insulation, Thermal (Mineral Fiber, for Pneumatic or Poured Application)*, HH-I-1030B, Federal Specification, 23 Feb. 1980.

[4] *Insulation Blankets, Thermal (Mineral Fiber, for Ambient Temperatures)*, HH-I-521F, Federal Specification, 4 Sept. 1980.

[5] *Federal Specification for Blocks, Boards, Blankets, Felts, Sleeving (Pipe and Tube Covering) and Pipe Fitting Covering, Thermal (Mineral Fiber, Industrial Type)*, HH-I-558B (Amendment 3), 24 Aug. 1976.

Sheldon W. Dean,[1] *Robert A. Woodroof,*[2] *and James Nichols*[1]

Electrochemical Methods for Evaluating Corrosion Inhibitors in Strong Acid Systems

REFERENCE: Dean S. W., Woodroof, R. A., and Nichols, J., "**Electrochemical Methods for Evaluating Corrosion Inhibitors in Strong Acid Systems,**" *Laboratory Corrosion Tests and Standards, ASTM STP 866*, G. S. Haynes and R. Baboian, Eds., American Society for Testing and Materials, Philadelphia, 1985, pp. 228–245.

ABSTRACT: Electrochemical techniques have been evaluated for determining the performance of corrosion inhibitors in oil well acidizing solutions. Tests have been made with a variety of corrosion inhibitor blends in hydrochloric acid over a range of concentrations using carbon steel electrodes. Two different scan rates were evaluated. Longer term immersion tests were made with the same inhibitors to evaluate the degree of inhibition and development of pitting.

Reverse scan polarization was found to produce anodic hysteresis loops similar to what is observed with passive alloys in chloride containing environments. A number of parameters from the reverse scan polarization hysteresis loop have been examined for correlation with pitting tendency. The return potential anodic corrosion rate appears to have merit for showing pitting tendency. The pitting tendency seems to be most severe when the inhibitor is at a relatively low concentration. The poor correlation seen between the 16-h mass loss corrosion rates and the electrochemical corrosion rate estimates is probably caused by inhibitor exhaustion in the mass loss results. Polarization scan rate effects also showed that inhibitor adsorption kinetics affected the anodic polarization parameters.

KEY WORDS: corrosion, acid treatment, inhibitors, potentiodynamic polarization, Tafel slope, polarization resistance, pitting potential, reverse scan polarization, corrosion potential, anodic hysteresis, mass loss corrosion rate, sign test

There are many occasions when it is desirable to contain strong acid solutions in steel vessels and pipes. In these cases, it is generally desirable to incorporate a corrosion inhibitor system into the strong acid in order to minimize corrosion of the steel [*1*]. The process of acidizing oil producing formations with hydrochloric acid solutions is a good example of this approach [*2*]. In this case, it is essential to formulate the hydrochloric acid solution with a balanced corrosion inhibitor system to protect the vessels and pipes that contain the acid on its way

[1]Chief engineer of materials and principal research chemist, respectively, Air Products and Chemicals, Inc., P.O. Box 538, Allentown, PA 18105.

[2]Manager of chemical research, The Western Company of North America, P.O. Box 186, Fort Worth, TX 76101.

Copyright© 1985 by ASTM International www.astm.org

to the oil producing formation. There are, of course, several other applications where inhibited acid is required, for example, in the pickling of steels.

In the use of inhibited acid, pitting sometimes occurs. In these cases, the rate of corrosive penetration exceeds the average rate of chemical attack. When pitting occurs, it is usually found that ferric ions or oxygen or some other oxidizing species is present in the acid. The stimulating effect of such species is qualitatively similar to what is seen in passive alloys, such as stainless steel, in chloride solutions. In laboratory tests on stainless steels when the potential is gradually increased, it is usually found that pitting initiates after a certain potential known as the critical pitting potential, is exceeded. In these cases, the pitting is accompanied by a sharp increase in the anodic current [*3*]. If the direction of polarization is now reversed to the negative direction, the potential-current density plot shows a marked hysteresis, which is caused by the presence of pits on the electrode surface [*4*]. Because pitting is observed in inhibited strong acid systems, it was of interest to know whether a similar electrochemical testing approach would show the presence of pitting and whether this approach could be used to rank inhibitor systems with regard to their tendency to cause pitting. In addition, it was of interest to examine electrochemical techniques for corrosion rate measurement to determine if these techniques could provide more information than mass loss measurements.

More specifically, the objectives of this study were to run mass loss measurements and forward and reverse polarization scans on a series of inhibitor systems to determine the effects caused by inhibitor blends in 15% hydrochloric acid. In the electrochemical runs corrosion rate estimates and polarization hysteresis effects during the reverse scan were of interest. Two different scan rates were used to assess the effect of polarization scan rate. A second objective was to examine the results of these polarization measurements to attempt to identify parameters that could be used to assess both corrosion rate and pitting tendencies in inhibited acid systems. These polarization studies were conducted over a range of inhibitor concentrations to determine the effects of inhibitor depletion.

Experimental Procedure

A series of organic inhibitor blends were prepared covering a range typical of commercial acidizing formulations. These blends included varying ratios of the components as well as similar formulations prepared with nominally identical compounds from different suppliers. All of these blends included the following components: heterocyclic amine quaternary salts, acetylenic alcohols, ethyoxylated alcohol surfactants, and organic amides. Because of the proprietary nature of these blends, it is not possible to provide further information on the formulations studied.

All of the tests were carried out using a 15% hydrochloric acid solution prepared from reagent grade acid and deionized water. The test temperature was 82 $\pm$1°C in all cases. A series of mass loss corrosion rate measurements were

TABLE 1—*Composition of N80 steel (all values in mass percent).*

Aluminum	Boron	Carbon	Chromium	Copper	Manganese	Molybdenum	Nickel	Phosphorus	Sulfur	Tin	Silicon	Vanadium
0.02	0.0002	0.36	0.054	0.14	1.2	0.016	0.08	0.009	0.012	0.006	0.26	0.11

made using American Petroleum Institute (API) Grade N80 steel. An analysis of this material is shown in Table 1. Specimens were 25 by 50 by 3 mm and were abraded with 600-grit silicon carbide to a smooth, bright finish before testing. The microstructure of this material is shown in Fig. 1 after polishing and etching with nital.

The 15% hydrochloric acid was prepared and placed in a glass vessel to a volume of 150 mL. The solution was brought to the test temperature and the desired amount of inhibitor was added to the vessel and allowed to equilibrate for about 15 min. A previously weighed steel specimen was placed into the container and the system was held at 82°C for 16 h. At the conclusion of the test, the specimen was removed from the vessel, rinsed with water, then with acetone. The specimen was rinsed again in isopropyl alcohol, then in water, and a final rinse with isopropyl alcohol was used to remove the water. The specimen was then air dried and a final weight obtained. Duplicate tests were run for each inhibitor concentration. The mass loss measurements were converted to corrosion rates in terms of miles per year (mpy) in accordance with ASTM Standard Practice for Preparing, Cleaning, and Evaluating Corrosion Test Specimens (G 1) procedures (Fig. 2). It was not necessary to do any post-test cleaning of these specimens because the acid left the surfaces clean and free of corrosion products.

The electrochemical measurements were carried out using the same N80 steel cut into disks. The specimens were placed in a flat panel specimen holder that exposed an area of 1 cm^2. The test cell contained approximately 800 mL of the 15% hydrochloric acid. It was brought to temperature in a water-bath and the inhibitor added to the solution after reaching the test temperature. The system was swept with nitrogen before beginning the test. After completing the deaeration step, the steel specimens were introduced into the vessel. The system was allowed to equilibrate for 1 h. A platinum counter electrode was used in these

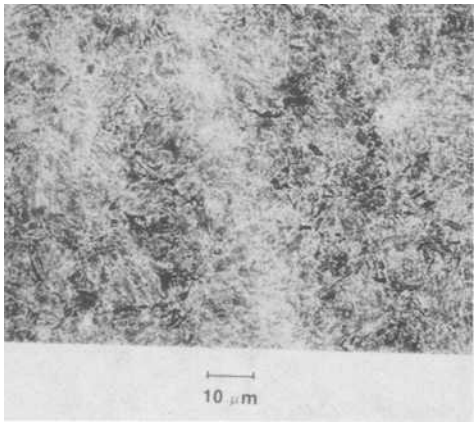


FIG. 1—*API Grade N80 steel sample nital etched showing bainite or tempered martensite structure.* (×*1000 original magnification in scanning electron microscope.*)

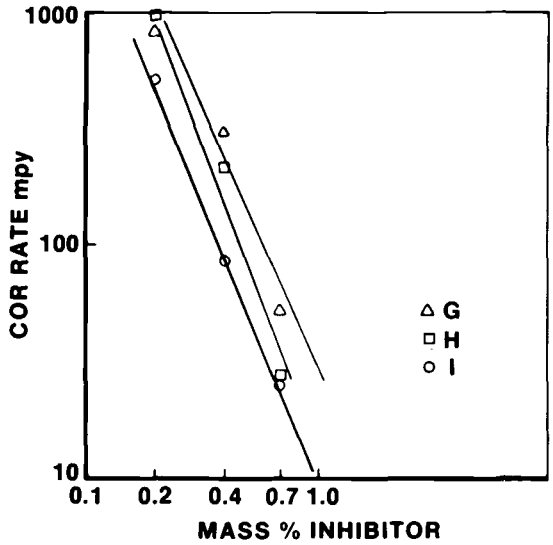


FIG. 2—*Typical mass loss corrosion rate results versus inhibitor concentration (log scale) for three inhibitors, G, H, and I, after a 16-h test in 15% hydrochloric acid at 82°C.*

tests, and the electrode potentials were measured by means of a salt bridge filled with the test solution. A calomel reference electrode was used in these tests. A Princeton Applied Research Model 350 corrosion measurement console was used for this work. This unit incorporates the potentiostat, *xy* recorder, programmer, electrometer, and scanner in a single unit and produces plots of potential versus log current density for the test conditions.

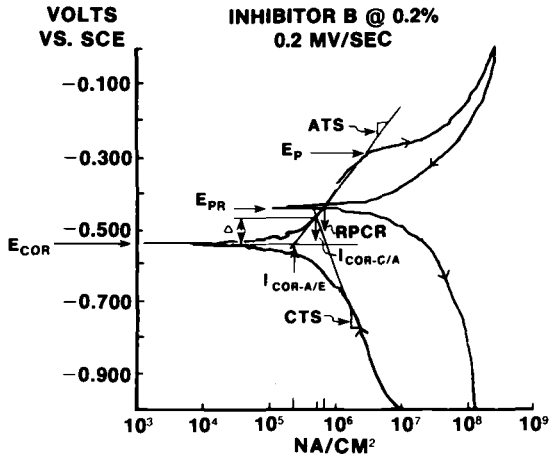


FIG. 3—*Typical polarization plot for N80 specimen in inhibited 15% hydrochloric acid at 82°C (Inhibitor B at 0.2%, scan rate 0.2 mV/s).*

In most of these tests the potential scan was begun at a value of −1.000 V with respect to calomel electrode and increased at either 1 or 0.2 mV/s until the potential reached 0.00 V. At this point, the potential scan was reversed and allowed to return to −1.000.

The instrument automatically recorded the corrosion potential at the beginning of the test and at each point at which current density was zero. The current density-potential data were recorded on tape for future reference. In some cases, a polarization resistance in the vicinity of the first zero current density point was determined. Two or three different runs were made on each solution. The specimen was removed from the bath at the conclusion of the potential scan, cleaned, and mechanically polished before beginning the next test. One or two runs at the 1.0 mV/s scanning rate were made and one run at the 0.2 mV/s rate with a single batch of solution.

Figure 3 shows a typical potential current density plot resulting from this procedure. The following data were recorded from these plots: The open circuit potential at the beginning of the polarization scan; the potential at which the current switched from positive to negative; the potential at which the anodic Tafel line showed a break; and the potential at which the current changed back from positive to negative.

An attempt was made to draw Tafel lines for the cathodic and anodic reactions. The cathodic current density potential plots all showed substantial curvature so that assignment of a linear portion was rather arbitrary. The linear portion of the anodic curve was usually apparent. The intersection of the cathodic Tafel line and the anodic Tafel line usually occurred between 10 and 100 mV more positive than the measured corrosion potential, confirming the nonlinear behavior of the cathodic reaction.

Three different approaches were used to calculate the corrosion rate. First was the intersection of cathodic and anodic Tafel lines. The second approach was to extrapolate the anodic Tafel line to the corrosion potential and read the current density. The third approach was to use the polarization resistance value together with the estimated anodic/cathodic Tafel slopes using the Stearn/Geary technique. For example, see ASTM Practice for Conducting Potentiodynamic Polrization Resistance Measurements (G 59). However, very few measurements of polarization resistance were obtained, and because of the ambiguity in the cathodic Tafel slope estimates, no further analyses were attempted on these values. The anodic current density was also read from the forward anodic Tafel line at the potential at which the return current went to zero. This value was termed the return potential corrosion rate or RPCR (see Fig. 3).

Surface examination was made on several of the specimens. This examination was carried out by means of the scanning electron microscope (SEM). The mass loss specimens were used in this phase of the study to determine if the attack on the specimen surface was relatively uniform or if there were elements of pitting involved in the corrosion.

Results

The results of this study are summarized in Tables 2 through 4 and Figs. 3 through 13. Table 2 contains the mass loss coupon results. Mean values of mass loss were used to determine the average corrosion rates on the duplicate specimens. Pitting assessments were made by rating scanning electron micrographs made both at low ($\times 100$ through $\times 400$) and high ($\times 1000$ through $\times 4000$) magnifications from the surface of coupons. Table 3 provides a summary of the average potentials and Tafel slopes that were measured in the electrochemical polarization tests that were made. Although the scan rate had some effect on the anodic Tafel slope, we felt that the average of all the measured values represented the inhibitor performance better than any smaller grouping. Thus, this average may show some bias as compared with either fast or slow scans, but the bias should be consistent throughout the inhibitor set. Table 4 gives the results of a number of statistical sign tests that were made to assess specific effects. The

TABLE 2—*Mass loss measurements of N80 steel in inhibited 15% hydrochloric acid at 82°C, 16-h test—duplicate specimens.*

Inhibitor ID[a]	Concentration, %	Mass Loss, g	Corrosion Rate		Pitting Rating
			mpy	mA/m^2[a]	
A	0.2	1.0254	903	197	severe
	0.4	0.2522	222	48.5	severe
	0.7	0.0229	20	4.1	light
B	0.2	0.7268	640	140	...
	0.4	0.1786	157	34.3	...
	0.7	0.0231	20	4.4	light
C	0.2	0.6978	614	134	...
	0.4	0.1587	140	30.6	light
	0.7	0.0232	20	4.4	few
D	0.2	0.9438	829	181	severe
	0.4	0.2368	209	45.7	moderate
	0.7	0.0223	19	4.2	none
E	0.2	0.8372	736	161	severe
	0.4	0.2704	238	52	moderate
	0.7	0.0211	18.5	4.0	none
F	0.2	0.7652	673	147	severe
	0.4	0.0970	85	18.6	moderate
	0.7	0.0213	19	4.2	none
G	0.2	0.9378	824	180	severe
	0.4	0.3494	307	67	few
	0.7	0.0600	53	11.6	edges only
H	0.2	1.1298	992	217	severe
	0.4	0.2604	229	50	few
	0.7	0.0316	28	6.1	none
I	0.2	0.5769	507	110	light
	0.4	0.0987	87	19.0	none
	0.7	0.0292	26	5.7	none

[a]ID is identification and mA/m^2 = 0.219 mpy.

TABLE 3—*Electrochemical parameters averaged from the polarization results (average of 1 and 0.2 mV/s scan results).*[a]

Inhibitor ID	Concentration, %	E_{cor} V versus SCE	ATS, mV/decade	CTS, mV/decade	E_P, V versus SCE	E_{PR}, V versus SCE
A	0.2	−0.502	213	580	−0.347	−0.425
	0.4	−0.456	256	335	−0.303	−0.388
	0.7	−0.438	275	423	−0.280	−0.404
B	0.2	−0.518	254	411	−0.295	−0.435
	0.4	−0.476	194	239	−0.269	−0.448
	0.7	−0.483	208	495	−0.290	−0.452
C	0.2	−0.480	204	567	−0.300	−0.446
	0.4	−0.462	109	314	−0.294	−0.449
	0.7	−0.462	211	322	−0.282	−0.451
D	0.2	−0.545	161	342	−0.285	−0.442
	0.4	−0.557	313	395	−0.278	−0.448
	0.7	−0.547	341	352	−0.272	−0.449
E	0.2	−0.542	169	411	−0.303	−0.406
	0.4	−0.508	284	600	−0.305	−0.411
	0.7	−0.517	305	454	−0.300	−0.439
F	0.2	−0.545	329	468	−0.325	−0.446
	0.4	−0.535	326	478	−0.316	−0.447
	0.7	−0.533	360	451	−0.283	−0.448
G	0.2	−0.536	197	342	−0.320	−0.458
	0.4	−0.543	276	424	−0.291	−0.452
	0.7	−0.529	281	370	−0.286	−0.452
H	0.2	−0.534	174	364	−0.298	−0.450
	0.4	−0.472	151	311	−0.290	−0.449
	0.7	−0.454	146	297	−0.290	−0.447
I	0.2	−0.514	184	329	−0.292	−0.455
	0.4	−0.541	320	272	−0.281	−0.454
	0.7	−0.468	148	329	−0.303	−0.436

[a] E_{cor} = averaged rest potential before beginning scan and first zero polarization potential for both fast and slow scans. ATS = anodic Tafel slope, graphical estimate from plot. CTS = cathodic Tafel slope, graphical estimate from plot. E_P = anodic polarization break potential (Fig. 3). E_{PR} = potential where polarization current becomes zero on return scan (Fig. 3).

TABLE 4—*Results of statistical sign test on electrochemical results.*

Effects	Significance Level
Scan rate	
I_{cor} C/A $F > S^a$	0.05
I_{cor} A/E_{cor} $F > S^b$	0.10
ATS $F > S$	0.05
E_P, E_{PR}, CTS, and RPCR	no effect
F = 1.0 mV/s, S = 0.2 mV/s	
Inhibitor concentration	
Comparing 0.2 to 0.7%	
E_{cor} increases	0.01
E_P increases	0.01
RPCR decreases	0.01
E_{PR}, CTS, ATS, I_{cor} C/A, or A/E_{cor}	no effect

[a] I_{cor} C/A corrosion rate estimated from intersection of cathodic and anodic Tafel lines.
[b] I_{cor} A/E_{cor} corrosion rate estimated from extrapolation of anodic Tafel line to corrosion potential.

sign test [5] is a nonparametric statistical test that is valuable for assessing the significance level of paired observations to determine: Is A greater than B?

Figure 2 shows a typical mass loss versus concentration plot for three of the inhibitors evaluated in this program. The results appear linear and parallel on log/log coordinates with a slope of about 2. Figure 3 shows a typical polarization plot for an inhibitor. This plot is useful in showing the various parameters that were considered in this study. Figures 4 through 9 contain plots of the various parameters versus inhibitor concentration. Figures 10 and 11 compare the mass loss results with corrosion rate estimates from the electrochemical polarization studies. Figure 12 shows a comparison between the pit ranking of the various inhibitors based on mass loss coupon examination and the geometric mean return potential corrosion rate values. The geometric mean was used because it cen-

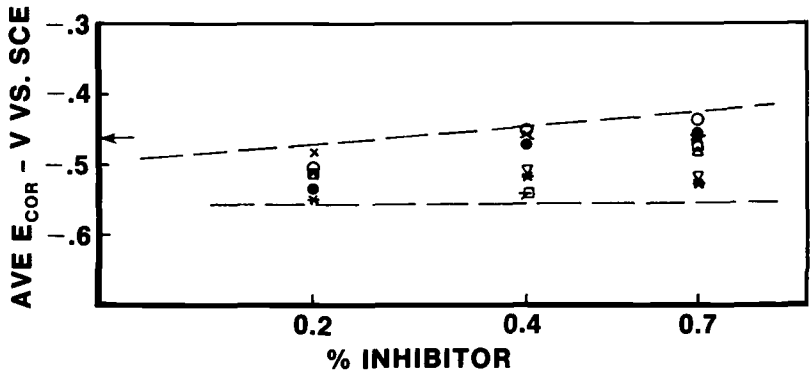


FIG. 4—*Mean corrosion potential versus inhibitor concentration (log scale) for all blends. Arrow on* E *axis shows corrosion potential of steel in uninhibited acid. (Average of initial corrosion potential plus first zero current potential on positive scan.) Symbol identity shown on Fig. 12.*

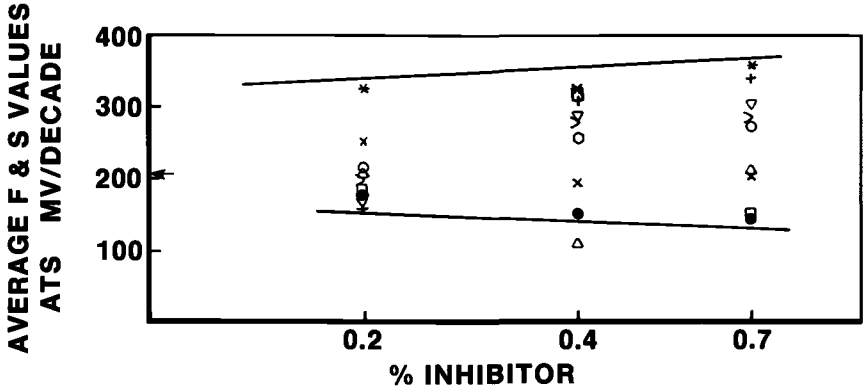


FIG. 5—*Mean anodic Tafel slope versus inhibitor concentration (log scale) for all blends. Arrow on* E *axis shows uninhibited acid value. Symbol identity shown on Fig. 12.*

tralizes the plotted value on a logarithmic scale. Figures 13 through 15 show typical mass loss specimen pitting as viewed in the scanning electron microscope.

Discussion

Initially, we attempted to correlate the electrochemical corrosion rate estimates with the mass loss results. Figure 10 shows a plot of one of these correlations on logarithmic axes. No statistical correlation was observed between the inter-

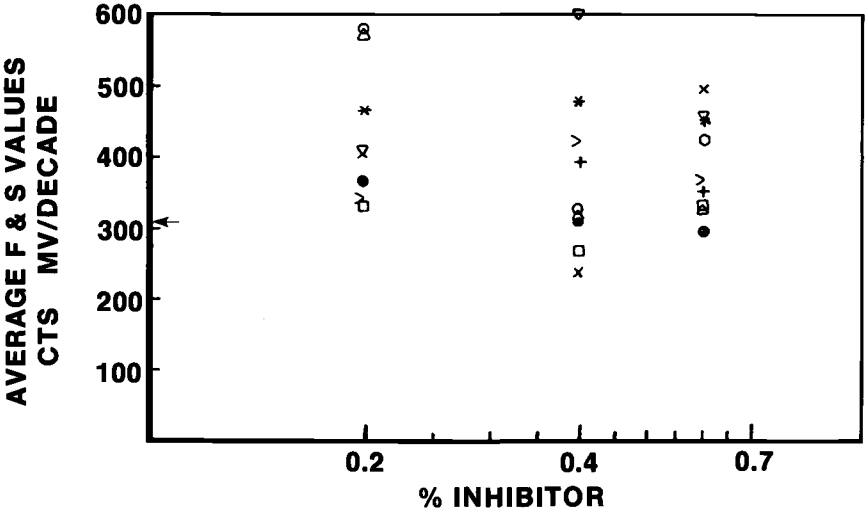


FIG. 6—*Mean cathodic Tafel slope versus inhibitor concentration (log scale) for all blends. Arrow on* E *axis shows uninhibited acid value. Symbol identity shown on Fig. 12.*

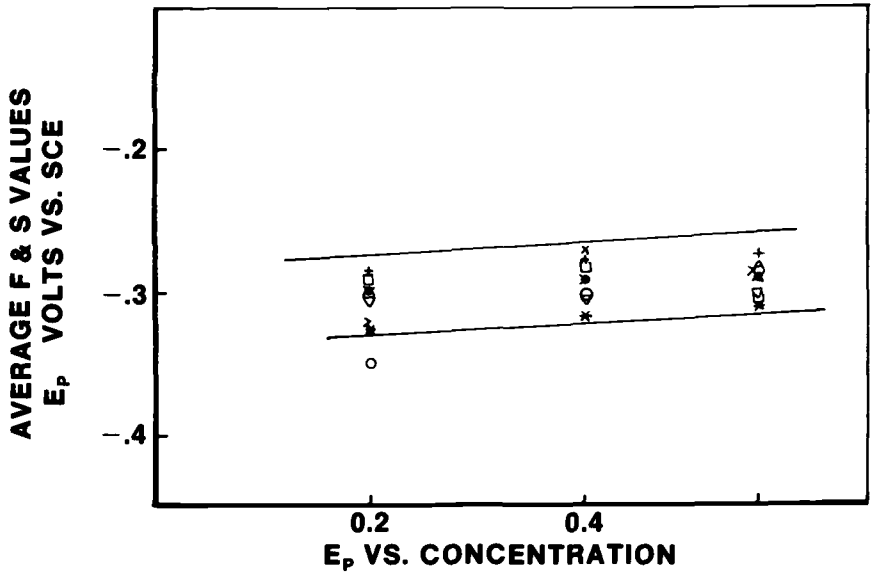


FIG. 7—*Mean pitting or anodic break potential* E_p *versus inhibitor concentration (log scale). Symbol identity shown on Fig. 12.*

section points of the anodic and cathodic Tafel lines from slow scan runs and the mass loss measurements. A slightly better correlation was observed between the anodic Tafel line extrapolation to the corrosion potential and the mass loss results, as seen in Fig. 11. This case was interesting because most of the electrochemical results were significantly below mass loss values, expecially at low inhibitor concentrations where the mass loss corrosion rates were highest. In

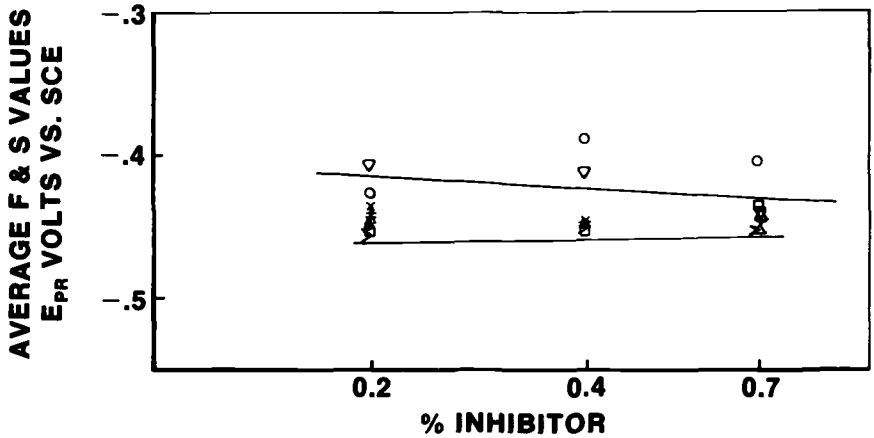


FIG. 8—*Mean return potential* E_{PR} *versus inhibitor concentration (log scale). Symbol identity shown on Fig. 12.*

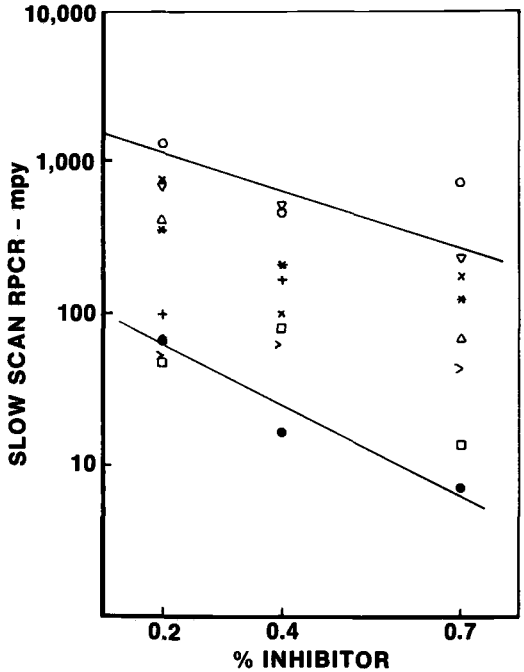


FIG. 9—*Return potential anodic corrosion rate (RPCR) values (log scale) versus inhibitor concentration (log scale), 0.2 mV/s value only. Anodic current converted to mpy. Symbol identity shown on Fig. 12.*

these cases, the inhibitor probably was exhausted over the 16-h period used in the mass loss measurements. The mass loss corrosion rate measurements may, in fact, have had a higher rate of attack than the specimens in the electrochemical runs. The electrochemical tests were completed within 7 h for each solution tested. Also, the ratio of solution volume to specimen area is substantially greater in the electrochemical tests (1 cm^2 to 800 mL versus 25 cm^2 to 150 mL in the mass loss runs) so that there was proportionately more inhibitor available to the specimen surface. These points give some credibility to the argument that inhibitor exhaustion did occur during the mass loss runs. However, we were disappointed that better correlations were not found.

The mass loss results did show a strong influence of inhibitor concentration on the degree of inhibition, as seen in Fig. 2 as we expected. In virtually every case, the corrosion rate of the steel at the lower concentration was greater than that at the higher concentration in the mass loss measurements. We had anticipated this behavior on the assumption that higher inhibitor concentrations were more effective in causing inhibition, but inhibitor exhaustion resulting in a progressively increasing corrosion rate during the mass loss runs could also explain this behavior.

The results of the electrochemical polarization scans showed more variability

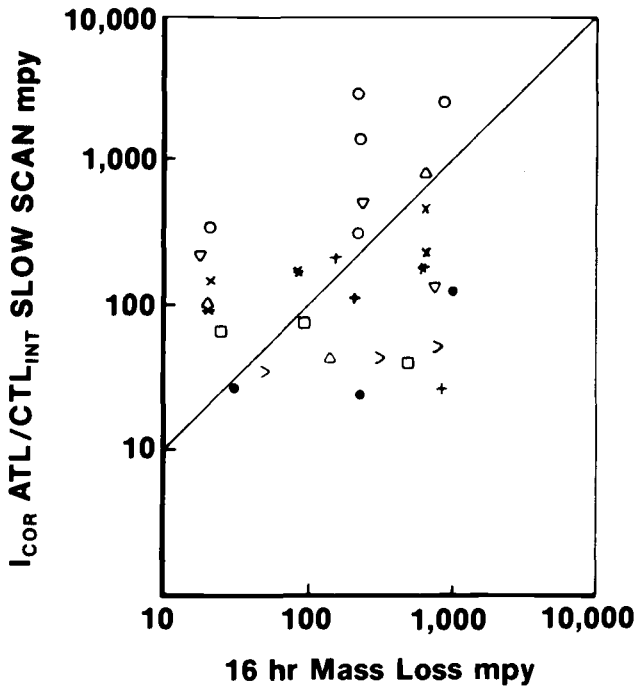


FIG. 10—*Comparison of corrosion rate from anodic Tafel line—cathodic Tafel line intersections based on 0.2 mV/s runs with 16-h mass loss rates. Line shows perfect correlation. Symbol identity shown on Fig. 12.*

than we had anticipated. In general, the anodic Tafel slopes were significantly less than the cathodic Tafel slopes. The strong curvature in the cathodic polarization curve made the assignment of a Tafel slope to this reaction rather arbitrary. It seems clear that the adsorption of the inhibitor system on the electrode and its subsequent influence on the cathodic reaction might be strongly affected by potential. The slope of the slow 0.2-mV/s scan rate tests did not show any significant difference in the cathodic polarization curves as compared to the faster 1-mV/s scan rate results.

On the other hand, the anodic Tafel slopes measured at the 1-mV/s scan rate tended to be greater than those measured at the 0.2-mV/s scan rate. This effect was more pronounced at the lower concentrations, therefore it seems likely that adsorption kinetics were affecting the polarization results, especially at higher potentials. A statistical sign test on the anodic Tafel slope data comparing slow and fast scans showed that this conclusion was valid at the 0.05 significance level (see Table 4). Similarly, it was found that the corrosion current values measured at the faster scan rate were greater than the values obtained at the slower scan rate. This again confirms that adsorption kinetics were probably influencing our estimates of the corrosion rates.

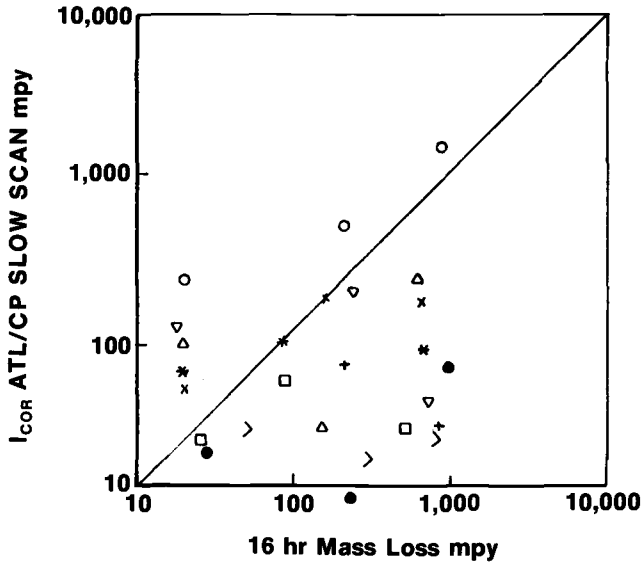


FIG. 11—*Comparison of corrosion rate from anodic Tafel line extrapolation to corrosion potential from 0.2 mV/s runs with 16-h mass loss rates. Line shows perfect correlation. Symbol identity shown on Fig. 12.*

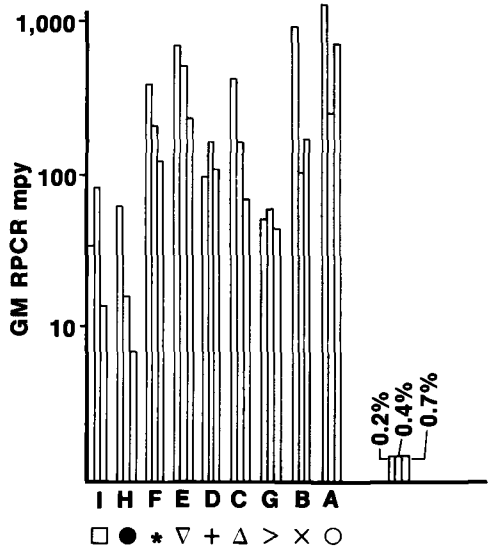


FIG. 12—*Geometric mean return potential corrosion rate versus inhibitor concentration and mass loss pit ranking.*

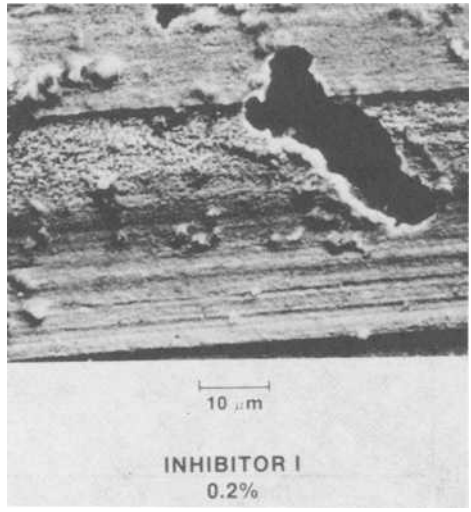


FIG. 13—*Scanning electron micrograph of pit in mass loss test coupon. Original magnification* ×*1500. Inhibitor 1, 0.2%, 16 h.*

All of the inhibitor blends tested in this study showed substantial anodic scan hysteresis, as illustrated by Fig. 3. It is significant that similar tests using uninhibited hydrochloric acid did not show this hysteresis, nor was there any break in the anodic Tafel line. Our interpretation of this polarization behavior was that the inhibitor blend significantly reduced the rate of the anodic reaction, but at higher potentials the inhibitor was either oxidized or desorbed. This seemed to occur at local sites causing pits to develop. On the return scan, the inhibitor was not able to enter these pits and reduce the rate of attack until the potential became substantially more negative than the breakaway or pitting potential. This may be caused in part by the high ferrous ion content within the pits. In any event, the anodic return scan behavior was similar to what had been observed on passive materials in chloride solutions. Because of this similarity to the pitting behavior of stainless alloys, it was decided to examine the hysteresis behavior in more detail to determine if this approach could be used to characterize pitting in strong acid systems.

The critical pitting potential E_p, is the potential at which the break occurs in the anodic polarization curve when the potential is scanned in the positive direction. There appears to be only small differences in the critical pitting potentials between the various inhibitor systems. Considering the similarity of the behavior seen in this study to pitting in passive alloys, we had expected the inhibitor systems with more positive pitting potentials to resist pitting better. There appears to be a slight tendency of this pitting potential to become more positive at higher concentrations of inhibitor (Fig. 7). This value did not seem to be affected by the scan rate. Because of the narrow range of values for this parameter, it did

not seem possible that the critical pitting potential would be a useful indication of pitting tendency for an inhibitor blend.

The potential at which the anodic current density became zero on the negative return scan, referred to as the "return potential" or E_{PR}, also did not seem to be affected either by the concentration of the inhibitor (Fig. 8) or by scan rate. With only two exceptions, all of the inhibitors seemed to give a value close to -0.45 for this return potential. The higher value for return potential of Inhibitor A was probably caused by experimental difficulties. The anomalously high value for the return potential of Inhibitor E had no explanation. It was originally thought that this potential might have significance in terms of evaluating differences in pitting behavior between inhibitor systems. However, at least within the variations observed in this study, this expectation appears not to be justified.

Another parameter that was identified as a possible indicator of pitting rate was the return potential corrosion rate. This value showed substantial variations among the different inhibitor blends. In addition, it showed a statistically significant tendency to decrease as the inhibitor concentration was increased. This value did not seem to show any statistically significant trend with the scan rate. This parameter may have significance in evaluating inhibitor systems for pitting

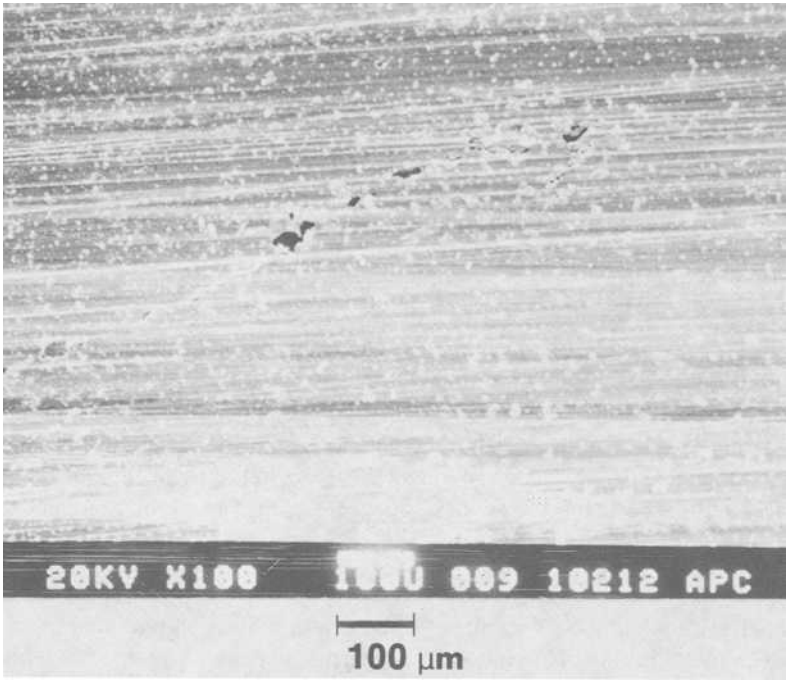


FIG. 14—*Scanning electron micrograph of pit in mass loss test coupon. Original magnification* $\times 110$. *Inhibitor G, 0.2%, 16 h.*

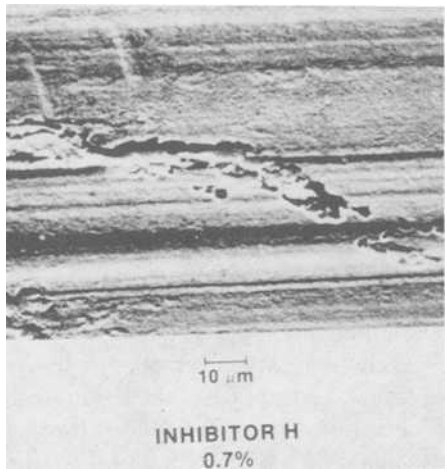


FIG. 15—*Scanning electron micrograph of pit in mass loss test coupon. Original magnification* × *1000. Inhibitor H, 0.7%, 16 h.*

tendencies, although our attempts to correlate it with degree of pitting, as seen in the mass loss coupons, were disappointing (Fig. 12). It is possible that the inhibitor exhaustion effects that we observed in the mass loss results were also confusing the correlation of coupon pit ranking and the electrochemical pit rating, as determined by this parameter.

It is also possible that the coupon pit rating approach was not sufficiently consistent to be reliable. Further work on this question would be very helpful. However, the fact that the RPCR does show the proper concentration dependence makes this parameter worth pursuing as a pitting severity indicator. An interpretation of the physical significance of this parametr is not apparent, however.

The scanning electron microscopy examinations of the mass loss specimens confirm that the specimens exposed at the lowest inhibitor concentration levels had the largest number of pits and also the deepest pits (Figs. 13 through 15). The pitting seemed to initiate at metallurgical features such as stringers of manganese sulfide. The SEM surface examination was not suited to give quantitative assessments of the pitting because the number of pits that could be examined in any reasonable area at × 100 was small. Thus, the ratings tended to be arbitrary at best and did not rank the depth of attack with any degree of confidence.

Conclusions

1. The correlation between the electrochemical corrosion rates and mass loss measurements is poor. The cause of this lack of agreement appears to be inhibitor exhaustion that occurs during the extended mass loss test period.

2. The cathodic polarization curves were very nonlinear, probably indicating cathodic desorption at more negative potentials. The anodic polarization curves

were closer to normal Tafel behavior. The intersection of the anodic Tafel line and the corrosion potential appeared to give more reliable corrosion rate estimates.

3. The reverse scan electrochemical polarization technique reveals hysteresis during the reverse or negative scan in inhibitor systems, which seems to be related to the tendency for pitting in these systems. The return potential corrosion rate provides a measure of this pitting tendency, which agrees, at least qualitatively, with surface examination.

4. Additional work is desirable to develop reliable electrochemical methods for evaluating pitting in inhibited strong acid systems.

Acknowledgment

The authors gratefully acknowledge the assistance of William Wagaman of Air Products in conducting the polarization measurements. Dr. J. V. Martinez and M. R. Anewalt of Air Products were very helpful in assisting with the scanning electron microscopic examination. D. L. Goode of Western assisted in preparations of the inhibitor blends. The authors also wish to thank Air Products and Chemicals, Inc. and The Western Company of North America for permission to publish this paper.

References

[*1*] Dean, S. W., Jr., Derby, R. and von dem Bussche, G. T., *Materials Performance*, Vol. 20, No. 12, Dec. 1981, pp. 47–51.

[*2*] Shreir, L. L., *Corrosion*, Vol. 2, Newnes Butterworths, London, 1976, pp. *18*: 28–29.

[*3*] Uhlig, H. H., *Corrosion and Corrosion Control*, 2nd ed., Wiley, New York, 1971, pp. 76–77.

[*4*] Wilde, B. E., *Corrosion*, Vol. 28, 1982, p. 283.

[*5*] Volk, W., *Applied Statistics for Engineers*, 2nd ed., Robert E. Krieger Publishing Company, Huntington, NY, 1969, pp. 374–376.

DISCUSSION

Stanley T. Hirozawa[1] *(written discussion)*—Did you run electrochemical corrosion rate as a function of immersion time? The time dependence of corrosion on rate can be positive, zero, or negative. A positive dependence could explain the larger mass loss relative to the electrochemically determined corrosion rate. This would indicate that the system was noninhibiting.

S. W. Dean (author's closure)—Unfortunately, we did not measure the variation of the corrosion rate with exposure time using the electrochemical procedure. Such measurements would have allowed us to verify the inhibitor exhaustion theory we proposed.

[1]BASF Wyandotte Corp., 1609 Biddle Ave., Wyndotte, MI 48192.

Robert D. Mack,[1] *S. Mark Wilhelm,*[2] *and Beverlee G. Steinberg*[3]

Laboratory Corrosion Testing of Metals and Alloys in Environments Containing Hydrogen Sulfide

REFERENCE: Mack, R. D., Wilhelm, S. M., and Steinberg, B. G., **"Laboratory Corrosion Testing of Metals and Alloys in Environments Containing Hydrogen Sulfide,"** *Laboratory Corrosion Tests and Standards, ASTM STP 866*, G. S. Haynes and R. Baboian, Eds., American Society of Testing and Materials, Philadelphia, 1985, pp. 246–259.

ABSTRACT: In recent years, the production of oil and gas from reservoirs containing significant partial pressures of hydrogen sulfide has become economical. Hydrogen sulfide is a toxic and highly flammable gas. Containment of the production fluid is critical from the view of safety and economics. The corrosion of metals and alloys used in these production environments therefore presents a serious problem. This paper discusses the test methods used for the laboratory corrosion testing of metals and alloys in simulated production environments containing hydrogen sulfide. The discussion includes the selection of the test method, test environment, and safety precautions taken during testing.

KEY WORDS: corrosion tests, electrochemistry, hydrogen embrittlement, hydrogen sulfide, oils, gases, safety, stress corrosion, double cantilever beam, slow strain rate, sulfide stress cracking

The worldwide shortage of oil and gas in the 1970s and early 1980s made the production of oil and gas from very sour formations (that is, those containing hydrogen sulfide [H_2S]) profitable. Although hydrogen sulfide has presented a corrosion problem in oil and gas production for over three decades, the very deep, high pressure, hot, sour gas wells present unusually difficult materials problems. An acceleration of the general corrosion, pitting, and crevice corrosion, and the increased susceptibility to environmentally assisted cracking (hydrogen embrittlement, sulfide stress cracking, and so forth) occur in many engineering alloys when in contact with aqueous solutions containing hydrogen sulfide. Catastrophic failures have occurred resulting in loss of life and in costly repairs.

[1]Research engineer, Shell Development Company, Westhollow Research Center, P.O. Box 1380, Houston, TX 77001.

[2]Principal research scientist, Battelle Memorial Institute's Petroleum Technology Center, 1100 Rankin Rd., Houston, TX 77073.

[3]Metallurgist, Baker Packers, 6023 Navigation Blvd., Houston, TX 77011.

Copyright© 1985 by ASTM International www.astm.org

The materials problems encountered in hydrocarbon production from sour wells has prompted a considerable amount of materials research. The purpose of this paper is to discuss the test methods used to evaluate the corrosion performance of metals and alloys in simulated, downhole environments containing hydrogen sulfide. The safety precautions taken and the criteria used to select the test method and test environment are also discussed. The scope of this paper is limited to a discussion of laboratory corrosion testing even though corrosion testing is frequently performed in actual "field" environments [*1–3*].

Corrosion Testing in Hydrogen Sulfide

Safety

Hydrogen sulfide is a highly toxic, flammable gas that can be detected in low concentrations by its characteristic rotten egg odor. Its toxicity to humans is so great that a safe concentration for an 8-h working period is only 10 ppm [*4*]. Higher concentrations of hydrogen sulfide can result in headaches, drowsiness, dizziness, eye irritation, respiratory malfunction, and even death. The effects depend upon concentration and period of exposure. A summary of these effects is given in Table 1.

There are precautions that can be taken to minimize the risk of exposure to hydrogen sulfide. These include adequate containment vessels, adequate ventilation, hydrogen sulfide "scrubbers," hydrogen sulfide detection systems, portable breathing apparatus, backup personnel, and evacuation plans.

The suitability of a test vessel for corrosion testing in aqueous solutions

TABLE 1—*Effects of inhalation of hydrogen sulfide by humans.*[a]

H_2S Concentration in Air, ppm	Effect
10	For most people, an 8-h exposure results in no discomfort
20 to 150	Eye irritation
100	In 2 to 15 min sense of smell may be lost; at higher concentrations loss occurs in shorter period of time. After 15 to 30 min, shortness of breath, coughing, eye pain, and drowsiness may occur
170 to 300	Maximum concentration without serious effects. Severe stinging in eyes and throat, blurred vision, and seeing halos around lights may result
500	After 30 min, headache, dizziness, excitement, staggering, and gastroenteric disorders will result; consciousness may be lost in 2 to 15 min, "breathing may stop" in 30 to 45 min
700	Consciousness lost and breathing stops in a very short period of time; death occurs if rescue and resuscitation does not occur promptly.
1000	Death occurs in a few minutes; loss of consciousness occurs immediately; permanent brain damage occurs if victim is not rescued and resuscitated immediately

[a]Some information contained in this table has been obtained from Ref *4*.

containing hydrogen sulfide depends upon the chloride concentration, temperature, and hydrogen sulfide partial pressure used in the test. At room temperature and 1-atm total pressure, Nalgene®, Teflon®, and glass are examples of good materials for hydrogen sulfide testing vessels provided no other species in the test solution affects these materials. At higher temperatures or total pressures or both, experiments must be conducted in autoclaves. These environments usually contain dissolved chlorides (or other halides); the presence of hydrogen sulfide and dissolved chlorides requires that all "wetted" parts in the autoclave be made of a corrosion resistant alloy, such as United Numbering System (UNS) N10276 (that is, Hastelloy C-276) with a hardness less than HRC 35 or of another material comparably resistant to cracking and pitting over the wide range of simulated downhole environments.

All experimentation involving hydrogen sulfide is carried out in laboratory hoods (preferably explosion-proof) with the hood fan on during testing. Adequate ventilation is of paramount importance; this is a backup for leaks.

The addition or removal of hydrogen sulfide before and after testing requires its safe disposal. This is accomplished by bubbling the hydrogen sulfide containing gas through a "scrubber" before venting it into the air in the hood. The "scrubber" usually contains a 2.5 to 3.0 *N* sodium hydroxide (aqueous) solution; another acceptable solution contains ferric chloride.

Portable hydrogen sulfide detectors in the form of self-contained rolls of lead acetate paper are used to check the concentration of hydrogen sulfide in the air (after a 180-s exposure) and are very useful as hydrogen sulfide leak detectors for test vessels, tubing connections, and scrubbers. A color change in the paper indicates the presence of hydrogen sulfide; the intensity of the change indicates the concentration of the hydrogen sulfide. Electronic hydrogen sulfide systems are commercially available to continuously monitor the air in the laboratory (outside of the hood) for the presence of hydrogen sulfide and activate an alarm if the concentration exceeds a pre-set value (usually 50 to 100 ppm).

Besides the selection of proper equipment to be used in hydrogen sulfide testing, there are a few other safety measures that can be taken. Laboratory personnel should never work alone with hydrogen sulfide; backup personnel are required. If large amounts of hydrogen sulfide are contained in the test vessel, portable breathing apparatus are necessary as are additional backup personnel. Portable breathing apparatus are especially needed for rapid evacuation or rescue or both. All those working in the proximity of hydrogen sulfide testing should be fully aware of the dangers of hydrogen sulfide and symptoms of hydrogen sulfide poisoning, instructed in cardiopulmonary resuscitation (CPR), instructed in the use of the portable breathing apparatus, and aware of all of the emergency measures needed for revival of those exposed to hydrogen sulfide. Finally, evacuation plans should be prepared and rehearsed in case of an emergency involving hydrogen sulfide. Safety is the primary concern in developing deep, sour gas reservoirs, and this is also true of testing in environments containing hydrogen sulfide.

Environments

The selection of the environment for materials testing in hydrogen sulfide depends entirely upon the intended application of the material in the oil field. Downhole environments vary considerably in hydrogen sulfide, carbon dioxide, and chloride concentration; downhole temperatures and pressures also vary depending upon the reservoir and location in the well, that is, wellhead versus bottom hole. Table 2 is a summary of oil and gas well environments found in the well. Pressure and temperature of the production fluid decrease as the fluid flows to the surface.

Frequently, as in the case of oil production, there are naturally occurring corrosion inhibitors or water present in the production fluid. A continuous aqueous phase presents the most severe conditions for corrosion of metals downhole; this can occur in sour gas and in high "water cut" oil wells. For this reason, almost all corrosion testing for metals in hydrogen sulfide service is performed in aqueous solutions containing hydrogen sulfide, carbon dioxide, or dissolved chlorides or any combination of these. The environmental parameters that must be controlled in these tests are the partial pressures of the cover gases, temperature, and the chloride content. The chloride content is usually controlled by the addition of sodium chloride. However, simulation of production brine may be attempted by starting with a simulated seawater solution prepared in accordance with ASTM Specification for Substitute Ocean Water (D 1141) followed by addition of sodium chloride to achieve the desired level of chloride. These solutions are deaerated before the addition of hydrogen sulfide; this prevents or minimizes the formation of elemental sulfur by the reaction between dissolved oxygen and hydrogen sulfide [*5,6*]. Sometimes, however, the aggressiveness of the test solution is increased by the intentional addition of elemental sulfur.

Although most materials testing is determined by the service environment, mention of an environment used as part of a standard test method in wide use is warranted. An aqeuous solution containing 5 weight % sodium chloride and 0.5% acetic acid, and in equilibrium with respect to 1-atm pressure of hydrogen sulfide at 24°C (75°F) is known as "NACE solution" (NACE is the National

TABLE 2—*Typical range of downhole environments in oil and gas wells.*

Parameters	Oil Wells	Gas Wells
Temperature of wellhead, °F[a]	100 to 150	150 to 275
Temperature at bottom of well, °F[a]	100 to 250	250 to 500
Total pressure, psi[b]	2000 to 7800	4300 to 23 000
Partial pressure of H_2S, psi	0 to 200	0 to 8 000
Partial pressure of CO_2, psi	0 to 200	0 to 3 000
Chloride concentration	0 to saturation	2 weight % to saturation

[a] t°C = (t°F − 32)/(1.8).

[b] Variation in pressure is due, in part, to well flowing (lower pressure) versus well shut-in (higher pressure) condition. 1 psi = 6895 Pa.

Association of Corrosion Engineers). It simulates an acidified brine containing hydrogen sulfide near wellhead temperatures; it also simulates conditions in distillation towers for sour crude [7]. The solution is used in the NACE Standard Test Method for Testing of Metals for Resistance to Sulfide Stress Cracking at Ambient Temperatures (TM-01-77). The NACE solution and test method was developed to detect the susceptibility of low alloy steels to sulfide stress cracking (SSC, a special case of hydrogen embrittlement) but has become a test method used (and misused) on a wide range of alloys to be used in sour oil or gas production.

Test Methods

The corrosion testing of metals and alloys in simulated oil field environments covers nearly the entire range of corrosion test methods. The choice of test method(s) depends upon the application, that is, stress state and environment; the problems anticipated, that is, general corrosion, pitting, environmentally assisted cracking, and so forth; the results of failure, for example, cost and danger to the workers or environment or both; and the economics of the specific metal or alloy usage in these environments.

The test methods used are placed in one of three groups: weight loss, pitting, and crevice corrosion; test methods for environmentally assisted cracking (EAC); and electrochemical. Advantages, disadvantages, purpose, and selection of a test method are discussed.

Weight Loss, Pitting, and Crevice Corrosion

Metals and alloys to be used in hydrogen sulfide containing oil field environments are exposed to environments simulating the expected service conditions and evaluated for general weight loss corrosion [*8,9*] to determine general corrosion rates, and for susceptibility to pitting [*9,10*] and to crevice corrosion [*11–13*]. The effect of coupling a specimen to a dissimilar metal should also be examined if such a couple is expected in service. The experiments are conducted in accordance with ASTM Recommended Practice for Laboratory Immersion Corrosion Testing of Metals (G 31). Test periods vary from 3 to 30 days; the longer the test, the greater the confidence is placed in the results.

Crevice corrosion testing [*11–13*] requires a Teflon or Ryton® washer or block (for creation of a crevice) to be held in place by a metal clamp or by a bolt through the specimen. The bolt or clamp is electrically isolated from the specimen if it is a dissimilar metal. Frequently rubber bands are used to hold the crevice-creating material in place, however, for hydrogen sulfide containing environments, the rubber may become embrittled and break or deteriorate in the test and, therefore, is entirely unsuitable for this application.

Evaluation of the weight loss corrosion and pitting tests is performed in accordance with ASTM G 31. Crevice corrosion tests can be evaluated in accordance with ASTM Recommended Test Method for Pitting and Crevice Corrosion

Resistance of Stainless Steels and Related Alloys by the Use of Ferric Chloride Solution (G 48). Frequently, materials are eliminated from certain applications in hydrogen sulfide service if they are susceptible to pitting or crevice corrosion; consequently an in-depth analysis of test results is usually not necessary.

Environmentally Assisted Cracking

Two groups of test methods are used to ascertain the susceptibility of metals and alloys to EAC in hydrogen sulfide containing environments. No effort is made to separate the mechanisms of EAC for discussion, that is, hydrogen embrittlement (HE), sulfide stress cracking (SSC), or stress corrosion cracking (SCC) by anodic dissolution. The combination of stress state and environment acting on the material system determines the mechanism. A large number of test methods are available to determine a material's resistance to EAC [*14*]. The test method used subjects the specimen to either "static" or dynamic loading.

"Static" loading test methods used in hydrogen sulfide testing include the constant or sustained loading of U-bend specimens; tensile bars; C rings; 2, 3, or 4-point bent beams; and double cantilever beams (DCB). These specimens should be electrically isolated from the test fixture, clamp, or bolt as applicable when the latter are made of a material different from the specimen. This prevents galvanic effects from influencing the test results.

U-bend specimens [*7,15–17*] are loaded by bending into a shape approaching a "U" to subject the material to severe plastic deformation during environmental exposure [*18*]. The specimens are held in this shape during the test by a variety of fixtures or by clamping or bolting (see ASTM Recommended Practice for Making and Using U-bend Stress Corrosion Test Specimens [G 30]); whichever method is chosen, the specimen should be electrically isolated from the fixture, and so forth if necessary. These specimens are suitable for use in any of the simulated downhold environments. They are typically exposed to the environment for 720 h, but longer or shorter periods of exposure may be deemed more appropriate. After exposure, the specimens are visually or metallographically, or both, examined for signs of EAC. No quantitative design information is derived from this test method, only cracking or no-cracking results are obtained from this simple and inexpensive specimen.

Tensile bars, C-rings, and bent beams are used to obtain useful quantitative design information for simulated hydrogen sulfide service. These tests are usually performed to determine threshold stresses below which no EAC is observed.

"Statically" loaded tensile bars [*19–23*] are usually limited to testing in environments near room temperature and at 1-atm total pressure. The bars are loaded to specified percentages of the measured 0.2% offset yield strength by either a dead load (constant loading) [*19–21,23*] or by using a proving ring (sustained loading) [*22*]; specimens are loaded in the presence of the environment, and time to failure is measured. Testing of tensile bars in hydrogen sulfide is most frequently done in NACE solution and in accordance with the procedures set forth in NACE TM-01-77. This 720-h test is the one most frequently used

when attempting to qualify a material for NACE Material Requirement for Sulfide Stress Cracking Resistant Metallic Materials for Oil Field Equipment (MR-01-75), though many other approaches to material acceptance are available. The smooth bar tension specimen can be used to test both base metal and welds for susceptibility to EAC. Test severity can be increased by introducing a circumferential notch in the gage section. A disadvantage of the tensile bar is that specimen orientation is usually limited to tube length when specimens are prepared from production tubing, casing, or coupling stock. Diametral stresses, however, can be imposed by stressing C-rings.

C-rings are prepared from tubes of the specified material and are bolt loaded to the desired stress level in accordance with ASTM Recommended Practice for Making and Using the C-ring Stress-Corrosion Cracking Test Specimen (G 38). The bolts are made of a corrosion resistant alloy. The specimens are suitable for testing in any hydrogen sulfide containing environment and are frequently used in high-temperature high-pressure corrosion tests [*13,24,25*]. The duration of the test depends upon the desired reliability of results. The length of the test is usually between 720 and 5000 h with 1000 h being a "popular" exposure time. The specimens are visually or metallographically examined, or both, for signs of EAC after testing; unfortunately, a simple method of determining time to failure or crack initiation is not available for this test specimen as is also true of bent beams.

The bent beam [*3,8,9,15,17,19,21,26–29*], typically 0.00254 m (0.10 in.) thick, is usually prepared with the same orientation relative to the product form as that found in the tensile bars. Bent beams are used in the entire range of hydrogen sulfide containing environments. They are held in corrosion resistant fixtures, from which they are electrically isolated, and are stressed in 2-, 3-, or 4-point bending according to ASTM Method for Preparation and Use of Bent-Beam Stress-Corrosion Specimens (G 39).

Beam geometry is an advantage relative to the larger tensile bar in that various locations within a tube or pipe wall can be tested for resistance to EAC in hydrogen sulfide containing environments. This is especially an advantage when circumferential pipe welds are being tested. The 4-point loading [*9,15,17*] is preferred over the 3-point loading [*3,8,19,21,27–29*] for welds because the entire weld can be stressed at the same stress level if so desired; 4-point loading also increases the chances of detecting EAC in specimens prepared from nonwelded base metal. The 2-point loading [*26*] is infrequently used. Beams are typically exposed for 30 days to the environment of interest and, like C-rings, have the disadvantage of no simple way to monitor cracking or detect failure without disturbing the test.

A special case of the bent beam was developed by Fraser and Treseder [*29–31*] in the 1950s and is referred to as the "Shell bent beam." Two #70 holes are drilled at the transverse centerline of the beam specimen. The holes are present to introduce a "stress-raiser" and increase the chance for EAC to occur if the material is susceptible. The holes are analogous to a V notch in a tensile bar or in a C-ring.

The purpose of the tensile bar, C-ring, and beam specimens is to determine a threshold stress below which no cracking occurs for the given material/environment (the Shell bent beam analysis yields a different value called S_c). This threshold stress is for the initiation of cracks in smooth specimens. Other types of "statically" loaded specimens can be used for the determination of a threshold stress intensity K_{Ith} for environmentally assisted crack propagation (in Mode I loading) [*32*]. The DCB specimen is the most widely used specimen of this type for corrosion testing in hydrogen sulfide [*19,24,33–35*].

The DCB is a fracture mechanics specimen that is fatigue precracked before wedge open loading at a pre-determined stress intensity K_I. The initial value of K_I is typically 88 to 110 MPa·m$^{1/2}$ but subject to the limitations of the fracture toughness of the test material. The DCB is flat if prepared from plate, forgings, or of sufficiently thick tubular material; if thinner wall tubular material is used, such as production tubing, then the DCB is curved and of full-wall thickness. For tubular materials the specimen is prepared in the C-L orientation (cylindrical bar stock designation). The DCBs are side-grooved to increase the degree of plane strain along the crack front.

Wedge open loaded DCBs are exposed to the environment of interest for 720 to 1000 h. At the conclusion of the test, the specimens are pulled apart in air, and the lift-off load (actual load imparted by the wedge at the conclusion of the test) and final crack length are measured. The final K_I is calculated using the lift-off load and the final crack length. If the test is sufficiently long for EAC to cease, then the final value of K_I is equated to K_{Ith}, the stress intensity below which no EAC is assumed to occur by "static" loading. The value of K_{Ith} is rarely used in minimum flaw tolerance design of downhole or wellhead "equipment" but rather used to rank materials according to their resistance to propagation of cracks by EAC.

The curved DCB presents some problems in determining the correct lift-off load because of the bending moment induced by the position of the clevis pins. This problem has not yet been resolved.

At the writing of this paper, NACE Committee T-1F-9 on Metals Testing Techniques for Sulfide Corrosion Cracking was collecting the results from a round-robin test program of DCB testing in hydrogen sulfide environments. The results from this program will be used to revise NACE TM-01-77 to incorporate an accepted standard procedure for DCB testing in hydrogen sulfide containing environments. A review of the use of the DCB for materials testing in hydrogen sulfide containing environments is available and provided by Heady [*35*].

Corrosion test methods using dynamic loading in hydrogen sulfide environments include the slow strain rate technique and fatigue testing. Fatigue testing of materials in hydrogen sulfide environments has been essentially limited to production of S-N curves [*36*] for materials used in drilling and for artificial lift (for example, sucker rods). Therefore, the discussion of dynamic loading techniques is limited to the slow strain rate technique.

The slow strain rate technique [*22,24,37–40*], also known as the constant extension rate test (CERT), is a very aggressive test for the susceptibility of a

material to SCC or HE under dynamic straining during exposure to the environment in question. It is considered by some to be a definite test of a material's susceptibility to EAC in that if susceptibility to SCC or HE exists then the CERT will expose it. This, of course, assumes that the strain rate to be used in the test is in the range suitable for the material/environment system in question.

The CERT specimen is a tensile bar (gage diameter is typically 0.00254 m [0.10 in.]) that is pulled to failure at a low strain rate of, typically, 10^{-6} to $5 \times 10^{-6}\ s^{-1}$ during environmental exposure. The ductility, as measured by the reduction in cross-sectional area or elongation, and fracture mode of CERT specimens pulled to failure in the environment are compared to that obtained by a CERT in air or another inert environment. A decrease in the ductility is one indication of the material's susceptibility to EAC as is a more "brittle" mode of fracture or evidence of secondary cracking in the gage section.

The CERT in hydrogen sulfide containing environments is performed in the same manner as in other environments. In the past, it has not been used extensively in corrosion testing in simulated oil field environments, but it appears to be gaining popularity in this area as a method of screening materials for downhole use before extensive DCB and C-ring testing. An extensive review of the CERT is provided in Ref *37*.

Hydrogen induced cracking (HIC), or stepwise cracking, is an EAC mode that affects line pipe steels exposed to wet sour gas or sour crude. It is a phenomena that results from internal hydrogen blisters linked by "stepwise" cracks in the steel and has posed significant problems to the oil/gas industry. Discussion of the test method(s) used to evaluate the susceptibility of these steels to HIC is outside the scope of this paper. However, the reader will find substantial coverage of the subject elsewhere in Refs *19*, *21*, and *41* through *48*.

Insight into EAC mechanisms can be obtained by polarization of (any) stressed specimens. Test results from specimens exposed to the environment under freely corroding, cathodically polarized, and anodically polarized conditions are compared. Cathodic polarization of a test specimen is effected if the material is expected to be coupled to a less noble material in service; cathodic polarization may make the material fail by HE. The purpose of cathodic polarization is to examine the susceptibility to failure by HE. Anodic polarization is performed if a material is expected to be coupled to a more noble metal in service. Anodic polarization may result in anodic SCC, no change in EAC, or prevention of EAC. Cathodic polarization is more frequently used than anodic polarization in hydrogen sulfide testing.

Polarization is accomplished by either coupling to an appropriate, dissimilar metal, or by galvanostatic or potentiostatic polarization. In high-temperature high-pressure autoclave experiments, it is simplest to couple a material or to use the galvanostatic technique; this alleviates the necessity for a reference electrode suitable for hydrogen sulfide testing. The problem of using reference electrodes in hydrogen sulfide containing environments is discussed in the next section of this paper.

Electrochemical Techniques

Several electrochemical techniques are used to determine the corrosion performance of metals in aqueous solutions containing hydrogen sulfide. These include linear polarization to measure corrosion rates; potentiodynamic polarization [*5,9,24,49*] to determine active-passive transitions, susceptibility to pitting [*9,10,49*], pitting potential, and so forth; potentiostatic or galvanostatic polarization of stressed specimens to measure susceptibility to EAC; and hydrogen permeation measurements to gather mechanistic information. In general, the methods used in electrochemical investigations in solutions containing hydrogen sulfide are analogous to those used for electrochemical studies in solutions that do not contain hydrogen sulfide (see ASTM Recommended Practice for Standard Reference Method for Making Potentiostatic and Potentiodynamic Anodic Polarization Measurements [G 5] and also Ref *50*). Two areas, however, require special attention: reference electrodes and high-temperature high-pressure experiments.

Commonly used reference electrodes (for example, H_2, Ag/AgCl, and calomel) are adversely affected by the sulfide anion. To circumvent this problem electrochemical cells have been designed to separate the reference system from the test environment with barriers that inhibit the diffusion of the sulfidic species to the compartment containing the reference electrode. Under ambient temperature and pressure conditions this requires only minor modifications of conventional electrochemical cells. For high-temperature high-pressure experiments, contamination by sulfidic species is a major impediment to the successful employment of electrochemical techniques.

An effective reference system for high-temperature high-pressure experiments involving sulfides has been reported by Danielson [*51*] and used by others [*9*]. This [*51*] consists of an Ag/AgCl reference electrode separated by a capillary from the test environment. A high-pressure pump is used to flow solution from the reference compartment to the test environment at a very low rate (a few mL/h), thus impeding the migration of sulfidic species to the reference electrode. This technique is useful when no contamination of the test environment by undesirable ions from the reference compartment occurs; during most electrochemical studies involving hydrogen sulfide this is not a problem as chlorides are already present in the test environment.

For some high-temperature high-pressure electrochemical measurements an absolute (reversible) potential reference is not necessary to perform certain electrochemical tests (for example, polarization). In such cases a "pseudo-reference" electrode that exhibits a stable potential at the conditions of interest is used. Actively corroding metals such as iron or nickel have been successfully used. The "pseudo-reference" can then be related, by independent measurement, to a reversible reference electrode outside of the high-temperature high-pressure autoclave environment. This technique is effective as long as the test environment does not change during the test; these changes can affect the potential of the "pseudo-reference" electrode.

Electrical isolation of the electrodes from the autoclaves in high-temperature high-pressure experiments is effected by using special fittings in the autoclave head. These fittings employ a Teflon pressure bushing/packing gland assembly that provides electrical isolation and pressure containment. Care must be exercised to prevent "ground loops" in the autoclave system as these can cause interference in electrochemical measurements.

Localized corrosion (that is, pitting and crevice corrosion) frequently occurs in metals exposed to environments containing hydrogen sulfide. Potentiodynamic polarization, when employed to detect susceptibility to pitting, is made somewhat difficult by reactions that occur simultaneously with the localized anodic dissolution of active-passive metals. Conventional methods of detecting pitting rely on low "background" currents, that is, anodic dissolution is the predominant reaction contributing to the measured current at potentials where pitting may occur. Oxidation of H_2S, HS^-, and/or $S^=$ to S^0 or metal sulfide formation [*9,24,52,53*] produce anodic currents that add to those produced by anodic dissolution (localized and otherwise) of the metal specimen. This additional current may be large enough in these systems to make active-passive metals and alloys appear to be active at all potentials above E_{corr} (that is, results can be misleading). Figure 1 is the polarization curve of platinum in an aqueous solution containing $S^=$ (0.1*M* NaOH + 0.03*M* Na_2S) and is taken from Ref *53*. The two anodic peaks, A1 and A2, correspond to the formation of one of the platinum sulfides PtS or PtS_2 by

$$\left.\begin{array}{l} Pt + S^= \rightarrow PtS + 2e^- \\ \text{or} \\ Pt + 2S^= \rightarrow PtS_2 + 4e^- \end{array}\right\} \text{A1 in Fig. 1}$$

and to the formation of elemental sulfur, S^0, by

$$S^= \rightarrow S^0 + 2e^- \qquad \text{A1 and A2 in Fig. 1}$$

respectively.

The same (or similar) reactions also occur on other metals and alloys and obfuscate the detection of pitting. Correct interpretation of potentiondynamic polarization experiments performed in aqueous solutions containing sulfidic species can be difficult.

Hydrogen embrittlement occurs in many metals and alloys exposed to hydrogen sulfide containing environments. Hydrogen permeation experiments [*54–58*] have been performed on many of these materials, some in aqueous solutions containing hydrogen sulfide. Electrochemical hydrogen permeation experiments have been used to investigate the mechanism of the interaction of hydrogen sulfide with metals and to measure relative permeation of hydrogen. These investigations have demonstrated that the increased susceptibility of some ferrous alloys to HE is a result of increased hydrogen flux caused by the hydrogen sulfide dissolved in the aqueous environment. Explanations for the increased hydrogen flux include the participation of sulfidic species [*54*] or metal sulfides [*59*].

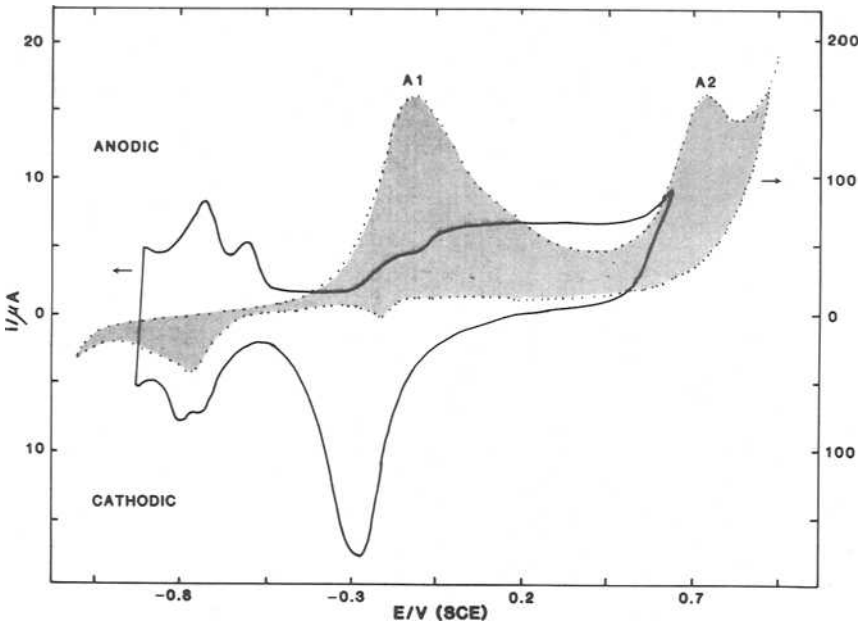


FIG. 1—*Current* i *versus potential* E *plot of a platinum electode in 0.1*M *NaOH* (solid line) *and 0.1*M *NaOH + 0.03*M Na_2S (dotted line) *solutions. Sweep rate = 0.01 V/s.*

Summary

Corrosion testing in hydrogen sulfide containing environments is primarily performed in simulated downhole environments. Test methods used in these environments include nearly the entire range of corrosion test methods used for weight loss corrosion, pitting, crevice corrosion, and environmentally assisted cracking. Emphasis is placed on safety, therefore, selection of materials for containment vessels, flow lines, and so forth, disposal of hydrogen sulfide, and training of personnel to form a sound program of safety are of paramount importance.

References

[*1*] Treseder, R. S., *Corrosion,* Vol. 8, No. 10., 1952, pp. 315–354.
[2] Dillon, C. P., Krisher, A. S., and Wissenberg, H., in *Handbook on Corrosion Testing and Evaluation,* W. H. Ailor, Ed., John Wiley and Sons, Inc., New York, 1971, pp. 599–615.
[*3*] Fraser, J. P. and Treseder, R. S., *Corrosion,* Vol. 8, No. 10, 1952, pp. 342–350.
[*4*] Braker, W., Mossman, A. L., and Siegel, D., *Effects of Exposure to Toxic Gases—First Aid and Medical Treatment,* 2nd ed., Matheson, Lyndhurst, NJ, 1977, pp. 75–77.
[*5*] Martin, R. L. and Annand, R. R., *Corrosion,* Vol. 37, No. 5, 1981, pp. 297–301.
[*6*] Rhodes, P. R., *Extended Abstracts of The Electrochemical Society,* Vol. 76-2, Abstract No. 107, 1976, p. 300.
[*7*] Takemura, S., Onoyama, M., and Ooka, T., in *Stress Corrosion—New Approaches, STP 610,* H. L. Craig, Jr., Ed., American Society for Testing and Materials, Philadelphia, 1976, pp. 338–348.

[8] Mack, R. D. and Bayes, M., *CORROSION/84*, Paper 221, National Association of Corrosion Engineers, Houston, TX, 1984.
[9] Miyuki, H., Myrayama, J., Kudo, T., and Moroishi, T., *CORROSION/84*, Paper 209, National Association of Corrosion Engineers, Houston, TX, 1984.
[10] Bond, A. P., in *Localized Corrosion—Cause of Metal Failure, STP 516*, M. Henthorne, Ed., American Society for Testing and Materials, Philadelphia, 1972, pp. 250–261.
[11] France, W. D., Jr., in *Localized Corrosion—Cause of Metal Failure, STP 516*, M. Henthorne, Ed., American Society for Testing and Materials, Philadelphia, 1972, pp. 164–200.
[12] Jackson, R. P. and van Rooyen, D., in *Localized Corrosion—Cause of Metal Failure, STP 516*, M. Henthorne, Ed., American Society for Testing and Materials, Philadelphia, 1972, pp. 210–221.
[13] Rice, P. W., *Materials Performance*, Vol. 17, No. 9, 1978, pp. 16–25.
[14] Craig, H. L., Jr., Sprowls, D. O., and Piper, D. E., in *Handbook on Corrosion Testing and Evaluation*, W. H. Ailor, Ed., John Wiley and Sons, Inc., New York, 1971, pp. 231–290.
[15] Bowers, C. N., McGuire, W. J., and Wiehe, A. E., *Corrosion*, Vol. 8, No. 10, 1952, pp. 333–341.
[16] Prange, F. A., *Corrosion*, Vol. 8, No. 10, 1952, pp. 355–357.
[17] Vollmer, L. W., *Corrosion*, Vol. 8, No. 10, 1952, pp. 326–332.
[18] Davis, R. D., *Materials Performance*, Vol. 22, No. 8, 1983, p. 21.
[19] Ikeda, A., Nagata, S., Tsumura, T., Nara, Y., and Kowaka, M., *Symposium on Line Pipe and Tubular Goods of the API Production Department 1977 Standardization Conference*, Paper SS-5:1, American Petroleum Institute, Dallas, TX, 1977.
[20] Baldy, M. F., *Corrosion*, Vol. 17, No. 11, 1961, pp. 509–513.
[21] Taira, T., Tsukada, K., Kobayashi, Y., Inagaki, H., and Watanabe, T., *Corrosion*, Vol. 37, No. 1, 1981, pp. 5–16.
[22] Yau, T. L., *Corrosion*, Vol. 38, No. 12, 1982, pp. 615–620.
[23] Burns, D. S., *Materials Performance*, Vol. 15, No. 1, 1976, pp. 21–27.
[24] Rhodes, P. R., Welch, G. A., and Abrego, L., in *Duplex Stainless Steels*, R. A. Lula, Ed., American Society for Metals, Metals Park, OH, 1983, pp. 757–803.
[25] Asphahani, A. I., *CORROSION/78*, Paper 42, National Association of Corrosion Engineers, Houston, TX, 1978.
[26] Asphahani, A. I., *Corrosion*, Vol. 37, No. 6, 1981, pp. 327–335.
[27] Grobner, P. J., Sponseller, D. L., and Cias, W. W., *Materials Performance*, Vol. 14, No. 6, 1975, pp. 35–43.
[28] Dunlop, A. K., *Corrosion*, Vol. 34, No. 3, 1978, pp. 88–96.
[29] Fraser, J. P. and Treseder, R. S., *Transactions of the American Society for Mechanical Engineers*, Vol. 77, Aug. 1955, pp. 817–826.
[30] Fraser, J. P., Eldredge, G. G., and Treseder, R. S., *Corrosion*, Vol. 14, No. 11, 1958, pp. 517t–523t.
[31] Fraser, J. P. and Eldredge, G. G., *Corrosion*, Vol. 14, No. 11, 1958, pp. 524t–530t.
[32] Smith, H. R. and Piper, D. E., in *Stress-Corrosion Cracking in High Strength Steels and in Aluminum and Titanium Alloys*, B. F. Brown, Ed., Naval Research Laboratory, Washington DC, 1978, pp. 17–77.
[33] Grobner, P. J., Sponseller, D. L., and Diesburg, D. E., *Corrosion*, Vol. 35, No. 6, 1979, pp. 240–249.
[34] Garber, R., *Corrosion*, Vol. 39, No. 3, 1983, pp. 83–91.
[35] Heady, R. B., *Corrosion*, Vol. 33, No. 3, 1977, pp. 98–107.
[36] Tsukada, K., Minakawa, K., and McEvily, A. J., *Metallurgical Transactions*, Vol. 14A, No. 8, 1983, pp. 1737–1742.
[37] Ugiansky, G. M. and Payer, J. H., Eds., *Stress Corrosion Cracking—The Slow Strain Rate Technique, STP 655*, American Society for Testing and Materials, Philadelphia, 1979.
[38] Payer, J. H., Berry, W. E., and Boyd, W. K., in *Stress Corrosion—New Approaches, STP 610*, H. L. Craig, Jr. Ed., American Society for Testing and Materials, Philadelphia, 1976, pp. 82–93.
[39] Lyle, F. F., and Norris, E. B., *Corrosion*, Vol. 34, No. 6, 1978, pp. 193–198.
[40] Turn, J. C., Jr., Wilde, B. E., and Troianos, C. A., *Corrosion*, Vol. 39, No. 9, 1983, pp. 364–370.
[41] Herbsleb, G., Poepperling, R. K., and Schwenk, W., *Corrosion*, Vol. 37, No. 5, 1981, pp. 247–256.

[42] Nakai, Y., Kurahashi, H., Emi, T., and Haida, O., "Kawasaki Steel Technical Report No. 1," Kawasaki Steel, Kawasaki, Japan, Sept. 1980, pp. 47–59.
[43] Ikeda, A. and Kowaka, M., *Chemical Economy and Engineering Review*, Vol. 10, No. 5–6, 1978, pp. 12–22.
[44] Bruno, T. V. and Hill, R. T., *CORROSION/80*, Paper 6, National Association of Corrosion Engineers, Houston, TX, 1980.
[45] Moore, E. M. and Warga, J. J., *Materials Performance*, Vol. 15, No. 6, 1976, pp. 17–23.
[46] Kim, C. D. and Loginow, A. W., *Corrosion*, Vol. 24, No. 10, 1968, pp. 313–318.
[47] Miyoshi, E., Tanaka, T., Terasaki, F., and Ikeda, A., *Petroleum Mechanical Engineering Conference*, Paper 75-Pet-2, American Society of Mechanical Engineers, New York, 1975.
[48] Baethmann, H. J., Graef, M., Hoh, B., Kleinen, J., and Poepperling, R., *CORROSION/84*, Paper 203, National Association of Corrosion Engineers, Houston, TX, 1984.
[49] Herbsleb, G. and Popperling, R. K., *CORROSION/80*, Paper 13, National Association of Corrosion Engineers, Houston, TX, 1980.
[50] Baboian, R., Ed., *Electrochemical Techniques for Corrosion*, National Association of Corrosion Engineers, Houston, TX, 1977.
[51] Danielson, M. J., *Corrosion*, Vol. 39, No. 5, 1983, p. 202.
[52] Ramasubramanian, N., *Journal of Electroanalytical Chemistry*, Vol. 64, 1975, pp. 21–37.
[53] Kapusta, S., Viehbeck, A., Wilhelm, S. M., and Hackerman, N., *Journal of Electroanalytical Chemistry*, Vol. 153, 1983, p. 157.
[54] McCright, R. D., in *Stress Corrosion Cracking and Hydrogen Embrittlement of Iron Base Alloys*, R. W. Staehle, J. Hochmann, R. D. McCright, and J. E. Slater, Eds., National Association of Corrosion Engineers, Houston TX, 1977, pp. 306–325.
[55] Xie, S. X. and Hirth, J. P., *Corrosion*, Vol. 38, No. 9, 1982, pp. 486–493.
[56] Latanision, R. M. and Kurkela, M., *Corrosion*, Vol. 39, No. 5, 1983, pp. 174–181.
[57] Zakroczymski, T., Szklarska-Smialowska, Z., and Smialowski, M., *Corrosion*, Vol. 39, No. 6, 1983, pp. 207–212.
[58] Zakroczymski, T., *Corrosion*, Vol. 38, No. 4, 1982, pp. 218–223.
[59] Wilhelm, S. M., Vera, J., and Hackerman, N., *Journal of Electrochemical Society*, Vol. 130, No. 10, 1983, pp. 2129–2132.

Robert Baboian[1] *and Gardner S. Haynes*[1]

Development of an Environmental Wear Corrosion Test for Coinage Materials

REFERENCE: Baboian, R. and Haynes, G. S., **"Development of an Environmental Wear Corrosion Test for Coinage Materials,"** *Laboratory Corrosion Tests and Standards, ASTM STP 866*, G. S. Haynes and R. Baboian, Eds., American Society for Testing and Materials, Philadelphia, 1985, pp. 260–274.

ABSTRACT: An accelerated environmental wear test has been developed that duplicates the behavior of coins in circulation mechanistically as well as visually. The environmental wear properties of monometal copper coins and of copper clad steel coins are improved by addition of zinc or nickel to the copper to form brass or copper-nickel (CuNi) alloys. Noble metal clad steel coins have similar environmental wear resistance to their respective noble monometal coins.

KEY WORDS: corrosion, wear tests, clad metals, coinage materials, cyclic humidity

Although the choice of a particular coinage material system depends on a number of factors (Table 1), one of the primary concerns is the durability of coins in circulation [*1,2*]. The relative durability is dependent on the physical, chemical, and mechanical properties of the material from which the coins are fabricated. These physical, chemical, and mechanical properties that are used as criteria for selection of coinage materials are listed in Table 2.

This paper primarily deals with the corrosion, wear, and soilage properties of coins. The laboratory coinage test program consisted of various tests to accelerate and simulate the environment to which coins are subjected. Since appropriate accelerated wear tests for coins did not exist, a test was developed to determine the comparative environmental wear resistance of coinage materials.

Experimental Procedure

The various coins used in this investigation are listed in Tables 3 and 4. The token coins listed in Table 3 were fabricated for this study by the Royal Mint in London from clad metal strip supplied by Texas Instruments, Inc. The currently minted coins in Table 4 were obtained locally in the uncirculated condition.

Wear properties of coins were investigated using a conventional wear (shaker)

[1]Head and member of technical staff, respectively, Texas Instruments Incorporated, Electrochemical and Corrosion Laboratory, Attleboro, MA 02703.

Copyright© 1985 by ASTM International www.astm.org

TABLE 1—*Criteria for selection of coinage materials.*

Availability and price
Public acceptability
Physical, chemical, and mechanical properties
Effect on coin-operated devices
Effect on mint operations
Counterfeiting, illegal duplication, and slugging

test apparatus and a newly developed environmental (cyclic humidity) wear test apparatus. Coins were degreased and weighed before and after each test period. Coin dimensions were also measured in order to determine wear mechanisms.

The wear (shaker) test apparatus is a modified version of one used by the Royal Mint in London (Fig. 1). Eight coins are placed in each of the three compartments (41.3 by 88.9 by 44.5 mm [1⅝ by 3½ by 1¾ in.]) of a Plexiglas® box, which is lined with cotton drill material. Four of these boxes are fixed to each of two reciprocating shafts whose amplitude is 63.5 mm (2½ in.) and whose frequency of reciprocation is 120/min. Once every 30 s the shaft and boxes rotate through an angle of 90°.

The environmental (cyclic humidity) wear apparatus (Fig. 2) was designed and constructed to evaluate the combined effects of wear and atmosphere on coinage materials. Each compartment of the rotating drum apparatus consists of a 139.7 mm (5½ in.) diameter by 76.2-mm (3-in.) Plexiglas cylinder (Fig. 3), which is lined with 6.35 mm (¼ in.) of foam rubber, a rubber backer, and cotton drill material from coin bags. A section of 19.05-mm (¾-in.) tubing beneath the liner creates a smooth hump that randomly upsets the coins. The compartments are separated by Plexiglas disks that are also lined with cotton drill and have a 12.7-mm (½ in.) hole in the center.

The apparatus consists of 16 cells with sliding seals on each end to allow the input and exit of a controlled atmosphere while the cells are rotating. In operation, the cylinders rotate at a rate of 40 rpm with a specified (usually 4) number of coins in each compartment while the humidity is automatically cycled using switching and timing devices.

TABLE 2—*Physical, chemical, and mechanical requirements for coinage materials.*

Color
Density
Electrical
Magnetic
Corrosion
Oxidation
Soilage
Toxicity
Hardness
Ductility
Wear
Fabricability

TABLE 3—*List of token coins tested.*

Cu/steel/Cu
75-25 CuNi/steel/75-25 CuNi
Ni/steel/Ni
90-10 Br/steel/90-1-Br
70-30 Br/steel/70-30 Br
Al/steel/Al
Ni/SS/Ni
75-25 CuNi/SS/75-25 CuNi
Ni/75-25 CuNi/Ni
75-25 CuNi/70-30 Br/75-25 CuNi
75-25 Cu/Ni/Ni silver/75-25 CuNi

A single humidity cycle consists of 2-h wet air and 6-h dry air. The relative humidity in the apparatus is monitored continuously and cycles between 10 and 90%. Wet air is obtained by passing air through a water bubble tower while dry air is obtained by passing air through a drying tower. Controlled amounts of various gases can be bled into the air to simulate various atmospheres (however, in this study, natural air was used).

Results and Discussion

Corrosion Properties

Corrosion, wear, and soilage characteristics are all interrelated. Although corrosion reactions occur independently, the rate can be affected by relative movement between materials at contact areas. The term wear corrosion or fretting corrosion is used to describe this specific type of degradation.

Alternatively, the wear rate of materials is affected by the presence of a corrosive environment. Thus, both corrosion and wear characteristics of materials are influenced by one another, the result being a form of degradation that can lead to rapid destruction of materials surfaces.

TABLE 4—*List of minted coins tested.*

U.S. penny (95-5 Br)
U.S. nickel (75-25 CuNi)
U.S. dime (CuNi/Cu/CuNi)
U.S. quarter (CuNi/Cu/CuNi)
English 5P (75-25 CuNi)
German 10Pf (70-30 Br/Steel/70-30 Br)
Columbian 5C (Cu/Steel/Cu)
Yugloslavia 50P (100 Al)
Argentina 5C (96 Al-4 Ni)
Austrian 10 Gr (98.5 Al-1.5 Mg)
Greek 5L (95 Al-5 Mg)

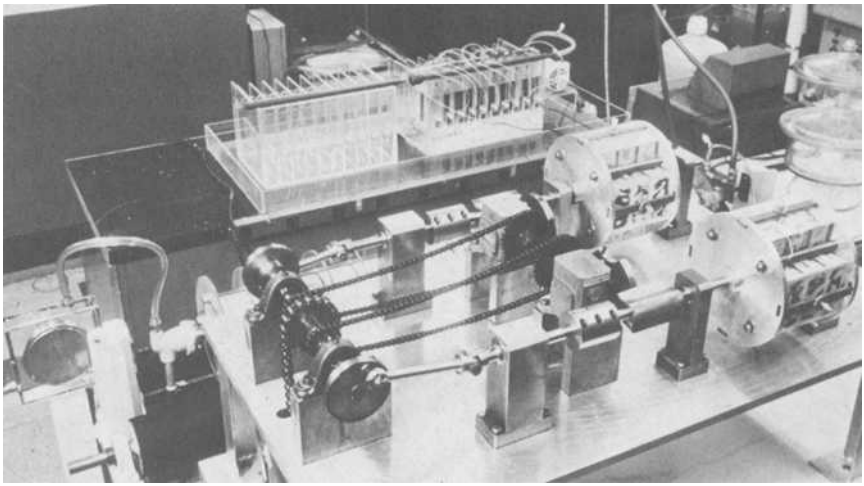


FIG. 1—*Wear (shaker) test apparatus developed by the Royal Mint (U.K.).*

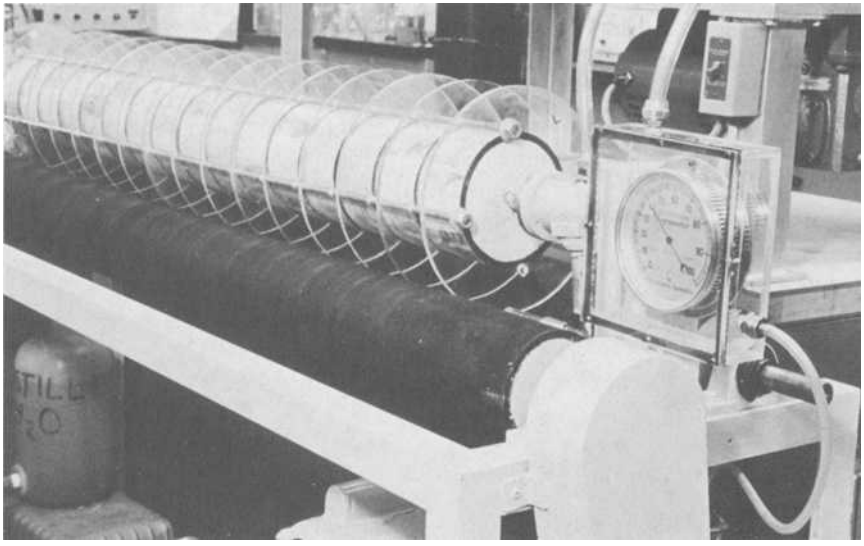


FIG. 2—*Environmental (cyclic humidity) wear test apparatus developed by Texas Instruments Incorporated.*

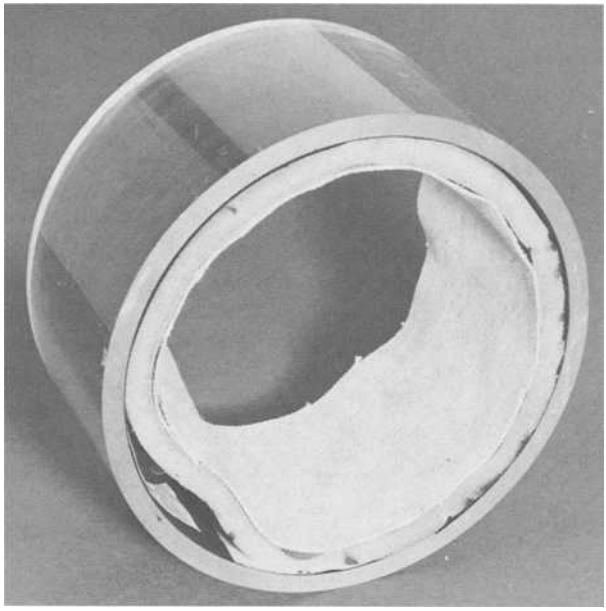


FIG. 3—*Coinage test compartment from environmental wear test apparatus.*

The degree of corrosion of metals is affected by the nature of the environment. Coins are subjected to environments of varying severity depending on location (coastal, inland, warm or cold, humid or dry regions) and mode of use (circulation frequency, social customs, and habits). The more severe environments include warm coastal and warm humid areas. Coins that are infrequently circulated or kept in storage may produce unsightly corrosion products after short periods of time in these environments (this is especially true for aluminum and its alloys). However, coins that are kept in constant circulation are continually wiped clean (such as the edge of clad metal coins), thus maintaining an unimpaired cosmetic condition.

One method of utilizing less noble (and less costly) materials in coins is by cladding. When steel, for example, is clad on both sides with a more noble metal, such as copper, nickel, and their alloys, the steel is only exposed at the coin edge. Since the edge is not part of the coin pattern, it is constantly wiped clean in circulation.

Wear and Wear Corrosion Properties

Wear is one of the most severe forms of materials degradation. It is a surface phenomenon consisting of the gradual mechanical deterioration of contacting surfaces. Wear occurs by the displacement and detachment of metallic particles

TABLE 5—*Factors affecting wear properties of coins.*

Environment
Coinage Material
Coin Design
Size
Density

from a metallic surface. The process is caused by contact with another material (metal or nonmetal) and is influenced by the factors listed in Table 5.

Coin design, including size and pattern, can have an important effect on wear rate. Spurr [*3*] and later on Cope [*4*] have shown that the wear rate of coins in circulation in the United Kingdom increases with the amount of wear. This behavior is confirmed for coins circulated in the United States by data for the U.S. penny. Coins were sorted into years and weighed after rejection of obviously damaged coins. The average weight of the coins is shown plotted against the year they were minted in Fig. 4. Notice that the weight change for U.S. pennies in circulation more than 25 years is much larger than the weight change for pennies in circulation less than 25 years. The photomicrographs (Fig. 5) of cross sections of uncirculated and circulated (35 years) U.S. pennies show the rim of the circulated coin has worn considerably. Visual examination of this coin, and all others with comparable high weight losses indicated that the faces of these coins were also worn. Alternately, coins with lower weight losses appeared to have worn mostly at the rim.

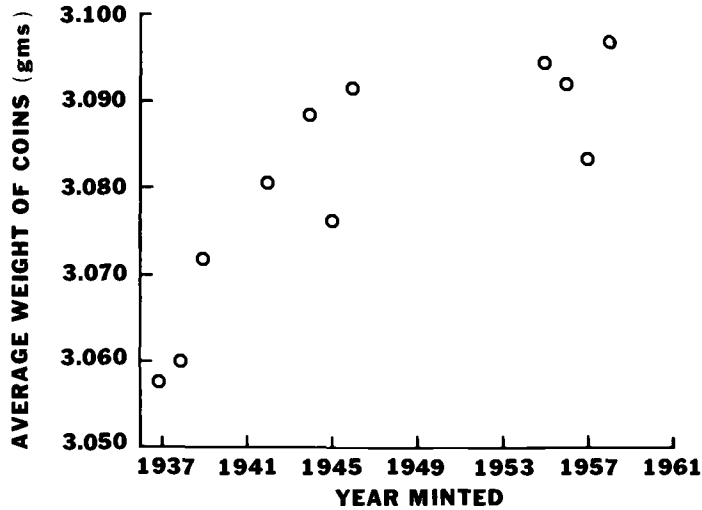


FIG. 4—*Graph showing average weight (measured in 1973) versus year minted for circulated U.S. pennies.*

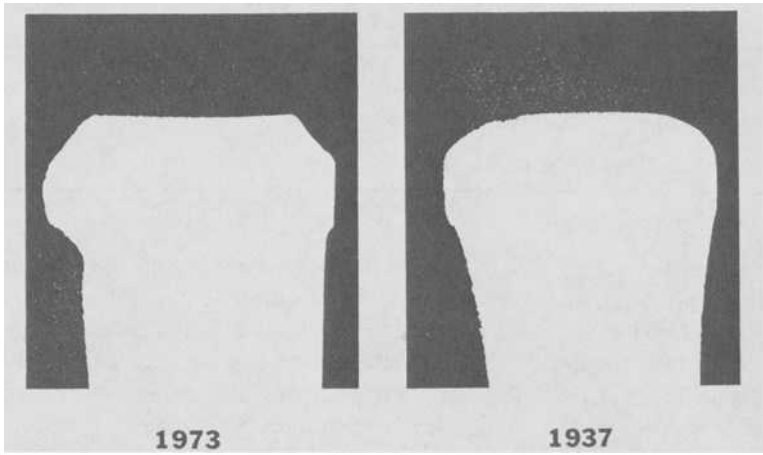


FIG. 5—*Photomicrographs of cross sections (approximately ×50) of new (1973) and circulated (1937) U.S. pennies.*

Thus, the wear rate of a particular coin is low until the rim is worn even with the face of the coin. The face of the coin then begins to wear yielding an increased wear rate proportional to the area exposed to wear. This change in wear rate occurs after about 30 years of circulation for the U.K. half penny, after about 20 years for the U.K. one shilling, and after about 25 years for the U.S. penny.

Measurement of the increasing area exposed to wear coupled with weight loss data led to the constant thickness wear rate hypothesis [*3*]. Cope [*4*] extended this work to show that the thickness wear rate (percent per annum) increases with decreasing size of coin.

The wear properties of coins are greatly affected by the choice of materials. The properties of materials affecting wear of coins are listed in Table 6. The complexity of the problem of choosing a suitable coinage material is emphasized by the many factors involved. In addition, all the other factors (Table 1) that are important in selecting a coin must be satisfied without considerable alteration

TABLE 6—*Properties of materials affecting wear of coins.*

Chemical composition
Corrosion
Oxide characteristics
Hardness
Ductility
Toughness

of the wear properties. However, use of monometals in coins generally requires a compromise of one or more of these properties.

A shift has therefore occurred in the choice of materials away from monometals to clad (sandwich) metal systems [*5–8*]. This has allowed the combining of properties of two metals into a single clad materials system. Frequently, the coinage material can be designed so that wear properties are not changed in going from the monometal to the same clad (sandwich) metal.

The wear (shaker) data in Fig. 6 for the English new pence (75-25 copper-nickel [CuNi]) and token coins (75-25 CuNi clad 70-30 brass and 75-25 CuNi clad steel) demonstrate this point. The wear data show that both CuNi/Br/CuNi and CuNi/steel/CuNi clad token coins have wear rates almost identical to the monometal CuNi English new pence.

Thus, the combination of CuNi with brass or steel allows more flexibility (over monolithic CuNi) in materials design without sacrifice of the surface wear properties.

Based on this initial data obtained in the wear (shaker) tests and the importance of the durability of coins in a real world, this study was extended to include the effects of environment on wear properties of coinage materials. The environmental, cyclic humidity wear test apparatus (as described above) was designed to simulate actual service conditions for coins. Since the mechanisms proposed for wear include the concept that atmospheric oxidation produces surface oxides that act as abrasives under repeated relative motion, cyclic humidity was introduced (during wear testing) similar to atmospheric conditions. The visual appearance of coins tested in this apparatus is very similar to that of coins in circulation for several years. For example, the U.S. penny takes on the characteristic brown coloration identical to that observed for coins in circulation.

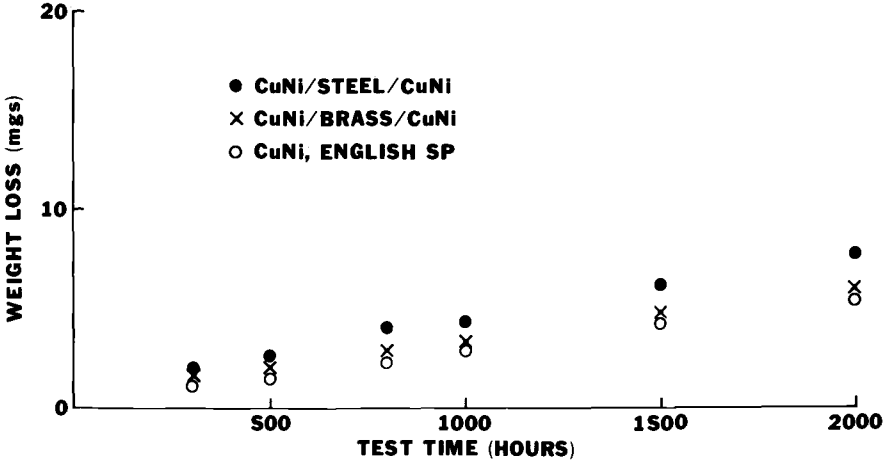


FIG. 6—*Weight loss data for coinage materials in wear (shaker) tests.*

The 600-h wear data in Fig. 7 are for a group of clad token coins having steel cores. For this series, only the material system is varied; that is, the coin pattern and size are identical.

Notice that there are significant differences observed in the environmental wear behavior of these coins. The differences are more clearly demonstrated by the data in Figs. 8 and 9. Figure 8 indicates that the addition of zinc to copper in the clad token coins improves the wear performance. The environmental wear rates decrease in the order: Cu/steel/Cu > 90-10 Br/steel/90-10 Br > 70-30 Br/Steel/70-30 Br.

Results were similar for the addition of nickel to copper (Fig. 9) and the environmental wear rates decrease in the order: Cu/steel/Cu > 75-25 CuNi/steel/75-25 CuNi > Ni/steel/Ni.

Figure 10 includes results with the U.S. penny (95-5 Br), U.S. nickel (75-25 CuNi), and German 10 Pfennig (Pf) (70-30 Br/steel/70-30 Br) in order to compare environmental wear data on token coins with data for currently minted coins. Since the currently minted coins are different with regards to pattern and size, care must be taken in evaluating these results. However, notice the lowest rates of environmental wear are observed with 70-30 Br/steel/70-30 Br, U.S. penny (95-5 Br), German 10 Pf (70-30 Br/steel/70-30 Br), 90-10 Br/steel/90-10 Br, and 75-25 CuNi/steel/75-25 CuNi.

For over 40 years, the German 2 Pf, 5 Pf, and 10 Pf have been coined from the clad (sandwich) material 70-30 Br/steel/70-30 Br. Although the steel edges are exposed in these coins, they are continuously wiped clean while in circulation. This behavior was observed with all clad metal coins (including the German 10 Pf) in the environmental (cyclic humidity) wear tests conducted in this program.

In Figures 7 and 10, the environmental wear data show that the rate of degradiation of Al/steel/Al (aluminum clad) token coins is extremely high compared to the other materials. This fact is clearly demonstrated by the photographs of several token coins in Fig. 11. The visual appearances after 600 h of testing can be compared to the U.S. penny (95-5 Br) and German 10 Pf.

To further study the effect of aluminum alloy composition on the environmental wear rate of coins, it was necessary to use uncirculated, currently minted monometal coins from several countries. Four U.S. pennies and four aluminum coins were tested in a single test cell. The coins utilized in this study include Greek 5 lepta (L) (95 Al-5 Mg), Austrian 10 Groschen (Gr) (98.5 Al-1.5 Mg), Yugoslavia 50 Paras (P) (100 Al), and Argentina 5 centavos (C) (96 Al-4 Ni). In addition to data on these coins, Fig. 12 includes environmental wear data for the U.S. penny (95-5 Br) and Columbian 5 centavos (C) (Cu/steel/Cu).

It can be seen from the weight loss data that there is a strong dependence on aluminum alloy composition. Only with the addition of 4% nickel or 5% magnesium to aluminum is there an appreciable reduction in wear rate; however, this is still three times the rate observed for the U.S. penny in the same test chamber. The rate for the 98.5 Al-1.5 Mg coin is five times greater, and the

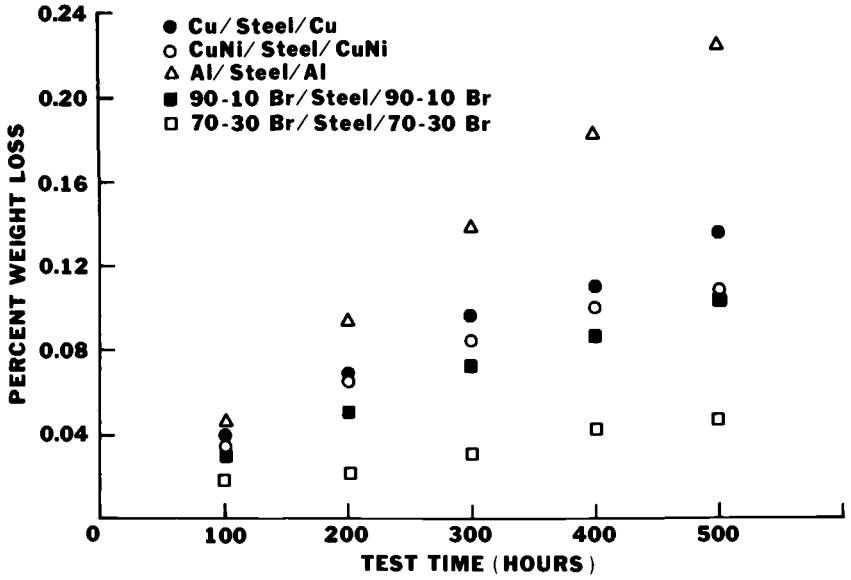


FIG. 7—*Weight loss data for steel cored token coins in environmental wear tests.*

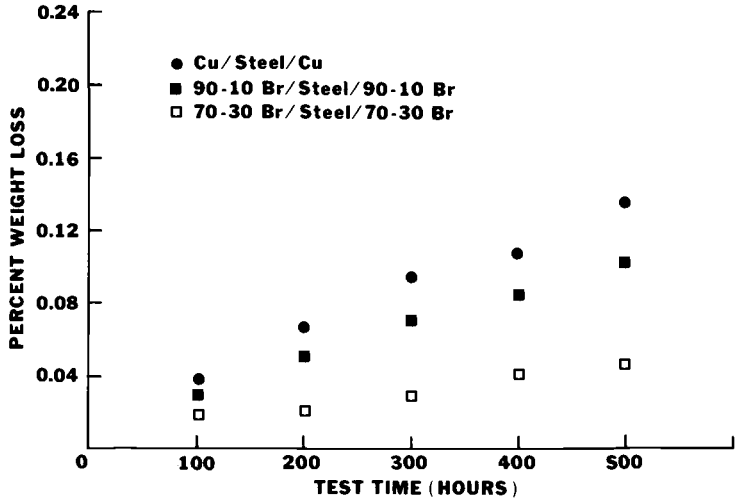


FIG. 8—*Weight loss data showing the effect of the addition of zinc to copper coinage materials in environmental wear tests.*

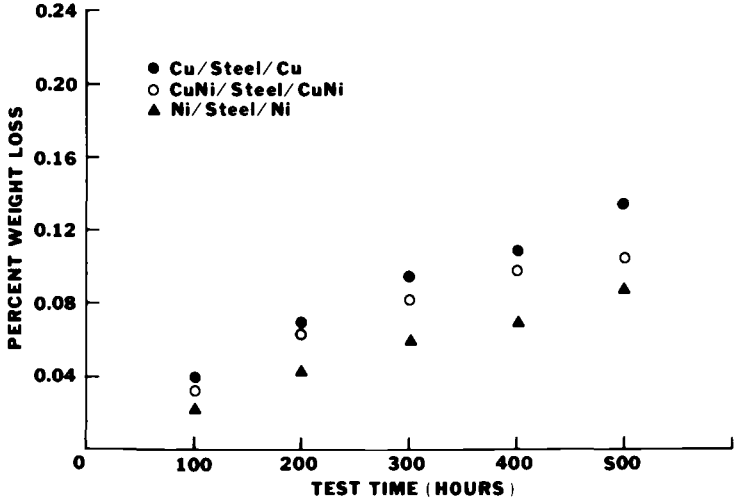


FIG. 9—*Weight loss data showing the effect of nickel additions to copper coinage materials in environmental wear tests.*

rate for the 100 Al coin is twelve times greater. This comparative behavior is also observed with coins in circulation.

Soilage Properties

During the environmental wear tests conducted on various coins, the cotton drill material used to line the test compartments became increasingly more dis-

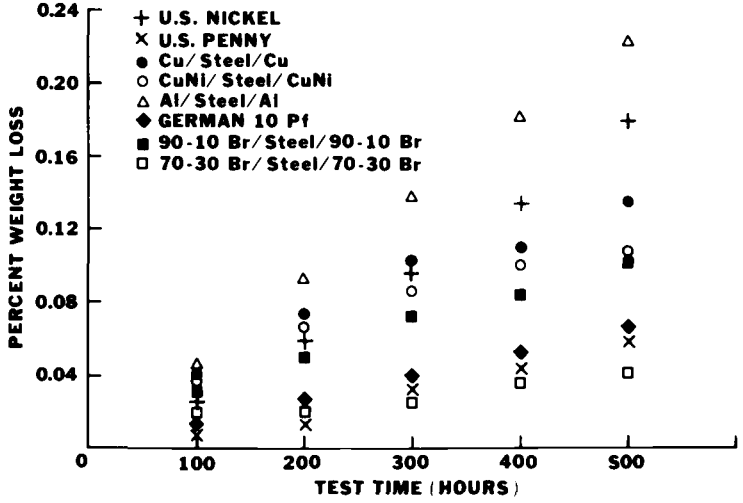


FIG. 10—*Weight loss data for various coinage materials in environmental wear tests.*

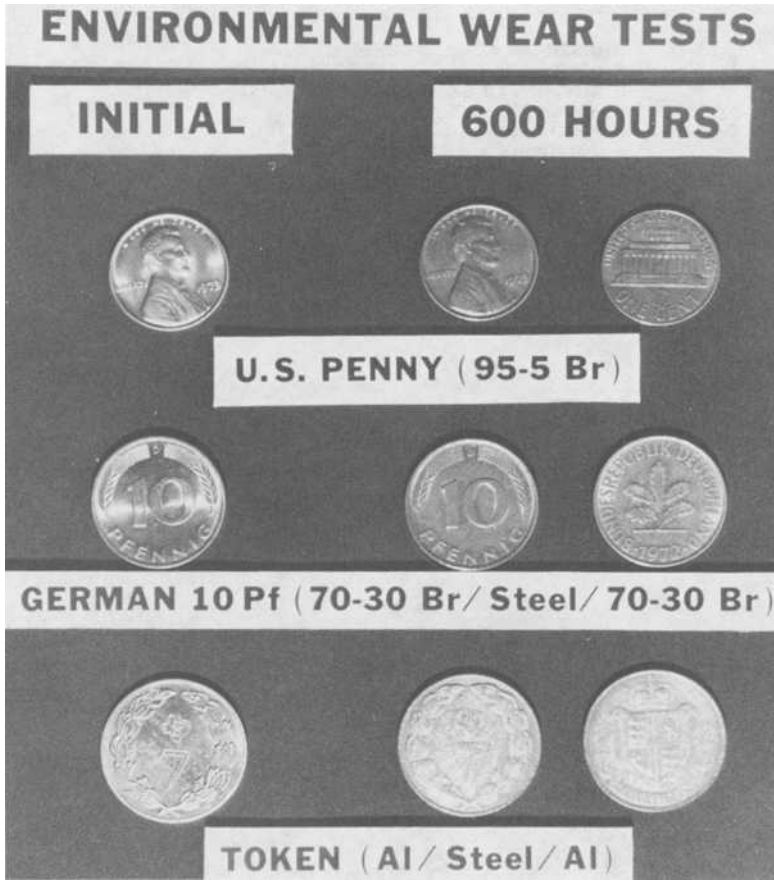


FIG. 11—*Photograph showing visual appearance of coins after environmental wear tests.*

colored. This can be attributed to the accumulation of oxide debris produced during the wear process.

The degree of soilage to cotton materials by coins during wear testing was dependent on coinage material and time of testing. Figure 13 shows the cotton drill linings (after 600-h environmental wear testing) for several token coins. Notice that there is an unusually high degree of soilage with Al/steel/Al token coins compared to all other coins. For steel cored token coin materials, the order of increasing soilage is

$$70\text{-}30\ \text{Br} < 90\text{-}10\ \text{Br} < \text{Cu} < 75\text{-}25\ \text{CuNi} < \text{Ni} < \text{Al}$$

The effect of aluminum alloying composition on soilage of cotton drill material

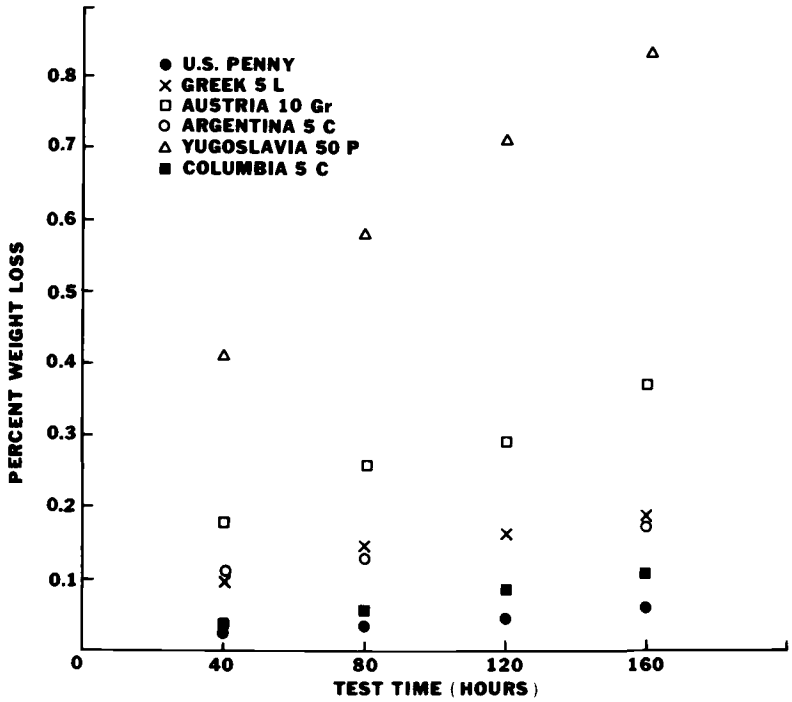


FIG. 12—*Weight loss data comparing aluminum and copper bearing coins in environmental wear tests.*

was determined. The order of increasing soilage is

$$95 \text{ Al-5 Mg} < 98.5 \text{ Al-1.5 Mg} < 100 \text{ Al}$$

It appears that the nature of the soilage properties of aluminum and its alloys are markedly different and quite extensive when compared to other coinage materials. The effect is more pronounced when aluminum coins are mixed with coins such as U.S. 1, 5, 10, and 25 cent pieces. This degree of discoloration of cotton material cannot be fully explained by the higher wear rate for aluminum coins. Possibly, this unusually high degree of soilage is explained by the nature of the aluminum oxide debris produced during wear testing. Further experimental work is necessary to confirm this hypothesis. However, it is important to note that the soilage characteristics of aluminum coins observed in the environmental wear test are also observed with aluminum coins in circulation.

Conclusions

An environmental (cyclic humidity) wear test apparatus has been designed and constructed, which simulates the environment of coins in circulation. The

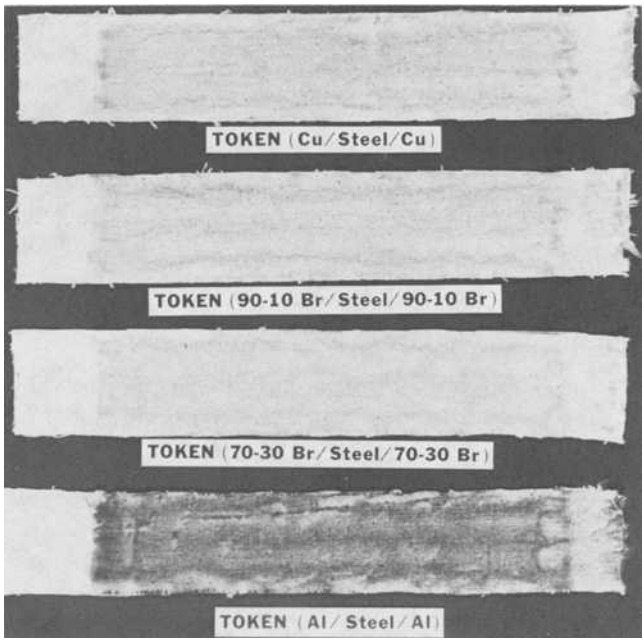


FIG. 13—*Photograph showing soilage (discoloration) of cotton drill after environmental wear tests (600 h).*

behavior of various coins in this test duplicates the behavior of coins in circulation mechanistically as well as visually.

The constant thickness wear rate hypothesis gives a good representation of the observed environmental wear characteristics of the U.S. penny (95-5 Br) in circulation.

Monometal coins fabricated from the more active metals, such as steel or aluminum, can build up unsightly corrosion products on the coin face depending on the degree of circulation. The worst situation occurs while these coins are in storage.

Although the edges of steel cored clad metal (covered on both sides with a more noble metal such as copper, nickel, or their alloys) coins are exposed to the environment, these edges are continuously wiped in circulation and no visual effects were observed.

The environmental wear properties of monometal copper coins and of copper clad steel coins are improved by addition of zinc or nickel to the copper to form brass or CuNi alloys. The noble metal clad (steel cored) sandwich coins performed similarly to their respective noble monometal coins in wear tests.

Addition of magnesium to aluminum in coins improves the environmental wear behavior, however, when compared to the U.S. penny (95-5 Br), the rate

was three times greater with 95 Al-5 Mg coins, five times greater with 98.5 Al-1.5 Mg coins, and twelve times greater with 100 Al coins. These rates could reflect a serious wear problem with aluminum coins if the constant thickness wear rate hypothesis is valid.

Soilage (discoloration of cotton drill materials) during environmental wear testing was exceptionally high with aluminum and very low with copper and copper alloys (especially brass) coins. The high degree of soilage with aluminum coins can be explained by their higher wear rate and the nature of the oxide debris produced during the wear process.

Acknowledgments

The authors acknowledge the assistance of William Gorman and the encouragement and cooperation of Edwin Miller and Richard Churchill of Texas Instruments Incorporated and Vincent Newman of the Royal Mint in London.

References

[*1*] "Annual Report of the Director of the Mint, Fiscal Year Ended June 30, 1972," U.S. Government Printing Office, Washington, DC, 1973.

[*2*] Rice, L. P., Emerson, M. E., Wagner, H. J., Hale, R. W., and Hall, A. M., "A Study of Alloys Suitable for Use as United States Coinage," U.S. Government Printing Office, Washington, DC, 1965.

[*3*] Spurr, R. T., "Wear of U.K. Coins," *Wear*, Vol. 8, 1965, p. 487.

[*4*] Cope, R. G., "The Wear of U.K. Coins in Circulation," *Wear*, Vol. 13, 1969, p. 217.

[*5*] Kimber, R. A. and Stokes, R. R., "Design Considerations and Proposals for Compatible U.S. Subsidiary Coinage," *Bell System Technical Journal*, April, 1966.

[*6*] Wagner, H. J. and Hall, A. M., "The New Coinage," *Journal of Metals*, March 1966.

[*7*] Deane, D. V., "Materials for Coinage," *Sheet Metal Industries*, Aug. 1967.

[*8*] Goldman, A. J., Jordon, R. W., and Winter, J., "Bond Degradation Mechanisms in the 75% Cu–25% Ni/Cu/75% Cu–25% Ni Coinage Composite," *Transactions of the Metallurgical Society of the American Institute of Mechanical Engineers*, AIME, Vol. 242, 1968, p. 295.

Philip A. Rosskopf[1] *and R. Craig Virnelson*[1]

Laboratory Tests for Corrosion of Steel in Concrete

REFERENCE: Rosskopf, P. A. and Virnelson, R. C., **"Laboratory Tests for Corrosion of Steel in Concrete,"** *Laboratory Corrosion Tests and Standards, ASTM STP 866*, G. S. Haynes and R. Baboian, Eds., American Society for Testing and Materials, Philadelphia, 1985, pp. 275–284.

ABSTRACT: The development of laboratory test methods for determining potential corrosion of steel imbedded in portland cement mortars is described in detail. Examples are given of the effects of chemical admixtures on the passive iron hydroxide protective layer surrounding reinforcing steel in concrete. Specific examples are shown that identify a threshold limit below which known corrosive materials are inert with respect to steel in concrete.

KEY WORDS: corrosion, concretes, reinforcing steels, anodic polarization, portland cements, alkaline passivity, chlorides, thiocyanates, acetates, formates

The corrosion of reinforcing steel in concrete can be the limiting factor in the life of a concrete structure [*1*]. The corrosion rate is usually slow and takes a substantial amount of time to study. An accelerated test for modeling corrosion is necessary for researchers to evaluate the effect of varied concrete environments or additives to concrete on corrosion of reinforcing steel. Especially, the effect of concrete set accelerators on corrosion can be modeled with a galvanostatic anodic polarization method. It can also aid in the establishment of realistic and meaningful limits for corrosion promoting materials.

The pH environment of concrete is basic enough to afford natural protection to steel. Corrosion can only occur when this environment is significantly altered. Alterations can result from carbonation, impurities in the mix, addition of large amounts of salt to the plastic concrete, deicing or marine salts diffused through the pores of the hardened concrete, or the exposure of reinforcing steel to moisture and oxygen through honeycombing or cracking. The latter physical cause for the corrosion of steel in concrete is a problem that is not the subject of this discussion.

The corrosion caused by excessive added salts or marine or deicing salts is due primarily to the chloride ion [*2*]. The cause for this kind of corrosion is an

[1] Senior research advisor and manager of analytical services, respectively, Master Builders, 23700 Chagrin Blvd., Cleveland, OH, 44122.

Copyright© 1985 by ASTM International www.astm.org

electrochemical phenomena, which is not explained easily in a matrix as complicated as concrete. Active corrosion can be detected as it develops by measuring the half cell potential produced by the corroding steel versus the copper/copper sulfate half cell as specified in ASTM Test Method for Half Cell Potentials of Reinforcing Steel in Concrete (C 876).

Efforts to prevent the corrosion of steel in concrete have taken many approaches; protective coatings on the surfaces of the steel [*3,4*], cathodic protection [*5*], waterproofers and sealers in the concrete [*6*] and anodic chemical inhibitors [*7*]. Each of the methods offers at least some protection, but all of the methods used for preventing corrosion have shortcomings. Most are expensive and are often installed as repair procedures [*1*]. Uncomplicated testing for establishment of realistic limits for potentially deleterious materials or for newly proposed concrete improvers or for different cement chemistries, is needed by the concrete construction industry.

Discussion

Techniques for predicting corrosion vary from theoretical computer simulation to direct measurements on actual concrete structures. Whatever the technique, it should as much as possible duplicate the real world of concrete. The test should represent the most rigorous or severe conditions to allow a safety factor.

From the point of view of specimen preparation, the most acceptable tests are those that incorporate actual steel bars embedded in mortar (portland cement, sand, and water) specimens. In this way the environment is not simulated but real. The use of specimens that have been cured under moist conditions for 24 h enhances the reactivity of the reinforcing bars and insures rigorous tests.

The age of the mortar specimens is very important in two opposing ways. Electrochemically the specimen should be tested at 24 h [*8*]. If it is allowed to cure for longer periods of time, the surface of the embedded steel bar becomes increasingly nonuniform. Also, the electrical resistance of the specimen increases with increased aging. Anodic polarization (galvanostatic) tests are most meaningful if the electrode (reinforcing bar) has not already undergone substantial changes. Age also affects the solution concentration of admixed salts. Monfore and Verbeck reported that chloride levels decrease rapidly as shown in Table 1 in the first 7 days and slowly until 28 days [*9*]. This decrease in chloride concentration is due to its reaction with tricalcium-aluminates of the portland cement as hydration occurs [*10*]. Corrosion is promoted by chlorides that remain

TABLE 1—*Percent calcium chloride by weight of cement in solution after 1 and 28 days for Type 1 cement.*

Calcium Chloride, % added	Calcium chloride, % at 1 day	Calcium chloride, % at 28 days
0.25	0.12	0.03
0.50	0.26	0.07
1.00	0.51	0.15
2.00	1.13	0.37

in solution [*1*]; therefore, it is the 28-day (and thereafter) chloride concentration that is most important. Testing specimens at one day requires a concentration correction for soluble chloride ions to be made, and in this way a close approximation of the real world is achieved. The following example will make this more clear:

A 2% by weight of cement addition of calcium chloride, which results in a 0.24% concentration of soluble chloride after 28-days of moist curing, is equivalent to an addition of 0.75% calcium chloride by weight of cement, which yields 0.24% soluble chloride after 24 h [*10*].

If this correction is not made, laboratory tests will not be interpreted in the manner known to occur naturally. Test results can vary between cements and are relative to the characteristics of the particular cement used.

Anodic polarization tests of mortars cause oxidation reactions to occur on the surface of the electrode (reinforcing bar). The electrochemical potential of these oxidation reactions is measured using a reference electrode such as the saturated calomel [*8*]. The polarization potential is great enough to allow almost any reaction that is possible in this system to occur, but relatively low current densities are used (typically 10 $\mu A/cm^2$) so that electrochemical reactions do not happen too rapidly to observe easily. The higher the current density the more rapid the reaction. The existence, stabilization, or destruction of the natural passive layer of the steel can be measured by this method. Destruction of the passive layer is an indication of a corrosive environment at the surface of the steel.

Test Apparatus

The first step in this investigation of corrosion potentials was construction of an instrument. Figure 1 shows an instrument that contains a constant current source, a digital readout microammeter, and a recording millivoltmeter. Linked to the instrument is a platinum electrode and a calomel reference electrode. Completing the circuit is a 10- by 20-cm cylindrical mortar specimen containing a steel rod. Before preparing the specimen, portions of the steel rod are coated with wax so that a known surface area is exposed within the mortar [*8*] (Fig. 2).

Under corrosive conditions in hardened concrete, steel reinforcing bars act as both the anode and cathode. The two halves of a cell may be very close or some distance apart (microcells or macrocells). As long as there is continuity between them, the resultant electrochemical reaction proceeds unchecked until the concrete dries to less than 60% relative humidity or reactants are exhausted. Corrosion occurs at the anode where iron is oxidized.

The technique that was chosen for accelerated tests generates an anodic condition at the surface of the steel rod in the specimen. The strength of the driving force, or current density, is measured in microamps. Normally, 10 $\mu A/cm^2$ is enough to overcome natural resistance of the system and force the steel to an

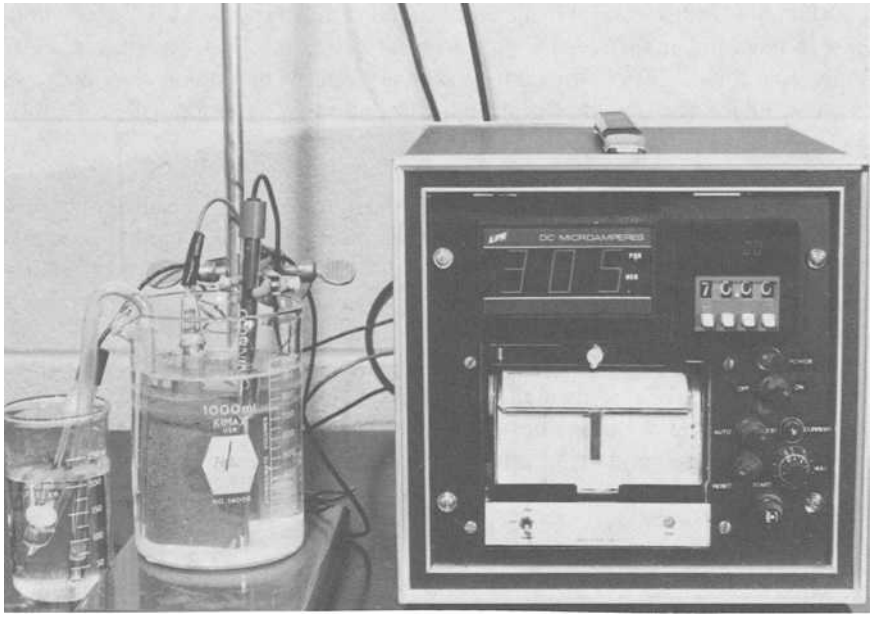


FIG. 1—*Galvanostatic corrosion test apparatus.*

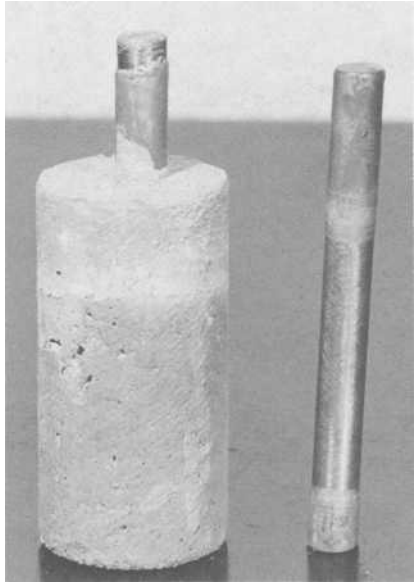


FIG. 2—*Corrosion test specimen and waxed steel rod.*

oxidized state. Once chosen, the current imposed upon the system is kept constant. Figure 3 contains a schematic diagram of the system.

The potential, or emf, of the reactions that occur as a result of the applied current density is measured in millivolts. The reference electrode and the platinum electrode potentials are well known and constant irrespective of the sample electrode. These potentials are the result of the following chemical reactions

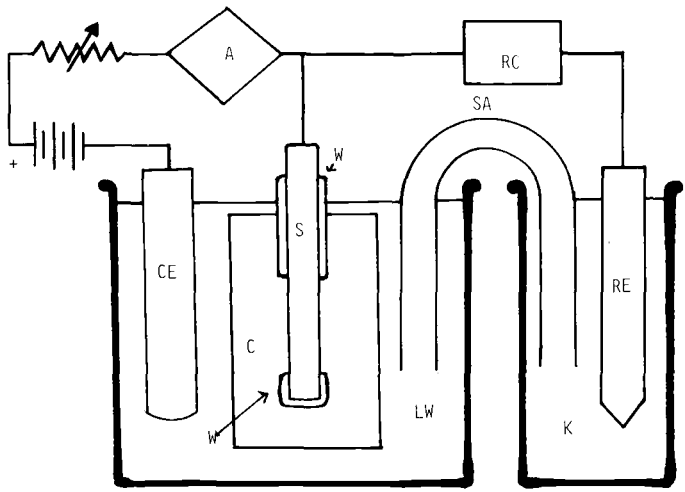
$$\text{platinum electrode: } 2H_2O + 2e^- \rightleftharpoons H_2 + 2OH^- \ (-828 \text{ mV})$$

$$\text{calomel electrode: } 2Hg + 2Cl \rightleftharpoons Hg_2Cl_2 + 2e^- \ (-242 \text{ mV})$$

Where mV are potentials versus hydrogen half cell.

The observed potential when measured empirically was between -1050 and -1100 mV. This value corresponds well with the theoretical value or the sum of the potentials shown above.

If a platinum electrode is substituted for the sample in the schematic shown



A - AMMETER
C - CONCRETE
CE - COUNTER ELECTRODE (Pt)
E - VOLTAGE SOURCE
G - GALVANOSTAT
K - POTASSIUM CHLORIDE SOLUTION
LW - LIME WATER (SATURATED)
RC - STRIP CHART RECORDER
RE - REFERENCE ELECTRODE
S - REINFORCING BAR
SA - SALT BRIDGE (KCL)
W - WAX

FIG. 3—*Schematic diagram of corrosion test apparatus.*

in Fig. 3, the reaction is

$$2H_2O \rightleftharpoons O_2 + 4H^+ + 4e \ (+1229 \text{ mV})$$

The combined potential between this electrode and the calomel is 1000 ± 50 mV. Again, measured values were found in this range.

Under normal test conditions, a reactive sample electrode is used in the system. Competing reactions occur between the oxidation of the metal and the electrolysis of water. The observed or measured potential of the system will be somewhere between the two. This value is 600 ± 50 mV and is obtained in a reasonably short time. Equilibrium exists and the potential remains constant as long as the steel surface remains passivated. Other ionic materials in the concrete or pore

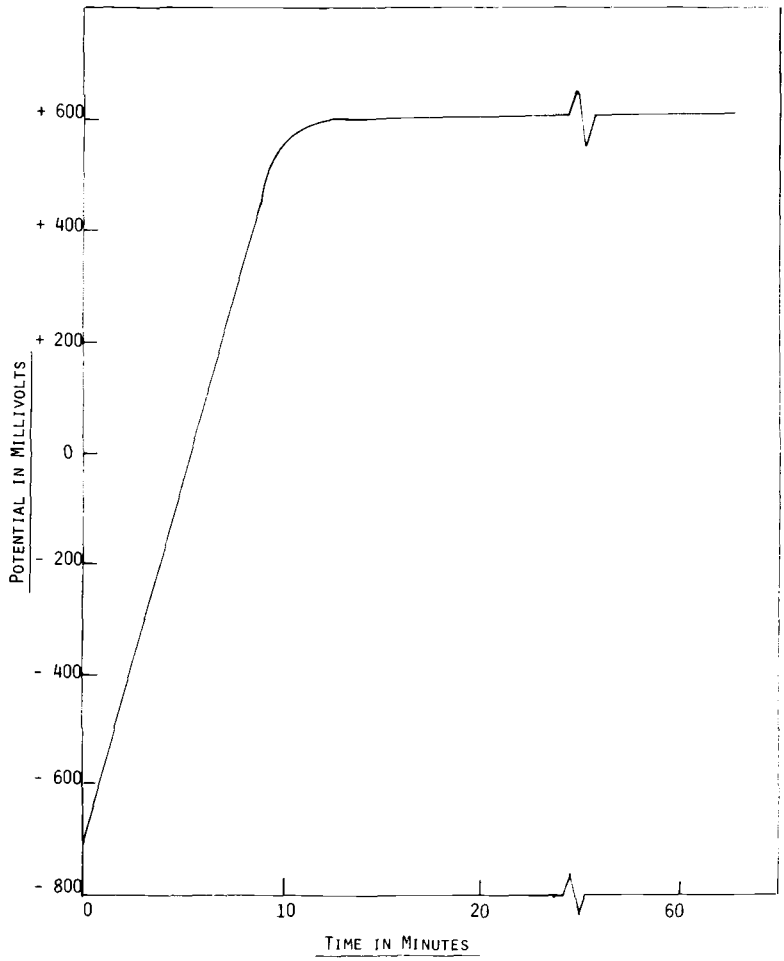


FIG. 4—*Galvanostatic tests on steel embedded in portland cement mortars.*

water, however, can participate in the reaction mechanism and complicate the system. Nevertheless, the system remains understandable from a qualitative point of view. For example, an abundance of chloride ion in the electrolyte (liquid within the sample) causes a passivation breakdown to occur at the steel or active electrode. Corrosion is observed by a dramatic change in the potential toward lower or even negative values.

Results

The data obtained when one-day old mortar specimens are tested under the conditions described above are shown graphically in Fig. 4. The cement to sand and water to cement weight ratios of the mixes were 0.36 and 0.64, respectively.

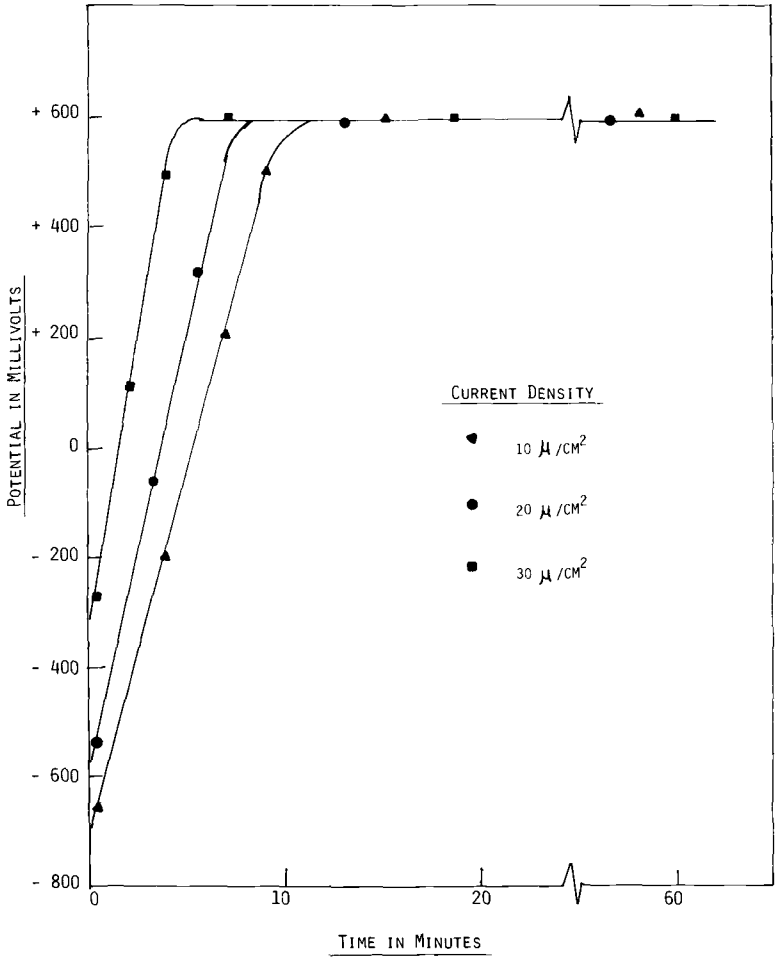


FIG. 5—*Effect of current density of the galvanostatic testing of steel in portland cement mortar mixes.*

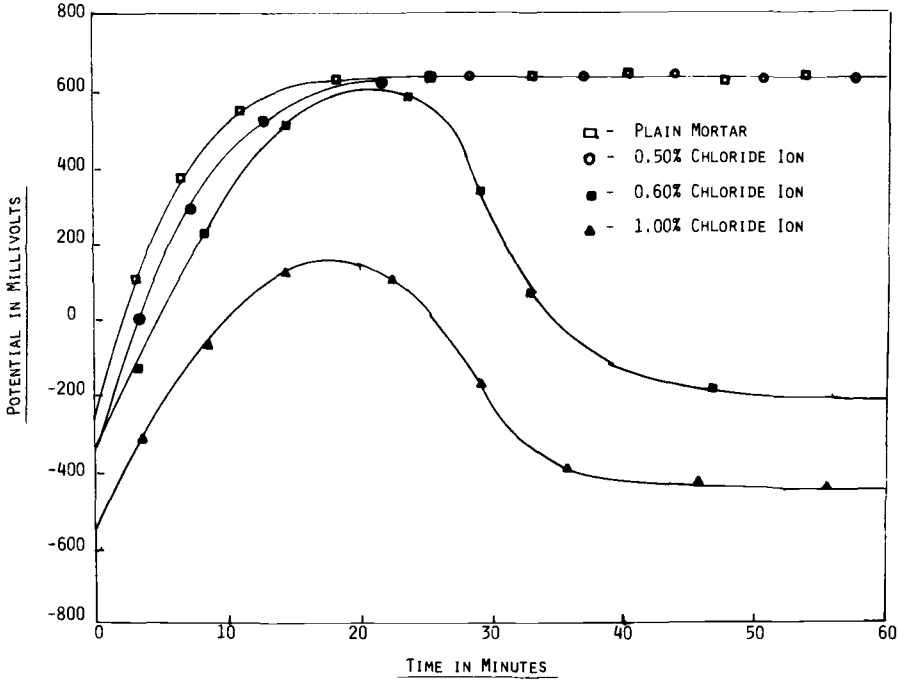


FIG. 6—*Effect of chloride ion concentration on the passive layer of reinforcing bars tested at one day.*

The curves for steel rods embedded in mortars made with either Type I, Type II, or Type III cement were essentially the same shape. Noncorroding conditions are evidenced by the maintenance of equilibrium potentials of 600 ± 50 mV.

Potential versus time curves for specimens run at higher current density are shown in Figs. 4 and 5. The only change noted is a decrease in the time required to reach equilibrium. Thereafter, the potential remains constant.

Steel rods in mortar specimens that contain large amounts of admixed calcium chloride will show unstable potentials when the concentration of the chloride ion exceeds a particular level. These curves are shown in Fig. 6. However, it appears that chloride tolerance for mortars made with different cements is dependent upon the portland cement composition. This dependency is summarized in Table 2 indicating the percentage of calcium chloride by weight of cement

TABLE 2—*Percent calcium chloride by weight of cement and one-day percent Cl^- necessary to breakdown the passive layer.*

Cement Type	Calcium Chloride Added, %	28-Day Cl^-, %
I	1.3 ± 0.1	0.5 ± 0.02
II	1.1 ± 0.1	0.5 ± 0.02
III	2.3 ± 0.1	0.5 ± 0.02

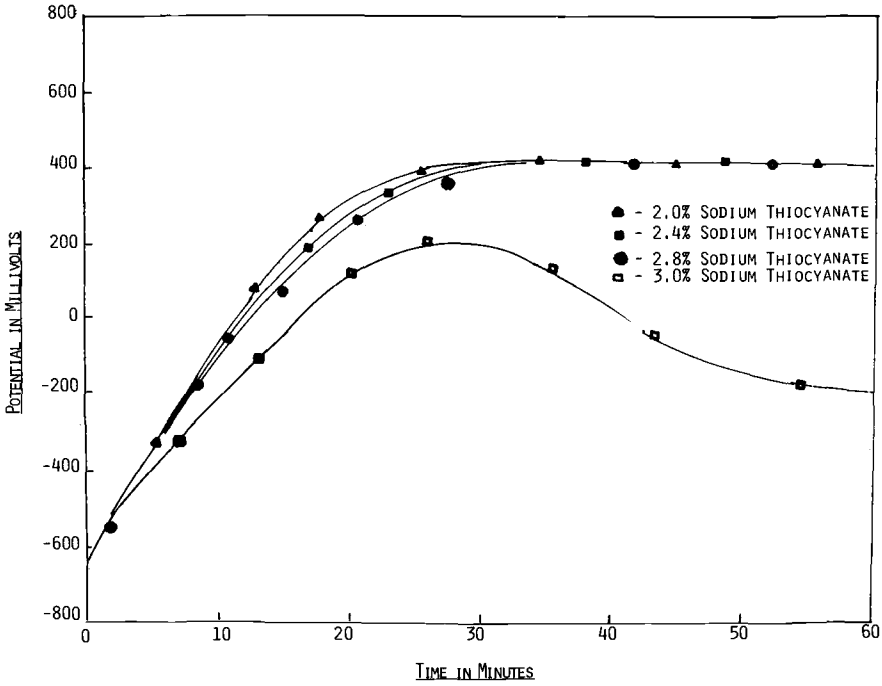


FIG. 7—*Effect of sodium thiocyanate concentration on the passive layer of reinforcing bars tested at one day.*

added, and the one-day equivalent soluble chloride level necessary to destroy the passive layer on the surface of the reinforcing bar under the influence of an externally applied current, as in this experiment. This is a "worst possible" situation that may not even occur in a particular real world situation.

Other inorganic ions are being offered for use as chloride substitute accelerators. One of these, namely, sodium thiocyanate (NaSCN), was tested. Figure 7 shows sodium thiocyanate additions of 2.0, 2.4, 2.8, and 3.0% by weight of Type I cement. There was no initiation of corrosion as high as 2.8%.

The galvanostatic technique was also used to test organic ionic constituents from other chloride substitute accelerators in mortar mixes. Calcium formate and calcium acetate were tested at rates of addition to mortar as high as 2.0% by weight of cement. In every test the potential versus time curves for the mixes containing the specific salts were similar to, if not identical with, those found for the plain passivated mortar mix.

Summary

The galvanostatic method is a valid technique for identifying environments that affect the passivity of steel embedded in concrete. This is demonstrated by the agreement between the laboratory test data and observations of actual concrete structures under equivalent conditions [*10*].

Corrosion caused by diffused salts is a separate problem and unrelated to normal additions of set accelerators such as chloride, nitrate, thiocyanate, formate, and so forth.

Accelerated (less than 28 days) tests must be corrected for any differences in salt concentrations between the 28-day concentration and the age of the specimen at the time it is tested.

References

[1] Cady, P. D., "Corrosion of Reinforcing Steel in Concrete—A General Overview of the Problem," *Chloride Corrosion of Steel in Concrete, STP 629*, D. E. Tonini and S. W. Dean, Jr., Eds., American Society for Testing and Materials, Philadelphia, 1977, pp. 3-11.

[2] Verbeck, G. J., "Mechanism of Corrosion of Steel in Concrete," SP-49, American Concrete Institute, 1975, pp. 21–38.

[3] Cook, A. R. and Radtke, S. F., "Recent Research on Galvanized Steel for Reinforcement of Concrete," *Chloride Corrosion of Steel in Concrete, STP 629*, D. E. Tonini and S. W. Dean, Jr., Eds., American Society for Testing and Materials, Philadelphia, 1977, pp. 51–60.

[4] Kilareski, W. P., "Epoxy Coatings for Corrosion Protection of Reinforcement Steel," *Chloride Corrosion of Steel in Concrete, ASTM STP 629*, D. E. Tonini and S. W. Dean, Jr., Eds., American Society for Testing and Materials, Philadelphia, 1977, pp. 82–88.

[5] Rog, J. W., Swait, W. J., and Hooker, W. H., "Cathodic Protection Prevents Corrosion Damage on Concrete Parking Structures," *Parking*, Winter 1982.

[6] Hagenbuch, J. J., Highway Research Board Record No. 257, 1975, p. 95.

[7] Griffin, D. F., "Corrosion Inhibitors for Reinforced Concrete," *Corrosion of Metals in Concrete*, SP-49, American Concrete Institute, 1975, pp. 95–102.

[8] Gouda, V. K. and Monfore, G. E., "A Rapid Method for Studying Corrosion Inhibition of Steel in Concrete," *Journal of the PCA Research and Development Laboratories*, Vol. 7, 1965, pp. 24–31.

[9] Monfore, G. E. and Verbeck, G. J., *Journal of American Concrete Institute*, Nov. 1960, pp. 491–515.

[10] Cook, H. K. and McCoy, W. J., "Influence of Chloride in Reinforced Concrete," *Chloride Corrosion of Steel in Concrete, STP 629*, D. E. Tonini and S. W. Dean, Jr., Eds., American Society for Testing and Materials, Philadelphia, 1977, pp. 20–29.

Stephen A. Dial,[1] *Ramon L. Carrasquillo,*[2] *and John E. Breen*[3]

Corrosion Induced Deformation Behavior of Brick Masonry Wall Panels

REFERENCE: Dial, S. A., Carrasquillo, R. L., and Breen, J. E., **"Corrosion Induced Deformation Behavior of Brick Masonry Wall Panels,"** *Laboratory Corrosion Tests and Standards, ASTM STP 866,* G. S. Haynes and R. Baboian, Eds., American Society for Testing and Materials, Philadelphia, 1985, pp. 285–296.

ABSTRACT: The main purpose of the work described herein was to study the magnitude of corrosion induced distress in brick masonry wall panels under service conditions in a structure exposed to an acid rain environment. For this purpose, some specimens were subjected to a constant sustained load during exposure testing typical of dead loading under service conditions.

Specimens consisted of nine masonry wall panels with a steel plate, representative of shelf angles used in construction, embedded in the mortar joints at the third and sixth courses. Following twelve weeks of strain readings after load application, an acid-water solution was sprayed on the face of the walls, and accelerated corrosion was electrically induced in the embedded steel plates. Corrosion was also induced in six steel plate specimens that were immersed in tubs filled with the acid-water solutions. Expansion strains and cracking caused by the corrosion of the embedded steel were recorded, and the weight loss of the steel plate specimens was measured. The corrosion products on the steel plates were analyzed under an electron microscope and using X-ray diffraction analysis.

The results show that the embedded plates do not affect the overall temperature and moisture deformation behavior of the wall panels except for local disturbances in the joints containing the plates. The plate regions in the loaded wall panels underwent larger creep strains than regions of the wall panels that did not contain embedded plates. The average creep strains for the loaded walls were 39% lower than the creep strains reported from a previous investigation using similar wall panels that did not contain embedded plates. The presence of the embedded plates appeared to decrease the magnitude and duration of creep.

The induced corrosion of the embedded steel plates caused expansion strains that were several orders of magnitude greater than the tensile strain of masonry at failure. The weight loss of the plates from the nonloaded walls generally was slightly greater than that of the plates from the loaded walls for similar exposure times and was approximately 50% less than the weight loss of the immersed plate specimens.

KEY WORDS: brick masonry, corrosion, creep properties, sustained load, wall panels, deformation, cracking (fracturing), acid rain

[1] Structural engineer, Cook Consultants, 4919 N. Central Expressway, Dallas, TX 75205.

[2] Assistant professor of civil engineering, The University of Texas at Austin, 10100 Burnet Rd., Austin TX 78758.

[3] Director, Phil M. Ferguson Structural Engineering Laboratory, 10100 Burnett Rd., Austin, TX 78758.

Copyright© 1985 by ASTM International www.astm.org

Brick masonry is one of the oldest forms of building construction and has been in use for thousands of years. In modern practice, masonry is combined with other structural materials, such as steel, concrete, and timber, to form an architectural cladding, and often serves as one of the main load-bearing components in the structural system of a building.

Reinforcing bars, joint reinforcement, wall ties, shelf angles, and other forms of steel are found embedded or in contact with the masonry for various reasons of structural integrity and construction assembly. The steel is subject to corrosion when exposed to air and moisture.

The corrosion of steel in a structure causes a reduction in its cross-sectional area and a corresponding loss of load-carrying capacity. More important, the corrosion products occupy a much greater volume than that of the steel destroyed, as much as three to seven times the volume of the original metal [*1–3*]. Expansion pressures of this magnitude from the steel embedded in masonry will create internal stresses that are much greater than can be resisted by the structural material [*1*]. The corrosion of embedded steel causes unsightly stains, cracking, and even failures of the masonry, which results in millions of dollars of damage per year.

A considerable amount of work has been conducted on various aspects of the corrosion of steel in concrete. However, there has been little research into the corrosion of steel in masonry [*2,4–12*]. Most of this research has been concerned with the durability and effectiveness of different coatings on wall ties and anchors. Generally, the problems encountered because of corrosion of ties and anchors have resulted in loss of serviceability in the form of cracking, leaching, or bulging. Occasionally, masonry walls have collapsed when subjected to high wind load. Rengaswami et al [*10*] reported on extensive damage in reinforced brickwork roofs in India caused by corrosion of the reinforcement, sometimes after exposure periods of only six months. The incidence of corrosion was reported to have been less where the reinforcement was adequately covered with mortar.

The work described herein consisted of a study of the deformation behavior of single wythe masonry wall panels made using Type S mortar containing embedded steel plates subjected to accelerated corrosion. This work reports on the amount of expansion caused by the corrosion of the embedded steel plates in the masonry wall panels and on the amount of corrosion protection provided by the mortar covering the embedded steel plate.

Experimental Program

Materials

The materials used in the construction of the test specimens were representative of those used in actual brick masonry construction. An acid-water solution and impressed current were used to accelerate the corrosion of the steel plates.

- *Bricks*—The bricks used to construct the masonry wall panels were five core jumbo bricks with nominal dimensions of 102 by 102 by 305 mm. The bricks had an average compressive strength of 90.78 MPa with a standard deviation of 5.17 MPa.
- *Sand*—Natural sand was used.
- *Mortar*—Type S portland cement-lime mortar according to Brick Institute of America Standard Specification for Portland Cements—Lime Mortar for Brick Masonry (MI-72) was used.
- *Steel Plates*—Steel plate specimens 6 by 64 by 965 mm and 6 by 64 by 203 mm were cut from ordinary A36 low carbon flat bar stock. A 0.8-mm-diameter hole was drilled and tapped at each end of the plates to provide an electrical connection. The plates were lightly brushed to remove any visible surface rust and were wiped clean using a dry cloth before weighing and embedding in the wall panels.
- *Water Solution*—The acid-water solution consisted of a dilute sulfuric acid solution having a pH of 3.5 ± 0.20. This pH level is in agreement with values reported for acid rain in several U.S. cities such as Pasadena, CA [*13*].

Specimens

The two types of specimens that were tested consisted of masonry wall panels and immersed steel plates.

- *Masonry Wall Panels*—Nine masonry wall panels were built on stainless steel drainage pans seated on rigid level bases. The walls were nine courses in height and had nominal dimensions of 915 by 915 by 102 mm. The walls were

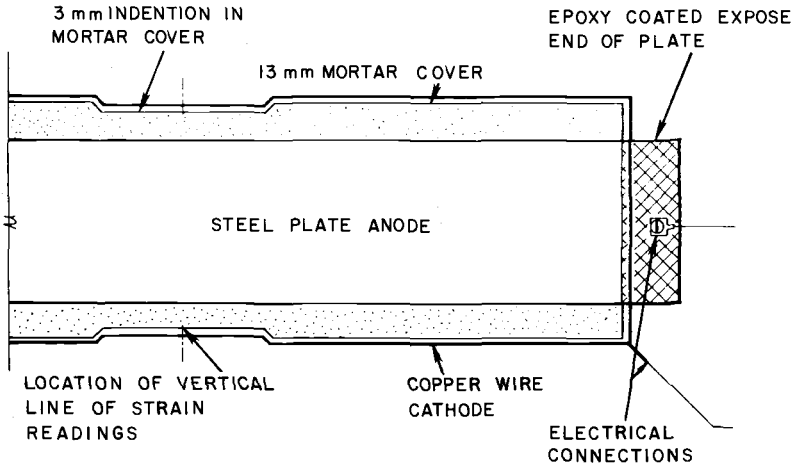


FIG. 1—*Schematic of steel plate embedded in wall panel.*

built by a skilled mason. Steel plates measuring 6 by 64 by 965 mm were embedded in the bed joints at the third and sixth courses to simulate support shelf angles typical of those used in actual structures. The width of the mortar bed joints containing the plates was typically 13 mm, and the other mortar joints were approximately 10 mm thick. A schematic of the steel plates embedded in the wall panels is shown in Fig. 1. As seen in the figure, the steel plates had an average mortar cover of 13 mm from the front and back faces of the wall panels. The mortar joints containing the plates were tooled approximately 3 mm deeper on each face at the locations where vertical strain gage readings were to be made using a demountable mechanical strain gage.

- *Immersed Plates*—Six steel plates 6 by 64 by 203 mm were suspended in 155-mm-deep plastic tubs filled with an acid-water solution flowing at a rate of 0.0009 m^3/min.

Method of Testing

Three of the nine masonry wall panels constructed were placed under a sustained uniform axial compressive stress of 2.76 MPa using the load frame shown in Fig. 2. The other six wall panels remained unloaded and were used to measure the temperature- and moisture-induced strains caused by changes in the room environment and to measure the unrestrained expansions caused by the corrosion of the embedded steel plates. The room temperature where all specimens were kept during testing ranged from 18.5 to 25.5°C, and the relative humidity varied from 35 to 90%. Starting twelve weeks after loading of the specimens, all nine wall specimens were continuously sprayed on the front and back faces with the acid-water solution at a rate of 0.006 m^3/min. At the same time, a similar acid-water solution flowed through the plastic tubs containing the immersed steel plate specimens at a rate of 0.0009 m^3/min. Corrosion was induced in the steel plates by an electrolytic process in which the steel plates constituted the anode; a ten gage solid-strand copper wire tightly wrapped around the mortar joint containing the steel plates was the cathode and the acid-water solution was the electrolyte. For the immersed steel plate specimens, the copper wire was suspended around each steel plate in the acid-water solution. A uniform current density of 646 mA/m^2 was applied to both the embedded and immersed steel plates. Daily adjustment of a variable resistor was necessary to maintain the currents at the specified levels because of the increase in the resistance of the plates as corrosion progressed.

Strain measurements on the wall specimens were made along two vertical lines on both surfaces for the walls at the locations shown in Fig. 3 using a 200- and 50-mm Demec mechanical strain gage. The 50-mm Demec strain gage was used to record deformations immediately across the mortar bed joints while the 200-mm readings spanned two bricks and two mortar joints.

In addition to strain measurements, steel plates were removed from the ma-

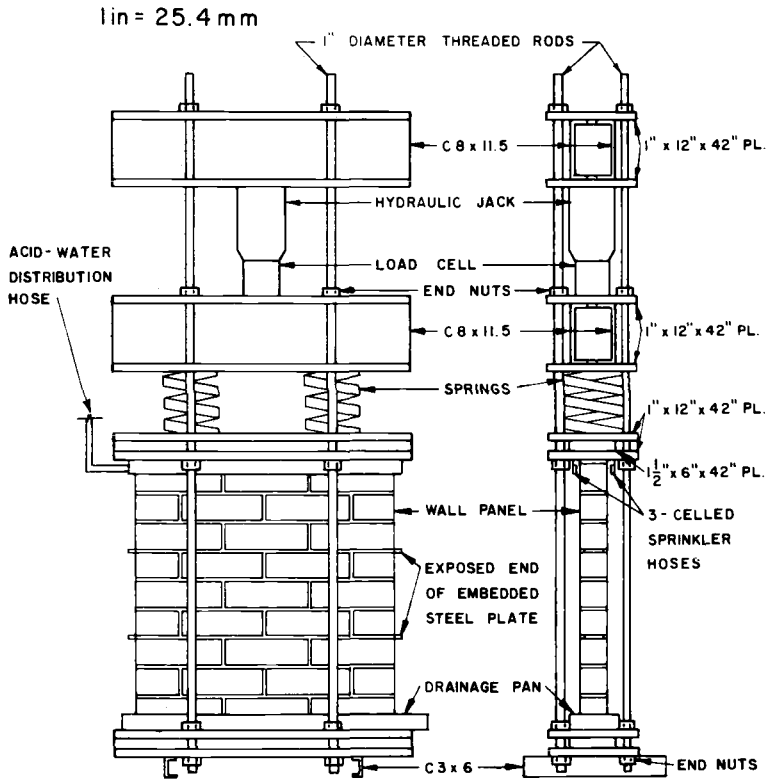


FIG. 2—*Schematic of wall panel in loading frame.*

sonry walls and the plastic tubs at regular time intervals to determine the weight loss and average pit depth caused by corrosion. The steel plates were cleaned using Clarke's solution according to ASTM Recommended Practice for Preparing, Cleaning, and Evaluating Corrosion Test Specimens (G 1). X-ray diffraction analyses of the corrosion products were performed to determine their composition.

Test Results and Discussion

Time-Dependent Deformations

• *Before Acid-Water Exposure*—A sustained load was placed on three of the masonry wall panels seven weeks after construction, and the time-dependent deformations were recorded for the following twelve weeks until start of the acid-water spray. At the same time, temperature and moisture-induced strains were measured from the nonloaded wall panels. The average total strains recorded in the wall panels both loaded and nonloaded are shown in Fig. 4. It is seen in

KEY

A. 20 cm GAUGE LENGTH - PLATE REGION

B. 20 cm GAUGE LENGTH - NO PLATE REGION

C. 5 cm GAUGE LENGTH

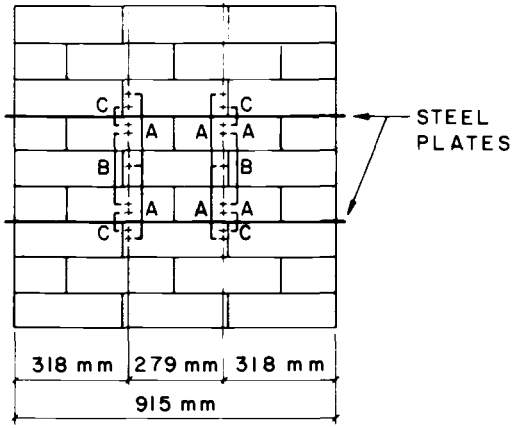


FIG. 3—*Schematic of location of strain readings on wall panels.*

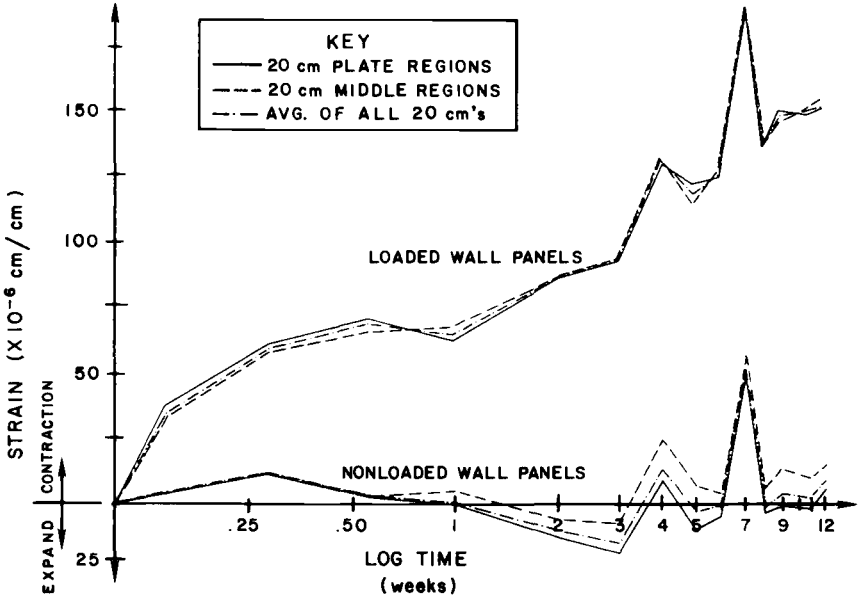


FIG. 4—*Comparison of average creep, temperature, and moisture-induced strains for loaded wall panels to average temperature and moisture-induced strains for nonloaded wall panels.*

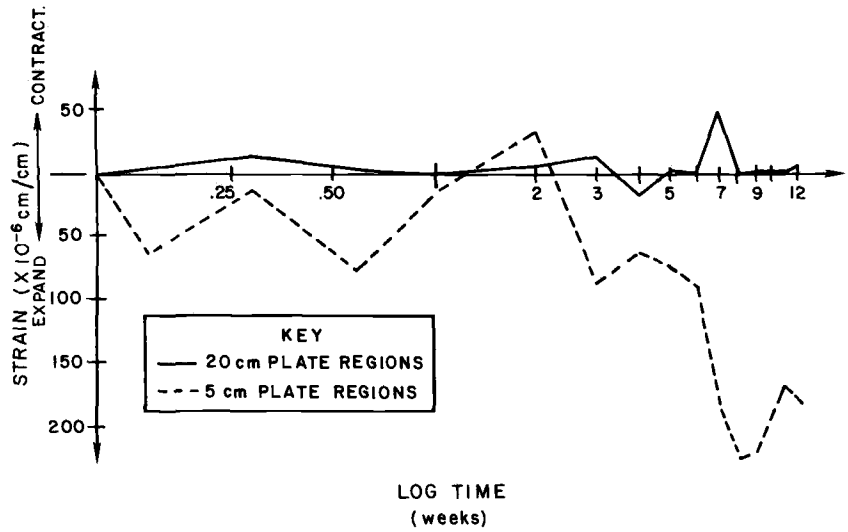


FIG. 5—*Comparison of average temperature and moisture-induced strains for plate regions to local strains at the joints containing the plates before acid-water.*

this figure that the total strains in the plate regions are essentially the same as the total strains in the middle regions that did not contain embedded plates for both loaded and nonloaded wall panels. However, comparing the measured strains on a plate region using the 20-cm strain gage with those measured immediately across the included mortar joint containing an embedded steel plate using the 5-cm strain gage for both loaded and nonloaded, it can be seen that

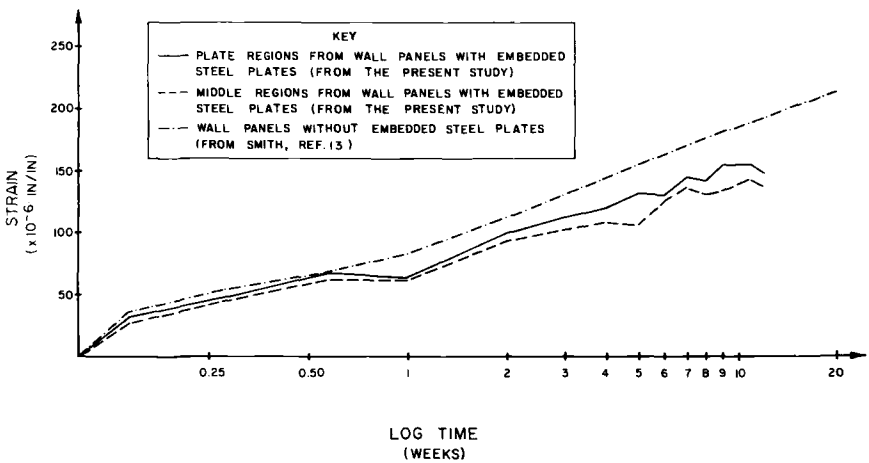


FIG. 6—*Comparison of average creep strains for wall panels with and without embedded steel plates.*

these are significantly different. This is shown in Fig. 5 for the nonloaded walls. This suggests that the local joint strains do not have a significant effect on the overall deformation of both loaded and nonloaded masonry walls. The observed creep behavior in the loaded walls after twelve weeks under load was compared to that reported by Smith [*14*] for the same time period using similar wall panels tested under similar conditions including the same masonry materials, size specimens, sustained load, and temperature. As shown in Fig. 6, after ten weeks under load, the creep strains for the panels tested by Smith containing no embedded steel plate were about 40% higher than the creep strains for the middle region of masonry wall panels from the present investigation. The wall panels that did not contain the steel plates had a strain ratio of 2.57 and the wall panels with the steel plates had a strain ratio of 2.16. This suggests that the presence of embedded plates affect the creep behavior in the masonry at least in the vicinity of the embedded steel plate.

Visual inspection and weight loss measurement on plates removed from nonloaded walls before acid-water exposure at 9 and 19 weeks after construction did not reveal any corrosion.

- *Corrosion-Induced Deformation*—After measuring creep, temperature, and moisture-induced strains for a period of twelve weeks, the wall panels were sprayed with an acid-water solution, and corrosion was electrically induced in the embedded steel plates. At the same time, corrosion was induced in six steel plate specimens immersed in acid-water tubs. The strains in the wall panels caused by expansions resulting from corrosion of the embedded plates were recorded. The maximum average expansion caused by saturation and temperature

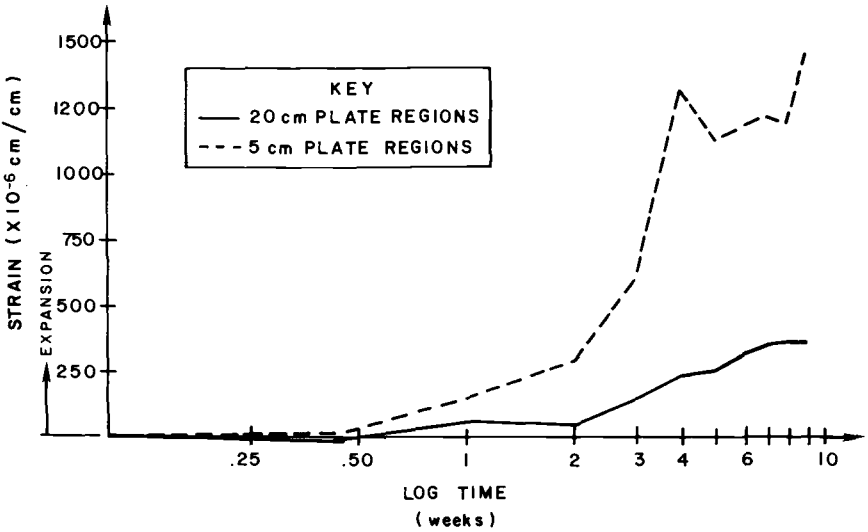


FIG. 7—*Average strains caused by induced corrosion of embedded steel in loaded wall panels.*

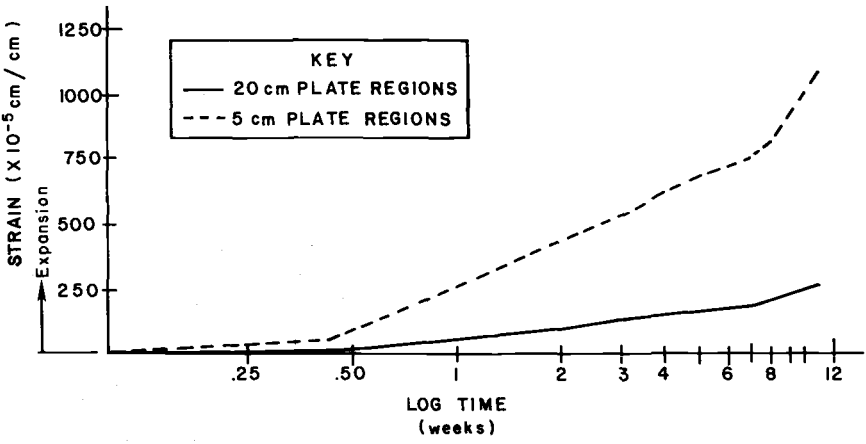


FIG. 8—*Comparison of expansion strains for plate regions and local strains at the embedded plate joint because of corrosion for nonloaded wall panels.*

measured in the nonloaded wall panels over the middle 20-cm region containing no embedded plate was 60×10^{-6} cm/cm.

For both the loaded and nonloaded walls, the corrosion induced strains measured on the plate regions using either the 20- or 5-cm strain gage increased with time at an increasing rate as shown in Fig. 7 for the loaded walls and in Fig. 8 for the nonloaded walls. The average corrosion induced strain recorded at the plate regions after eleven weeks of acid-water spray for the nonloaded walls was 11 130 $\times 10^{-6}$ mm/mm and 2 865 $\times 10^{-6}$ mm/mm for the 5- and 20-cm Demec strain gage readings, respectively. For the loaded walls, the corrosion induced expansions at the plate regions after exposure to acid-water spray for eleven weeks were 1455 $\times 10^{-6}$ mm/mm and 360 $\times 10^{-6}$ mm/mm for the 5- and 20-cm Demec strain gage readings, respectively. The observed expansion was at least several times greater than the expected tensile strain at cracking of brick masonry.

As can be seen from Figs. 7 and 8, the strains of the loaded walls are considerably lower than those of the nonloaded wall panels for the same exposure time. The unrestrained local joint expansions in the nonloaded walls were 6.5 times greater than the local joint expansions in the loaded wall panels, and plate region expansions for the nonloaded panels were seven times greater than the corresponding corrosion expansions in the loaded wall panels. This indicates that a small applied load across the joint helps to reduce the expansion strains caused by corrosion.

Cracks measuring 0.05 to 0.10 mm in width were observed in a nonloaded wall panel after one week of induced corrosion. Crack widths at the brick-mortar interface in the nonloaded wall panels after eleven weeks of acid-water spray were greater than 0.70 mm. Crack widths of the order of 0.20 mm were measured in the loaded wall specimens after nine weeks of acid-water spray.

Time-dependent deformation behavior of the loaded walls tested in this study containing embedded steel plates and exposed to acid-water spray is compared in Fig. 9 to that of similar specimens not exposed to acid-water spray and without embedded steel plates subjected to the same sustained loads. From this figure, it is seen that the corrosion induced expansion is 1.9 times greater in magnitude than the creep strains of the wall panels with no embedded plates after eight weeks under sustained loading. In fact, after eight weeks of exposure time, a net expansion occurred in specimens containing embedded steel plates while shrinkage strains occurred in the specimens containing no steel plate even though both type specimens were subjected to sustained loading.

For any exposure time, the immersed plate specimens had a greater weight loss caused by corrosion than the embedded steel plates in the masonry wall panels. In general, the loaded wall panel plate specimens had less weight loss than those in the nonloaded wall panels for the same exposure time. This indicates that because of the applied sustained load, the expansions caused by corrosion of the embedded plate and the initiation and opening of cracks at the brick-mortar interface decreased.

A correlation between the weight loss of the embedded plates and the expansion strains for the loaded and nonloaded wall panel specimens is shown in Fig. 10. It is seen in this figure that the expansion strains of the nonloaded walls increased

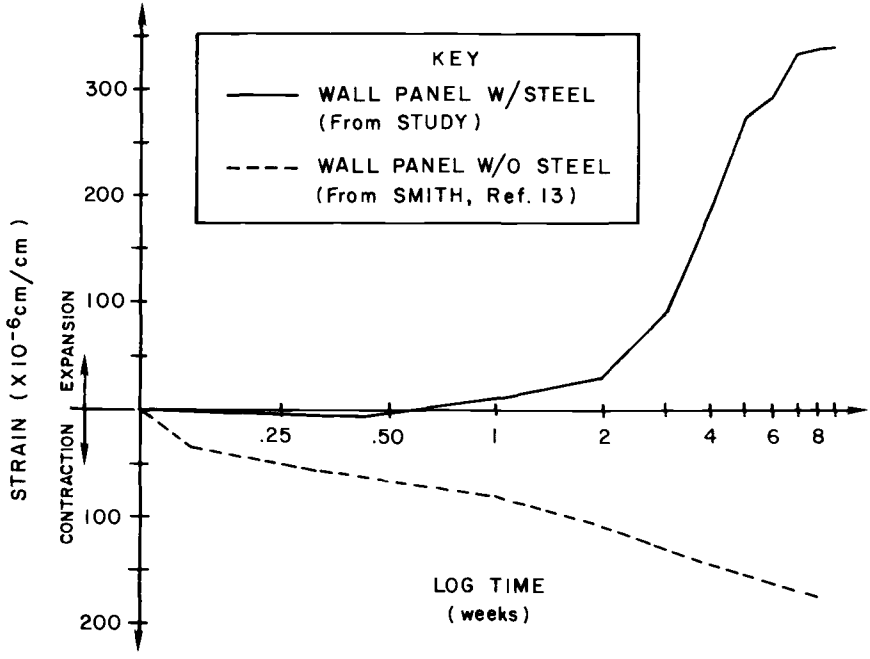


FIG. 9—*Comparison of corrosion expansions from loaded wall panels without embedded steel plates.*

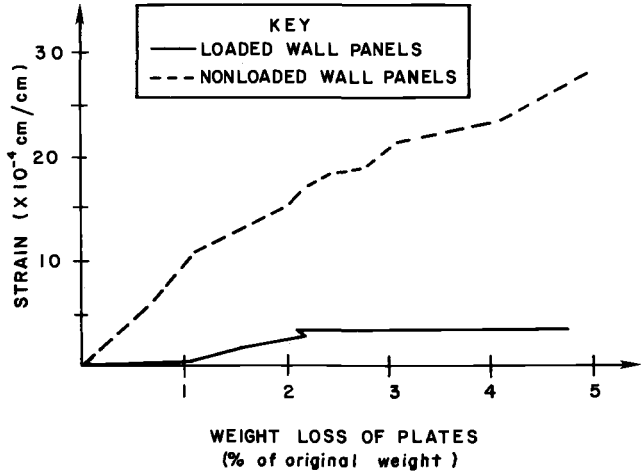


FIG. 10—*Comparison of weight loss of embedded plates to measured expansion strains caused by corrosion of embedded plates.*

proportionally to the amount of weight loss of the plate specimens. However, this behavior was not similar to that observed in the plates from the loaded walls. For the plates in the loaded wall panels, a similar weight loss as that of the plates in the nonloaded walls occurred at a much smaller strain in the masonry. This is another indication that the applied load resists the expansions caused by corrosion; however, it does not significantly affect the amount of weight loss in the embedded plates and consequently the load carrying capacity of the embedded plate.

The corrosion products that were removed from the plate specimens were examined under an electron microscope and were found to contain iron and small amounts of sulfur, chlorine, chromium, and manganese. The X-ray diffraction analysis of the corrosion products indicated that the corrosion principally consisted of magnetite with smaller amounts of goethite and lepidocrocite.

Conclusions

The following conclusions are based on the experimental work described herein:

1. Before start of corrosion at time of acid-water exposure, the effect of the embedded steel plates on the overall total deformation behavior with time for both loaded and nonloaded walls is negligible.
2. Corrosion induced strains caused by corrosion of embedded steel plates in brick masonry could result in cracking of the masonry leading to serviceability and aesthetic problems.
3. Corrosion induced strains are greater in nonloaded wall panels than in loaded wall panels.

4. Corrosion of embedded plates in brick masonry could result in an expansion behavior of the brick masonry with time even for walls under sustained loads.

5. In general, the weight loss of plates embedded in nonloaded walls was slightly greater than that of the plates from the loaded walls for similar exposure times.

6. For the same exposure conditions and exposure time, crack widths caused by corrosion of embedded plates in masonry are much greater for nonloaded walls than for loaded walls.

7. Weight loss prediction of plates embedded in loaded walls based on observations made on measured weight losses of plates embedded in nonloaded walls under similar exposure conditions could be very misleading.

8. The presence of embedded steel plates results in a decrease in the measured creep strain in the masonry at least in the vicinity of the embedded plate.

References

[1] *Corrosion in Action*, 6th ed., International Nickel Company, Inc., New York, 1977, 44 pp.

[2] Moore, J. F. A., *The Performance of Cavity Wall Ties*, Building Research Establishment, Garston, Great Britain, April 1981.

[3] Beeby, A. W., "Cracking, Cover, and Corrosion of Reinforcement," presented at the 1981 Annual Convention, American Concrete Institute, Dallas, TX. 9-13 Feb. 1981, pp. 1–13.

[4] Brown, B., "Leaky Walls Endanger Steel Buildings," *Engineering News Record*, 8 Dec. 1949, pp. 42–43.

[5] De VeKey, R. C., *Corrosion of Steel Wall Ties: Recognition, Assessment, and Appropriate Action*, Building Research Establishment Information Paper, IP 28/79, Garston, Great Britain, Oct. 1979.

[6] Fearnside, P. P., "Rust Wreaks Havoc in Cavity Brickwork," *Illustrated Carpenter and Builder*, 7 Dec. 1962, pp. 3904–3905.

[7] Fishburn, C. C., *Strength and Resistance to Corrosion of Ties for Cavity Walls*, Building Materials and Structures Report BMS 101, National Bureau of Standards, Washington, DC, 1 July 1943.

[8] Foster, D. and Thomas, A., "Some Interim Comments on the Corrosion of Reinforcement in Brickwork," *Proceedings of the British Ceramic Society*, No. 24, Sept. 1975, pp. 197–222.

[9] Kaminetzky, D., "Corrosion Problems in Structural Systems," *Corrosion and the Building Industry*, National Bureau of Standards, Gaithersburg, MD, 17 May 1977, pp. 1–24.

[10] Rangaswami, N. S., Balasuramangam, T. M., Venkataraman, H. S., and Rajagopalan, K. S., "Corrosion of Reinforcement in Reinforced Concrete and Reinforced Brickwork," *Indian Concrete Journal*, Vol. 38, No. 6, June 1964, pp. 233–237.

[11] Roberts, J. J., "The Development of a Technique for Investigating the Durability of Reinforcing Steel in Reinforced Concrete Blockwork," *Proceedings of the North American Masonry Conference*, University of Colorado, Boulder, CO, Aug. 1978, pp. 2.2–2.16.

[12] Roberts, J. J., *The Development of an Electrical-Resistance Technique for Assessing the Durability of Reinforcing Steel in Reinforced Concrete Blockwork*, Cement and Concrete Association, London, Technical Report 532, May 1980.

[13] Liljestrand, H. H. and Morgan, J. J., "Chemical Composition of Acid Precipitation in Pasadena, California," *Environmental Science and Technology*, Vol. 12, No. 12, Nov. 1978, pp. 1271–1273.

[14] Smith, D. A., "Creep, Shrinkage, and Physical Properties of Masonry Using Type S Mortar and High Strength Latex Mortar," Master's thesis, The University of Texas at Austin, Austin, TX, May 1981.

Tests for Corrosion Type

Robert M. Kain[1] *and Thad S. Lee*[1]

Recent Developments in Test Methods for Investigating Crevice Corrosion

REFERENCE: Kain, R. M. and Lee, T. S., **"Recent Developments in Test Methods for Investigating Crevice Corrosion,"** *Laboratory Corrosion Tests and Standards, ASTM STP 866,* G. S. Haynes and R. Baboian, American Society for Testing and Materials, Philadelphia, 1985, pp. 299–323

ABSTRACT: The ultimate successful utilization of stainless steels and related alloys in marine and other chloride containing environments will depend on a more complete understanding of the factors affecting crevice corrosion. To this end, numerous test methods have been devised to investigate the effects of various metallurgical and environmental parameters. While not totally ignored in past research, more recent investigations have also emphasized the importance of crevice geometry considerations. For example, mathematical modelling of chemistry changes in the crevice electrolyte indicates a strong dependency on crevice gap and crevice depth dimensions. In addition, the bulk environment chloride level will affect the ultimate crevice electrolyte pH and chloride level. Accordingly, a given stainless steel may encounter a range of crevice solutions of varying pH and chloride level dependent upon the crevice geometry and bulk environment conditions encountered.

Two experimental approaches for studying crevice corrosion are presented. A remote crevice assembly and a compartmentalized cell have been used to study both the initiation and propagation phases of crevice corrosion. Both methods make use of two specimen components consisting of physically separated but electrically connected anodes (crevice portion) and cathode members. Accordingly, corrosion potential and current data along with conventional mass loss and penetration data can be gathered. A significant feature of these methods is that neither requires the application of current from an external source. Both initiation and propagation of crevice corrosion occur spontaneously. The two techniques differ slightly in that the remote crevice assembly requires creation of a physical crevice on the anode while the compartmentalized cell approach uses a nonoccluded anode in a simulated crevice electrolyte. With the compartmentalized cell, crevice electrolytes are simulated based on the predictions of a mathematical model of crevice corrosion.

Results from recent tests investigating the effects of variations in crevice tightness, bulk solution composition, and crevice solution pH are described in the present article. Remote crevice assembly research has focused on efforts to provide a consistent and reproducible condition of crevice tightness on the anode. The compartmentalized cell research has dealt with the effects of changes in both bulk environment conditions and crevice solution pH. Insights gained on the relative influence of these various factors on crevice corrosion lend credence to the testing concepts embodied by both the remote crevice assembly and the compartmentalized cell.

KEY WORDS: seawater, stainless steels, crevice corrosion test methods, multiple crevice assembly, remote crevice assembly, compartmentalized cell, mathematical modelling,

[1] Corrosion scientist and vice-president of research and engineering, respectively, LaQue Center for Corrosion Technology, Inc., P. O. Box 656, Wrightsville Beach, NC 28480.

Copyright© 1985 by ASTM International www.astm.org

crevice geometry, crevice solution chemistry, natural seawater, synthetic seawater, crevice corrosion initiation, crevice corrosion propagation, temperature effects

The phenomenon of crevice corrosion has been investigated by many researchers using a variety of methodologies. The test techniques have ranged from actual immersion tests in the specific environment of interest to accelerated tests using synthetic environments or electrochemical stimulation or both. The objective of these tests has ranged from determining mechanisms to evaluating relative alloy performance.

One area of crevice corrosion research that has received a considerable degree of attention involves the performance of stainless steels in chloride environments. Since the major chloride-containing environment is the world's oceans, much of this research has been specifically oriented to characterizing crevice corrosion behavior in seawater. Several approaches to these characterizations have been taken. It is the intent of this paper to review some of the approaches applied in seawater and to discuss two recent experimental developments in some detail.

Mathematical Modelling

Perhaps the most significant accomplishment in the understanding of crevice corrosion in recent years is the development of a mathematical model of the phenomenon. The Oldfield and Sutton model [*1*,*2*] is based on the widely accepted four stage mechanism of crevice corrosion [*3*] as summarized in Fig. 1.

The model has a series of inputs that allow predictions of initiation behavior of various stainless steels:

(1) oxygen content of the bulk solutions,
(2) crevice geometry, that is, gap and depth,
(3) passive current,
(4) bulk solution pH and chloride content,
(5) chemical hydrolysis equilibria,
(6) alloy composition, and
(7) critical crevice solution composition.

With these inputs the model can predict:

(1) time required to deplete oxygen in the crevice,
(2) pH of the crevice solution and composition of the solution as a function of time, and
(3) the time required to "breakdown" of the passive film and initiation of crevice corrosion.

The theoretical factors and assumptions and the interrelation of the above inputs have been described in detail by Oldfield and Sutton. Of these inputs, 1, 4, and

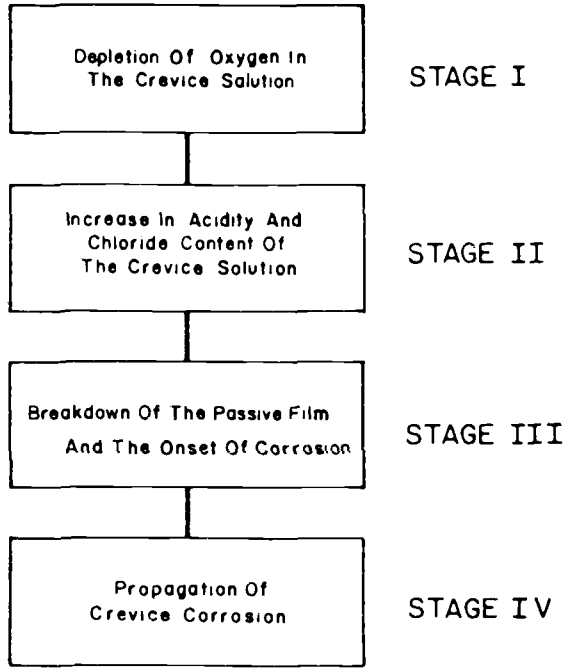


FIG. 1—*Generally accepted four stage mechanism for crevice corrosion.*

6 represent known factors for a given situation. Factor 5 represents a theoretical input, and Factor 2 represents a variable (somewhat unmeasurable, as will be discussed later), which is assumed. Factors 3 and 7 represent experimental inputs that are determined electrochemically using the methods described by Oldfield and Sutton [2].

Recent extensions [*4–7*] of the model to incorporate the propagation stage of crevice corrosion have further enhanced the utility of this approach. The propagation model considers crevice corrosion propagation in terms of an electrochemical cell with an anode, the actively dissolving alloy within the crevice, and a cathode, usually sustaining oxygen reduction outside the crevice or hydrogen evolution within the crevice or both. This model has shown the importance of additional parameters such as the corrosion cell voltage and the electrochemical response of an alloy in acid-chloride solutions on crevice corrosion behavior of stainless steels.

The overall model of crevice corrosion presents a vehicle for an organized assessment of the effect of various factors on crevice corrosion of stainless steels in aqueous chloride environments. Environmental, metallurgical, electrochemical, and geometric factors can be considered for their relative influence on the crevice corrosion process. Ultimately, this provides a guideline for both the development of relevant experimental data from laboratory crevice corrosion

research as well as a basis for optimizing the application of materials where crevice corrosion could otherwise limit their utility.

Multiple Crevice Assembly

This device was originally developed by Anderson [*8*] for the purpose of providing a convenient and economical means of screening relative alloy performance in natural seawater. It consists of two serrated washers each with a series of plateaus such that 20 separate crevice sites are created beneath each washer. Two such washers when attached with a nut and bolt to a test specimen, create 40 individual crevice sites.

Initially, a probability concept was used to describe initiation and propagation behavior since the phenomena appeared random in their occurrence. The data were thus presented as a probability that a given material would be susceptible. However, the previously described development of a model of crevice corrosion helped to identify a number of factors that would affect the occurrence of crevice corrosion. The modelling showed that experimental factors, such as reproducibility of the crevice geometry, could be as important as metallurgical variables in accounting for the observed crevice corrosion behavior of a given stainless steel. As such, the probability concept was abandoned since it implied a material property, when in reality it more likely represented the probability that a given crevice site was sufficiently severe to initiate crevice corrosion.

The multiple crevice assembly has been frequently used to evaluate material behavior in seawater as well as in other chloride-containing environments [*9–13*]. Many of the test programs have resulted in some variability between seemingly replicate tests. This can be attributed to many factors including the lack of reproducible crevice geometries which is inherent with other crevice formers as well. However, the data generally do provide a consistent picture in assessing cause and effects in the crevice corrosion process.

A recent analysis [*14*] of multiple crevice assembly data revealed some interesting insights on effects of alloy additions to stainless steels. However, this analysis also promoted an oversimplification of the process by the advocacy of an arbitrary "crevice corrosion index." This index treats the initiation and propagation phases as being equally affected by the same factors when many researchers have clearly indicated that the two phases should be treated separately [*4,15,16*]. Additionally, the basic data used to establish the index do not consistently show a direct dependent relationship between the chosen initiation and propagation parameters with several alloys not fitting the arbitrary relationship.

A more theoretically credible approach is to treat initiation and propagation separately as independent phenomena. Evaluating alloy performance based on initiation and propagation separately was the subject of an analysis of multiple crevice assembly data by the authors [*16*]. This approach is more practical in that a designer or engineer can select an alloy that may be subject to crevice corrosion initiation under certain conditions but for which an acceptably low

degree of propagation will exist. The index approach allows no such delineation of behavior and literally forces an engineer into a go or no-go decision on materials selection.

Experimental Procedure

While the preceding methodologies have provided significant utility in the study of localized corrosion, each has its own limitations. The application of additional test concepts that resolve some of these limitations has been the subject of recent research at the LaQue Center for Corrosion Technology, Inc. Two test techniques have been developed and are continuing to be refined and expanded in their application. The following describes some recent uses of these two methods: the remote crevice assembly and the compartmentalized cell.

Remote Crevice Assembly

General—By separating the crevice area from the larger boldly exposed surface, the remote crevice assembly method [*17*] enables measurement (through a zero resistance ammeter) of any current between a large boldly exposed cathode member and the smaller shielded anode (crevice member). This offers the advantages of electrochemical data collection with the uncertainties of electrochemical stimulation employed by various applied current test methods. The potential of the coupled members as well as other corrosion data can also be monitored.

The primary advantage of this method is its ability to clearly identify initiation and subsequent propagation. The current measurements at any time provide an indication of the instantaneous rate of crevice corrosion propagation. Since previous work [*17*] has shown good correlations between the corrosion rates determined from the total current and mass loss, these instantaneous measurements are accurate reflectors of ongoing propagation rates.

Procedure—The continued use of the remote crevice assembly concept has evolved variations in the method of forming and controlling the geometry of the crevice. In one case, the crevice member is positioned between two acrylic blocks to which plastic tape has been applied [*18*]. The tape provides a deformable cushion to help enhance crevice tightness. A torque wrench is used when tightening the constraining bolt to provide some degree of consistency from one assembly to another. All of the tests described in the present paper utilized an assembly torque of 2.8 Nm (25 in·lb). For the most part, a nominal crevice area of 4.5 cm^2 (cathode:anode area ratio ~ 37:1) was used. Surfaces of the anode members were wet ground with 120-grit silicon carbide paper before cleaning (pumice scrub, water rinse, and acetone degrease) and weighing. Depending on test objectives, cathode members were either ground or left in their respective mill finish. Drilled holes in the stem of both anode and cathode members allowed electrical connections to be made above the waterline.

As described previously [*17*] waterline attack may be a problem for some

TABLE 1—*Summary of environments used in remote crevice assembly and compartmentalized cell tests.*

Remote Crevice Assembly 30 ± 2°C	Compartmentalized Cell, 25 ± 2°C
Nonmarine	*bulk environment* (cathode)
1 000-mg/L Cl^- at pH = 3 and pH = 6	natural (filtered) seawater, dissolved oxygen varied
10 000-mg/L Cl^- at pH = 3 and pH = 6	*simulated crevice solutions*
15 000-mg/L Cl^- at pH = 3 (above prepared with NaCl and HCl)	synthetic seawater
3.5% NaCl (neutral)	(0.5*M* Cl^-) + 3.5*M* Cl^-
Marine	(0.5*M* Cl^-) + 4.0*M* Cl^-
natural (filtered) seawater	(0.5*M* Cl^-) + 4.5*M* Cl^-
19 000-mg/L Cl^-	(0.5*M* Cl^-) + 5.5*M* Cl^-
35 000-mg/L TDS (salinity)[a]	(above prepared with NaCl and HCl)
pH = 8, dissolved oxygen, 80% saturation	
synthetic seawater [2]	

[a]TDS is total dissolved solids.

alloy/environment combinations. Periodic cleaning of the waterline area by simple swabbing with the bulk environment has been moderately successful. Additional improvement in this regard is necessary, particularly for tests involving less resistant materials.

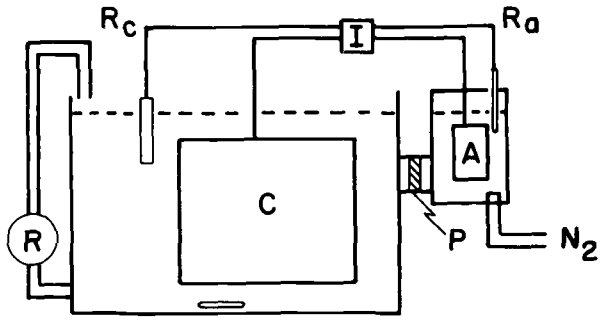
To further study the influence of crevice geometry control, an air operated crevice loading device has been constructed in which regulated air pressure is used to replace the load screw used previously. Loading was applied at a level of 69 000 Pa (~10 psi) to wetted anode members.

Environments—Results are presented for tests conducted in a variety of natural and synthetic solutions. In addition to natural and synthetic seawater, other chloride containing environments, which have been used, are given in Table 1. All remote crevice tests described in the present paper were conducted at a controlled temperature of 30 ± 2°C, and low velocity conditions (<0.01 m/s) prevailed. Except for the natural seawater tests that were continuously refreshed, all other tests were closed loop.

Compartmentalized Cell Test

General—Compartmentalized cell methodologies have been previously used to investigate general and localized corrosion [*19–21*]. The present cell design, as shown in Fig. 2, has been used to study the effects of differences in cathode and anode electrolyte compositions on propagation and cessation of crevice corrosion. The technique is similar to the remote crevice assembly tests in that the respective members are again physically separated but electrically connected. The anode and cathode compartments are separated by an agar gel prepared with the crevice solution and held in place between two fritted glass disks.

The anode member is exposed without a crevice former in a predetermined crevice solution. As reported elsewhere [*21*] selection of the crevice solution



COMPARTMENTALIZED CELL

A=Anode Cell
C=Cathode Cell
Ra,Rc=Reference Electrodes
P=Cell Partition
I=Instrumentation
R=Recirculation Pump/Reservoir

FIG. 2—*Schematic identifying various components of the compartmentalized cell apparatus.*

concentrations is based on mathematical modelling predictions for specific inputs of alloy composition, bulk environment and known, but frequently uncontrollable, crevice geometries. One of the primary advantages of this method is that the time factor for development of a critical crevice solution (CCS) is eliminated. Second, it allows for characterization of the polarization behavior of cathode and anode member under purely spontaneous conditions, that is, without the application of external current.

Procedure—Specimen configuration and preparation were typical of those described for remote crevice assembly tests. However, the exposed area (~10 cm^2) for anode members, which include wetted portions of the stem as well as edges, were larger. The exposed surface area of the cathodes was ~170 cm^2. Each cell contained two specimens of the respective size. After a 1-h exposure under freely corroding conditions in the bulk environment and simulated crevice solution, one set of cathode and anode members were coupled through a zero resistance ammeter. The remaining uncoupled "cathode" and "anode" members served as freely corroding control specimens. Potential data were also collected via reference electrode connections in both environments. Potentials measured for the coupled "cathode" member in the bulk environment are analogous to potentials measured for the remote crevice assembly or any other crevice bearing specimen. Conventional mass loss data determined at the conclusion of the test

were compared with the electrochemical data. The results described herein are from short-term 24-h exposures.

Environments—Natural seawater was used as the cathode, or bulk, environment in the present study. Crevice solutions were prepared by the addition of sodium chloride and hydrochloric acid to a stock solution of synthetic seawater yielding the concentrations shown in Table 1.

Effects of bulk oxygen environment concentration, achieved by purging with various gas mixtures, and crevice solution pH at ambient temperatures (25 ± 2°C) were examined.

Results and Discussion

Remote Crevice Assembly Experiments

Alloy Resistance in Nonmarine Environments: Effects of Alloying and Environment—Remote crevice assembly tests were conducted to determine the propagation resistance of a number of stainless steels in nonmarine environments. In one such study [*18*], several austenitic and ferritic stainless steels were exposed to a 10 000-mg/L chloride, pH = 6 solution at 30°C. Although the 18Cr-2Mo material exhibited some increase in resistance to initiation over Type 316, an order of magnitude improvement in progagation resistance was measured for the Type 316 stainless steel. Similar results were shown for comparisons between Type 304 and Type 430 stainless steels. In addition, both classes of materials show an order of magnitude beneficial effect of molybdenum when considering the overall extent of crevice corrosion. However, significant differences in actual penetration (average depth measurements) were not detected between molybdenum-free and molybdenum-containing materials.

Additional studies, as indicated by the results given in Table 2, describe the effects of variation in bulk environment pH and chloride content on the behavior of Type 316 stainless steel. Type 316 initiated within 24 h upon exposure to a 10 000-mg/L Cl^- solution of pH = 6. Similar behavior was noted at pH = 3. Decreasing the chloride level to 1000 mg/L resulted in longer times to initiation at pH = 3 and no initiation at pH = 6 within 40 days.

For Type 316 in the high chloride solution, changes in the bulk environment pH from 6 to 3 resulted in an order of magnitude increase in overall propagation. Again, however, this effect is not as strongly evident from the average depth of penetration data. Considering differences in initiation times, the instantaneous propagation rate in the low chloride, pH = 3 solution approached that observed in the corresponding high chloride solution.

Crevice Corrosion Propagation Resistance of High Alloy Materials—The crevice corrosion propagation resistance of a number of high alloy materials identified in Table 3 has been determined. In this series of tests, remote crevice assemblies were exposed to a 15 000-mg/L chloride, pH = 3 solution at 30°C. Except for Alloy 254SMO, duplicate specimens of the other six alloys corroded during the

TABLE 2—*Effect of bulk environment chloride and pH levels on crevice corrosion resistance of Type 316 stainless steel.*

Test Environment		Initiation	Maximum Anode	Potential at	Total	Mass Loss	Average Penetration	Affected Crevice
Cl^-, mg/L	pH	Time, h	Current, A	I_{max}, V	Charge, C	Gravimetric, g	Depth, mm	Area, cm^2
1 000	6	>960	0.89×10^{-6}	+0.021	1	0.0010	0	0
10 000	6	24	5.12×10^{-6}	−0.199	10	0.0050	0.02	0.23
1 000	3	144 to 168	1.81×10^{-5}	−0.072	36	0.0057	0.06	0.34
10 000	3	24	7.7×10^{-5}	−0.143	118	0.0262	0.04	1.20

TABLE 3—*Summary of results describing relative alloy ranking in acid-chloride solution.*

Alloy	Total Charge, C	Current, A × 10^{-5}	Current Density, A/cm^2 × 10^{-5}	Penetration Depth, mm
254SMO			did not initiate	
G	27	2.1	1.7	0.03
904L	48	3.7	4.5	0.05
317L+	73	6.2	8.4	0.15
Type 316	87	7.7	18	0.37
Type 317	90	7.8	6.0	0.11
28Cr-4Ni-2MO	115	9.0	7.1	0.48
26Cr-1Mo	147	11.5	19.8	0.34

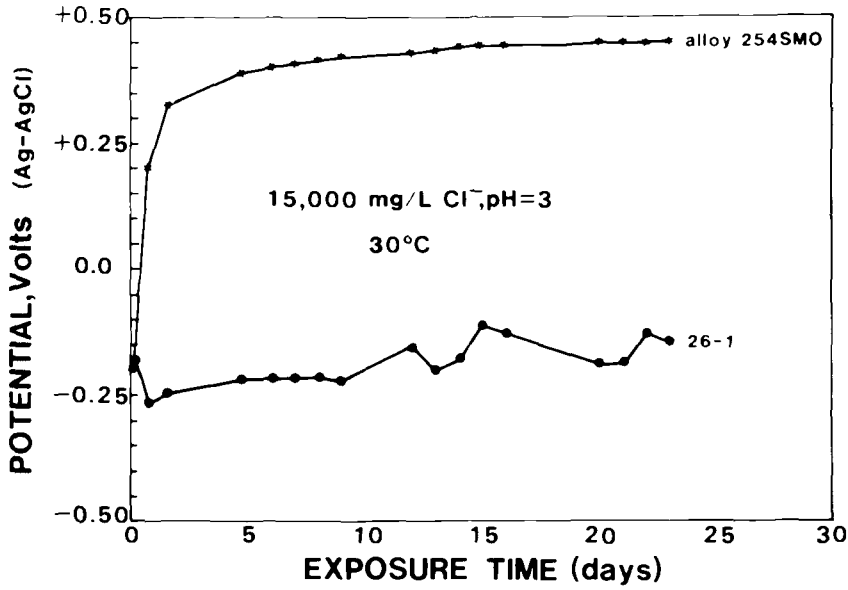


FIG. 3—*Variation in remote crevice assembly potentials for two different alloys: alloy 254SMO was resistant, while 26Cr-1Mo alloy initiated within 1 day in the 23-day test.*

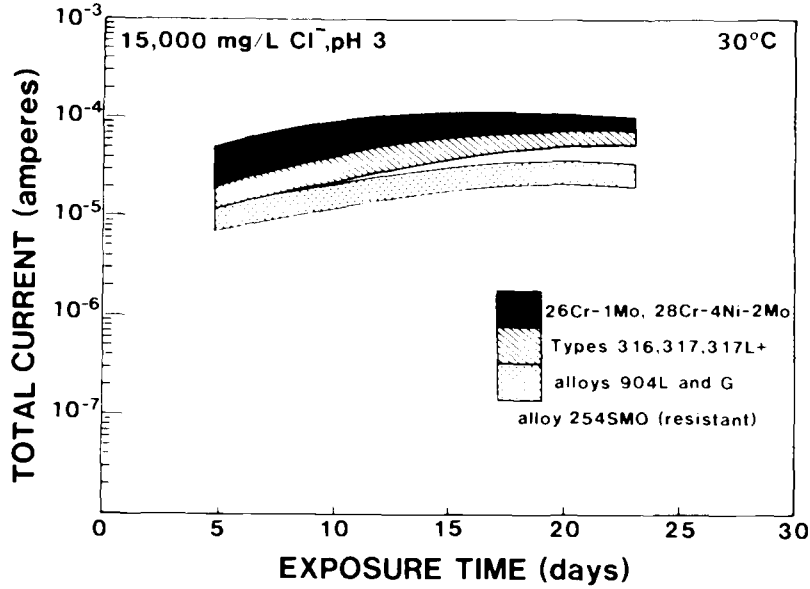


FIG. 4—*Relative current levels for various classes of materials during propagation stage of crevice corrosion.*

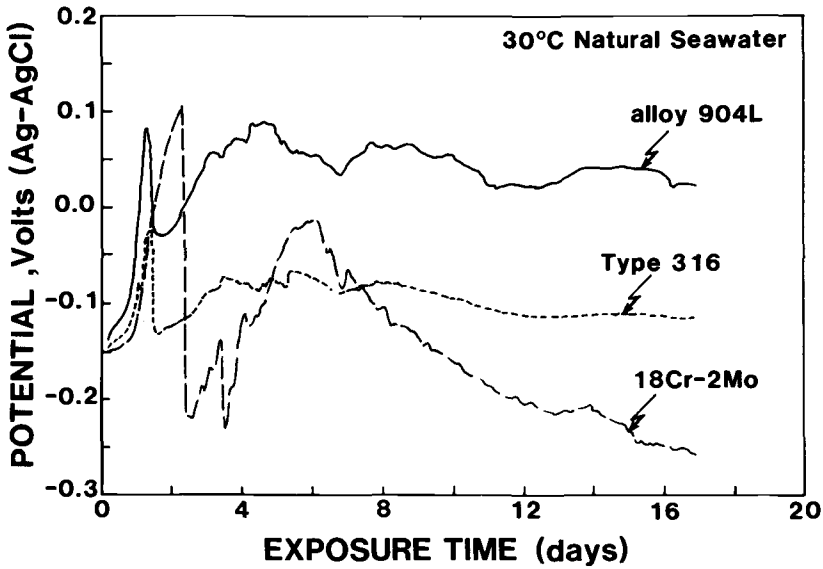


FIG. 5—*Differences in corrosion potentials for remote crevice assemblies for three different stainless alloys in natural seawater.*

23-day test period. Although most alloys initiated within one to two days, somewhat longer times were required for Alloy G (5 to 8 days). In the case of Alloy 26-1, one specimen clearly initiated within 1 day, while a duplicate specimen did not exhibit sustained propagation until about day 17.

Data shown in Fig. 3, for one of the two resistant 254SMO specimens, describe very noble potentials. Conversely, data for the rapidly initiated Alloy 26-1 specimen describe more active potentials. For the most part, potentials exhibited by the other materials were between these two examples. Figure 4 compares the relative current levels for the various classes of materials once propagation was established. Overall propagation behavior based on the maximum current and maximum total charge and the average total charge for duplicate specimens provides the same ranking of materials. A somewhat different ranking can be established by comparisons of the maximum penetration (physical measurement) and maximum current density at the end of the test (I/affected area).

Natural Versus Synthetic Environments—Testing in natural or proposed service environments has long been recognized as the preferred method for determining an alloy's resistance to corrosion. Frequently, however, it is expedient to use synthetic media for initial screening purposes. In the present series of remote crevice assembly tests, the behavior of three stainless alloys of varied composition is compared in natural and synthetic seawater and 3.5% sodium chloride solution at 30°C.

Figure 5 compares typical corrosion potential data obtained for Type 316, Alloy 18-2 and Alloy 904L in low-velocity filtered seawater. In each case, the

onset of crevice corrosion is illustrated by a decrease (more active) in potential. As will be discussed, this was accompanied by a sharp increase in current, which occurred after one to two days exposure. By the end of the 400-h test, substantial differences in the corrosion potential of the three materials are quite apparent.

Data for currents measured in the above natural seawater tests are shown along with similar data for 800-h tests conducted in synthetic seawater and the 3.5% sodium chloride solution in Figs. 6 through 8. While the initiation response for Type 316 was about the same in both the natural and synthetic environments, Alloy 18-2 and especially Alloy 904L exhibited greater resistance in the synthetic environments.

The overall propagation resistance can be expressed in terms of the total charge for the various alloy/environment combinations. The results from the seawater tests show similar charge values for Type 316 and Alloy 904L while those for Alloy 18-2 are nearly doubled. While differences in initiation times would certainly affect the total charge for a fixed duration test, comparison as a function of bulk environment can be made in at least two specific cases. For example, total current and total charge values (after 400 h testing) for Type 316 in natural seawater are an order of magnitude greater than those determined in synthetic seawater and 3.5% sodium chloride. Similar, if not greater, differences are evident from data for Alloy 904L in natural seawater and 3.5% sodium chloride.

It is perhaps of interest to note that once the propagation stage of crevice corrosion was established, the relative ranking (total charge) of the three alloys was nominally the same in all three environments. The similarity in behavior

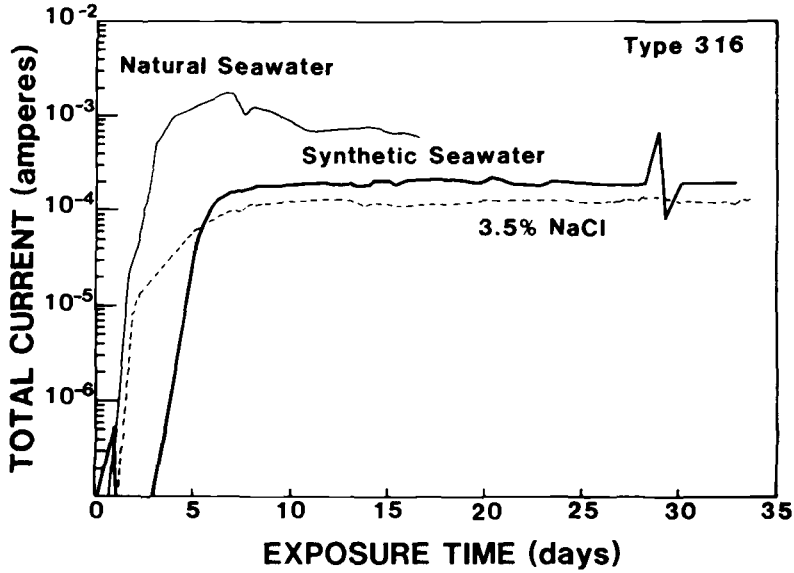


FIG. 6—*Variation in current measurements for remote crevice assemblies of Type 316 stainless steel exposed in natural and synthetic environments.*

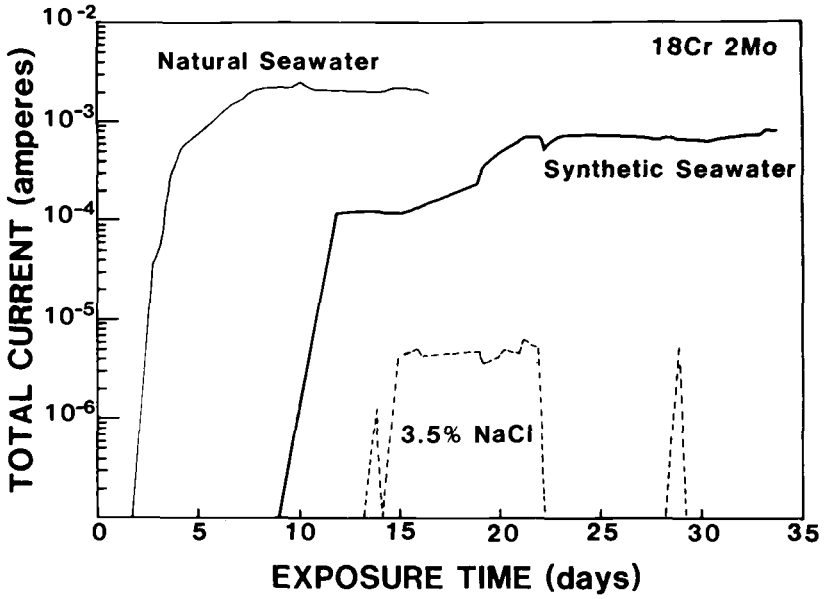


FIG. 7—*Variation in current measurements for remote crevice assemblies of 18Cr-2Mo stainless alloy exposed in natural and synthetic environments.*

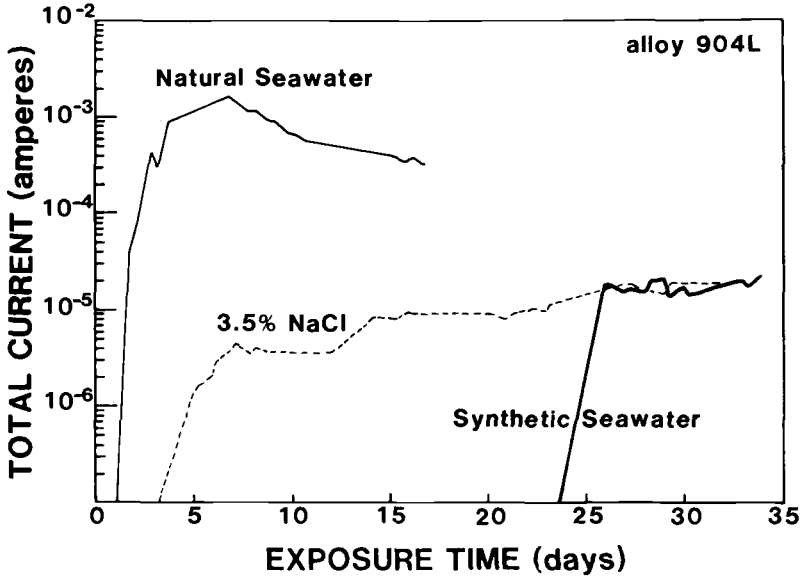


FIG. 8—*Variation in current measurements for remote crevice assemblies of Alloy 904L exposed in natural and synthetic environments.*

for Type 316 and Alloy 904L in the above seawater test is consistent with seawater test results reported by Hack [*11*]. On the other hand, the apparent improved resistance of the higher Alloy 904L in the synthetic environment is consistent with that previously shown in Fig. 4.

Monitoring the Effects of Environmental Variables—One of the more attractive features of the remote crevice assembly technique is that it enables measurement of changes in the rate of crevice corrosion propagation during the course of testing. This is extremely useful, for example, in establishing any effect of changes in the bulk environment on continued propagation or cessation of crevice corrosion.

It has been shown [*17,22*] that crevice corrosion tests in seawater at 50°C and higher, for example, 70°C, have resulted in substantially less attack than that observed in tests at lower temperatures, that is, ambient or controlled at 25 to 35°C. These differences, which are generally an order of magnitude or more, have been detected in tests using a variety of crevice formers on both sheet and tube material.

Figure 9 shows results for tests with continuously refreshed/recirculated natural seawater in which temperature was varied after initiation, and sustained propagation was established. The solid graph shows data collected for one of two Alloy 904L specimens initially exposed to seawater at 30°C. As evidenced

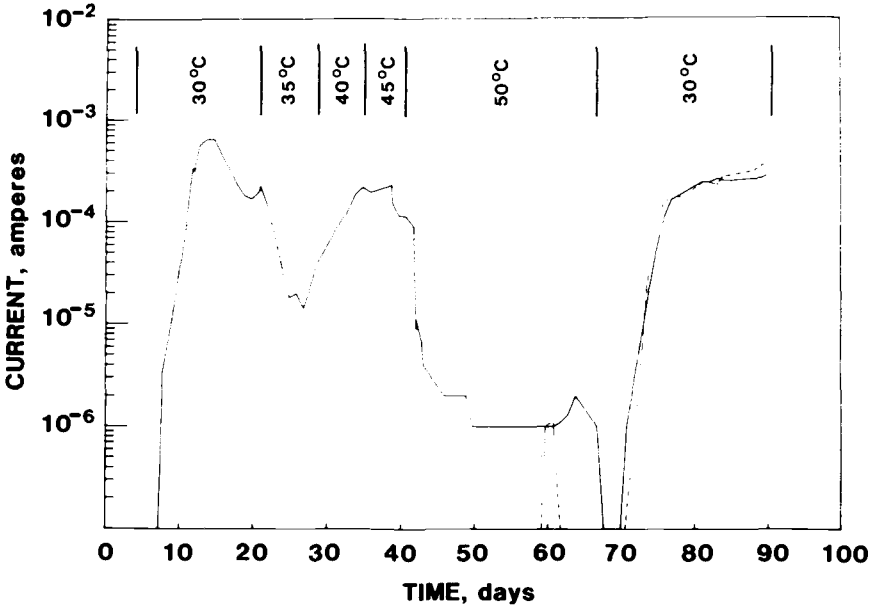


FIG. 9—*Remote crevice assembly data describing changes in current measurements for Alloy 904L as a function of time and controlled variation in seawater temperature during testing. Solid line shows current data for specimen exposed initially in 30°C seawater. Dashed line is for specimen exposed initially in 50°C seawater.*

by the sharp increase in current, initiation occurred at about the seventh day of exposure. The magnitude of this current is consistent with the total current shown earlier in Fig. 8. During the course of testing, the temperature of the seawater was elevated in 5°C increments approximately every 5 days. While some perturbations are noted through the first 40 days (temperature up to 45°C), the magnitude of current remains relatively high. Upon a further increase in temperature to 50°C, the magnitude of total current dramatically decreased by several orders of magnitude. After almost four weeks of corroding at this low rate, the propagation rate was returned to its earlier higher level by allowing the seawater to cool back to 30°C.

The dashed graph shows current data for a companion specimen that was introduced after the above test temperature was established at 50°C. As can be seen, initiation in this case did not occur until the seawater was cooled to 30°C. Note that the time at 50°C was more than twice that required for initiation at 30°C.

Effects of Crevice Tightness—Mathematical modelling of crevice corrosion has shown that decreasing the gap dimension (that is, degree of tightness) will reduce the time to initiation while wider gaps will have an opposite effect. This can be related to the decreased volume of crevice solution that must undergo deoxygenation and become sufficiently acidified to cause breakdown of passivity. Some critical gap dimension can be predicted for each alloy, environment, and crevice depth combination. The authors [*9,16*] have used this geometric influence to help explain the frequently observed variability in crevice corrosion behavior for stainless steels in seawater tests and have quantified a number of different crevice assemblies. It is postulated that laboratory crevice devices, such as multiple crevice assemblies, may produce a range of tight crevice gaps, which may vary according to the actual degree of tightness at the time of the exposure.

Differences in crevice tightness can also be related to physical properties of the crevice former. It is easy to appreciate, for example, that nonmetallics are more readily deformable than metal and hence are likely to produce more severe crevices. If, however, equal geometries could be produced for metal to metal and nonmetal to metal crevices, the former would be expected to cause more rapid initiation. This is because of the fact that metal ions enter the same volume of solution from two metal surfaces causing more rapid hydrolysis and hence acidification, than that from a single metal surface.

Controlled Crevice Loading Device—An air operated loading device used in concert with the previously described remote crevice assembly concept has been used to further study the effects of crevice tightness. In these tests, the anode members were positioned between acetal resin blocks. Tests were conducted with and without plastic tape inserts between the blocks and both metal surfaces. Again, it is presumed that the tape would be more deformable and hence provides for a tighter crevice at the same applied constant load of 69 000 Pa (~10 psi).

Figure 10 shows the remote crevice assembly current and potential data for duplicate assemblies exposed without the inserts. While anodic currents were

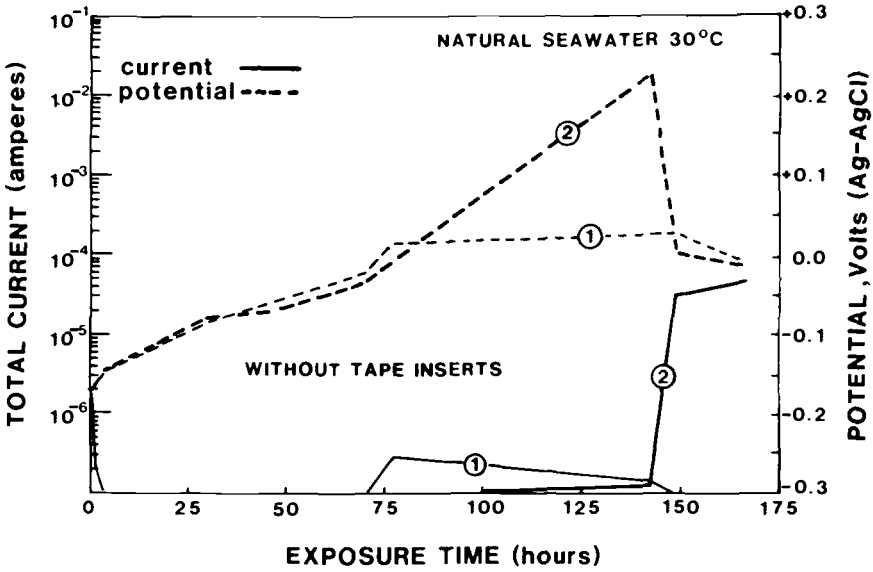


FIG. 10—*Remote crevice assembly current and potential data for Type 316 stainless steel in air-operated loading test without plastic tape inserts between crevice former and metal.*

recorded, the levels were fairly low. Results for Specimen 1 indicate that while conditions leading to initiation were developing, the crevice area repassivated. In the case of Specimen 2, initiation did not occur until about 145 h. This was later confirmed when examination revealed a trace of crevice attack on Specimen 2 and no corrosion for Specimen 1.

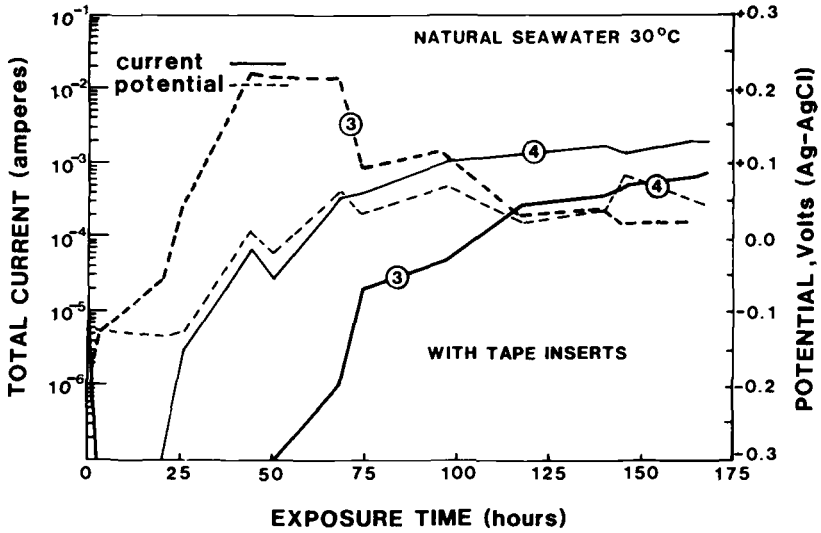


FIG. 11—*Remote crevice assembly current and potential data for Type 316 stainless steel in air-operated loading test with plastic tape inserts between crevice former and metal.*

It is also interesting to note the differences in the spontaneous polarization behavior exhibited by the two assemblies. While the potentials for both were comparable up to about 75 h, those for Specimen 2 continued to rise to more noble values until the crevice area was sufficiently active to cause a shift in the couple potential. The behavior described in Fig. 10 is also significant in that while two crevice assemblies of the same material exhibited similar potentials at the end of seven days, one was actively corroding while the other was not.

Figure 11 shows results for tests using the tape inserts in the crevice formers. In both cases, conditions were sufficiently severe to cause initiation within 50 h. While two additional specimens initiated within 5 h, one of these spontaneously repassivated and reinitiated several times during the seven-day test. The average initiation time (~20 h) is consistent with the results described earlier for Type 316 in seawater tests using the bolt loading type remote crevice assembly fixture (with tape inserts). In addition, the degree of reproducibility in this regard is extremely good considering that initiation occurred within the time frequently allowed for standard laboratory tests, such as the 72-h ferric chloride test described in ASTM Test Method for Pitting and Crevice Corrosion Resistance of Stainless Steels and Related Alloys by the Use of Ferric Chloride Solution (G 48).

Table 4 summarizes results describing the overall resistance for the six specimens in this preliminary series. For this relatively short test, differences in the area for which propagation occurred are evident. The most severe attack with respect to total area and total mass loss was exhibited by Assembly 5. This was reflected by the order of magnitude increase in current that occurred toward the end of the test period, as well as the earlier initiation time. Figure 12 shows the current increases for the three most severely corroded specimens. The curves have been normalized to a common initiation time so that data can be compared from the onset of crevice corrosion. Observed differences in propagation behavior from one crevice assembly to another are consistent with the frequently reported [*16*] orders of magnitude differences in penetration for single specimens having multiple crevice sites, for example, multiple crevice assemblies.

Tests of this nature can be used to quantify the resistance of different alloys to crevice corrosion. Ranking of alloys based on identification of critical load levels for several types of crevice geometries is envisioned to be of a more practical value than other types of rankings such as critical temperatures in ferric chloride [*23*].

Compartmentalized Cell Experiments

Effect of Crevice Solution pH—For Type 316 stainless steel, the effects of decreasing crevice solution pH on freely corroding anode members and on anode members coupled to a larger cathode member in an adjacent compartment containing recirculated, natural seawater are shown in Fig. 13. In each case, decreases in crevice solution pH resulted in the anticipated increase in mass loss for the anodes. As can be seen, coupling to the seawater cathode member resulted

TABLE 4—*Remote crevice assembly test results for Type 316 in seawater (air-operated loading device).*

Specimen	Time to Initiation, h	Area Corroded, cm^2	Total Charge, C	Mass Loss, g	Potential at Day 7, V	Current Density at Day 7, mA/cm^2
1[a]	OK[b]	0	0	0.0003	−0.008	0.000
2[a]	145	0.10	2	0.0003	−0.016	0.001
3[c]	50	0.75	46	0.0300	+0.008	1.2
4[c]	20	1.80	229	0.0251	+0.043	1.0
5[c]	5 to 10	2.00	513	0.1699	+0.039	10.0
6[c]	5[d]	0.24	12	0.0030	+0.271	0.4

[a]Without tape.
[b]Repassivated without measureable propagation.
[c]With tape.
[d]Repassivated with measureable propagation.

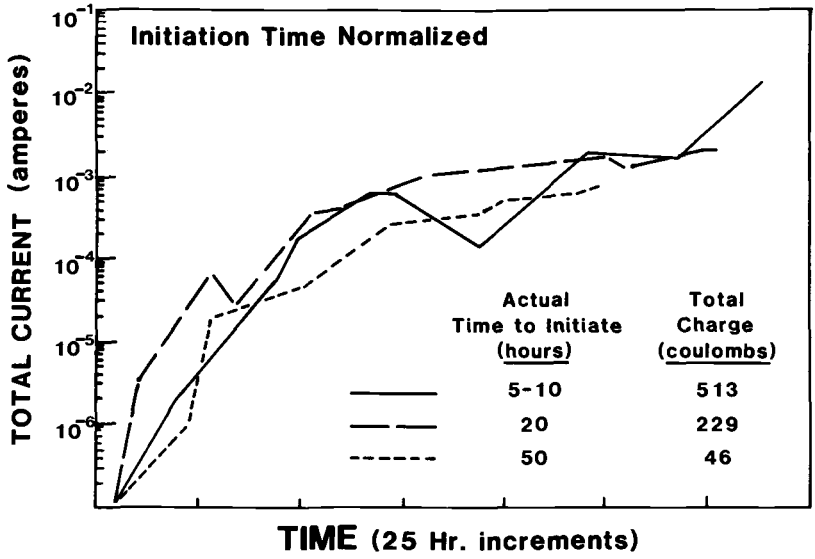


FIG. 12—*Comparison of crevice corrosion propagation currents for Type 316 stainless steel remote crevice assemblies (air-operated with tape inserts) after normalizing initiation times.*

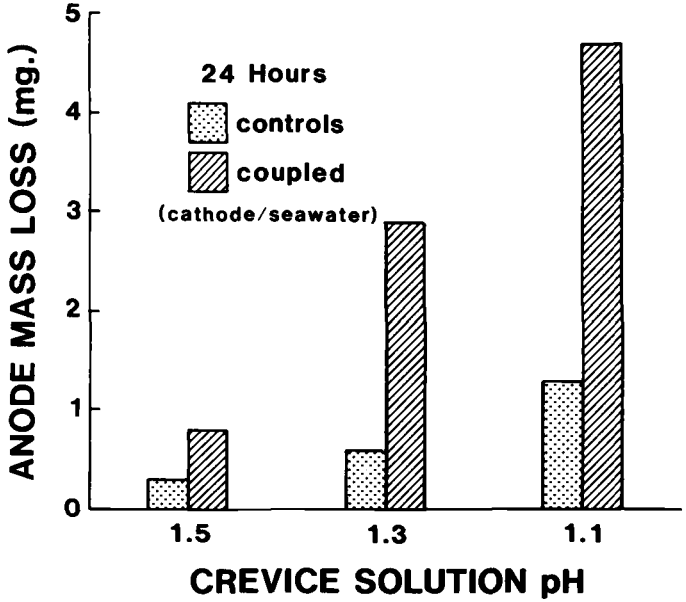


FIG. 13—*Effect of crevice solution pH on mass loss for "control anodes" and coupled anode members in compartmentalized cell tests for Type 316 stainless steel.*

in dramatic increases in mass loss to an extent greater than any of the incremental decreases in pH. These results, as discussed previously [*21*], correlate well with amperometric data. In addition, it was shown that the relative potential domain of the anodes during the course of the tests in pH = 1.5 and 1.3 solutions shift to a passive state while those at pH = 1.1 remained active at values closely associated with the anodic peak as evidenced by potentiodynamic polarization curves (at 0.6 V/h).

The compartmentalized cell has also been used to monitor the overall couple potential as a function of crevice solution pH. Figure 14 shows the average potentials for freely corroding, crevice free cathode members in natural seawater and those for freely corroding anode members in deaerated crevice solutions at the indicated pH value. Data points plotted on the graph identify the couple potentials measured in the bulk environment compartment. As can be seen, these values decreased with decreasing crevice solution pH. In general, these results are consistent with published potential data describing differences in potentials of active and passive stainless steel in seawater [*24*]. In a general way, these data also typify the differences in potentials for the tests described earlier in Fig. 5.

Area Ratio Effects—It is noted that the potentials shown in Fig. 14 are somewhat more active than those identified for Type 316 in the seawater remote crevice assembly test. This difference can be attributed to differences in the actual anode area. In the crevice free compartmentalized cell tests, the anodes

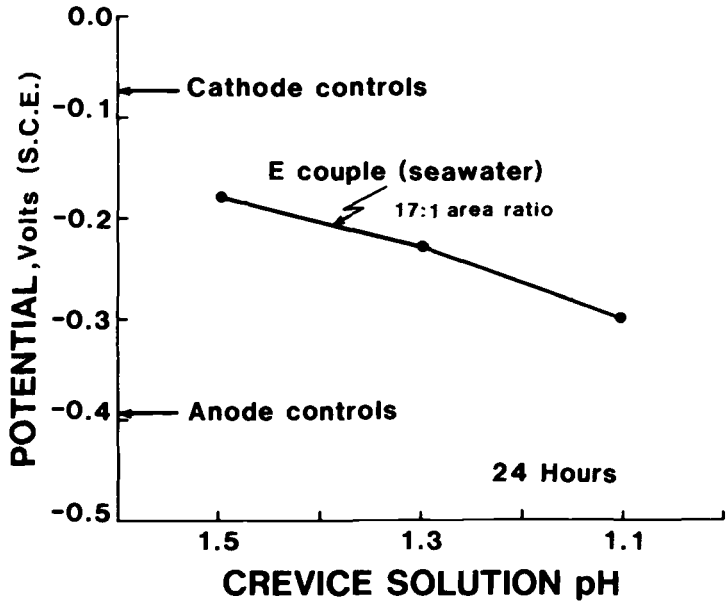


FIG. 14—*Effect of crevice solution pH on the couple potential for Type 316 stainless steel in compartmentalized cell tests using natural seawater in cathode compartment.*

have a surface area of ~10 cm^2. In contrast, the nominal contact area for the remote crevice assembly anodes is only 4.5 cm^2. In most cases, however, only a portion of that crevice area has initiated in the time allowed. As a result, studies have been undertaken to assess the effects of cathode to anode area ratio. In one test conducted with the anode members in a pH = 0.8 solution, the couple potential for a 17:1 cathode to anode area ratio approximated −0.35 V saturated calomel electrode (SCE). Increasing the cathode to anode ratio by an order of magnitude provides couple potentials close to −0.20 V.

Figure 15 describes the anodic potentiodynamic polarization behavior (0.6-V/h scan rate) for Type 316 in the above crevice electrolyte. Changes in area ratio, as determined in compartmentalized cell tests, can result in a shift in the anode member potential from the active region to more noble potential regions describing the breakdown of passivity.

Effect of Bulk Environment Oxygen Concentration—Figure 16 describes the effect of bulk seawater environment oxygen concentration on the potential of coupled anodes for Alloy 904L in a series of compartmentalized cell tests. At this pH level, deaeration of the seawater (~1-mg/L dissolved oxygen) resulted in the material remaining active with some low measure of corrosion currents. Increasing the oxygen concentration by purging with various gas mixtures, that is, 95% nitrogen and 5% oxygen, compressed air (80% nitrogen and 20% oxide) and 50% nitrogen and 50% oxygen, resulted in an increase in the anode potential

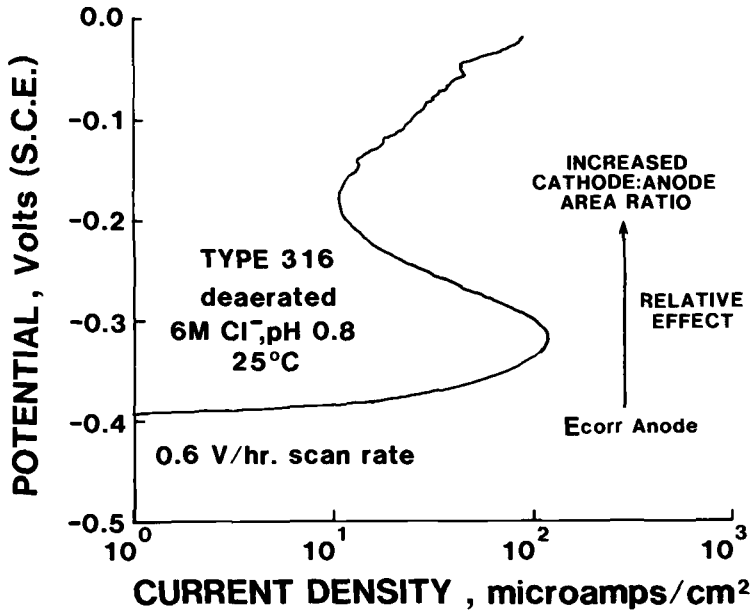


FIG. 15—*Potentiodynamic polarization curve for Type 316 stainless steel in simulated crevice solution. Relative effect of cathode to anode area ratio from compartmentalized cell tests is indicated schematically.*

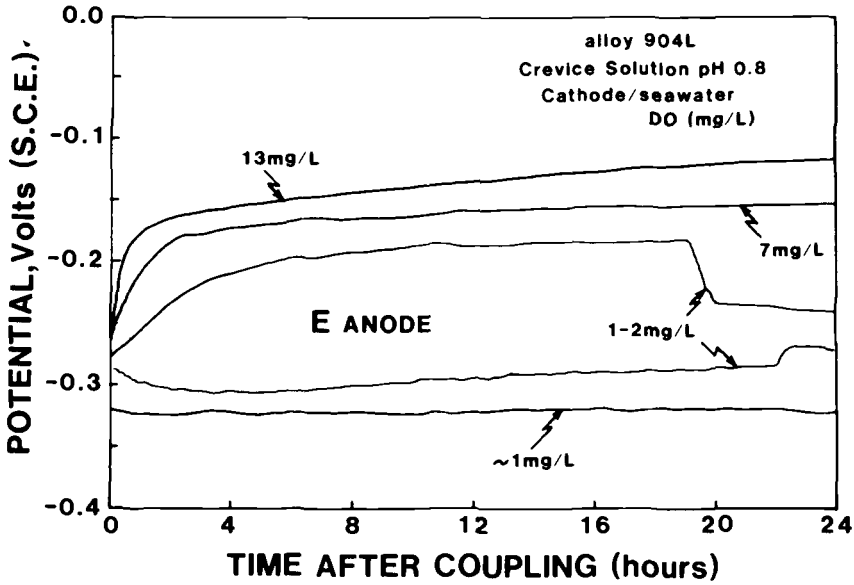


FIG. 16—*Effect of bulk seawater dissolved oxygen level (cathode compartment) on potential of Alloy 904L anode member in pH = 0.8 simulated crevice solution.*

to more noble values. Under these alloy-environment conditions, polarization to the passive state was described by decay in current densisties to ~1 $\mu A/cm^2$ or less. Other effective area ratios or more concentrated crevice solutions or both could account for the results described by the remote crevice assembly test (Fig. 5), that is, ongoing crevice corrosion at a couple potential around +0.05 V.

Summary

Crevice corrosion has been shown to be a complex phenomenon that can be treated as being composed of two discrete phases. The initiation phase and the propagation phase can be influenced by a wide range of factors that can be classified as metallurgical, environmental, or geometric in nature. The processes can be described mathematically, which allows convenient assessments of cause and effect relationships. This, in turn, enhances the understanding of factors influencing the processes and aids in the design of appropriate experiments to study crevice corrosion.

Application of relevant test methods allows a characterization of the crevice corrosion process and can yield data of practical engineering utility. The proper interpretation of results from tests that are designed to truly control the critical parameters affecting the result is an equally important consideration.

Relevant use and interpretation of results from tests using devices, such as the remote crevice assembly and compartmentalized cell, can expand understanding of many variables in the crevice corrosion behavior of engineering

materials. It is possible to establish the relative effects of environmental factors such as bulk environment chloride level and dissolved oxygen content as well as effects of crevice solution pH on both crevice initiation and propagation. The unique nature of natural seawater in promoting an order of magnitude more extensive degree of crevice corrosion than synthetic seawater can be clearly established with these techniques. The effect of increasing temperature of natural seawater on reducing the extent of crevice corrosion can also be documented in a unique manner.

A multifaceted approach to investigating crevice corrosion has been described, which involves use of mathematical modelling and various compatible experimental methodologies. The continued evolution of this approach holds promise for achieving the ultimate goal of developing the capacity to accurately predict and define alloy crevice corrosion performance in engineering applications.

References

[1] Oldfield, J. W. and Sutton, W. H., *British Corrosion Journal,* Vol. 13, No. 1, Jan. 1978, p. 13.

[2] Oldfield, J. W. and Sutton, W. H., *British Corrosion Journal,* Vol. 13, No. 3, March 1978, p. 104.

[3] Fontana, M. G. and Greene, N. C., *Corrosion Engineering,* McGraw-Hill, New York, 1967, Chapter 3, pp. 41–44.

[4] Oldfield, J. W., Lee, T. S., and Kain, R. M., *Corrosion and Corrosion Protection,* Vol. 81-8, The Electrochemical Society, Pennington, NJ, 1981, p. 213.

[5] Oldfield, J. W., Lee, T. S., and Kain, R. M., "A Mathematical Model of Crevice Corrosion Propagation of Stainless Steel," presented at CORROSION/81—Research in Progress Symposium, Toronto, Canada, April 1981.

[6] Lee, T. S., Oldfield, J. W., Kain, R. M., and O'Dell, C. S., "Assessing Crevice Corrosion Behavior of Stainless Steels in Natural Waters Via Mathematical Modelling," presented at CORROSION/82—Research in Progress Symposium, Houston, TX, April 1982.

[7] Lee, T. S., Oldfield, J. W., and Kain, R. M., "The Role of Oxygen Reduction in Crevice Corrosion of Stainless Steels," presented at 162nd Electrochemical Society Meeting, Detroit, MI, 17-22 Oct. 1982.

[8] Anderson, D. B., *Galvanic and Pitting Corrosion—Field and Laboratory Studies, STP 576,* American Society for Testing and Materials, Philadelphia, 1976, pp. 261–275.

[9] Kain, R. M., "Crevice Corrosion and Metal Ion Concentration Cell Corrosion Resistance of Candidate Materials for OTEC Heat Exchangers, Parts I and II," ANL/OTEC-BCM-022, Argonne National Laboratory, Argonne, IL, May 1981.

[10] Kain, R. M., "Crevice Corrosion Resistance of Several Iron Base and Nickel Base Cast Stainless Alloys in Seawater," *CORROSION/82,* Paper No. 66, National Association of Corrosion Engineers, Houston, TX, March 1982.

[11] Hack, H. P., *Materials Performance,* Vol. 22, No. 6, June 1983, p. 24.

[12] Bond, A. P., Bertoli, C., and Dundas, H. J., "Corrosion Resistance of Stainless Steels in Seawater," *Proceedings of Symposium on Advanced Stainless Steels for Seawater Applications,* Piacenze, Italy, 28 Feb. 1980.

[13] Garner, A., *Corrosion,* Vol. 37, No. 3, March 1981, p. 178.

[14] Streicher, M. A., *Materials Performance,* Vol. 22, No. 5, May 1983, p. 37.

[15] Streicher, M. A., *Journal of the Electrochemical Society,* Vol. 103, No. 7, July 1956, p. 375.

[16] Lee, T. S. and Kain, R. M., "Factors Influencing the Crevice Corrosion Behavior of Stainless Steels in Seawater," *CORROSION/83,* Paper No. 69, National Association of Corrosion Engineers, Houston, TX, April 1983.

[17] Lee, T. S., *Electrochemical Corrosion Testing, STP 727,* American Society for Testing and Materials, Philadelphia, 1981, pp. 43–68.

[18] Kain, R. M., *Materials Performance,* Vol. 23, No. 2, Feb. 1984, pp. 24–30.

[19] Rosenfeld, I. T. and Marshakov, I. K., *Corrosion*, Vol. 20, No. 4, April 1964, p. 115t.
[20] Verink, E. D., Starr, K. K., and Bowers, J. M., "Chemistry of Crevice Corrosion as Observed in Certain Cu-Ni and Fe-Cr Alloys," *Corrosion*, Vol. 32, No. 2, Feb. 1976, p. 60.
[21] Kain, R. M. and Lee, T. S., "Polarization Characteristics of Stainless Steel Cathode and Anode Areas Involved in Crevice Corrosion," Presented at 162nd Meeting of Electrochemical Society Meeting, Detroit, MI, 17-22 Oct. 1982.
[22] Kain, R. M., "Crevice Corrosion Resistance of Austenitic Stainless Steels in Ambient and Elevated Temperature Seawater," *CORROSION/79*, Paper No. 230, National Association of Corrosion Engineers, Houston, TX, March 1979.
[23] Brigham, R. J., *Corrosion*, Vol. 30, No. 11, Nov. 1974, p. 396.
[24] LaQue, F. L., *Marine Corrosion—Causes and Prevention*, Wiley Interscience, New York, 1975, Chapter 6, p. 179.

DISCUSSION

B. Rosborg[1] *(written discussion)*—You mentioned that an increased temperature may result in a lowered tendency for crevice corrosion in a natural environment. Does this apply both to initiation and propagation?

R. M. Kain (author's response)—Reduction in crevice corrosion associated with elevated seawater temperature testing have been primarily noted with respect to the observed extent of propagation.

While increased seawater temperature, as described herein, does not appear to accelerate initiation, it is premature to conclude that the tendency for initiation is actually reduced. Some susceptible stainless alloys have exhibited reduced incidences of attack in some tests. However, time required for visible detection may be affected by lowered propagation rates.

In somewhat related studies, Tipton and Kain[2] have shown that both pit initiation and pit propagation for Monel alloy 400 is significantly lower in 50°C seawater as compared to tests in seawater at 19 or 30°C.

H. Jain[3] *(written discussion)*—A very recent publication by a Canadian group shows that the observed crevice potential depends on where the reference electrode is placed. Have you investigated this phenomenon? What would be its explanation?

R. M. Kain (author's response)—The potential of freely corroding stainless steel in an aggressive, deaerated crevice solution is likely to be several hundred millivolts more active than passive stainless steel in aerated seawater. As shown in Figs. 14 and 15, measured potentials in compartmentalized cell tests for stainless steels with "ongoing crevice corrosion" can vary considerably as a function of crevice solution pH and cathode to anode (active crevice area) ratio.

[1] Studevik Energiteknik AB, S-611 82 Nykoping, Sweden.
[2] Tipton, D. G. and Kain, R. M., "The Effect of Temperature on the Resistance to Pitting of Monel Alloy 400 in Seawater, NACE Annual Conference, 1980, unpublished Paper No. 36.
[3] Brookhaven National Laboratory, Building 830, Upton, NY 11973.

In addition, depending on where the reference electrode was placed, potentials for coupled members (that is, cathode in seawater and anode in simulated crevice solution) varied by 9 to 15 mV. More active values were obtained when the reference electrode was placed in contact with the crevice solution. Accordingly, it would be expected that placement of a reference capillary in the bulk environment immediately adjacent to the active crevice site would yield potentials somewhat more active than those obtained by remote measurements.

M. Hubbell,[1] *C. Price,*[2] *and R. Heidersbach*[3]

Crevice and Pitting Corrosion Tests for Stainless Steels: A Comparison of Short-Term Tests with Longer Exposures

REFERENCE: Hubbell, M., Price, C., and Heidersbach, R., **"Crevice and Pitting Corrosion Tests for Stainless Steels: A Comparison of Short-Term Tests with Longer Exposures,"** *Laboratory Corrosion Tests and Standards, ASTM STP 866,* G. S. Haynes and R. Baboian, Eds., American Society for Testing and Materials, Philadelphia, 1985, pp. 324–336.

ABSTRACT: Several methods for determining the "protection potential" of stainless steels have been reported in the literature. As most commonly defined, this potential is the potential below which metals will not corrode by pitting or crevice corrosion. This report presents a discussion on how the protection potential, if it were accurately known, could be utilized to control corrosion of stainless steels. The results of four different experimental methods for determining the protection potential for American Iron and Steel Institute 304 (Unified Numbering System [UNS] S30400) stainless steel are presented and compared.

KEY WORDS: corrosion, stainless steels, concentration cell corrosion, protection potential

At low temperatures the principal problems of stainless steels are pitting and crevice corrosion. Many authorities consider these forms of corrosion to be virtually the same, that is, a pit is a form of crevice corrosion that is self initiating. Stainless steel equipment suffering from pitting corrosion can be expected to also have crevice corrosion problems, but the reverse is not true. Thus, if the engineer can avoid crevice corrosion, pitting corrosion will also be avoided.

One possible indicator of crevice corrosion activity is the "protection potential." As this terminology is applied to pitting and crevice corrosion, the protection potential is the potential below which crevice corrosion and pitting corrosion will not occur. Above the protection potential crevice corrosion will

[1] Materials Engineering Laboratory, Eastman Kodak Company, Bldg. 23, Fifth Floor, Rochester, NY 14650.

[2] School of Mechanical and Aerospace Engineering, Oklahoma State University, Stillwater, OK 74078.

[3] Professor, School of Chemical Engineering, Oklahoma State University, Stillwater, OK 74078.

Copyright© 1985 by ASTM International www.astm.org

occur, but, supposedly, pits will not initiate, although if present they will grow. Above a second potential, known as the pitting potential or rupture potential, pits will initiate, and both crevices and pits will grow. Unfortunately, while the concept of a protection potential has been known for many years, disagreement exists as to how it should be determined, and long-term confirmation of the concept is lacking [*1–28*]. Recent work by Galvele [*29*] confirms earlier work by Wilde and Williams [*30*], which showed that for stainless steels the protection potential, or breakdown potential [*26*], for crevice corrosion will be much lower than the repassivation potential, frequently referred to as the "protection potential" for pitting corrosion.

While laboratory reports are available that discuss the potential inside an occluded cell or crevice [*31*], the potential inside a crevice cannot be measured on operating equipment. Thus all references to potentials in this report refer to potentials of the bulk specimen outside the crevice. France [*28*], Galvele [*29*], and others have reviewed experiments that show that the potential inside a crevice is related to the potential outside the crevice.

The existence of a protection potential against crevice corrosion is confirmed by experience on cathodic protection of stainless steel marine equipment having crevices [*32,33*]. Cathodic protection is now being used to control crevice corrosion of stainless steels in coastal power plants [*34*].

Other practical applications of the protection potential include potential monitoring of operating process equipment and anodic protection below the protection potential [*35*].

Careful examination of the research literature on pitting and crevice corrosion revealed at least four fundamentally different methods for experimentally determining the protection potential.

Verink et al modified existing potentiodynamic polarization curve techniques to identify the protection potential [*36–38*]. Their method, which they termed the "electrochemical hysteresis technique," involves a reverse potentiodynamic scan in the active direction. During the reverse scan portion of the potentiodynamic polarization curve method, the current density approaches zero. The potential where the anodic current becomes zero, labeled E_p in Fig. 1, is defined as the "protection potential" by researchers using this technique.

Several electrode potential regions are shown in Fig. 1:

1. Above (more noble than) the rupture potential, new pits can intiate and propagate and existing pits can continue to propagate [*36*].
2. Between the rupture potential and the protection potential, existing pits can continue to propagate but no new pits can initiate [*37*].
3. Below (more active than) the protection potential pits can neither initiate nor propagate [*36*].
4. Below the corrosion potential the region of immunity exists. In this region there is a resistance to corrosion or anodic dissolution of a metal caused by thermodynamic stability of the metal [*37*].

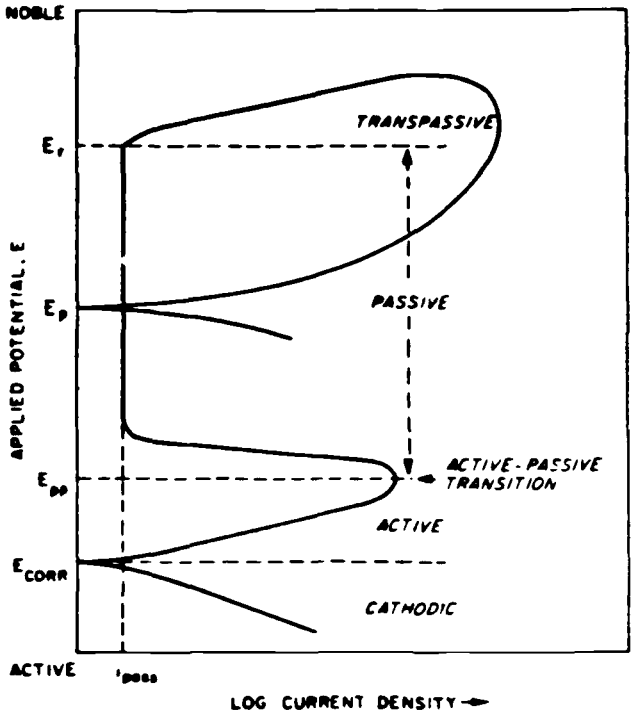


FIG. 1—*Idealized polarization curve modified to include the electrochemical hysteresis loop.*

ASTM Practice for Conducting Cyclic Potentiodynamic Polarization Measurements for Localized Corrosion (G 61) is based on the procedure described above.

Figure 1 is an idealized polarization curve used to illustrate the concepts discussed above. Actual polarization curves are usually more complicated and difficult to interpret. Fortunately, the protection potential, as defined above, is easy to identify on many of these more complex curves [*39*]. Some environments produce hysteresis curves, which are hard to explain using the logic above. Baboian and Haynes and Price et al have reported hysteresis curves for stainless steels where the "protection potential" is below the "corrosion potential [*18,40*]." No curves of this type were obtained during the research discussed in this report [*39*].

Many authorities have questioned the validity of this short-term test procedure. The most frequent criticism is that these tests may not adequately predict long-term corrosion behavior [*6,26,32*].

Sedriks described a second method for determining the protection potential [*41*]. According to Sedriks when a specimen is held potentiostatically at its pitting potential, the current decays to a value that becomes constant with time. When held at a potential more noble than its pitting potential, the current increases with time because of localized corrosion on the specimen. When held at a

potential more active than its pitting potential, the current decreases with time because of the repassivation of any localized corrosion sites on the specimen. The same logic should hold true for crevice corrosion specimens held above or below the protection potential.

Intuitively, it would seem that this test more accurately reflects conditions on operating equipment. Wilde and Williams [*30*] and Galvele [*29*] have suggested that long-term crevice corrosion potential will be lower than the repassivation potential determined by the cyclic polarization, or hysteresis technique, which supposedly represents repassivation of pitting corrosion initiated above E_r on Fig. 1.

Hultquist and Leygraf described a "potential step" method for determining the protection potential [*42*]. After immersion of the specimen for 1 min in the test solution, the potential is switched to a predetermined value more active than the protection potential. Every 2 min the potential is increased in steps of 50 mV. The sample current is monitored as a function of time. The protection potential is determined to be the lowest potential at which the current is found to increase within 2 min. It might seem like the procedure described by Hultquist and Leygraf should describe a potential-step method of determining the rupture potential in Fig. 1. However, the authors clearly refer to crevices in their manuscript. The reason for this emphasis is the frequent observation that crevice corrosion almost invariably occurs on flat specimens exposed to successively increasing potentials during potentiodynamic experiments. Very careful procedures are necessary to avoid crevice corrosion in pitting experiments.[4]

A modification of Hultquist's and Leygraf's potential step method is also possible. In this technique the specimen surface is first "activated" by polarizing at a potential noble to the rupture potential determined by a potentiodynamic scan (E_r on Fig. 1). After initiating active sites, the specimen is polarized to a predetermined potential active to the protection potential. Again, every 2 min the potential is increased in steps of 50 mV, and the protection potential is determined to be the lowest potential at which the current is found to increase within 2 min.

There are other possible methods of determining the protection potential, but the four techniques described above are representative of current research and understanding of the protection potential concept.

Experimental Procedure

American Iron and Steel Institute Type 304 (Unified Numbering System [UNS] S30400) stainless steel was exposed to a series of electrolytes, which have been used in other research in our laboratories and elsewhere [*43–46*]. The composition of these electrolytes is shown in Table 1. It should be noted that the pH of these electrolytes will be somewhat different at elevated temperatures.

Potentiodynamic curves were generated using a commercial potentiostat with a flat specimen holder. ASTM Recommended Practice for Standard Reference

[4] Hakkarainen, R., in this publication, pp. 91–107.

TABLE 1—*Electrolytes.*

pH, ±0.2	Composition
3.0	0.001M H_2SO_4
	0.005M $KHC_8H_4O_4$
4.1	0.088M $KHC_8H_4O_4$
	0.002M NaOH
4.5	0.016M NaOH
	0.074M $KHC_8H_4O_4$
5.0	0.030M NaOH
	0.060M $KHC_8H_4O_4$
5.5	0.038M NaOH
	0.052M $KHC_8H_4O_4$
5.9	0.042M NaOH
	0.048M $KHC_8H_4O_4$
7.1	0.046M NaOH
	0.045M $KHC_8H_4O_4$
8.3	0.100M $NaHCO_3$
	0.001M $KHC_8H_4O_4$
8.6	0.100M $NaHCO_3$
9.0	0.100M $NaHCO_3$
	0.010M NaOH
9.5	0.100M $NaHCO_3$
	0.020M NaOH
10.0	0.001M NaOH
	0.003M $NaHCO_3$
11.0	0.001M NaOH
12.0	0.10M NaOH

Method for Making Potentiostatic and Potentiodynamic Anodic Polarization Measurements (G 5) and ASTM G 61 were used as guides in measuring these curves.

All cyclic scans were performed at a scan rate of 0.833 mV/s, 3 V/h, so that data would be comparable. This scan rate was used because it yielded very reproducible data and was fast enough to obtain the large number of scans necessary to produce the experimental Pourbaix diagrams, which were another objective of this research [*39*]. Scan rates from 0.6 to 3 V/h were tested with no effect on the results obtained.

Two very different working electrode holders were used. The working electrode holder shown in Fig. 2 was used in the development of the potentiodynamic polarization curves described above. The working electrode holder shown in Fig. 3 was used for the verification of protection potentials during long-term potentiostatic exposures. As its name, "multiple crevice assembly," implies, it is a specimen holder that purposely creates crevice sites. It is a modified design of the specimen holders used by Anderson [*47*].

The multiple-crevice electrode holder was used for the long-term potentiostatic tests suggested by Sedriks and for the potential-step experiments suggested by Hultquist and Leygraf. The flat specimen holder (Fig. 3) was used for determination of the protection potential using the electrochemical hysteresis method

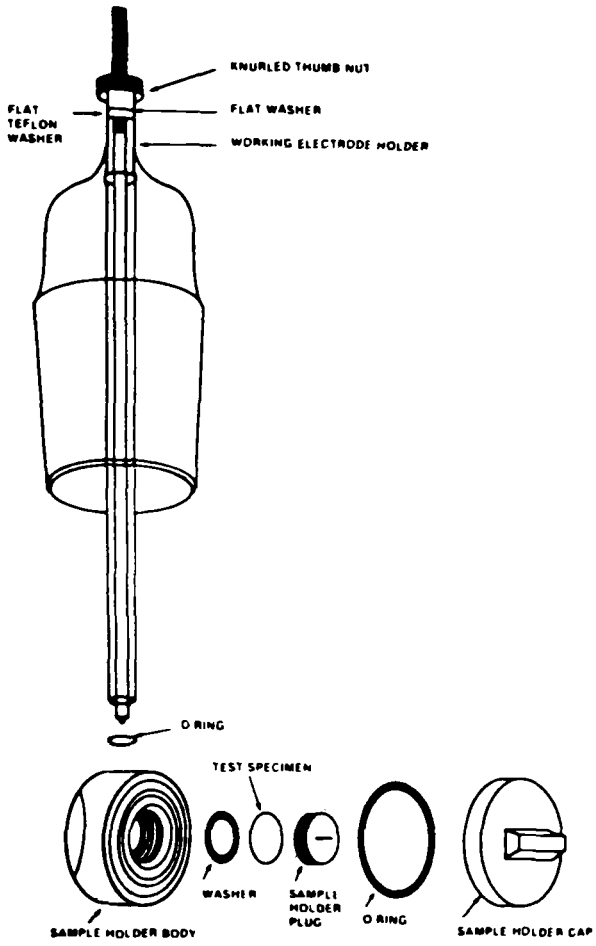


FIG. 2—*Commercial specimen holder.*

of Verink et al. It was also used for modified "potential-step" experiments where the surface was "activated" by exposing it for 1 min at a potential 250 mV more active than the rupture potential determined using the electrochemical hysteresis technique.

Visual inspection under × 10 magnification was used to determine whether or not pitting corrosion, or crevice corrosion under the multiple crevice assembly, had occurred during long-term potentiostatic exposures. The protection potentials were determined by successive iterations at the correct value until the potential was narrowed down to within ±50 mV. This procedure is similar to that reported by Manning in his pitting corrosion tests [*1*]. The potentiostatic tests were 2 to 4 h long for the 80°C environments tested and 1 to 2 weeks long for the 20°C environments tested.

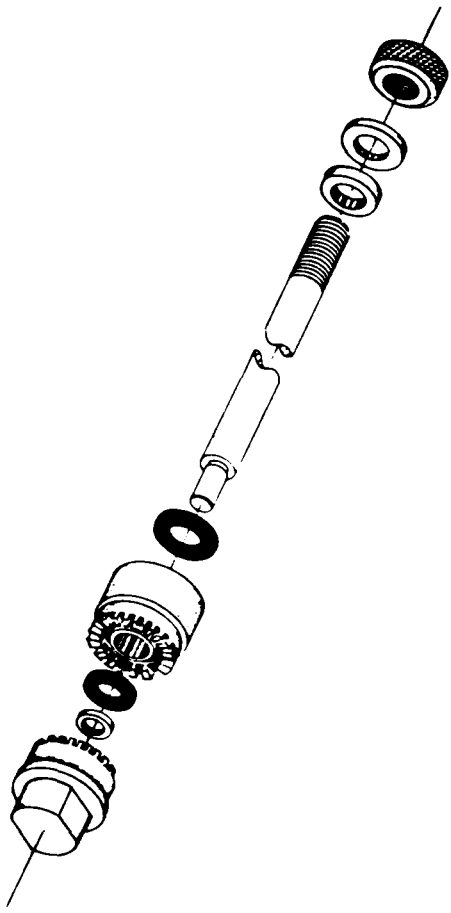


FIG. 3—*Multiple crevice assembly working electrode holder.*

Complete details on specimen preparation and experimental procedures are available in the extended report on this research [*39*].

Results and Discussion

Tables 2 through 4 summarize the results of the crevice and pitting corrosion tests described in detail in the earlier sections of this report. The lack of consistency between the four methods of determining the protection potential is apparent.

Data obtained from the two "stepping" techniques were identical. The potential where current increased within a 2-min step period was independent of whether the specimen was exposed to crevice sites or was purposely activated before testing. Data from these tests were generally less conservative than po-

TABLE 2—*Summary of protection potential experimental results Alloy 304, 20°C, 0.10M sodium chloride (potential versus saturated calomel electrode).*

Method	pH					
	3	5	7	9	11	13
Electrochemical hysteresis [*37,38*]	−0.108	0.059	−0.144	−0.278	−0.176	0.136
Long-term potentiostatic [*41*]	−0.200	−0.150	−0.170	−0.225	−0.150	0.175
Step method multiple crevice assembly specimen holder [*42*]	0.050	0.050	0.100	0.100	0.050	0.450
Step method flat specimen holder-activated specimens [*42*]	0.050	0.050	0.100	0.100	0.050	0.450
Most conservative results	−0.200	−0.150	−0.170	−0.278	−0.176	0.136

TABLE 3—*Summary of protection potential experimental results Alloy 304, 80°C, nil-Cl (potential versus SCE).*

Method	pH					
	3	5	7	9	11	13
Electrochemical hysteresis [*37,38*]	0.762	0.612	0.169	0.034	0.330	−0.07
Long-term potentiostatic-current decay [*41*]	0.900	0.850	0.650	0.600	0.535	0.750
Step method multiple crevice assembly specimen holder [*42*]	1.100	1.100	0.900	0.850	0.300	0.500
Step method flat specimen holder-activated specimens [*42*]	1.100	1.100	0.900	0.850	0.300	0.500
Most conservative results	0.762	0.612	0.169	0.034	0.300	−0.07

TABLE 4—*Summary of protection potential experimental results Alloy 304, 80°C, 0.10M sodium chloride (potential versus SCE).*

Method	pH					
	3	5	7	9	11	13
Electrochemical hysteresis [*37,38*]	−0.293	−0.012	−0.158	−0.262	−0.246	−0.09
Long-term potentiostatic-current decay [*41*]	−0.300	−0.075	−0.075	−0.050	−0.000	0.150
Step method multiple crevice assembly specimen holder [*42*]	0.000	0.100	0.100	0.100	0.050	0.450
Step method flat specimen holder-activated specimens [*42*]	0.000	0.100	0.100	0.100	0.050	0.450
Most conservative results	−0.300	−0.075	−0.158	−0.262	−0.246	−0.09

tentiostatically derived protection potentials. The fact that these two tests produced identical results shows that the use of the two different specimen holders did not alter the results obtained. It also suggests that pitting corrosion, supposedly initiated by "activating" the specimen at elevated potentials, and crevice corrosion can be prevented at the same potentials. Whether or not pits were actually "activated" by this process is subject to controversy [*26–27*].

Comparison of the hysteresis results with the long-term potentiostatic results is also interesting. One of these two techniques was likely to produce the most conservative results in the environments tested in this study. The introduction to this report mentioned studies by Galvele [*29*] and by Wilde and Williams [*30*], which suggested that the potentials associated with protection from crevice corrosion would be more cathodic than the potentials associated with protection from or repair of pits. The present results do not confirm this idea. Whereas long-term crevice tests produced more cathodic, or conservative, results in room temperature acids with 0.1M sodium chloride additions (Table 2), the hysteresis technique suggested by Verink and Pourbaix (and adopted with modifications as per ASTM G 61) produced more conservative results in bases at room temperature (Table 2) and for many elevated-temperature exposures (Tables 3 and 4).

Intuitively, it would seem that the potentiostatic crevice corrosion tests should yield the results most likely to be confirmed by engineering practice. The relatively short duration of the potentiostatic tests in this research (2 h to 2 weeks depending on temperature) may account for this descrepancy. Longer tests may yield more conservative results for potentiostatic exposures.

At this point no reasons can be identified for the lack of consistency between techniques reported. Conservative engineering practice would require that all three types of tests (both step methods yielded the same results) be performed and the most conservative results be used.

Conclusions

Since pitting or crevice corrosion can perforate and destroy thin-walled industrial equipment, the protection potential E_p represents a limiting potential that should not be exceeded.

One criticism of relatively rapid laboratory corrosion tests (both freely corroding and with externally applied current) has been that results might not correlate with in-service tests. The longer term potentiostatically derived protection potentials derived in this work tend to substantiate this criticism. Even longer term tests may prove to produce still more conservative results.

The lack of consistency between the protection potential results described in this research and the lack of a single most conservative test indicate a need for further research into the concept of a protection potential. This research should be confirmed by long-term industrial exposure tests.

Acknowledgments

This work was performed at Oklahoma State University and the University of Rhode Island under the sponsorship of the Materials Technology Institute of the Chemical Process Industries.

References

[1] Manning, P., *Corrosion*, Vol. 36, 1980, p. 468.
[2] Leckie, H., *Journal of the Electrochemical Society*, Vol. 117, 1970, p. 1152.
[3] Wilde, B. and Williams, E., *Journal of the Electrochemical Society*, Vol. 117, 1970, p. 775.
[4] Wilde, B. and Williams, E., *Journal of the Electrochemical Society*, Vol. 118, 1971, p. 1057.
[5] Steigerwald, R., *Corrosion*, Vol. 22, 1966, p. 107.
[6] Wilde, B., *Corrosion*, Vol. 22, 1972, p. 283.
[7] Leckie, N. and Uhlig, H., *Journal of Electrochemical Society*, Vol. 113, 1966, p. 1262.
[8] Streicher, M., *Journal of the Electrochemical Society*, Vol. 103, 1956, p. 375.
[9] Wilde, B., *Localized Corrosion*, National Association of Corrosion Engineers, Houston, TX, 1974, p. 342.
[10] France, W. and Greene, N., *Corrosion*, Vol. 26, 1970, p. 1.
[11] Defranoux, J., *Corrosion Science*, Vol. 3, 1963, p. 75.
[12] Lizlovs, E. and Bond, A., *Corrosion*, Vol. 31, 1975, p. 219.
[13] Smialowska, Z. and Czachor, *British Corrosion Journal*, Vol. 4, 1969, p. 138.
[14] Schwenk, W., *Corrosion Science*, Vol. 5, 1965, p. 245.
[15] Kolotyrkin, J., *Journal of the Electrochemical Society*, Vol. 108, 1961, p. 209.
[16] Morris, P., "Use of Rapid-Scan Potentiodynamic Techniques to Evaluate Pitting and Crevice Corrosion Resistance of Iron-Chromium-Nickel Alloys," *Galvanic and Pitting Corrosion—Field and Laboratory Studies, STP 576*, American Society for Testing and Materials, Philadelphia, 1976, pp. 261–275.
[17] Lee, T., "A Method for Quantifying the Initiation and Propagation Stages of Crevice Corrosion," *Electrochemical Corrosion Testing, STP 727*, American Society for Testing and Materials, Philadelphia, 1981, pp. 43–68.
[18] Baboian, R. and Haynes, G., "Cyclic Polarization Measurements—Experimental Procedure and Evaluation of Test Data," *Electrochemical Corrosion Testing, STP 727*, American Society for Testing and Materials, Philadelphia, 1981, pp. 274–281.
[19] Newman, R., Isaacs, H., and Alman, B., *Corrosion*, Vol. 38, 1982, p. 261.
[20] Suzuki, T. and Kitamura, Y., *Corrosion*, Vol. 28, 1972, p. 1.
[21] Zakipour, S. and Leygraf, C., *Corrosion*, Vol. 37, 1981, p. 21; and Vol. 38, 1982, p. 180.
[22] Man, H. and Gabe, D., *Corrosion Science*, Vol. 21, 1981, p. 713.
[23] Asphahani, A., *Materials Performance*, Aug. 1980, p. 9.
[24] Hronsky, P. and Duquette, D., *Corrosion*, Vol. 38, 1982, p. 63.
[25] McCafferty, E., *Journal of the Electrochemical Society*, Vol. 121, 1974, p. 1007.
[26] LaQue, F., *Materials Performance*, Aug. 1984, p. 34.
[27] Uhlig, H., *Materials Performance*, Aug. 1983, p. 35.
[28] France, W., "Crevice Corrosion of Metals," *Localized Corrosion—Cause of Metal Failure, STP 516*, American Society for Testing and Materials, Philadelphia, 1976, pp. 164–200.
[29] Galvele, J., "Pitting Corrosion," *Corrosion: Aqueous Processes and Passive Films*, Academic Press, New York, 1982, pp. 1–57.
[30] Wilde, B. and Williams, E., *Electrochimica Acta*, Vol. 16, 1971, p. 1971.
[31] Tromans, D. and Frederick, L., *Corrosion*, Vol. 39, 1983, p. 305.
[32] Bates, J., *Corrosion*, Vol. 29, 1972, p. 28.
[33] Allen, B., Heidersbach, R., and Mealy, S., *Proceedings of the Offshore Technology Conference*, Paper 3856, Houston, TX, May 1980.
[34] Lee, T. and Tuthill, A., *Materials Performance*, Vol. 22, No. 1, Jan. 1983, p. 48.
[35] Riggs, O. and Locke, C., *Anodic Protection*, Plenum Press, New York, 1981.
[36] Pourbaix, M., *Corrosion*, Vol. 26, 1970, p. 26.
[37] Verink, E., *Corrosion*, Vol. 23, 1967, p. 371.

[38] Verink, E., "Construction of Pourbaix Diagrams for Alloys with Special Application to the Binary Fe-Cr System, Report to the Advanced Research Projects Agency, University of Florida, Gainesville, FL, June 1970.
[39] Hubbell, M., "Experimental Potential-Pit Diagrams for Stainless Steel," Masters thesis, University of Rhode Island, Kingston, RI, 1982.
[40] Price, C., Maschino, S., and Traylor, L., *Proceedings of the 6th Heat Pump Technology Conference*, Tulsa, OK, 1983.
[41] Sedricks, A. J., *Corrosion of Stainless Steels*, John Wiley and Sons, New York, 1979.
[42] Hultquist, G. and Leygraf, C., *Materials Science and Engineering*, Vol. 42, 1980, p. 199.
[43] Cusamano, R., "The Establishment of a Three Dimensional (Potential-pH-Composition) Diagram for Binary Fe-Cr Alloys in 0.1 Molar Chloride Solutions," Masters thesis, University of Florida, Gainesville, FL, 1971.
[44] Thibeau, R., Brown, C., Goldfarb, A., and Heidersbach, R., *Journal of the Electrochemical Society*, Vol. 127, 1980, p. 37.
[45] Thibeau, R., Brown, C., Goldfarb, A., and Heidersbach, R., *Journal of the Electrochemical Society*, Vol. 127, 1980, p. 1702.
[46] Thibeau, R., Brown, C., Goldfarb, A., and Heidersbach, R., *Journal of the Electrochemical Society*, Vol. 127, 1980, p. 1913.
[47] Anderson, D., Statistical Aspects of Crevice Corrosion in Sea Water," *Galvanic and Pitting Corrosion—Field and Laboratory Studies, STP 576*, American Society for Testing and Materials, Philadelphia, 1976, pp. 231–242.

Himashu Jain,[1] *Tae-Moon Ahn,*[2] *and Peter Soo*[1]

A Technique for Characterizing Crevice Corrosion Under Hydrothermal Conditions

REFERENCE: Jain, H., Ahn, T.-M., and Soo, P., **"A Technique for Characterizing Crevice Corrosion Under Hydrothermal Conditions,"** *Laboratory Corrosion Tests and Standards, ASTM STP 866,* G. S. Haynes and R. Baboian, Eds., American Society for Testing and Materials, Philadelphia, 1985, pp. 337–357.

ABSTRACT: A technique was developed to monitor crevice corrosion of Grade-12 titanium in a high magnesium synthetic brine under hydrothermal conditions. The current between the cathode and anode and the potential of the whole crevice assembly provide information on the various stages of corrosion. Occasionally, the decoupled potential of the cathode and anode are measured to give supporting information about the crevice conditions. A parallel test is run on a specimen that has small wells to collect crevice solution whose pH is determined at room temperature.

The current/potential results show that the crevice corrosion incubation period for a Grade-12 titanium crevice formed between two Teflon® plates is approximately two days at 150°C. Optical and scanning electron microscopy (SEM) observations show that the corrosion starts as isolated pitting that spreads along the surface as shallow pits. The corrosion conditions change significantly as the titanium oxide corrosion product fills the crevice, and the rate of corrosion may be greatly reduced after several days. The rate of crevice corrosion of commercial purity (Grade-2) titanium under similar conditions is approximately three orders of magnitude higher. In this case, active dissolution of metal starts during the initial heating of the autoclave, and the incubation period is negligible.

KEY WORDS: crevice corrosion, titanium alloys, brines, pitting, hydrothermal conditions, electrochemical techniques, incubation period

In the disposal of high-level radioactive waste in a deep rock salt repository the metal container must retain its integrity for a period of 300 to 1000 years while the fission product nuclei decay to low levels. Titanium Grade-12 is a candidate container material that in high-temperature brine is susceptible to corrosion, and this material must be adequately characterized to determine its capability to withstand failure by corrosion for very extended times. Commercially pure titanium is known to be susceptible to pitting and crevice corrosion

NOTE: This work was performed under the auspices of the U.S. Nuclear Regulatory Commission.

[1]Associate metallurgist and metallurgist, respectively, Department of Nuclear Energy, Brookhaven National Laboratory, Upton, NY 11973.

[2]Metallurgist, IBM Thomas Watson Research Center, Yorktown Heights, NY 10598.

Copyright© 1985 by ASTM International www.astm.org

in seawater and other chloride containing environments above room temperature [*1–4*]. Grade-12 titanium was initially believed [*5*] to be resistant to these types of corrosion. Recently, an investigation [*6*] at Brookhaven National Laboratory gave the first indication of crevice corrosion of Grade-12 titanium in brine at 150°C. Continuation of this work has confirmed the initial observation and determined that the severity of corrosion is enhanced when the brine solution is oxygenated. The corrosion product is found to be a mixture of anatase, rutile, and lower oxides of titanium. In general, the extent of crevice corrosion of Grade-12 titanium is much less than that for Grade-2 titanium, and its presence may be limited to certain ranges of test conditions.

Usually the crevice corrosion of passive metals in a chloride solution is believed to proceed in four stages [*7–11*]. In the first stage, oxygen is consumed within the crevice at a faster rate than can be supplied from outside, thus forming an oxygen concentration cell. As the thickness of passive oxide film within the crevice increases, the potential of the metal rises. In the second stage, the cathodic reaction is slowly moved to the freely exposed external surface. As this stage proceeds, the pH decreases and the concentration of chloride ion within the crevice solution increases in order to maintain charge neutrality. During the third stage, the crevice solution becomes sufficiently aggressive for the passive film to break down. In the final stage, the metal within the crevice continues to dissolve actively and crevice corrosion propagates in a self-sustaining manner.

This model of crevice corrosion is very general, and details of the mechanisms for each stage may vary considerably from metal to metal. For example, Oldfield and Sutton [*9*] have listed ten different categories of variables that determine the behavior of a particular crevice. Therefore, considering the complexity of a realistic crevice, an experimental characterization of each stage is very important. Note, also, that the stages of crevice corrosion may be divided into two parts. There is an incubation period during which corrosion conditions develop within the crevice but no major loss of metal results, and there is a propagation period commencing with rapid corrosion in the crevice region.

In the past, several direct and indirect experimental methods have been developed to monitor various stages of crevice corrosion [*12–25*]. The direct methods [*12–15,18,22*] use an artificial crevice and monitor its current or potential without disturbing the electrochemistry, whereas indirect methods make use of external electrochemical measurements. Most of these methods have been primarily developed for measurements under ambient conditions. However, Taylor [*24*] and more recently Taylor and Caramitas [*23*] and Diegle [*4*] have developed techniques suitable for testing under hydrothermal conditions. In the cell and specimen design by Diegle, the current between the cathode and anode and the potential of the whole crevice assembly are monitored continuously to determine the end of incubation and onset of active corrosion. In the experimental designs developed by Taylor et al in-situ crevice pH is also monitored; however, the crevice gap is too large for Grade-12 titanium to attain active corrosion conditions. In the present work we have used very small crevice gaps (sufficient

to initiate crevice corrosion of TiCode-12) as well as incorporated certain features to determine the final pH of the crevice solution at room temperature. Also, a plane circular crevice geometry has been used to make future modeling of corrosion kinetics mathematically simple. For the purpose of comparison, results on a Grade-2 titanium crevice are also included. To support the predictions from electrochemical measurements, the surface and morphology of corroded specimens were extensively studied using optical and scanning electron microscopes. Presently, the experiments are conducted at 150°C in brines of different concentration and pH, but do not include any studies on the effect of irradiation on crevice corrosion.

Equipment Design and Experimental Procedures

Materials

The chemical compositions of Grade-12 and Grade-2 titanium sheets as supplied by the vendor are given in Table 1. A thicker sheet was used for pH measurements to provide sufficiently deep wells for crevice solution to be collected.

The chemical composition of the test solution, commonly referred to as WIPP Brine A in the nuclear waste management literature, is given in Table 2. This is a high-magnesium, nearly-saturated brine solution representative of one that would be present at one of the proposed sites for nuclear waste disposal in New Mexico [*26*]. To lower the pH of the solution appropriate amounts of hydrochloric acid were added. To increase the dilution, doubly distilled water was added.

Cell Design

A schematic diagram of the autoclave assembly and the measuring equipment is shown in Fig. 1*a*. The bolted top of a 3.8-L (1-gal) Type 316 (Unified Numbering System [UNS] 531600) stainless steel vessel (A) was modified to allow the access of a reference electrode (RE), a thermocouple (TC), and two leads that were connected to the cathode (CC) and crevice specimen (CS). In all cases insulated feed-through assemblies (Conax type) provided leak tight connections. The titanium lead wires were covered with Teflon® for electrical insulation from the solution. An inlet near the top of the cylindrical surface of the autoclave was machined to connect a pressure gage (PG), a safety rupture disk (RD), and a gas control valve (GV). An electrical furnace (H) with a temperature controller heated the autoclave to the desired temperature. To avoid corrosion of the autoclave, a Teflon® liner (L) was used to isolate brine from the steel parts; the chromel-alumel thermocouple was encased in a titanium sheath.

The silver/silver chloride reference electrode (RE) consisted of a thick wall Teflon tube that was fixed to the autoclave head through a Conax fitting, and whose lower end provided a junction with the brine solution through a porous

TABLE 1—*Vendor supplied chemical analysis of Grade-12 and Grade-2 titanium, weight percent.*

Titanium Alloy	Carbon	Iron	Nitrogen	Molybdenum	Hydrogen	Oxygen	Nickel	Titanium
Grade-12								
current specimen	0.009	0.10	0.010	0.27	0.007	0.13	0.84	balance
pH specimen	0.013	0.13	0.012	0.31	0.008	0.13	0.7	balance
Grade-2								
current specimen	0.008	0.05	0.004	...	0.005	0.07	...	balance

TABLE 2—*Composition of WIPP Brine A.*

Component	Concentration, ppm by weight
Na^+	42 000
K^+	30 000
Mg^{+2}	35 000
Ca^{+2}	600
Sr^{+2}	5
Cl^-	190 000
SO_4^{-2}	3 500
I^-	10
HCO_3^-	700
Br^-	400
BO_3^{-3}	1 200

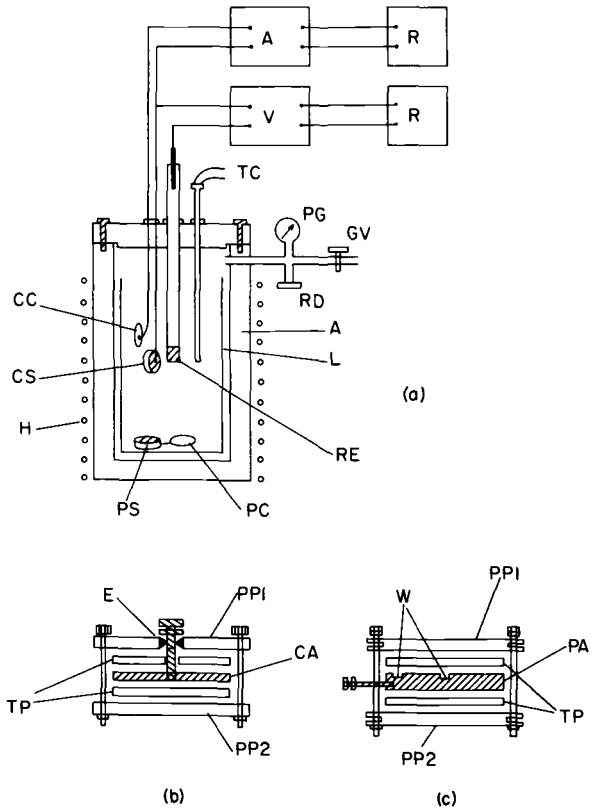


FIG. 1—*Design of the testing equipment for crevice corrosion under hydrothermal conditions (diagram not to scale).* (a) *Autoclave and current/potential measuring assembly.* (b) *Details of the anode assembly used in the current/potential measurements.* (c) *Details of the anode assembly used in the measurement of pH of the crevice solution.*

zirconia plug. The top end of the tube was closed with a Teflon plug with a silver wire passing through its center. The wire had a layer of silver chloride deposited by electrolysis to form a silver/silver chloride junction, which along with the upper half of the tube was maintained at room temperature. No correction was made for possible thermal junction potential that is expected to be a small constant factor and will not change present conclusions. The Teflon tube was filled with a saturated solution of potassium chloride. Additional solid potassium chloride was added to maintain saturation at an elevated temperature, which was found to be necessary to prevent local boiling of the potassium chloride under the test conditions used. The potential (versus silver/silver chloride) of the crevice assembly, consisting of a freely exposed cathode (CC) connected through an ammeter (Keithley 150AR) (A) to the anode (CS), was monitored with EG and G Model 173 potentiostat (V). No potential drop was observed across the ammeter. The values of current and potential were recorded on strip chart recorders (R). A separate crevice assembly was used to obtain specimens for pH measurements at room temperature. It consisted of an anode specimen (PS) connected to a freely exposed cathode (PC), and this was placed at the bottom of the Teflon liner.

Specimen Preparation and Configuration

In the present tests the cathode and anode of a crevice assembly were physically separated. The cathode, both in the case of current and pH measurement assemblies, was a polished 5-cm-diameter circular disk. The anode part of the current assembly is shown schematically in Fig. 1*b*. Here, the anode disk (CA) was mirror polished so that it could form a tight crevice when sandwiched between two Teflon plates (TP) of the same diameter. Thus, the crevice was formed on both sides of the specimen, and its area was equal to the total cathode area. A screw made of the same metal as the specimen was used to provide the electrical connection from the anode to the outside of the autoclave. The screw and the connecting leads were insulated from the test solution by an enamel (Glyptal, General Electric Company) layer (E). Only the edge of the specimen was freely exposed to the solution. Finally, a very narrow crevice was formed by tightening the titanium screws that pressed the Teflon disks under two larger titanium disks (PP1 and PP2). These disks did not show any signs of crevice corrosion.

As shown schematically in Fig. 1*c*, the design of the anode part of the pH assembly is essentially the same as that of the current assembly. In this case, however, a thicker disk (PA) was used to provide small wells (W) of diameter 0.14 cm (one at the center and another near the edge) to collect crevice solution. Also, the electrical connection to the cathode was placed at the side, and no enamel was used. The titanium pressure disks (PP1 and PP2) had partly open holes to accommodate titanium screws so that this assembly can be quickly opened even after quenching it to liquid nitrogen temperature.

Test Procedure

Before starting a test, all the cathode and anode specimens were mirror polished and weighed to allow subsequent examination of the effects of crevice corrosion. The anode specimens were submerged in the test solution at room temperature and then assembled as shown in Figs. 1*b* and 1*c*. In this manner any uncertainty regarding the ingress of solution to the inside of the crevice was eliminated. The current-anode assembly was kept for one day under ambient conditions to cure the enamel. Before closing the autoclave, the brine solution was saturated with oxygen by bubbling the gas through it for a minimum of 1 h. Next, the electrical connections were made as shown in Fig. 1*a*, and the autoclave was kept under an oxygen pressure overnight to check for leaks in the system. This leak check became necessary because of highly corrosive effects of brine on stainless steel components, as evidenced by stress corrosion cracking of the autoclave after several tests. If no leak was detected, the oxygen overpressure was reduced to atmospheric level, and the autoclave was heated to the test temperature (~150°C). At this temperature, the equilibrium pressure of the brine solution was approximately 0.414 MPa.

During the recording of current and potential, the anode and cathode were coupled most of the time via the ammeter. Occasionally, the two electrodes were decoupled for a short time. After a few minutes the potential of the two electrodes reached stationary values, which were recorded, and then the usual connections were restored. In the present experimental arrangement the anode potential is measured with a reference electrode, which is placed outside the crevice. Therefore, at a later stage a change in crevice chemistry (from the bulk composition) will contribute junction potentials to the observed crevice potential. However, since the starting solution itself was highly concentrated, the relative change in composition was not expected to be very large. In the crevice corrosion testing of stainless steels where much larger crevices can be used, a reference electrode is placed internally to circumvent this problem [*23,25*]. Because of the requirement of very tight crevices in the case of Grade-12 titanium (see below), similar arrangements are not likely to produce crevice corrosion. Also, generally the metal surface does not corrode uniformly and, therefore, the error caused by junction potential cannot be eliminated completely.

The duration of a test at an elevated temperature was typically two weeks. At the end of the test, to facilitate rapid cooling, the furnace around the autoclave was replaced by a bucket containing ice and water. During this cooling, the contraction of crevice solution is likely to draw in the bulk solution and, therefore, affect the pH measurements. However, the data for pure water [*27*] suggest that cooling from 150 to 90°C causes contraction in volume by only 5%. When the temperature within the autoclave was below the boiling point of brine, an aliquot of the gases generated during corrosion was collected for chemical analysis by mass spectrometry. Then the autoclave was opened, and the pH-anode assembly was immediately quenched in liquid nitrogen to minimize any changes in the

chemistry of crevice solution while disassembling the crevice. The pH was measured with a microcombination probe (Model MI-410, Microelectrodes Inc.) after the crevice solution in the wells had warmed up to room temperature. The tip of the pH probe required the well diameter to be larger than 1.2 mm. Some error in the pH measurements might have been incurred because of the condensation of atmospheric moisture.

Finally, all four anode and cathode specimens were ultrasonically cleaned three or four times in distilled water and weighed after drying. The anode specimens were examined under optical and scanning electron microscopes (SEM) to determine the morphology of crevice corrosion. The corrosion on Grade-12 titanium surfaces was in the form of pitting rather than uniform crevice corrosion. Therefore, some of the specimens were sectioned across the thickness at low cutting speeds and examined in SEM to determine the shape of the pits. For Grade-2 titanium, which showed extensive crevice attack, the corrosion product was also analyzed by X-ray powder methods.

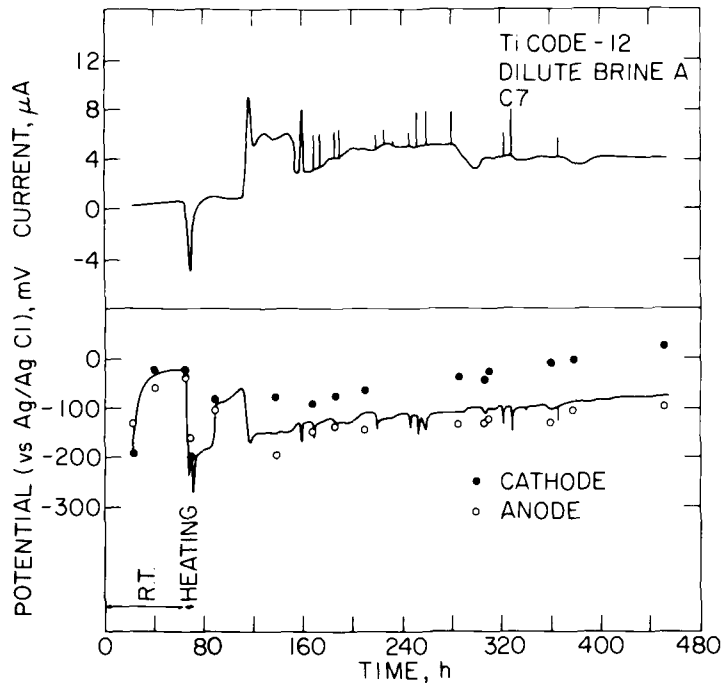


FIG. 2—*Time dependence of current and potential for Grade-12 titanium crevice in diluted (by a factor of ten) Brine A. The closed and open circles represent uncoupled potentials of the freely exposed cathode disk and the anode assembly, respectively. The steady state test temperature is ~150°C.*

Results

Current and Potential Measurements

The time dependent variation of current from cathode to anode, and of potential of the coupled crevice assembly, as shown typically in Fig. 2 for a Grade-12 titanium crevice in dilute Brine A (diluted from the composition given in Table 1 by a factor of ten) appears to be very complex. However, the behavior of all the tests shows the following common features:

1. In the beginning when the whole assembly is at room temperature, the crevice potential increases at a rate that decreases with time. During this period, the current is essentially zero and the uncoupled potential of the "cathode" specimen is higher than that of the anode assembly.
2. During heating of the autoclave, which takes a few hours, a strong negative current accompanied by a sharp decrease in crevice potential is recorded.
3. As the temperature approaches the testing value, the current again becomes zero and the crevice potential shows an increase. At this stage the uncoupled potentials of the cathode and anode specimens are about the same. For approximately one day, as the temperature is kept constant, the current and potential values do not show any appreciable change.
4. In the next stage, the current shows an abrupt increase, usually as a spike that subsequently returns to a high positive value. The crevice potential, at the same time, shows an abrupt decrease. After this abrupt change, the uncoupled cathode potential remains at a much higher value than that of the anode assembly.
5. In the following period, which covers most of the test time, the variation of current and potential does not show any reproducible pattern. However, on a positive background, many sharp peaks in current accompanied by decreases in potential are observed.

The general features described above for Grade-12 titanium crevices in dilute Brine A are also found for acidified undiluted Brine A (starting pH at room temperature = 4.2) (Fig. 3). Note that in this case, the current during the last few days of the test is reduced to a considerably lower value. In a similar test in neutral and undiluted Brine A (results not shown), the crevice current was reduced to such low values at an even earlier time. Figure 3 shows that after 300 h, although the difference between the uncoupled cathode and anode potentials does not change appreciably, the crevice current continues to decrease. This suggests an increasing resistance to the corrosion process. Also note that during this period the potential of the whole crevice assembly increases gradually.

The current/potential behavior of Grade-2 (commercially pure) titanium crevice in neutral Brine A is shown in Fig. 4; the decoupled potentials were not measured in this case. This figure shows several important differences as compared to Grade-12 titanium crevices. First, the crevice current is approximately three orders of magnitude higher. Although the behaviors of the crevice potential

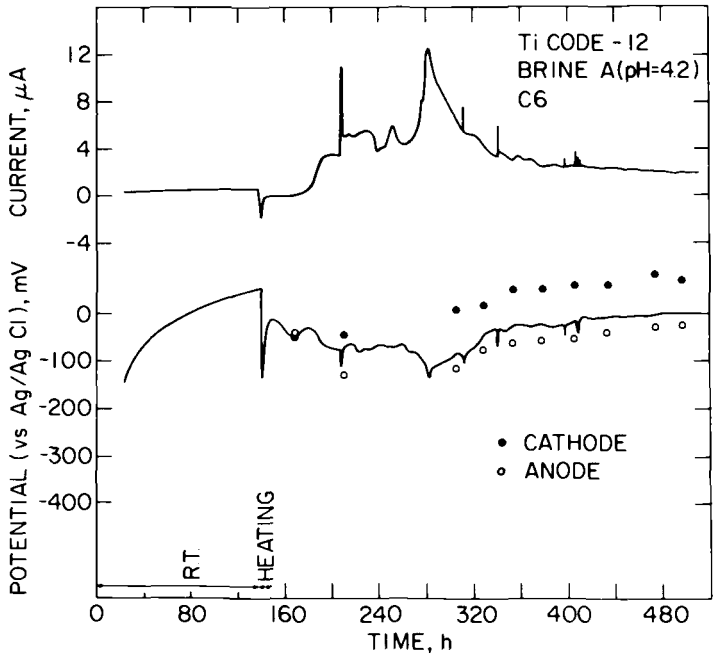


FIG. 3—*Time dependence of current and potential for a Grade-12 titanium crevice in acidic Brine A (pH = 4.2). The closed and open circles represent the uncoupled potentials of the cathode and anode. The steady state test temperature is ~150°C.*

and current at room temperature are similar for both metals, the Grade-2 titanium crevice does not show any negative current during heating. Instead, the next stage of abrupt increase in current starts during heating. There are no further spike-like features. Finally, after about 125 h the crevice current not only approaches zero, but changes polarity.

Morphological Observations

The extensive crevice corrosion of the Grade-2 titanium specimen, which is initially mirror polished and circular in shape, is evident from the picture taken after the test (Fig. 5). Although the whole metal surface corroded, the attack was most severe near the edge. The loss of metal from an isolated area of the cathode specimen, an unusual feature, is shown in Fig. 6. Otherwise, the cathode specimens developed a thin strongly adherent oxide film. The X-ray powder diffraction analysis of the anode corrosion product identifies it as mostly rutile (titanium oxide), but a few lines could only be related to titanium hydride.

In the case of Grade-12 titanium crevices, the extent of corrosion was much less and the crevice gap appeared to be a critical parameter for the development of corrosive conditions within the crevice. Thus, a specimen corroded more or less uniformly (on a coarse macroscopic scale) if the crevice gap was small and

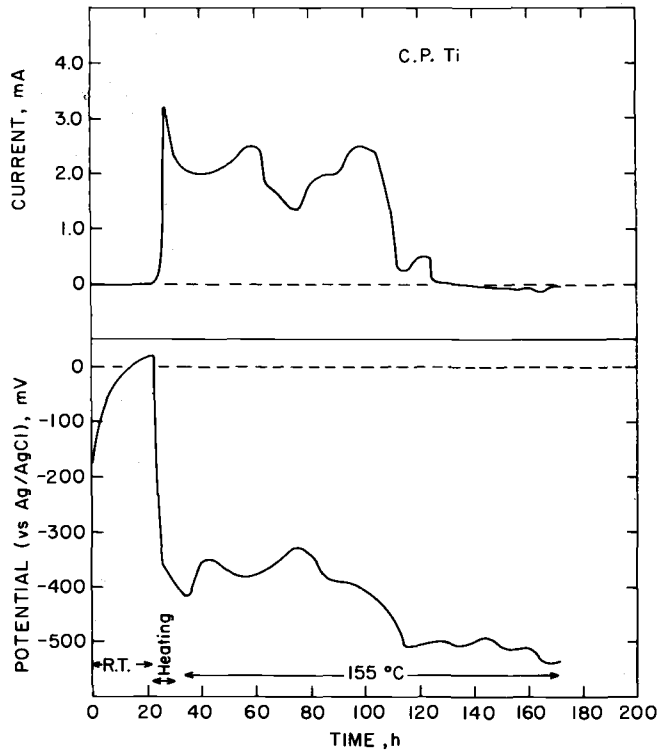


FIG. 4—*Time dependence of current and potential for a Grade-2 titanium crevice in Brine A.*

uniform. The corrosion was much less in the areas containing relatively large volumes of the solution such as in the center of a specimen (Fig. 7) or around the pH-wells (Fig. 8).

An examination of the corroded surface under an optical microscope shows that corrosion starts in small isolated areas. During the early stages (Fig. 9), a pit is formed, which at a later stage becomes filled with a white corrosion product. The arrow in the macrograph of Fig. 10 (taken under oblique light incidence) points to one such pit that has been covered under a mound of corrosion product. This product has been identified as mostly rutile, although initial oxidation of titanium results in the formation of a protective layer of anatase (titanium oxide). Transformation of titanium to rutile requires a 5.3% increase in volume. Thus, corrosion will produce large stresses in the crevice and the oxide prefers to grow in a direction that would accommodate such stresses. This is demonstrated in Fig. 11 by the alignment of oxide covered pits along the scratches in the adjoining Teflon disk.

Figure 12 shows a vertical cross section through a pit formed on a Grade-12 titanium crevice specimen. As the metal corrodes, the oxide grows above (Area A) as well as under (Area B) the original surface of the specimen. Because of

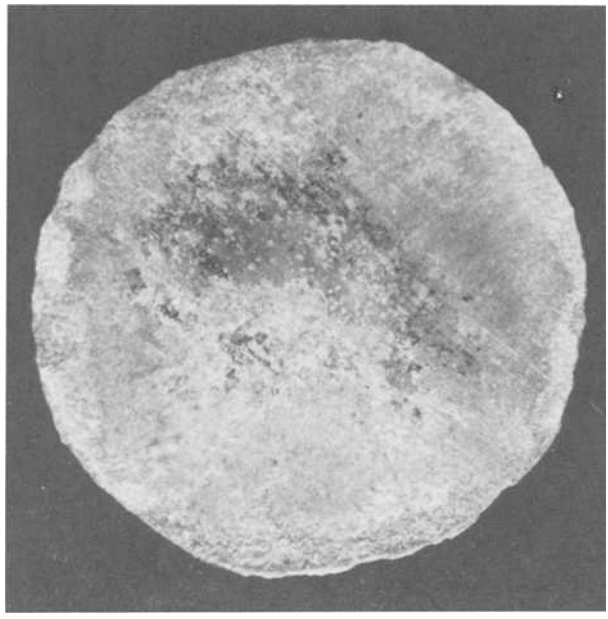


FIG. 5—*Severely corroded Grade-2 titanium crevice anode after test described in Fig. 4.*

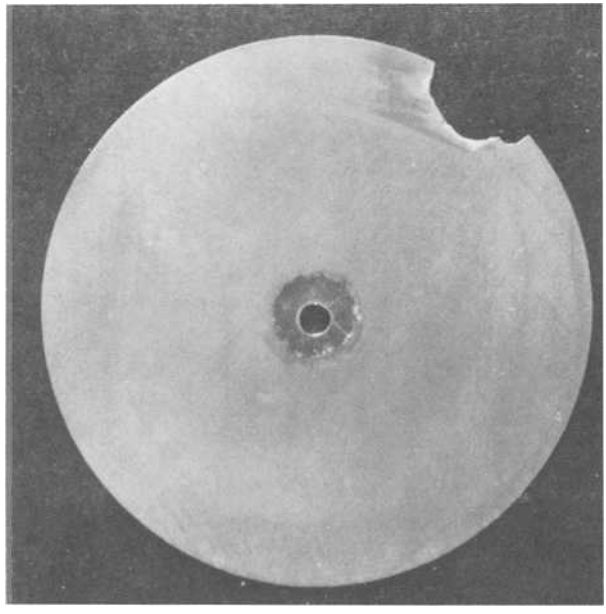


FIG. 6—*Freely exposed Grade-2 titanium crevice cathode after the test described in Fig. 4. Note the unusual loss of metal in the upper corner.*

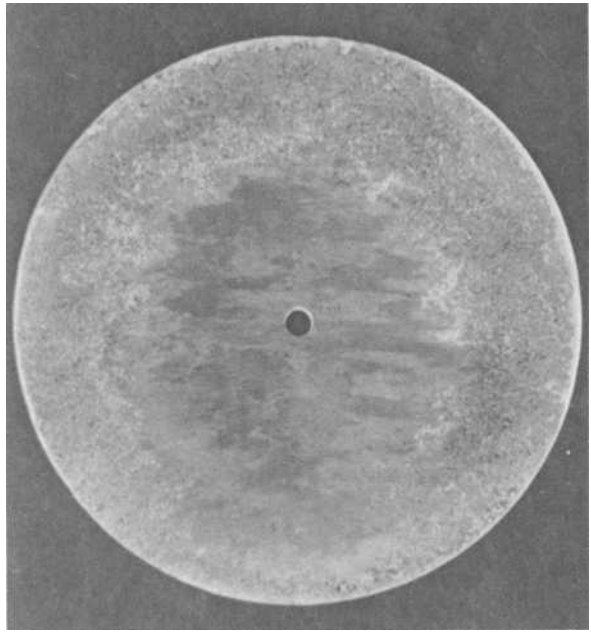


FIG. 7—*A Grade-12 titanium crevice anode after the test in dilute Brine A showing corroded areas around the circumference. The central area shows only minor oxide film formation.*

the constraints on oxide growth in the vertical direction, the pit tends to grow horizontally. For this reason most of the pits are found to be rather shallow. Area C in Fig. 12 is also oxidized to some extent. Note that a large crack has been initiated in the pit region that propagates parallel to the crevice surface.

pH and Weight Measurements

In the initial experiments with Grade-12 titanium, the wells to collect crevice solution were 2.8 mm in diameter. Very little corrosion occurred in the vicinity of such large wells, and, therefore, the pH of the solution could not be considered representative of the crevice conditions. It was concluded that for crevice corrosion to occur in a Grade-12 titanium, the crevice volume should be very small. Therefore, in later experiments, the well diameter was reduced to 1.4 mm, which was the minimum possible to use the pH probe. Even for a well of this size, in some cases (for example, the central area in Fig. 8) much less corrosion occurred in its vicinity. Thus, the observed value of pH within a Grade-12 titanium crevice (listed in Table 3) may be considered as an upper estimate of the true value in the rest of the crevice. In the case of dilute Brine A, the pH of condensed moisture in the uniformly corroded area was as low as 1.8. The condensed moisture outside the crevice had a pH of 5.9.

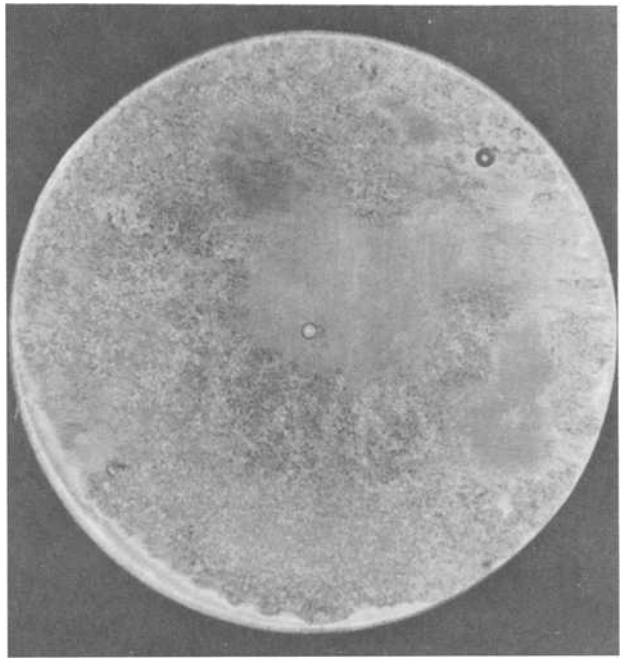


FIG. 8—*The pH measuring anode used in the same test as in Fig. 7. Note decreased corrosion near the wells.*

In all experiments with Grade-12 titanium, the weight of both current and pH anode specimens increased as a result of corrosion. The weight increase of the pH-anode (Table 3) was approximately one and a half times the increase for the current specimen. There are three possible reasons for this observation:

1. The freely exposed edge area of an anode acts as a cathode. This area, which contributes to the corrosion reaction, was appreciably larger for the thicker pH specimen.
2. The electrical resistance of the connecting path between cathode and anode was smaller for the pH assembly.
3. As suggested by one of the reviewers, the decoupling of cathode and anode of the current assembly might have caused temporary passivation of the anode surfaces. However, the fact that the crevice current and potential remained the same before and after the decoupling (for a few minutes) suggests that this step did not modify the crevice properties.

The weight increases for the cathode specimens were approximately two orders of magnitude smaller than for the anodes. The chemical analysis of the gas phase in the autoclave after the test showed large fractions of hydrogen (up to 60 mole

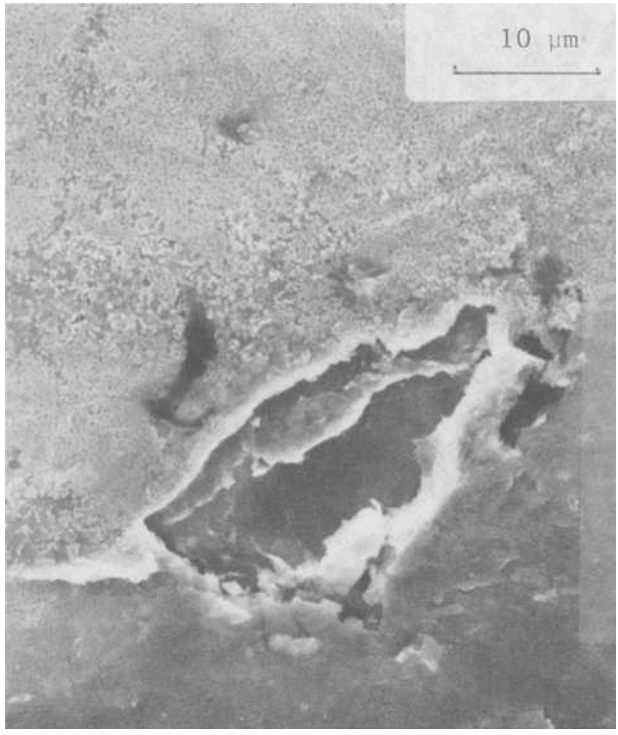


FIG. 9—*An SEM micrograph of early stages of pit formation in a Grade-12 titanium crevice where the crevice product has not filled the pit.*

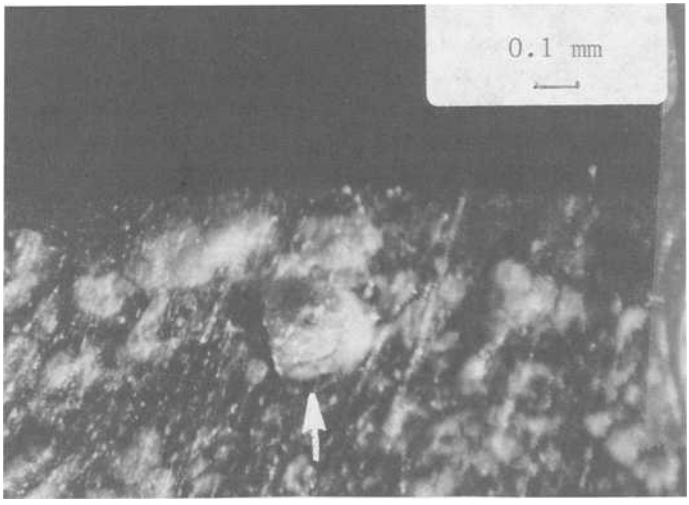


FIG. 10—*An optical micrograph of the pits on a Grade-12 titanium crevice specimen. Note the outgrowth of oxide as corrosion continues.*

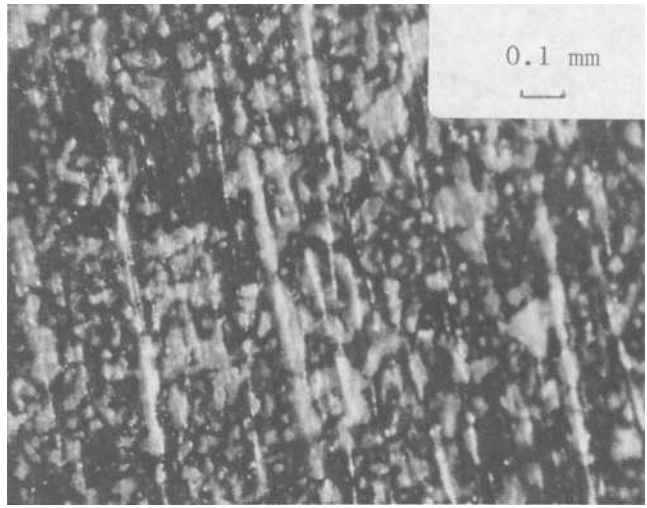


FIG. 11—*An optical micrograph of the surface of a Grade-12 titanium crevice specimen showing the alignment of oxide.*

percent). However, in these tests severe corrosion of the titanium screws was noticed and may be responsible for the generation of this gas.

In the case of the Grade-2 titanium crevice, the current anode was very severely corroded. After simple scraping, the specimen showed a 6.8% loss in its weight. Since all of the corrosion product could not be removed, the actual loss in weight was probably much larger.

Discussion

The present electrochemical and pH measurement results for a Grade-12 titanium crevice in Brine A at 150°C are in general agreement with the usually accepted model of crevice corrosion according to which the corrosion proceeds with oxygen depletion, increase in proton and chloride ion concentration, breakdown of the passive film, and then propagation by active dissolution. However,

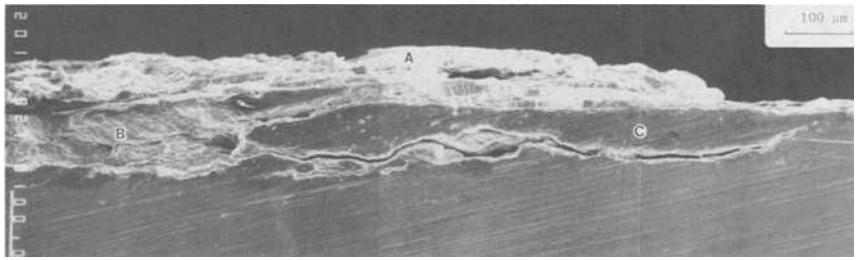


FIG. 12—*A vertical cross section through a pit formed on a Grade-12 titanium anode specimen.*

TABLE 3—*pH of the crevice solution and weight gain of the crevice anode after two-week tests in three brines.*

Bulk Solution	Crevice Solution, pH	Weight Gain of pH Specimen, g/cm^2
Neutral Brine A	3.2	7.0×10^{-4}
Acidic Brine A	3.8	9.5×10^{-4}
Dilute Brine A	2.8	12.3×10^{-4}

there are a few observations that point to additional details of the corrosion mechanism. With reference to Fig. 2, we find that initially at room temperature the crevice potential increases because of more or less uniform growth of oxide film both inside and outside the crevice. In the very early stage of testing, the anode specimen has been in contact with brine for a longer duration than the cathode specimen and therefore has a thicker oxide film and higher potential. At a later time (the second and third sets of uncoupled potentials) the oxide film on the cathode specimen has grown thicker than that on the anode specimen, but the temperature is too low to initiate the second stage of crevice corrosion, and the current remains negligibly small. Next, during heating of the autoclave to the test temperature the crevice potential shows a sharp decrease in response to the equilibrium conditions at the higher temperature. The reason behind the negative corrosion current during this period is not clear. After reaching the test temperature (~150°C), the growth of oxide film both on the anode and cathode specimens continues in a similar way to that at room temperature, but at a much faster rate. At the same time proton and chloride ion (as well as possibly some other anion) concentrations within the crevice change according to local potential, concentration gradients, and the diffusion coefficient of the various species. The variation of crevice potential in this time period is very complex and is determined by the contributions from all these sources. The current, however, remains very small, thus suggesting that the metal has not yet corroded significantly.

As the chemistry within the crevice becomes increasingly corrosive, the protective anatase film breaks down at least in parts of the crevice, and fresh metal is exposed to the solution. The active dissolution of the metal (Fig. 9) is characterized by a sudden increase in current and lowering of potential. This is the beginning of observable corrosion within the crevice. The ultimate corrosion product is porous rutile, which presumably is formed via the hydrolysis of some type of titanium-chloride complex. The production of rutile fills the actively corroding pit (Fig. 10) and thus inhibits metal dissolution to some extent as shown by a decrease in current. Once the metal dissolution state has commenced, the cathode remains at a much higher potential than the anode. This observation of decoupled potentials is direct proof of separation of anodic and cathodic parts in the present design.

The irregular variation of current as well as physical examination of the crevice specimens (Figs. 7 and 8) shows the inhomogeneous nature of corrosion within

the crevice, probably because of the high sensitivity of crevice solution chemistry with respect to crevice gap size, which may not have been constant throughout the crevice. The spikes in crevice current, which are always associated with lowering of potential, represent the onset of active dissolution in a new area within the crevice.

The extent of corrosion in a crevice is most simply determined from weight loss measurements. However, in the present case, such an approach will be very misleading for two reasons:

1. The corrosion product, rutile, cannot be easily removed from the specimen surface, and, therefore, we find a weight gain rather than a loss. However, the weight gain may not be a true measure of corrosion since some of the corrosion products may have dissolved in the solution or did not completely adhere to the specimen. Since the extent of corrosion is proportional to the total flow of electrical charge between anode and cathode, a better estimate of crevice corrosion can be obtained from the area under the current-time curve. In this respect physical observations agree with the integrated current obtained from data such as those shown in Figs. 2 through 4.
2. The mechanism of crevice corrosion is found to start as pitting. From the point of view of containment of nuclear waste, the maximum penetration rather than average metal loss is important. Development of cracks within the crevice (Fig. 12) would further reduce the container penetration time.

From earlier crevice corrosion test data [*28*], temperature has been shown to be a very important parameter, and no crevice corrosion in chloride-ion-containing environments is found at room temperatures. Therefore, to determine the incubation period in the present experiments we may assume the start of the incubation period to be when the crevice has just attained the test temperature. The end of the period would correspond to the sudden jump in current thereafter. With this definition, the incubation periods are determined to be 68, 45, and 44 h for the neutral, acidic, and dilute Brine A solutions, respectively. Within the uncertainty of the various experimental parameters these values are similar. We may therefore conclude that all three test solutions are equally corrosive as defined by the initiation time for active crevice corrosion. In the case of a Grade-2 titanium crevice the solution is so corrosive that the incubation period is essentially zero.

An important observation from all of the present current versus time measurements is that the current decreases after a few days, and in some cases (Fig. 3) it even approaches zero. Similar observations were made by Diegle [*4*] on Grade-2 titanium crevices. This suggests that eventually the rate of crevice corrosion approaches a near-zero value. One possible explanation for this observation is that the cathodic reaction is slowly stifled as oxygen is being consumed. However, in the present tests on Grade-12 titanium there was considerably more oxygen present than expected to be consumed from the weight

change measurements. Alternatively, such behavior is possible because of the corrosion products (oxides and so forth) within the crevice. This suggestion is supported by the increase in the crevice resistance as shown in Fig. 3 where at the end of the test the current is reduced to a very small value although the difference in decoupled cathode and anode potentials has not changed appreciably. Thus, if by some mechanism rate-inhibiting corrosion products are removed, crevice attack will be restarted.

Finally, the unusual observation of loss of metal from the Grade-2 titanium cathode specimen (Fig. 6) may be explained as follows. Initially, the crevice corrosion of Grade-2 titanium follows the four-stage mechanism described earlier. Then (after about 100 h, Fig. 4), sufficiently large amounts of corrosion products were deposited within the crevice to change the nature of corrosion reaction. At this stage, the cathodic reaction moved within the crevice and, therefore, the observed current approached zero; note that unlike the Grade-12 titanium crevice, the crevice potential did not show any increase in this case. The presence of titanium hydride in the corrosion product is consistent with the observations by Griess [2] who observed a large fraction of cathodic reaction to be reduction of hydrogen. With further changes in the crevice (during the period of negative current in Fig. 4) the cathodic reaction within the crevice became sufficiently strong to make the external cathode specimen act as an anode and, therefore, undergo dissolution.

Conclusions

By measuring the variation of current and potential with time, the experimental technique described above can be used to monitor the progress of crevice corrosion under hydrothermal conditions. The measurement of final pH of the crevice solution and of decoupled potentials of cathode and anode of the crevice assembly provide further information about the mechanisms of corrosion.

The results show that Grade-12 titanium is much less susceptible to crevice corrosion than Grade-2 titanium in Brine A at 150°C. Increasing the acidity of the brine solution to a pH = 4.2 or diluting it ten times has little effect on the incubation period. This suggests that the critical chloride concentration needed for the breakdown of passivity is already present in dilute Brine A.

Acknowledgment

The authors are thankful to R. L. Sabatini and G. Spira for their technical help, and to one of the reviewers for helpful comments.

References

[1] Beck, T. R., *Proceedings*, International Conference on Localized Corrosion, NACE, Williamsburg, VA, Dec. 1971.

[2] Griess, J. C., *Corrosion*, NACE, Vol. 24(4), 1968, p. 96.

[3] Bohlmann, E. G. and Posey, F. A., in *Proc. First International Symposium on Water Desalination*, Washington, DC, Oct. 1965, p. 306.

[4] Diegle, R. B., *Materials Performance*, National Association of Corrosion Engineers, March 1982, p. 43.
[5] Abrego, L. and Braithwaite, J. W., *Transactions*, American Nuclear Society, Vol. 34, 1980, p. 34.
[6] Ahn, T. M. and Soo, P., "Container Assessment—Corrosion Study of HLW Container Materials," BNL-NUREG-51449, NUREG/CR-2317, Vol. 1, No. 3, Brookhaven National Laboratory, Upton, NY, Jan. 1982.
[7] France, W. D., Jr., "Crevice Corrosion of Metals," *Localized Corrosion—Cause of Metal Failure, STP 516*, American Society for Testing and Materials, Philadelphia, 1972, p. 164–200.
[8] Fontana, M. G. and Greene, N. D., *Corrosion Engineering*, McGraw-Hill, New York, 1967.
[9] Oldfield, J. W. and Sutton, W. H., *British Corrosion Journal*, Vol. 13, Man. 1978, p. 13.
[10] Schreir, L. L., *Corrosion*, Vol. 1, Newnes-Butterworths, London, 1976, Chapter 1.6.
[11] Kruger, J. and Rhyne, K., *Nuclear and Chemical Waste Management*, Vol. 3, 1982, p. 205.
[12] Oldfield, J. W. and Sutton, W. H., *British Corrosion Journal*, Vol. 13, March 1978, p. 104.
[13] France, W. D. and Greene, N. D., *Corrosion*, National Association of Corrosion Engineers, Vol. 24, No. 8, 1968, p. 247.
[14] Bates, J. F., *Corrosion*, National Association of Corrosion Engineers, Vol. 29, No. 1, 1973, p. 28.
[15] Karlberg, G. and Wranglen, G., *Corrosion Science*, Vol. 11, 1971, p. 499.
[16] Peterson, M. H. and Lennox, T. J., *Corrosion*, National Association of Corrosion Engineers, Vol. 29, No. 10, 1973, p. 406.
[17] Efird, K. D. and Verink, E. D., *Corrosion*, National Association of Corrosion Engineers, Vol. 33, No. 9, 1977, p. 328.
[18] Rosenfeld, I. L. and Marshakov, I. K., *Corrosion*, SBIIA, Vol. 20, 1964, p. 115t.
[19] Jones, D. A. and Greene, N. D., *Corrosion*, National Association of Corrosion Engineers, Vol. 25, No. 9, 1969, p. 367.
[20] Wilde, B. E., *Corrosion*, National Association of Corrosion Engineers, Vol. 28, No. 8, 1972, p. 283.
[21] Lee, T. S., "A Method for Quantifying the Initiation and Propagation Stages of Crevice Corrosion," *Electrochemical Corrosion Testing, STP 727*, American Society for Testing and Materials, Philadelphia, 1981, p. 43–68.
[22] Siitari, D. W. and Alkire, R. C., *Journal of Electrochemical Society*, Vol. 129, No. 3, 1982, p. 481.
[23] Taylor, D. F. and Caramihas, C. A., *Journal of Electrochemical Society*, Vol. 129, No. 11, 1982, p. 2458.
[24] Taylor, D. F., *Corrosion*, National Association of Corrosion Engineers, Vol. 35, No. 12, 1979, p. 550.
[25] Tromans, D. and Frederick, L., *Corrosion*, National Association of Corrosion Engineers, Vol. 39, No. 8, 1983, p. 305.
[26] Molecke, M. A., "A Comparison of Brines Relevant to Nuclear Waste Experimentation," SAND83-0516, Sandia National Laboratory, Los Alamos, NM, May 1983.
[27] *Handbook of Physics and Chemistry*, CRC Press, 1982.
[28] *Titanium Information Bulletin*, IMI-5020/220, Imperial Metal Industries, Inc., Titanium, Birmingham, England, 1976.

DISCUSSION

N. Berke (written discussion)—Could nonsoluable corrosion products in the crevice displace corrosive solution and thus lower the measured currents in time? At the very least, would not the resistive path be increased?

[1]W. R. Grace, CPD Research, 62 Whittemore Ave., Cambridge, MA.

H. Jain (author's closure)—Yes, it is true that insoluble corrosion products (such as titanium oxide) displace the crevice solution and, therefore, increase the resistance to the corrosion reaction. However, considering the relative area of corroded surface the decrease in current appears to be larger than can be explained by this mechanism alone.

Masanobu Matsumura,[1] *Yoshinori Oka,*[1] *Satofumi Okumoto,*[1] *and Hiroyuki Furuya*[1]

Jet-in-Slit Test for Studying Erosion-Corrosion

REFERENCE: Matsumura, M., Oka, Y., Okumoto, S., and Furuya, H., **"Jet-in-Slit Test for Studying Erosion-Corrosion,"** *Laboratory Corrosion Tests and Standards, ASTM STP 866*, G. S. Haynes and R. Baboian, Eds., American Society for Testing and Materials, Philadelphia, 1985, pp. 358–372.

ABSTRACT: "Jet-in-slit" was used for erosion-corrosion tests on 6/4 yellow brass in a 3% sodium chloride solution together with free jet and submerged jet (common nozzle diameter of 1.6 mm). The latter jets are typical testing methods for evaluating the resistance of alloys to erosion-corrosion. Each specimen sustained a characteristic damage on its surface after 24-h running under common flow rate (0.4 L/min) of the test liquid. The most critical damage occurred on the jet-in-slit specimen.

Measurements through hydrodynamic as well as electrochemical techniques have proved that on a free jet specimen, the damage occurs only on the place of maximum shear stress, and on the submerged jet and jet-in-slit specimens occurs not only at the place of maximum shear stress but also at a place downstream where the flow velocity is considerably low but where impulsive pressure occurs intermittently. Based upon the experimental results obtained, the authors recommended the jet-in-slit for a standard testing method of erosion-corrosion resistance.

KEY WORDS: erosion-corrosion, tests, impingement corrosion, shear stress, yellow brass, sodium chloride solution, inlet tube corrosion, mass transfer rate, turbulence corrosion

Since copper-based alloys have excellent resistance to corrosion in seawater, they are widely used in ship propellers, marine heat exchanger tubes, and other applications where seawater is used. Copper-based alloys, however, have a weak point in that they are attacked by erosion-corrosion when they are brought into contact with flowing seawater at a high velocity. Erosion, referred to here, is not the same as defined by ASTM Terminology Relating to Erosion and Wear (G 40) (that is mechanical damage to materials caused by cavitation, impingement of liquid or solid particles) but is the type of erosion that may accelerate corrosion even though there is no mechanical damage to the material.

The most widely accepted mechanism of erosion-corrosion of this kind is as follows [*1*]. The surface of a copper alloy in a corrosive environment is covered

[1]Professor, assistant, and graduate students, respectively, Department of Chemical Engineering, Hiroshima University, Higashi-Hiroshima, Japan 724.

Copyright© 1985 by ASTM International www.astm.org

with a relatively thick but low-strength protective film of corrosion products. Copper-based alloys possess a corrosion resistant quality because of the film that acts as an insulation of the materials from corrosive environments. As fluid velocity on the copper alloy surface increases, shear stress on the metal surface increases accordingly. The film is broken away in a few areas as the shear stress reaches its critical value at a certain velocity (breakaway velocity). The underlying metal surface comes in direct contact with the corrosive liquid, and the portion acts as a local anode. The remaining oxide film serves as a local cathode.

The above mentioned explanation of the mechanism is not entirely applicable to the localized attack that occurs near the inlet ends of heat exchanger tubes (inlet tube corrosion). This type of attack is caused at a distance three or four time the tube diameter away from the tube inlet ends [*2*]. Shear stress in this area will never rise locally according to fluid dynamics. If the shear stress in the tube should vary locally, the testing method may be useless in which case the testing parameter is the average shear stress at the tube wall, calculated from the static pressure difference between the upstream and downstream of the tube [*3*]. Then, is this kind of erosion-corrosion caused by turbulence of the fluid flow rather than by shear stress? Turbulence intensity however is said to increase monotonously as the stream runs downward provided that Reynold's number is higher than a certain value. There are many other points to question: (1) Is the shear stress large enough in the impingement test? (2) Is the turbulence intensified? or (3) Are impingement attack, turbulence corrosion, and inlet tube corrosion caused by a common mechanism?

Loss and Heitz [*4*] proposed another mechanism for this kind of erosion-corrosion, that is, it may not come from a mechanical breakaway of the oxide film but may result from dissolution of the protective film in a high-velocity area where the mass transfer rate through the boundary layer increases. Fluid dynamics, however, points out that in general the area of larger fluid shear stress coincides with the area of larger mass transfer rate. Therefore, even this explanation is not sufficient to answer the foregoing questions.

An exception where no analogy exists between mass transfer and shear stress is the point of reattachment downstream of flow separation. At the reattachment point the average wall shear stress is zero, nevertheless the rate of mass transfer is considerably high in this region because of the high turbulence intensity. Realizing this fact Sydberger and Lotz [*5*] have recently conducted electrochemical measurements of mass transfer in turbulent pipe flow and found that sudden expansion or reduction of the tube diameter causes an evident increase in the mass transfer rate downstream. A sudden reduction of the pipe diameter, however, made the mass transfer rate maximum at the upstream edge, and it decreased monotonously downstream. This result cannot explain the general observation of the inlet tube corrosion where severe damage occurs at three or four times the tube diameter downstream from the inlet ends.

As the testing device for determining the erosion-corrosion resistance of metals to high-velocity boiler feed water, Wagner et al [*6*] used a unit successfully

about 40 years ago in which the water impinges upward on the face of a plain disk specimen and escapes at right angles through the slot in the face of the lower disk. The reason why the unit could simulate erosion-corrosion has not been explained.

In this study, the mechanism of erosion-corrosion of this kind has been investigated for 6/4 yellow brass in 3% sodium chloride solution using the conventional impingement test apparatus as well as jet-in-slit testing apparatus. As a result, it has been made clear that the erosion-corrosion is caused by two kinds of forces, and we proposed the jet-in-slit test as a standard testing apparatus for erosion-corrosion of this kind because it is capable of generating these two forces.

Test Apparatus and Test Results

Three types of jets were used in this study, namely, free jet, submerged jet, and jet-in-slit. Free jet is, as illustrated in Fig. 1, is the same as the one used in conventional impingement tests in which the liquid jet strikes at right angles with the specimen surface in the air. Submerged jet is a jet submerged in water. In the jet-in-slit, jet is injected into a narrow gap. The jets have the geometry and the flow conditions of the test liquid in common. The inside diameter of the nozzles is 1.6 mm; the gap between the nozzle top end and the specimen is 0.8 mm; and the flow rate of test liquid is 0.4 L/min. At this flow rate, the fluid velocity at the nozzle outlet was 3.3 m/s and the Reynold's number at that point was 8100.

The liquid film depth distribution under the above conditions on the free jet specimen is shown in Fig. 2 (upper). The average radial flow velocity distributions that were calculated by the following equation are also shown in the figure (lower)

$$\bar{u} = Q/2\pi rh$$

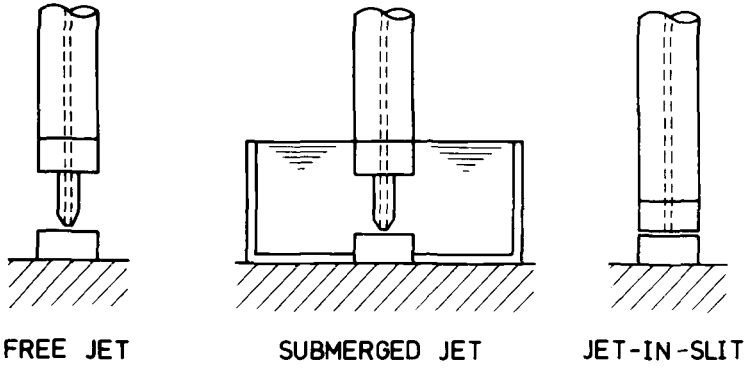


FIG. 1—*Three types of jets used in experiment.*

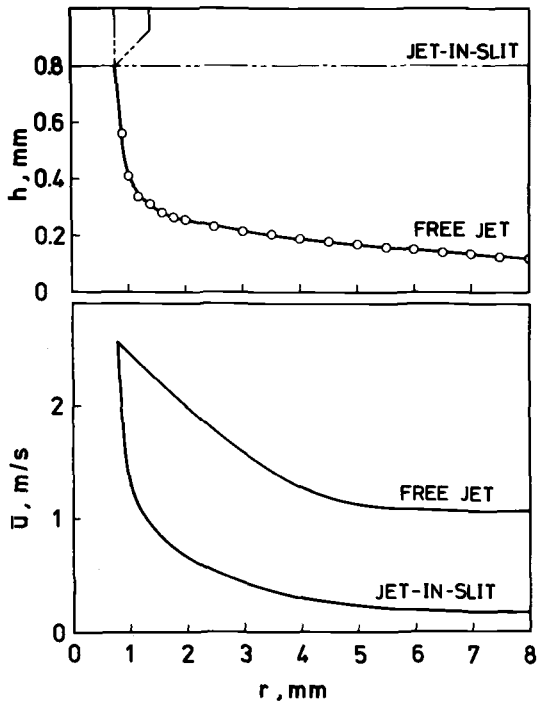


FIG. 2—*Liquid film depth distribution on free jet specimen* (upper) *and radial flow velocity distributions on specimens of free jet and jet-in-slit* (lower).

where

$\bar{u}$ = average radial flow velocity,
Q = flow rate (0.4 L/min),
r = distance from the center, and
h = liquid film depth.

The average radial flow velocity of the free jet is higher than that of the jet-in-slit because the liquid film of the free jet is thinner than that of the jet-in-slit in which liquid flow fills up the gap. The average radial flow rate distribution in the submerged jet is presumed to be intermediate between the free jet and the jet-in-slit.

A test with 6/4 yellow brass specimens (16 mm in diameter with a chemical composition of 59.77 copper, 0.28 iron, and the remainder zinc) in 3% sodium chloride solution (40°C) indicated that the weight loss of the specimens after 24 h was 9.7, 10.0, and 11.3 mg for the free jet, submerged jet, and jet-in-slit, respectively. Inspection of surface and cross section of the specimen after the tests showed that extreme corrosion was seen with the submerged jet and jet-in-slit as shown in Fig. 3. The cross section was measured with a surface

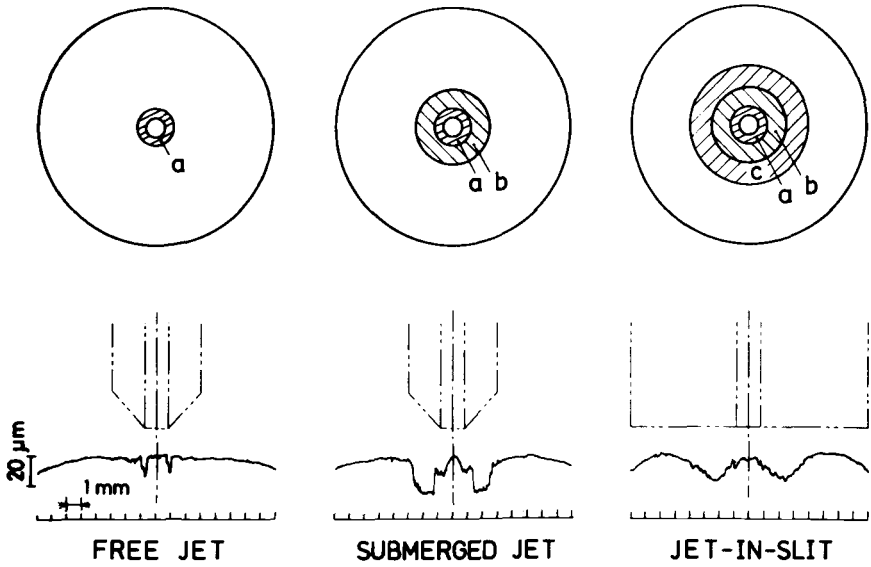


FIG. 3—*Sketches of surface and cross sections of specimens after 24-h test under flowing sodium chloride solution.*

roughness meter, so that the longitudinal direction is magnified 100 times with respect to the transverse direction. Attack *a* occurred at same position on each specimen. In addition, attacks *b* and *c* were recognized on the jet-in-slit specimen. In the cross section, however, the distinction between *b* and *c* was not clear. Figure 4 shows the scanning electron micrograph of the surface of specimens deeply and scarcely attacked with the jet-in-slit. The surface of the unattacked area is covered with a thick oxide film. On the contrary the attacked surface is stripped of the surface film, exposing metal grains as well as the hill and valley structure on the grain surface.

The test liquid used contains no solid particles, and it was confirmed that the fluid velocity was too slow to develop cavitation. The localized corrosion of the test specimen under such conditions may be regarded as erosion-corrosion.

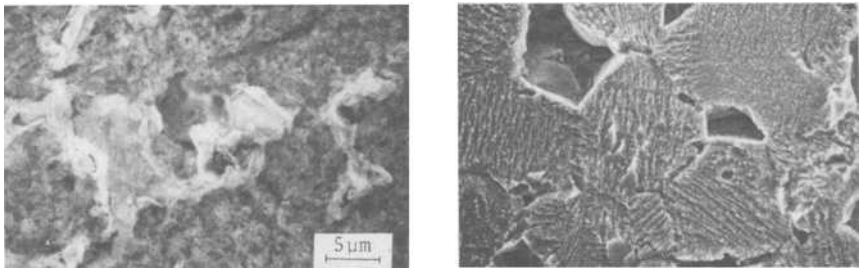


FIG. 4—*Scanning electron micrographs of jet-in-slit specimen surface attacked deeply* (right) *and scarcely* (left).

Discussion on Attack Mechanism

Shear Stress Distribution on Specimen Surface

The textbooks of fluid dynamics indicate that shear stress τ_0 caused by fluid running on the surface of an object is defined by the following equation

$$\tau_0 = \mu (du/dy)_{y=0} \tag{2}$$

where

μ = viscosity of the fluid and
$(du/dy)_{y=0}$ = velocity gradient normal to the wall (Fig. 5).

As it is impossible to measure directly the velocity gradient in the close vicinity of the wall, an arrangement was used in order to measure a pressure difference that is proportional to the velocity gradient: holes of 0.3 mm diameter were provided on the surface at a 0.5 mm interval and a hair was plastered in between (Fig. 5). The principle on which τ_0 is measured by the pressure difference Δp across two holes can be represented by the following equation

$$\tau_0 = \mu (du/dy)_{y=0} \propto u_1/y_1 \propto u_1 \tag{3}$$

$$\Delta p = p_1 - p_2 \propto u_1^2 \tag{4}$$

$$\tau_0 \propto \sqrt{\Delta p} \tag{5}$$

where

y_1 = a distance normal to the wall and smaller than the thickness of the boundary layer and
u_1 = fluid velocity at $y = y_1$.

If the velocity gradient from the wall surface to a distance y_1 is approximated to be constant, τ_0 is proportional to u_1/y_1 (Eq 3). On the other hand, the flow

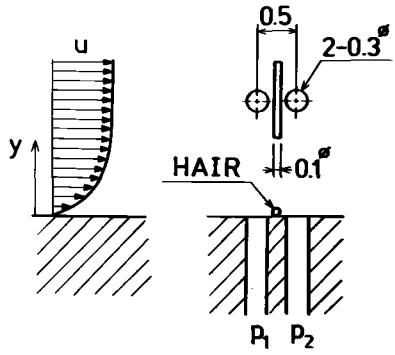


FIG. 5—*Velocity gradient normal to surface wall and arrangement to measure the velocity gradient.*

on the upstream side of the hair is prevented, which results in a pressure rise by the value corresponding to dynamic pressure, that is, Δp (Eq 4). If we put y_1 equal to the diameter of the hair, we obtain Eq 5. Although this method is inadequate for quantitative measurement because of the many approximations involved, it indicates at least the situations on the surface where τ_0 reaches maximum or zero.

The radial distribution of $\sqrt{\Delta p}$ was measured by the arrangement (Fig. 5). The results obtained for each nozzle are shown in Fig. 6. The dotted line in the figure indicates the nozzle's inside radius. In each of the jet types, $\sqrt{\Delta p}$ reaches maximum at near the parimeter of the jet and then falls as it moves toward the periphery of the specimen. Localized attack *a* in Fig. 3 is found on the section of each specimen where $\sqrt{\Delta p}$ is maximized. Therefore it may be determined that the attack *a* was caused by shear stress.

It should be also noticed that $\sqrt{\Delta p}$ of the jet-in-slit is zero at $r = 2.6$ mm, where the large attack *c* is observed and is negative thereafter. The fact that τ_0 reduces to zero at a point and then takes a reverse sign indicates that the flow is separated at that point, producing a vortex downstream. A theoretical computation by fluid dynamics revealed that a radial flow in a narrow slit causes separations [7]. The flow condition at the separation point gives zero shear stress.

It should be also pointed out that at the separation point the analogy exists between mass transfer and shear stress. Consequently zero mass transfer is expected at that point. Thus, it is true that a separation occurs in the neighborhood

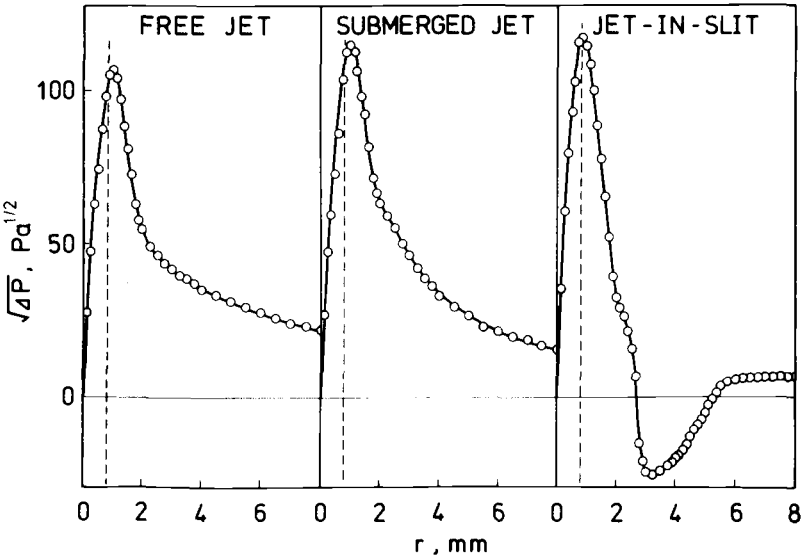


FIG. 6—*Distribution of* $\sqrt{\Delta p}$ *on each specimen.*

of the point where attack *c* is initiated in the jet-in-slit test, but this phenomenon does not give good reason for the development of the local attack that occurs in this neighborhood.

Measurement of Mass Transfer Rate on Specimen Surface

In order to determine whether or not attacks *b* and *c* were caused by acceleration of mass transfer in the attacked areas, as suggested by Loss and Heitz [*4*], a distribution of limiting currents that corresponds to the mass transfer rate, was measured by use of the electrochemical method, which was used by Sydberger and Lotz [*5*]. The arrangement consists of an anode of nickel plate with a relatively large area and a cathode of copper with a sufficiently small area (wire of 0.6 mm diameter) surrounded by another copper electrode that was also polarized separately in order to eliminate the mass transfer entry region (refer to Ref *5* for the reason) (Fig. 7). The electrolyte is composed of 0.01 mol/L each of potassium ferricyanide and potassium ferrocyanide and 1 mol/L of sodium chloride. When current is measured by gradually increasing the voltage applied across both electrodes, the current shows a constant value in a certain range irrespective of the voltage. This is the limiting current i_o, that is, generated when $Fe(CN)_6^{-3}$ ions reaching the cathode electrode surface by diffusion are reduced to $Fe(CN)_6^{-4}$, that is, i_o is proportional to the mass transfer rate.

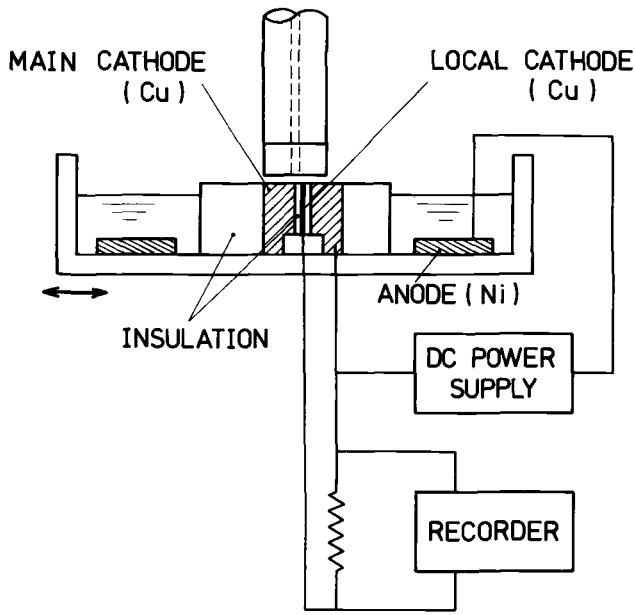


FIG. 7—*Arrangement for measuring distributions of limiting current.*

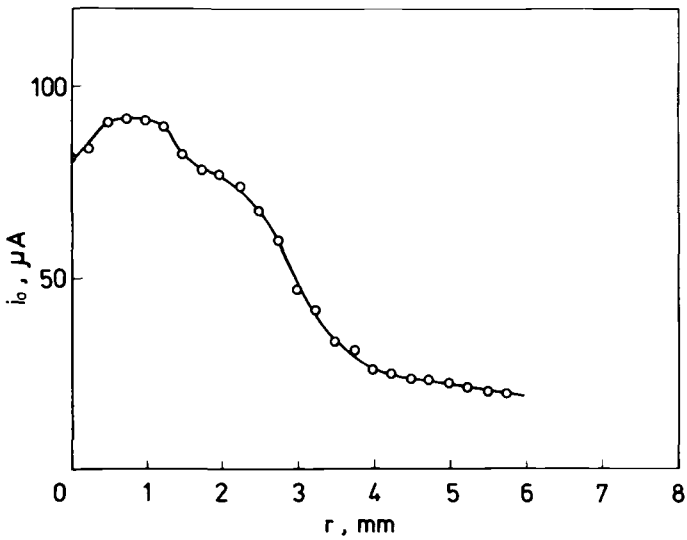


FIG. 8—*Distribution of limiting currents on a jet-in-slit specimen.*

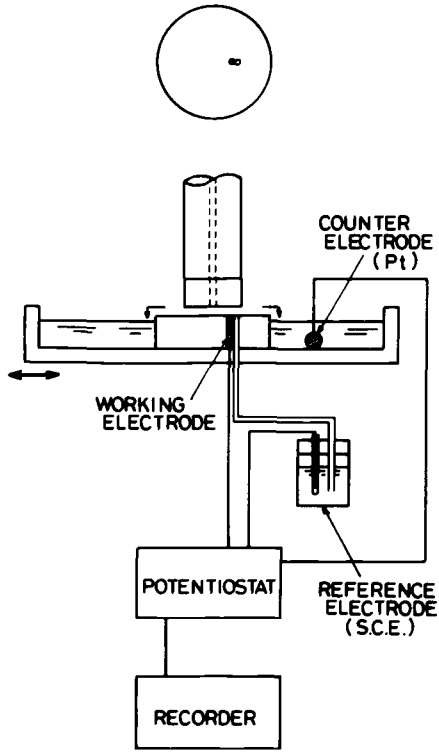


FIG. 9—*Arrangement for measuring polarization curves.*

Distributions of i_o on the surface of jet-in-slit specimen was measured by moving the cathode electrode in a horizontal direction. The i_o distribution (Fig. 8) has a close resemblance to the $\sqrt{\Delta p}$ distribution; it shows a peak near the perimeter of the jet, falling as it moves to the periphery of the specimen. Namely, the mass transfer rate is large where shear stress is large, as is generally recognized with respect to the mass transfer rate in the boundary layers.

No increase in i_o was recognized downstream from the separation point where the reattachment was expected. This may be attributed to the fact that flow velocity at the place is too slow to cause a definite reattachment. For these reasons, the mass transfer rate cannot account for the large attacks initiated at points *b* and *c*.

Measurement of Polarization Curve

A measuring apparatus as illustrated in Fig. 9 was set up for measurements of polarization behavior at various sections of the jet-in-slit specimen. The electrode was 6/4 yellow brass of 1 mm diameter. The capillary of the reference electrode (saturated calomel cell) was placed in polymethyl methacrylate resin in contact with the specimen to minimize the ohmic (IR) drop. The test liquid was 3% sodium chloride solution (40°C), and the sweep rate was 40 mV/min (stepwise 20 mV at intervals of 30 s).

Cathodic polarization curves were obtained for various sections of the specimen. The current value at which a sharp potential drop occurs is known as the limiting oxygen diffusion current density i_e, which was the largest at the perimeter of the jet, decreasing towards the periphery of the specimen. This tendency coincides with the result in Fig. 8.

Anodic polarization curves were obtained at the section of $r = 2.8$ mm on the jet-in-slit specimen as well as in static liquid (3% sodium chloride solution), (Fig. 10). Comparison of these curves indicates the following:

1. Jet-in-slit gives a far larger current density at the rising of the curve as compared with the one in static liquid.
2. On the curve of static liquid, two peaks are observed in the neighborhood of -80 and 360 mV, but in that of jet-in-slit the one at -80 mV is not observed.
3. On the curve of jet-in-slit, a multiple of peaks are observed over 400 mV, which are not observed with that of static liquid.

The fact that the jet-in-slit polarization curve showed a higher rising current density as compared with that of static liquid agrees with the result that the attack in jet-in-slit is larger than that of static liquid. Disappearance of peaks seems to be the result of the separation of oxides such as copper oxide or copper dioxide from the surface that sticks to the surface in static liquid. Many peaks that appeared at the potentials over 400 mV did not occur at the same potentials in repeated runs. This gave us the impression that generation of peaks depend not upon specific potentials but upon time.

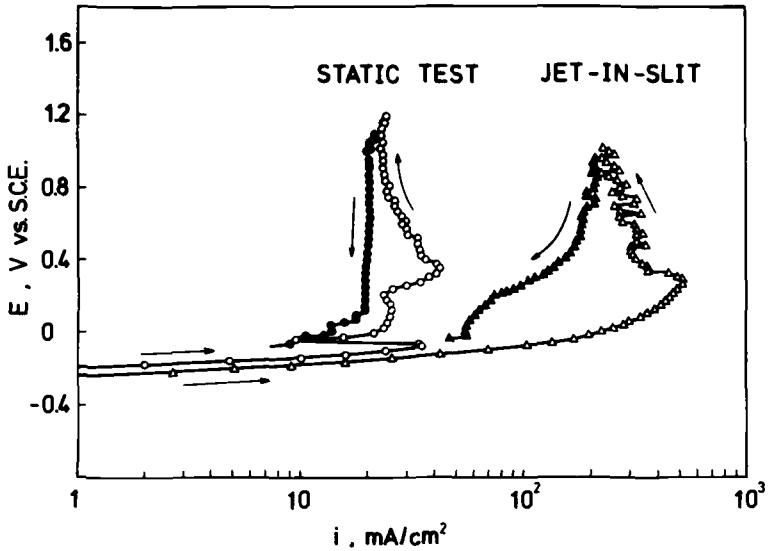


FIG. 10—*Anodic polarization curves in static test liquid and in jet-in-slit.*

In order to prove the above mentioned view, a potentiostatic polarization sweep was performed until the potential reached 360 mV, where the potential was maintained constant, and the variation of current with time was recorded. The results are shown in Fig. 11. Peaks appeared repeatedly even at a constant potential with intervals of several minutes. This suggests that growth and fracture of oxide films were repeated on the electrode surface.

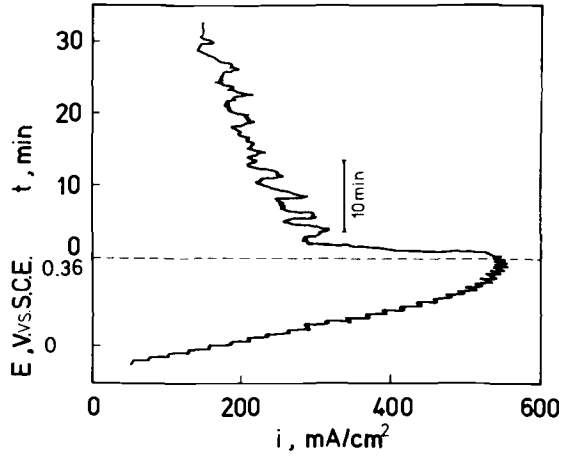


FIG. 11—*Anodic polarization curves, potentiostatic sweep* (lower half) *and current variation with time* (upper half).

The measurement of current was interrupted when a peak or valley appeared on the current-time curve at a constant potential, and the electrode surface was observed using a scanning electron microscope (Fig. 12). It can be clearly recognized that oxide films scarcely exist on the electrode surface at the peak (Fig. 12 upper), whereas thick oxide films cover the surface at the valley (Fig. 12 lower).

Separation of Grease Film

The above-mentioned experimental results clarified that the oxide film is broken away intermittently on the electrode surface. In order to identify the force that causes the breakaway of the oxide film, we made a thin film (0.1 mm thickness) of grease on a glass surface, placed it under the jet-in-slit nozzle, and watched the process of the film being broken away. Figure 13 (lower) is a photograph of the grease film directly under the jet, which shows that the grease film was continuously forced out by the shear stress toward the periphery. On the contrary, at the place where attack *b* or *c* occurs, the breakaway of the grease film progressed not continuously but suddenly, resulting in a small wedge shape at one time (Fig. 13, upper). This indicates that the force is an impulsive one that acts locally and momentarily.

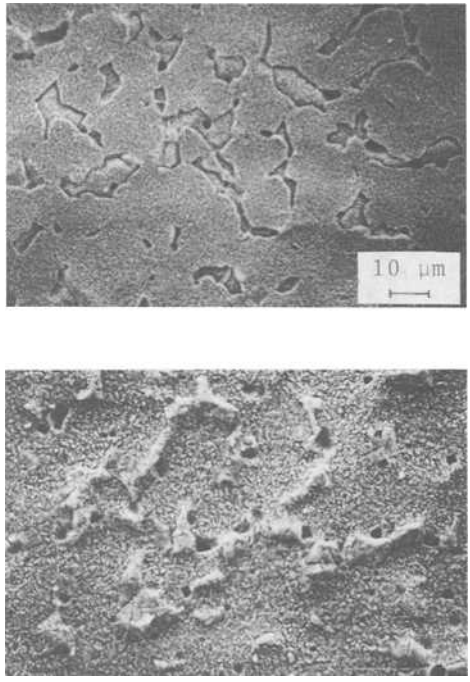


FIG. 12—*Scanning electron micrographs of electrode surface at peak* (upper) *and valley* (lower) *on a current-time curve.*

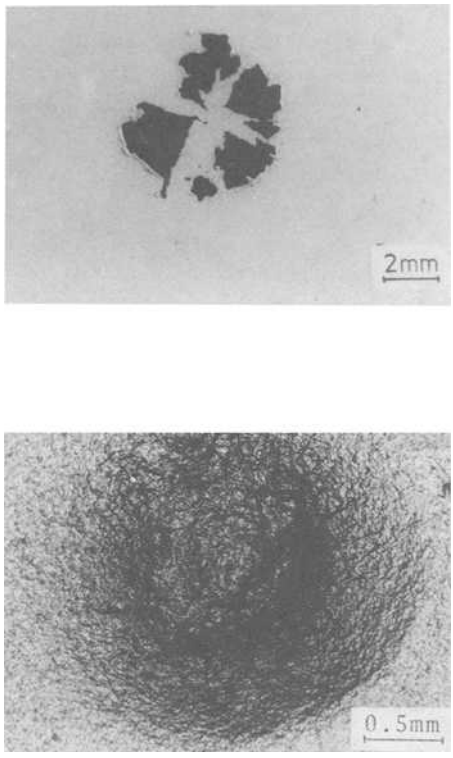


FIG. 13—*Separation of grease film on a glass surface under jet-in-slit nozzle* (upper) *and behavior of grease film directly under nozzle* (lower). (*The nozzle is nearly at the center of the upper photograph.*)

It is clear that the grease film and the oxide film are not the same, and the grease film can not exactly simulate the oxide film. But the grease film is insoluble in the solution. Thus it proves that the film breakaway was caused not by dissolution but by mechanical force. It has also been made clear that the force is different from the shear stress.

The sudden separation of the grease film occurred on the submerged jet specimen as well, but no separation was recognized on the free jet specimen.

The force occurs intermittently and acts impulsively. This would be the main reason why the force was not detected during the measurements of mass transfer and shear stress distribution. The mechanism of generating such impulsive force has not been established to date, but it should be noticed that such force is produced where the flow is decelerated abruptly. This may account for the reason why the erosion-corrosion is observed not at the highest velocity region but on the downstream side of deposited obstacles.

Conclusions

This study has established that in addition to the shear stress so far pointed out, there exists an intermittently occurring impulsive force that attacks the oxide film on copper alloy surfaces exposed to 3% sodium chloride solution. This kind of force can occur in areas subjected to a flow velocity of below 1 m/s, under normal pressure. This level of flow velocity can not cause cavitation to occur.

The jet-in-slit test brought about the oxide film fracture by impulsive force in addition to shear stress that was observed in the conventional impingement test. For this reason, the jet-in-slit method is suitable to test the resistance of metals to the erosion-corrosion.

Acknowledgments

The authors wish to express their gratitude to Messrs. A. Murata, Y. Tanaka, H. Funaya, and T. Ogasawara for their assistance in the experiments.

References

[1] Syrett, B. C., *Corrosion*, Vol. 32, No. 6, June 1976, pp. 242–252.
[2] Bremhost, K. and Lai, J. C. S., *Wear*, Vol. 54, No. 1, May 1979, pp. 87–100.
[3] Efird, K. D., *Corrosion*, Vol. 33, No. 1. Jan. 1977, pp. 3–8.
[4] Loss, C. and Heiz, E., *Werkstoffe und Korrosion*, Vol. 24, No. 1, 1973, pp. 38–48.
[5] Sydberger, T. and Lotz, U., *Journal of the Electrochemical Society*, Vol. 129, No. 2, Feb. 1982, pp. 276–283.
[6] Wagner, H. A., Decker, J. M., and Marsh, J. C., *Transactions, American Society of Mechanical Engineers*, Vol. 69, No. 4, May 1947, pp. 389–403.
[7] Ishizawa, S., *Transactions, Japan Society of Mechanical Engineers*, Vol. 31, No. 224, April 1965, pp. 535–552.

DISCUSSION

T. S. Lee[1] *(written discussion)*—What would be the expected effects of a longer test duration than the 24 h used? Specifically, would the pattern of attack exhibited after 24 h continue to evolve with each of the three methods? Would the shear stress calculations still be applicable to a more high roughened surface that might exist with longer test durations?

M. Matsumura (author's response)—The longest test duration so far was 24 h. With a prolonged test duration, for example 50 h, the patterns of attack will continue to develop until the surfaces of the specimen would be so roughened that they would affect the shear stress and flow conditions. Then, new patterns of attack may develop according to the altered shear stress distributions and flow conditions.

[1]LaQue Center for Corrosion Technology, Inc., P.O. Box 656, Wrightsville Beach, NC 28480.

T. S. Lee—The results of jet impingement tests in seawater have shown that the cathode surface area submerged in "quiescent" seawater strongly affects the depth of erosion-corrosion attack. What is the effective cathode area in the jet-in-slit method given the narrow gap between the nozzle top and specimen? Would IR drop considerations down this gap preclude use of a submerged cathode specimen connected to the smaller specimen subjected to the impinging jet?

M. Matsumura—The cathode area on the jet-in-slit specimen was mainly the area outside of the attack c. When a square plate (50 by 50 mm) was placed under the jet-in-slit nozzle for the disk specimen, the attack patterns were scarcely changed but the depth of erosion-corrosion was slightly larger than that of the disk specimen. This may be attributed to the increase of cathode area. Thus, our experience agrees with yours.

Richard S. Treseder[1] *and Edward A. Kachik*[2]

MTI Corrosion Tests for Iron- and Nickel-Base Corrosion Resistance Alloys

REFERENCE: Treseder, R. S. and Kachik, E. A., **"MTI Corrosion Tests for Iron- and Nickel-Base Corrosion Resistance Alloys,"** *Laboratory Corrosion Tests and Standards, ASTM STP 866,* G. S. Haynes and R. Baboian, Eds., American Society for Testing and Materials, Philadelphia, 1985, pp. 373–399.

ABSTRACT: The Materials Technology Institute (MTI) of the Chemical Process Industries, Inc. has selected a series of laboratory corrosion tests to provide guideline information on new wrought iron- and nickel-base corrosion resistant alloys. Data obtained from these procedures are expected to provide the materials engineer with a reasonable assessment of the probable utility of a new alloy in a variety of environments or corrosion conditions and thus facilitate the commercial usage of such alloys. The test procedures are based essentially on ASTM methods. Test procedures are specified in sufficient detail to insure comparable data being obtained by different laboratories. Two basic concepts are used: (1) in each test a critical test factor is selected as the criterion for corrosion resistance of the alloys and (2) a control alloy is selected for each test, specimens of the control alloy being supplied by MTI. There are five test procedures: one for general corrosion, two for crevice corrosion, and two for stress corrosion cracking.

KEY WORDS: corrosion, corrosion testing, concentrated cell corrosion, stress corrosion, MTI, iron-base alloys, nickel-base alloys

The Materials Technology Institute (MTI) of the Chemical Process Industries, Inc. has selected a series of laboratory corrosion tests to provide guideline information on new wrought iron- and nickel-base corrosion resistant alloys. Data from these tests are expected to provide the materials engineer with a reasonable assessment of the probable utility of a new alloy in a variety of environments or corrosion conditions and thus facilitate commercial usage of such alloys. This paper describes the test methods and the thinking that led to their selection. There are five tests: one for general corrosion, two for crevice corrosion, and two for stress corrosion cracking. The corrosion data from these tests are intended to supplement the alloy property and other corrosion data usually supplied by the manufacturer.

[1]Consulting corrosion engineer, 6272 Girvin Dr., Oakland, CA 94611.
[2]Technical director, MTI, Benge Rd., R.D.F. 2, Box 80, Hockessin, DE 19707.

Copyright© 1985 by ASTM International www.astm.org

The MTI laboratory corrosion tests were based on corrosion tests in the ASTM standards in so far as feasible; however, it was necessary to specify some details that were not covered in the ASTM standards, to assure that different laboratories would obtain comparable data. In so far as possible, test procedures were selected to conform to those currently used by alloy manufacturers.

The test methods incorporate two basic concepts. The first of these involves selecting for each test a critical test factor to be used as the criterion of corrosion resistance. For example, in the corrosion test for evaluating general corrosion resistance, the test factor selected was temperature. A critical temperature was determined for each combination of alloy and corrosive environment that defined a certain level of corrosion damage. This is thought to be a more definitive way of comparing the corrosion resistance of alloys than the conventional way of comparing corrosion rates under a fixed set of environmental conditions.

The second concept is that of selecting a control alloy for each test environment. The control alloy selected is a commercial alloy that can be considered as useful for the test environment, and one for which corrosion behavior in the test environment has been well established. Alloy manufacturers who are using the MTI tests are provided with specimens of the control alloys from standard stocks maintained by MTI. Use of the control alloy specimens allows a manufacturer to confirm the correctness of his laboratory procedures.

In the following sections of this paper the individual MTI tests are summarized and the critical features of each test are discussed. These MTI tests are presented in Appendixes A through E.

Method MTI-1

Laboratory Testing of Wrought Iron- and Nickel-Base Alloys for Relative Resistance to Corrosion in Selected Media (MTI-1) (see Appendix A) provides

TABLE 1—*Corrosion test solutions and control alloys for Method MTI-1.*

Corrosive	Concentration, %weight	Control Alloy, UNS
Hydrochloric acid	0.2	S30400
Hydrochloric acid	1.0	N10276
Hydrochloric acid + ferric chloride	1.0 + 0.3	N10276
Sulfuric acid	10	N08020
Sulfuric acid	60	N08020
Sulfuric acid	95	S30400
Phosphoric acid	85	S31600
Phosphoric acid + hydrofluoric acid	83 + 2	S31600
Nitric acid	10	N10276
Nitric acid	65	S31600
Nitric acid + hydrochloric acid	60 + 2	N10276
Acetic acid	80	S30400
Acetic acid + acetic anhydride	50 + 50	S30400
Sodium hydroxide	50	S30400
Formic acid	50	S31600

data that will permit comparison of the general corrosion resistance of a new alloy relative to other alloys. The test environments selected are listed in Table 1 along with the control alloys to be used. They represent a wide spectrum of corrosive systems of interest to the chemical industry. An additional consideration in the selection of test environments was ease of reproducibility in testing.

The testing plan involves varying the test temperature in order to establish the temperature above which the general corrosion rate exceeds 0.1 mm/y (5 mpy). This critical temperature is a means for rank ordering alloys for each corrosive system. Three specimens are used in a planned interval test sequence (0 to 48, 48 to 96, 0 to 96 h) to provide information on initial corrosion effects that might influence interpretation of the data.

Specimens have an abraded surface and are exposed totally immersed, with a nitrogen atmosphere above the solution. The critical temperature is first determined with as-manufactured material in the annealed or solution treated condition. Then sensitized and welded specimens are exposed at the same temperature and the corrosion rates determined. Where indicated, metallographic examination is made of these specimens after exposure.

The detailed procedures for preparing, cleaning, and evaluating specimens follow ASTM Recommended Practice for Preparing, Cleaning, and Evaluating Corrosion Test Specimens (G 1) and ASTM Recommended Practice for Examination and Evaluation of Pitting Corrosion (G 46). ASTM Recommended Practice for Laboratory Immersion Corrosion Testing of Metals (G 31) was the guide used in preparing the solution testing procedures.

Method MTI-2

Laboratory Testing of Wrought Iron- and Nickel-Base Alloys for Relative Resistance to Crevice Corrosion in a Standard Ferric Chloride Solution (MTI-2) (see Appendix B) is a procedure for determining the relative resistance of alloys to crevice corrosion in an oxidizing acidic chloride solution. The method is patterned after ASTM Test Method for Pitting and Crevice Corrosion of Stainless Steels and Related Alloys by the Use of Ferric Chloride Solution (G 48), with the added feature of using the crevice corrosion temperature (CCT) proposed by Bingham [*1*] as the means for rank ordering alloys. A 6% ferric chloride solution is used. The multiple crevice assembly (MCA) is made of grooved tetrafluoroethylene (TFE) fluorocarbon blocks held against the specimen by a Unified Numbering System (UNS) N10276 alloy bolt and nut assembly torqued to 0.28 N·M (40 oz·in). The specimens are made from as-supplied material that has been abraded to a standard finish. The test duration is 24 h. If no pitting (defined as <1.0 mil) is observed at the first temperature tried, the test is repeated with fresh solution at a temperature 2.5°C higher than the previous test. This procedure is repeated until the CCT is determined.

The control alloys for this test are UNS S31600 and N10276.

Method MTI-3

Laboratory Testing of Wrought Iron- and Nickel-Base Alloys for Relative Resistance to Stress Corrosion Cracking in a Boiling Magnesium Chloride Solution (MTI-3) (see Appendix C) is based on ASTM Recommended Practice for Performing Stress Corrosion Cracking Tests in a Boiling Magnesium Chloride Solution (G 36) and ASTM Recommended Practice for Making and Using U-Bend Stress Corrosion Test Specimens (G 30), with certain details specified in order to assure that different laboratories will perform the test the same way. The test provides a number, time to failure, which can be used to rank order alloys for their relative resistance to stress corrosion cracking in this one environment. This rank ordering may or may not be applicable to other chloride environments. The magnesium chloride test was selected despite the objections that have been raised about its severity, because it is the most widely used test for evaluating the stress corrosion cracking resistance of austenitic stainless steels and related nickel alloys.

The specimens are of the U-bend type with abraded surfaces and are testing in triplicate. The solution composition is adjusted to give a boiling temperature of 155°C. Tests are of fixed duration: 24, 96, and 500 h. The reported time of failure for an alloy is the shortest test duration at which one or more of the specimens develop stress corrosion cracks. Alloy behavior is divided into four categories based on time to failure: less than 24 h, between 24 and 96 h, between 96 and 500 h, and greater than 500 h. No attempt was made to make more precise definitions of resistance to cracking, since it is believed that such definitions are without practical significance.

The control alloys for this test method are UNS S30400 and S31600.

Method MTI-4

Laboratory Testing of Wrought Iron- and Nickel-Base Alloys for Relative Resistance to Crevice Corrosion in Sodium Chloride Solutions (MTI-4) (see Appendix D) is a corrosion test procedure for determining the relative resistance of alloys to crevice corrosion in a neutral sodium chloride solution. It is intended to measure the minimum (critical) concentration of sodium chloride necessary to produce crevice corrosion at room temperature (20 to 24°C).

The specimens and multiple crevice assembly are identical to those used in MTI-2. The test solution is one of the following:

0.10% NaCl	0.4% NaCl	1.0% NaCl	2.0% NaCl
0.20% NaCl	0.7% NaCl	1.5% NaCl	3.0% NaCl

The test duration is 1000 h; the test solution is replaced with fresh solution every two weeks. Crevice corrosion is considered to have occurred if a pit is found which is equal to or greater than 1.0 mil in depth. The critical sodium

chloride concentration for crevice corrosion (CCC) is the lowest concentration at which crevice corrosion is observed.

This procedure provides a much less severe crevice corrosion environment than MTI-2. It is intended to evaluate the pitting resistance of alloys with relatively low contents of chromium and molybdenum, and those that can be considered for applications in mild chloride environments. It is based on a procedure suggested by Bednar.[3]

The control alloys are UNS S30400 and S31600.

Method MTI-5

Laboratory Testing of Wrought Iron- and Nickel-Base Alloys for Relative Resistance to Stress Corrosion Cracking in a Sodium Chloride Drop Evaporation System (MTI-5) (see Appendix E) is a corrosion test procedure for determining the relative resistance of alloys to stress corrosion cracking in a neutral sodium chloride solution under evaporative conditions, in air, at a metal temperature of 300°C. This is a variation of the wick test and is based on the method described by Henrikson and Asberg [2]. It is less severe than the magnesium chloride test and has the potential advantage of providing a test environment representative of the many neutral chloride environments found in the chemical industry, such as cooling waters and seaside atmospheric exposures, which can result in stress corrosion cracking of austenitic stainless steels. Since it is relatively new, the method is optional until there is more experience with it.

The test consists of a horizontal cylindrical test specimen subjected to a constant tensile stress, heated electrically to a metal temperature of 300°C, and exposed to a drop-wise stream of 0.6% NaCl solution. The test is continued until failure occurs, or for a maximum of 500 h. The rank ordering test variable is the applied stress. The test is started with a load application corresponding to 10% of the 0.2% offset yield strength, and repeated at 30, 50, 70, and 90% of the 0.2% offset yield strength until failure occurs in less than 500 h. The minimum stress for failure thus determined is reported.

The control alloy is UNS S31600.

Summary

1. MTI has selected five corrosion test methods (one for general corrosion, two for crevice corrosion, and two for stress corrosion cracking) to provide guideline information to materials engineers on wrought iron- and nickel-base alloys to facilitate commercial usage of such alloys.

2. The MTI test methods were based on existing ASTM standards as far as feasible. Test details, including test environments, were selected so as to permit different laboratories to obtain comparable data.

[3]Bednar, L., private communication, Aug. 1978.

3. In each test the critical value of a test variable (temperature, concentration, or stress) is used to rank order the corrosion resistance of the alloy being tested.

4. MTI supplies specimens of control alloys for each test environment to allow laboratories to confirm the correctness of their interpretation of the laboratory procedures.

APPENDIX A

Method MTI-1 for Laboratory Testing of Wrought Iron- and Nickel-Base Alloys for Relative Resistance to Corrosion in Selected Media

1. Scope

1.1 This method describes the procedure for corrosion tests to determine the relative resistance of wrought iron- and nickel-base alloys to corrosion in selected media. Data from these corrosion tests will be included in the MTI compilation of properties of new alloys. These tests are intended to provide corrosion data suitable for preliminary evaluation prior to testing for specific chemical-process applications.

1.2 Each alloy is tested in the as-manufactured condition, in an as-welded condition, and in a sensitized condition.

1.3 The corrosion test media have been selected to provide a wide spectrum of corrosive environments which are economically important to the chemical industry. In addition, the corrosion media and test conditions were selected to provide ease of reproducibility so as to minimize this factor in the comparative evaluation of different alloys by different laboratories.

1.4 Specimen evaluation procedures provide for weight loss measurements for evaluation of general corrosion, pit depth measurements of pitting corrosion, and microscopic examination for evaluation of intergranular corrosion.

2. Applicable Documents

2.1 ASTM Recommended Practice for Preparing, Cleaning, and Evaluating Corrosion Test Specimens (G 1).

2.2 ASTM Recommended Practice for Laboratory Immersion Corrosion Testing of Materials (G 31).

2.3 ASTM Recommended Practice for Examination and Evaluation of Pitting Corrosion (G 46).

2.4 ASTM Detecting Susceptibility to Intergranular Attack in Wrought Nickel-Rich, Chromium-Bearing Alloys (G 28).

2.5 ASTM Recommended Practices for Detecting Susceptibility to Intergranular Attack in Stainless Steels (A 262).

3. Apparatus

3.1 The apparatus shall consist of a 1000-mL flask equipped with a reflux condenser, a sparger for controlling the atmosphere within the flask (certain tests only), a specimen support system, and a means for controlling the temperature of the contents of the flask.

3.2 All components of the apparatus described in 3.1 which are in contact with the test environment (liquid and gas phases) shall be made of glass or polytetrafluoroethylene (PTFE).

3.3 The temperature-regulating device used for tests at temperatures other than the boiling temperature shall be capable of controlling the temperature of the contents of the flask to within ±1 C of the selected test temperature.

3.4 The specimen support system shall be designed so that the specimens are separated from each other and from the flask and its internal components. The specimens are to be maintained, in a vertical position, totally immersed in the test solution. One possible support system involves the use of individual glass cradles for each specimen.

3.5 The sparging system which is used only in tests at temperatures below boiling, shall be capable of sparging nitrogen at a rate of 10-100 ml per minute. The sparging gas shall be bubbled through about 100 ml of the test solution contained in a suitable glass container prior to entering the test flask. This is to provide an easy means of indicating the gas flow rate as well as a means of scrubbing possible contaminants from the gas stream.

4. Test Specimens

4.1 The specimens shall be made from sheet, plate or strip produced by commercial methods.

4.2 Material from which the specimens are made shall be in the annealed condition, the final heat treatment being done after any cold rolling. Temperature of the final heat treatment and method of cooling shall be reported.

4.3 Specimens are to be cut to size by a machining operation. If sheared specimens are used, the sheared edges are to be removed by machining; the amount of metal removed by machining shall equal the thickness of the specimen.

4.4 Thickness of the sheet material used for specimens shall be between 0.06 and 0.188 in. (1.5 and 4.8 mm). Width of the specimens shall be 0.8 in. (20 mm) and the length shall be 2.0 in. (50 mm). Tolerances for these dimensions shall be ±0.04 in. (1 mm).

4.5 Specimens are to be measured prior to test and the area calculated and reported to the closest 0.1 $in.^2$ (65 mm^2).

4.6 Prior to test, all specimens are to be abraded to provide a uniform surface finish free of scale and dirt, and to remove any sharp edges or burrs due to machining or drilling operations. The final step in this abrading operation shall be done with wet No. 80 or dry No. 120 grit abrasive paper. Care should be taken to avoid overheating the surface.

4.7 Following the abrasive treatment, the specimens shall be cleaned with a magnesium oxide paste or detergent solution to remove any residual dirt or grease, rinsed in water, and dipped in acetone and air dried.

4.8 The dried specimens shall be weighed to an accuracy of at least ±0.2 mg. Weighed specimens shall be stored in a desiccator until used.

4.9 Three kinds of specimens shall be used: (a) as-manufactured specimens, (b) as-welded specimens, and (c) sensitized specimens.

4.9.1 *As-manufactured Specimens*—These specimens shall be prepared according to the procedure described in Sections 4.1 through 4.8 above.

4.9.2 *As-welded Specimens*—The reason for using these specimens is to evaluate the corrosion resistance of the weld deposit. Although some information may be gained regarding intergranular corrosion in the heat-affected zone of the weld, it is intended that such effects will be evaluated primarily by the sensitized specimens (4.9.3). The welded specimens shall be prepared from material described in 4.1 and 4.2. The minimum thickness of material for these specimens shall be 0.125 in. (3.2 mm). The weld shall be made so that it will be in the center of the specimen and be parallel to the long direction of the specimen. The weld shall be a gas-tungsten arc (GTA) weld with filler metal. The filler metal and welding procedure shall correspond to that recommended by the manufacturer for fabrication of process equipment. The weld bead shall be ground

or machined flush with the base metal. The final preparation of the specimen shall be as specified in 4.3 through 4.8. There shall be no post-weld heat treatment.

4.9.3 *Sensitized Specimens*—Since the preferred sensitization treatment varies with type of alloy, the sensitization treatment to be used for a specific alloy shall be determined by mutual agreement between the manufacturer and MTI. The manufacturer will submit details of his proposed sensitization treatment, which can be a simple heat treatment or a procedure involving welding, together with laboratory data supporting his choice. The laboratory data shall include that obtained from tests such as ASTM A 262 and G 28. MTI will either approve the procedure submitted or will suggest an alternative which shall be subject to the manufacturer's approval.

5. Test Solutions

5.1 Test solutions shall be prepared accurately from reagent grade chemicals conforming to the Specifications of the Committee on Analytical Reagents of the American Chemical Society and distilled water.

5.2 The compositions of the various test solutions are given in Table 2.

5.3 The sparging gas in those tests made at temperatures other than the boiling temperature shall be nitrogen. The purity of the nitrogen shall be at least 99.9%, and the oxygen content shall be less than 0.02%. To insure that it is free of oil and dirt, the nitrogen should be passed through at least 2 ft (610 mm) of a suitable cleaning material such as asbestos, sheep's wool, excelsior, slag wool, or activated alumina. Prior to entering the test container, the nitrogen should be bubbled through at least 100 mL of the test solution contained in a small flask or bottle. The volume of this scrubbing solution should be maintained during the test.

6. Procedure

6.1 The test solutions to be used are listed in Table 2. The test temperatures are to be selected from the following list: 30, 50, 70, 90, 110, and 130°C (boiling temperature can be substituted for either of the last two, as appropriate). With the tests of the as-manufactured specimens, the aim is to determine the lowest temperature at which the corrosion rate exceeds 5 mpy (0.13 mm/y); thus, tests should be made at a minimum of two temperatures with each test solution unless the 5 mpy rate is exceeded at 30°C, or this rate is not exceeded at the maximum listed temperature. With the welded and the sensitized specimens, tests shall be made only at the critical temperature as defined above.

6.1.1 The corrosion rate value to be used in determining the critical corrosion temperature shall be the value obtained in the 96-h test (6.7).

6.1.2 If the manufacturer expects that the corrosion rate value for a specific alloy in one of the test solutions will be very high (for example, greater than 100 mpy) at 30°C, he may elect not to make tests with that solution, provided he agrees that a statement can be placed in the MTI manual that the alloy in question is not recommended for that specific corrosive/concentration combination.

6.2 For each test temperature there shall be two specimens in the flask. The specimens shall be totally immersed in the liquid phase and shall be located so that the long dimension is vertical. The specimens shall be located so as to avoid any direct impingement of the sparging gas on the specimen surface.

6.3 The volume of the test solution shall be 600 mL.

6.4 The rate of heating shall be such as to bring the test solution to temperature as rapidly as possible. Boiling chips or other boiling aids shall be added. The specimens are to be added just prior to the time the solution reaches the test temperature.

6.5 For tests at temperatures other than the boiling temperature, the temperature shall be controlled to within ±1°C (1.8°F) of the desired temperature. For boiling temperature

TABLE 2—*Corrosion test solutions.*

Test Solution		
Corrosive	Concentration, %weight	Control Alloy, UNS
Hydrochloric acid	0.2	S30400
Hydrochloric acid	1.0	N10276
Hydrochloric acid + ferric chloride	1.0 + 0.3	N10276
Sulfuric acid	10	N08020
Sulfuric acid	60	N08020
Sulfuric acid	95	S30400
Phosphoric acid	85	S31600
Phosphoric acid + hydrofluoric acid	83 + 2	S31600
Nitric acid	10	N10276
Nitric acid	65	S31600
Nitric acid + hydrochloric acid	60 + 2	N10276
Acetic acid	80	S30400
Acetic acid + acetic anhydride	50 + 50	S30400
Sodium hydroxide	50	S30400
Formic acid	50	S31600

NOTE: For concentrations in the range of 50 to 100%, the concentration used shall be within 0.5% of the specified concentration. For concentrations in the range of 1 to 10%, the concentration used shall be within 0.1% of the specified value. For the 0.2% hydrochloric acid solution, the concentration shall be within 0.01% of the specified value.

tests, the rate of boiling shall be controlled so as to avoid excessive turbulence and bubble impingement.

6.6 In tests at the boiling temperature, the condenser is to be open to the air with no sparging gas used. For tests at temperatures below the boiling temperature, a sparging gas (nitrogen) shall be used. The rate of flow of the sparging gas shall be approximately 100 mL/min for the first ½ h of the test, and then reduced to approximately 10 mL/min.

6.7 The duration of tests shall be 96 h. For tests with as-manufactured specimens, one specimen is to be removed after 48 h and replaced with a new specimen.

6.8 At the conclusion of the test, the specimens shall be removed from the test solution and immediately rinsed in cold water. Following this, the specimens should be rinsed in distilled water, then in acetone, and dried in air. If not cleaned immediately, they shall be stored in a desiccator.

6.9 After the above cleaning operation, the specimens shall be examined visually and the color, thickness, and physical nature of any deposits and corrosion products on the metal surface shall be noted.

6.10 The specimens shall be cleaned of corrosion products and deposits by light scrubbing using water and a soft brush. Ultrasonic cleaning is permitted. Any remaining deposits or corrosion products shall be removed by rubbing with a soft rubber eraser. The specimen shall be washed in acetone, dried in air, and stored in a desiccator until weighed.

6.11 If an additional cleaning procedure is required, the electrolytic cleaning procedure described in ASTM G 1 shall be used.

6.12 For each alloy, "blank" specimens shall be weighed before and after being subjected to the specimen cleaning procedure in order to establish a correction factor for the cleaning procedure.

6.13 If the weight-loss corrosion rate values (7.1) for the three as-manufactured specimens at a given test temperature (6.7) differ by a factor greater than 4 (ratio of highest corrosion rate to lowest corrosion rate), the test shall be repeated unless the maximum corrosion rate is less than 5 mpy. The same criterion for repeating the test applies to the tests of welded specimens and of sensitized specimens.

7. Evaluation of Specimens After the Test

7.1 The cleaned specimens shall be weighed to an accuracy of at least ±0.2 mg, and the weight loss during test determined making an appropriate correction for the "blank" loss during cleaning (6.12). The corrosion rate shall be calculated from this corrected weight loss using the following formula:

$$\text{corrosion rate (mpy)} = \frac{534 \times \text{weight loss (mg)}}{\text{area (in.}^2\text{)} \times \text{time (h)} \times \text{metal density (g/cm}^3\text{)}}$$

$$\text{corrosion rate (mm/y)} = 0.0254 \times \text{corrosion rate (mpy)}$$

7.2 The cleaned specimens shall be inspected using a low-power (×20) binocular microscope and a record made of the surface appearance, noting any irregularities of the corrosive attack and including a qualitative description of the number and distribution of pits. The nature of the pits shall be characterized; that is, shallow or deep, rounded or steep-sided, narrow or wide.

7.3 The pit depths shall be measured to an accuracy of 1.0 mil using a micrometer or depth gage according to the procedure in Section 6.2.3 of ASTM G 46. Alternatively, the microscopical procedure in section 6.2.4 of ASTM G 46 can be used. A record shall be made of the five deepest pits. Corrosion rates shall be calculated from these measurements using the formula:

$$\text{corrosion rate (mpy)} = \text{pit depth (mil)} \times \frac{24 \times 365}{\text{time (h)}}$$

$$\text{corrosion rate (mm/y)} = 0.0254 \times \text{corrosion rate (mpy)}$$

7.4 Sensitized specimens shall be examined metallographically to determine the severity of any subsurface corrosion effects, such as intergranular corrosion, if there are indications of such attack by either weight loss measurements or by a ×20 examination following a bend test. For the metallographic examination, the specimens shall be cut in half parallel to the 0.8-in. dimension, and the entire cross section examined at a magnification of ×100 after polishing and etching using standard metallographic techniques for the alloy being tested. A typical photomicrograph shall be supplied. The maximum depth of subsurface attack shall be reported together with a description of its nature.

7.5 For welded specimens the metallographic examination shall be similar to that in 7.4, except that the area examined shall include the weld metal and the heat-affected zone on both sides of the weld. In all cases, the depth of attack shall be reported in mils.

8. Control Tests

8.1 Using the above procedure, control tests shall be made with the control alloys listed in Table 2 for the test environments indicated. Samples of the control alloys will be supplied by MTI. Tests will be made only with as-manufactured specimens except in the case of UNS S31600 where tests shall be made also with sensitized specimens. MTI

will supply the sensitized specimens that will have been heat treated at 677°C (1250°F) for 1 h and air cooled.

9. Reporting the Data

9.1 For each corrosion test, a report sheet shall be prepared. The items to be reported are discussed individually below.

9.2 *Alloy Description*—The alloy tested shall be described by its commercial name, manufacturer, UNS number (if any), and nominal composition as specified by the manufacturer.

9.3 *Alloy Composition*—The heat number of the material tested shall be reported together with the heat analysis.

9.4 *Alloy Manufacture*—The method of alloy manufacture shall be briefly summarized; the information given shall include method of ingot manufacture, final descaling, and finishing treatments. The final heat treatment conditions of temperature and cooling method shall be reported.

9.5 *Alloy Mechanical Properties*—The yield strength, tensile strength, elongation and reduction in area, and hardness shall be given for the heat of material tested. Units shall be English units followed by SI units in parentheses.

9.6 *Specimen Source*—The size and gage dimension of the sheet, plate, or strip from which the specimen was cut shall be reported together with information on the orientation of the specimen relative to the rolling direction.

9.7 *Specimen Area*—The nominal dimensions of the specimen and its measured area shall be reported.

9.8 *Test Apparatus*—The apparatus shall be identified in the report by reference to the appropriate section of this method, with any pertinent additional details added.

9.9 *Test Solution*—The volume and composition of the test solution shall be reported.

9.10 *Sparging Gas*—The identity and purity of the sparging gas shall be reported for those tests made at temperatures below boiling.

9.11 *Temperature* of the test solution shall be reported for the normal test period.

9.12 *Welded Specimens*—The welding procedure and the filler metal used shall be reported together with the dimensions of the welded sheet from which the specimens were cut.

9.13 *Sensitized Specimens*—The heat treatment or welding conditions used to produce sensitization shall be reported in detail.

9.14 *Appearance* of the test specimens at the end of the test shall be reported (6.9 and 7.2). For those specimens examined metallographically, there shall be a description of the nature of any subsurface attack plus a photomicrograph.

9.15 *Corrosion rates* calculated from weight loss measurements (7.1), shall be reported for each specimen. Corrosion rates shall be reported to two significant figures only, with the minimum unit being 0.1 mpy (0.01 mm/y). Values less than 0.1 mpy shall be reported as "<0.1 mpy" ("<0.01 mm/y").

9.15.1 Corrosion rates calculated from pit depth measurements shall be reported for each specimen which shows any visual indication of pitting. Values reported shall be either "<*Y*" (where *Y* is the corrosion rate calculated from the sensitivity of the pit depth measuring device), or two values each given to one significant figure, which shall be the corrosion rates calculated from the deepest measured pit depth and from the average of the five deepest pits. Pit depths in mils shall be reported in addition to the corrosion rates.

9.15.2 The corrosion rates reported for the depth of intergranular attack shall be the corrosion rate calculated form the deepest measured intergranular penetration (see 7.4). The depth of intergranular attack in mils shall also be reported.

9.15.3 All corrosion rates are to be reported as mpy with mm/y values in parentheses.

9.16 A summary report sheet shall be prepared for each alloy and each test solution which shall include only items 9.2, 9.9, 9.11, 9.12, 9.13, 9.15, 9.15.1, and 9.15.2.

9.17 Data from all tests made are to be reported unless the test can be rejected for a known gross experimental error (for example, loss of temperature control).

APPENDIX B

Method MTI-2 for Laboratory Testing of Wrought Iron- and Nickel-Base Alloys for Relative Resistance to Crevice Corrosion in a Standard Ferric Chloride Solution

1. Scope

1.1 This method describes a procedure for corrosion tests to determine relative resistance of wrought iron- and nickel-base alloys to crevice corrosion in a standard ferric chloride solution. Data from these corrosion tests will be included in the MTI compilation of properties of new alloys.

1.2 The method is designed to determine the relative resistance of alloys to crevice corrosion in an oxidizing chloride environment by measuring the minimum (critical) temperature for crevice corrosion (CCT).

2. Applicable Documents

2.1 ASTM Test for Pitting and Crevice Corrosion Resistance of Stainless Steels and Related Alloys by the Use of Ferric Chloride Solution (G 48).

2.2 ASTM Recommended Practice for Examination and Evaluation of Pitting Corrosion (G 46).

3. Ferric Chloride Test Solution

3.1 Dissolve 100 g of reagent grade ferric chloride, $FeCl_3 \cdot 6H_2O$, in 900 mL of distilled water (about 6% $FeCl_3$ by weight). Filter through glass wool or filter paper to remove insoluble particles.

4. Test Specimens

4.1 The test specimens shall be made from sheet, plate, or strip made by commercial methods.

4.2 The material from which the specimens are made shall be in the annealed condition, the final heat treatment being done after any cold rolling. The temperature of the final heat treatment and the method of cooling shall be reported.

4.3 The specimens are to be cut to size by a machining operation. If sheared specimens are used, the sheared edges are to be removed by machining; the amount of metal removed by machining shall equal the thickness of the specimens.

4.4 Thickness of the material used for the specimens shall be between 0.06 and 0.188 in. (1.5 and 4.8 mm). Width of the specimens shall be 1.0 in. (25 mm) and the length shall be 3.0 in. (76 mm). The tolerances for these dimensions shall be ±0.04 in. (1 mm). One ⅜ in. (10 mm) hole shall be drilled in the center of the specimen.

4.5 The specimens are to be cut so that the long direction of the specimen is parallel to the rolling direction of the original sheet, plate, or strip.

4.6 Prior to the test the specimens are to be abraded to provide a uniform surface finish free of scale and dirt, and to remove any sharp edges or burrs due to machining

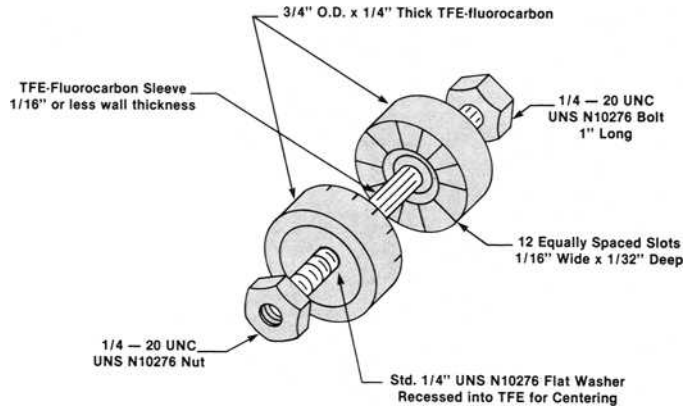


FIG. 1—*Crevice block assembly.*

or drilling operations. The final step in this abrading operation shall be done with either wet No. 80 or dry No. 120 grit paper. Care should be taken to avoid overheating the surface.

4.7 Following the abrasive treatment the specimens shall be cleaned with a magnesium oxide paste or detergent solution to remove any residual dirt or grease, rinsed in water, dipped in acetone, and air dried.

5. Apparatus

5.1 Cylindrical TFE-fluorocarbon crevice blocks, two for each test specimen. Each block shall be 0.75 in. (19 mm) in diameter and 0.25 in. (6.4 mm) thick, with 12 radial slots 0.063 in. (1.6 mm) wide and 0.03 in. (0.8 mm) deep cut in one side (Fig. 1).

5.2 Bolt, nut, and washers of UNS N10276 shall be used to fasten the crevice blocks to the specimen (Fig. 1). Also, a TFE-fluorocarbon sleeve, having a wall thickness of 0.063 in. (1.6 mm) or less, shall be used over the bolt.

5.3 Test tube, 1.5 in. (38 mm) in diameter and 7.9 in. (200 mm) long.

5.4 Rubber stopper, with center hole for insertion of 0.25 in. (6.4 mm) diameter, 4 in. (102 mm) long glass tube (medicine dropper tube may be conveniently used) to serve as a vent and condenser. For test temperatures above about 80°C, it may be necessary to use a small water-cooled condenser in place of the long glass tube so as to minimize evaporation losses.

5.5 Water or oil bath, thermostatically controlled.

6. Procedure

6.1 Add 125 mL of ferric chloride solution to each test tube, insert a rubber stopper, and place the tube in a thermostatically controlled bath until it comes to the equilibrium temperature of interest.

6.2 Fasten the two crevice blocks to the test specimen by passing the sleeved bolt through the hole in the specimen and positioning a block on either side of the specimen as shown in Fig. 2. The torque on the bolt shall be 0.280 N·m (40 oz·in.) and shall be accomplished using an adjustable 6.35-mm (¼-in.) drive torque limiting screwdriver. Use plastic gloves to avoid hand contact with metal surfaces during this operation. There shall be no metallic contact between the bolt assembly and the specimen.

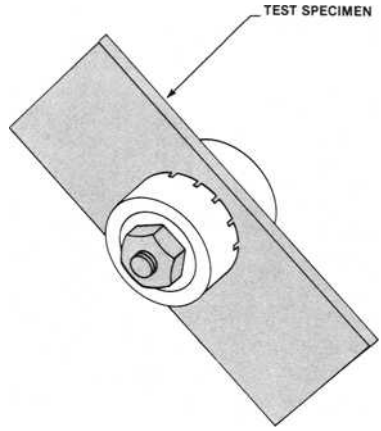


FIG. 2—*Crevice block assembly with specimen.*

6.3 After the test solution has reached the desired temperature, tilt the tube at a 45° angle and slide the test specimen to the bottom of the tube, replace the stopper, and return the tube to the bath. Maintain at temperature for 24 h.

6.4 At the end of the 24-h test period, the specimen assembly is removed by decanting the test solution into a beaker and sliding the assembly from the tube. After disassembly, rinse the specimen in water and examine the surface that was under the crevice blocks. Inspection is done according to the procedure of 7.1. If attack is observed under the crevice blocks, discontinue the test. If no attack is observed, raise the bath temperature by 2.5°C, replace test container plus fresh ferric chloride solution in constant-temperature bath, and repeat procedures 6.2, 6.3, and 6.4.

6.5 The minimum temperature of test is 0°C and the maximum temperature of test is 100°C.

6.6 The pH of the test solution shall be measured at the beginning and end of the test.

7. Examination and Evaluation

7.1 Examine areas under the crevice blocks for crevice attack using low-power (× 20) magnification. Crevices are considered corroded if the local attack is 1.0 mil or greater, as estimated by either a needle-point micrometer gage or microscope with calibrated fine-focus knob.

8. Control Tests

8.1 Using the above procedure, control tests shall be made with samples of alloys supplied by MTI. The control alloys are UNS S31600 and N10276.

9. Reporting the Data

9.1 For each crevice corrosion test, a report sheet shall be prepared which will include the items discussed below.

9.2 *Alloy Description*—The alloy tested shall be described by its commercial name, manufacturer, UNS number (if any), and nominal composition as specified by the manufacturer.

9.3 *Alloy Composition*—The heat number of the material tested shall be reported together with the heat analysis.

9.4 *Alloy Manufacture*—The method of manufacture shall be summarized briefly; the information given shall include method of ingot manufacture and final descaling and finishing treatments. The final heat treatment conditions of temperature and cooling method shall be reported.

9.5 *Alloy Mechanical Properties*—The yield strength, tensile strength, elongation and reduction in area, and hardness shall be given for the heat of material tested.

9.6 *Specimen Source*—The size and gage dimension of the sheet, plate, or strip from which the specimen was cut shall be reported together with information on the orientation of the specimen relative to the rolling direction. The final surface preparation of the specimen shall be reported.

9.7 Report the number of areas of crevice attack greater than 1.0 mil in depth found under the crevice blocks for each test temperature, and indicate the minimum temperature for crevice corrosion (CCT) to the closest 2.5°C. Report the initial and final pH of the test solution for the test made at the minimum temperature for crevice corrosion.

APPENDIX C

Method MTI-3 for Laboratory Testing of Wrought Iron- and Nickel-Base Alloys for Relative Resistance to Stress-Corrosion Cracking in a Boiling Magnesium Chloride Solution

1. Scope

1.1 This method describes the procedure for corrosion tests to determine the relative resistance of wrought iron- and nickel-base alloys to stress-corrosion cracking in a boiling magnesium chloride solution. Data from these corrosion tests will be included in the MTI compilation of properties of new alloys.

1.2 This method results in a number, time to failure, which can be used to rank order alloys for their relative resistance to stress-corrosion cracking in a boiling magnesium chloride solution. This rank ordering may or may not be applicable to other chloride environments.

2. Applicable Documents

2.1 ASTM Recommended Practice for Performing Stress-Corrosion Cracking Tests in a Boiling Magnesium Chloride Solution (G 36).

2.2 ASTM Recommended Practice for Making and Using U-Bend Stress-Corrosion Test Specimens (G 30).

3. Apparatus

3.1 The following test apparatus is specified for its ability to maintain a constant temperature and solution concentration over a long period of time.

3.2 *Components*—The suggested test apparatus is shown in Fig. 3, and the design details are given below.

3.2.1 *Flask*—The 1-L Erlenmeyer flask (Fig. 4) has a 45/50 ground-glass outer joint at the mouth and a 10/30 ground-glass outer joint to hold the thermometer.

3.2.2 *Condenser*—(Fig. 5) A modified Allihn condenser with a 45/50 ground-glass inner joint. In place of the drip tip on the conventional condenser, the exit must be formed as shown in Fig. 5. A smooth exit on the condenser is essential to prevent dripping. The water jacket of the condenser should be at least 250 mm long. At the top of the condenser, a 29/26 ground-glass outer joint is required to hold the trap in place.

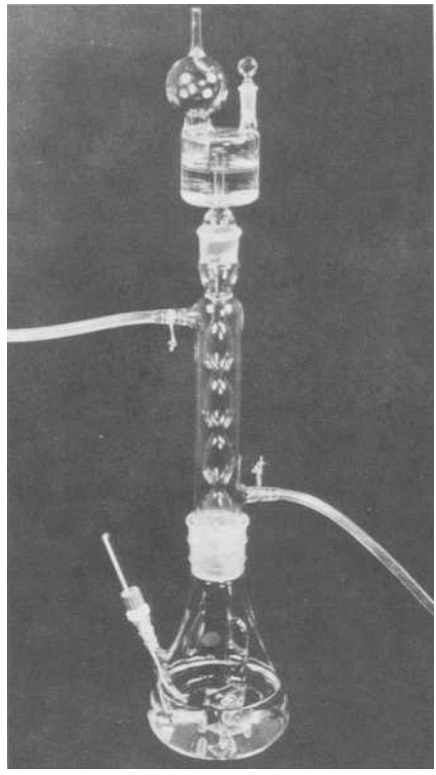


FIG. 3—*Assembly of glass apparatus for stress-corrosion test in boiling magnesium chloride with U-bend specimen in place (ASTM G 36). Reprinted/adapted with permission from the* Annual Book of ASTM Standards, *Part 10.*

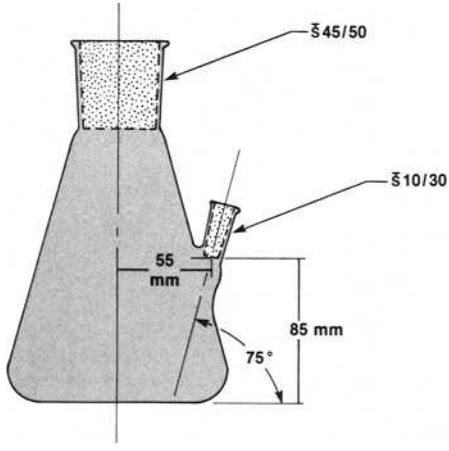


FIG. 4—*Modified Erlenmeyer flask (1000 mL) (ASTM G 36). Reprinted/adapted with permission from the* Annual Book of ASTM Standards, *Part 10.*

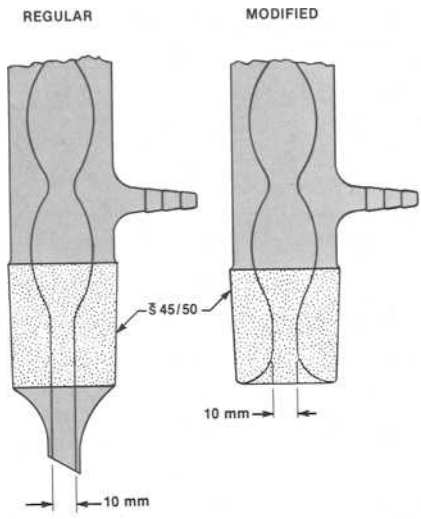


FIG. 5—*Modifications of Allihn condenser to prevent loss of vapor (ASTM G 36). Reprinted/adapted with permission from the* Annual Book of ASTM Standards, *Part 10.*

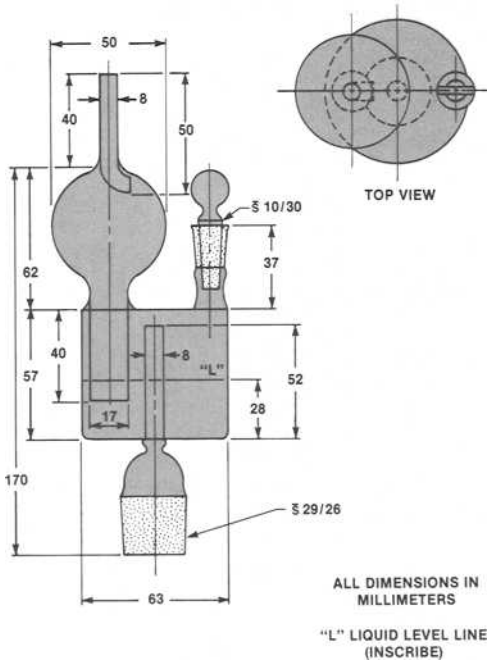


FIG. 6—*Trap for top of condenser to prevent loss of vapor (ASTM G 36). Reprinted/adapted with permission from the* Annual Book of ASTM Standards, *Part 10.*

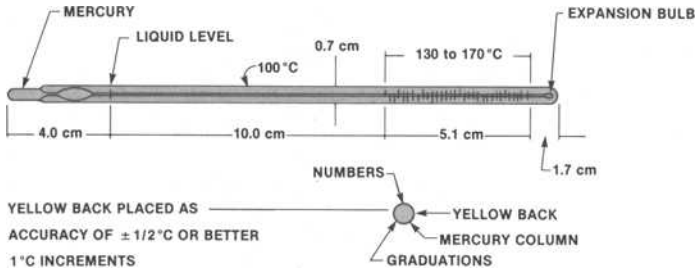


FIG. 7—*Design of thermometer for use in flask of Fig. 4 (ASTM G 36). Reprinted/adapted with permission from the* Annual Book of ASTM Standards, *Part 10*

NOTE: Dripping of condensate into hot magnesium chloride solution from the "drip tip" of a conventional Allihn condenser results in a pulsating generation of water vapor. These pressure waves lead to loss of water vapor at the top of the condenser. Initially, there may be some dripping from the condenser until there is complete wetting of the walls of the flask by the condensate.

3.2.3 *Trap*—Containing a 25 weight % solution of magnesium chloride (Fig. 6), and affixed to the top of the condenser to eliminate vapor losses by diffusion during tests in excess of 7 days. The trap is joined to the condenser by the 29/26 ground-glass inner joint.

3.2.4 *Thermometer*—Required to adjust the boiling point, and thereby the concentration of the magnesium chloride solution when it is prepared, and to monitor the solution temperature throughout the test. The graduations must clearly show 1°C increments in the range of 130 to 170°C (266 to 338°F). When the specially designed thermometer of Fig. 7 is used in the 1-L Erlenmeyer flask of Fig. 4, no more space is needed on hot plates than that taken up by the flasks themselves. A modified ASTM Thermometer 86D with a temperature range from 95 to 170°C (203 to 338°F) in 1°C subdivisions can also be used with this apparatus.

NOTE: The thermometer should be checked for the presence of gas bubbles before each use. These can be removed by cooling the lower part of bulb (dry ice) and gently tapping the thermometer. Storage of a thermometer in a vertical position will prevent appearance of bubbles.

3.2.5 *Adapter*—A fluorocarbon resin adapter containing a rubber O-ring seal for a 10/30 ground-glass outer joint must be used to hold the thermometer in place in the flask.

NOTE: Use of a thermometer with a ground-glass inner joint in place of the adapter results in appreciable loss of water vapor at this hot joint.

3.2.6 When assembling the above components, *do not* use any lubricants on any of the ground-glass joints.

3.3 Assembly.

3.3.1 The thermometer along with its adapter is inserted into the side arm of the Erlenmeyer flask and positioned so that the bulb is located about 7.5 mm (5/16 in.) from the bottom of the flask. The adapter is tightened to prevent loss of water during the test; then the $MgCl_2 \cdot 6H_2O$/distilled water solution, prepared according to Section 5, and boiling

aids are added to the flask. After positioning the water-cooled condenser on top of the flask, the whole assembly is placed on a hot plate or other suitable source of heat. Do not attach the trap at this time.

3.3.2 The solution concentration is adjusted by slowly adding small portions (4 to 5 mL) of distilled water until the constant boiling temperature of 155 ± 1°C (311 ± 1.8°F) is attained. The previously prepared test specimens and holder are now ready to be placed in the flask. This is accomplished by removing the condenser from the flask, immersing the specimen and specimen holder in the boiling solution (with caution), and quickly replacing the condenser.

3.3.3 Cut a 50- by 450-mm (2- by 18-in.) strip of commercial aluminum foil. Wrap this foil around the outside of the joint between the condenser and the flask and press the foil against the glass so that the joint is well covered and none of the foil is in contact with the hot flask below the joint.

NOTE: The purpose of the aluminum foil is to prevent loss of condensate by evaporation where the top of the ground-glass surface of the joint is exposed to the air. Condensate rises by capillary action in the joint and evaporates in the warm air.

3.3.4 If the period of exposure exceeds 7 days, a liquid trap is required at the top of the condenser to maintain the constant boiling point of 155 ± 1.0°C (311 ± 1.8°F) without new additions of water to the boiling $MgCl_2$ solution. Fill the trap to the liquid level line with 25% solution of $MgCl_2$ (see 5.4). As soon as the condensate stops dripping from the condenser and flows down the wall of the Erlenmeyer flask in a continuous stream, place the trap on top of the condenser.

NOTE: Whenever the trap is needed, it must be used with the modified condenser because the pressure pulses generated by "drip tip" condensers exceed the capacity of the trap to absorb sudden changes in pressure within the flask.

3.3.5 During long-time tests, there may be a slow drop in the level of liquid in the trap because of evaporation of water at the top of the trap from the 25 weight % $MgCl_2$ solution. This level should be brought up to the liquid-level line by additions of distilled water every 7 to 14 days.

4. Test Specimens

4.1 The test specimens shall be U-bend specimens.

4.2 The specimens shall be made from sheet, plate, or strip made by commercial methods.

4.3 The material from which the specimens are made shall be in the annealed condition, the final heat treatment being done after any cold rolling. The temperature of the final heat treatment and the method of cooling shall be reported.

4.4 Specimens are to be cut to size by a machining operation. If sheared specimens are used, the sheared edges are to be removed by machining. The amount of metal removed by machining shall equal the thickness of the specimen.

4.5 Thickness of the material used for the specimens shall be between 0.06 and 0.188 in. (1.5 and 4.8 mm). Width of the specimens shall be 0.5 in. (13 mm), and the length shall be 5.0 in. (127 mm). The tolerances for these dimensions shall be ±0.04 in. (1 mm). Two holes, each ¼ in. (6.35 mm) in diameter shall be drilled along the center line of the specimen, the center of each hole being ½ in. (12.7 mm) from an end.

4.6 The specimens are to be cut so that the long direction of the specimen is parallel to the rolling direction of the original sheet, plate or strip.

4.7 Prior to test, the specimens are to be abraded to provide a uniform surface finish

free of scale and dirt, and to remove any sharp edges or burrs due to machining or drilling operations. The final step in this abrading operation shall be done with either wet No. 80 or dry No. 120 grit paper. Care should be taken to avoid overheating the surface.

4.8 Following the abrasive treatment, the specimens shall be cleaned with a magnesium oxide paste or detergent solution to remove any residual dirt or grease, rinsed in water, dipped in acetone, and air dried.

4.9 The test specimens shall be stressed by a two-stage operation which involves first forming the approximate U-shape over a 1.0 in. diameter mandrel then allowing the elastic strain to relax completely before the second stage of applying the stress. The sequence of operations shall be as shown in Fig. 8. In order to ensure that additional strain is applied in the second stage significantly beyond that applied in the first stage, the distance between the specimen ends shall be measured at the end of the first stage before the load on the preforming device is released, and then the final stressing shall be done so that the distance between the ends of the specimen after the final stressing operation shall be 0.50 in. (12.7 mm) less then the first measurement. A single stage stressing operation can be used if the equipment is such that there is no opportunity for relaxation of stress during loading.

4.10 The bolt, washers, and nut used for stressing the U-bend shall be made of the same alloy as the specimen or an alloy more resistant to general corrosion and stress-corrosion cracking in the magnesium chloride solution. If the latter alloy is used, silica-filled TFE-fluorocarbon insulators shall be used to insulate electrically the specimen from the stressing components.

4.11 Means shall be provided for supporting three stressed specimens in the test solution. The support system shall be made of either glass or polytetrafluoroethylene (PTFE) and shall be designed so that the stressed portion of the specimens is totally immersed in the test solution, and with no contact of the specimen support system or the flask or flask internals with the stressed area of the specimen.

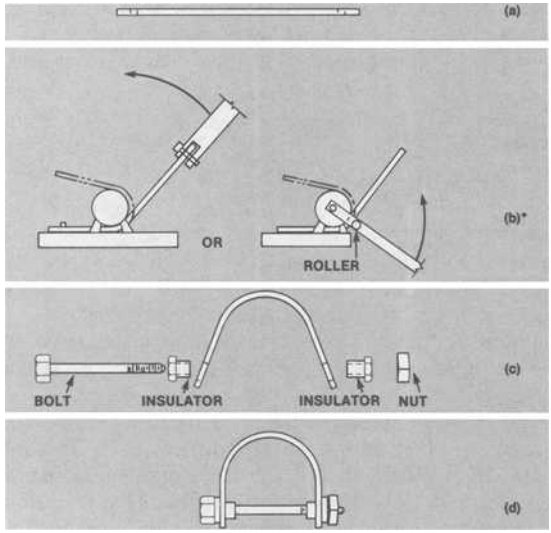


FIG. 8—*Method of stressing U-bend—two stage method (ASTM G 30). Reprinted/adapted with permission from the* Annual Book of ASTM Standards, *Part 10.*

5. Test Solution

5.1 *Purity of Reagents*—Reagent grade chemicals shall be used in all tests. Unless otherwise indicated, it is intended that all reagents shall conform to the specifications of the Committee on Analytical Reagents of the American Chemical Society. Other grades may be used, provided it is first ascertained that the reagent is of sufficiently high purity to permit its use without lessening the accuracy of the determination.

5.2 *Purity of Water*—Distilled water or water of equal purity shall be used to prepare the test solutions.

5.3 *Magnesium Chloride* ($MgCl_2 \cdot 6H_2O$)—A solution of magnesium chloride that boils at 155 ± 1.0°C (311 ± 1.8°F) is used in this test. The boiling temperature of 155°C corresponds to a $MgCl_2$ concentration of 45%. A second 25 weight % solution of magnesium chloride is required for the trap if the test duration exceeds 7 days without a solution change.

5.3.1 To prepare about 400 mL of the test solution for use in a 1-L Erlenmeyer flask, weigh 600 g of reagent grade $MgCl_2 \cdot 6H_2O$ and add this to the flask containing a thermometer along with 15 mL of distilled water.

5.3.2 Add 10 to 15 boiling chips or other boiling aids.

5.3.3 Heat by placing the flask on a hot plate or other suitable source of heat and put the condenser in place, leaving off the trap. Hook up the cooling water supply to the condenser.

5.3.4 When the solution boils vigorously and there is no more dripping of condensate, slowly add small quantities (4 to 5 mL) of distilled water at the top of the condenser to reduce the temperature to 155°C (311°F). Use extreme caution when adding the water to the boiling magnesium chloride solution. Cool water can form a layer on top of the magnesium chloride solution, and when it reaches the bottom of the flask, bumping can occur. Use a protective shield.

NOTE: If too much water has been added, add some crystals of $MgCl_2 \cdot 6H_2O$ through the condenser until a temperature of 155°C (311°F) is attained.

5.4 To prepare the 25 weight % solution for the trap (Fig. 6), place 53.4 g of $MgCl_2 \cdot 6H_2O$ and 46.6 mL of distilled water in a flask and allow the crystals to dissolve at room temperature.

6. Procedure

6.1 After the solution's boiling temperature has been adjusted to the specified value of 155 ± 1.0°C (311 ± 1.8°F), the three test specimens shall be added to the flask; the stressed portion of the test specimens shall be totally immersed in the test solution.

6.2 The specified test temperature shall be maintained throughout the test.

6.3 Three separate tests shall be made; one of 24-h duration, one of 96-h duration, and one of 500-h duration.

6.4 The specimens shall be examined at the end of each test for signs of cracking. This shall be done by removing the specimen from the test solution, washing it in water, drying it, and examining the areas stressed in tension under a ×20 binocular microscope. Any positively identified crack shall be sufficient to constitute "failure."

6.5 It is not necessary to do the 500-h test if a total of two or more specimens failed in the 24-h test and the 96-h test.

7. Reporting the Data

7.1 For each stress-corrosion test, a report sheet shall be prepared which will include the items discussed below.

7.2 *Alloy Description*—The alloy tested shall be described by its commercial name,

manufacturer, UNS number (if any), and nominal composition as specified by the manufacturer.

7.3 *Alloy Composition*—The heat number of the material tested shall be reported together with the heat analysis.

7.4 *Alloy Manufacture*—The method of alloy manufacture shall be summarized briefly; the information given shall include method of ingot manufacture and final descaling and finishing treatments. The final heat treatment conditions of temperature and cooling method shall be reported.

7.5 *Alloy Mechanical Properties*—The yield strength, tensile strength, elongation and reduction in area, and hardness shall be given for the heat of material tested.

7.6 *Specimen Source*—The size and gage dimension of the sheet, plate, or strip from which the specimen was cut shall be reported together with information on the orientation of the specimen relative to the rolling direction.

7.7 *Temperature* of the test solution shall be reported for the normal test period. The average temperature shall be given together with the minimum and maximum values.

7.8 The *visual appearance* of the specimens ($\times 20$) at the end of the test shall be reported.

7.9 The *number of specimens* tested and the number of specimens that failed in each test shall be reported, each test being identified by duration.

7.10 The *time to failure* shall be reported for the alloy being tested. It shall be one of the following: 24, 96, 500, or >500-h duration, and shall be the shortest test duration at which one or more failures were observed.

APPENDIX D

Method MTI-4 for Laboratory Testing of Wrought Iron- and Nickel-Base Alloys for Relative Resistance to Crevice Corrosion in Sodium Chloride Solutions

1. Scope

1.1 This method describes a procedure for corrosion tests to determine relative resistance of wrought iron- and nickel-base alloys to crevice corrosion in sodium chloride solutions. Data from these corrosion tests will be included in the MTI compilation of properties of new alloys.

1.2 The method is designed to determine the relative resistance of alloys to crevice corrosion in a neutral chloride environment by measuring the minimum (critical) concentration for crevice corrosion (CCC).

2. Applicable Documents

2.1 Laboratory Testing of Wrought Iron- and Nickel-Base Alloys for Relative Resistance to Crevice Corrosion in a Standard Ferric Chloride Solution (MTI-2).

3. Sodium Chloride Test Solutions

3.1 Dissolve reagent grade sodium chloride in distilled water in appropriate amounts to make the following solutions:

0.10% NaCl	1.0% NaCl
0.20% NaCl	1.5% NaCl
0.40% NaCl	2.0% NaCl
0.70% NaCl	3.0% NaCl

4. Test Specimens

4.1 The test specimens shall be made from sheet, plate, or strip made by commercial methods.

4.2 The material from which the specimens are made shall be in the annealed condition, the final heat treatment being done after any cold rolling. The temperature of the final heat treatment and the method of cooling shall be reported.

4.3 The specimens are to be cut to size by a machining operation. If sheared specimens are used, the sheared edges are to be removed by machining; the amount of metal removed by machining shall equal the thickness of the specimens.

4.4 Thickness of the material used for the specimens shall be between 0.06 and 0.188 in. (1.5 and 4.8 mm). Width of the specimens shall be 1.0 in. (25 mm) and the length shall be 3.0 in. (76 mm). The tolerances for these dimensions shall be ±0.04 in. (1 mm). One ⅜ in. (10 mm) hole shall be drilled in the center of the specimen.

4.5 The specimens are to be cut so that the long direction of the specimen is parallel to the rolling direction of the original sheet, plate, or strip.

4.6 Prior to test, the specimens are to be abraded to provide a uniform surface finish free of scale and dirt, and to remove any sharp edges or burrs due to machining or drilling operations. The final step in this abrading operation shall be done with either wet No. 80 or dry No. 120 grit paper. Care should be taken to avoid overheating the surface.

4.7 Following the abrasive treatment, the specimens shall be cleaned with a magnesium oxide paste or detergent solution to remove any residual dirt or grease, rinsed in water, dipped in acetone, and air dried.

5. Apparatus

5.1 Cylindrical TFE-fluorocarbon crevice blocks, two for each test specimen. Each block shall be 0.75 in. (19 mm) in diameter and 0.25 in. (6.4 mm) thick, with 12 radial slots 0.063 in. (1.6 mm) wide and 0.03 in. (0.8 mm) deep cut in one side (Fig. 9).

5.2 Bolt, nut and washers of UNS N10276 alloy shall be used to fasten the crevice blocks to the specimen (Fig. 9). Also, a TFE-fluorocarbon sleeve, having a wall thickness of .063 inch (1.6 mm) or less, shall be used over the bolt.

5.3 A 500-mL wide-mouth Erlenmeyer flask provided with a method of specimen support made of glass or TFE-fluorocarbon so that the specimen is vertical (within 10°), and there is minimum contact between the specimen surface and the specimen support and the flask. The flask shall be covered so as to avoid evaporation.

6. Procedure

6.1 Add 450 mL of sodium chloride solution ot the flask and place the flask in a room where the temperature is 68 to 75°F (20 to 24°C). As many different test solutions with concentrations as given in 3.1 shall be tested at one time as is considered necessary to establish the critical concentration for crevice corrosion.

6.2 Fasten the two crevice blocks to the test specimen by passing the sleeved bolt through the hole in the specimen and positioning a block on either side of the specimen, as shown in Fig. 10. The torque on the bolt shall be 40 oz-in. (0.280 N·m) and shall be accomplished using an adjustable ¼ in. (6.35 mm) torque limiting screwdriver. Use plastic gloves to avoid hand contact with metal surfaces during this operation. There shall be no metallic contact between the bolt assembly and the specimen.

6.3 The specimen shall be totally immersed in the test solution.

6.4 Duration of the test is 1000 h, with fresh solution being added every two weeks.

6.5 At the end of the test period, the assembly is removed from the test solution, the test specimen is removed from the assembly, rinsed in water, and dried. The surface of the specimen which was under the crevice blocks is examined for crevice corrosion according to the procedure of 7.1.

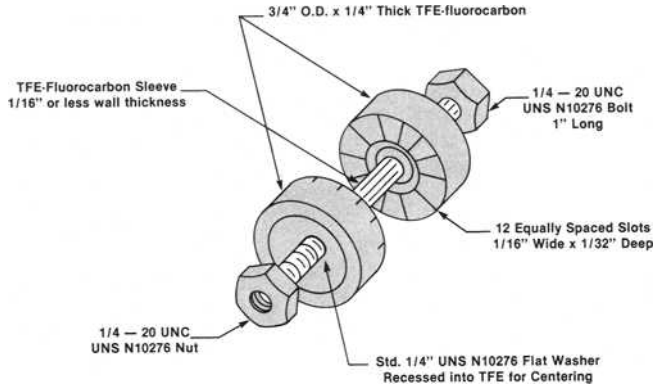


FIG. 9—*Crevice block assembly.*

6.6 The test is repeated until two test series are made which give the same critical sodium chloride concentration for crevice corrosion.

7. Examination and Evaluation

7.1 Examine areas under the crevice blocks for crevice attack using low power ($\times 20$) magnification. Crevices are considered corroded if the local attack is 1.0 mil or greater, as estimated by either a needle-point micrometer gage or microscope with calibrated fine-focus knob.

8. Control Tests

8.1 Using the above procedure, control tests shall be made with samples of alloys supplied by MTI. The control alloys are UNS S30400 and S31600.

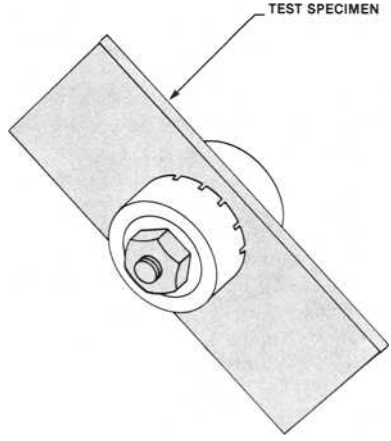


FIG. 10—*Crevice block assembly with specimen.*

9. Reporting the Data

9.1 For each crevice corrosion test, a report sheet shall be prepared which will include the items discussed below.

9.2 *Alloy Description*—The alloy tested shall be described by its commercial name, manufacturer, UNS number (if any), and the nominal composition as specified by the manufacturer.

9.3 *Alloy Composition*—The heat number of the material tested shall be reported together with the heat analysis.

9.4 *Alloy Manufacture*—The method of manufacture shall be summarized briefly; the information given shall include method of ingot manufacture and final descaling and finishing treatments. The final heat treatment conditions of temperature and cooling method shall be reported.

9.5 *Alloy Mechanical Properties*—The yield strength, tensile strength, elongation and reduction in area, and hardness shall be given for the heat of material tested.

9.6 *Specimen Source*—The size and gage dimension of the sheet, plate, or strip from which the specimen was cut shall be reported together with information on the orientation of the specimen relative to the rolling direction. The final surface preparation of the specimen shall be reported.

9.7 Report the number of areas of crevice attack greater than 1.0 mil in depth found under the crevice blocks for each test. Report the critical sodium chloride concentration for crevice corrosion (CCC) for the alloy being tested as being the lowest concentration among the series of concentrations in 3.1 at which crevice corrosion was observed.

APPENDIX E

Method MTI-5 for Laboratory Testing of Wrought Iron- and Nickel-Base Alloys for Relative Resistance to Stress-Corrosion Cracking in a Sodium Chloride Drop Evaporation System

1. Scope

1.1 This method describes the procedure for corrosion tests to determine the relative resistance of wrought iron- and nickel-base alloys to stress-corrosion cracking in a sodium chloride drop evaporation system. Data from these corrosion tests will be included in the MTI compilation of properties of new alloys.

1.2 This method results in a number, minimum stress for failure, which can be used to rank order alloys for their relative resistance to stress-corrosion cracking in a sodium chloride solution. This rank ordering may or may not be applicable to other chloride environments.

2. Applicable Documents

2.1 Method for Laboratory Testing of Wrought Iron- and Nickel-Base Alloys for Relative Resistance to Stress-Corrosion Cracking in a Boiling Magnesium Chloride Solution (MTI-3).

3. Apparatus

3.1 Horizontal constant-load machine capable of applying a measured load of up to 400 lb (1800 N), and equipped with gripping devices to handle the specimens described in 4.5.

3.2 Equipment for applying an alternating current of approximately 24 A at a voltage of 1 V or less to the specimen so as to provide resistance heating of the specimen.

3.3 Contact thermocouple to measure the temperature of the specimen.

3.4 A reservoir for the sodium chloride solution and a micropump connected to a 180 mm long vertical glass tube (0.5 mm internal diameter, 4.5 mm external diameter) located so that the tube orifice is 10 mm above the center of the specimen. The system shall be capable of delivering a controlled flow of salt solution of 40 drops per minute.

4. Test Specimens

4.1 The test specimens shall be tension specimens with a circular cross section in the gage length.

4.2 The specimens shall be made from sheet, plate, or strip made by commercial methods.

4.3 The material from which the specimens are made shall be in the annealed condition, the final heat treatment being done after any cold rolling. The temperature of the final heat treatment and the method of cooling shall be reported.

4.4 Specimens are to be cut to size by a machining operation.

4.5 The specimens are to be cut so that the long direction of the specimen is parallel to the rolling direction of the original sheet, plate, or strip.

4.6 The specimen dimensions are 0.08 × 0.08 × 4.0 inches (2 × 2 × 100 mm), with a 0.4 inch (10 mm) long cylindrical gage length 0.07 inch (1.8 mm) in diameter. The gage length should be faired into the grip sections with a suitable gradual radius.

4.7 Prior to test, the specimen shall be degreased by washing in a detergent solution, rinsed in distilled water, and electropolished for 3 minutes in an electrolyte of the following composition: 150 g citric acid, 600 ml H_3PO_4 of density 1.70, 450 ml H_2SO_4 of density 1.84 and 300 ml H_2O.

5. Test Solution

5.1 The test solution is a 0.6% solution of reagent grade sodium chloride in distilled water.

6. Procedure

6.1 The specimen is attached to the gripping devices and the specified load is applied by direct loading in tension.

6.2 The load applied shall be one of the following fractions of the 0.2% offset yield strength of the alloy at 400°F (204°C): 0.1, 0.3, 0.5, 0.7, or 0.9.

6.3 The specimen is resistance heated to a temperature of 570°F (300°C) as measured by the contact thermocouple.

6.4 The test solution is dripped onto the test section of the specimen at a rate of 40 drops a minute.

6.5 The test is continued until the specimen ruptures, up to a maximum time of 500 h. The time to rupture is recorded.

6.6 The ruptured specimen shall be examined metallographically to confirm that the failure was due to stress-corrosion cracking.

6.7 The test is repeated at other fractions of the yield strength until the minimum stress for failure in 500 h is determined. This value shall be the fraction of the yield strength (from the list in 6.2) at which failure did occur, but which was just above the stress at which no failure occurred in 500 h. The test shall be repeated until two similar values are obtained for the minimum stress for failure by stress-corrosion cracking.

7. Control Tests

7.1 Using the above procedure, control tests shall be made with UNS alloy S31600. Samples of the control alloy will be supplied by MTI.

8. Reporting the Data

8.1 For each stress-corrosion test, a report sheet shall be prepared which will include the items discussed below.

8.2 *Alloy Description*—The alloy tested shall be described by its commercial name, manufacturer, UNS number (if any), and nominal composition as specified by the manufacturer.

8.3 *Alloy Composition*—The heat number of the material tested shall be reported together with the heat analysis.

8.4 *Alloy Manufacture*—The method of alloy manufacture shall be summarized briefly; the information given shall include method of ingot manufacture and final descaling and finishing treatments. The final heat treatment conditions of temperature and cooling method shall be reported.

8.5 *Alloy Mechanical Properties*—The yield strength, tensile strength, elongation and reduction in area, and hardness shall be given for the heat of material tested.

8.6 *Specimen Source*—The size and gage dimension of the sheet, plate or strip from which the specimen was cut shall be reported together with information on the orientation of the specimen relative to the rolling direction.

8.7 *Temperature* of the test speciment shall be reported. The average temperature shall be given together with the minimum and maximum values.

8.8 The *visual appearance* of the failed specimens ($\times 20$) at the end of the test shall be reported together with the results of the metallographic examination.

8.9 The *time for failure* shall be given for each test plus the value of the minimum stress for failure, expressed as a fraction of the yield strength at 400°F (204°C).

References

[1] Brigham, R. J., *Corrosion*, Vol. 30, No. 11, Nov. 1974, pp. 396–398.
[2] Henrikson, S. and Asberg, M., *Corrosion*, Vol. 35, No. 9, Sept. 1979, pp. 429–431.

Timothy D. Whitehead[1] *and Calvin H. Baloun*[2]

Evaluating the Suitability of the NACE Standard Test, TM-01-77, for Testing 13% Chromium Martensitic Stainless Steels for Sulfide Stress Cracking Resistance

REFERENCE: Whitehead, T. D. and Baloun, C. H., **"Evaluating the Suitability of the NACE Standard Test, TM-01-77, for Testing 13% Chromium Martensitic Stainless Steels for Sulfide Stress Cracking Resistance,"** *Laboratory Corrosion Tests and Standards, ASTM STP 866*, G. S. Haynes and R. Baboian, Eds., American Society for Testing and Materials, Philadelphia, 1985, pp. 400–414.

ABSTRACT: Potentiostatic anodic polarization curves were used to study the pitting resistance of American Iron and Steel Institute (AISI) Type 420 (Unified Numbering System [UNS] S42000) stainless steel in solutions containing bicarbonate, sodium chloride, hydrogen sulfide, and carbon dioxide. The effect of applied potential on the sulfide stress cracking (SSC) of this material was also investigated. The appropriateness of the test solution, described in the National Association of Corrosion Engineers (NACE) (TM-01-77), for determining the SSC of Type 420 stainless steel is then evaluated in light of the results of this investigation.

KEY WORDS: stress corrosion tests, chromium, passivity, sulfide stress cracking, sulfide stress corrosion cracking, AISI Type 420, AISI Type 410, polarization measurement, pitting corrosion

The most widely used laboratory environment for determining material resistance to sulfide stress cracking (SSC) is that recommended in the National Association of Corrosion Engineers (NACE) Standard Testing of Metals for Resistance to Sulfide Stress Cracking at Ambient Temperatures (TM-01-77). It is a solution of 0.5% weight acetic acid and 5% weight sodium chloride, saturated with hydrogen sulfide under a partial pressure of 0.1 MPa (1 atm). This will be referred to as the "NACE solution" throughout the rest of the paper. The various stress cracking test methods, in conjunction with the NACE solution, have been very useful in identifying and ranking medium and high strength carbon steels for their SSC susceptibility and have played an important role in the successful

[1]Research chemist, Petrolite Corp., 369 Marshall Ave., St. Louis, MO 63119.
[2]Professor, Department of Chemical Engineering, Ohio University, Athens, OH 45701.

Copyright© 1985 by ASTM International www.astm.org

development of deep sour gas wells. However, the results of SSC tests on 12 to 13% chromium martensitic stainless steels, such as AISI Type 410 and 420 (Unified Numbering System [UNS] S41000 and S42000), in the NACE solution were not consistent with the eventual, successful use of these materials [*1–3*].

The purpose of this investigation was to study the factors influencing the corrosion behavior of 12 to 13% chromium martensitic stainless steels (12-13Cr steels) and to use this information to evaluate the suitability of the NACE solution for testing the SCC susceptibility of these materials.

Experimental Procedure

Material

All specimens were machined from a section of AISI Type 420 stainless steel tubing, having the nominal chemical composition and physical properties given in Table 1. The tubing was heat treated in the following manner: austenitized at 980°C, air cooled, then tempered at 700°C [*3*].

The specimens for the anodic polarization curves were cylindrical buttons with surface areas ranging from 3 to 5 cm^2. Before use, the specimens were polished and prepared as described in the ASTM Recommended Practice Standard Reference Method for Making Potentiostatic and Potentiodynamic Anodic Polarization Measurements (G 5), except xylene was used for degreasing them.

The stress specimens were machined to the dimensions given in NACE TM-01-77. Except for approximately 5 cm^2 in the reduced section, the specimen surfaces were painted with a beeswax resin to isolate them from the corrosive environment. No additional treatment of the specimen surfaces was made except for degreasing with xylene and ultrasonic cleaning before use.

Solutions

The solutions were 0.001, 0.1, and 1.0 *N* sodium hydroxide, saturated either with carbon dioxide or a 1% hydrogen sulfide, 99% carbon dioxide gas mixture under a total pressure of 0.1 MPa at 30°C. The resulting equilibrium pH values were 4.9, 6.7, and 7.7, respectively. The calculated bicarbonate concentrations and pH values are presented in Table 2 as a function of the initial sodium hydroxide concentration. These values were approximated using the assumption of unit activities. The correlation between calculated and experimental pH values is excellent. The chloride ion concentrations were adjusted by adding the required weight of dried sodium chloride to the solutions as needed. Distilled water was used, and all chemicals were American Chemical Society (ACS) certified reagent grade.

Potentiostatic Anodic Polarization Curves

The polarization cell and electrical apparatus were in accordance with ASTM G 5. The polarization cell was filled with 900 mL of the sodium hydroxide

TABLE 1—*Nominal chemical composition and physical properties of AISI Type 420 stainless steel.*[a]

Composition, Weight %									
Chromium	Carbon	Silicon	Manganese	Phosphorus	Sulfur	Iron	Yield Strength, psi	Tensile Strength, psi	Elongation 2 in. %
13	0.2	0.25	0.47	...	0.006	balance	95 000	117 000	21

[a] 1 psi = 6.8948 MPa and 1 in. = 25.4 mm.

TABLE 2—*Equilibrium concentrations in the NaOH/CO_2 (0.1 MPa) solutions.*

Concentration of NaOH, *M*	Experimental pH	Calculated pH	Concentration of HCO_3^-, *M*
9.389×10^{-4}	4.89	4.83	9.4×10^{-4}
9.389×10^{-3}	5.75	5.82	9.5×10^{-3}
9.389×10^{-2}	6.70	6.73	9.3×10^{-2}
9.389×10^{-1}	7.49	7.46	9.3×10^{-1}

solution, and 100 mL was placed in the reference electrode cell. The solution was deaerated using a biological grade anaerobic carbon dioxide gas until the equilibrium pH was reached. If hydrogen sulfide was to be included in a particular run, then a 1% hydrogen sulfide, 99% carbon dioxide gas mixture was bubbled through the solution for an additional 30 to 45 min to insure that the equilibrium concentrations of sulfide species (H_2S, HS^-, $S^=$) were achieved. The concentration of total sulfide species was calculated to be approximately 40 ppm. The relative amounts of each species depend upon the pH.

The platinum auxiliary electrodes and the working electrode were then immersed into the solution. The working electrode was allowed to corrode freely for 1 h before beginning the polarization run. At the end of this period, the open circuit potential (OCP) was recorded, and the anodic polarization test was started from this value. The potential was first stepped in the negative direction until the current changed from anodic to cathodic, and then the scan direction was reversed. The potential step interval was 10 mV with the current being recorded at the end of 1 min. The scans were continued until a definite pitting potential could be determined or the transpassive region was reached. All polarization curves were run at 30°C, except where indicated. An anodic polarization curve was also run in the standard NACE solution.

Linear strip chart recordings were made of the current transients that occurred after each potential step change. Examples of these are shown in Figs. 1 and 2. It is observed from Figs. 1 and 2 that, at potentials below the pitting potential, the current transients relax in a very reproducible pattern. However, at the potential indicated by "pitting" in the figures, the current transient behavior becomes more erratic. The type of erratic behavior was not consistent, but the potential at which it began was found to be reproducible in a given system. The potential at which the erratic current behavior began was taken to be the pitting potential whether or not the current density was larger than in the passive region.

The potentials were measured and reported as millivolts versus the Ag/AgCl/0.1 *N* potassium chloride standard reference electrode (standard hydrogen electrode [SHE] = potential E + 288mV and standard calomel electrode [SCE] = E + 47mV) and the current as microamperes per cm^2. The data were plotted in accordance with ASTM Recommended Practice for Conventions Applicable to Electrochemical Measurements in Corrosion Testing (G 3).

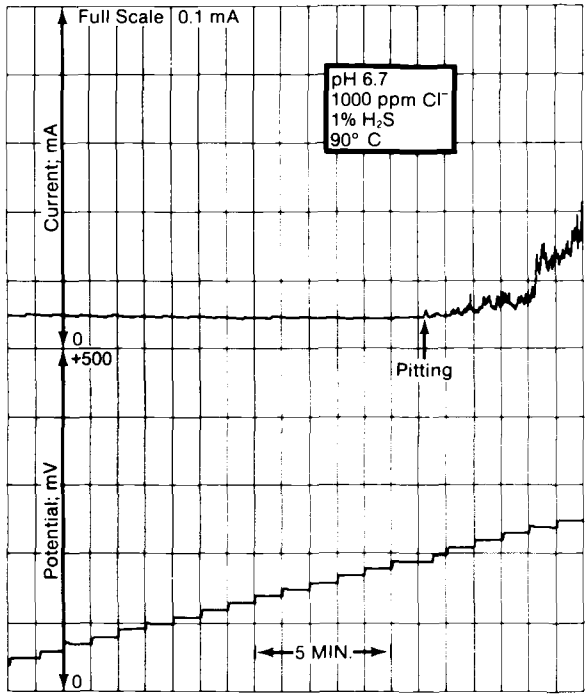


FIG. 1—*Chart recording of polarization curve at pH 6.7, showing pitting potential.*

Applied Potential, Step-Stress Tension Tests

The corrosion cells were 250-mL-thick-bottomed glass beakers through which a hole had been drilled to accommodate the stress specimens. The specimens were bolted into the cell using nylon nuts and rubber washers to insure a leak proof seal. Number 13 rubber stoppers were used as cell covers. Holes were bored through the stoppers to accommodate the working electrode (stress specimen), two 6.35-mm (¼-in) graphite auxiliary electrodes, a Luggin probe, and inlet and outlet tubes. A disposable glass pipet was used as the Luggin probe, with the remainder of the salt bridge being fabricated from polyvinyl and glass tubing. The reference cell leg of the salt bridge was filled with a 1% agar gel solution containing 1000-ppm chloride ion concentration to eliminate siphoning and hydrogen sulfide poisoning of the Ag-AgCl reference electrode. A schematic diagram of the cell assembly is shown in Fig. 3.

The cell assemblies were placed in the stress corrosion testing machines and the solutions added. The test solutions (1000-ppm Cl^-, pH 4.9 and 6.7) had previously been brought to equilibrium pH under carbon dioxide atmosphere in a separate vessel to avoid exposing the specimens to hydroxide ions. The 1%

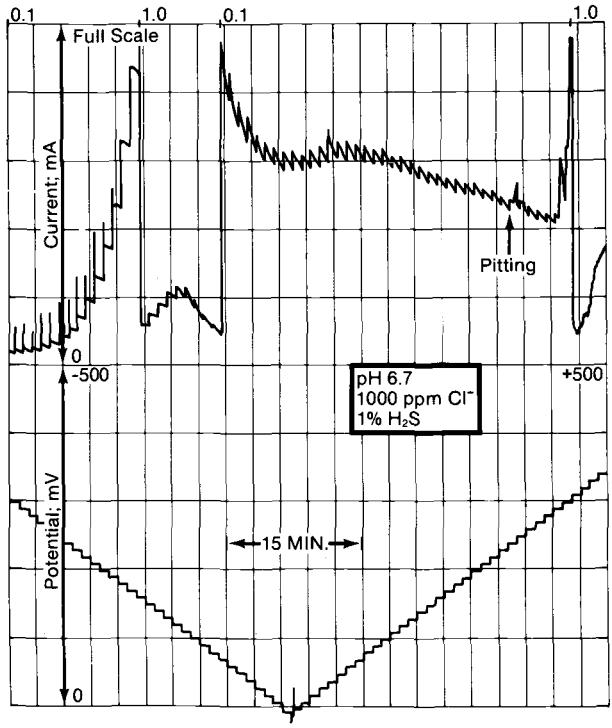


FIG. 2—*Chart recording of polarization curve at pH 6.7 showing current transient and pitting potential.*

hydrogen sulfide 99% carbon dioxide gas mixture was then bubbled through the test cells. The open current potential (OCP) was monitored for 1 h, then an initial load of 75% of the minimum yield strength (YS) was applied, and the specimens were polarized to predetermined potentials. The gas flow was continued throughout the test. The potential and current were continuously recorded for the duration of the test. The tests were run at room temperature (approximately 25°C).

The stress load was increased by 5% of the minimum YS every ten days to a maximum of 85%. Since it has been shown that the majority of failures occur within a short time (90% in 5 days) [*1,3*], it was felt that this time period was sufficient to determine if cracking would occur at each level of applied stress. The tests were continued for a total of 1000 h. Running the tests in this manner allowed each 10-day period (240 h) to be treated as its own SSC test at that level of applied load. The results were plotted as applied potential versus total hours to failure. The number of hours at a given applied load were then superimposed upon the master plot (Figure 10).

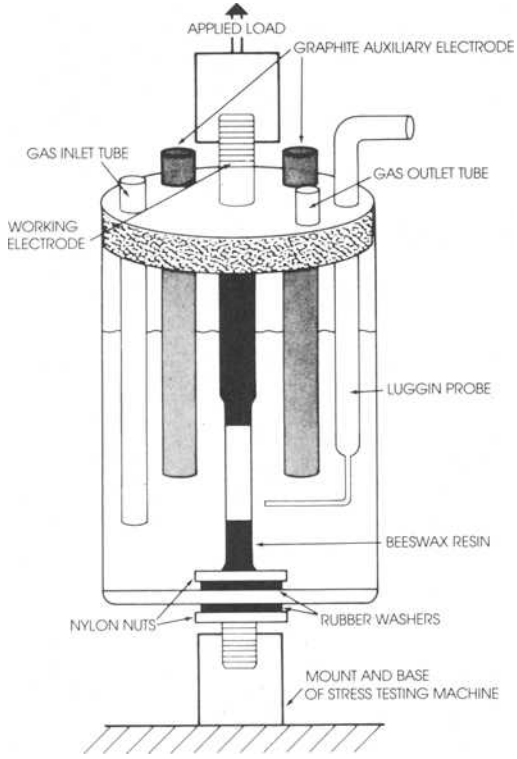


FIG. 3—*Schematic diagram of corrosion cell used in the constant applied potential, SSC tests.*

Results

Effects of Hydrogen Sulfide, pH and Chloride Concentration

A series of curves showing the effect of hydrogen sulfide is given in Fig. 4. These curves were run in sodium chloride free solutions at three pH levels. These curves show that the presence of hydrogen sulfide significantly lowers the OCP, and increases the magnitude of the passive current densities from the values observed when only carbon dioxide is used. These increases in current density have been shown to be caused mostly by the oxidation of HS^- [*4*] and not by large increases in the passive corrosion currents. The curves of Fig. 4 support this conclusion since the current density increases with increases in pH, which would correspond to higher and higher concentrations of HS^-.

The effect of hydrogen sulfide on the pitting potential of AISI Type 420 stainless steel is shown in Fig. 5 for a 1000-ppm chloride solution at pH 6.7. The pitting potentials, as determined from the chart recordings, are indicated with arrows on the curves. Again it is observed that the presence of hydrogen sulfide drastically lowers the OCP, but it does not change the value of the pitting

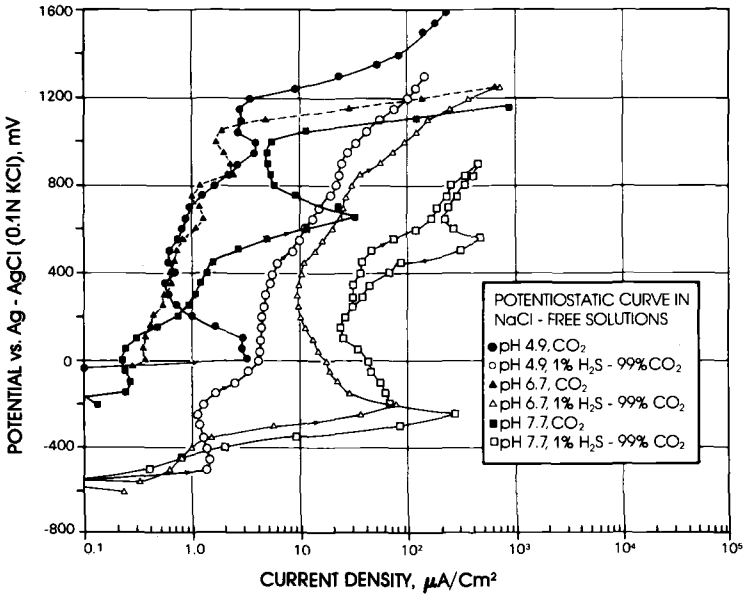


FIG. 4—*Effect of hydrogen sulfide on the polarization curves in chloride-free solutions.*

potential by any observable amount. This phenomenon was observed for all combinations of pH and chloride concentrations.

Potentiostatic polarization curves were run at all three levels of pH to investigate the interactive effects of pH and chloride concentration. At each pH the chloride concentration was increased by a factor of 10 with each sequential run, starting from 0 ppm until pitting was observed to occur at some potential above the OCP. The highest chloride concentration tested for which no pitting occurred is referred to as the maximum chloride concentration $(Cl^-)_{max}$, and the first chloride concentration at which pitting occurred is referred to as the critical chloride concentration for that pH $(Cl^-)_{crit}$. These series of curves were run both with and without hydrogen sulfide. The values of $(Cl^-)_{max}$ and $(Cl^-)_{crit}$ were shown to be independent of hydrogen sulfide. The series of curves for pH 7.7, carbon dioxide saturated, and for pH 4.7 with the 1% hydrogen sulfide, 99% carbon dioxide gas mixture are shown in Figs. 6 and 7, respectively.

The two parameters, $(Cl^-)_{max}$ and $(Cl^-)_{crit}$, are both plotted in Fig. 8 as functions of pH. In the region above the solid line AISI Type 420 stainless steel is susceptible to pitting at some potential above OCP, while in the region below the dashed line it is immune to pitting. The exact behavior in the hatch-marked region is not known, but it is obvious that somewhere in this region the values of $(Cl^-)_{max}$ and $(Cl^-)_{crit}$ are identical. The point at which they coincide would be the true critical chloride concentration for pitting at that particular pH. It is seen that the resistance to chloride pitting decreases as the pH decreases.

In Fig. 8 the series of polarization curves was carried out beyond $(Cl^-)_{crit}$.

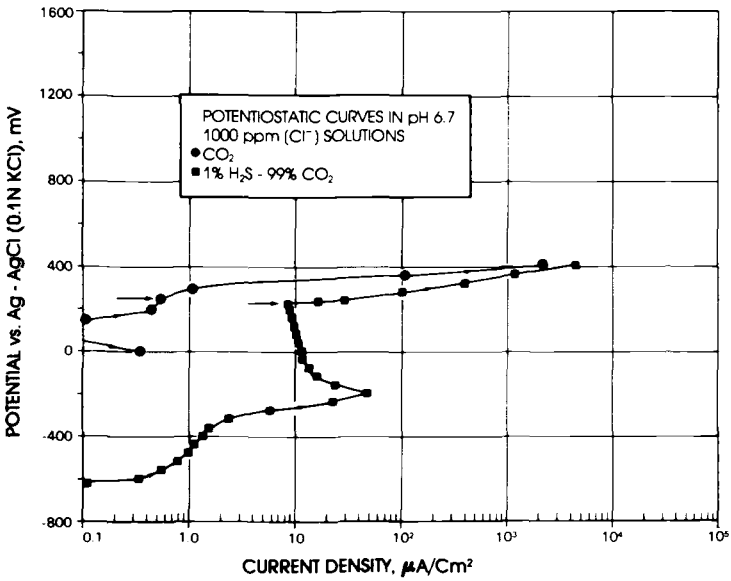


FIG. 5—*Effect of hydrogen sulfide on the pitting potential in pH 6.7, 1000-ppm chloride solutions.*

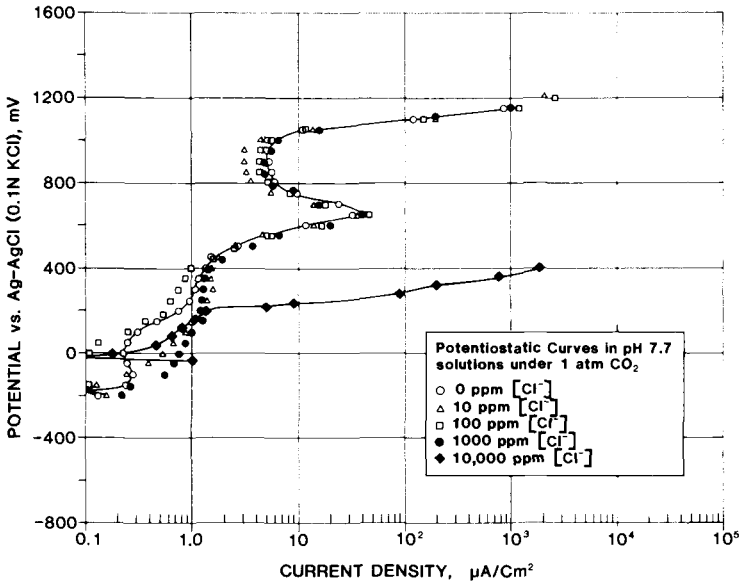


FIG. 6—*Effect of Cl^- concentration in pH 7.7 solutions, 0.1 MPa carbon dioxide.*

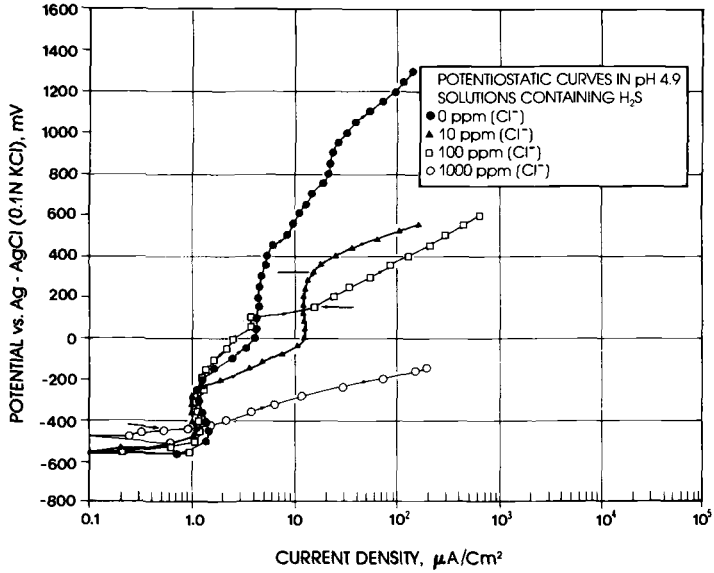


FIG. 7—*Effect of chloride ion concentration on the pitting potential.*

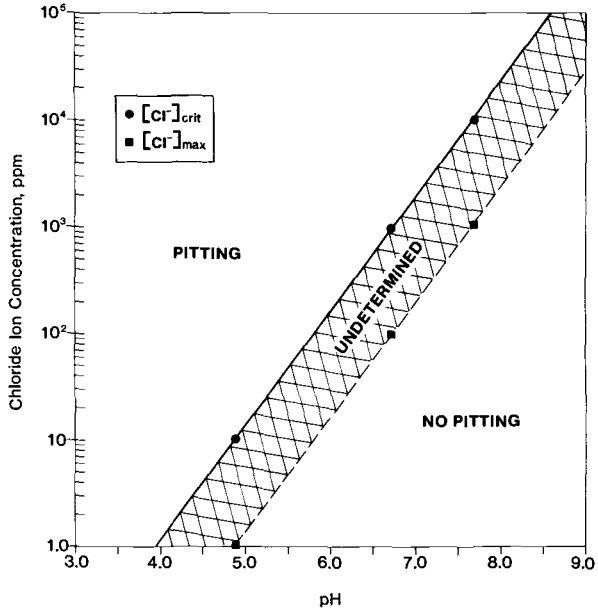


FIG. 8—$(Cl^-)_{max}$ *and* $(Cl^-)_{crit}$ *as functions of pH.*

Increasing the chloride concentration beyond $(Cl^-)_{crit}$ shifts the pitting potential in the negative direction toward the OCP.

The curve run in the standard NACE solution is shown in Fig. 9. Small anodic shifts in potential away from the OCP result in large increases in polarization current, and passivation is never achieved in this solution.

SSC

The results of the SSC tests are given in Table 3 and presented graphically in Fig. 10. It is important to note that pitting preceded and accompanied all failures, but that cracking did not necessarily initiate at pit sites. The most obvious observation from the data of Fig. 10 is that, even if the effect of the differences in applied load is acknowledged, shifting the potential to values more positive than the OCP reduces the hours-to-failure because of the increased amount of pitting. The two data points at 85% minimum YS, (−430 mV, 152 h) and (−470 mV, no failure [NF]) indicate that this behavior occurs at a constant applied load as well.

Consider the three data points at pH 4.9 that failed at 75% minimum YS. A curve representing the hypothetical potential/time-to-failure behavior was drawn through these points. At potentials far more noble than the OCP (solid portion of curve), corrosion is very severe and failure occurs by ductile rupture brought about by the reduction of cross-sectional area. As the applied potential is shifted to more negative values, the severity of the pitting is decreased and the time-to-failure is increased, and approaches infinity as the OCP is approached. The

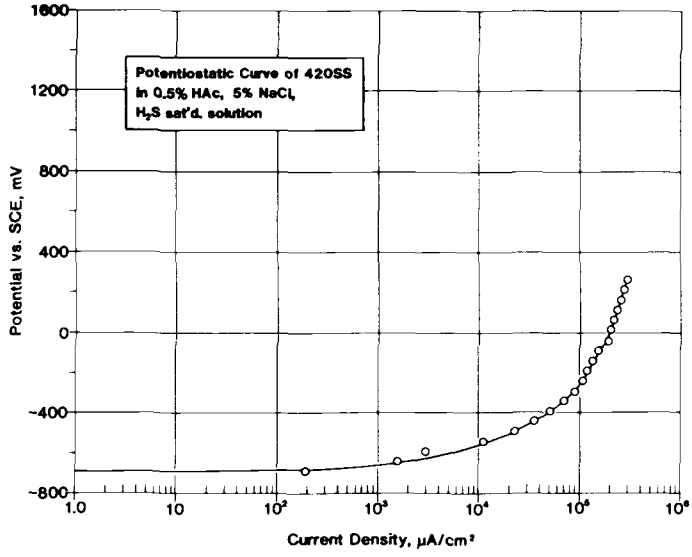


FIG. 9—*Potentiostatic curve on AISI Type 420 stainless steel in the NACE solution.*

TABLE 3—*Results of constant applied potential SCC tests.*[a]

pH	Potential, mV	HRC	Total Hours to Failure	Maximum Applied Stress, % of minimum YS	Hours to Failure at Maximum Stress	Mode of Failure
4.9	−150	23.0	5	75	5	ductile rupture
4.9	−250	21.4	11.5	75	11.5	ductile rupture
4.9	−350	20.3	195	75	195	SSC
4.9	−390	22.1	356	80	116	SSC
4.9	−430	21.5	632	85	152	SSC
4.9	−470 (OCP)	20.6	NF (1152 h)	85	NF (672 h)	...
6.7	+230	22.8	NF (1000 h)	85	NF (520 h)	...
6.7	+170	20.0	NF (1000 h)	85	NF (520 h)	...
6.7	+50	21.1	NF (1000 h)	85	NF (520 h)	...
6.7	−240	21.5	NF (1000 h)	85	NF (520 h)	...
6.7	−370 (OCP)	22.1	NF (1000 h)	85	NF (520 h)	...

[a]HRC is Rockwell hardness C-scale, and NF is no failure.

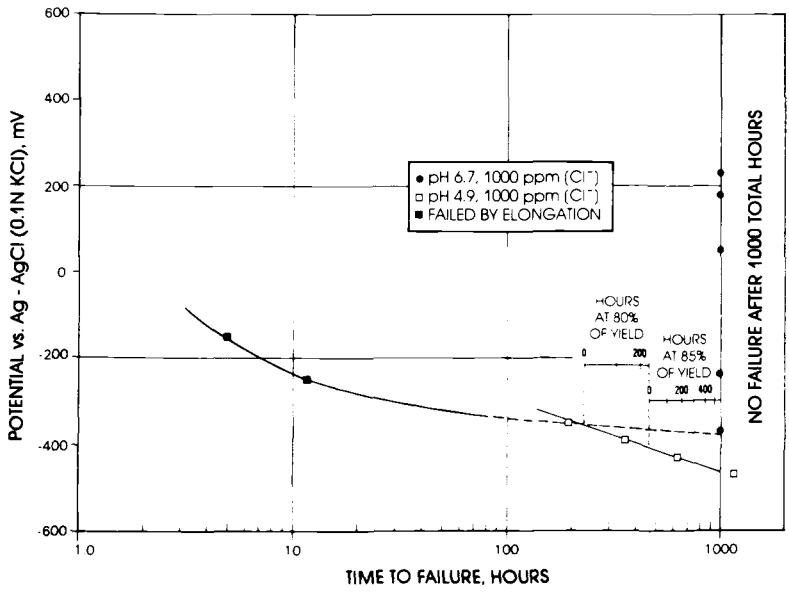


FIG. 10—*Results of the constant applied potential step-stress tension tests.*

following additional information at 75% minimum YS can be deduced from the other data: at −390 mV failure occurs some time after 356 h, at −430 mV failure occurs at some time after 632 h, and at −470 mV (OCP) failure occurs at some time after 1152 h, if at all. This additional information, although not conclusive, does lend support to the validity of the hypothetical curve drawn for a constant applied load of 75% minimum YS.

Although the exact interaction between applied potentials and load cannot be determined from the data in Table 3, it is clear that, as a general rule, an increase in the anodic potential above the OCP has a more critical effect on the time-to-failure than does an increase in the applied load.

No failure occurred for any specimen tested in the pH 6.7 solutions, even at potential above the pitting potential. From the chart recordings of these tests, it was observed that, although pitting initiated, it did not propagate for more than several hours before repassivating. No pitting or failures occurred for specimens at OCP at either pH.

Discussion

It has been shown that pitting is necessary, but not sufficient, for cracking of AISI Type 420 stainless steel to occur. It was also shown that the susceptibility to cracking increased with the severity of the pitting, as simulated by increased anodic potentials. The fact that no failures occurred at pH 6.7, even though pitting had initiated and propagated for some time before repassivating, indicates that an active corrosion process is also a necessary requirement for cracking.

Pitting, therefore, does not merely provide an initiation site for cracking to begin, but provides a mechanism for active corrosion and hydrogen generation. In light of the above observations and conclusions, it is logical to further conclude that the factors that control the pitting of 12-13Cr steels would also play a major role in controlling the SSC susceptibility.

The likelihood of AISI Type 420 stainless steel to pit increases as the pH is lowered and as the chloride concentration is increased beyond the critical value for a given pH. The pH of the NACE sour solution is between 3 and 4. According to Fig. 8 the critical chloride concentration lies between 0.1 and 1.0 ppm in this pH range. The chloride concentration in the NACE solution is 30 000 to 300 000 times larger than the critical value in this pH range. Therefore, it would be expected that AISI Type 420 stainless steel would pit and undergo severe corrosion in the NACE solution. This predicted behavior is confirmed by the polarization curve of Figure 9, which shows that no degree of passivation is achieved in the NACE solution. The importance of the breakdown of passivation to SSC susceptibility of stainless steels has been observed by other experimenters who found that the chloride concentration had no effect on SSC susceptibility, except in the case of stainless steels [*1*].

Although the results presented in this paper have shown that hydrogen sulfide does not effect the pitting potential, it cannot be concluded that hydrogen sulfide does not play an important role in the cracking mechanism, once passivation has been disturbed and pitting initiated. On the contrary, the detrimental effects of hydrogen sulfide on the corrosion and the SSC of ferrous alloys in general are well established, and it is reasonable to conclude that its effect on depassivated stainless steels could be quite significant.

The 12-13Cr steels are often chosen for downhole use in gas wells because of their high resistance to corrosion induced by aqueous carbon dioxide, and in spite of the poor SSC results obtained in the NACE solution. This resistance to carbon dioxide corrosion is due to the ability of these materials to passivate in the presence of aqueous carbon dioxide as is demonstrated by the polarization curves presented in this paper. These materials are not intended for use under very severe environmental conditions, such as during well acidizing, where passivity can not be achieved or maintained. Nor are they intended for environments with high hydrogen sulfide concentrations and little carbon dioxide. Therefore, it does not seem reasonable to test and evaluate materials that depend on passivity to resist SSC in environments where passivation cannot be achieved.

It is not the purpose of this paper to propose a more relevant test environment for evaluating SSC of stainless steels, but only to bring to light the fact that the current NACE solution is not appropriate for testing these materials. There are other environmental factors, such as temperature, carbon dioxide partial pressure, HCO_3^- concentration, and the presence of other pit inhibiting anionic species [*6*], which might effect the passivation, and consequently the SSC resistance of 12-13Cr steels. The effect of these variables needs to be assessed before a better accelerated test method can be developed.

Conclusion

The standard NACE sour solution described in NACE TM-01-77 is not appropriate for testing the SSC resistance of 12 to 13% chromium martensitic stainless steels because their SSC resistance is due to their ability to passivate in the presence of aqueous carbon dioxide, which is not present in this solution. The severity of the NACE solution does not permit passivation of these materials to occur.

References

[1] Treseder, R. S., in *H_2S Corrosion in Oil and Gas Production: A Compilation of Classic Papers*, R. N. Tuttle and R. D. Kane, Eds., National Association of Corrosion Engineers, Houston, TX, 1981, pp. 162–175.

[2] Tuttle R. N. and Kochera J. W., in *H_2S Corrosion in Oil and Gas Production: A Compilation of Classic Papers*, R. N. Tuttle and R. D. Kane, Eds., National Association of Corrosion Engineers, Houston, TX, 1981, pp. 193–197.

[3] Combes, J. D., Kerr, J. G., and Klein, L. J., *Petroleum Engineer International*, March 1983, pp. 50–70.

[4] Martin, R. L., *Application of Electrochemical Polarization to Corrosion Problems*, Petrolite Instruments, Houston, TX, 1981, pp. 35.

[5] Whitehead, T. D., "Factors Influencing Pitting and Cracking Resistance of AISI Type 420 Stainless Steel in CO_2 Environments," Master's Thesis, Department of Chemical Engineering, Ohio University, Athens, OH, 1984.

[6] Szklarsha-Smialowska, Z., *Corrosion*, Vol. 27, No. 6, June 1971, pp. 223–233.

Bo Rosborg[1] *and Anders Rosengren*[1]

Slow Strain Rate Testing in High-Purity Water at Controlled Electrode Potentials

REFERENCE: Rosborg, B. and Rosengren, A., **"Slow Strain Rate Testing in High-Purity Water at Controlled Electrode Potentials,"** *Laboratory Corrosion Tests and Standards, ASTM STP 866,* G. S. Haynes and R. Baboian, Eds., American Society for Testing and Materials, Philadelphia, 1985, pp. 415–427.

ABSTRACT: A closed-loop oxygen dosage and electrode potential control system has been designed for slow strain rate testing in high-purity water at controlled electrode potentials. It is used instead of a potentiostat in order to circumvent the experimental difficulty with an IR drop caused by the high resistivity of the environment. By means of this system slow strain rate testing of sensitized American Iron and Steel Institute (AISI) Type 304 (Unified Numbering System [UNS] 530400) stainless steel has been performed in high-purity high-temperature water at different electrode potentials, the occurrence of intergranular stress corrosion cracking being revealed by fractography. In this way the electrode potential below which intergranular stress corrosion cracking does not occur has been estimated; at 200°C a critical potential of −250 mV versus the standard hydrogen electrode (SHE) was obtained.

KEY WORDS: stress corrosion, electrode potentials, high-temperature tests, high purity water, slow strain rate testing

It has been known for quite some time that austenitic stainless steels, when sensitized and heavily stressed, are prone to intergranular stress corrosion cracking (IGSCC) in oxygenated high-purity water at high temperatures [*1*]. Failures because of IGSCC of weld sensitized American Iron and Steel Institute (AISI) Type 304 (Unified Numbering System [UNS] 530400) stainless steel piping in boiling water reactors (BWRs) have occurred and are a matter of concern [*2,3*].

Several remedies for BWR pipe cracking have been developed [*3*]. It has been proposed that IGSCC of sensitized austenitic stainless steel in oxygenated high-purity water at high temperatures can be avoided by keeping the corrosion potential below a certain electrode potential, that is, the critical potential for IGSCC [*4,5*]. This paper describes an experimental method of estimating this critical potential by means of slow strain rate testing (SSRT) in high-purity water at controlled electrode potentials, without the addition of any supporting electrolyte to increase the conductivity of the water.

[1]Section head and corrosion specialist, respectively, Studsvik Energiteknik AB, Department of Industrial Technology, S-611 82 Nyköping, Sweden.

Copyright© 1985 by ASTM International www.astm.org

Slow Strain Rate Testing

In SSRT the specimen is subjected to an increasing strain while exposed to a specified environment (International Organization for Standardization (ISO) Recommendations for Conducting Slow Strain Rate Stress Corrosion Tests [ISO/DP 7539/7]). The merits of SSRT compared to other methods of stress corrosion testing are described in Ref. *6*.

Sensitized Austenitic Stainless Steels

SSRT is a very useful accelerated test method for determining the susceptibility to IGSCC of sensitized austenitic stainless steels in oxygenated high-purity water at elevated temperatures [*7*]. Besides shorter exposure times than constant deformation and constant load testing, it also gives a better reproducibility [*8*]. SSRT also has the great advantage of invariably producing failure of the specimen.

Autoclave Equipment

SSRT in high-temperature water differs from SSRT in media under ambient conditions only by the necessity of using an autoclave system. The SSRT described below was performed in a once-through flow autoclave system, which has been described previously [*8*].

The autoclave with its specimen holder is shown in Fig. 1. The specimen (Fig. 2) is galvanically insulated from the specimen holder by means of alumina pieces. Only the gauge section of the specimen is exposed to the aqueous environment. The autoclave is designed for electrochemical testing.

The volume of the small autoclave is 0.8 L. In the testing described below the flow rate was 5 L/h. In order to obtain a desired oxygen content in the water inside the autoclave, oxygenated water is dosed into the deoxygenated water as shown in Fig. 3.

Controlled Electrode Potential Testing

There are several problems when performing controlled electrode potential testing in high-purity water at elevated temperatures:

1. the selection of a suitable reference electrode,
2. the insulation and sealing of the electrode leads, and
3. the high resistivity of the environment giving rise to a high IR-drop when using a potentiostat (in the ordinary manner).

A compilation of techniques for electrochemical measurements in high-temperature aqueous solutions is found in Ref *9*.

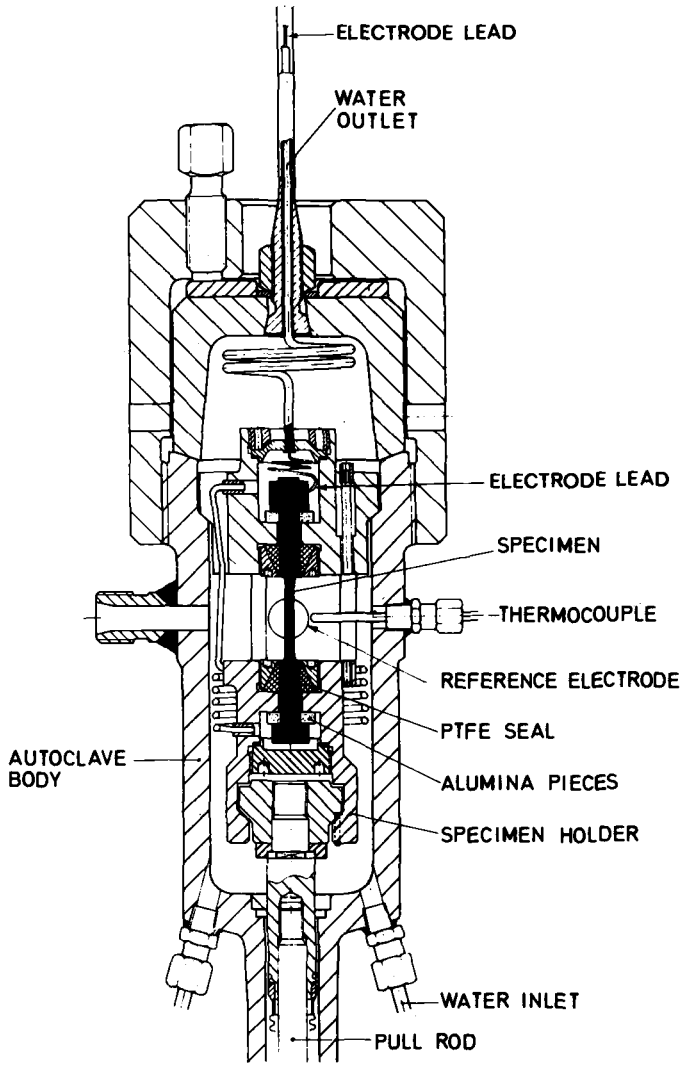


FIG. 1—*Autoclave with specimen holder.*

Reference Electrode

Reference electrode designs for electrochemical measurements in aqueous media at high temperatures are described in the literature [*10,11*]. The most commonly used reference electrode for corrosion testing in high-temperature aqueous solutions is the silver chloride electrode.

The internal silver chloride electrode (Ag, $AgCl_2$ (solid)/0.01-molal potassium chloride) used in the present work is similar to a reference electrode design that

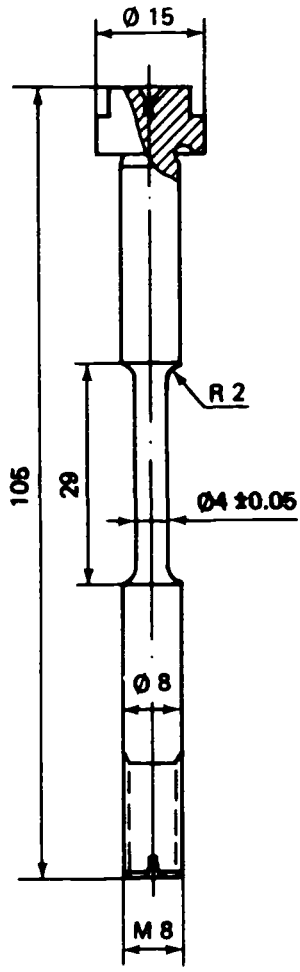


FIG. 2—*Specimen with dimensions in millimetres.*

has previously been reported on [*12*]. It is shown in Fig. 4 and is briefly described below.

The electrode consists of a silver rod, one end of which has repeatedly been dipped into molten silver chloride. The silver rod is surrounded by zirconia sand and a 0.01-molal potassium chloride solution enclosed in a polytetrafluoroethylene (PTFE) electrode body. A "buffer" reservoir, also filled with zirconia sand and the same solution, is attached to the electrode body. The electrode body and the "buffer" reservoir are seperated by a porous zirconia plug. A zirconia tube forms the liquid junction between the "buffer" reservoir and the test solution.

Measured electrode potentials were converted to the standard hydrogen electrode (SHE) scale by a method described in Ref. *13*.

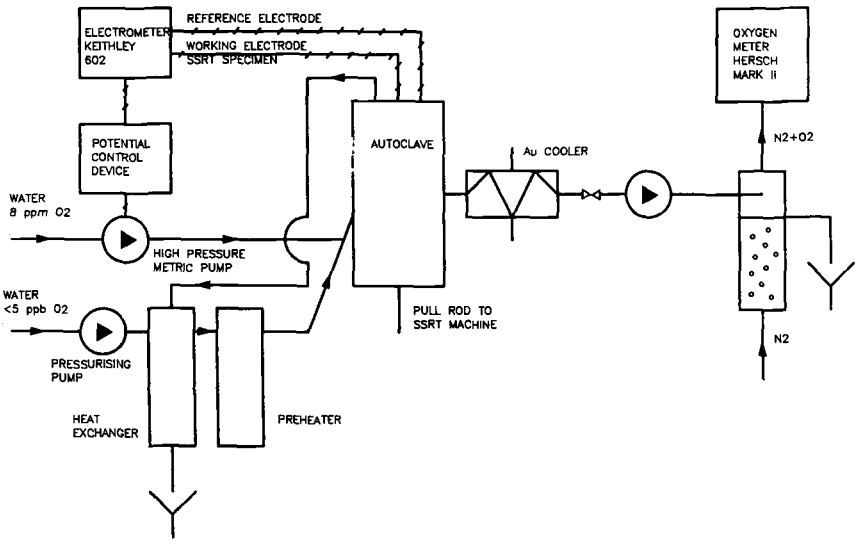


FIG. 3—*Experimental setup for SSRT at controlled electrode potential.*

Electrode Leads

It is important that the electrode leads have adequate insulation. This is particularly true for so-called polarizable electrodes.

As the working electrode of interest often is an easily polarizable electrode, its electrode lead insulation should be high and reliable in order to ensure that the measurements solely refer to the working electrode. We use an electrode lead design for which the PTFE insulation is not in contact with the aqueous environment, but only with a cover gas (Fig. 1). Thus, its impedance to the ground is satisfactory.

For the reference electrode lead we use a thick PTFE insulation (Fig. 4). It is in contact with the aqueous environment. However, the reference electrode is a nonpolarizable electrode.

IR Drop

One way to circumvent the problem with a high IR drop is to add a supporting electrolyte to increase the conductivity of the water, but such an addition may have an influence on the result [*4,14,15*]. Another is to compensate for the IR drop by electronic means. A third way is to control the electrode potential by means of a closed-loop oxygen dosage and electrode potential control system instead of a potentiostat. The latter technique was adopted for the present work.

Electrode Potential Control System

The experimental setup for SSRT under electrode potential control is shown in Fig. 3. The electrode potential is continuously measured by an electrometer,

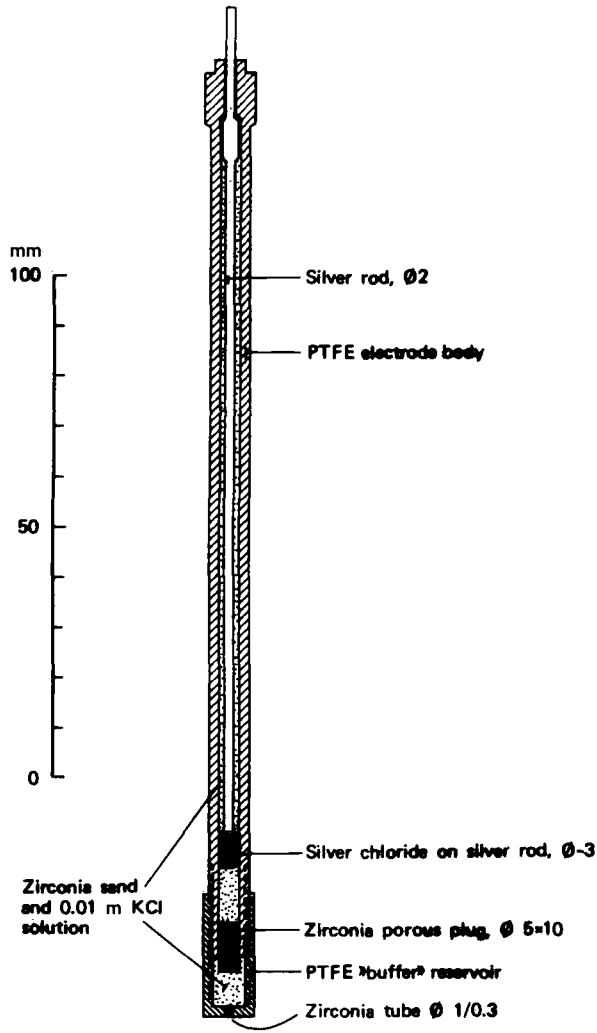


FIG. 4—*Internal silver chloride reference electrode design.*

and the recorded value is compared to the preset value on the potential control device. Any deviation acts upon the servomechanism on the high-pressure dosage pump, thus increasing or lowering the dosage rate of oxygenated water to the deoxygenated water and maintaining the electrode potential on the preset value. The dosage point is situated close to the water inlet of the autoclave in order to decrease the response time of the system.

Compared to potentiostatic control the electrode potential control by means of oxygen dosage involves no separation of the anode and the cathode process, that is, the working electrode is still a freely corroding electrode. The obvious

disadvantage of the oxygen dosage method is that no quantitative electrode kinetic information is directly obtained.

Critical Potential for IGSCC

Using the electrode potential control system described above the critical potential for IGSCC of a sensitized Type 304 stainless steel in high-purity water at 200°C has been determined by means of SSRT of heavily furnace sensitized specimens at different electrode potentials, the occurrence of IGSCC being revealed by fractography. The conductivity of the high-purity water was less than 0.1 μS/cm.

Material and Specimens

The composition of the Type 304 stainless steel used is shown in Table 1. Smooth cylindrical tension test specimens of the dimensions shown in Fig. 2 were used. After machining from 15-mm bar, they were first quench annealed (1060°C/15 min), then heavily sensitized (620°C/40 h), and finally wet polished with 600-mesh paper.

The electrochemical potentiokinetic reactivation (EPR) method according to the procedure described in ASTM STP 656 was used for determining the degree of sensitization [*16*]. The integral charge normalized to the grain boundary area was found to be P_a (C/cm^2) = 70. The EPR etched microstructure is shown in Fig. 5.

Experimental Procedure

The SSRT to estimate the critical potential for IGSCC was performed according to the following procedure. The unloaded specimen was exposed to deoxygenated high-purity water during heating to 200°C and until a stable corrosion potential was established at this temperature. Then oxygenated water was added and controlled by means of the closed-loop oxygen dosage and electrode potential control system so that the electrode potential was maintained on the preset value. The straining was finally initiated after about 15-h exposure at the selected electrode potential.

In all tests the elongation rate was 5.8×10^{-4} mm/min, equivalent to a nominal strain rate of 3.9×10^{-7} s^{-1} for the smooth specimens used.

After failure each specimen was examined in a scanning electron microscope.

Results and Discussion

The results from the SSRT at electrode potentials between −250- and −100-mV SHE are shown in Figs. 6 through 8. While IGSCC was obtained at −200-mV SHE and above, no IGSCC was obtained at −250-mV SHE. Thus, the results show that the critical potential for IGSCC of the sensitized Type 304

TABLE 1—*Composition of the Type 304 stainless steel, weight %.*

Carbon	Silicon	Manganese	Phosphorus	Sulfur	Chromium	Nickel	Molybdenum	Copper	Nitrogen
0.050	0.57	1.25	0.020	0.014	18.38	9.10	0.18	0.13	0.052

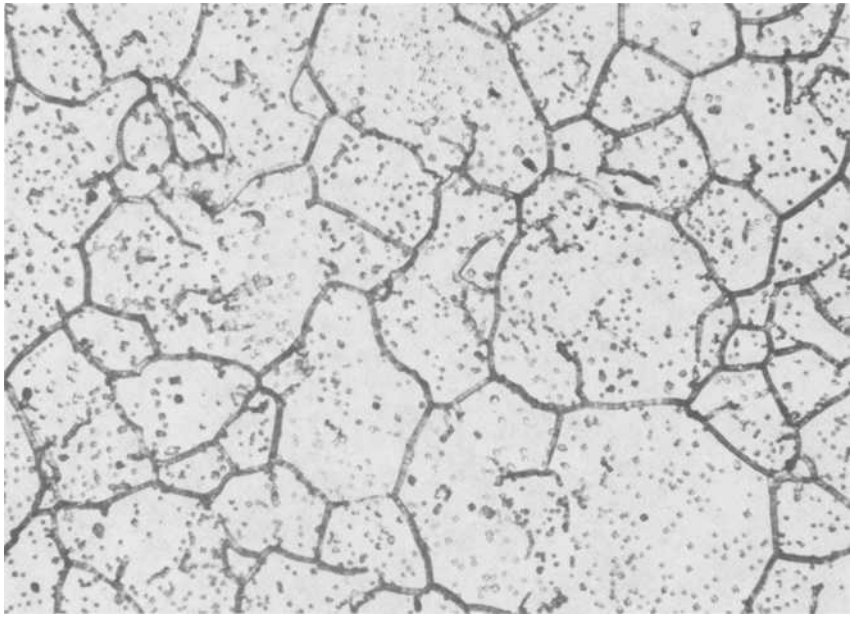


FIG. 5—*The EPR etched microstructure* (×200).

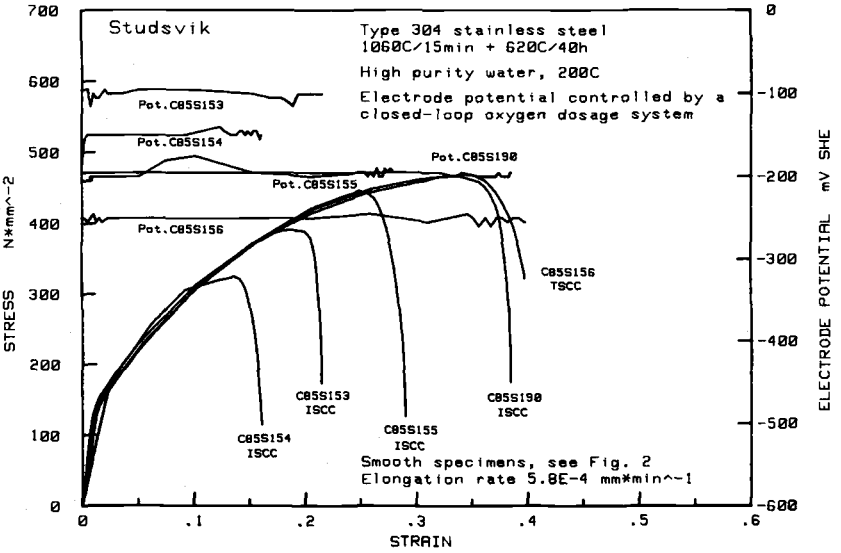


FIG. 6—*Stress-strain curves from SSRT at 200°C.*

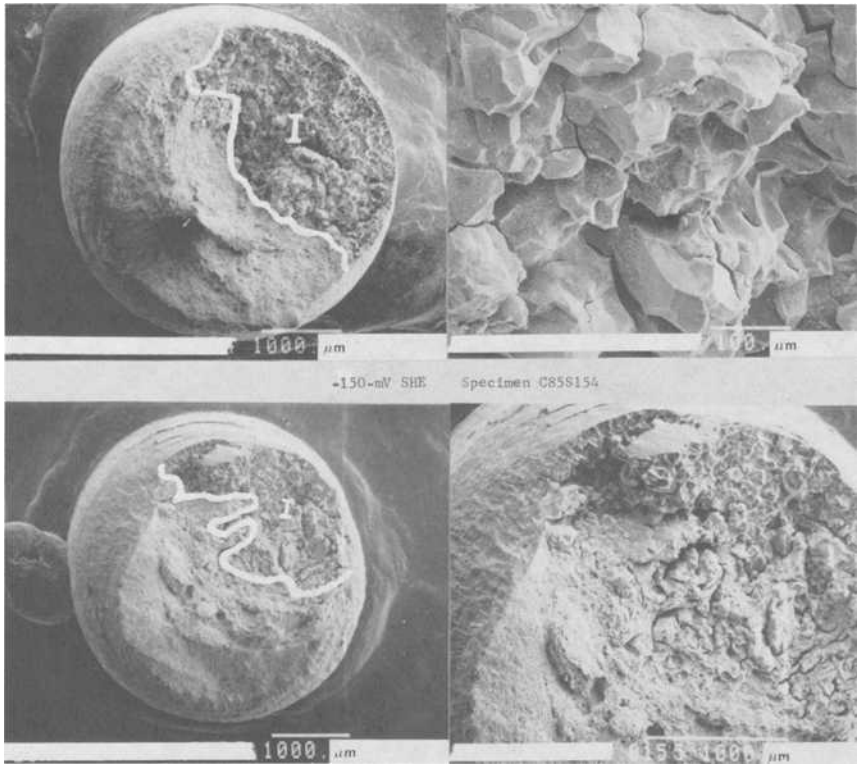


FIG. 7—*Fractographs from SSRT at 200°C: Specimen C85S154, −150-mV SHE; and Specimen C85S155, −200-mV SHE.*

stainless steel in high-purity water at 200°C falls in the range −250- to −200-mV SHE, and −250-mV SHE is chosen as an estimate of the critical potential.

In comparison SSRT of sensitized Type 304 stainless steel in dilute aqueous solutions at 200°C using a potentiostat to control the electrode potential has given the following critical potentials for IGSCC:

1. in 10^{-2}-molal sodium chloride solution, −300- to −200-mV SHE [5],
2. in 10^{-2}-molal sodium sulfate solution, −270- to −220-mV SHE,[2]
3. in 10^{-2}-molal boric acid + 10^{-3}-molal lithium hydroxide solution, 75- to 100-mV SHE [*17*].

While the results obtained in the dilute sodium chloride and sodium sulfate solutions fall in the same potential range as the above result obtained in high-purity water, the borate solution gave a substantially higher critical potential for IGSCC.

[2]Tanno, K., Iwate University, 4-3-5-, Ueda, Morioka, 020 Japan, personal communication.

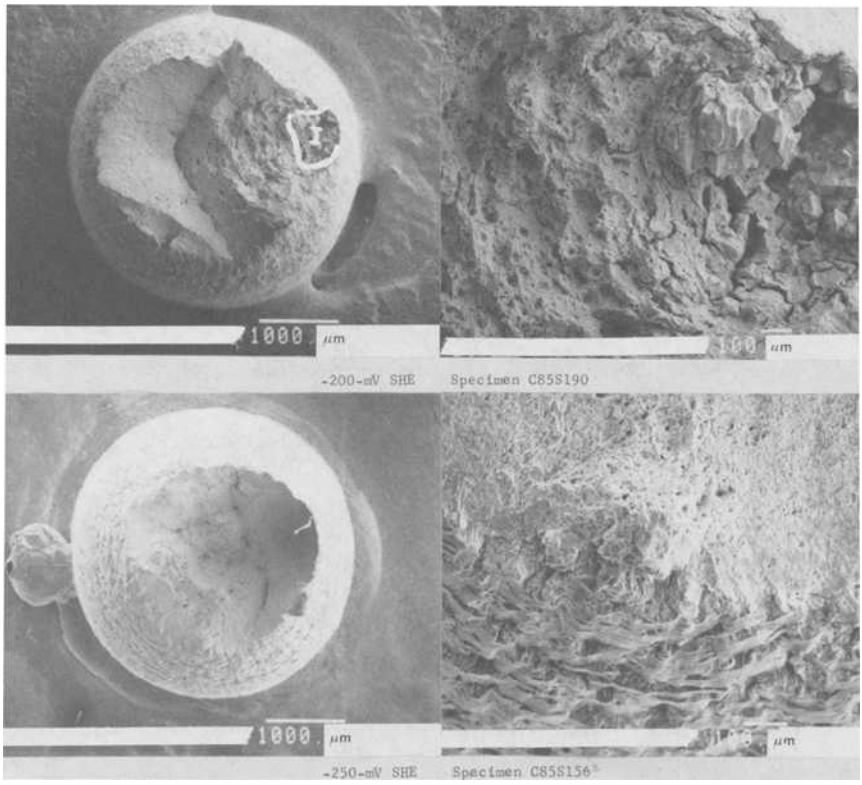


FIG. 8—*Fractographs from SSRT at 200°C: Specimen C85S190, −200-mV SHE; and Specimen C85S156, −250-mV SHE.*

For the very same heat and heat treatment, and using the same experimental method as described in this paper, the critical potential for IGSCC in high-purity water at 250°C has been estimated to −300-mV SHE [*18*].

Summary

SSRT at controlled electrode potentials has been performed to estimate the electrode potential below which IGSCC does not occur in sensitized Type 304 stainless steel exposed to oxygenated high-purity water at elevated temperatures. By using a closed-loop oxygen dosage and electrode potential control system instead of a potentiostat, a supporting electrolyte addition was not necessary. Thus, the testing has been performed in a high-purity water-oxygen environment.

At 200°C the critical potential for IGSCC has been estimated to −250-mV SHE, compared to −300-mV SHE at 250°C for the same material and experimental method.

Acknowledgments

This work has partly been sponsored by the National Swedish Board for Technical Development and partly by the following companies: Swedish State Power Board, OKG Aktiebolag, Southern Sweden Power Supply, ASEA-ATOM, and Studsvik Energiteknik AB.

Many of our colleagues have contributed to this work and their assistance is gratefully acknowledged.

References

[*1*] Hübner, W. and Johansson, B. J. E., "Stress Corrosion Cracking of Austenitic Fe-Cr-Ni Alloys in High Temperature Water With and Without Chlorides," *Reviews on High-Temperature Material*, Vol. 2, No. 1/2, 1974, pp. 159–195.

[*2*] Klepfer, H. H. et al, "Investigation of Cause of Cracking in Austenitic Stainless Steel Piping," NEDO-21000, General Electric, San José, CA, 1975.

[*3*] Fox, M. "An Overview of Intergranular Stress Corrosion Cracking in BWRs," *Journal of Materials Energy Systems*, Vol. 1, No. 3, Dec. 1979, pp. 3–13.

[*4*] Indig, M. E. and McIlree, A. R., "High Temperature Electrochemical Studies of the Stress Corrosion of Type 304 Stainless Steel," *Corrosion*, Vol. 35, No. 7, July 1979, pp. 288–295.

[*5*] Lin, L. F., Cragnolino, G., Szklarska-Smialowska, Z., and Macdonald, D. D., "Stress Corrosion Cracking of Sensitized Type 304 Stainless Steel in High Temperature Chloride Solutions," *Corrosion*, Vol. 37, No. 11, Nov. 1981, pp. 616–627.

[*6*] Ugiansky, G. M. and Payer, J. H., Eds., *Stress Corrosion Cracking—The Slow Strain-Rate Technique, STP 665*, American Society for Testing and Materials, Philadelphia, 1979.

[*7*] Solomon, H. D., Povich, M. J., and Devine, T. M., "Slow Strain-Rate Testing in High Temperature Water," *Stress Corrosion Cracking—The Slow Strain-Rate Technique, STP 665*, American Society for Testing and Materials, Philadelphia, 1979, pp. 132–148.

[*8*] Rosengren, A. and Rosborg, B., "Constant Elongation Rate Testing of Sensitized Austenitic Stainless Steels in Oxygenated High Purity Water at 300°C," *Proceedings of the 8th Scandinavian Corrosion Congress*, Vol. 1, Helsinki University of Technology, Helsinki, Finland, 1978, pp. 296–304.

[*9*] Jones, D. de G., Slater, J., and Staehle, R. W., "High Temperature High Pressure Electrochemistry in Aqueous Solutions," NACE-4, National Association of Corrosion Engineers, Houston, TX, 1976.

[*10*] Jones, D. de G. and Masterson, H. G., "Techniques for the Measurement of Electrode Processes at Temperatures Above 100°C," *Advances in Corrosion Science and Technology*, Vol. 1, M. G. Fontana and R. W. Staehle, Eds., Plenum Press, New York, 1970, pp. 1–49.

[*11*] Macdonald, D. D., "Reference Electrodes for High Temperature Aqueous Systems—A Review and Assessment," *Corrosion*, Vol. 34, No. 3, March 1978, pp. 75–84.

[*12*] Agrawal, A. K. and Staehle, R. W., "A Silver-Silver Chloride Reference Electrode for the High Temperature and High Pressure Electrochemistry," *Corrosion*, Vol. 33, No. 11, Nov. 1977, pp. 418–419.

[*13*] Greeley, R. S., Smith, W. T., Jr., Stoughton, R. W., and Lietzke, M. H., "Electromotive Force Studies in Aqueous Solutions at Elevated Temperatures. I. The Standard Potential of the Silver-Silver Chloride Electrode," *Journal of Physical Chemistry*, Vol. 64, No. 5, May 1960, pp. 652–657.

[*14*] Rosengren, A. and Rosborg, B., unpublished research, Studsvik Energiteknik AB, Sweden, 1980.

[*15*] Andresen, P. L. and Indig, M. E., "Effects of Impurities and Supporting Electrolytes on SCC of 304 Stainless Steel in High Temperature Aqueous Environments," *Corrosion*, Vol. 38, No. 10, Oct. 1982, pp. 531–541.

[*16*] Clarke, W. L., Cowan, R. L., and Walker, W. L. "Comparative Methods for Measuring Degree of Sensitization in Stainless Steel," *Intergranular Corrosion of Stainless Alloys, STP 656*, American Society for Testing and Materials, Philadelphia, 1978, pp. 99–132.

[17] Park, H. C., Cragnolino, G., and Macdonald, D. D., "Stress Corrosion Cracking of Sensitized Type 304 Stainless Steel in Borate Solutions at Elevated Temperatures," presented at the International Symposium on Environmental Degradation of Materials in Nuclear Power Systems—Water Reactors, Myrtle Beach, SC, 22–25 Aug. 1983.

[18] Rosengren, A. and Rosborg, B., "Critical Potential for IGSCC of Type 304 Stainless Steel in High Purity Water at 250°C," presented at the International Symposium on Environmental Degradation of Materials in Nuclear Power Systems—Water Reactors, Myrtle Beach, SC, 22–25 Aug. 1983.

DISCUSSION

Martin Kendig[1] (*written discussion*)—Was there any influence of extension rate on the critical potential?

Bo Rosborg and Anders Rosengren (*authors' closure*)—We have selected a sufficiently low extension rate to make the initiation of IGSCC possible and easy, but we have not specifically examined the influence of the extension rate. However, testing of the same heat and heat treatment as in the present work with nominal strain rates of 5×10^{-8} s^{-1} and 3.9×10^{-7} s^{-1} in high-purity water at 275°C gave the same estimate of the critical potential for IGSCC within the chosen resolution of 50 mV.

[1]Rockwell International Science Center, Thousand Oaks, CA.

V. Sánchez Gálvez,[1] *Luis Caballero,*[1] *and Manuel Elices*[1]

The Effect of Strain Rate on the Stress Corrosion Cracking of Steels for Prestressing Concrete

REFERENCE: Sánchez Gálvez, V., Caballero, L., and Elices, M., "**The Effect of Strain Rate on the Stress Corrosion Cracking of Steels for Prestressing Concrete,**" *Laboratory Corrosion Tests and Standards, ASTM STP 866*, G. Haynes and R. Baboian, Eds., American Society for Testing and Materials, Philadelphia, 1985, pp. 428–436.

ABSTRACT: The aim of the paper is to investigate the stress corrosion cracking behavior of prestressing steels under general practical conditions. An aqueous solution of calcium hydroxide with small additions of sodium chloride has been used, the pH being 12.5 and the potential −0.6-V standard calomel electrode (SCE) as well as −1.2-V (SCE). Both tension tests at constant load and constant strain rate have been performed on specimens precracked by fatigue. The experimental results show that the constant load test, as proposed by the Prestressing International Federation (FIP), may be improved by the constant slow strain rate test in a realistic environment, needing a smaller number of tests and showing that in some cases fractures happen at stress intensity factor K_I values below the stress intensity threshold factor K_{ISCC} value as determined by a constant load test.

KEY WORDS: corrosion, prestressing steels, stress corrosion, slow strain rate tests, constant load tests, calcium hydroxide solution, fatigue precracked specimens

There are several types of high-strength steels (ultimate tensile strength $\geq$ 1500 MPa) that can be used for prestressing concrete. The most common is cold drawn eutectoid carbon-manganese steel. Other types achieve a high-tensile strength by heat treatment, such as quenching and tempering.

The importance of prestressing steels may be reckoned from the world production, over 10^6 metric tons per year.

Stress corrosion cracking (SCC) of prestressing steel is currently the subject of many studies, and three international symposia have been organized by the Prestressing International Federation (FIP) on this subject [*1–3*] showing the interest driven by such a problem.

In 1978, the FIP proposed the ammonium thiocyanate test [*4*] to standardize the SCC behavior of prestressing steels. In spite of some objections to this standard test proposal [*5*], the third international symposium has recognized that

[1]Professors, E. T. S. Ingenieros de Caminos, Universidad Politecnica de Madrid, Madrid-3, Spain.

Copyright© 1985 by ASTM International www.astm.org

it clearly distinguishes the susceptibility of prestressing steels to hydrogen embrittlement [3]. Recent results [6] tend to support that residual stresses at the surface of the specimens are the main cause of the observed differences in time to rupture, and, hence, comparisons between different types of steels should be done on specimens with similar surface stresses.

However, among the general conclusions of this symposium is the need to develop another test to investigate the behavior of prestressing steels under general practical conditions and the possibility of improvement by replacing the constant load test by a constant slow strain rate test [3].

Water in contact with concrete usually has pH values in the vicinity of 12.5, being essentially a saturated solution of calcium hydroxide ($Ca(OH)_2$), although other substances are likely to be present in small amounts [7].

Therefore, calcium hydroxide solutions with a pH value of 12.5 have been selected as one of the simplest realistic environments because calcium hydroxide can be leached from concrete. On the other hand the influence of noxious ions, especially of chloride ions, on the stress corrosion behavior is well known. These ions may be expected to be present in many applications of concrete structures. Small additions of chloride ions to the solution are thus advisable.

The majority of the tests performed to study the SCC of prestressing steels in the past have been constant load tests. However, the strain rate is found to be an important parameter affecting the SCC behavior of other alloys and environments [8]. Following these ideas and the conclusions of the third symposium, the slow strain rate test has been extensively used in this work, although some constant load tests have also been performed at potential values of -0.6 and -1.2 V with respect to the standard calomel electrode (SCE) for which the SCC susceptibility is the highest.

Experiments

Three commercial prestressing steels have been used. Their chemical compositions are shown in Table 1, and their mechanical properties are summarized in Table 2.

Alloy A, is an eutectoid cold drawn steel, while the other two are heat treated steels. Steel A was patented by cooling from the austenitic condition in a molten lead bath to produce fine pearlite, after which the 12-mm-diameter rods were cold drawn to produce 7-mm-diameter wires. Finally, the drawn wires were stress relieved at 400°C for a few seconds. Steels B and C were obtained by water quenching from the austenitic condition, tempering at 350°C and final water cooling. They are 7- and 9-mm-diameter steel rods, respectively.

Specimens used for testing were precracked by fatigue. Their surfaces were firstly ground to a 600-grit finish, then a starter notch about 1 mm deep was introduced with a jeweller's file. Finally they were degreased in boiling acetone and fatigue precracked. To ensure sharp cracks that were readily reproducible, the stress intensity factor range was adjusted so that the last 1 mm of crack

TABLE 1—*Chemical compositions.*

Steel	Carbon, %	Silicon, %	Manganese, %	Chromium, %	Aluminum, %	Sulfur, %	Phosphorus, %	Iron, %
A	0.85	0.27	0.64	...	...	0.027	0.012	balance
B	0.52	1.56	0.63	0.46	0.54	0.023	0.020	balance
C	0.47	1.71	0.83	0.50	...	0.011	0.023	balance

TABLE 2—*Mechanical properties.*

Steel	Ultimate Tensile Strength, MPa	0.2% Proof Stress, MPa	Elongation Under Maximum Load, %[a]
A	1749	1518	5.6
B	1650	1530	4.9
C	1500	1380	6.5

[a]Gage length = 50 mm.

propagation involved not less than 40 000 cycles. The total crack depth was between 1.5 and 2.5 mm for Steels A and B, while it was about 3 mm for Steel C. All specimens were coated with an insulating lacquer except for a narrow band about 1 mm wide on each side of the notch and precrack.

The test environment used was an aqueous solution of 1-g/L calcium hydroxide plus 0.1-g/L sodium chloride. Demineralized water with an electrical conductivity below 1 μS/cm was used in the preparation of the solution, and both the calcium hydroxide and the sodium chloride were analytical grade. The pH value was 12.5, and the testing was performed at ambient temperature (between 15 and 25°C).

All tests have been performed at a constant potential set by means of an electronic potentiostat and a classical three electrode assembly. Corrosion cells were cut from glass cylindrical tubes, containing about 100 mL of solution, to which air had access, closed at each end with rubber stoppers that allowed the passage of the specimen for external gripping. A platinum counter electrode and a bridge to an external calomel reference electrode were used to set and measure the electrochemical parameters.

Tension tests at both constant load and constant strain rate have been performed. In the first case dead weight loading through a system of levers was used while constant strain rate tests were carried out in an Instron® testing machine.

To avoid the use of a definite expression of the stress intensity factor K_I for the geometry of the specimens, calibration curves representing fracture load in air versus crack depth have been previously obtained for each steel, and they are shown in Fig. 1. For a definite crack depth a, K_I is proportional to the load

$$K_I = F f(a)$$

where F is the load applied, and $f(a)$ is a function of the crack depth. Also, the fracture toughness K_{IC} is proportional to the fracture load in air F_R

$$K_{IC} = F_R f(a)$$

Hence, if F_{env} is the fracture load in the SCC test

$$K_{Ienv}/K_{IC} = F_{env}/F_R$$

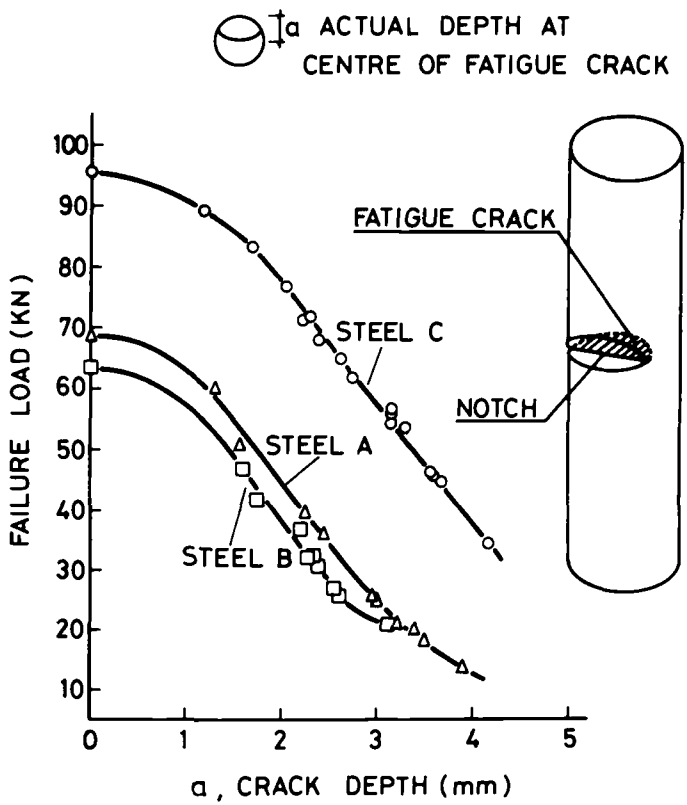


FIG. 1—*Calibration curves, fracture load in air versus crack depth a for the steels tested.*

where K_{Ienv} is the K_I value for fracture in the SCC test. In this way, the method followed has been to first measure the initial crack depth a after fracturing the specimen in the SCC test. Second, from this value a and the calibration curve to determine the fracture load in air F_R. Finally the last equation shows that the K_I for fracture as a percentage of K_{IC} is the same as the fracture load in the SCC test as a percentage of F_R.

Results and Discussion

Constant Load Tests

In constant load tests, the K_I value for fracture, as a percentage of the K_{IC}, is a function of the fracture time. If no fracture occurred after some time, the specimen was unloaded and that time recorded, in order to obtain a stress intensity threshold factor K_{ISCC} value. This was never before 140 h. For test durations over 24 h the solution was renewed every day.

Tests have been performed at potentials of -0.6- and -1.2-V SCE as characteristic values of the anodic and cathodic regimes of cracking, respectively,

to establish whether the SCC susceptibility of prestressing steels is higher under anodic or cathodic conditions. The results are shown in Fig. 2. All three steels are less susceptible to SCC at −0.6 V than at −1.2 V.

Also, at the cathodic potential, all the results are fairly similar, with K_{ISCC} values between 40 and 60% of K_{IC}, but at the anodic potential the cold drawn steel (Steel A) shows less susceptibility to SCC than the quenched and tempered steels (K_{ISCC} value of Steel A as high as 95% of K_{IC} while the K_{ISCC} for Steels B and C are 65 or 75% of K_{IC}).

Slow Strain Rate Tests

First, strain rate tests at different potentials but at a definite crosshead speed of 3×10^{-5} mm/s have been performed. This choice is based on the fact that for this speed, the SCC susceptibility of Steel A is the highest. Tests have been carried out at potentials between −1.5- and −0.2-V SCE.

Figure 3 illustrates the results obtained with all three steels tested. As can be seen, the SCC susceptibility is quite high for potentials below −0.9-V SCE, showing a potential regime of cracking that will be called cathodic. The behavior

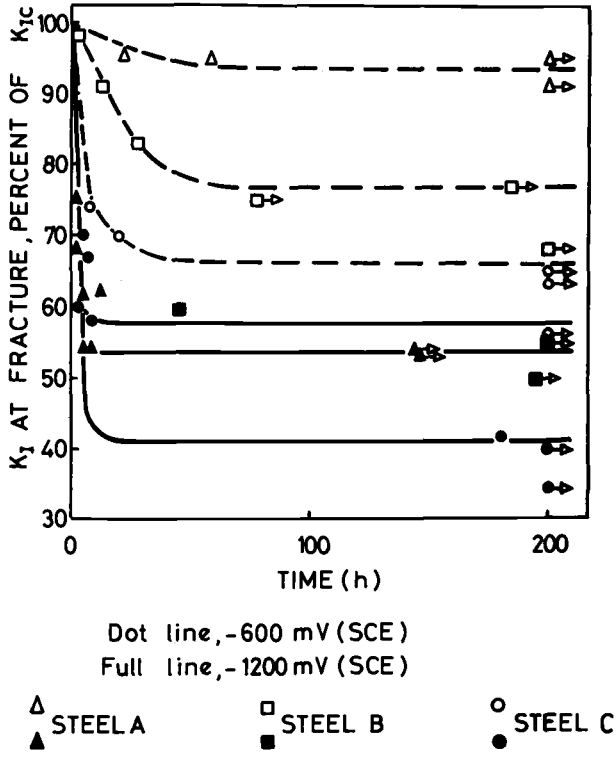


FIG. 2—*Constant load test results at −0.6- and −1.2-V SCE.*

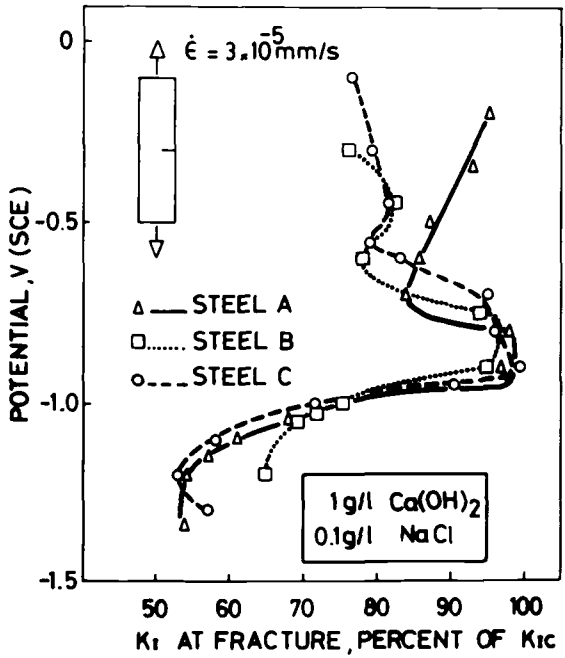


FIG. 3—*Slow strain rate test results at a crosshead speed of* 3×10^{-5} *mm/s.*

of all steels tested in this potential range is similar. In this region, steels will suffer failure by hydrogen induced cracking. In between −0.9- and −0.8-V SCE, the susceptibility is negligible and another regime of high susceptibility appears above this latter potential, which is called the anodic regime. In this region the behavior of the steels is different. While the cold drawn steel shows a maximum at −0.7-V SCE, and above that a continuous decrease in the SCC susceptibility, the quenched and tempered steels show also a maximum around −0.6-V SCE, but for higher potentials after a low decrease, they are again much more susceptible.

Finally, strain rate tests at different crosshead speeds have been performed. The tests have been carried out at potentials of −0.6- and −1.2-V SCE, representatives of the two regimes of cracking found.

The results are shown in Fig. 4, together with the K_{ISCC} results obtained at constant load. As can be seen at −1.2-V SCE the behavior of all steels is fairly similar, and within the speed range used (10^{-6} to 10^{-4} mm/s) the K_I value for fracture is never lower than the K_{ISCC} obtained in constant load tests. This result can be easily understood, since in this region cracking of steel is hydrogen induced, and the hydrogen embrittlement is time dependent. The longer the time, the higher the susceptibility to SCC. Nevertheless for strain rate tests at crosshead speeds as low as about 10^{-6} mm/s some stabilization appears, and the K_I value obtained is similar to the K_{ISCC} value obtained in constant load tests.

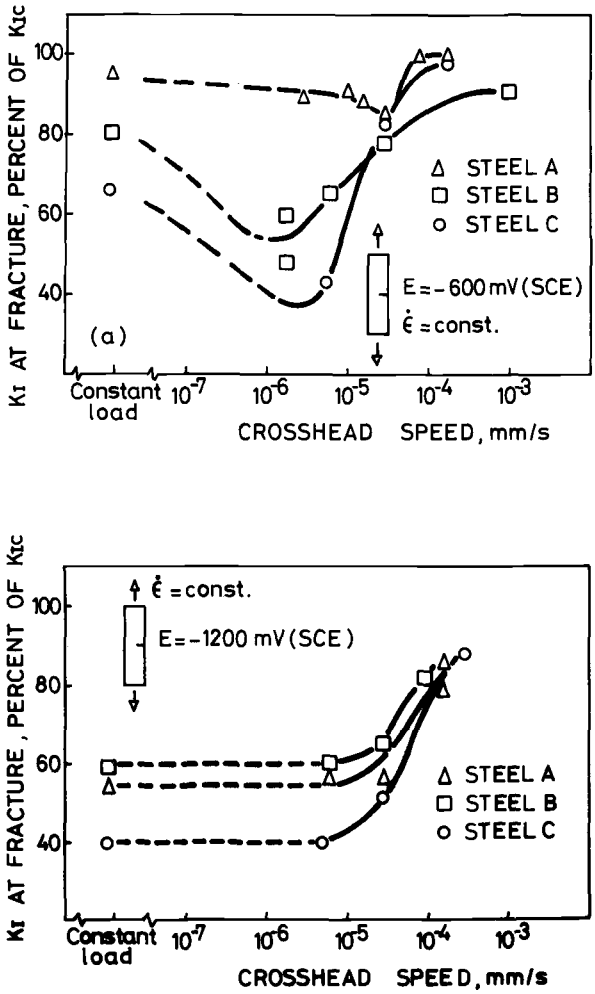


FIG. 4—*Slow strain rate test results at different crosshead speeds and comparison with the constant load test results:* (a) *tests at a potential of −0.6-V SCE and* (b) *tests at a potential of −1.2-V SCE.*

On the other hand, at −0.6-V SCE the behavior is different. In all cases, there is a speed range for which the K_I value at fracture is lower than the K_{ISCC} obtained in constant load tests, and there is a clearly different behavior of the quenched and tempered steels with respect to the cold drawn one. The former steels show a very high SCC susceptibility with K_I values below 50% of K_{IC} for crosshead speeds between 10^{-5} and 10^{-6} mm/s while the cold drawn steel shows a much better behavior, the lowest K_I value for fracture being 85% of K_{IC} obtained for a crosshead speed of 3×10^{-5} mm/s.

Conclusions

A new SCC test, using an aqueous solution of calcium hydroxide with small additions of sodium chloride, has been extensively used throughout this work to study the SCC behavior of prestressing steels. This solution bears some relation to the types of conditions to which prestressing steels may be subjected in service. In this solution, at potentials below −0.9-V SCE steels will suffer failure by hydrogen embrittlement, but at higher potentials above about −0.8-V SCE a second regime of cracking is found, with the two regimes separated by a potential range in which environment sensitive fracture is not observed. In the hydrogen induced cracking regime, the behavior of all steels is fairly similar and can be easily studied with a constant load test. As it is the FIP test proposal, although a strain rate test, could save time by reducing the number of tests required.

However, the values quoted of the free corrosion potential for prestressing steels in contact with concrete are usually in the range −0.65- to −0.2-V SCE [*9*], therefore, it is necessary to complement the study of the hydrogen embrittlement behavior by studying the SCC behavior in the anodic regime. In this case the slow strain rate test in the calcium hydroxide solution used in this work has many advantages because it needs fewer tests as compared with constant load tests. It distinguishes the behavior of different types of prestressing steels, and finally the fracture loads in this test can be lower than in a constant load test, indicating that this latter test could be unsafe in some cases.

References

[*1*] Prestressing International Federation, Wexham Spring, Slough, England, *First International Symposium on Stress Corrosion of Prestressing Steel*, 1971.

[*2*] *Second International Symposium on Stress Corrosion of Prestressing Steel*, Prestressing International Federation, Wexham Spring, Slough, England, 1973.

[*3*] *Third International Symposium on Stress Corrosion of Prestressing Steel*, Prestressing International Federation, Wexham Spring, Slough, England, 1981.

[*4*] Brachet, M., "Report on Prestressing Steel: 5—Stress Corrosion Cracking Resistance Test for Prestressing Tendons," Prestressing International Federation, and Cement and Concrete Association, London, 1980.

[*5*] Parkins, R. N., Elices, M., and Sánchez Gálvez, V., in *Proceedings of the 3rd FIP Symposium on Stress Corrosion of Prestressing Steel*, Prestressing International Federation, Wexham Spring, Slough, England, 1981.

[*6*] Elices, M., Maeder, G., and Sánchez Gálvez, V., *British Corrosion Journal*, Vol. 18, No. 2, 1983, pp. 80–81.

[*7*] Parkins, R. N., Elices, M., Sánchez Gálvez, V., and Caballero, L., *Corrosion Science*, Vol. 22, No. 5, April–June 1982, pp. 379–405.

[*8*] Parkins, R. N., "Development of Strain-Rate Testing and Its Implications," *Stress Corrosion Cracking—The Slow Strain Rate Technique*, *STP 665*, American Society for Testing and Materials, Philadelphia, 1979, pp. 5–23.

[*9*] Bergsma, F., Boon, J. W., and Etienne, C. F., *Heron*, Vol. 22, No. 1, 1977, pp. 46–75.

Paul E. Manning[1]

An Improved Intergranular Corrosion Test for HASTELLOY® Alloy C-276

REFERENCE: Manning, P. E., **"An Improved Intergranular Corrosion Test for HASTELLOY® Alloy C-276,"** *Laboratory Corrosion Tests and Standards, ASTM STP 866*, G. S. Haynes and R. Baboian, Eds., American Society for Testing and Materials, Philadelphia, 1985, pp. 437–454.

ABSTRACT: Presently, the most widely used susceptibility test for intergranular corrosion of HASTELLOY® Alloy C-276 is the ferric sulfate-sulfuric acid test. The corrosion rate obtained by this test has uniform and intergranular corrosion components. The uniform corrosion rate, which is a function of minor variations in alloy chemistry, may easily mask the intergranular corrosion component of the overall corrosion rate. A new solution chemistry identified through laboratory tests resolves the problem and displays a step function response in corrosion rate when there are high levels of grain boundary precipitation. Over 700 production specimens have been comparatively tested in both solutions, spanning a time period of two years. The new test consistently detects undesirable microstructural conditions in HASTELLOY Alloy C-276 that, in many cases, are not detected by the ferric sulfate-sulfuric acid test.

KEY WORDS: corrosion, intergranular corrosion, pitting, NiCrMo alloy, sensitization, ASTM G 28

The use of the ferric sulfate-sulfuric acid test (ASTM Detecting Susceptibility to Intergranular Attack in Wrought Nickel-Rich, Chromium-Bearing Alloys G 28) in production over many years has pointed out its relative insensitivity in detecting intergranular corrosion tendency for HASTELLOY® Alloy C-276. The currently used test (50% sulfuric acid + 42-g/L ferric sulfate) results in a very high uniform corrosion rate on Alloy C-276. In fully solution-annealed material, limited, if any, intergranular corrosion takes place. Therefore, the corrosion rate that results from these specimens identifies the uniform corrosion rate. In past experience, the uniform corrosion rate varies in a range of 2.5 to 12.5 mm/year (100 to 500 mpy where mpy is mils per year) and is a function of the heat chemistry. Small variations of chromium or molybdenum contents or both within the chemistry range of the alloy dramatically change the uniform corrosion component of the overall corrosion rate [*1,2*] in this test. In cases where grain boundary precipitation exists and intergranular corrosion occurs, a high uniform corrosion rate range may easily mask the intergranular corrosion component of

[1]Corrosion group leader, Cabot Corporation, 1020 W. Park Ave., Kokomo, IN 46901.

Copyright© 1985 by ASTM International www.astm.org

TABLE 1—*Chemistry of HASTELLOY Alloy C-276.*

Element	Weight Percent
Carbon	0.002
Cobalt	2.03
Chromium	15.46
Iron	5.63
Molybdenum	15.41
Nitrogen	0.019
Nickel	55.14
Phosphorus	0.007
Sulfur	0.002
Silicon	0.03
Vanadium	0.17
Tungsten	3.74

the overall corrosion rate. The ideal susceptibility test for intergranular corrosion is one that will give a very high ratio of intergranular corrosion component to uniform corrosion component when grain boundary precipitation is present in the alloy.

The goal of this research effort was to identify a screening test environment for HASTELLOY Alloy C-276, which would result in a step function response in corrosion rate at a predetermined level of grain boundary precipitation in the alloy. The use of such an improved screening test would ensure a well defined standard quality product.

It must be emphasized that the purpose for the screening test is to detect susceptibility to intergranular corrosion as influenced by variations in processing or composition or both. Material shown to be susceptible may or may not be intergranularly attacked in another environment. This must be established independently by specific tests or by service experience [*3*].

Experimental Procedure

All corrosion testing was performed according to the procedure indicated in ASTM G 28 with the following exceptions:

(1) changes in solution chemistry (all reagent grade chemicals) and
(2) immersion time.

The initial investigation to identify a solution chemistry that is more sensitive to intergranular precipitation in HASTELLOY Alloy C-276 was accomplished by corrosion testing heat-treated specimens that possessed differences in the extent of grain boundary precipitation. The chemistry of the material used in this study is shown in Table 1. The thermal profiles of the eight heat treatments are shown in Figs. 1 and 2. Mill-annealed material is designated as heat treatment 1 and is not shown in Fig 1 or 2. Heat treatment 2 is a 3-min age of mill-annealed

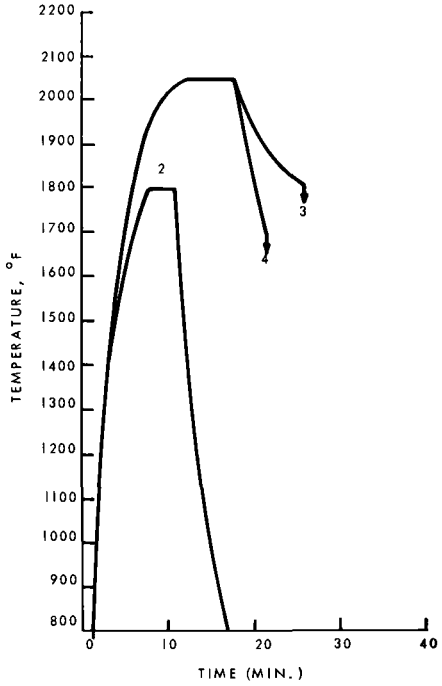


FIG. 1—*Thermal profiles of heat treatments 2 through 4. t (°C) = t (°F) − 32/1.8.*

product at 982°C (1800°F) followed by an air cool. Heat treatments 3 through 8 are mill-annealed specimens that were double annealed (no deformation before the second anneal) at 1121°C (2050°F) for 5 min and cooled to yield the thermal profiles shown in Figs. 1 and 2.

Results and Discussion

Typical microstructures of the mill-annealed product (heat treatment 1) and the heat-treated specimens (heat treatments 2 through 8) are shown in Figs. 3 through 10. Specimens given heat treatments 2, 6, 7, and 8 have grain boundary precipitation conditions that should be detected by an intergranular corrosion screening test.

Corrosion tests were performed on specimens heat treated as indicated above. In addition to the two most widely used intergranular corrosion screening tests for HASTELLOY Alloy C-276 (50% sulfuric acid + 42 g/L ferric sulfate and boiling 10% hydrochloric acid), twelve developmental solution chemistries were used. The solution chemistries, immersion time, temperature, and the corresponding corrosion rates of specimens given the eight different heat treatment conditions are shown in Table 2. Note that the boiling 10% hydrochloric acid test results in corrosion rates between 5.6 to 7.3 mm/year (225 to 290 mpy) for

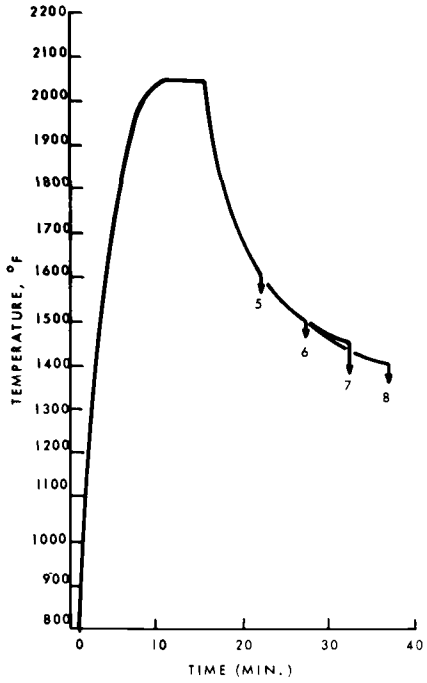


FIG. 2—*Thermal profiles of heat treatments 5 through 8. t* (°C) = *t* (°F) − *32/1.8.*

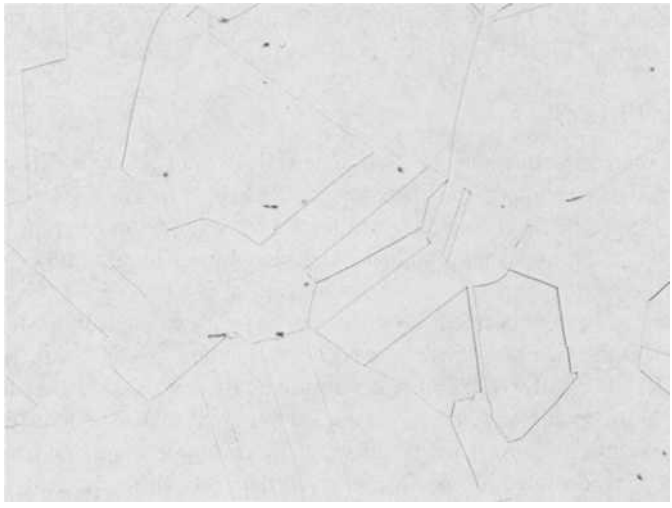


FIG. 3—*High magnification of mill-annealed specimen (heat treatment 1) (X500).*

FIG. 4—*High magnification micrograph of heat treatment 2 (X500).*

all specimen conditions tested. Additionally, the ferric sulfate-sulfuric acid test solution results are similar for specimens with heat treatments 1 through 5. Specimens subjected to heat treatment 6 have a ferric sulfate-sulfuric acid corrosion rate that is high (11 mm/year [439 mpy]); however, the specimens pass the rejection criteria (12 mm/year > 480 mpy) specified by some members of the chemical process industry for HASTELLOY Alloy C-276 [*4*]. Specimens

FIG. 5—*High magnification micrograph of heat treatment 3 (X500).*



FIG. 6—*High magnification micrograph of heat treatment 4 (X500).*

with heat treatments 7 and 8 have ASTM G 28 corrosion rates, which slightly exceed the (12 mm/year [480 mpy]) criteria. There are only 2 of the 14 solution chemistries examined that yield corrosion rates which dramatically distinguish microstructures with significant grain boundary precipitation (heat treatments 2, 6, 7, and 8). The most sensitive of these two tests is the 23% sulfuric acid, 1.2% hydrochloric acid, 1% ferric chloride, 1% cupric chloride solution, which

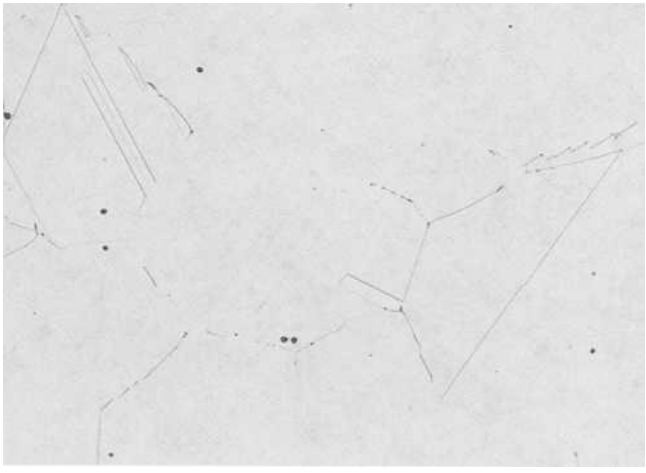


FIG. 7—*High magnification micrograph of heat treatment 5 (X500).*

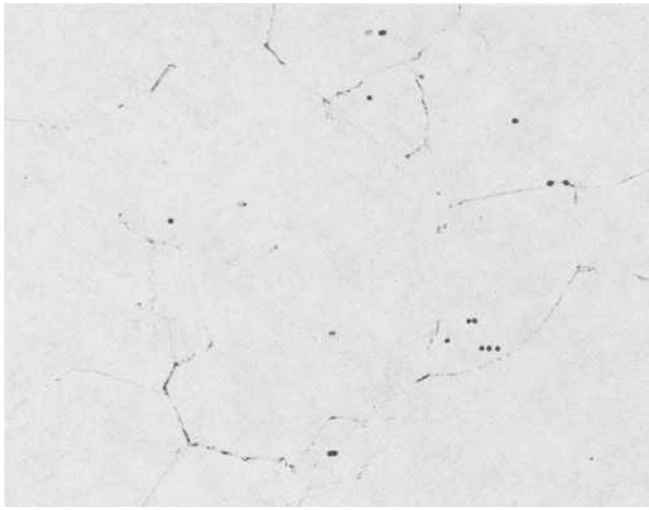


FIG. 8—*High magnification micrograph of heat treatment 6 (X500).*

will be designated the PEMT solution. In this test solution, specimens with heat treatments 1, 3, 4, and 5 resulted in corrosion rates of 1.3 to 1.9 mm/year (50 to 75 mpy), while specimens of the remaining heat treatments resulted in corrosion rates over 25 mm/year (1000 mpy). A direct comparison of the corrosion rates in the ferric sulfate-sulfuric acid environment, the new environment (PEMT solution), and a qualitative description of the microstructures (Figs. 3 through 10) of the specimens is shown in Table 3.

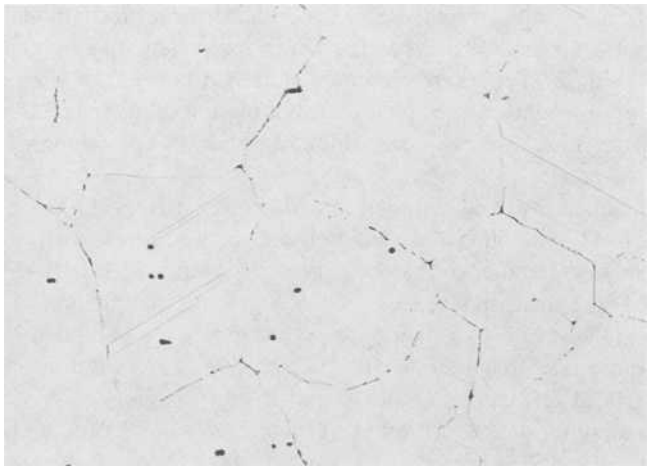


FIG. 9—*High magnification micrograph of heat treatment 7 (X500).*



FIG. 10—*High magnification micrograph of heat treatment 8 (X500).*

A photomacrograph of the heat-treated specimens after corrosion testing in the PEMT solution is shown in Fig. 11. Specimens exposed to heat treatments 2, 6, 7, and 8 suffered pitting attack. A photomicrograph of a PEMT solution corrosion tested specimen that was exposed to heat treatment 5 (1.8 mm/year, 73 mpy) is shown in Fig. 12. Minor pitting corrosion is apparent on this specimen. Other specimens that exhibited low corrosion rates (heat treatments 1, 3, and 4) were somewhat less pitted than the specimen shown in Fig. 12. Severe pitting attack is apparent in specimens that received heat treatments 2 (Figs. 13 and 14), 6 (Figs. 15 and 16), 7, and 8 (Fig. 17). The mode of rapid propagation of pits, which causes high weight loss in a 24-h corrosion test, is intergranular attack (Fig. 14, 16, and 17). When a grain is completely undermined within a pit (Fig. 14 and 16), the severe pit anolyte totally dissolves the grain. If nearly continuous grain boundary precipitation is not present in the microstructure, the rapid pit propagation does not occur (Fig. 12), and low corrosion rates (weight losses) are observed.

The mechanism involved in the observed attack on HASTELLOY Alloy C-276 in the PEMT solution is a combination of two basic corrosion forms, pitting corrosion and intergranular corrosion. Pitting corrosion occurs on HASTELLOY Alloy C-276 specimens independent of the degree of precipitation of the grain boundaries in the severely oxidizing (ferric and cupric ions), high-chloride containing acidic environment of the PEMT solution (23% sulfuric acid, 1.2% hydrochloric acid, 1% cupric chloride, and 1% ferric chloride, that is, 90-mL reagent grade sulfuric acid, 18-mL reagent grade hydrochloric acid, 475-mL H_2O, 7.2-g $CuCl_2 \cdot 2H_2O$, and 10.1-g $FeCl_3 \cdot 6H_2O$). In fact, the environment is so severe that other high-performance alloys (625 alloy or HASTELLOY

TABLE 2—*Corrosion rate (mpy)[a] of heat treated specimens.*

Media	Immersion Time, h	Temperature	Heat Treatment 1	2	3	4	5	6	7	8
10% chromic + 5% HCl	24	boil	25	29	26	29	37	56	54	74
12% H_2SO_4 + 1.2% HCl + 1% $FeCl_3$ + 1% $CuCl_2$	24	boil	24	26	25	25	26	35	36	128
23% H_2SO_4 + 1.2% HCl + 1% $FeCl_3$ + 1% $CuCl_2$	24	boil	50	1093	53	55	73	1285	1555	1733
23% H_2SO_4 + 2.4% HCl + 1% $FeCl_3$ + 1% $CuCl_2$	24	boil	47	941	45	49	60	1046	1285	1435
10% chromic	96	boil	48	78	49	80	96	161	167	165
10% chromic + 1% HCl	24	boil	54	70	53	68	86	140	158	171
50% H_2SO_4 + 44-g/L $Fe_2(SO_4)_3$	24	boil	215	274	214	257	297	439	484	485
50% H_2SO_4 + 44-g/L $Fe_2(SO_4)_3$	24	70°C	6.4	5.7	7.3	6.6	6.9	6.1	6.0	7.2
30% H_2SO_4 + 19-g/L $Fe_2(SO_4)_3$	24	boil	46	46	45	44	48	52	53	57
10% HCl	24	boil	240	290	227	242	238	258	257	266
10% H_2SO_4 + 44-g/L $Fe_2(SO_4)_3$	24	boil	16	18	17	15	16	15	15	16
12% H_2SO_4 + 1.2% HCl + 1% $FeCl_3$ + 1% $CuCl_2$	24	70°C	1.7	2.4	1.4	1.4	2.9	1.7	6.0	7.2
12% H_2SO_4 + 2.4% HCl + 1% $FeCl_3$ + 1% $CuCl_2$	24	boil	28	30	28	29	31	34	36	38
5% chromic + 5% HCl	24	boil	5.3	5.9	6.0	5.5	6.3	5.5	6.1	5.0

[a]mm/year = mpy × 0.0254.

TABLE 3—*Comparison of the ferric sulfate-sulfuric acid and PEMT results.*

Sample Heat Treatment	Corrosion Rate, mpy[a]		Qualitative Microstructure Description
	$Fe_2(SO_4)_3 \cdot H_2SO_4$	PEMT	
1 (mill annealed)	215	50	excellent
2	273	1093	poor
3	214	53	excellent
4	256	55	good
5	296	73	good
6	439	1285	poor
7	484	1555	poor
8	486	1733	poor

[a]mm/year = mpy × 0.0254.

Alloys G and C-4) suffer severe pitting attack independent of grain boundary precipitation with overall weight losses that translate to a 50 to 88 mm/year (2000 to 3500 mpy) corrosion rate. In the case of Alloy C-276 possessing nearly continuous grain boundary precipitation, the rapid propagation of the pit that results in very high corrosion rates occurs by intergranular attack. The mechanism for this attack was established by Streicher [5] and involves preferential dissolution of molybdenum-rich precipitates (carbides or intermetallic precipitates or both) by the highly oxidizing, acidic environment. If nearly continuous grain boundary precipitation is not present in the microstructure, pit propagation is

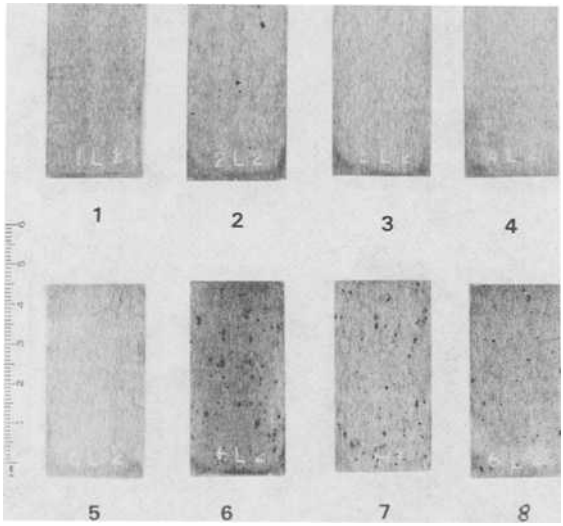


FIG. 11—*Corrosion test coupons given heat treatments 1 through 8 and exposed to boiling PEMT solution for 24 h.*

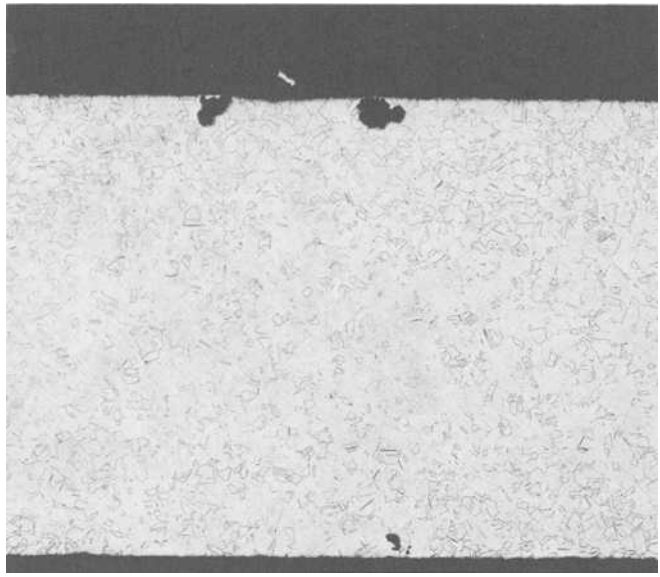


FIG. 12—*Corrosive attack (PEMT solution) on a specimen that was given heat treatment 5 (~X18).*

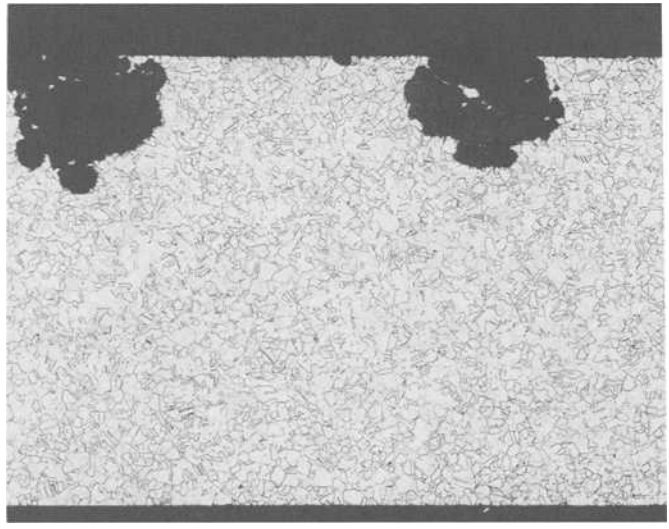


FIG. 13—*Corrosive attack (PEMT solution) on a specimen that was given heat treatment 2 (~X18).*

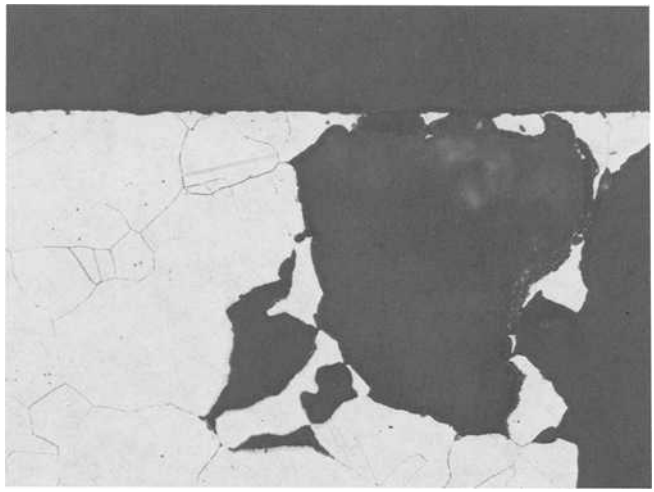


FIG. 14—*Corrosive attack (PEMT solution) on a specimen that was given heat treatment 2 (~X200).*

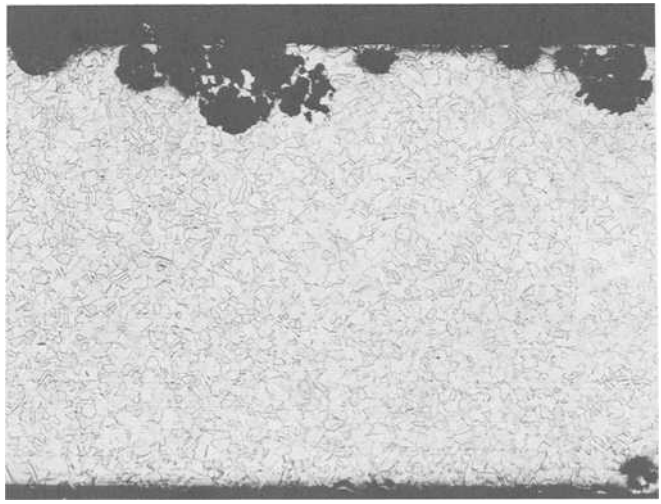


FIG. 15—*Corrosive attack (PEMT solution) on a specimen that was given heat treatment 6 (~X18).*

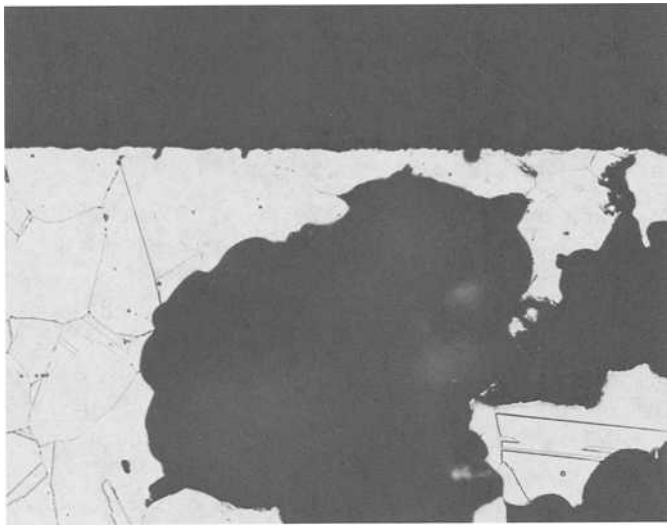


FIG. 16—*Corrosive attack (PEMT solution) on a specimen that was given heat treatment 6 (~X200).*

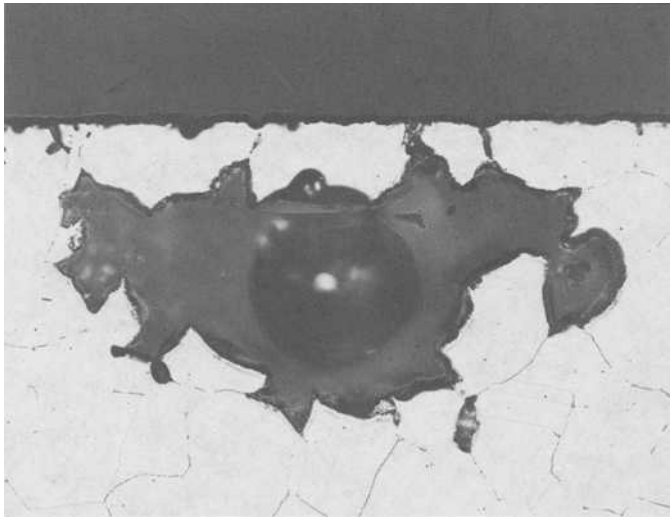


FIG. 17—*Corrosive attack (PEMT solution) on a specimen that was given heat treatment 8 (~X200).*

considerably slower (uniform corrosion within the pit), and the resulting weight loss is low. Therefore, a step function response of corrosion rate as a function of microstructure is obtained to clearly distinguish material with unacceptable levels of grain boundary precipitation.

Production Experience

For a two-year period, all HASTELLOY Alloy C-276 product that was tested by the ferric sulfate-sulfuric acid test (ASTM G 28) procedure was concurrently tested in the PEMT solution. Currently, more than 700 specimens have been comparatively tested in each media. All specimens that resulted in high corrosion rates in either test procedure were examined metallographically.

Corrosion tests in the PEMT solution consistently detected undesirable microstructural conditions that in many cases are not detected by the ferric sulfate-sulfuric acid (ASTM G 28) test (Figs. 18 through 20). Examples of production sample corrosion test results from both environments, displaying the above mentioned microstructure problems, are shown in Table 4. The specimens used for both corrosion test environments were cut out next to one another on the supplied production material in all cases.

A study of welded and annealed product was undertaken to assure that the PEMT solution defines a standard quality annealed weld structure. Over 150 welded and annealed specimens were examined. The test specimens were approximately ⅓ weld metal and ⅔ base metal. Several welded and annealed specimens contained nearly continuous weld metal precipitation (Fig. 21) and

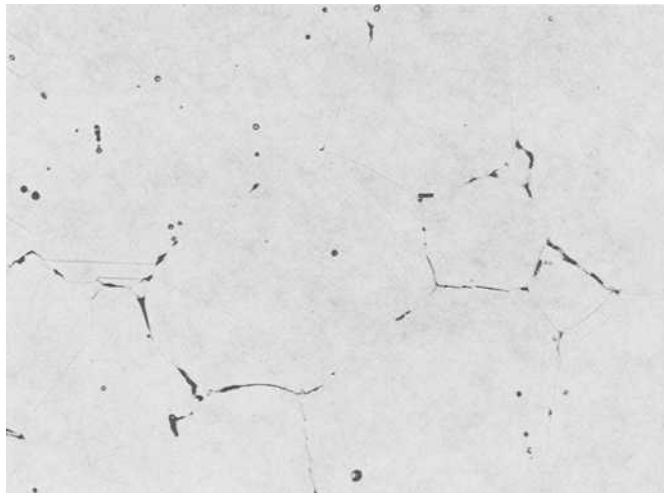


FIG. 18—*Grain boundary precipitation from a slow rate of cooling from the annealing temperature through the sensitizing temperature range; (~X500).*

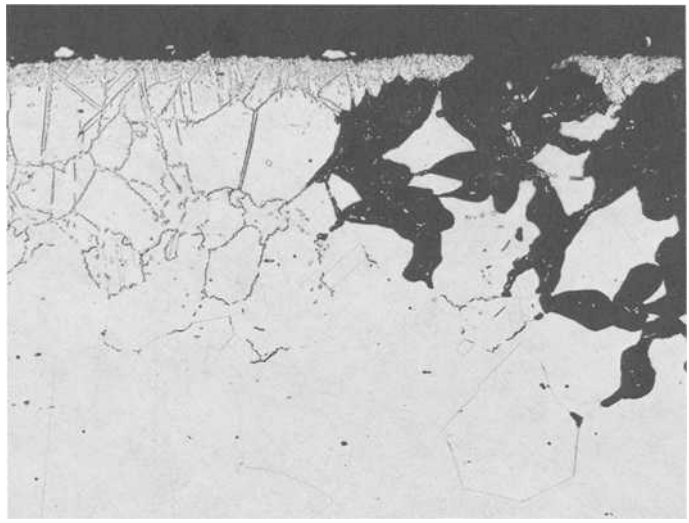


FIG. 19—*Microstructure of corrosion tested specimens that have a surface contamination problem. Corrosive attack resulting in high weight loss by the PEMT solution (~X200).*

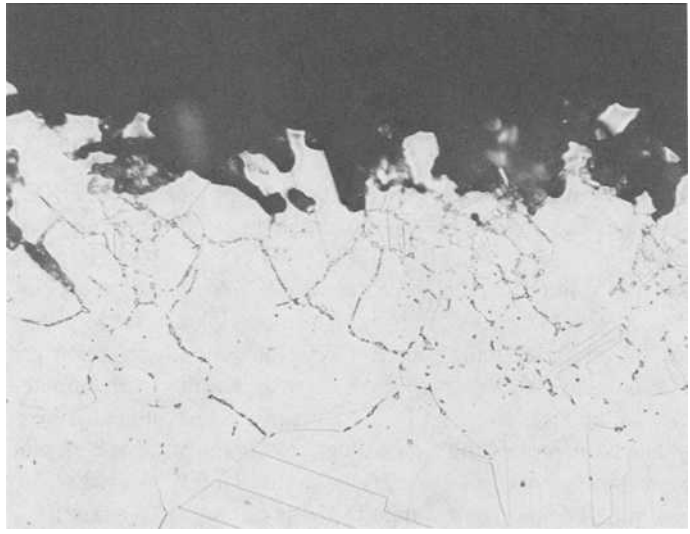


FIG. 20—*Microstructure of corrosion tested specimens that have a surface contamination problem. Corrosive attack resulting in low weight loss by the ASTM G 28 test (~X500).*

TABLE 4—*Comparison of corrosion test results of production specimens.*[a]

Corrosion Rate	
PEMT Solution, mpy[b]	$Fe_2(SO_4)_3 \cdot H_2SO_4$, mpy
3298	335
4535	347
1555	376
1803	458
4426	407
4529	397
1776	178
4044	350
1267	264
3850	1963
1580	311
5794	545
1537	418
2064	438
4409	306
2516	374
1135	274
3827	346
1537	418
1325	296
1564	323
2008	216

[a]In each of these cases, microstructural examination determined that the PEMT results were correct and the material should be held. Two examples of the microstructures found are shown in Figs. 18 through 20.

[b]mm/year = mpy × 0.0254.

resulted in very high corrosion rates in the PEMT solution and low corrosion rates in the ASTM G 28 test (Table 5). One of these specimens was examined to characterize the precipitate. Chemical analysis of the weld metal determined the carbon content was 0.005%. Another piece from the weld of the same specimen was examined by energy dispersive X-ray analysis (EDX). The precipitate was found to contain 28.8% molybdenum, 5.2% tungsten, 14.8% chromium, 4.3% iron, and 43.3% nickel (HASTELLOY Alloy C-276 contains 16% molybdenum, 4% tungsten, 16% chromium, 5% iron, and a balance of nickel). It should be noted that EDX analysis of the precipitates usually involves the precipitate and the surrounding matrix; therefore, the composition provided is not precise but clearly demonstrates a molybdenum-rich precipitate. Carbon content can not be measured by EDX analysis; therefore, it is unknown whether the precipitate is an intermetallic, a carbide, or a combination of both precipitates. In any case, the presence of a nearly continuous molybdenum-rich ($\geq$28.8% versus 16% molybdenum) precipitate explains the high corrosion rate obtained in the PEMT solution. The absence of high ASTM G 28 corrosion rates further demonstrates the insensitivity of that test solution to Alloy C-276.



FIG. 21—*Nearly continuous weld metal precipitation, which resulted in high corrosion rates in the PEMT solution* (~*X500*).

In view of the PEMT solution mechanism of corrosive attack (molybdenum-enriched areas), preferential weld attack from macrosegregation in multipass, unannealed weld specimens may occur. This was observed with several as-welded 9.53-mm (3.8-in.) plate specimens, which suffered preferential weld metal attack without possessing a microstructure that could be classified as a weld metal precipitation problem (Fig. 21). In as-welded specimens there may be sufficient macrosegregation of molybdenum in the weldment to result in preferential attack in the PEMT solution. Further work is required to resolve the mechanism of preferential attack in as-welded specimens. Therefore, the PEMT solution should not be used as a quality control test on as-welded product. An annealing heat treatment presumably reduces the molybdenum macrosegregation of weldments to an extent where the PEMT solution will successfully detect microstructural problems in the base and weld metal.

TABLE 5—*Comparison of corrosion test results on welded and annealed production specimens.*

Corrosion Rate	
PEMT Solution, mpy[a]	$Fe_2(SO_4)_3 \cdot H_2SO_4$, mpy[a]
2543	258
2308	240
3142	251

[a]mm/year = mpy × 0.0254.

Conclusions

1. The ASTM G 28 test (50% sulfuric acid + 42 g/L ferric sulfate) on HASTELLOY Alloy C-276 results in a corrosion rate that combines a high and variable uniform corrosion rate (strong function of chromium and molybdenum content) with an intergranular component (on sensitized specimens) that may be masked by the high and variable uniform corrosion rate.

2. The PEMT solution test (23% sulfuric acid + 1.2% hydrochloric acid + 1% cupric chloride + 1% ferric chloride) on HASTELLOY Alloy C-276 results in minor pitting attack and low corrosion rates on material that is not sensitized and provides a step function increase in corrosion rates on sensitized material by an intergranular corrosion mechanism that results in rapid pit propagation.

3. The PEMT solution corrosion test results have consistently detected undesirable microstructural problems in mill-produced material for over two years, which in many cases were not detected by the ferric sulfate-sulfuric acid (ASTM G 28) test.

4. The PEMT solution test will properly screen wrought product as well as welded and annealed product. Macrosegregation of molybdenum in unannealed weldments may be sufficient to cause preferential weld metal attack. Therefore, the test should not be used for quality control of as-welded structures.

References

[1] Hodge, F. G. and Kirchner, R. W., "A Third Generation Ni-Cr-Mo Alloy for Corrosion," European Federation of Corrosion, Paris, 24–28 Sept. 1973.
[2] Hodge, F. G. and Kirchner, R. W., *Corrosion*, Vol. 32, No. 8, Aug. 1976, p. 332.
[3] Brown, M. H., *Corrosion*, Vol. 25, No. 10, Oct. 1969, p. 439.
[4] Kirchner, R. W. and Silence, W. L., *Materials Protection and Performance*, Vol. 10, No. 1, Jan. 1971, p. 11.
[5] Streicher, M. A., *Corrosion*, Vol. 32, No. 3, March, 1976, p. 79.

John M. Schluter[1] *and Joseph A. Chivinsky*[2]

Surface Preparation Requirements for ASTM A 262

REFERENCE: Schluter, J. M. and Chivinsky, J. A., **"Surface Preparation Requirements for ASTM A 262,"** *Laboratory Corrosion Tests and Standards, ASTM STP 866,* G. S. Haynes and R. Baboian, Eds., American Society for Testing and Materials, Philadelphia, 1985, pp. 455–464.

ABSTRACT: Variations in the ASTM Recommended Practices for Detecting Susceptibility to Intergranular Attack in Stainless Steels (A 262), Practice A and C results, between the producer and purchaser of a heat of American Iron and Steel Institute (AISI) 304 L (Unified Numbering System [UNS] S30403) stainless steel, resulted in a round-robin test. The four laboratories involved (two producers and two purchaser locations) each prepared one-quarter of the specimens tested by each of the laboratories to the ASTM A 262 Practice A and C requirements. The resulting data indicated that a specific practice of surface preparation on the test specimens should be specified and mutually accepted by the participating laboratories. Variations in the amount of metal removed from the specimen's surface can make a pass/fail difference. The current specification does not require a specific surface preparation or point out the importance of a mutually accepted surface preparation. The parties involved in ASTM A 262 Practice C testing should be aware of the significant effects of surface preparation on the reproducibility of test data.

KEY WORDS: intergranular corrosion, surface finishing, cold working, stainless steels, sensitization, chemical tests

Two years ago, Union Carbide Corporation (UCC) refused delivery of five plates of American Iron and Steel Institute (AISI) 304 L (Unified Numbering System [UNS] S30403) stainless steel manufactured by Allegheny Ludlum Steel Corporation (ALSC) based on the results of the ASTM Recommended Practices for Detecting Susceptibility to Intergranular Attack in Stainless Steels (A 262), Practice A and C, tests run on these plates. However, the Practice C data of ALSC showed that the material met the UCC requirements. As a result of this controversy, a round-robin test involving two ALSC and two UCC laboratories was initiated to investigate the differences in the test data. The UCC locations involved were the corrosion laboratories of the Engineering and Technology Services Division. Each laboratory tested a set of specimens prepared by them-

[1]Lead corrosion engineer, Engineering and Technology Services Division, Union Carbide Corporation, P.O. Box 471, Texas City, TX 77590.

[2]Supervisor of quality assurance, Allegheny Ludlum Steel Corp., Quality Assurance and Specifications, Leechburg, PA 15656.

Copyright© 1985 by ASTM International www.astm.org

selves and the other three laboratories per ASTM A 262, Practice A and C. The resulting data allowed an evaluation of such variables as specimen preparation, corrosion test practices, evaluation criteria, and as-shipped condition of the plates.

Procedure

Equipment

The decision was made to allow each lab to use the Practice C equipment, which they had been normally using up to this time. The equipment by location is listed in Table 1.

Specimen Preparation

The four participating labs received material from four plates representing Heat A (Type 304 [UNS S30400]), Heat B (Type 304 L), and Heat C (Type 304 L, Plates 1 and 2). The ladle analyses, product analyses, and mill condition of the four plates are listed in Tables 2 and 3, respectively. Sixteen identical specimens were prepared from each of the four plate samples. Half of these specimens were left in the mill annealed condition and half were sensitized at 675°C (1250°F) for 1 h and air cooled. These mill annealed and sensitized specimens then received the surface preparation and cleaning normally used at the respective laboratories. The ready to test Practice C specimens were then distributed evenly to the four test locations. Therefore, each laboratory received four sets of completely prepared duplicate mill annealed and sensitized specimens from each plate for a total of 64 specimens.

The four plates were also to be tested to ASTM A 262, Practice A. Therefore each laboratory using their normal techniques prepared eight micro-specimens from each of the four plates. Two coupons (one mill annealed and one sensitized specimen) per plate were retained and the other 24 specimens distributed equally to the other three laboratories.

The Practice A specimens were used with little or no preparation before being mounted, polished, and etched. The UCC laboratories produced a metallurgical polish (1-μ diamond) on the specimen before etching. The ALSC laboratories used 600-grit silicon carbide paper to prepare the specimens for the etch.

The preparation of specimens for the Practice C tests is shown in Table 4. The ALSC Leechburg and UCC Texas City laboratories used a similar surface preparation for both mill annealed and sensitized specimens. The one exception is the nitric acid passivation used after grinding by the Leechburg laboratory.

ALSC Brackenridge laboratory prepared the mill annealed specimens using hot alkaline degreasing and acid pickling. The sensitized specimens were pickled in 10% nitric acid, 3% hydrofluoric acid at 66°C (150°F) for 3 min to remove scale and then detergent cleaned, rinsed, and dried.

The mill annealed specimens of the UCC South Charleston Laboratory were

TABLE 1—*ASTM A 262, Practice C test equipment.*

Location Test Equipment	ALSC Leechburg	UCC Texas City	ALSC Brackenridge	UCC South Charleston
Flask	1 1.-L flask	1 1.-L erlenmeyer	1 1.-L flask	2 1.-L resin flask
Condenser	cold finger	West	cold finger	West
Specimen Holder	glass cradle	trifluoroethylene tree	glass basket	glass tree

TABLE 2—*Ladle chemistry.*

Heat Number	Type	Plate Number	Carbon	Manganese	Phosphorus	Sulfur	Silicon	Chromium	Nickel	Aluminum	Molybdenum	Nitrogen	Copper
A	304	...	0.055 0.050[a]	1.69	0.023	0.016	0.64	18.26	8.52	0.002	0.24	0.065	0.27
B	304 L	...	0.022	1.69	0.035	0.002	0.65	19.05	10.54	0.004	0.29	0.061	0.21
B			0.022[a]	1.69	...	...	0.67	19.07	10.58	...	...	...	0.27
C	304 L	...	0.024	1.71	0.028	0.002	0.62	18.51	9.93	0.002	0.28	0.065	...
C	304 L	1	0.026[a]	1.77	0.030	0.002	0.63	18.50	9.92	0.002	0.27	0.062	0.31
C	304 L	2	0.028[a]	1.76	0.031	0.002	0.64	18.52	9.96	0.002	0.27	0.062	0.32

[a]Product Analysis

TABLE 3—*Mill condition of the plates.*

Heat Number	Plate Number	Type	Condition[a]
A	...	304	0.500-in. hot rolled, annealed and descaled
B	...	304 L	0.500-in. hot rolled, annealed and descaled
C	1	304 L	0.375-in. hot rolled, annealed and descaled
C	2	304 L	0.375-in. hot rolled, annealed and descaled

[a]1 in. = 25.4 mm.

cleaned with a bristle brush and detergent, rinsed, and dried. The sensitized specimens were prepared similar to those of the Brackenridge laboratory with the addition of a nitric acid passivation (15% nitric acid, 66°C [150°F], 20 min) after the descaling treatment.

Experimental Work

The testing of the appropriate specimens were performed according to the procedures in ASTM A 262, Practices A and C. No significant deviations from ASTM A 262 testing procedures were noted at any of the four laboratories. However, variations did exist in the test equipment and specimen preparation at the various laboratories as noted earlier in Tables 1 and 4.

The Practice A specimens were tested as outlined in Sections 4.4 and 4.5 of ASTM A 262. The only notable difference in technique was in the polish on the specimen before etching. The results of the Practice A tests for the four laboratories is shown in Table 5.

The specimens prepared for the Practice C tests were run at each of the four laboratories using their own normal practice. Each laboratory recorded the equipment used for the test, the acid concentrations, and the techniques for cleaning specimens before and after testing together with any other pertinent information.

TABLE 4—*ASTM A 262, Practice C Specimen Preparation.*

ALSC Leechburg	UCC Texas City	ALSC Brackenridge	UCC South Charleston
	MILL ANNEALED		
120-grit ground finish	120-grit ground finish	alkaline degrease	detergent clean
HNO_3 passivation	detergent clean	acid pickle	water rinse
Water rinse	water rinse	detergent clean	acetone dried
Detergent clean	acetone dried	water rinse	
Water rinse		dried	
Dried			
	SENSITIZED		
120-grit ground finish	120-grit ground finish	HNO_3/HF pickle	HNO_3/HF pickle
HNO_3 passivation	detergent clean	water rinse	HNO_3 passivation
Water rinse	water rinse	detergent clean	detergent clean
Detergent clean	acetone dried	water rinse	water rinse
Water rinse		dried	acetone dried
Dried			

TABLE 5—*Results of ASTM A 262, Practice A, sensitized coupons.*

Heat	Specimen Supplier	Laboratory Performing Practice A Test			
		ALSC Leechburg	UCC Texas City	ALSC Brackenridge	UCC South Charleston
B	Leechburg	dual	dual	dual	dual
(304L)	Texas City	dual	dual	dual	dual
	Brackenridge	dual	dual	dual	dual
	South Charleston	ditch	dual	dual	dual
C	Leechburg	ditch	dual	ditch	dual
Plate 1	Texas City	ditch	dual	ditch	dual
(304L)	Brackenridge	ditch	dual	ditch	dual
	South Charleston	ditch	dual	dual	dual
C	Leechburg	ditch	ditch	ditch	ditch
Plate 2	Texas City	ditch	ditch	ditch	ditch
(304L)	Brackenridge	ditch	ditch	ditch	ditch
	South Charleston	ditch	dual	ditch	dual
A	Leechburg	ditch	ditch	ditch	ditch
(304)	Texas City	ditch	ditch	ditch	ditch
	Brackenridge	ditch	ditch	ditch	ditch
	South Charleston	ditch	ditch	dual	ditch

These laboratory to laboratory variations were retained in the test since, at the onset of this test, there was only the vaguest notion as to the factors that were responsible for the original discrepancies. The effects of some of these variations were checked during the actual Practice C test work. One of these items was the effect of different condensers on the acid concentration during the test. The acid was tested before and after several 48-h exposures. Any varitions in concentration fell within the 0.2% tolerance and the analytical tolerances. The Practice C test results are shown in Table 6.

Discussion

The accumulation of the Practice A and C test data from the four laboratories provided the first insights into the testing differences. The first interesting point to come out of the composite data showed up in the Practice A testing. Initially, this phase of the round-robin testing was simply a prelude to the Practice C test, which was our primary concern. From Table 5, it is apparent that the results of the Practice A testing on sensitized specimens varied considerably between the ALSC and the UCC Labs, especially in the Heat C, Plate 1, specimens. It is unlikely that the minor differences in surface area measurements, test current, and elapsed time were responsible for these discrepancies. One difference could easily explain the data involved in the evaluation of the etched surface for ditching. ALSC evaluated the entire etched face except for any grain cut by the surfaces. UCC did not evaluate the zone several grains deep on the mill surfaces. This area tended to be more severely etched for a number of possible reasons including surface phenomena (for example, contamination, roughness, residual cold work, and so forth) or higher current densities at an edge. This difference in evaluation techniques would explain the discrepancies in the Practice A data.

The second and principal phase of the testing was the performance of the Practice C testing and analysis of the data. The summary of the average corrosion rates on the individual specimens for the various laboratories is contained in Table 6. All of the 304 L specimens in the mill annealed condition met the 0.0015-ipm (where ipm is inch per month) criteria in UCC Specification MOC-403. The data show a marked difference in the results of tests on sensitized specimens performed by the Leechburg and Texas City laboratories as opposed to the results from the Brackenridge and South Charleston labs. No sensitized 304 L stainless steel specimens prepared by Leechburg and Texas City failed when tested by the four laboratories. The only sensitized 304 L stainless steel specimens prepared by Brackenridge and South Charleston to pass the 0.0020-ipm maximum criteria were South Charleston's Heat B specimens tested by the ALSC Laboratories. The 304 specimens failed in every case, which was to be expected for material tested in the sensitized condition.

At this point, we began checking into the procedures used by the four labo-

TABLE 6—*Average results of ASTM A 262, Practice C, sensitized coupons, ipm.*

Heat Number	Specimen Supplier	Laboratory Performing Practice C Test							
		ALSC Leechburg		UCC Texas City		ALSC Brackenridge		UCC South Charleston	
B	Leechburg	0.0009	0.0008	0.0009	0.0009	0.0007	0.0008	0.0009	0.0008
(304L)	Texas City	0.0014	0.0012	0.0010	0.0011	0.0010	0.0010	0.0009	0.0009
	Brackenridge	0.0024[b]	0.0025[b]	0.0027[b]	0.0028[b]	0.0024[b]	0.0024[b]	0.0026[b]	0.0026[b]
	South Charleston	0.0019	0.0020	0.0023[b]	0.0023[b]	0.0019	0.0019	0.0023[b]	0.0022[b]
C	Leechburg	0.0012	0.0012	0.0012	0.0012	0.0010	0.0010	0.0010	0.0010
Plate 1	Texas City	0.0010	0.0009	0.0014	0.0014	0.0012	0.0011	0.0012	0.0012
(304L)	Brackenridge	0.0031[b]	0.0032[b]	0.0030[b]	0.0030[b]	0.0028[b]	0.0028[b]	0.0027[b]	0.0028[b]
	South Charleston	0.0026[b]	0.0025[b]	0.0030[b]	0.0029[b]	0.0025[b]	0.0025[b]	0.0027[b]	0.0028[b]
C	Leechburg	0.0027[b]	0.0024[b]	0.0021[b]	0.0019	0.0017	0.0017	0.0020	0.0019
Plate 2	Texas City	0.0017	0.0018	0.0018	0.0018	0.0014	0.0015	0.0017	0.0015
(304L)	Brackenridge	0.0048[b]	0.0038[b]	0.0043[b]	0.0036[b]	0.0070[b]	0.0069[b]	0.0034[b]	0.0036[b]
	South Charleston	0.0025[b]	0.0024[b]	0.0035[b]	0.0033[b]	0.0032[b]	0.0030[b]	0.0032[b]	0.0031[b]
A	Leechburg	0.0103[b]	discontinued	0.0094[b]	0.0103[b]	0.0077[b]	0.0078[b]	0.0055[b]	0.0065[b]
(304)	Texas City	0.0056[b]	0.0044[b]	0.0064[b]	0.0072[b]	0.0051[b]	0.0040[b]	0.0052[b]	0.0053[b]
	Brackenridge	0.0647[b]	0.0691[b]	0.0435[a]	0.0367[b]	0.0472[b]	0.0474[b]	0.0570[b]	0.0564[b]
	South Charleston	0.0166[b]	0.0115[b]	0.0045[b]	0.0065[b]	0.0061[b]	0.0049[b]	0.0082[b]	0.0054[b]

[a]Two run average.
[b]Failed 0.0020-ipm maximum criteria.

ratories to determine which, if any, of the procedures could be responsible for the discrepancies of the test data. A variety of specimen supports, flasks, and condensing apparatus were in use, but there was no clear reason to suspect any of the variety of apparatus used for the tests. Note 10 in the Practice C discusses alternate condensers and states that corrosion rates tend to be slightly higher using the 762-mm (30-in.) reflux condenser than with the cold finger. Before and after data on several test runs indicated that acid concentrations remained within the 0.2% tolerance of ASTM A 262, Section 17.1 with the West condensers. The nitric acid, while from different suppliers, all met the specification limits of ASTM A 262, Practice C, Note 11. The cleaning methods used after each test were all very similar to the method in ASTM A 262, Section 19.3.

The single significant difference in the various laboratory techniques which could account for the trends in the Practice C data was in the surface preparation of the coupons. The two labs showing the lowest corrosion rates on sensitized specimens (Leechburg and Texas City) ground their specimens with a 120-grit abrasive. The two other labs (Brackenridge and South Charleston) prepared their specimens without abrading the surface. As the mill surface makes up a significant portion of the surface of the Practice C coupons, the finish (shot blasting or residual cold work) or carbon contamination of this surface could be responsible for the higher corrosion rates during the nitric acid exposures.

Conclusion

The round-robin test data indicated that for any given surface preparation, the reproducibility among the four participating laboratories was excellent even with the variations in corrosion testing procedures. The variations in surface preparation, however, were capable of making a significant difference in the ability of specimens to pass the Practice C tests. While ASTM A 262, Practice C describes the surface preparation in general terms, the test data point out that several specific items should be included in the buyer's testing agreement. This agreement should clearly specify the surface preparation required on the test specimens.

Differences in the test results in this round-robin test arose from an interpretation of the word "abrasive paper" in ASTM A 262, Section 18.4. If belt sanders can be included under this term, significant metal removal can result. If the intention was to include the belt sander in the machining or heavy grinding restriction of Section 18.5, this should be made clear. If the stainless steel product has a surface condition (for example, carbon contamination, shot blasted surface, residual cold work, and so forth) which may affect the corrosion test, the clarity of this statement can make a pass/fail difference in the Practice C test results. Therefore, the appropriate ASTM committee should consider revisions to Sections 18.4 and 18.5 of ASTM A 262 to clarify the surface preparation requirements.

Acknowledgments

We would like to recognize the assistance of the personnel at the four participating laboratories for their invaluable help in performing the Practice A and C tests and accumulating the resultant data. We also acknowledge the technical and financial assistance of both the Allegheny Ludlum Steel Corporation and Union Carbide Corporation for their support of the test work.

Appendix of Selected ASTM Standards

APPENDIX OF SELECTED ASTM STANDARDS

This appendix contains the ASTM standards most often referred to in this special technical publication. These voluntary consensus standards were developed under the direct jurisdiction of ASTM Committee A-1 on Steel, Stainless Steel, and Related Alloys and Committee G-1 on Corrosion of Metals. Specific subcommittee jurisdiction is indicated in the first footnote to each standard. Membership in the Society is open to all concerned with the fields in which ASTM is active.

Purpose and Use of ASTM Standards

An ASTM standard represents a common viewpoint of those parties concerned with its provisions, namely, producer, users, consumers, and general interest groups. It is intended to aid industry, government agencies, and the general public. The use of an ASTM standard is purely voluntary. It is recognized that, for certain work or in certain regions, ASTM specifications may be either more or less restricted than needed. The existence of an ASTM standard does not preclude anyone from manufacturing, marketing, or purchasing products, or using products, processes, or procedures not conforming to the standard.

The standards included in this appendix were the latest editions available at the time of publication. Because ASTM standards are subject to periodic review and revision, those who use them are cautioned to use the latest revision. A new edition of the ASTM Book of Standards is issued annually and individual standards are available as separate copies. All of the standards in this appendix are currently published in the *Annual Book of ASTM Standards*, Section 03 on Metals Test Methods and Analytical Procedures, Volume 03.02 on Metal Corrosion, Erosion, and Wear.

Precautionary Caveat

In January 1983, the Board of Directors approved the inclusion of the following precautionary caveat in ASTM standards: This standard may involve hazardous materials, operations, and equipment. This standard does not purport to address all of the safety problems associated with its use. It is the responsibility of whoever uses the standard to consult and establish appropriate safety and health practices and determine the applicability of regulatory limitations prior to use.

Copyright© 1985 by ASTM International www.astm.org

Designation: A 262 - 85

Standard Practices for DETECTING SUSCEPTIBILITY TO INTERGRANULAR ATTACK IN AUSTENITIC STAINLESS STEELS[1]

This standard is issued under the fixed designation A 262; the number immediately following the designation indicates the year of original adoption or, in the case of revision, the year of last revision. A number in parentheses indicates the year of last reapproval. A superscript epsilon (ε) indicates an editorial change since the last revision or reapproval.

These practices have been approved for use by agencies of the Department of Defense and for listing in the DoD Index of Specifications and Standards.

1. Scope

1.1 These practices cover the following five tests:

1.1.1 *Practice A*—Oxalic Acid Etch Test for Classification of Etch Structures of Austenitic Stainless Steels (Sections 3 to 7, inclusive),

1.1.2 *Practice B*—Ferric Sulfate-Sulfuric Acid Test for Detecting Susceptibility to Intergranular Attack in Austenitic Stainless Steels (Sections 8 to 14, inclusive),

1.1.3 *Practice C*—Nitric Acid Test for Detecting Susceptibility to Intergranular Attack in Austenitic Stainless Steels (Sections 15 to 21, inclusive),

1.1.4 *Practice D*—Nitric-Hydrofluoric Acid Test for Detecting Susceptibility to Intergranular Attack in Molybdenum-Bearing Austenitic Stainless Steels (Sections 22 to 28, inclusive), and

1.1.5 *Practice E*—Copper-Copper Sulfate-Sulfuric Acid Test for Detecting Susceptibility to Intergranular Attack in Austenitic Stainless Steels (Sections 29 to 38, inclusive).

1.2 The following factors govern the application of these practices:

1.2.1 Susceptibility to intergranular attack associated with the precipitation of chromium carbides is readily detected in all five tests.

1.2.2 Sigma phase in wrought chromium-nickel-molybdenum steels, which may or may not be visible in the microstructure, can result in high corrosion rates only in nitric acid.

1.2.3 Sigma phase in titanium or columbium stabilized alloys, which may or may not be visible in the microstructure, can result in high corrosion rates in both the nitric acid and ferric sulfate-sulfuric acid solutions.

1.3 The oxalic acid etch test is a rapid method of identifying, by simple etching, those specimens of certain stainless steel grades which are essentially free of susceptibility to intergranular attack associated with chromium carbide precipitates. These specimens will have low corrosion rates in certain corrosion tests and therefore can be eliminated (screened) from testing as "acceptable."

1.4 The ferric sulfate-sulfuric acid test, the nitric acid test, and the nitric-hydrofluoric acid test are based on weight loss determinations and, thus, provide a quantitative measure of the relative performance of specimens evaluated. In contrast, the copper-copper sulfate-sulfuric acid test is based on visual examination of bend specimens and, therefore, classifies the specimens only as acceptable or nonacceptable.

1.5 In most cases either the 24-h copper-copper sulfate-sulfuric acid test or the 120-h ferric sulfate-sulfuric acid test, combined with the oxalic acid etch test, will provide the required information in the shortest time. All stainless grades listed in the accompanying table may be evaluated in these combinations of screening and corrosion tests, except those specimens of molybdenum-bearing grades (for

[1] These practices are under the jurisdiction of ASTM Committee A-1 on Steel, Stainless Steel and Related Alloys and are the direct responsibility of Subcommittee A01.14 on Methods of Corrosion Testing.

Current edition approved March 29, 1985. Published July 1985. Originally published as A 262 - 43 T. Last previous edition A 262 - 81.

example 316, 316L, 317, and 317L), which represent steel intended for use in nitric acid environments.

1.6 For AISI Grades 316, 316L, 317, and 317L only, the nitric-hydrofluoric acid test may be used to provide test results in 4 h.

1.7 The 240-h nitric acid test must be applied to stabilized and molybdenum-bearing grades intended for service in nitric acid and to all stainless steel grades which might be subject to end grain corrosion in nitric acid service.

1.8 Only those stainless steel grades are listed in Table 1 for which data on the application of the oxalic acid etch test and on their performance in various quantitative evaluation tests are available.

1.9 Extensive test results on various types of stainless steels evaluated by these practices have been published in Ref **(10)**.[2]

1.10 *This standard may involve hazardous materials, operations, and equipment. This standard does not purport to address all of the safety problems associated with its use. It is the responsibility of whoever uses this standard to consult and establish appropriate safety and health practices and determine the applicability of regulatory limitations prior to use.* Specific precautionary statements are given in 5.6, 11.1.1, 11.1.9, and 25.1.4.1.

2. Applicable Document

2.1 *ASTM Standard:*

A 370 Methods and Definitions for Mechanical Testing of Steel Products[3]

PRACTICE A—OXALIC ACID ETCH TEST FOR CLASSIFICATION OF ETCH STRUCTURES OF AUSTENITIC STAINLESS STEELS (1)

3. Scope

3.1 The oxalic acid etch test is used for acceptance of material but not for rejection of material. This may be used in connection with other evaluation tests to provide a rapid method for identifying those specimens which are certain to be free of susceptibility to rapid intergranular attack in these other tests. Such specimens have low corrosion rates in the various hot acid tests, requiring from 4 to 240 h of exposure. These specimens are identified by means of their etch structures which are classified according to the following criteria:

3.2 The oxalic acid etch test may be used to screen specimens intended for testing in Practice B—Ferric Sulfate-Sulfuric Acid Test, Practice C—Nitric Acid Test, Practice D—Nitric-Hydrofluoric Acid Test, and Practice E—Copper-Copper Sulfate-Sulfuric Acid Test.

3.2.1 Each practice contains a table showing which classifications of etch structures on a given stainless steel grade are equivalent to acceptable, or possibly nonacceptable performance in that particular test. Specimens having acceptable etch structures need not be subjected to the hot acid test. Specimens having nonacceptable etch structures must be tested in the specified hot acid solution.

3.3 The grades of stainless steels and the hot acid tests for which the oxalic acid etch test is applicable are listed in Table 2.

3.4 Extra low carbon grades, and stabilized grades, such as 304L, 316L, 317L, 321, and 347, are tested after sensitizing heat treatments at 1200 to 1250°F (650 to 675°C), which is the range of maximum carbide precipitation. These sensitizing treatments must be applied before the specimens are submitted to the oxalic acid etch test. The most commonly used sensitizing treatment is 1 h at 1250°F.

4. Apparatus

4.1 *Source of Direct Current*—Battery, generator, or rectifier capable of supplying about 15 V and 20 A.

4.2 *Ammeter*—Range 0 to 30 A (Note 1).

4.3 *Variable Resistance* (Note 1).

4.4 *Cathode*—A cylindrical piece of stainless steel or, preferably, a 1-qt (0.946-L) stainless steel beaker.

4.5 *Large Electric Clamp*—To hold specimen to be etched.

4.6 *Metallurgical Microscope*—For examination of etched microstructures at 250 to 500 diameters.

4.7 *Electrodes of the Etching Cell*—The specimen to be etched is made the anode, and a stainless steel beaker or a piece of stainless steel as large as the specimen to be etched is made the cathode.

[2] The boldface numbers in parentheses refer to the list of references found at the end of these practices.

[3] *Annual Book of ASTM Standards*, Vols 01.01 to 01.05.

4.8 *Electrolyte*—Oxalic acid, ($H_2C_2O_4 \cdot 2H_2O$), reagent grade, 10 weight % solution.

NOTE 1—The variable resistance and the ammeter are placed in the circuit to measure and control the current on the specimen to be etched.

5. Preparation of Test Specimens

5.1 *Cutting*—Sawing is preferred to shearing, especially on the extra-low carbon grades. Shearing cold works adjacent metal and affects the response to subsequent sensitization. Microscopical examination of an etch made on a specimen containing sheared edges, should be made on metal unaffected by shearing. A convenient specimen size is 1 by 1 in. (25 by 25 mm).

5.2 The intent is to test a specimen representing as nearly as possible the surface of the material as it will be used in service. Therefore the preferred sample is a cross section including the surface to be exposed in service. Only such surface finishing should be performed as is required to remove foreign material and obtain a standard, uniform finish as described in 5.3. For very heavy sections, specimens should be machined to represent the appropriate surface while maintaining reasonable specimen size for convenient testing. Ordinarily, removal of more material than necessary will have little influence on the test results. However, in the special case of surface carburization (sometimes encountered, for instance, in tubing or castings when lubricants or binders containing carbonaceous materials are employed) it may be possible by heavy grinding or machining to completely remove the carburized surface. Such treatment of test specimens is not permissible, except in tests undertaken to demonstrate such effects.

5.3 *Polishing*—On all types of materials, cross sectional surfaces should be polished for etching and microscopical examination. Specimens containing welds should include base plate, weld heat-affected zone, and weld metal. Scale should be removed from the area to be etched, by grinding to an 80 or 120-grit finish on a grinding belt or wheel without excessive heating, and then polishing on successively finer emery papers, No. 1, ½, ⅛, ⅔, and ⅜, or finer. This polishing operation can be carried out in a relatively short time since all large scratches need not be removed. Whenever practical, a polished area of 1 cm^2 or more is desirable. If any cross sectional dimension is less than 1 cm, a minimum length of 1 cm should be polished. When the available length is less than 1 cm, a full cross section should be used.

5.4 *Etching Solution*—The solution used for etching is prepared by adding 100 g of reagent grade oxalic acid crystals ($H_2C_2O_4 \cdot 2H_2O$) to 900 mL of distilled water and stirring until all crystals are dissolved.

5.5 *Etching Conditions*—The polished specimen should be etched at 1 A/cm^2 for 1.5 min. To obtain the correct current density:

5.5.1 The total immersed area of the specimen to be etched should be measured in square centimetres, and

5.5.2 The variable resistance should be adjusted until the ammeter reading in amperes is equal to the total immersed area of the specimen in square centimetres.

5.6 *Etching Precautions:*

5.6.1 **Caution**—Etching should be carried out under a ventilated hood. Gas, which is rapidly evolved at the electrodes with some entrainment of oxalic acid, is poisonous and irritating to mucous membranes.

5.6.2 A yellow-green film is gradually formed on the cathode. This increases the resistance of the etching cell. When this occurs, the film should be removed by rinsing the inside of the stainless steel beaker (or the steel used as the cathode) with an acid such as 30 % HNO_3.

5.6.3 The temperature of the etching solution gradually increases during etching. The temperature should be kept below 50°C by alternating two beakers. One may be cooled in tap water while the other is used for etching. The rate of heating depends on the total current (ammeter reading) passing through the cell. Therefore, the area etched should be kept as small as possible while at the same time meeting the requirements of desirable minimum area to be etched.

5.6.4 Immersion of the clamp holding the specimen in the etching solution should be avoided.

5.7 *Rinsing*—Following etching, the specimen should be thoroughly rinsed in hot water and in acetone or alcohol to avoid crystallization of oxalic acid on the etched surface during drying.

5.8 On some specimens containing molybdenum (AISI 316, 316L, 317, 317L) which are free of chromium carbide sensitization, it may be difficult to reveal the presence of step structures by electrolytic etching with oxalic acid. In such

cases, an electrolyte of a 10 % solution of ammonium persulfate, $(NH_4)_2S_2O_8$, may be used in place of oxalic acid. An etch of 5 or 10 min at 1 A/cm^2 in a solution at room temperature readily develops step structures on such specimens.

6. Classification of Etch Structures

6.1 The etched surface is examined on a metallurgical microscope at 250× to 500× for wrought steels and at about 250× for cast steels.

6.2 The etched cross-sectional areas should be thoroughly examined by complete traverse from inside to outside diameters of rods and tubes, from face to face on plates, and across all zones such as weld metal, weld-affected zones, and base plates on specimens containing welds.

6.3 The etch structures are classified into the following types (Note 2):

6.3.1 *Step Structure* (Fig. 1)—Steps only between grains, no ditches at grain boundaries.

6.3.2 *Dual Structure* (Fig. 2)—Some ditches at grain boundaries in addition to steps, but no single grain completely surrounded by ditches.

6.3.3 *Ditch Structure* (Fig. 3)—One or more grains completely surrounded by ditches.

6.3.4 *Isolated Ferrite* (Fig. 4)—Observed in castings and welds. Steps between austenite matrix and ferrite pools.

6.3.5 *Interdendritic Ditches* (Fig. 5)—Observed in castings and welds. Deep interconnected ditches.

6.3.6 *End-Grain Pitting I* (Fig. 6)—Structure contains a few deep end-grain pits along with some shallow etch pits at 500×. (Of importance only when nitric acid test is used.)

6.3.7 *End-Grain Pitting II* (Fig. 7)—Structure contains numerous, deep end-grain pits at 500×. (Of importance only when nitric acid test is used.)

NOTE 2—All photomicrographs were made with specimens that were etched under standard conditions: 10 % oxalic acid, room temperature, 1.5 min at 1 A/cm^2.

6.4 The evaluation of etch structures containing steps only and of those showing grains completely surrounded by ditches in every field can be carried out relatively rapidly. In cases that appear to be dual structures, more extensive examination is required to determine if there are any grains completely encircled. If an encircled grain is found, the steel should be evaluated as a ditch structure. Areas near surfaces should be examined for evidence of surface carburization.

6.4.1 On stainless steel castings (also on weld metal) the steps between grains formed by electrolytic oxalic acid etching tend to be less prominent than those on wrought materials, or are entirely absent. However, any susceptibility to intergranular attack is readily detected by pronounced ditches.

6.5 Some wrought specimens, especially from bar stock, may contain a random pattern of pits. If these pits are sharp and so deep that they appear black (Fig. 7) it is possible that the specimen may be susceptible to end grain attack in nitric acid only. Therefore, even though the grain boundaries all have step structures, specimens having as much or more end grain pitting than that shown in Fig. 7 cannot be safely assumed to have low nitric acid rates and should be subjected to the nitric acid test whenever it is specified. Such sharp, deep pits should not be confused with the shallow pits shown in Figs. 1 and 6.

7. Use of Etch Structure Classifications

7.1 The use of these classifications depends on the hot acid corrosion test for which stainless steel specimens are being screened by etching in oxalic acid and is described in each of the practices. Important characteristics of each of these tests are described below.

7.2 *Practice B—Ferric Sulfate-Sulfuric Acid Test* is a 120-h test in boiling 50 % solution that detects susceptibility to intergranular attack associated primarily with chromium carbide precipitate. It does not detect susceptibility associated with sigma phase in chromium-nickel-molybdenum stainless steels (316, 316L, 317, 317L) which is known to lead to rapid intergranular attack only in certain nitric acid environments. It does not detect susceptibility to end grain attack which is also found only in certain nitric acid environments. The ferric sulfate-sulfuric acid test does reveal susceptibility associated with a sigma-like phase constituent in stabilized stainless steels, AISI 321 and 347.

7.3 *Practice C—Nitric Acid Test* is a 240-h test in boiling, 65 % nitric acid which detects susceptibility to rapid intergranular attack associated with chromium carbide precipitate and with sigma-like phase precipitate. The latter may be formed in molybdenum-bearing and in stabilized grades of austenitic stainless steels and may or may not be visible in the microstructure. This test also reveals susceptibility to end grain attack in all grades of stainless steels.

7.4 *Practice D—Nitric-Hydrofluoric Acid*

Test is a 4-h test in a solution of 10 % nitric acid and 3 % hydrofluoric acid at 70°C. It is applicable only to molybdenum-bearing grades of austenitic stainless steels (AISI 316, 316L, 317, 317L) and detects only susceptibility to intergranular attack associated with chromium carbide precipitates. It does not detect susceptibility to intergranular attack associated with sigma phase or end grain corrosion, which, so far, are known to lead to rapid intergranular attack only in certain nitric acid environments.

7.5 *Practice E—Copper-Copper Sulfate-Sulfuric Acid Test* is a 24-h test in a boiling solution containing 16 % sulfuric acid and 6 % copper sulfate with the test specimen embedded in metallic copper shot or grindings, which detects susceptibility to intergranular attack associated with the precipitation of chromium-rich carbides. It does not detect susceptibility to intergranular attack associated with sigma phase, or end-grain corrosion, both of which have been observed to date only in certain nitric acid environments.

PRACTICE B—FERRIC SULFATE-SULFURIC ACID TEST FOR DETECTING SUSCEPTIBILITY TO INTERGRANULAR ATTACK IN AUSTENITIC STAINLESS STEELS (2)

8. Scope

8.1 This practice describes the procedure for conducting the boiling, 120-h ferric sulfate-50 % sulfuric acid test (Note 3) which measures the susceptibility of stainless steels to intergranular attack. The presence or absence of intergranular attack in this test is not necessarily a measure of the performance of the material in other corrosive environments. The test does not provide a basis for predicting resistance to forms of corrosion other than intergranular, such as general corrosion, pitting, or stress-corrosion cracking.

NOTE 3—See Practice A for information on the most appropriate of the several test methods available for the evaluation of specific grades of stainless steel.

8.1.1 The ferric sulfate-sulfuric acid test detects susceptibility to intergranular attack associated with the precipitation of chromium carbides in unstabilized austenitic stainless steels. It does not detect susceptibility to intergranular attack associated with sigma phase in austenitic stainless steels containing molybdenum, such as Types 316, 316L, 317, and 317L.

NOTE 4—To detect susceptibility to intergranular attack associated with sigma phase in austenitic stainless steels containing molybdenum, the nitric acid test, Practice C, should be used.

8.2 In stabilized stainless steel, Type 321 (and perhaps 347) the ferric sulfate-sulfuric acid test detects susceptibility associated with precipitated chromium carbides and with a sigma phase which may be invisible in the microstructure.

8.3 The ferric sulfate-sulfuric acid test may be used to evaluate the heat treatment accorded as-received material. It may also be used to check the effectiveness of stabilizing columbium or titanium additions and of reductions in carbon content in preventing susceptibility to rapid intergranular attack. It may be applied to wrought products (including tubes), castings, and weld metal.

8.4 Specimens of extra low carbon and stabilized grades are tested after sensitizing heat treatments at 1200 to 1250°F (650 to 675°C), which is the range of maximum carbide precipitation. The length of time of heating used for this sensitizing treatment determines the maximum permissible corrosion rate for such grades in the ferric sulfate-sulfuric acid test. The most commonly used sensitizing treatment is 1 h at 1250°F.

9. Rapid Screening Test

9.1 Before testing in the ferric sulfate sulfuric acid test, specimens of certain grades of stainless steels (see Table 3) may be given a rapid screening test in accordance with procedures given in Practice A, Oxalic Acid Etch Test for Classification of Etch Structures of Austenitic Stainless Steels. Preparation, etching, and the classification of etch structures are described therein. The use of etch structure evaluations in connection with the ferric sulfate-sulfuric acid test is specified in Table 3.

9.1.1 Corrosion test specimens having acceptable etch structures in the oxalic acid etch test will be essentially free of intergranular attack in the ferric sulfate-sulfuric acid test. Such specimens are acceptable without testing in the ferric sulfate-sulfuric acid test. All specimens having nonacceptable etch structures must be tested in the ferric sulfate-sulfuric acid test.

10. Apparatus

10.1 The apparatus (Note 6) is illustrated in Fig. 8.

10.1.1 A four-bulb Allihn or Soxhlet condenser with a 45/50 ground glass joint. Overall length: about 13 in. (330 mm), condensing section, 9½ in. (241 mm).

10.1.2 A 1-L Erlenmeyer flask with a 45/50 ground glass joint. The ground glass opening is somewhat over 1½ in. (38 mm) wide.

10.1.3 The glass cradle (Note 5) can be supplied by a glass-blowing shop. To pass through the ground glass joint on the Erlenmeyer flask, the width of the cradle should not exceed 1½ in., and the front-to-back distance must be such that the cradle will fit the 1⅓-in. (34-mm) diameter opening. It should have three or four holes to increase circulation of the testing solution around the specimen.

NOTE 5—Other equivalent means of specimen support, such as glass hooks or stirrups, may also be used.

10.1.4 Boiling chips must be used to prevent bumping.

10.1.5 A silicone grease[4] is recommended for the ground glass joint.

10.1.6 During testing, there is some deposition of iron oxides on the upper part of the Erlenmeyer flask. This can be readily removed, after test completion, by boiling a solution of 10 % hydrochloric acid in the flask.

10.1.7 A device such as an electrically heated hot plate which provides heat for continuous boiling of the solution.

10.1.8 An analytical balance capable of weighing to the nearest 0.001 g.

NOTE 6—No substitutions for this equipment may be used. The cold-finger type of condenser with standard Erlenmeyer flasks may not be used.

11. Ferric Sulfate-Sulfuric Acid Test Solution

11.1 Prepare 600 mL of 50 % (49.4 to 50.9 %) solution as follows:

11.1.1 **Caution**—Protect the eyes and use rubber gloves for handling acid. Place the test flask under a hood.

11.1.2 First, measure 400.0 mL of distilled water in a 500-mL graduate and pour into the Erlenmeyer flask.

11.1.3 Then measure 236.0 mL of reagent grade sulfuric acid of a concentration which must be in the range from 95.0 to 98.0 % by weight in a 250-mL graduate. Add the acid slowly to the water in the Erlenmeyer flask to avoid boiling by the heat evolved.

NOTE 7—Loss of vapor results in concentration of the acid.

11.1.4 Weigh 25 g of reagent grade ferric sulfate (contains about 75 % $Fe_2(SO_4)_3$) and add to the sulfuric acid solution. A trip balance may be used.

11.1.5 Drop boiling chips into the flask.

11.1.6 Lubricate ground glass joint with silicone grease.

11.1.7 Cover flask with condenser and circulate cooling water.

11.1.8 Boil solution until all ferric sulfate is dissolved (see Note 7).

11.1.9 **Caution**—It has been reported that violent boiling resulting in acid spills can occur. It is important to ensure that the concentration of acid does not become more concentrated and that an adequate number of boiling chips (which are resistant to attack by the test solution) are present.[5]

12. Preparation of Test Specimens

12.1 A specimen having a total surface area of 5 to 20 cm^2 is recommended. Specimens containing welds should be cut so that no more than ½-in. (13-mm) width of base metal is included on either side of the weld.

12.2 The intent is to test a specimen representing as nearly as possible the surface of the material as used in service. Only such surface finishing should be performed as is required to remove foreign material and obtain a standard, uniform finish as specified. For very heavy sections, specimens should be machined to represent the appropriate surface while maintaining reasonable specimen size for convenience in testing. Ordinarily, removal of more material than necessary will have little influence on the test results. However, in the special case of surface carburization (sometimes encountered, for instance, in tubing or castings when lubricants or binders containing carbonaceous materials are employed) it may be possible by heavy grinding or machining to remove the carburized layer completely. Such treatment of test specimens is not permissible, except in tests undertaken to demonstrate such surface effects.

[4] Dow Corning Stopcock Grease has been found satisfactory for this purpose.

[5] Amphoteric alundum granules, Hengar Granules, from the Hengar Co., Philadelphia, PA have been found satisfactory for this purpose.

12.3 When specimens are cut by shearing, the sheared edges should be refinished by machining or grinding prior to testing.

12.4 All surfaces of the specimen, including edges, should be finished using No. 80 or 120 grit abrasive paper. If dry abrasive paper is used, polish slowly to avoid overheating. Sand blasting should not be used.

12.5 All traces of oxide scale formed during heat treatments must be thoroughly removed. Any scale which cannot be removed by grinding, for example, in stamped numbers, must be removed by immersing the specimen in concentrated nitric acid at about 200°F (93°C). (Residual oxide scale causes galvanic action and consequent activation in the test solution.)

12.6 The specimen should be measured including the inner surfaces of any holes and the total exposed area calculated.

12.7 The specimen should then be degreased and dried using suitable nonchlorinated agents, such as soap and acetone, and then weighed to the nearest 0.001 g.

13. Procedure

13.1 Place specimen in glass cradle and immerse in boiling solution.

13.2 Mark liquid level on flask with wax crayon to provide a check on vapor loss which would result in concentration of the acid. If there is an appreciable change in the level, the test must be repeated with fresh solution and a reground specimen.

13.3 Continue immersion of the specimen for a total of 120 h, then remove specimen, rinse in water and acetone, and dry.

13.4 Weigh specimen and subtract weight from original weight.

13.5 No intermediate weighings are usually necessary. The tests can be run without interruption for 120 h. However, if preliminary results are desired, the specimen can be removed at any time for weighing.

13.6 No changes in solution are necessary during the 120-h test periods.

13.7 Additional ferric sulfate inhibitor may have to be added during the test if the corrosion rate is extraordinarily high as evidenced by a change in the color of the solution. More ferric sulfate must be added if the total weight loss of all specimens exceeds 2 g. (During the test, ferric sulfate is consumed at a rate of 10 g for each 1 g of dissolved stainless steel.)

13.8 Several specimens may be tested simultaneously. The number (3 or 4) is limited only by the number of glass cradles that can be fitted into the flask.

14. Calculation and Report

14.1 The effect of the acid solution on the material shall be measured by determining the loss of weight of the specimen. The corrosion rates should be reported as inches of penetration per month (Note 8), calculated as follows:

$$\text{Inches per month} = (287 \times W)/(A \times t \times d)$$

where:

t = time of exposure, h,
A = area, cm^2,
W = weight loss, g, and
d = density, g/cm^3.

for chromium-nickel steels, $d = 7.9\ g/cm^3$

for chromium-nickel-molybdenum steels, $d = 8.00\ g/cm^3$

NOTE 8—Conversion factors to other commonly used units for corrosion rates are as follows:

inches per month × 12 = inches per year
inches per month × 1000 = mils per month
inches per month × 12 000 = mils per year
inches per month × 8350 × density = milligrams per square decimetre per day
inches per month × 34.8 × density = grams per square metre per hour
1.00 $in.^2$ = 6.45 cm^2

PRACTICE C—NITRIC ACID TEST FOR DETECTING SUSCEPTIBILITY TO INTERGRANULAR ATTACK IN AUSTENITIC STAINLESS STEELS

15. Scope

15.1 This practice describes the procedure for conducting the boiling nitric acid test (3) as employed to measure the relative susceptibility of austenitic stainless steels to intergranular attack. The presence or absence of intergranular attack in this test is not necessarily a measure of the performance of the material in other corrosive environments; in particular, it does not provide a basis for predicting resistance to forms of corrosion other than intergranular, such as general corrosion, pitting, or stress-corrosion cracking.

15.2 The boiling nitric acid test may be used to evaluate the heat treatment accorded "as-received" material. It is also sometimes used to check the effectiveness of stabilizing elements and of reductions in carbon content in preventing susceptibility to rapid intergranular attack.

NOTE 9—Intergranular attack in nitric acid is asso-

ciated with one or more of the following: (*1*) intergranular precipitation of chromium carbides, (*2*) sigma or transition phases in molybdenum-bearing grades, and (*3*) sigma phase constituents in stabilized grades. The boiling nitric acid test should not be used for extra low carbon molybdenum-bearing grades unless the material tested is to be used in nitric acid service. See Practice A, Oxalic Acid Etching Test, for information on the most appropriate of the several test methods available for the evaluation of specific grades of stainless steel.

15.3 Specimens of extra low carbon and stabilized grades are tested after sensitizing heat treatments at 1200 to 1250°F (650 to 675°C), which is the range of maximum carbide precipitation. The length of time used for this sensitizing treatment determines the maximum permissible corrosion rate in the nitric acid test. The most commonly used sensitizing treatment is 1 h at 1250°F.

15.4 This practice may be applied to wrought products (including tubes), castings, and weld metal of the various grades of stainless steel (Note 9).

16. Rapid Screening Test

16.1 Before testing in the nitric acid test, specimens of certain grades of stainless steel as given in Table 1 may be given a rapid screening test in accordance with procedures given in Practice A, Oxalic Acid Etch Test for Classification of Etch Structures of Austenitic Stainless Steels. The use of the etch structure evaluations in connection with the nitric acid test is specified in Table 4.

16.1.1 Corrosion test specimens having acceptable etch structures in the oxalic acid etch test will be essentially free of intergranular attack in the nitric acid test; such specimens are acceptable without testing in the nitric acid test. All specimens having nonacceptable etch structures must be tested in the nitric acid test.

17. Apparatus

17.1 *Container*—A 1-L Erlenmeyer flask equipped with a cold finger-type condenser, as illustrated in Fig. 9, is recommended.

NOTE 10—Two other types of containers have been employed in the past and may be used if agreed upon between the supplier and purchaser. One of these consists of a 1-L Erlenmeyer flask with a ground glass joint and equipped with a 30-in. (762-mm) reflux condenser; it has been shown that results obtained with a reflux condenser tend to be somewhat higher than with the cold finger-type condenser due to greater vapor loss. The second type of container is the so called multi-sample testing apparatus (**4**) which was designed to permit the testing of a large number of specimens simultaneously by providing for replacement of the acid in contact with the specimens several times per hour with redistilled acid. Because of the lesser accumulation of corrosion products in the testing solution, the rates obtained with the multi-sample tester are consistently lower than those obtained with the conventional apparatus; the differences are small on properly annealed or stabilized material which will show low rates in both types of test but can be very large for sensitized specimens. For research purposes or where results are to be compared directly, it is essential that the same type of apparatus be used for all tests.

17.2 *Specimen Supports*—Glass hooks, stirrups, or cradles for supporting the specimens in the flask fully immersed at all times during the test and so designed that specimens tested in the same container do not come in contact with each other.

17.3 *Heater*—A means for heating the test solutions and of keeping them boiling throughout the test period. An electrically heated hot plate is satisfactory for this purpose.

17.4 *Balance*—An analytical balance capable of weighing to at least the nearest 0.001 g.

18. Nitric Acid Test Solution

18.1 The test solution shall be 65 ± 0.2 weight % as nitric acid determined by analysis. This solution may be prepared by adding distilled water to concentrated nitric acid (reagent grade HNO_3, sp gr 1.42) (Note 11) at the rate of 108 mL of distilled water per litre of concentrated nitric acid.

NOTE 11—The nitric acid used should conform to the recommended specifications for analytical reagent chemicals of the American Chemical Society (**5**) as follows:

Nonvolatile matter, max, %	0.0005
Sulfate (SO_4), max, %	0.0002
Arsenic, max, %	0.000003
Chlorine, max, % about	0.00007
Heavy metals, max, % about lead	0.0005
and iron	0.0001

In addition, the fluorine content shall not exceed 0.0001 % and phosphate (PO_4) shall not exceed 0.00002 %.

19. Preparation of Test Specimens

19.1 The size and shape of the specimen must be considered with respect to available facilities for accurate weighing and the volume of test solution to be used. Normally, the maximum convenient weight of specimen is about 100 g. Specimens containing welds should be cut so that

no more than ½ in. (13 mm) width of base metal is included on either side of the weld. Furthermore, in the case of bar, wire, and tubular products, the proportion of the total area represented by the exposed cross section may influence the results. Cross-sectional areas in these products may be subject to end grain attack in nitric acid. The proportion of end grain in the specimen should therefore be kept low unless such surface is actually to be exposed in service involving nitric acid. When specimens of such products are being tested in research investigations, the ratio of the cross-sectional area exposed to the total area should be kept constant from test to test. For inspection tests, specimens cut from bars, wires, or tubes should be proportioned so that the areas of the exposed cross sections shall not exceed half the total exposed area of the specimen.

19.2 Special heat treatment of specimens prior to testing or the use of specimens which contain a weld may be specified.

19.3 When specimens are cut by shearing, the sheared edges should be refinished by machining or grinding prior to testing.

19.4 All surfaces of the specimen, including edges, should be finished using No. 80 or 120 grit abrasive paper. If dry abrasive paper is used, polish slowly to avoid overheating. Sandblasting should not be used.

19.5 The intent is to test a specimen representing as nearly as possible the surface of the material as it will be used in service. Only such surface machining should be performed as is required to remove foreign material and obtain a standard uniform finish as specified in 19.4. For very heavy sections, specimens should be machined to represent the appropriate surface while maintaining reasonable specimen size for convenience in testing. Ordinarily, removal of more material than necessary will have little influence on the test results. However, in the special case of surface carburization (sometimes encountered, for instance, in tubing or castings when lubricants or binders containing carbonaceous materials are employed), it may be possible by heavy grinding or machining to remove the carburized surface completely. Such treatment of test specimens is not permissible except in tests undertaken to demonstrate such surface effects.

19.6 The specimen should be measured including the inner surfaces of any holes and the total exposed area calculated.

19.7 The specimen should then be degreased and dried using suitable nonchlorinated agents, such as soap and acetone (Note 12), and then weighed to the nearest 0.001 g (see 17.4).

NOTE 12—The cleaning treatment described may be supplemented by immersing the specimen in nitric acid (for example, 20 weight % at 120 to 140°F (49 to 60°C) for 20 min), followed by rinsing, drying, and weighing. In the case of small-diameter tubular specimens which cannot be conveniently resurfaced on the inside, it is desirable to include in the preparation an immersion in boiling nitric acid (65 %) for 2 to 4 h using the same apparatus as for the actual test. The purpose of these treatments is to remove any surface contamination that may not be accomplished by the regular cleaning method and which may increase the apparent weight loss of the specimen during the early part of the test.

19.8 It is common practice to test only one specimen of each material or lot of material, as defined by those using the test for specification purposes. However, the use of at least two specimens for check purposes is recommended.

20. Procedure

20.1 Use a sufficient quantity of the nitric acid test solution to cover the specimens and to provide a volume of at least 125 mL/in.^{2} (20 mL/cm^2) of specimen surface. Normally, a volume of about 600 cm^3 is used.

20.2 The best practice is to use a separate container for each test specimen.

NOTE 13—For routine evaluations, it is acceptable to test as many as three specimens in the same container provided that they all are of the same grade and all show satisfactory resistance to corrosion. If more than one of the specimens tested in the same container fail to pass the test, it is necessary to retest all specimens in separate containers, since excessive corrosion of one specimen may result in accelerated corrosion of the other specimens tested with it. Excessive corrosion may often be detected by changes in the color of the test solution, and it may be appropriate to provide separate containers for such specimens without waiting until the end of the test period. A record should be made showing which specimens were tested together.

NOTE 14—If the multi-sample testing apparatus (see Note 10) is employed, a large number of specimens may be tested in the large container provided.

20.3 After the specimens have been placed in the acid in the container, pass cooling water through the condenser and bring the acid to a boil on the hot plate and then keep boiling throughout the test period (Note 15). After each test period, rinse the specimens with water and treat by scrubbing with rubber or a nylon brush under running water to remove any adhering

corrosion products, after which they should be dried and weighed. Drying may be facilitated, if desired, by dipping the specimens in acetone after they are scrubbed.

NOTE 15—Care should be taken to prevent contamination of the testing solution, especially by fluorides, either before or during the test. Experience has shown that the presence of even small amounts of hydrofluoric acid will increase the corrosion rate in the nitric acid test. It is not permissible, for example, to conduct nitric-hydrofluoric acid tests in the same hood with nitric acid tests.

20.4 For most consistent results, the test should consist of five boiling periods of 48 h each (Note 16) with a fresh test solution being used in each period.

NOTE 16—For specification purposes, those experienced in the use of the test may, by mutual agreement, shorten the standard test to three 48-h boiling periods. However, if with this shorter test procedure the rate of attack in the third period should exceed that in either the first or second periods to some previously agreed-upon extent, then the test should be continued for a total of five periods. As an alternative, when the test is being used for inspection prior to approval of steel for shipment, a procedure may be agreed upon by the purchaser and the manufacturer whereby the material will be released for shipment following satisfactory performance in three 48-h boiling periods with final acceptance being dependent upon satisfactory performance in the longer test of five 48-h boiling periods. Also, by mutual agreement, a combination of one 48-h period and two 96-h periods (not necessarily in that order) instead of five 48-h test periods may be acceptable for routine evaluations.

21. Calculation and Report

21.1 *Calculation*—The effect of the acid on the material shall be measured by determining the loss of weight of the specimen after each test period and for the total of the test periods. Such weight-loss determinations should be made with the accuracy prescribed in 17.1.4. The corrosion rates are usually reported as inches per month (Note 17), calculated in the following rate of corrosion equation:

$$\text{Inches per month} = (287 \times W)/(A \times d \times t)$$

where:

t = time of exposure, h,
A = total surface area, cm^2,
W = weight loss, g, and
d = density of the sample, g/cm^3.

NOTE 17—Conversion factors to other commonly used units for corrosion rates are as follows:

inches per month × 12 = inches per year
inches per month × 1000 = mils per month
inches per month × 12 000 = mils per year
inches per month × 8350 × density = milligrams per square decimetre per day
inches per month × 34.8 × density = grams per square metre per hour
1.00 $in.^2$ = 6.45 cm^2

21.2 *Report*—Results should be reported for the individual periods, as well as the average for the three or five test periods.

PRACTICE D — NITRIC - HYDROFLUORIC ACID TEST FOR DETECTING SUSCEPTIBILITY TO INTERGRANULAR ATTACK IN MOLYBDENUM - BEARING AUSTENITIC STAINLESS STEELS (6)

22. Scope

NOTE 18—See Practice A for information on the most appropriate of the several test methods available for the evaluation of specific grades of stainless steel.

22.1 This practice describes the procedure for conducting the 70°C 4-h, 10 % nitric-3 % hydrofluoric acid test as employed to measure the susceptibility of molybdenum-bearing stainless steels to intergranular attack. The presence or absence of intergranular attack in this test is not necessarily a measure of the performance of the material in other corrosive environments. The test does not provide a basis for predicting resistance to forms of corrosion other than intergranular, such as general corrosion, pitting, or stress-corrosion cracking.

22.1.1 The 10 % nitric-3 % hydrofluoric acid test detects susceptibility to intergranular attack associated with the precipitation of chromium carbides in molybdenum-bearing stainless steels (Types 316, 317, 316L, and 317L). It does not detect susceptibility to intergranular attack associated with sigma phase in these same types of stainless steel.

22.2 The 10 % nitric-3 % hydrofluoric acid test may be used to evaluate the heat treatment accorded as-received material (Types 316 and 317 stainless steel). It may also be used to check the effectiveness of reduction in carbon content in preventing susceptibility to rapid intergranular attack (Types 316L and 317L). It may be applied to wrought products (including tubes), castings, and weld metal.

22.3 Specimens of extra low carbon grades (Types 316L and 317L) are tested after sensitizing heat treatments at 1200 to 1250°F (650 to 675°C), which is the range of maximum carbide precipitation. The length of time of heating used for this

sensitizing treatment will generally be 1 or 2 h. The most commonly used sensitizing treatment is 1 h at 1250°F.

23. Summary of Practice

23.1 *Types 316 and 317 Stainless Steel*—The material submitted for evaluation is tested in each of two conditions of heat treatment: (*1*) as-received (commercially annealed) and (*2*) laboratory-annealed for 1 h at 1900 to 2000°F (1040 to 1095°C), and water quenched.

23.2 *Types 316L and 317L Stainless Steel*—The material submitted for evaluation test is tested in each of two conditions of heat treatment: (*1*) a sensitized specimen, and (*2*) a baseline specimen, which usually is the as-received (commercially annealed) specimen. If the as-received specimen does not show a step structure in the oxalic acid etch test, a portion of it must be laboratory annealed to give a step structure and that sample used as the baseline specimen (see footnote *C* of Table 5).

24. Rapid Screening Test

24.1 Before testing in the 10 % nitric-3 % hydrofluoric acid test, specimens of the stainless steels as given in Table 5 may be given a rapid screening test in accordance with procedures given in Practice A, Oxalic Acid Etch Test for Classification of Etch Structures of Austenitic Stainless Steels. Preparation, etching, and the classification of etch structures are described therein. The use of etch-structure evaluations in connection with the 10 % nitric-3% hydrofluoric acid test is specified in Table 5.

24.1.1 Corrosion test specimens having acceptable etch structures in the Oxalic Acid Etch Test will be largely free of intergranular attack in the 10 % nitric-3% hydrofluoric acid test. Such specimens are acceptable without testing in the 10 % nitric-3 % hydrofluoric acid test. All specimens having nonacceptable etch structures must be tested in the 10 % nitric-3 % hydrofluoric acid test.

25. Apparatus

25.1 The apparatus is illustrated in Fig. 9.

25.1.1 *Test Cylinders* (Note 19)—The tests are conducted in cylinders of poly(vinyl chloride) (PVC) as shown in Fig. 10. The test cylinders can be made from 12-in. (305-mm) lengths of 1¼-in. PVC pipe (3/16-in. (4.76 mm) wall) by either of the following two techniques: (*1*) one end of each pipe length is plugged with a disk of 3/16-in. PVC sheet and the disk is then heat-welded in place with PVC filler rod, or (*2*) one end of each pipe length is plugged by solvent-welding a 1¼-in. NPS (Schedule 80) socket-type PVC cap onto the end of the pipe.

25.1.2 *Specimen Holders* (Note 19)—The specimens may be suspended in the test solution by means of either a specimen holder (as described in this paragraph) or a TFE-fluorocarbon string through an appropriate hole drilled in one end of the specimen. The specimen holders may be made in either of two ways: (*1*) a 1-in. (25-mm) length of TFE-fluorocarbon tubing (1-in. inside diameter) is drilled at one end to accommodate a 3/16-in. (4.76-mm) TFE-fluorocarbon rod. The holders are flattened into an elliptical shape which is maintained by inserting the rod through the two holes and upsetting the ends of the rod with a hammer, or (*2*) a ½-in. NPS (Schedule 80) socket-type PVC cap is machined to reduce the outer diameter of the cap to 1 1/16 in. (27.0 mm). Holes ¼ in. (6.35 mm) in diameter are then drilled in the bottom and sides of the machined PVC caps to allow free circulation of the test solution. Smaller holes are drilled at the top of the PVC cap to attach the TFE-fluorocarbon string. A loop of the same string is attached to each specimen holder and used to suspend it in the test cylinder.

NOTE 19—All poly(vinyl chloride) materials should be specified on the order as Schedule 80, rigid unplasticized normal impact PVC.

25.1.3 *Constant-Temperature Bath*—The desired solution test temperature of 70°C is obtained by placing the PVC cylinders within a rack in a constant-temperature water bath. The temperature of the bath is maintained at 72 to 73°C to offset the low thermal conductivity of the poly(vinyl chloride).

25.1.4 *10 % Nitric-3 % Hydrofluoric Acid Test Solution:*

25.1.4.1 **Caution**—The 10 % nitric-3 % hydrofluoric acid solution will cause severe burns if it comes into contact with the skin. Therefore, extreme care should be exercised in handling this solution. Rubber gloves should be worn. Spilled acid should immediately be washed from the skin with an excess of water and emergency first-aid treatment obtained.

25.1.4.2 A 10 % nitric-3 % hydrofluoric acid

solution (by weight) is prepared by mixing 111 mL of 65 % nitric acid (sp gr 1.39), 54 mL of 48 % hydrofluoric acid (sp gr 1.16), and 784 mL of distilled water in a polyethylene carboy. Fresh test solution should be made up daily to avoid changes in concentration due to evaporation.

26. Preparation of Test Specimens

26.1 A specimen having a total surface area of 5 to 20 cm^2 is recommended. Specimens containing welds should be cut so that no more than a ½-in. (13-mm) width of base metal is included on either side of the weld.

26.2 The intent is to test a specimen representing as nearly as possible the surface of the material as it will be used in service. Only such finishing should be performed as is required to remove foreign material and obtain a standard, uniform finish as specified. For very heavy sections, specimens should be machined to represent the appropriate surface while maintaining reasonable specimen size for convenience in testing. Ordinarily, removal of more material than necessary will have little influence on the test results. However, in the special case of surface carburization (sometimes encountered, for instance, in tubing or castings when lubricants or binders containing carbonaceous materials are employed), it may be possible by heavy grinding or machining to remove the carburized layer completely. Such treatment of test specimens is not permissible.

26.3 When specimens are cut by shearing, the sheared edges should be refinished by machining or grinding prior to testing.

26.4 All surfaces of the specimen, including edges, should be finished using No. 80 or 120 grit abrasive paper. If dry abrasive paper is used, polish slowly to avoid overheating. Sand blasting should not be used.

26.5 The specimen should be measured and the total exposed area, including the inner surfaces of any holes, calculated in square centimetres.

26.6 The specimen should then be degreased and dried using suitable nonchlorinated agents, such as soap and acetone, and then weighed to the nearest 0.001 g.

27. Procedure

27.1 *Types of Test Specimens:*

27.1.1 *Types 316 and 317*—Test two specimens, one representing the as-received condition and one representing the laboratory-annealed condition. (The laboratory-annealed specimen must show a step structure in the oxalic acid etch test.)

27.1.2 *Types 316L and 317L*—Test two specimens, one representing the sensitized condition and the other a base-line specimen, which is usually the as-received (commercially annealed) specimen. If the as-received specimen does not show a step structure in the oxalic acid etch test, laboratory anneal a portion of it to give a step structure and use that sample as the base-line specimen (see footnote *C* of Table 5).

27.2 Fill the PVC test cylinders with 200 mL of 10 % nitric-3 % hydrofluoric acid solution and then heat in the constant temperature water bath until the solution temperature, as measured with a thermometer, is 70 ± 0.5°C.

NOTE 20—It is important that the test solution be maintained at 70 ± 0.5°C because small changes in solution temperature produce large changes in the corrosion rate.

27.3 When the solution temperature is 70 ± 0.5°C, lower the specimens into the solution by means of the specimen holders or string. After a 2-h exposure, remove the specimens from the test, wash in distilled water and acetone, dry, and weigh. Then expose the two specimens for an additional 2-h test period in fresh test solutions at 70 ± 0.5°C.

27.4 Test only one specimen in each cylinder. In addition, it is preferable to test simultaneously the two specimens representing each of the two conditions of heat treatment for each material evaluated.

28. Calculation and Report

28.1 *Calculation of Individual Corrosion Rates*—The effect of the acid solution on each of the two specimens of each material shall be measured by determining the loss of weight of the specimen. The average corrosion rate in inches per month (Note 21), based on the 4-h test exposure, is calculated for each specimen as follows:

$$\text{Inches per month} = (287 \times W)/(A \times t \times d)$$

where:

t = time of exposure, h,
A = area, cm^2,
W = weight loss, g, and
d = density, g/cm^3, for chromium-nickel-molybdenum steels, $d = 8.0\ g/cm^3$.

28.2 *Calculations of Corrosion-Rate Ratios:*

28.2.1 *Types 316 and 317 Stainless Steel*—The ratio of the corrosion rate for the as-received specimen to the corrosion rate for the laboratory-annealed specimen is determined.

28.2.2 *Types 316L and 317L Stainless Steel*—The ratio of the corrosion rate for the sensitized specimen to the corrosion rate for the as-received specimen is determined.

28.3 *Significance of Corrosion Rate Ratios*—A value of 1.5 or less for the above ratios indicates that the degree of intergranular attack in the 10 % nitric-3 % hydrofluoric acid test was not significant. A ratio of greater than 1.5 indicates that significant intergranular corrosion has occurred in the 10 % nitric-3 % hydrofluoric acid test.

NOTE 21—Conversion factors to other commonly used units for corrosion rates are as follows:

inches per month × 12 = inches per year
inches per month × 1000 = mils per month
inches per month × 12 000 = mils per year
inches per month × 8350 × density = milligrams per square decimetre per day
inches per month × 34.8 × density = grams per square metre per hour
1.00 $in.^2$ = 6.45 cm^2

PRACTICE E—COPPER-COPPER SULFATE-SULFURIC ACID TEST FOR DETECTING SUSCEPTIBILITY TO INTERGRANULAR ATTACK IN AUSTENITIC STAINLESS STEELS (7) (8)

29. Scope

29.1 This practice describes the procedure by which the copper-copper sulfate-sulfuric acid test is conducted to determine the susceptibility of austenitic stainless steels to intergranular attack. The presence or absence of intergranular corrosion in this test is not necessarily a measure of the performance of the material in other corrosive media. The test does not provide a basis for predicting resistance to other forms of corrosion, such as general corrosion, pitting, or stress-corrosion cracking.

29.2 The copper-copper sulfate-sulfuric acid test indicates susceptibility to intergranular attack associated with the precipitation of chromium-rich carbides. It does not detect susceptibility associated with sigma phase. This test may be used to evaluate the heat treatment accorded as-received material. It may also be used to evaluate the effectiveness of stabilizing element additions (Cb, Ti, etc.) and reductions in carbon content to aid in resisting intergranular attack.

29.3 All wrought products and weld material of austenitic stainless steels can be evaluated by this test.

30. Rapid Screening Test

30.1 Before testing in the copper-copper sulfate-sulfuric acid test, specimens of certain grades of stainless steel (see Table 6) may be given a rapid screening test in accordance with the procedures given in Practice A (Sections 3 through 7). Preparation, etching, and the classification of etch structures are described therein. The use of etch-structure evaluations in connection with the copper-copper sulfate-sulfuric acid test is specified in Table 6.

30.1.1 Corrosion test specimens having acceptable etch structures in the oxalic acid etch test will be essentially free of intergranular attack in the copper-copper sulfate-sulfuric acid test. Such specimens are acceptable without testing in the copper-copper sulfate-sulfuric acid test. All specimens having nonacceptable etch structures must be tested in the copper-copper sulfate-sulfuric acid test.

31. Summary of Practice

31.1 A suitable sample of an austenitic stainless steel, embedded in copper shot or grindings, is exposed to boiling acidified copper sulfate solution for 24 h. After exposure in the boiling solution, the specimen is bent. Intergranular cracking or crazing is evidence of susceptibility.

32. Apparatus

32.1 A 1-L glass Erlenmeyer flask with a ground 45/50 glass joint and four-bulb Allihn condenser with 45/50 ground glass joint (as in 10.1.1 and 10.1.2 and Fig. 8) are required. A silicone grease is recommended for the ground glass joint.

32.2 *Specimen Supports*—An open glass cradle capable of supporting the specimens and copper shot or grindings in the flask is recommended.

NOTE 22—It may be necessary to embed large specimens, such as from heavy bar stock, in copper shot on the bottom of the test flask. A copper cradle may also be used.

32.3 *Heat Source*—Any gas or electrically heated hot plate may be utilized for heating the

test solution and keeping it boiling throughout the test period.

33. Acidified Copper Sulfate Test Solution

33.1 Dissolve 100 g of copper sulfate ($CuSO_4 \cdot 5H_2O$) in 700 mL of distilled water, add 100 mL of sulfuric acid (H_2SO_4, cp, sp gr 1.84), and dilute to 1000 mL with distilled water.

NOTE 23—The solution will contain approximately 6 weight % of anhydrous $CuSO_4$ and 16 weight % of H_2SO_4.

34. Copper Addition

34.1 Electrolytic grade copper shot or grindings may be used. Shot is preferred for its ease of handling before and after the test.

34.2 A sufficient quantity of copper shot or grindings is to be used to cover all surfaces of the specimen whether it is in a vented glass cradle or embedded in a layer of copper shot on the bottom of the test flask.

34.3 The amount of copper used, assuming an excess of metallic copper is present, is not critical. The effective galvanic coupling between copper and the test specimen may have importance (9).

34.4 The copper shot or grindings may be reused if they are cleaned in warm tap water after each test.

35. Specimen Preparation

35.1 The size of the sample submitted for test and the area from which it is to be taken (end or middle of coil, midway surface and center, etc.) is generally specified in the agreement between the purchaser and the seller. The testing apparatus dictates the final size and shape of the test specimen. The specimen configuration should permit easy entrance and removal through the neck of the test container.

35.1.1 Table 7 may be used as a guide to determine acceptable specimen sizes. There may be restrictions placed on specimen size by the testing apparatus.

35.1.2 Specimens obtained by shearing should have the sheared edges machined or ground off prior to testing. Care should be taken when grinding to avoid overheating or "burning." A "squared" edge is desirable.

35.2 Any scale on the specimens should be removed mechanically unless a particular surface finish is to be evaluated. Chemical removal of scale is permissible when this is the case. Mechanical removal of scale should be accomplished with 120-grit iron-free aluminum oxide abrasive.

35.2.1 Each specimen should be degreased using a cleaning solvent such as acetone, alcohol, ether, or a vapor degreaser prior to being tested.

35.3 All austenitic material in the "as-received" (mill-annealed) condition should be capable of meeting this test.

35.3.1 Specimens of extra low carbon and stabilized grades are tested after sensitizing heat treatments at 1200 to 1250°F (650 to 675°C), which is the range of maximum carbide precipitation. The most commonly used sensitizing treatment is 1 h at 1250°F. Care should be taken to avoid carburizing or nitriding the specimens. The heat treating is best carried out in air or neutral salt.

NOTE 24—The sensitizing treatment (1250°F) is performed to check the effectiveness of stabilized and 0.03 % maximum carbon materials in resisting carbide precipitation, hence, intergranular attack.

36. Test Conditions

36.1 The volume of acidified copper sulfate test solution used should be sufficient to completely immerse the specimens and provide a minimum of 50 mL/in.^{2} (8 mL/cm^2) of specimen surface area.

36.1.1 As many as three specimens can be tested in the same container. It is ideal to have all the specimens in one flask to be of the same grade, but it is not absolutely necessary. The solution volume-to-sample area ratio is to be maintained.

36.1.2 The test specimen(s) should be immersed in ambient test solution which is then brought to a boil and maintained boiling throughout the test period. Begin timing the test period when the solution reaches the boiling point.

NOTE 25—Measures should be taken to minimize bumping of the solution when glass cradles are used to support specimens. A small amount of copper shot (8 to 10 pieces) on the bottom of the flask will conveniently serve this purpose.

36.1.3 The time of the test shall be a minimum of 24 h unless a longer time is agreed upon between the purchaser and the producer. If not 24 h, the test time shall be specified on the test report. Fresh test solution would not be needed if the test were to run 48 or even 72 h. (If any adherent copper remains on the specimen, it may

be removed by a brief immersion in concentrated nitric acid at room temperature.)

NOTE 26—Results in the literature indicate that this test is more sensitive if it is run for longer times (**11**), (**12**).

37. Bend Test

37.1 The test specimen shall be bent through 180° and over a diameter equal to the thickness of the specimen being bent (see Fig. 11). In no case shall the specimen be bent over a smaller radius or through a greater angle than that specified in the product specification. In cases of material having low ductility, such as severely cold worked material, a 180° bend may prove impractical. Determine the maximum angle of bend without causing cracks in such material by bending an untested specimen of the same configuration as the specimen to be tested.

37.1.1 Duplicate specimens shall be obtained from sheet material so that both sides of the rolled samples may be bent through a 180° bend. This will assure detection of intergranular attack resulting from carburization of one surface of sheet material during the final stages of rolling.

NOTE 26—Identify the duplicate specimen in such a manner as to ensure both surfaces of the sheet material being tested are subjected to the tension side of the 180° bends.

37.1.2 Samples machined from round sections or cast material shall have the curved or original surface on the outside of the bend.

37.1.3 The specimens are generally bent by holding in a vise and starting the bend with a hammer. It is generally completed by bringing the two ends together in the vise. Heavy specimens may require bending in a fixture of suitable design. An air or hydraulic press may also be used for bending the specimens.

37.1.4 Tubular products should be flattened in accordance with the flattening test, prescribed in Methods and Definitions A 370.

37.1.5 When agreed upon between the purchaser and the producer, the following shall apply to austenitic stainless steel plates 0.1875 in. (4.76 mm) and thicker:

37.1.5.1 Samples shall be prepared according to Table 7.

37.1.5.2 The radius of bend shall be two times the sample thickness, and the bend axis shall be perpendicular to the direction of rolling.

37.1.5.3 Welds on material 0.1875 in. (4.76 mm) and thicker shall have the above bend radius, and the weld-base metal interface shall be located approximately in the centerline of the bend.

37.1.5.4 Face, root, or side bend tests may be performed, and the type of bend test shall be agreed upon between the purchaser and the producer. The bend radius shall not be less than that required for mechanical testing in the appropriate material specification (for base metal) or in ASME Code Section IX (for welds).

38. Evaluation

38.1 The bent specimen shall be examined under low (5 to 20×) magnification (see Fig. 12). The appearance of fissures or cracks indicates the presence of intergranular attack (see Fig. 13).

38.1.1 When an evaluation is questionable (see Fig. 14), presence or absence of intergranular attack shall be determined by metallographic examination of a longitudinal section of the specimen at a magnification of 100 to 250×.

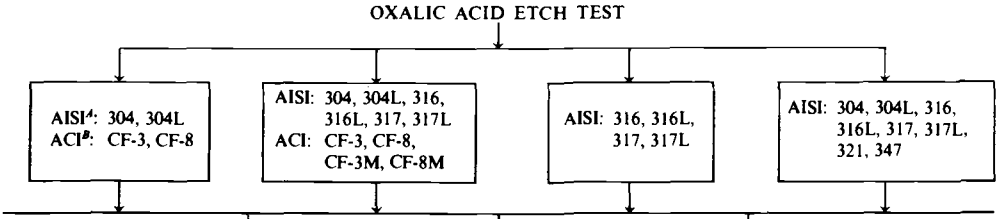
NOTE 27—Cracking that originates at the edge of the specimen should be disregarded. The appearance of deformation lines, wrinkles, or "orange peel" on the surface, without accompanying cracks or fissures, should be disregarded also.

NOTE 28—Cracks suspected as arising through poor ductility may be investigated by bending a similar specimen which was not exposed to the boiling test solution. A visual comparison between these specimens should assist in interpretation.

TABLE 1 Application of Evaluation Tests for Detecting Susceptibility to Intergranular Attack in Austenitic Stainless Steels

NOTE 1—For each corrosion test, the types of susceptibility to intergranular attack detected are given along with the grades of stainless steels in which they may be found. These lists may contain grades of steels in addition to those given in the rectangles. In such cases, the acid corrosion test is applicable, but not the oxalic acid etch test.

NOTE 2—The oxalic acid etch test may be applied to the grades of stainless steels listed in the rectangles when used in connection with the test indicated by the arrow.



Nitric Acid Test[C] (240 h in boiling solution)	Ferric Sulfate-Sulfuric Acid Test (120 h in boiling solution)	Nitric-Hydrofluoric Acid Test (4 h at 70°C)	Copper-Copper Sulfate-Sulfuric Acid Test (24 h in boiling solution)
Chromium carbide in: 304, 304L, CF-3, CF-8 Chromium carbide and sigma phase in:[D] 316, 316L, 317, 317L, 321, 347, CF-3M, CF-8M End-grain in: all grades	Chromium carbide in: 304, 304L, 316, 316L, 317, 317L, CF-3, CF-8 Chromium carbide and sigma phase in: 321, CF-3M, CF-8M[E]	Chromium carbide in: 316, 316L, 317, 317L	Chromium carbide in: 304, 304L, 316, 316L, 317, 317L, 321, 347

[A] AISI: American Iron and Steel Institute designations for austenitic stainless steels.
[B] ACI: Alloy Casting Institute designations.
[C] The nitric acid test may be also applied to AISI 309, 310, 348, and AISI 410, 430, 446, and ACI CN-7M.
[D] Must be tested in nitric acid test when destined for service in nitric acid.
[E] To date, no data have been published on the effect of sigma phase on corrosion of AISI 347 in this test.

TABLE 2 Applicability of Etch Test

	AISI Grade No.	ACI Grade No.
Practice B—Ferric Sulfate-Sulfuric Acid Test	304, 304L, 316, 316L, 317, 317L	CF-3, CF-8, CF-3M, CF-8M
Practice C—Nitric Acid Test	304, 304L	CF-8, CF-3
Practice D—Nitric Hydrofluoric Acid Test	316, 316L, 317, 317L	...
Practice E—Copper-Copper Sulfate-Sulfuric Acid Test	304, 304L, 316, 316L, 317, 317L, 321, 347	...

TABLE 3 Use of Etch Structure Classifications from the Oxalic Acid Etch Test with Ferric Sulfate-Sulfuric Acid Test

NOTE—Grades AISI 321 and 347 cannot be screened because these grades may contain a type of sigma phase which is not visible in the etch structure but which may cause rapid corrosion in the ferric sulfate-sulfuric acid test.

Grade	Acceptable Etch Structures	Nonacceptable Etch Structures[A]
AISI 304	Step, Dual, End Grain, I & II	Ditch
AISI 304L	Step, Dual, End Grain, I & II	Ditch
AISI316	Step, Dual, End Grain, I & II	Ditch
AISI316L	Step, Dual, End Grain, I & II	Ditch
AISI 317	Step, Dual, End Grain, I & II	Ditch
AISI 317L	Step, Dual, End Grain, I & II	Ditch
AISI 321	None	...
ACI CF-3	Step, Dual, Isolated Ferrite Pools	Ditch, Interdendritic Ditches
ACI CF-8	Step, Dual, Isolated Ferrite Pools	Ditch, Interdendritic Ditches
ACI CF-3M	Step, Dual, Isolated Ferrite Pools	Ditch, Interdendritic Ditches
ACI CF-8M	Step, Dual, Isolated Ferrite Pools	Ditch, Interdendritic Ditches

[A] Specimens having these structures must be tested in the ferric sulfate-sulfuric acid test.

TABLE 4 Use of Etch Structure Classification from Oxalic Acid Etch Test with Nitric Acid Test

NOTE—AISI 316, 316L, 317, 317L, 347, and 321 cannot be screened because these steels may contain sigma phase not visible in the etch structure. This may cause rapid intergranular attack in the nitric acid test.

Grade	Acceptable Etch Structures	Nonacceptable Etch Structures[A]
AISI 304	Step, Dual, End Grain I	Ditch, End Grain II
AISI 304L	Step, Dual, End Grain I	Ditch, End Grain II
ACI CF-8	Step, Dual, Isolated Ferrite Pools	Ditch, Interdendritic Ditches
ACI CF-3	Step, Dual, Isolated Ferrite Pools	Ditch, Interdendritic Ditches

[A] Specimens having these structures must be tested in the nitric acid test.

TABLE 5 Use of Etch Structure Classifications from the Oxalic Acid Etch Test with 10 % Nitric-3 % Hydrofluoric Acid Test

Grade	Condition of Heat Treatment	Acceptable Etch Structures	Nonacceptable Etch Structures[A]
AISI 316	As-received[B]	Step, Dual, End Grain I and II	Ditch
AISI 317	As-received[B]	Step, Dual, End Grain I and II	Ditch
AISI 316L	As-received[C]	Step, End Grain I and II	Dual, Ditch
	Sensitized	Step, Dual, End Grain I and II	Ditch
AISI 317L	As-received[C]	Step, End Grain I and II	Dual, Ditch
	Sensitized	Step, Dual, End Grain I and II	Ditch

[A] Specimens having these structures must be tested in 10 % nitric-3 % hydrofluoric acid test.

[B] If the as-received specimen shows a ditch structure and the HNO_3-HF test is to be applied, then a duplicate specimen must be laboratory-annealed in order to produce a base-line specimen having a step structure. The laboratory-annealed specimen (step structure) along with the original as-received specimen (ditch structure) is subjected to the HNO_3-HF test. The final criterion is then the ratio of the corrosion rate for the as-received specimen to the corrosion rate for the laboratory-annealed specimen.

[C] When the oxalic acid etch test is used with the HNO_3-HF test for Types 316L and 317L, the as-received specimens should show a step structure (free from precipitated carbides). If it does not, a portion of the as-received specimen must be laboratory annealed to produce a base-line specimen having a step structure and that sample used for the HNO_3-HF test. This requirement is necessary because the base-line specimen must be completely free of intergranular attack in the HNO_3-HF test in order to obtain an indicative ratio of the corrosion rate of the sensitized specimen to the corrosion rate of the base-line specimen.

TABLE 6 Use of Etch Structure Classifications from the Oxalic Acid Etch Test with the Copper-Copper Sulfate-Sulfuric Acid Test

Grade	Acceptable Etch Structures	Non-acceptable Etch Structures[A]
AISI 304	Step, Dual, End Grain I and II	Ditch
AISI 304L	Step, Dual, End Grain I and II	Ditch
AISI 316	Step, Dual, End Grain I and II	Ditch
AISI 316L	Step, Dual, End Grain I and II	Ditch
AISI 317	Step, Dual, End Grain I and II	Ditch
AISI 317L	Step, Dual, End Grain I and II	Ditch
AISI 321	Step, Dual, End Grain I and II	Ditch
AISI 347	Step, Dual, End Grain I and II	Ditch

[A] Specimens having these structures must be tested in the copper-copper sulfate-sulfuric acid test.

TABLE 7 Sizes of Test Specimens

Type of Material	Size of Test Specimen
Wrought wire or rod:	
Up to ¼ in. in diameter, incl	Full diameter by 3 in. (min) long
Over ¼ in. in diameter	Cylindrical segment ¼ in. thick by 1 in. (max) wide by 3 to 5 in. long[A]
Wrought sheet, strip, plates, or flat rolled products:	
Up to 3/16 in. thick, incl	Full thickness by ⅜ to 1 in. wide by 3 in. (min) long
Over 3/16 in. thick	3/16 to ½ in. thick by ⅜ to 1 in. wide by 3 in. (min) long[B]
Tubing:	
Up to 1½ in. in diameter, incl	Full ring, 1 in. wide[C]
Over 1½ in. in diameter	A circumferential segment 3 in. (min) long cut from a 1-in. wide ring[D]

[A] When bending such specimens, the curved surface shall be on the outside of the bend.

[B] One surface shall be an original surface of the material under test and it shall be on the outside of the bend. Cold-rolled strip or sheets may be tested in the thickness supplied.

[C] Ring sections are not flattened or subjected to any mechanical work before they are subjected to the test solution.

[D] Specimens from welded tubes over 1½ in. in diameter shall be taken with the weld on the axis of the bend.

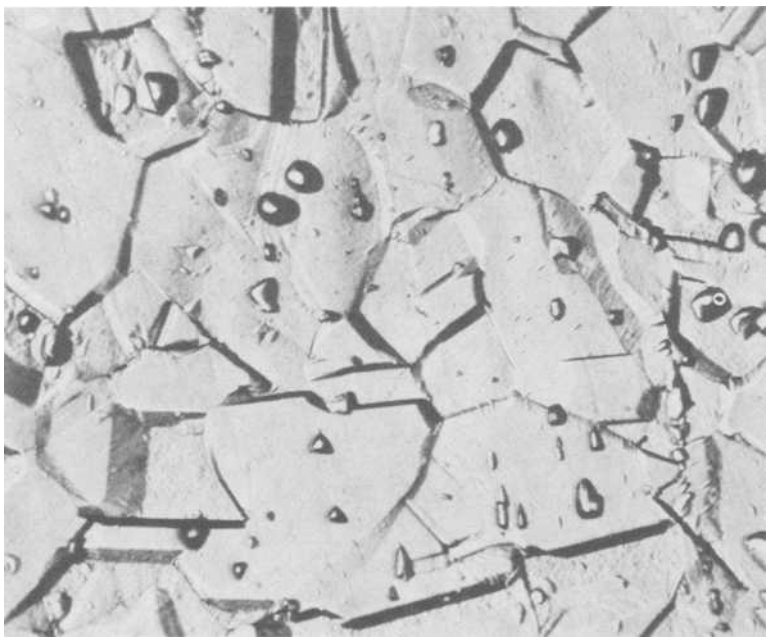


FIG. 1 Step Structure (500×) (Steps between grains, no ditches at grain boundaries)

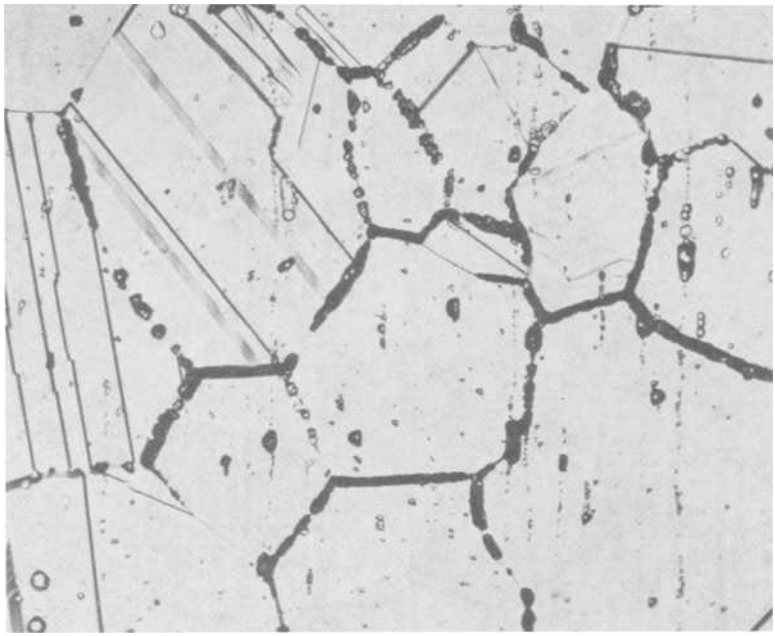


FIG. 2 Dual Structure (250×) (Some ditches at grain boundaries in addition to steps, but no one grain completely surrounded)

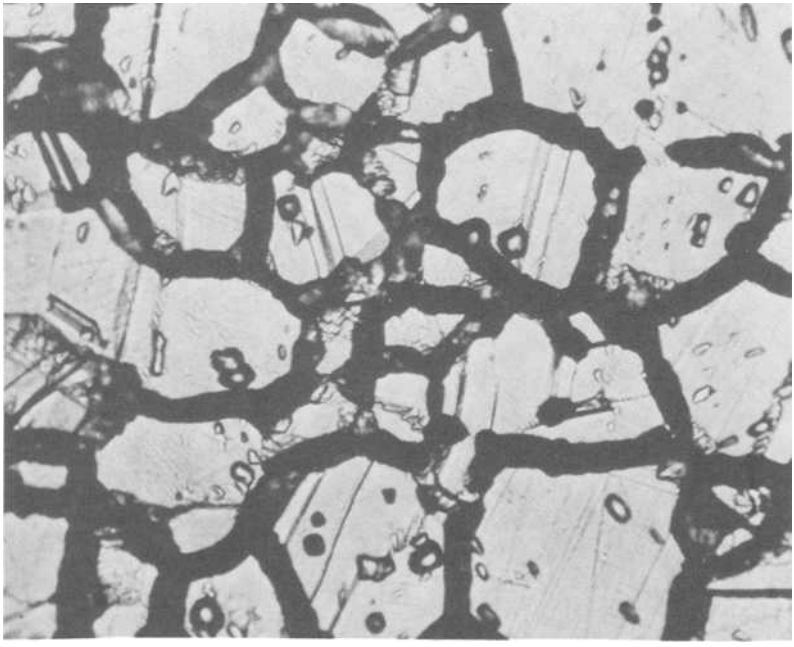


FIG. 3 Ditch Structure (500×) (One or more grains completely surrounded by ditches)

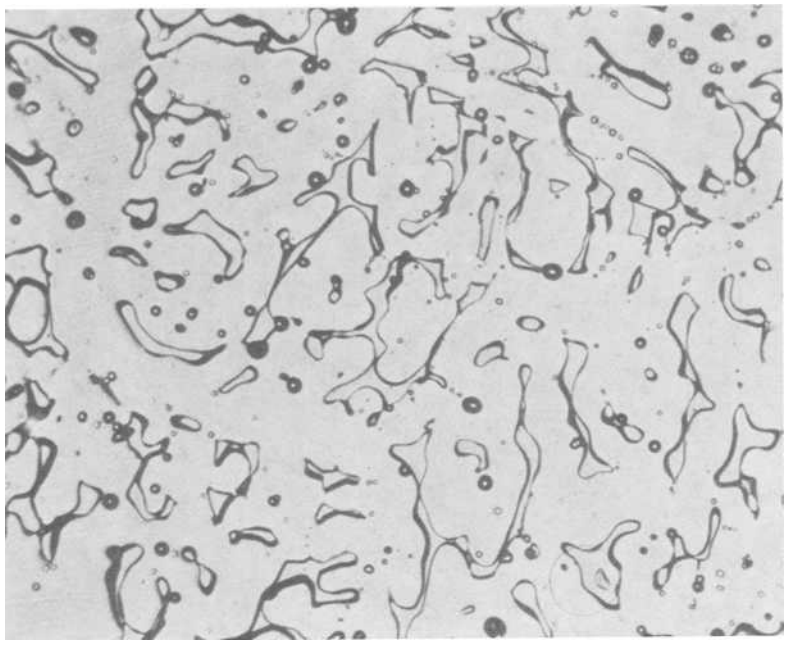


FIG. 4 Isolated Ferrite Pools (250×) (Observed in castings and welds. Steps between austenite matrix and ferrite pools)

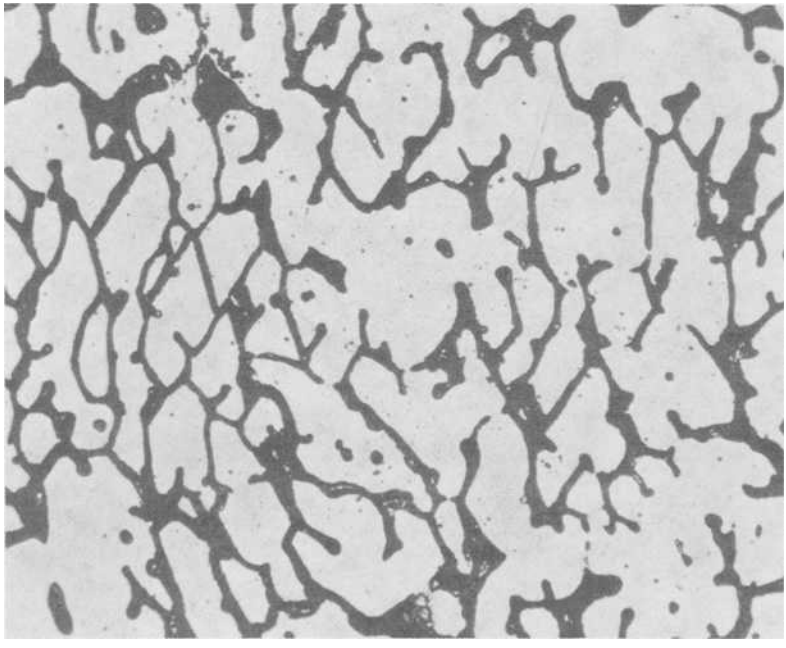
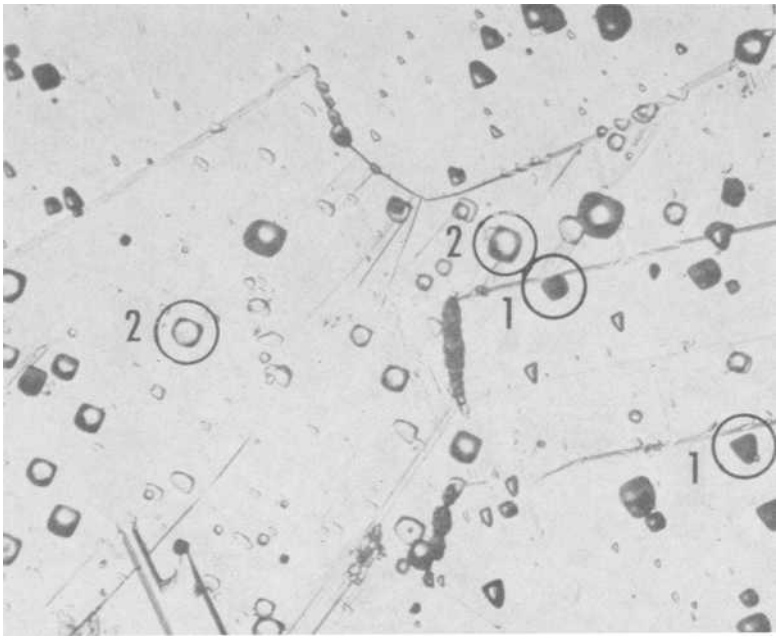
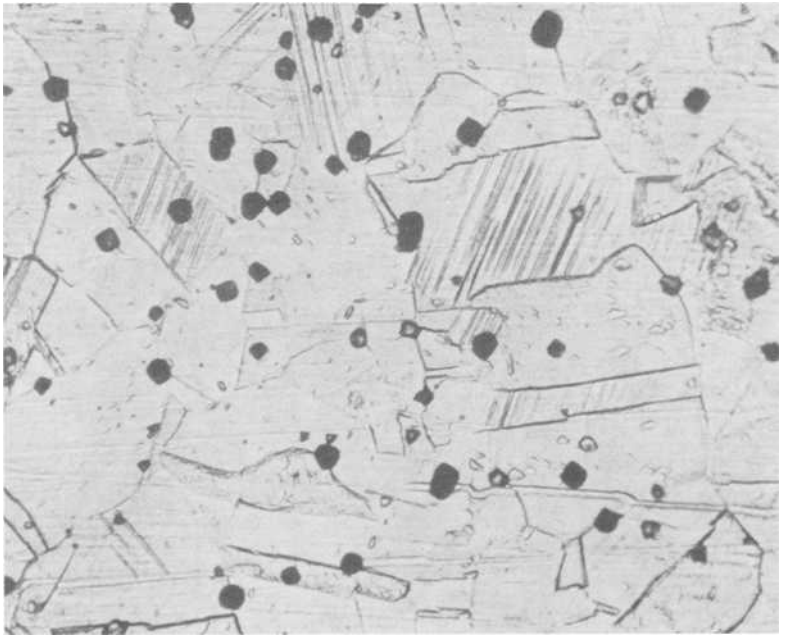


FIG. 5 Interdendritic Ditches (250×) (Observed in castings and welds. Deep interconnected ditches)



To differentiate between the types of pits, use a magnification of 500× and focus in the plane of etched surface. The pits which now appear completely black are end grain pits.

FIG. 6 End Grain Pitting I (500×) (A few deep end grain pits (see 1 in figure) and shallow etch pits (2))



This or a greater concentration of end grain pits at 500× (using standard etching conditions) indicates that the specimen must be tested when screening is for nitric acid test.

FIG. 7 End Grain Pitting II (500×)

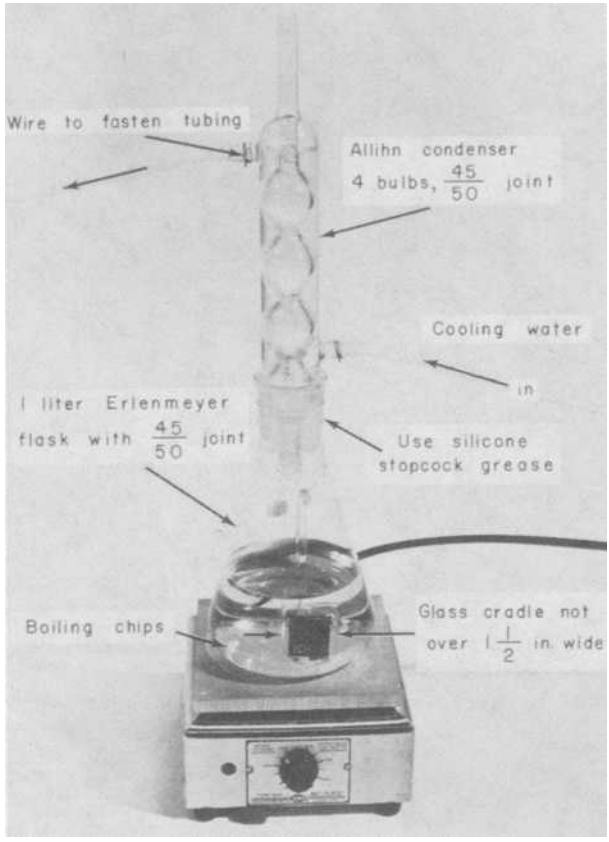


FIG. 8 Apparatus for Ferric Sulfate-Sulfuric Acid Test

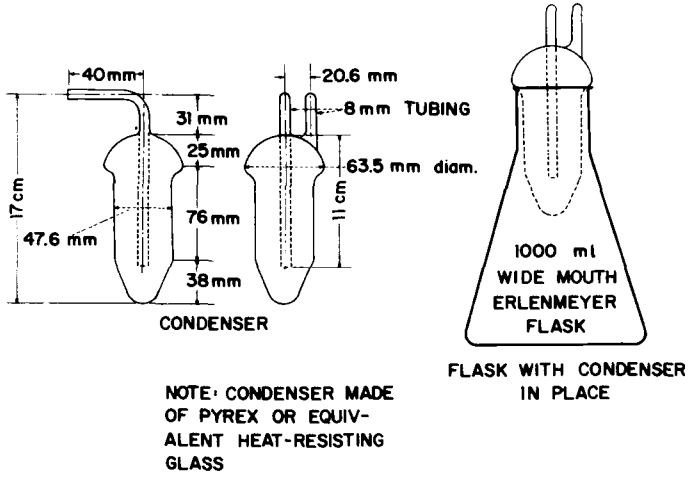


FIG. 9 Flask and Condenser for Nitric Acid Test

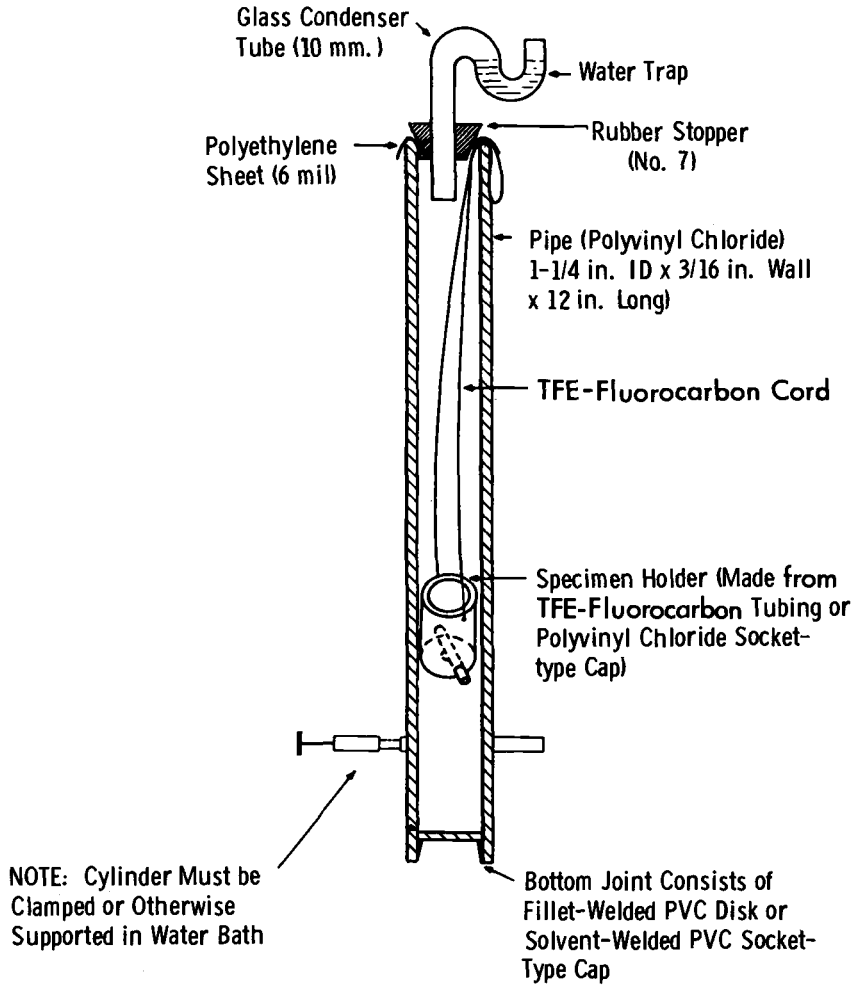


FIG. 10 Apparatus for Nitric-Hydrofluoric Acid Test

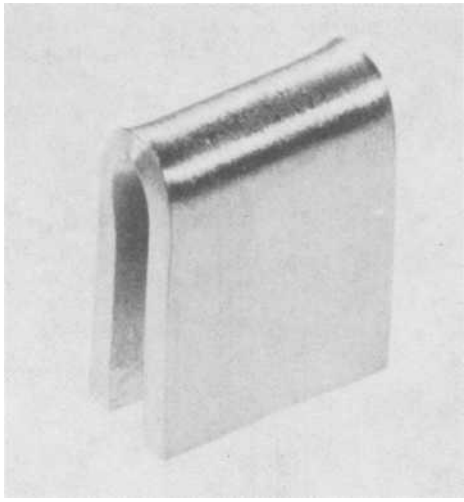


FIG. 11 A Bent Copper-Copper Sulfate-Sulfuric Acid Test Specimen

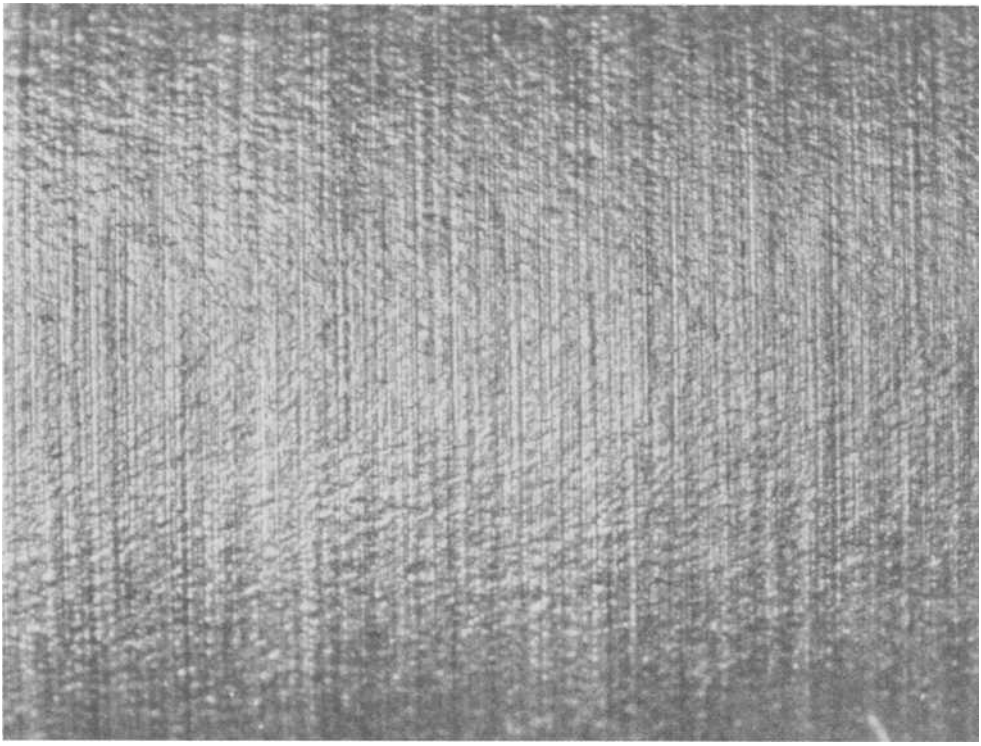


FIG. 12 Passing Test Specimen—View of the Bent Area (20× magnification before reproduction)

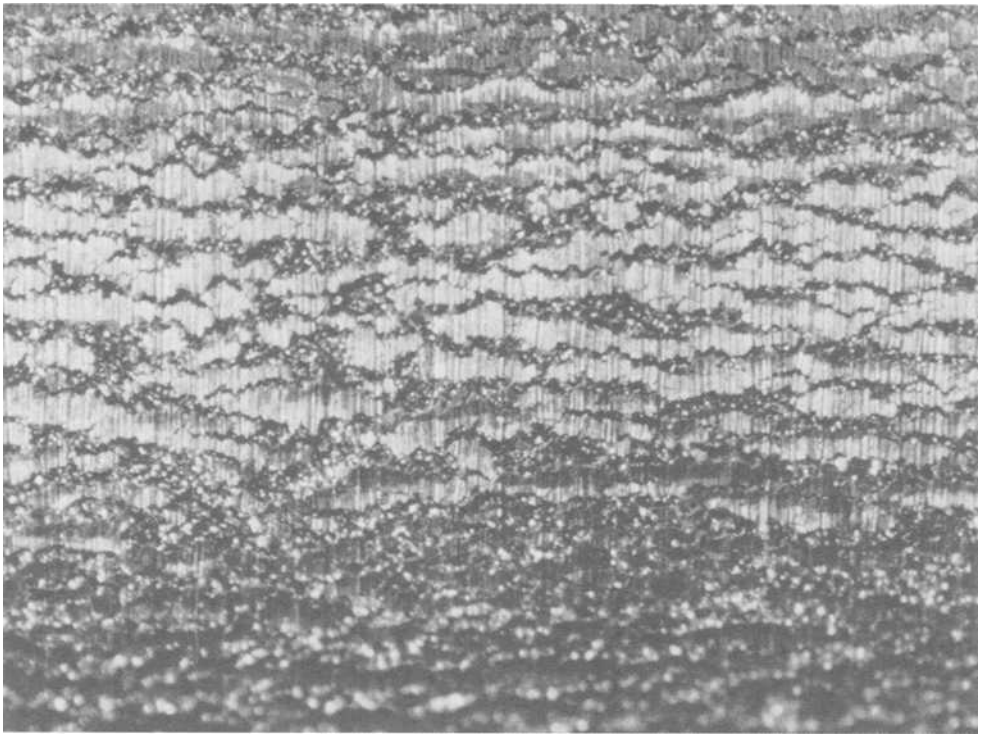


FIG. 13 Failing Test Specimen (Note the many intergranular fissures. Bent area at 20× magnification before reproduction.)

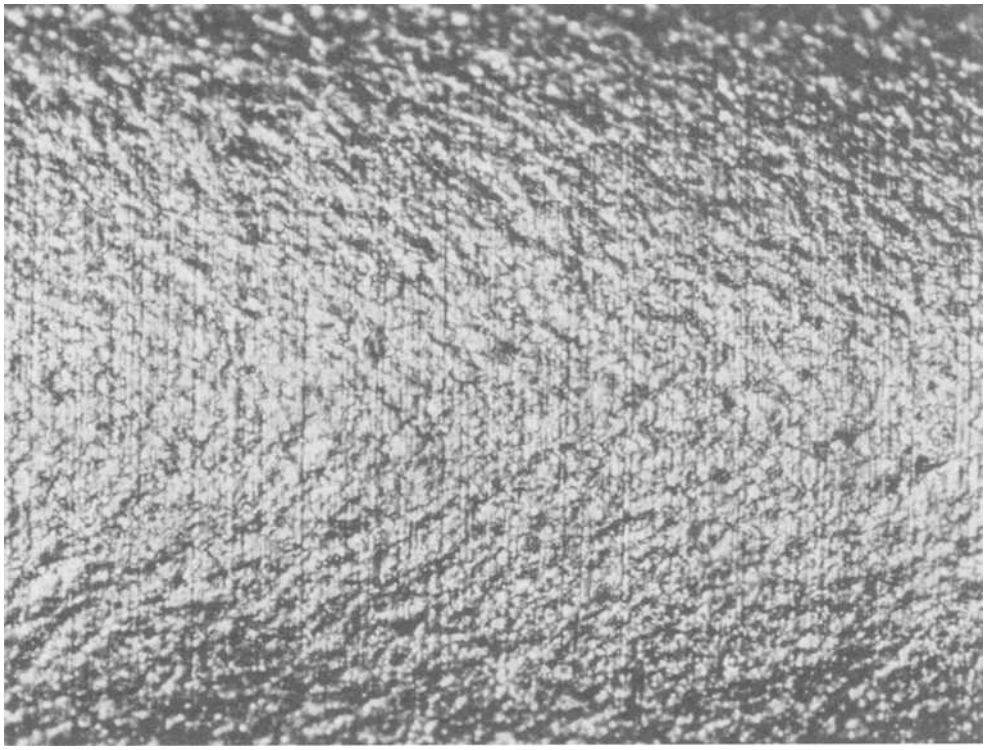


FIG. 14 Doubtful Test Result (Note the traces of intergranular fissures and "orange-peel" surface. Bent area at 20× magnification before reproduction.)

REFERENCES

(1) For original descriptions of the use of etch structure classifications, see Streicher, M. A., "Screening Stainless Steels from the 240-h Nitric Acid Test by Electrolytic Etching in Oxalic Acid," *ASTM Bulletin,* No. 188, February 1953, p. 35; also "Results of Cooperative Testing Program for the Evaluation of the Oxalic Acid Etch Test," *ASTM Bulletin,* No. 195, January 1954, p. 63.

(2) For original description of ferric sulfate-sulfuric acid test, see Streicher, M. A., "Intergranular Corrosion Resistance of Austenitic Stainless Steels: A Ferric Sulfate-Sulfuric Acid Test," *ASTM Bulletin,* No. 229, April 1958, (*STP 95*), pp. 77–86.

(3) For original descriptions of the boiling nitric acid test, see Huey, W. R., "Corrosion Test for Research and Inspection of Alloys," *Transactions, Am. Soc. Steel Treating,* Vol 18, 1930, p. 1126; also, "Report of Subcommittee IV on Methods of Corrosion Testing," *Proceedings,* ASTM, Vol 33, Part I, 1933, p. 187.

(4) For details, see DeLong, W. B., "Testing Multiple Specimens of Stainless Steels in a Modified Boiling Nitric Acid Test Apparatus," *Symposium on Evaluation Tests for Stainless Steels, ASTM STP 93,* ASTM, 1950, p. 211.

(5) See *Industrial and Engineering Chemistry,* Vol 17, 1925, p. 756; also, "A.C.S. Analytical Reagents. Specifications Recommended by Committee on Analytical Reagents." Am. Chem. Soc., March 1941.

(6) For original description of 10 % nitric-3 % hydrofluoric acid test, see Warren, D., "Nitric-Hydrofluoric Acid Evaluation Test for Type 316L Stainless Steel," *ASTM Bulletin,* No. 230, May 1958, pp. 45–56.

(7) The use of copper to accelerate the intergranular corrosion of sensitized austenitic stainless steels in copper sulfate-sulfuric acid was first described by H. J. Rocha in the discussion of a paper by Brauns, E., and Pier, G., *Stahl und Eisen,* Vol 75, 1955, p. 579.

(8) For original evaluation of the copper-copper sulfate-sulfuric acid test, see Scharfstein, L. R., and Eisenbrown, C. M., "An Evaluation of Accelerated Strauss Testing," *ASTM STP* 369, ASTM, 1963, pp. 235–239.

(9) Subtle effects due to variations in copper surface areas, galvanic contact, condenser design, etc., are described by Herbsleb, G., and Schwenk, W., "Untersuchungen zur Einstellung des Redoxpotentials der Strausschen Lösung mit Zusatz von Mettalischem Kupfer," *Corrosion Science,* Vol 7,

1967, pp. 501–511.
(10) Brown, M. H., "Behavior of Austenitic Stainless Steels in Evaluation Tests for the Detection of Susceptibility to Intergranular Corrosion," *Corrosion*, Vol 30, January 1974, pp. 1–12.
(11) Streicher, M. A., "Theory and Application of Evaluation Tests for Detecting Susceptibility to Intergranular Attack in Stainless Steels and Related Alloys-Problems and Opportunities," *Intergranular Corrosion of Stainless Alloys, ASTM STP 656*, R. F. Steigerwald ed, ASTM, 1978, 3–84.
(12) Walker, W. L., "Variatins in the Evaluation of ASTM A262, Practice E, Results (ASTM Subcommittee A01.14 Round Robin)," *Intergranular Corrosion of Stainless Alloys, ASTM STP 656*, R. F. Steigerwald ed; 1978, pp. 146–153.

The American Society for Testing and Materials takes no position respecting the validity of any patent rights asserted in connection with any item mentioned in this standard. Users of this standard are expressly advised that determination of the validity of any such patent rights, and the risk of infringement of such rights, are entirely their own responsibility.

This standard is subject to revision at any time by the responsible technical committee and must be reviewed every five years and if not revised, either reapproved or withdrawn. Your comments are invited either for revision of this standard or for additional standards and should be addressed to ASTM Headquarters. Your comments will receive careful consideration at a meeting of the responsible technical committee, which you may attend. If you feel that your comments have not received a fair hearing you should make your views known to the ASTM Committee on Standards, 1916 Race St., Philadelphia, PA 19103.

Designation: B 117 – 85

Standard Method of SALT SPRAY (FOG) TESTING[1]

This standard is issued under the fixed designation B 117; the number immediately following the designation indicates the year of original adoption or, in the case of revision, the year of last revision. A number in parentheses indicates the year of last reapproval. A superscript epsilon (ε) indicates an editorial change since the last revision or reapproval.

This method has been approved for use by agencies of the Department of Defense to replace Method 811.1 of Federal Test Method Standard No. 151b and for listing in DoD Index of Specifications and Standards.

1. Scope

1.1 This method sets forth the conditions required in salt spray (fog) testing for specification purposes. Suitable apparatus which may be used to obtain these conditions is described in Appendix X1. The method does *not* prescribe the type of test specimen or exposure periods to be used for a specific product, nor the interpretation to be given to the results. It should be noted that there is seldom a direct relation between salt spray (fog) resistance and resistance to corrosion in other media, because the chemistry of the reactions, including the formation of films and their protective value, frequently varies greatly with the precise conditions encountered. Comments on the use of the test in research will be found in Appendix X2.

NOTE 1—This method is applicable to salt spray (fog) testing of ferrous and non-ferrous metals, and is also used to test inorganic and organic coatings, etc., especially where such tests are the basis for material or product specifications.

1.2 The values stated in SI units are to be regarded as standard. The inch-pound units in parentheses are provided for information.

1.3 *This standard may involve hazardous materials, operations, and equipment. This standard does not purport to address all of the safety problems associated with its use. It is the responsibility of whoever uses this standard to consult and establish appropriate safety and health practices and determine the applicability of regulatory limitations prior to use.*

2. Applicable Documents

2.1 *ASTM Standards:*

B 287 Method of Acetic Acid-Salt Spray (Fog) Testing[2]

B 368 Method for Copper-Accelerated Acetic Acid-Salt Spray (Fog) Testing (CASS Test)[3]

D 609 Method for Preparation of Steel Panels for Testing Paint, Varnish, Lacquer, and Related Products[4]

D 1193 Specification for Reagent Water[5]

D 1654 Method for Evaluation of Painted or Coated Specimens Subjected to Corrosive Environments[4]

E 70 Test Method for pH of Aqueous Solutions with the Glass Electrode[6]

3. Apparatus

3.1 The apparatus required for salt spray (fog) testing consists of a fog chamber, a salt solution reservoir, a supply of suitably conditioned compressed air, one or more atomizing nozzles, specimen supports, provision for heating the chamber, and necessary means of control. The size and detailed construction of the apparatus are optional, provided the conditions obtained meet the requirements of this method.

3.2 Drops of solution which accumulate on the ceiling or cover of the chamber shall not be permitted to fall on the specimens being tested.

---

[1] This method is under the jurisdiction of ASTM Committee G-1 on Corrosion of Metals, and is the direct responsibility of Subcommittee G01.05 on Laboratory Corrosion Tests.

Current edition approved April 26, 1985. Published August 1985. Originally published as B 117 – 39 T. Last previous edition B 117 – 64.

[2] *Annual Book of ASTM Standards*, Vols 02.05 and 03.02.

[3] *Annual Book of ASTM Standards*, Vol 02.05.

[4] *Annual Book of ASTM Standards*, Vol 06.01.

[5] *Annual Book of ASTM Standards*, Vol 11.01.

[6] *Annual Book of ASTM Standards*, Vol 15.05.

3.3 Drops of solution which fall from the specimens shall not be returned to the solution reservoir for respraying.

3.4 Material of construction shall be such that it will not affect the corrosiveness of the fog.

4. Test Specimens

4.1 The type and number of test specimens to be used, as well as the criteria for the evaluation of the test results, shall be defined in the specifications covering the material or product being tested or shall be mutually agreed upon by the purchaser and the seller.

5. Preparation of Test Specimens

5.1 Metallic and metallic-coated specimens shall be suitably cleaned. The cleaning method shall be optional depending on the nature of the surface and the contaminants, except that it shall not include the use of abrasives other than a paste of pure magnesium oxide nor of solvents which are corrosive or will deposit either corrosive or protective films. The use of a nitric acid solution for the chemical cleaning, or passivation, of stainless steel specimens is permissible when agreed upon by the purchaser and the seller. Care shall be taken that specimens are not recontaminated after cleaning by excessive or careless handling.

5.2 Specimens for evaluation of paints and other organic coatings shall be prepared in accordance with applicable specification(s) for the material(s) being tested, or as agreed upon by the purchaser and supplier. Otherwise, the test specimens shall consist of steel meeting the requirements of Methods D 609 and shall be cleaned and prepared for coating in accordance with applicable procedure of Method D 609.

5.3 Specimens coated with paints or nonmetallic coatings shall not be cleaned or handled excessively prior to test.

5.4 Whenever it is desired to determine the development of corrosion from an abraded area in the paint or organic coating, a scratch or scribed line shall be made through the coating with a sharp instrument so as to expose the underlying metal before testing. The conditions of making the scratch shall be as defined in Method D 1654, unless otherwise agreed upon between the purchaser and seller.

5.5 Unless otherwise specified, the cut edges of plated, coated, or duplex materials and areas containing identification marks or in contact with the racks or supports shall be protected with a suitable coating stable under the conditions of the test, such as ceresin wax.

NOTE 2—Should it be desirable to cut test specimens from parts or from preplated, painted, or otherwise coated steel sheet, the cut edges shall be protected by coating them with paint, wax, tape, or other effective media so that the development of a galvanic effect between such edges and the adjacent plated or otherwise coated metal surfaces, is prevented.

6. Position of Specimens During Test

6.1 The position of the specimens in the salt spray chamber during the test shall be such that the following conditions are met:

6.1.1 Unless otherwise specified, the specimens shall be supported or suspended between 15 and 30° from the vertical and preferably parallel to the principal direction of horizontal flow of fog through the chamber, based upon the dominant surface being tested.

6.1.2 The specimens shall not contact each other or any metallic material or any material capable of acting as a wick.

6.1.3 Each specimen shall be so placed as to permit free settling of fog on all specimens.

6.1.4 Salt solution from one specimen shall not drip on any other specimen.

NOTE 3—Suitable materials for the construction or coating of racks and supports are glass, rubber, plastic, or suitably coated wood. Bare metal shall not be used. Specimens shall preferably be supported from the bottom or the side. Slotted wooden strips are suitable for the support of flat panels. Suspension from glass hooks or waxed string may be used as long as the specified position of the specimens is obtained, if necessary by means of secondary support at the bottom of the specimens.

7. Salt Solution

7.1 The salt solution shall be prepared by dissolving 5 ± 1 parts by weight of sodium chloride in 95 parts of water conforming to Type IV water in Specification D 1193. The salt used shall be sodium chloride substantially free of nickel and copper and containing on the dry basis not more than 0.1 % of sodium iodide and not more than 0.3 % of total impurities. Some salts contain additives that may act as corrosion inhibitors; careful attention should be given to the chemical content of the salt. Upon agreement between purchaser and seller, analysis may be required and limits established for elements or com-

pounds not specified in the chemical composition given above.

7.2 The pH of the salt solution shall be such that when atomized at 35°C (95°F) the collected solution will be in the pH range of 6.5 to 7.2 (Note 4). Before the solution is atomized it shall be free of suspended solids (Note 5). The pH measurement shall be made electrometrically at 25°C (77°F) using a glass electrode with a saturated potassium chloride bridge in accordance with Method E 70, or colorimetrically using bromothymol blue as indicator, or short range pH paper which reads in 0.2 or 0.3 of a pH unit (Note 6).

NOTE 4—Temperature affects the pH of a salt solution prepared from water saturated with carbon dioxide at room temperature and pH adjustment may be made by the following three methods:

(*1*) When the pH of a salt solution is adjusted at room temperature, and atomized at 35°C (95°F), the pH of the collected solution will be higher than the original solution due to the loss of carbon dioxide at the higher temperature. When the pH of the salt solution is adjusted at room temperature, it is therefore necessary to adjust it below 6.5 so the collected solution after atomizing at 35°C (95°F) will meet the pH limits of 6.5 to 7.2. Take about a 50-mL sample of the salt solution as prepared at room temperature, boil gently for 30 s, cool, and determine the pH. When the pH of the salt solution is adjusted to 6.5 to 7.2 by this procedure, the pH of the atomized and collected solution at 35°C (95°F) will come within this range.

(*2*) Heating the salt solution to boiling and cooling to 95°F for maintaining it at 95°F for approximately 48 h before adjusting the pH produces a solution the pH of which does not materially change when atomized at 35°C (95°F).

(*3*) Heating the water from which the salt solution is prepared to 35°C (95°F) or above, to expel carbon dioxide, and adjusting the pH of the salt solution within the limits of 6.5 to 7.2 produces a solution the pH of which does not materially change when atomized at 35°C (95°F).

NOTE 5—The freshly prepared salt solution may be filtered or decanted before it is placed in the reservoir, or the end of the tube leading from the solution to the atomizer may be covered with a double layer of cheesecloth to prevent plugging of the nozzle.

NOTE 6—The pH can be adjusted by additions of dilute cp hydrochloric acid or cp sodium hydroxide solutions.

8. Air Supply

8.1 The compressed air supply to the nozzle or nozzles for atomizing the salt solution shall be free of oil and dirt (Note 7) and maintained between 69 and 172 kN/m^2 (10 and 25 psi) (Note 8).

NOTE 7—The air supply may be freed from oil and dirt by passing it through a water scrubber or at least 610 mm (2 ft) of suitable cleaning material such as sheep's wool, excelsior, slag wool, or activated[7] alumina.

NOTE 8—Atomizing nozzles may have a "critical pressure" at which an abnormal increase in the corrosiveness of the salt fog occurs. If the "critical pressure" of a nozzle has not been established with certainty, control of fluctuation in the air pressure within plus or minus 0.7 kN/m^2 (0.1 psi), by installation of a suitable pressure regulator valve[8] minimizes the possibility that the nozzle will be operated at its "critical pressure."[9]

9. Conditions in the Salt Spray Chamber

9.1 *Temperature*—The exposure zone of the salt spray chamber shall be maintained at 35 + 1.1 − 1.7°C (95 + 2 − 3°F). The temperature within the exposure zone of the closed cabinet shall be recorded at least twice a day at least 7 h apart (except on Saturdays, Sundays, and holidays when the salt spray test is not interrupted for exposing, rearranging, or removing test specimens or to check and replenish the solution in the reservoir).

NOTE 9—A suitable method to record the temperature is by a continuous recording device or by a thermometer which can be read from outside the closed cabinet. The recorded temperature must be obtained with the salt spray chamber closed to avoid a false low reading because of wet-bulb effect when the chamber is open.

9.2. *Atomization and Quantity of Fog*—At least two clean fog collectors shall be so placed within the exposure zone that no drops of solution from the test specimens or any other source shall be collected. The collectors shall be placed in the proximity of the test specimens, one nearest to any nozzle and the other farthest from all nozzles. The fog shall be such that for each 80 cm^2 of horizontal collecting area there will be collected in each collector from 1.0 to 2.0 mL of solution per hour based on an average run of at least 16 h (Note 10). The sodium chloride concentration of the collected solution shall be 5 ±

[7] Registered U. S. Patent Office.

[8] The Nullmatic pressure regulator (or equivalent) manufactured by Moore Products Co., H and Lycoming Sts., Philadelphia, PA 19124, is suitable for this purpose.

[9] It has been observed that periodic fluctuations in air pressure of ±3.4 kN/m^2 (0.5 psi) resulted in about a twofold increase in the corrosivity of the fog from a nozzle which was being operated at an average pressure of 110 kN/m^2 (16 psi). Controlling the fluctuations within ±0.7 kN/m^2 (0.1 psi), however, avoided any increase in the corrosivity of the salt fog. See Darsey, V. M. and Cavanagh, W. R., "Apparatus and Factors in Salt Fog Testing," *Proceedings*, ASTM, Vol 48, 1948, p. 153.

1 weight % (Note 11). The pH of the collected solution shall be 6.5 to 7.2. The pH measurement shall be made electrometrically or colorimetrically using bromothymol blue as the indicator.

NOTE 10—Suitable collecting devices are glass funnels with the stems inserted through stoppers into graduated cylinders, or crystallizing dishes. Funnels and dishes with a diameter of 10 cm have an area of about 80 cm^2.

NOTE 11—A solution having a specific gravity of 1.0255 to 1.0400 at 25°C (77°F) will meet the concentration requirement. The concentration may also be determined as follows: Dilute 5 mL of the collected solution to 100 mL with distilled water and mix thoroughly; pipet a 10-mL aliquot into an evaporating dish or casserole; add 40 mL of distilled water and 1 mL of 1 % potassium chromate solution (chloride-free) and titrate with 0.1 *N* silver nitrate solution to the first appearance of a permanent red coloration. A solution that requires between 3.4 and 5.1 mL of 0.1 *N* silver nitrate solution will meet the concentration requirements.

9.3 The nozzle or nozzles shall be so directed or baffled that none of the spray can impinge directly on the test specimens.

10. Continuity of Test

10.1 Unless otherwise specified in the specifications covering the material or product being tested, the test shall be continuous for the duration of the entire test period. Continuous operation implies that the chamber be closed and the spray operating continuously except for the short daily interruptions necessary to inspect, rearrange, or remove test specimens; to check and replenish the solution in the reservoir, and to make necessary recordings as described in Section 9. Operations shall be so scheduled that these interfuptions are held to a minimum.

11. Period of Test

11.1 The period of test shall be as designated by the specifications covering the material or product being tested or as mutually agreed upon between the purchaser and the seller.

NOTE 12—Recommended exposure periods are to be as agreed upon by the purchaser and seller, but exposure periods of multiples of 24 h are suggested.

12. Cleaning of Tested Specimens

12.1 Unless otherwise specified in the specifications covering the material or product being tested, specimens shall be treated as follows at the end of the test:

12.1.1 The specimens shall be carefully removed.

12.2 Specimens may be gently washed or dipped in clean running water not warmer than 38°C (100°F) to remove salt deposits from their surface, and then immediately dried. Drying shall be accomplished with a stream of clean, compressed air.

13. Evaluation of Results

13.1 A careful and immediate examination shall be made for the extent of corrosion of the dry test specimens or for other failure as required by the specifications covering the material or product being tested or by agreement between the purchaser and the seller.

14. Records and Reports

14.1 The following information shall be recorded, unless otherwise prescribed in the specifications covering the material or product being tested:

14.1.1 Type of salt and water used in preparing the salt solution,

14.1.2 All readings of temperature within the exposure zone of the chamber,

14.1.3 Daily records of data obtained from each fog-collecting device including the following:

14.1.3.1 Volume of salt solution collected in milliliters per hour per 80 cm^2,

14.1.3.2 Concentration or specific gravity at 35°C (95°F) of solution collected, and

14.1.3.3 pH of collected solution.

14.4 Type of specimen and its dimensions, or number or description of part,

14.5 Method of cleaning specimens before and after testing,

14.6 Method of supporting or suspending article in the salt spray chamber,

14.7 Description of protection used as required in 5.5,

14.8 Exposure period,

14.9 Interruptions in test, cause and length of time, and

14.10 Results of all inspections.

NOTE 13—If any of the atomized salt solution which has not contacted the test specimens is returned to the reservoir, it is advisable to record the concentration or specific gravity of this solution also.

15. Precision and Bias

15.1 The reproducibility of results in the salt spray test is highly dependent on the type of

specimens tested and the evaluation criteria selected as well as the control of the operating variables. In any testing program, sufficient replicates should be included to establish the variability of the results. Substantial variability is often observed when similar specimens are tested in different fog chambers even though the testing conditions are nominally similar and within the ranges specified in this method.

15.2 The salt spray (fog) test is intended to reproduce the corrosion that occurs in atmospheres containing salt spray or splash. It has been widely observed, however, that rankings of different alloys or coating systems, or both, do not necessarily fall in the same order as atmospheric tests in marine or road salt splash environments. This test has been more useful in rating the relative resistance of a specific type of protective coating, for example, hot-dip zinc coatings on steel. Interpretation of the results of this method beyond this purpose must be verified by actual exposure tests.

APPENDIXES

(Nonmandatory Information)

X1. CONSTRUCTION OF APPARATUS

X1.1 Cabinets

X1.1.1 Standard salt spray cabinets are available from several suppliers, but certain pertinent accessories are required before they will function according to this method and provide consistent control for duplication of results.

X1.1.2 The salt spray cabinet consists of the basic chamber, an air-saturator tower, a salt solution reservoir, atomizing nozzles, specimen supports, provisions for heating the chamber, and suitable controls for maintaining the desired temperature.

X1.1.3 Accessories such as a suitable adjustable baffle or central fog tower, automatic level control for the salt reservoir, and automatic level control for the air-saturator tower are pertinent parts of the apparatus.

X1.1.4 The cabinet should be of sufficient size to test adequately the desired number of parts without overcrowding. Small cabinets have been found difficult to control and those of less than 0.43-m^3 (15-ft^3) capacity should be avoided.

X1.1.5 The chamber may be made of inert materials such as plastic, glass, or stone, but most preferably is constructed of metal and lined with impervious plastics, rubber, or epoxy-type materials or equivalent.

X1.2 Temperature Control

X1.2.1 The maintenance of temperature within the salt chamber can be accomplished by several methods. It is generally desirable to control the temperature of the surroundings of the salt spray chamber and to maintain it as stable as possible. This may be accomplished by placing the apparatus in a constant-temperature room, but may also be achieved by surrounding the basic chamber of a jacket containing water or air at a controlled temperature.

X1.2.2 The use of immersion heaters in an internal salt solution reservoir or of heaters within the chamber is detrimental where heat losses are appreciable, because of solution evaporation and radiant heat on the specimens.

X1.2.3 All piping which contacts the salt solution or spray should be of inert materials such as plastic. Vent piping should be of sufficient size so that a minimum of back pressure exists and should be installed so that no solution is trapped. The exposed end of the vent pipe should be shielded from extreme air currents that may cause fluctuation of pressure or vacuum in the cabinet.

X1.3 Spray Nozzles

X1.3.1 Satisfactory nozzles may be made of hard rubber, plastic, or other inert materials. The most commonly used type is made of plastic. Nozzles calibrated for air consumption and solution atomized are available. The operating characteristics of a typical nozzle are given in Table X1.1.

X1.3.2 It can readily be seen that air consumption is relatively stable at the pressures normally used, but a marked reduction in solution sprayed occurs if the level of the solution is allowed to drop appreciably during the test. Thus, the level of the solution in the salt reservoir must be maintained automatically to ensure uniform fog delivery during the test.[10]

X1.3.3 If the nozzle selected does not atomize the salt solution into uniform droplets, it will be necessary to direct the spray at a baffle or wall to pick up the larger drops and prevent them from impinging on the test specimens. Pending a complete understanding of air-pressure effects, etc., it is important that the nozzle selected shall produce the desired condition when operated at the air pressure selected. Nozzles are not necessarily located at one end, but may be placed in the center and can also be directed vertically up through a suitable tower.

---

[10] A suitable device for maintaining the level of liquid in, either the saturator tower, or reservoir of test solution may be designed by a local engineering group, or may be purchased from manufacturers of test cabinets as an accessory.

X1.4 Air for Atomization

X1.4.1 The air used for atomization must be free of grease, oil, and dirt before use by passing through well-maintained filters. Room air may be compressed, heated, humidified, and washed in a water-sealed rotary pump, if the temperature of the water is suitably controlled. Otherwise cleaned air may be introduced into the bottom of a tower filled with water, through a porous stone or multiple nozzles. The level of the water must be maintained automatically to ensure adequate humidification. A chamber operated according to this method and Appendix will have a relative humidity between 95 and 98 %. Since salt solutions from 2 to 6 % will give the same results (though for uniformity the limits are set at 4 to 6 %), it is preferable to saturate the air at temperatures well above the chamber temperature as insurance of a wet fog. Table X1.2 shows the temperatures, at different pressures, that are required to offset the cooling effect of expansion to atmospheric pressure.

X1.4.2 Experience has shown that most uniform spray chamber atmospheres are obtained by increasing the atomizing air temperature sufficiently to offset heat losses, except those that can be replaced otherwise at very low-temperature gradients.

X1.5 Types of Construction

X1.5.1 A modern laboratory cabinet is shown in Fig. X1.1. Walk-in chambers are not usually constructed with a sloping ceiling due to their size and location. Suitably located and directed spray nozzles avoid ceiling accumulation and drip. Nozzles may be located at the ceiling, or 0.91 m (3 ft) from the floor directed upward at 30 to 60° over a passageway. The number of nozzles depends on type and capacity and is related to the area of the test space. A 11 to 19-dm^3 (3 to 5-gal) reservoir is required within the chamber, with the level controlled. The major features of a walk-in type cabinet, which differs significantly from the laboratory type, are illustrated in Fig. X1.2. Construction of a plastic nozzle, such as is furnished by several suppliers, is shown in Fig. X1.3.

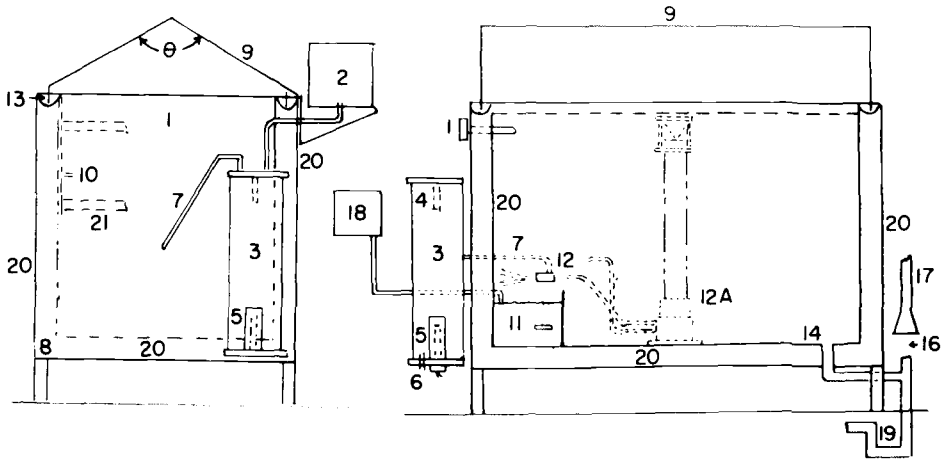
TABLE X1.1 Operating Characteristics of Typical Spray Nozzle

Siphon Height, in.	Air Flow, L/min				Solution Consumption, mL/h			
	Air Pressure, psi				Air Pressure, psi			
	5	10	15	20	5	10	15	20
4	19	26.5	31.5	36	2100	3840	4584	5256
8	19	26.5	31.5	36	636	2760	3720	4320
12	19	26.5	31.5	36	0	1380	3000	3710
16	19	26.6	31.5	36	0	780	2124	2904

Siphon Height cm	Air Flow, dm^3/min				Solution Consumption, cm^3/h			
	Air Pressure, kPa				Air Pressure, kPa			
	34	69	103	138	34	69	103	138
10	19	26.5	31.5	36	2100	3840	4584	5256
20	19	26.5	31.5	36	636	2760	3720	4320
30	19	26.5	31.5	36	0	1380	3000	3710
40	19	26.6	31.5	36	0	780	2124	2904

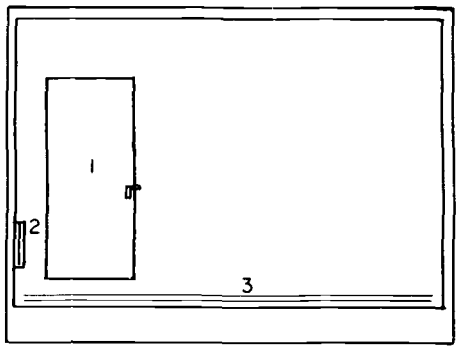
TABLE X1.2 Temperature and Pressure Requirements for Operation of Test at 95°F

	Air Pressure, psi			
	12	14	16	18
Temperature, °F	114	117	119	121
	Air Pressure, kPa			
	83	96	110	124
Temperature, °C	46	47	48	49



θ—Angle of lid, 90 to 125°
1—Thermometer and thermostat for controlling heater (Item No. 8) in base
2—Automatic water levelling device
3—Humidifying tower
4—Automatic temperature regulator for controlling heater (Item No. 5)
5—Immersion heater, non-rusting
6—Air inlet, multiple openings
7—Air tube to spray nozzle
8—Strip heater in base
9—Hinged top, hydraulically opeated, or counterbalanced
10—Brackets for rods supporting specimens, or test table
11—Internal reservoir
12—Spray nozzle above reservoir, suitably designed, located, and baffled
12A—Spray nozzle housed in dispersion tower located preferably in center of cabinet
13—Water Seal
14—Combination drain and exhaust. Exhaust at opposite side of test space from spray nozzle (Item 12), but preferably in combination with drain, waste trap, and forced draft waste pipe (Items 16, 17, and 19).
16—Complete separation between forced draft waste pipe (Item 17) and combination drain and exhaust (Items 14 and 19) to avoid undesirable suction or back pressure.
17—Forced draft waste pipe.
18—Automatic levelling device for reservoir
19—Waste trap
20—Air space or water jacket
21—Test table or rack, well below roof area

FIG. X1.1 Typical Salt Spray Cabinet.



NOTE—The controls are the same, in general as for the laboratory cabinet (Fig. X1.1), but are sized to care for the larger cube. The chamber has the following features:

(*1*) Heavy insulation,

(*2*) Refrigeration door with drip rail, or pressure door with drip rail, inward-sloping sill,

(*3*) Low-temperature auxiliary heater, and

(*4*) Duck boards on floor, with floor sloped to combination drain and air exhaust.

FIG. X1.2 Walk-in Chamber, 1.5 by 2.4 m (5 by 8 ft) and Upward in Over-all Size

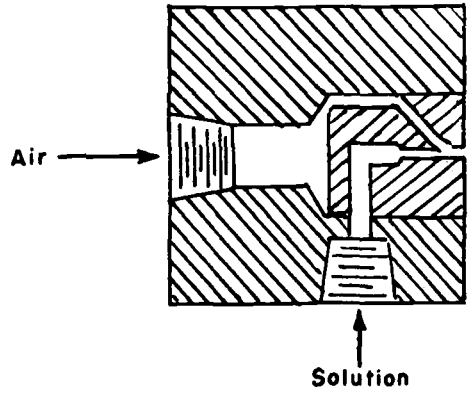


FIG. X1.3 Typical Spray Nozzle

X2. USE OF THE SALT SPRAY (FOG) TEST IN RESEARCH

X2.1 The detailed requirements of this method are primarily for quality acceptance and should not be construed as the optimum conditions for research studies. The test has been used to a considerable extent for the purpose of comparing different materials or finishes with an acceptable standard. The recent elimination of many cabinet variables and the improvement in controls have made the three ASTM Salt Spray Tests: Method B 117, B 287, and B 368, into useful tools for many industrial and military production and qualification programs.

X2.2 The test has been used to a considerable extent for the purpose of comparing different materials or finishes. It should be noted that there is seldom a direct relation between salt spray (fog) resistance and resistance to corrosion in other media, because the chemistry of the reactions, including the formation of films and their protective value, frequently varies greatly with the precise conditions encountered. Informed personnel are aware of the erratic composition of basic alloys, the possibility of wide variations in quality and thickness of plated items produced on the same racks at the same time, and the consequent need for a mathematical determination of the number of specimens required to constitute an adequate sample for test purposes. In this connection it is well to point out that Method B 117 is not applicable to the study or testing of decorative chromium plate (nickel-chromium or copper-nickel-chromium) on steel or on zinc-base die castings or of cadmium plate on steel. For this purpose Methods B 287 and B 368 are available, which are also considered by some to be superior for comparison of chemically-treated aluminum (chromated, phosphated, or anodized), although final conclusions regarding the validity of test results related to service experience have not been reached. Method B 117 is considered to be most useful in estimating the relative behavior of closely related materials in marine atmospheres, since it simulates the basic conditions with some acceleration due to either wetness or temperature or both.

X2.3 When a test is used for research, it may prove advantageous to operate with a different solution composition or concentration or at a different temperature. In all cases, however, it is desirable to control the temperature and humidity in the manner specified, and to make certain that the composition of the settled fog and that of the solution in the reservoir are substantially the same. Where differences develop, it is necessary to control conditions so that the characteristics of the settled fog meet the specified requirements for the atmosphere.

X2.4 Material specifications should always be written in terms of the standard requirements of the appropriate salt spray method, thereby making it possible to test a variety of materials from different sources in the same equipment.

The American Society for Testing and Materials takes no position respecting the validity of any patent rights asserted in connection with any item mentioned in this standard. Users of this standard are expressly advised that determination of the validity of any such patent rights, and the risk of infringement of such rights, are entirely their own responsibility.

This standard is subject to revision at any time by the responsible technical committee and must be reviewed every five years and if not revised, either reapproved or withdrawn. Your comments are invited either for revision of this standard or for additional standards and should be addressed to ASTM Headquarters. Your comments will receive careful consideration at a meeting of the responsible technical committee, which you may attend. If you feel that your comments have not received a fair hearing you should make your views known to the ASTM Committee on Standards, 1916 Race St., Philadelphia, PA 19103.

Designation: G 1 - 81

Standard Practice for PREPARING, CLEANING, AND EVALUATING CORROSION TEST SPECIMENS[1]

This standard is issued under the fixed designation G 1; the number immediately following the designation indicates the year of original adoption or, in the case of revision, the year of last revision. A number in parentheses indicates the year of last reapproval. A superscript epsilon (ε) indicates an editorial change since the last revision or reapproval.

1. Scope

1.1 This practice gives suggested procedures for preparing bare, solid metal specimens for laboratory corrosion tests, for removing corrosion products after the test has been completed, and for evaluating the corrosion damage that has occurred. Emphasis is placed on procedures related to the evaluation of corrosion by mass-loss and pitting measurements.

NOTE 1: **Caution**—In many cases the corrosion product on the reactive metals titanium and zirconium is a hard and tightly bonded oxide that defies removal by chemical or ordinary mechanical means. In many such cases, corrosion rates are established by weight gain rather than weight loss.

2. Applicable Documents

2.1 *ASTM Standards:*

A 262 Practices for Detecting Susceptibility to Intergranular Attack in Austenitic Stainless Steels[2]

D 1384 Method for Corrosion Test for Engine Coolants in Glassware[3]

G 31 Recommended Practice for Laboratory Immersion Corrosion Testing of Metals[4]

G 46 Recommended Practice for Examination and Evaluation of Pitting Corrosion[4]

3. Significance and Use

3.1 A significance and use statement is not applicable to this practice.

4. Sampling

4.1 The bulk sampling of products is outside the scope of this practice.

5. Methods for Preparing Specimens for Test

5.1 *Surface Condition:*

5.1.1 For laboratory corrosion tests that simulate exposure to service environments, a commercial surface, closely resembling the one that would be used in service, will yield the most significant results.

5.1.2 For more searching tests of either the metal or the environment, standard surface finishes may be preferred. A suitable procedure might be:

5.1.2.1 Degrease in an organic solvent or hot alkaline cleaner.

NOTE 2—Hot alkalies and chlorinated solvents may attack some metals.

NOTE 3—Ultrasonic cleaning may be beneficial in both pre-test and post-test cleaning procedures.

5.1.2.2 Pickle in an appropriate solution (in some cases the chemical cleaners described in Section 7 will suffice) if oxides or tarnish are present.

5.1.2.3 Abrade with a slurry of an appropriate abrasive or with an abrasive paper (see Practices A 262, D 1384, and G 31). The edges as well as the faces of the specimens should be abraded to remove burrs.

5.1.2.4 Rinse thoroughly and dry.

5.2 *Metallurgical Condition*—When speci-

---

[1] This practice is under the jurisdiction of ASTM Committee G-1 on Corrosion of Metals and is the direct responsibility of Subcommittee G01.05 on Laboratory Corrosion Tests.

Current edition approved April 24, 1981. Published July 1981. Originally published as G 1 - 67. Last previous edition G 1 - 72 (1979).

[2] *Annual Book of ASTM Standards*, Vols 01.03 and 03.02.

[3] *Annual Book of ASTM Standards*, Vol 15.05.

[4] *Annual Book of ASTM Standards*, Vol 03.02.

men preparation changes the metallurgical condition of the metal, other methods should be chosen or the metallurgical condition must be corrected by subsequent treatment. For example, shearing a specimen to size will cold work and may possibly fracture the edges. Edges should be machined or the specimen annealed.

5.3 The clean, dry specimens should be measured and weighed. Dimensions determined to the third significant figure and mass determined to the fifth significant figure are suggested.

6. Method for Electrolytic Cleaning After Testing

6.1 Electrolytic cleaning is a satisfactory method for many common metals.

6.1.1 The following method is typical; after scrubbing to remove loosely attached corrosion products, electrolyze the specimen as follows:

Sulfuric acid (H_2SO_4, sp gr 1.84)	28 ml
Organic inhibitor	2 ml (see Note 4)
Water to make	1 litre
Temperature	75 C (167 F)
Time	3 min
Anode	carbon or lead (see Note 5)
Cathode	test specimen
Current density	20 A/dm^2

NOTE 4—Instead of using 0.2 volume percent of any proprietary inhibitor, about 0.5 g/litre of such inhibitors as diorthotolyl thiourea, quinoline ethiodide, or betanaphthol quinoline may be used.

NOTE 5—If lead anodes are used, lead may deposit on the specimen and cause an error in the mass loss. If the specimen is resistant to nitric acid, the lead may be removed by a flash dip in 1 + 1 nitric acid. Except for this possible source of error, lead is preferred as an anode as it gives more efficient corrosion-product removal.

6.2 It should be noted that this electrolytic treatment may result in the redeposition of metal, such as copper, from reducible corrosion products and, thus, lower the apparent mass loss.

7. Methods for Chemical Cleaning After Testing

NOTE 6: **Caution**—These methods may be hazardous to personnel. They should not be carried out by the uninitiated or without professional supervision.

7.1 *Copper and Nickel Alloys*—Dip in:

Hydrochloric acid (HCl, sp gr 1.19)	500 ml
Water to make	1 litre
Temperature	room
Time	1 to 3 min

NOTE 7—To avoid metal loss during cleaning, deaerate solution with purified nitrogen before cleaning specimens.

7.2 *Aluminum Alloys*—The following methods are suitable:

7.2.1 Dip in:

Chromic acid (CrO_3	20 g
Phosphoric acid (H_3PO_4 sp gr 1.69)	50 ml
Water to make	1 litre
Temperature	80°C (176°F)
Time	5 to 10 min, or until clean

7.2.1.1 If a film remains, dip in:

Nitric acid (HNO_3, sp gr 1.42)	...
Temperature	room
Time	1 min

7.2.2 Dip in:

Nitric acid (HNO_3, sp gr 1.42)	...
Temperature	room
Time	15 min, or until clean

NOTE 8: **Caution**—Remove extraneous deposits as well as bulky corrosion products before the HNO_3 treatment to avoid violent reactions that may result in attack of the aluminum alloy (see 7.9).

7.3 *Tin Alloys*—Dip in:

Trisodium phosphate (Na_3PO_4)	150 g
Water to make	1 litre
Temperature	boiling
Time	10 min

7.4 *Lead Alloys*—Suitable methods include:

7.4.1 Preferably, use the electrolytic cleaning procedure of Section 6.

7.4.2 Dip in:

Acetic acid (99.5 percent)	10 ml
Water to make	1 litre
Temperature	boiling
Time	5 min

7.4.3 Alternatively dip in:

Ammonium acetate	50 g
Water to make	1 litre
Temperature	hot
Time	5 min

7.4.3.1 This removes lead oxide (PbO) and lead sulfate ($PbSO_4$).

7.5 *Zinc*—The following methods are suitable:

7.5.1 Dip in:

Ammonium hydroxide (NH_4OH, sp gr 0.90)	150 ml
Water to make	1 litre
Temperature	room
Time	several minutes

7.5.2 Then dip in:

Chromic acid (CrO_3)	50 g
Silver nitrate ($AgNO_3$)	10 g
Water to make	1 litre
Temperature	boiling
Time	15 to 20 s

NOTE 9—In making up the chromic acid solution, it is advisable to dissolve the silver nitrate separately and add it to the boiling chromic acid to prevent excessive crystallization of the silver chromate. The chromic acid must be free from sulfate to avoid attack on the zinc.

7.5.2 Dip in:

Hydriodic acid (HI, sp gr 1.5)	85 ml
Water to make	1 litre
Temperature	room
Time	15 s

7.5.2.1 This procedure dissolves a little zinc and corrections must be made as noted in 8.1.

7.5.6 *Magnesium Alloys*—Dip in:

Chromic acid (CrO_3)	150 g
Silver chromate (Ag_2CrO_4)	10 g
Water to make	1 litre
Temperature	boiling
Time	1 min

7.7 *Iron and Steel*—The following methods are suitable:

7.7.1 The hot sodium hydride method is excellent for cleaning iron and steel both from the point of view of ease of removal of corrosion products and minimum attack on the metal.[5] Because of the hazard involved and the somewhat more sophisticated equipment required, other methods may be preferred. An alternative choice is electrolytic cleaning (see Section 6).

7.7.2 Dip in Clarke's solution:

Hydrochloric acid (HCl, sp gr 1.19)	1 litre
Antimony trioxide (Sb_2O_3)	20 g
Stannous chloride ($SnCl_2$)	50 g
Temperature	room
Time	up to 25 min

7.7.2.1 Solution should be vigorously stirred or the specimen should be rubbed with a nonabrasive implement of wood or rubber.

7.7.3 Dip in:

Sulfuric acid (H_2SO_4, sp gr 1.84)	100 ml
Organic inhibitor	1.5 ml
Water to make	1 litre
Temperature	50 C (120 F)
Temperature	70 C (158 F)
Time	10 to 60 min

7.8 *Stainless Steels:*

7.8.1 Methods in 7.7.1 are also applicable.

7.8.2 Dip in:

Nitric acid (HNO_3, sp gr 1.42)	100 ml
Water to make	1 litre
Temperature	60 C (140 F)
Time	20 min

7.8.3 Alternatively dip in:

Ammonium citrate	150 g
Water to make	1 litre

7.9 Mechanical cleaning in some cases may be used in place of, or as supplement to, chemical treatments to remove bulky adherent deposits. A relatively soft scraper or stiff fiber bristle brush should be used to avoid scratching or removal of metal from the surface of the specimen. However, this method may not remove all the products from pits.

NOTE 10—Such vigorous mechanical cleaning is applicable when mass losses are large and hence errors in mass loss will produce only small errors in corrosion rates. Blank corrections will be difficult to apply.

7.10 In all the foregoing methods, specimens should be rinsed following cleaning and scrubbed lightly with a bristle brush under running water. The cleaning dip may be repeated as necessary. After the final rinse, specimens should be dried and weighed.

8. Calculation of Corrosion Rate

8.1 Whatever cleaning method is used, the possibility of removal of solid metal is present; this results in error in the determination of the corrosion rate. To check this, one or more cleaned and weighed specimens may be recleaned by the same method and reweighed. Loss due to this second weighing may be used as an approximate correction to the first one (see Appendix X2 for a more exact method).

8.2 The initial total surface area of the specimen (making allowances for the change in area due to mounting holes) and the mass lost during the test are determined. The average corrosion rate may then be obtained as follows:

$$\text{Corrosion rate} = (K \times W)/(A \times T \times D)$$

where:

K = a constant (see 8.2.1),
T = time of exposure in hours to the nearest 0.01 h,
A = area in cm^2 to the nearest 0.01 cm^2,
W = mass loss in g, to nearest 1 mg, and
D = density in g/cm^3 (see Appendix X1).

8.2.1 Many different units are used to express corrosion rates. Using the above units for T, A, W, and D the corrosion rate can be

[5] *Technical Information Bulletin SP29–370* "DuPont Sodium Hydride Descaling Process Operating Instructions," available from E. I. duPont de Nemours & Co. (Inc.), Electrochemicals Dept., Wilmington, Del. 19898.

calculated in a variety of units with the following appropriate value of K:

Corrosion Rate Units Desired	Constant (K) in Corrosion Rate Equation
mils per year (mpy)	3.45×10^6
inches per year (ipy)	3.45×10^3
inches per month (ipm)	2.87×10^2
millimetres per year (mm/y)	8.76×10^4
micrometres per year (μm/y)	8.76×10^7
picometres per second (pm/s)	2.78×10^6
grams per square metre per hour (g/$m^2 \cdot h$)	$1.00 \times 10^4 \times D^A$
milligrams per square decimetre per day (mdd)	$2.40 \times 10^6 \times D^A$
micrograms per square metre per second ($\mu g/m^2 \cdot s$)	$2.78 \times 10^6 \times D^A$

[A] Density is not needed to calculate the corrosion rate in these units; the density in the constant K cancels out the density in the corrosion rate equation.

NOTE 11—If desired, these constants may also be used to convert corrosion rates from one set of units to another. To convert a corrosion rate in units X to a rate in units Y, multiple by K_Y/K_X for example:

$$15 \text{ mpy} = 15 \times (2.78 \times 10^6)/(3.45 \times 10^6) \text{ pm/s}$$

8.3 Corrosion rates calculated from mass losses can be misleading when deterioration is highly localized, as in pitting or crevice corrosion. If corrosion is in the form of pitting, it may be measured with a depth gage or micrometer calipers with pointed anvils (see Recommended Practice G 46). Microscopical methods will determine pit depth by focusing from top to bottom of the pit, when it is viewed from above (using a calibrated focusing knob) or by examining a section that has been mounted and metallographically polished. The pitting factor is the ratio of the deepest metal penetration to the average metal penetration (as measured by mass loss).

8.4 Other methods of assessing corrosion damage are:

8.4.1 *Appearance*—The degradation of appearance by rusting, tarnishing, or oxidation.

8.4.2 *Mechanical Properties*—An apparent loss in tensile strength will result if the cross-sectional area of the specimen (measured before exposure to the corrosive environment) is reduced by corrosion. Loss in tensile strength will result if a metasomatic change, such as parting has taken place. Loss in tensile strength and elongation will result from localized attack, such as cracking.

8.4.3 *Electrical Properties*—Loss in apparent conductivity will result from cracking or pitting.

8.4.4 *Microscopical Examination*—Parting, exfoliation, cracking, or intergranular attack may be measured by metallographic examination of suitably prepared sections.

9. Report

9.1 The report should include the compositions and sizes of specimens, their metallurgical conditions, surface preparations, and post-corrosion cleaning methods, as well as measures of corrosion damage such as corrosion rates (calculated from mass losses), maximum depths of pitting, or losses in mechanical properties.

10. Precision and Accuracy

10.1 A precision and accuracy statement cannot be made for this practice.

APPENDIXES

X1. DENSITIES FOR A VARIETY OF METALS AND ALLOYS

Aluminum Alloys	Density g/cm^3
1100, 3004	2.72
1199, 5005, 5357, 6061, 6062, 6070, 6101	2.70
2024	2.77
2219, 7178	2.81
3003, 7079	2.74
5050	2.69
5052, 5454	2.68
5083, 5086, 5154, 5456	2.66
7075	2.80

Copper Alloys	Density g/cm^3
Copper	8.94
Brasses:	
Commercial bronze 220	8.80
Red brass 230	8.75
Cartridge brass 260	8.52
Muntz metal 280	8.39
Admiralty 442, 443, 444, 445	8.52
Aluminum brass 687	8.33

Aluminum Alloys	Density g/cm³
Bronzes:	
Aluminum bronze, 5 percent 608	8.16
Aluminum bronze, 8 percent 612	7.78
Composition M	8.45
Composition G	8.77
Phosphor bronze, 5 percent 510	8.86
Phosphor bronze, 10 percent 524	8.77
85-5-5-5	8.80
Silicon bronze 655	8.52
Copper nickels 706, 710, 715	8.94
Nickel silver 752	8.75
Ferrous Metals	
Gray cast iron	7.20
Carbon steel	7.86
Silicon iron	7.00
Low alloy steels	7.85
Stainless steels:	
Types 201, 202, 302, 304, 304L, 321	7.94
Types 309, 310, 311, 316, 316L, 317, 329, 330	7.98
Type 347	8.03
Type 410	7.70
Type 430	7.72
Type 446	7.65
Type 502	7.82
Durimet 20	8.02
Carpenter Stainless No. 20 Cb 3	8.05
Lead	
Antimonial	10.80
Chemical	11.33
Nickel Alloys	
Nickel 200	8.89
Monel Alloy 400	8.84
Inconel Alloy 600	8.51
Incoloy Alloy 825	8.14
Illium G	8.31
Hastelloy B	9.24
Hastelloy C	8.93
Hastelloy G	8.27
Other Metals	
Magnesium	1.74
Molybdenum	10.22
Platinum	21.45
Silver	10.49
Tantalum	16.60
Tin	7.30
Titanium	4.54
Zinc	7.13
Zirconium	6.53

X2. METHOD FOR DETERMINING MASS LOSS WHERE CLEANING MAY ATTACK THE BASE METAL OF THE SPECIMEN

X2.1 Repeat the cleaning procedure a number of times. Weigh after each cleaning and plot the mass loss against the total time of cleaning or the number of cleanings, see Fig. X2.1. The ordinate at the intersection of the two lines is the mass loss caused by removal of corrosion products alone. The method is particularly applicable to electrolytic cleaning, see Section 6.

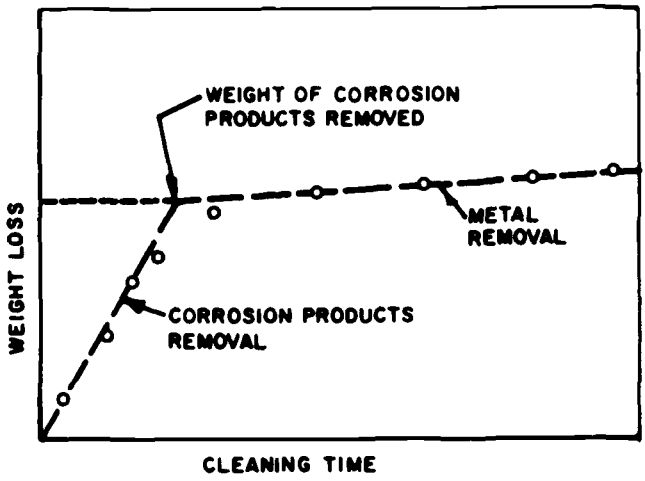


FIG. X2.1 Mass Loss Versus Exposure Time for Specimens During Cleaning

The American Society for Testing and Materials takes no position respecting the validity of any patent rights asserted in connection with any item mentioned in this standard. Users of this standard are expressly advised that determination of the validity of any such patent rights, and the risk of infringement of such rights, are entirely their own responsibility.

This standard is subject to revision at any time by the responsible technical committee and must be reviewed every five years and if not revised, either reapproved or withdrawn. Your comments are invited either for revision of this standard or for additional standards and should be addressed to ASTM Headquarters. Your comments will receive careful consideration at a meeting of the responsible technical committee, which you may attend. If you feel that your comments have not received a fair hearing you should make your views known to the ASTM Committee on Standards, 1916 Race St., Philadelphia, Pa. 19103.

Designation: G 5 - 82[ε1]

Standard Practice for STANDARD REFERENCE METHOD FOR MAKING POTENTIOSTATIC AND POTENTIODYNAMIC ANODIC POLARIZATION MEASUREMENTS[1]

This standard is issued under the fixed designation G 5; the number immediately following the designation indicates the year of original adoption or, in the case of revision, the year of last revision. A number in parentheses indicates the year of last reapproval. A superscript epsilon (ε) indicates an editorial change since the last revision or reapproval.

[ε1] NOTE—A revised Fig. 4B was included editorially in July 1983. (See Note in Fig 4B.)

1. Scope

1.1 This practice describes an experimental procedure which can be used to check one's experimental technique and instrumentation. If followed, this practice will provide repeatable potentiostatic and potentiodynamic anodic polarization measurements that will reproduce data determined by others at other times and in other laboratories.

1.2 Standard potentiostatic and potentiodynamic polarization plots are included. These reference data are based on the results from different laboratories (15 for the potentiostatic and 12 for the potentiodynamic) that followed the standard procedure, using a specific ferritic Type 430 stainless steel in 1.0 *N* H_2SO_4. Maximum and minimum current values are shown at each potential to indicate the acceptable range of values.

1.3 Deviations from the standard reference plots and the causes for such deviations are discussed in the Appendix.

1.4 Samples of the standard ferritic Type 430 stainless steel used in obtaining the standard reference plots are available for those who wish to check their own test procedure and equipment.[2]

1.5 *This standard may involve hazardous materials, operations, and equipment. This standard does not purport to address all of the safety problems associated with its use. It is the responsibility of whoever uses this standard to consult and establish appropriate safety and health practices and determine the applicability of regulatory limitations prior to use.*

2. Applicable Document

2.1 *ASTM Standard:*

G 3 Practice for Conventions Applicable to Electrochemical Measurements in Corrosion Testing[3]

3. Apparatus

3.1 The test cell should be constructed to allow the following items to be inserted into the solution chamber: the test electrode, two counter electrodes, a Luggin capillary with salt-bridge connection to the reference electrode, inlet and outlet for an inert gas, and a thermometer. The test cell shall be constructed of materials that will not corrode, deteriorate, or otherwise contaminate the test solution.

NOTE 1—Borosilicate glass and TFE-fluorocarbon have been found suitable.

3.1.1 A suitable cell is shown in Fig. 1 (1).[4] A 1-L, round-bottom flask has been modified by the addition of various necks to permit the introduction of electrodes, gas inlet and outlet tubes, and a thermometer. The Luggin probe-salt bridge separates the bulk solution from the saturated calomel reference electrode, and the

[1] This practice is under the jurisdiction of ASTM Committee G-1 on Corrosion of Metals.

Current edition approved Sept. 24, 1982. Published December 1982. Originally published as G 5 - 69. Last previous edition G 5 - 78.

[2] These standard samples are available from ASTM Headquarters. Generally, one sample can be repolished and reused for many runs. This procedure is suggested to conserve the available material. Order PCN 12-700050-00.

[3] *Annual Book of ASTM Standards*, Vol 03.02.

[4] The boldface numbers in parentheses refer to the list of references at the end of this practice.

probe tip can be easily adjusted to bring it in close proximity with the working electrode.

3.2 *Electrode Holder* (**1**):

3.2.1 The auxiliary and working electrodes are mounted in the type of holder shown in Fig. 2. A longer holder is required for the working electrode than for the auxiliary electrode. A leak-proof assembly is obtained by the proper compression fit between the electrode and a TFE-fluorocarbon gasket. (Too much pressure may cause shielding of the electrode or breakage of the glass holder, and too little pressure may cause leakage.)

3.3 *Potentiostat* (Note 2):

3.3.1 A potentiostat that will maintain an electrode potential within 1 mV of a preset value over a wide range of applied currents should be used. For the type and size of standard specimen supplied, the potentiostat should have a potential range of −0.6 to 1.6 V and an anodic current output range of 1.0 to 10^5 μA. Many commercial potentiostats meet the specific requirements for these types of measurements.

3.4 *Potential-Measuring Instruments* (Note 2):

3.4.1 The potential-measuring circuit should have a high input impedance on the order of 10^{11} to 10^{14} Ω to minimize current drawn from the system during measurements. Such circuits are provided with most modern potentiostats. Instruments should have sufficient sensitivity and accuracy to detect a change of 1.0 mV over a potential range between −0.6 and 1.6 V.

3.5 *Current-Measuring Instruments* (Note 2):

3.5.1 An instrument that is capable of measuring a current accurately to within 1 % of the absolute value over a current range between 1.0 and 10^5 μA for the approximately 5-cm^2 specimen of Type 430 stainless steel that is supplied should be used. Many commercial instruments are satisfactory for this purpose.

3.6 *Anodic Polarization Circuit:*

3.6.1 A schematic potentiostatic anodic polarization wiring diagram (**2**) is illustrated in Fig. 3. Note that the milliammeter is placed between the potentiostat and the auxiliary electrode. The potentiometer-electrometer combination provides the high impedance necessary for potential measurement. Most modern potentiostats have outputs of potential and current as a voltage for connection to appropriate recorders. This makes the use of a milliammeter, potentiometer, and electrometer null detector shown in Fig. 3 unnecessary.

3.6.2 A scanning potentiostat is used for potentiodynamic measurements. A record of the potential and current is plotted continuously using such instruments as an *X-Y* recorder and a logarithmic converter incorporated into the circuit described in 3.6.1. Some potentiostats have an output of the logarithm of the current as a voltage, which allows direct plotting of the potential log current curve using an *X-Y* recorder.

NOTE 2—The instrumental requirements are based upon values typical of the instruments in the 15 laboratories that provided the data used in determining the standard polarization plot.

3.7 *Electrodes:*

3.7.1 *Working Electrode*, prepared from a ½-in. (12.7-mm) length of ⅜-in. (9.5-mm) diameter rod stock. Each electrode is drilled, tapped, and mounted in the manner discussed in 3.2.1.

NOTE 3—If specimen forms are used other than those called for by this practice, for example, flat sheet specimen, care should be taken since it was shown that crevices may be introduced which can lead to erroneous results (see Fig. X1).

3.7.1.1 The standard AISI Type 430 stainless steel should be used if one wishes to reproduce the standard reference plot. This material was prepared from a single heat of metal that was mill-annealed for ½ h at 1500°F (816°C) and air cooled. The chemical composition of the standard stainless steel is shown in Table 1.

3.7.2 *Platinum Electrodes*—Two platinum auxiliary electrodes are prepared from high-purity rod stock. Each electrode is drilled, tapped, and mounted with a TFE-fluorocarbon gasket in the same manner as the working electrode. A large platinum sheet sealed into a glass holder is also acceptable.

3.7.2.1 A platinized surface is recommended because of the increased surface area. This may be accomplished by cleaning the surface in hot aqua regia (3 parts concentrated HCl and 1 part concentrated HNO_3), washing, and then drying. Both electrodes are platinized by immersing them in a solution of 3 % platinic chloride and 0.02 % lead acetate and electrolyzing at a current density of 40 to 50 mA/cm^2 for 4 or 5 min (**1,3**). The polarity is reversed every minute. Occluded chloride is removed by electrolyzing in a dilute (10 %) sulfuric acid solution for several minutes with a reversal in polarity every minute. Electrodes are rinsed thoroughly and stored in distilled water until ready for use. Since certain ions can poison these

electrodes, periodic checks of platinized platinum potentials against a known reference electrode should be made.

3.7.2.2 Alternatively, graphite auxiliary electrodes can be used, but material retained by the graphite may contaminate subsequent experiments. This contamination can be minimized by using high-density graphite or avoided by routinely replacing the graphite electrode.

3.8 *Calomel Electrode* (**4**)—A saturated calomel electrode with a controlled rate of leakage (about 3 μl/h) is recommended. This type of electrode is durable, reliable, and commercially available. The normal precautions should be taken to ensure that it is maintained in the proper condition. The potential of the calomel electrode should be checked at periodic intervals to ensure the accuracy of the electrode.

4. Standard Experimental Procedure

4.1 *Test Specimen Preparation:*

4.1.1 Prepare the surface within 1 h of the experiment. Wet grind with 240-grit SiC paper, wet polish with 600-grit SiC paper until previous coarse scratches are removed, rinse, and dry. (Drilled and tapped specimens can be threaded onto an electrode holder rod and secured in a lathe or electric drill for this operation.)

4.1.2 Determine the surface area by measuring all dimensions to the nearest 0.01 mm, subtracting the area under the gasket (usually 0.20 to 0.25 cm^2).

4.1.3 Mount the specimen on the electrode holder as described in 3.2.1. Tighten the assembly by holding the upper end of the mounting rod in a vise or clamp while tightening the mounting nut until the gasket is properly compressed.

4.1.4 Clean the specimen just prior to immersion by degreasing for 5 min in boiling benzen (**Caution:** Use under hood), followed by rinsing in distilled water.

4.2 Prepare 1 L of 1.0 *N* H_2SO_4 from reagent grade acid and distilled water, using 27.2 mL of 98 % H_2SO_4/L of solution. Transfer 900 mL of solution to clean polarization cell.

4.3 Bring the temperature of the solution to 30 ± 1°C by immersing the test cell in a controlled-temperature water bath or by other convenient means.

4.4 Place the platinized auxiliary electrodes, salt-bridge probe, and other components in the test cell and temporarily close the center opening with a glass stopper. Fill the salt bridge with test solution.

NOTE 4—The levels of the solution in the reference and polarization cells should be the same to avoid siphoning. If this is impossible, a closed solution-wet (not greased) stopcock can be used in the salt bridge to eliminate siphoning.

4.5 Purge the solution prior to immersion of the test specimen, for a minimum of ½ h with oxygen-free hydrogen gas at the rate of 150 cm^3/min to remove oxygen from solution.

4.6 Transfer the specimen to the test cell and adjust the salt-bridge probe tip so it is about 2 mm from the specimen electrode.

4.7 Record the open-circuit specimen potential, that is, the corrosion potential, after 55 min immersion. Record the platinized platinum potential 50 min after immersion of the specimen.

4.8 *Potential Scan:*

4.8.1 Start the potential scan 1 h after specimen immersion, beginning at the corrosion potential (E_{corr}) for potentiodynamic measurements and the nearest 50-mV increment above E_{corr} for the potentiostatic measurements. Proceed through +1.60 V versus saturated calomel electrode (SCE) (active to noble).

4.8.2 Use a potentiostatic potential step rate of 50 mV every 5 min, recording the current at the end of each 5-min period at potential.

4.8.3 Use a potentiodynamic potential sweep rate of 0.6 V/h (±5 %) recording the current continuously with change in potential.

4.9 Plot anodic polarization data on semilogarithmic paper in accordance with Practice G 3, (potential-ordinate, current density-abscissa). If a potentiostat with a logarithmic converter is used, this plot can be produced directly during the measurement.

5. Standard Reference Plots

5.1 Standard polarization plots based on potentiostatic data from 15 different laboratories and potentiodynamic data from 12 different laboratories are shown in Figs. 4A and 4B (**5**). The plots show a range of acceptable current density values at each potential. The average corrosion potential is −0.52 V, and the average platinized platinum potential is −0.26 V.

5.2 These plots were prepared from data obtained by following the standard procedure discussed in this practice.

5.3 Typical deviations from the standard potentiostatic plot are shown and discussed in Appendix X1. Reference to this discussion may be helpful in determining the reasons for dif-

ferences between an experimental curve and the standard plots.

5.4 The potentiodynamic standard curve shows good agreement with the potentiostatic standard curve determined at an equivalent overall polarization rate.

6. Reproducibility

6.1 It is possible to show excellent repeatability in the same laboratory when following a set procedure. However, these data may not agree with that in another laboratory. An example of repeatable data is shown in Fig. 5, but the curve does not agree completely with the standard plot in that the secondary current density maximum occurs at a potential of about 100 mV more active than the standard.

6.2 The small spread in data obtained from a number of laboratories and used in the preparation of the standard plot demonstrated that good reproducibility is possible when a standard procedure is followed.

6.3 The availability of a standard procedure, standard material, and a standard plot should make it easy for an investigator to check his techniques. This should lead to polarization curves in the literature which can be compared with greater confidence than is possible now.

TABLE 1 Chemical Composition of Standard Type 430 Stainless Steel, Weight Percent.

Chromium	16.52
Carbon	0.052
Manganese	0.40
Silicon	0.49
Phosphorus	0.013
Sulfur	0.009
Nickel	0.27
Molybdenum	0.03
Copper	0.07
Iron	balance

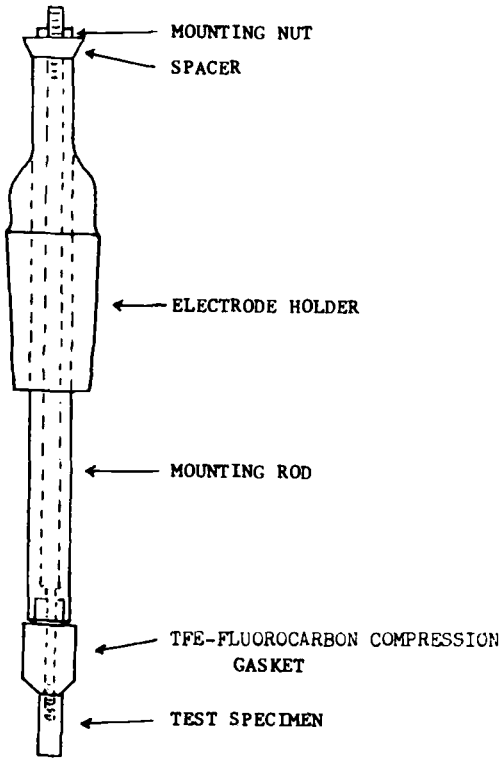


FIG. 2 Specimen Mounted on Electrode Holder

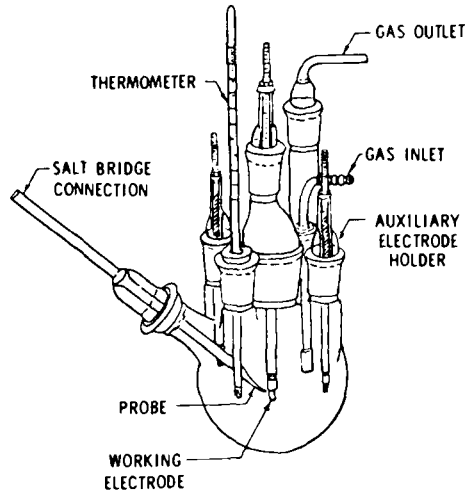


FIG. 1 Schematic Diagram of Polarization Cell (1)

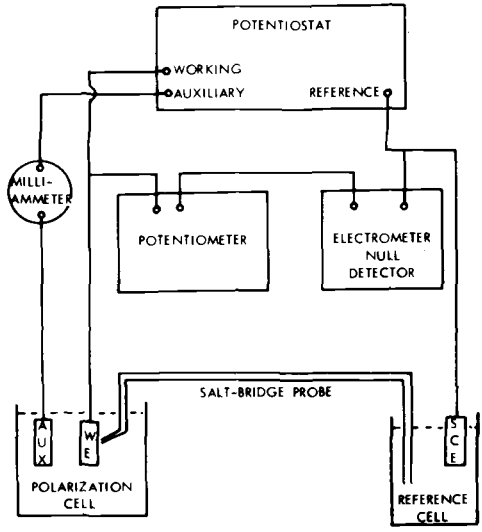


FIG. 3 Schematic Potentiostatic Anodic Polarization Wiring Diagram (2)

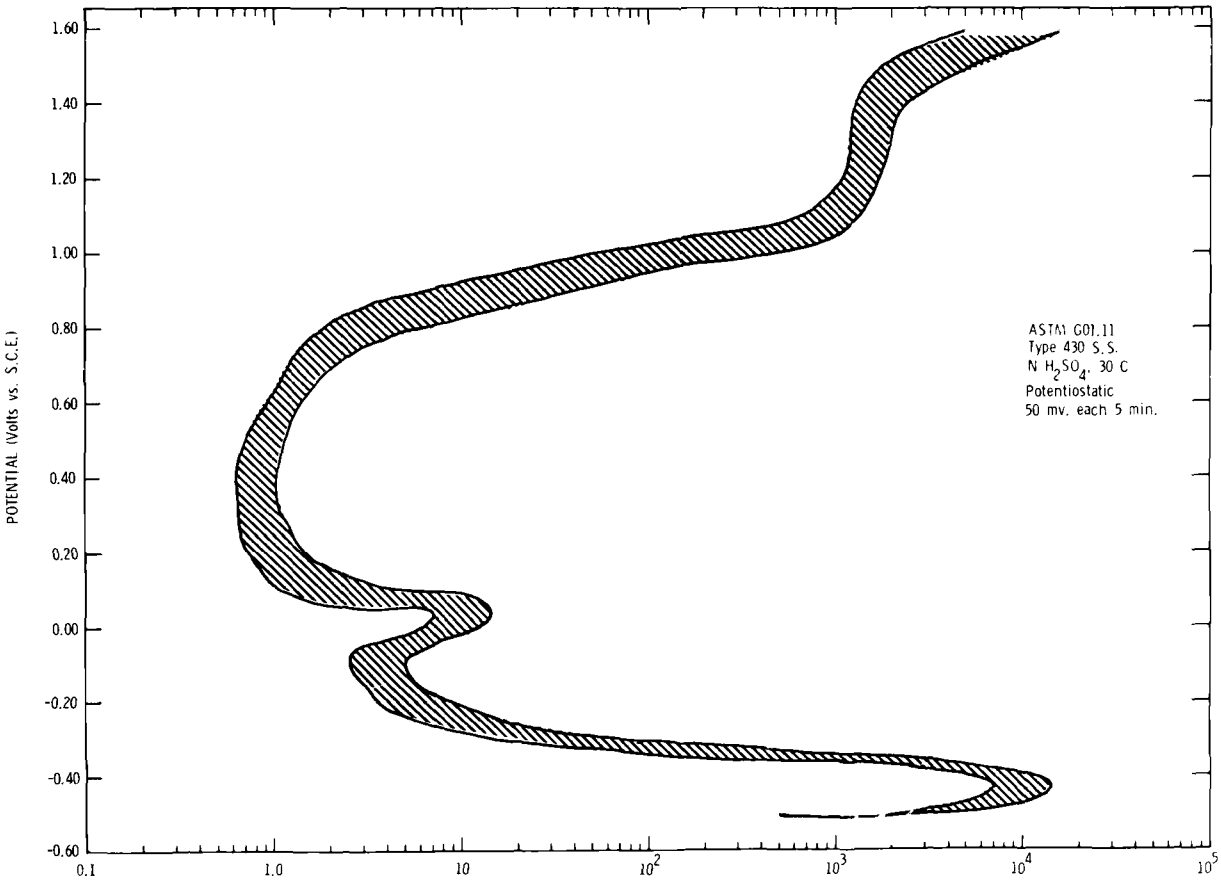
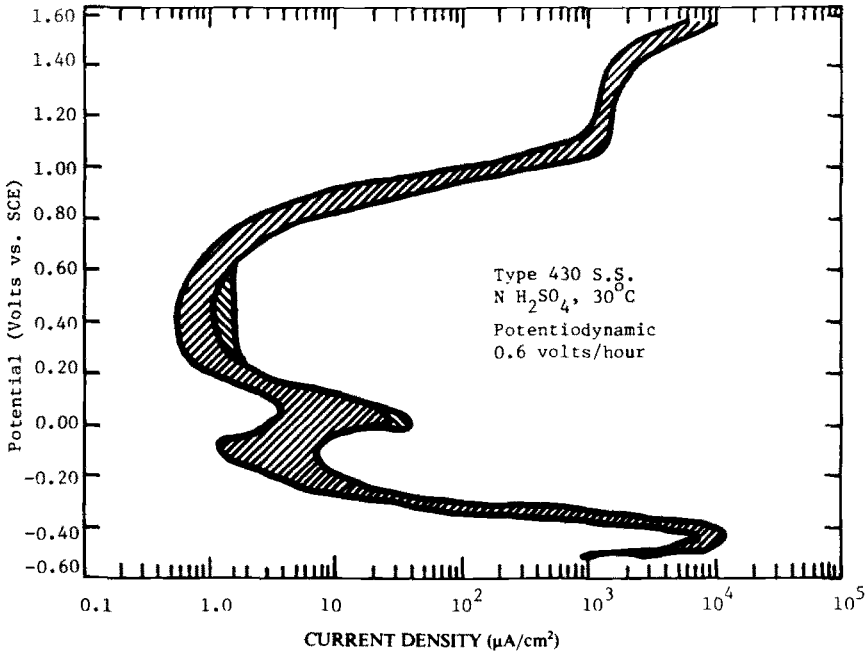


FIG. 4A Standard Potentiostatic Anodic Polarization Plot



NOTE—This practice is being revised within Subcommittee G01.11. A new heat of Type 430 S.S. is being used for standard material, and the standard curve has been shown through round-robin testing to be slightly off in terms of the maximum passive current density and the maximum secondary peak current density for this new material. This plot shows the standard curve and the revised areas (crosshatched in the opposite direction). This revised curve has not been balloted and is offered for information only for your convenience until a revised practice appears.

FIG. 4B Standard Potentiodynamic Anodic Polarization Plot

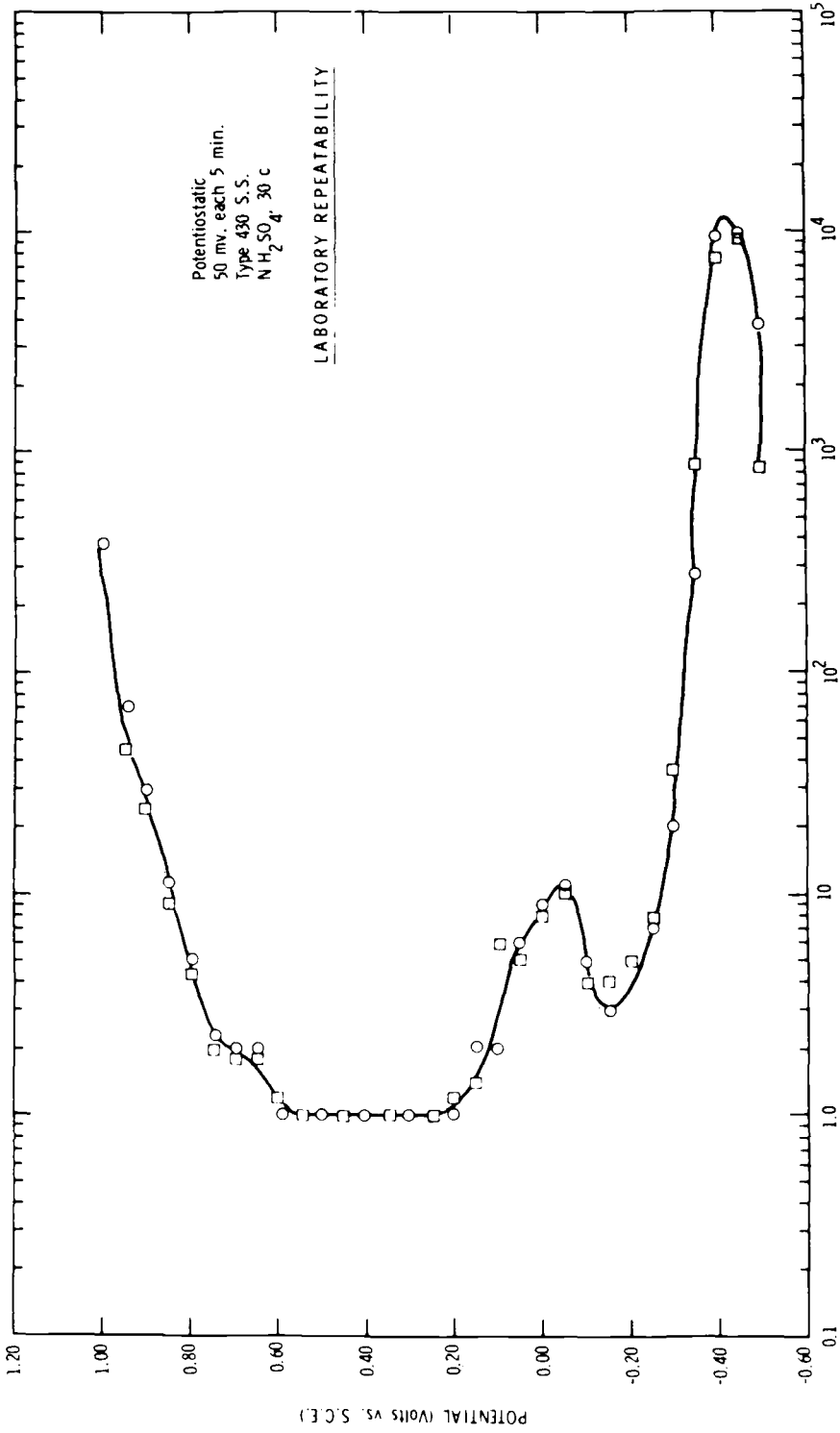


FIG. 5 Laboratory Repeatability of Potentiostatic Anodic Polarization Curve

APPENDIX

(Nonmandatory Information)

X1. DEVIATIONS FROM STANDARD POLARIZATION PLOTS

X1.1 High Passive Current Densities (Crevice Effect)

X1.1.1 Examples of passive current densities which are greater than those for the standard potentiostatic plot are shown in Fig. X1. This effect is attributable to a crevice between the specimen and mounting material (6). The crevice may be the result of the mounting technique or the material used for mounting.

X1.1.2 The potential drop along the narrow path of the electrolyte within the crevice between the specimen and the mounting material prevents this area from passivating. Although the face of the specimen passivates, the high current density associated with the active crevice contributes to an increase in the measured current density. Specimen electrodes for polarization measurements must be mounted without crevice sites to avoid such erroneous passive current densities.

X1.2 Low Passive Current Densities (Instrumental Effect)

X1.2.1 The low passive current densities shown in Fig. X2 are undoubtedly the result of instrumental problems. This effect can be eliminated by calibrating the current over the entire range of interest before conducting an experiment.

X1.3 Cathodic Currents During Anodic Polarization (Oxygen Effect)

X1.3.1 The "negative loop" at potentials between −0.350 V and −0.050 V, shown by dashed lines in Fig. X3, occurs when the total cathodic current exceeds the total anodic current. Such results are characteristic of oxygen being present in the solution (7). This effect can be anticipated if the recorded platinum potential is considerably more noble than −0.26 V. The hydrogen purge should remove oxygen from the system, but there may be an air leak or the hydrogen may be contaminated with oxygen. It is necessary to take extreme care in the design of glassware equipment and to ensure a high order of purity in the gas that is used to avoid oxygen contamination.

REFERENCES

(1) Greene, N. D., *Experimental Electrode Kinetics*, Rensselaer Polytechnic Institute, Troy, N. Y., 1965.

(2) France, Jr., W. D., "Controlled Potential Corrosion Tests, Their Applications and Limitations," *Materials Research and Standards*, Vol 9, No. 8, 1969, p. 21.

(3) Mellon, M. G., *Quantitative Analysis*, Thomas Y. Crowell Co., New York, 1955.

(4) Ives, D. J., and Janz, G. J., *Reference Electrodes, Theory and Practice*, Academic Press, New York, N. Y., 1961.

(5) "The Reproducibility of Potentiostatic and Potentiodynamic Anodic Polarization Measurements," ASTM Subcommittee G-1/XI, Section I, Interlaboratory Testing Program, June, 1967. Available from ASTM Headquarters as RR: G01-1000.

(6) Greene, N. D., France, Jr., W. D., and Wilde, B. E., "Electrode Mounting for Potentiostatic Anodic Polarization Studies," *Corrosion*, CORRA, Vol 21, 1965, p. 275.

(7) Greene, N. D., "Effect of Oxygen on the Active-Passive Behavior of Stainless Steel," *Journal of the Electrochemical Society*, JESOA, Vol 107, 1960, p. 457.

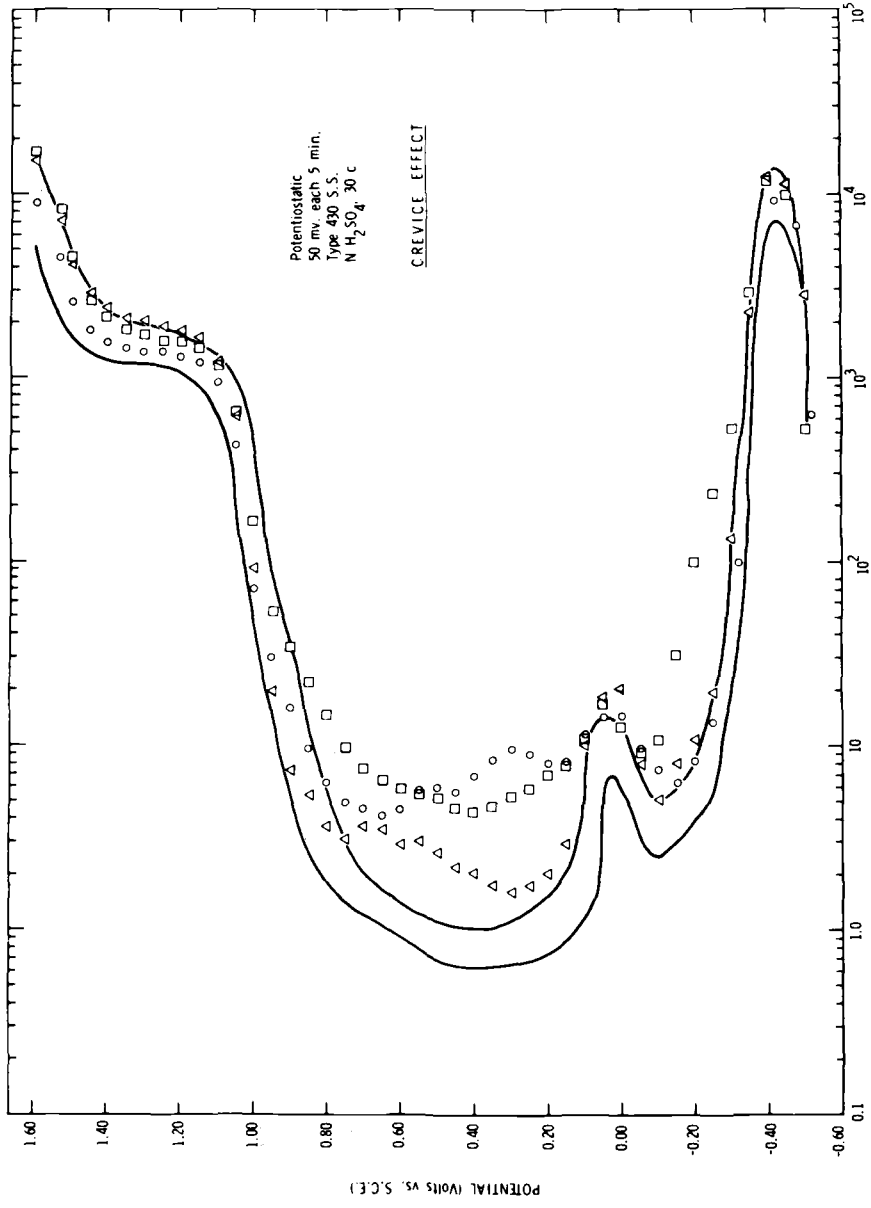


FIG. X1 Crevice Effect During Potentiostatic Anodic Polarization

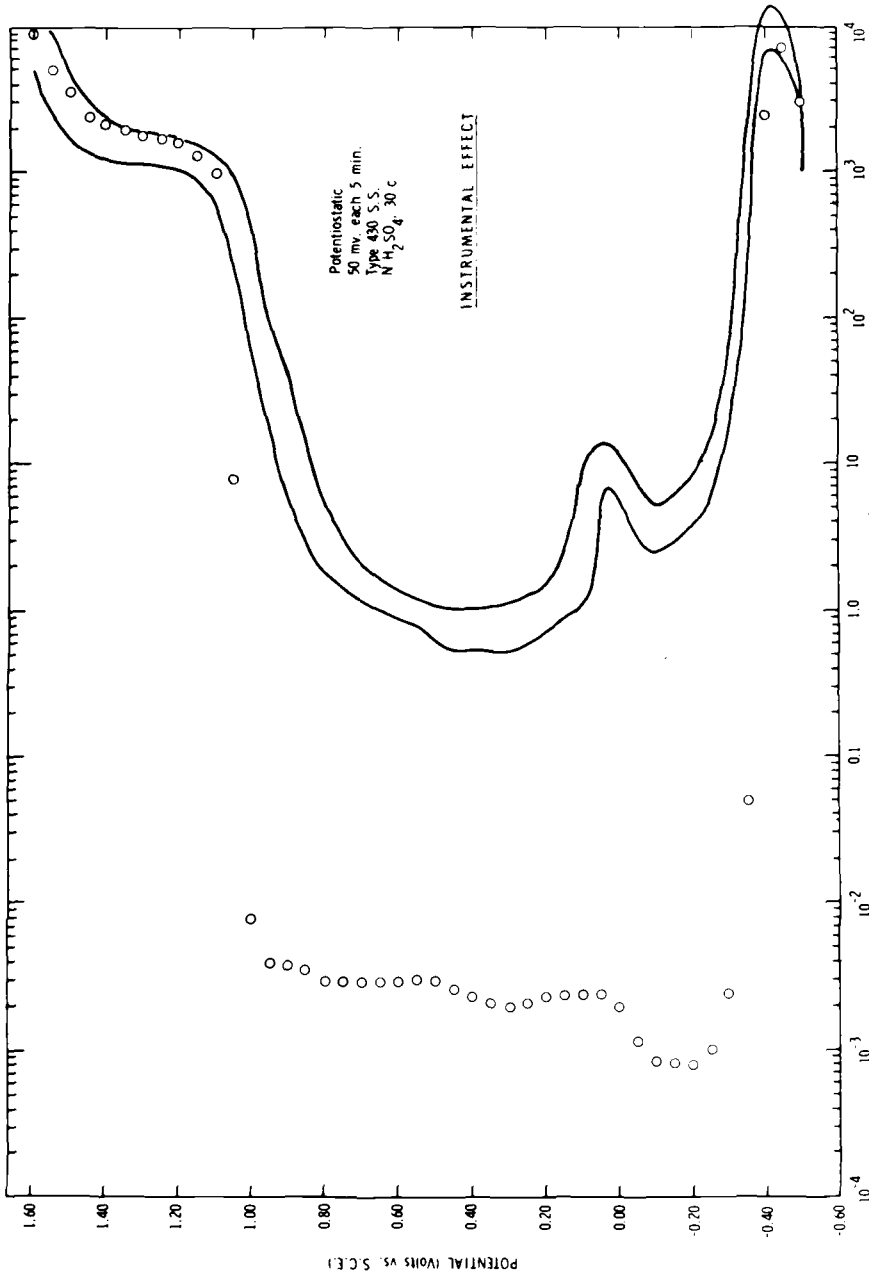


FIG. X2 Instrumental Effect During Potentiostatic Anodic Polarization

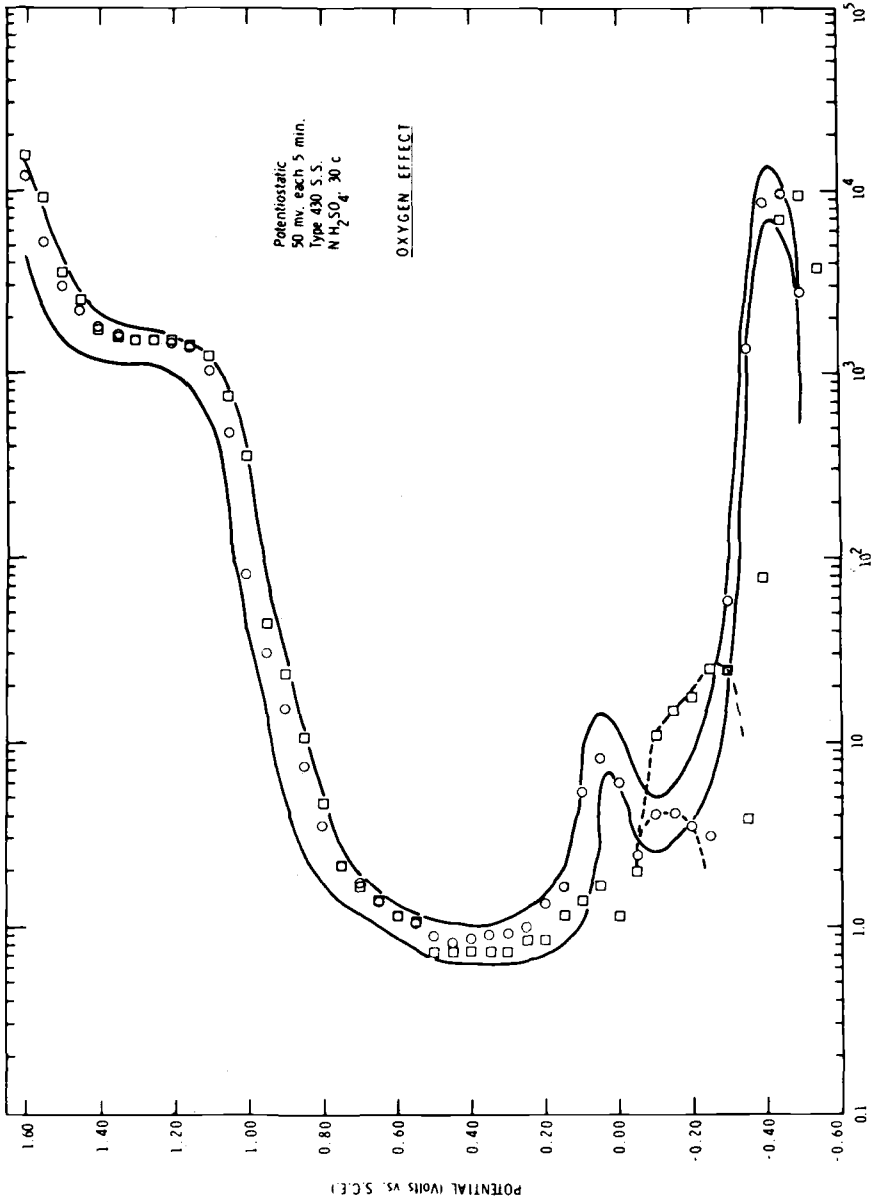


FIG. X3 Oxygen Effect During Potentiostatic Anodic Polarization

The American Society for Testing and Materials takes no position respecting the validity of any patent rights asserted in connection with any item mentioned in this standard. Users of this standard are expressly advised that determination of the validity of any such patent rights, and the risk of infringement of such rights, are entirely their own responsibility.

This standard is subject to revision at any time by the responsible technical committee and must be reviewed every five years and if not revised, either reapproved or withdrawn. Your comments are invited either for revision of this standard or for additional standards and should be addressed to ASTM Headquarters. Your comments will receive careful consideration at a meeting of the responsible technical committee, which you may attend. If you feel that your comments have not received a fair hearing you should make your views known to the ASTM Committee on Standards, 1916 Race St., Philadelphia, Pa. 19103.

Designation: G 15 - 85a

Standard Definitions of Terms Relating to CORROSION AND CORROSION TESTING[1]

This standard is issued under the fixed designation G 15; the number immediately following the designation indicates the year of original adoption or, in the case of revision, the year of last revision. A number in parentheses indicates the year of last reapproval. A superscript epsilon (ε) indicates an editorial change since the last revision or reapproval.

These definitions have been approved for use by agencies of the Department of Defense and for listing in the DoD Index of Specifications and Standards.

active—the negative direction of electrode potential. (Also used to describe corrosion and its associated potential range when an electrode potential is more negative than an adjacent depressed corrosion rate [passive] range.)

anion—a negatively charged ion.

anode—the electrode of an electrolytic cell at which oxidation is the principal reaction. (Electrons flow away from the anode in the external circuit. It is usually the electrode where corrosion occurs and metal ions enter solution.)

anode corrosion efficiency—the ratio of the actual corrosion (weight loss) of an anode to the theoretical corrosion (weight loss) calculated by Faraday's law from the quantity of electricity that has passed.

anodic inhibitor—an inhibitor of metal corrosion that reduces the rate of the anodic or oxidation reaction.

anodic polarization—the change of the electrode potential in the noble (positive) direction due to current flow. (See **polarization**.)

anodic protection—a technique to reduce the corrosion rate of a metal by polarizing it into its passive region where dissolution rates are low.

anolyte—the electrolyte adjacent to the anode of an electrolytic cell.

auxiliary electrode—the electrode in an electrochemical cell that is used to transfer current to or from a test electrode.

breakdown potential—the least noble potential where pitting or crevice corrosion, or both, will initiate and propagate.

cathode—the electrode of an electrolytic cell at which reduction is the principal reaction. (Electrons flow toward the cathode in the external circuit.)

cathodic corrosion—corrosion of a metal when it is a cathode. (It usually happens to metals because of a rise in pH at the cathode or as a result of the formation of hydrides.)

cathodic inhibitor—an inhibitor of metal corrosion that reduces the rate of the cathodic or reduction reaction.

cathodic polarization—the change of the electrode potential in the active (negative) direction due to current flow. (See **polarization**.)

cathodic protection—a technique to reduce the corrosion rate of a metal surface by making it the cathode of an electrochemical cell.

catholyte—the electrolyte adjacent to the cathode of an electrolytic cell.

cation—a positively charged ion.

caustic cracking—stress corrosion cracking of metals in caustic solutions. (See also **stress corrosion cracking**.)

caustic embrittlement—see **caustic cracking.**

cavitation—the formation and rapid collapse within a liquid of cavities or bubbles that contain vapor or gas or both.

cavitation damage—the degradation of a solid body resulting from its exposure to cavitation. (This may include loss of material, surface deformation, or changes in properties or appearance.)

cavitation-erosion—progressive loss of original material from a solid surface due to continuing exposure to cavitation.

[1] These definitions are under the jurisdiction of ASTM Committee G-1 on Corrosion of Metals and are the direct responsibility of Subcommittee G01.02 on Nomenclature.

Current edition approved March 29, and April 26, 1985. Published July 1985. Originally published as G 15 - 71. Last previous edition G 15 - 83a.

chemical conversion coating—a protective or decorative nonmetallic coating produced *in situ* by chemical reaction of a metal with a chosen environment. (It is often used to prepare the surface prior to the application of an organic coating.)

concentration cell—an electrolytic cell, the emf of which is caused by a difference in concentration of some component in the electrolyte. (This difference leads to the formation of discrete cathode and anode regions.)

corrosion—the chemical or electrochemical reaction between a material, usually a metal, and its environment that produces a deterioration of the material and its properties.

corrosion fatigue—the process in which a metal fractures prematurely under conditions of simultaneous corrosion and repeated cyclic loading at lower stress levels or fewer cycles than would be required in the absence of the corrosive environment.

corrosion fatigue strength—the maximum repeated stress that can be endured by a metal without failure under definite conditions of corrosion and fatigue and for a specific number of stress cycles and a specified period of time.

corrosion potential—the potential of a corroding surface in an electrolyte relative to a reference electrode measured under open-circuit conditions.

corrosion rate—the amount of corrosion occurring in unit time. (For example, mass change per unit area per unit time; penetration per unit time)

counter electrode—See **auxiliary electrode.**

crazing—a network of checks or cracks appearing on a coated surface.

crevice corrosion—localized corrosion of a metal surface at, or immediately adjacent to, an area that is shielded from full exposure to the environment because of close proximity between the metal and the surface of another material.

critical anodic current density—the maximum anodic current density observed in the active region for a metal or alloy electrode that exhibits active-passive behavior in an environment.

critical humidity—the relative humidity above which the atmospheric corrosion rate of some metals increases sharply.

critical pitting potential—the least noble potential where pitting corrosion will initiate and propagate. (See breakdown potential.)

current density—the current flowing to or from a unit area of an electrode surface.

current efficiency—the ratio of the electrochemical equivalent current density for a specific reaction to the total applied current density.

deactivation—the process of prior removal of the active corrosive constituents, usually oxygen, from a corrosive liquid by controlled corrosion of expendable metal or by other chemical means, thereby making the liquid less corrosive.

dealloying—see **parting.**

depolarization—not a preferred term. (See **polarization.**)

deposit corrosion—localized corrosion under or around a deposit or collection of material on a metal surface. (See also **crevice corrosion.**)

dezincification—See **parting;** specific to copper-zinc alloys.

differential aeration cell (oxygen concentration cell)—a concentration cell caused by differences in oxygen concentration along the surface of a metal in an electrolyte. (See **concentration cell.**)

diffusion limited current density—the current density, often referred to as limiting current density, that corresponds to the maximum transfer rate that a particular species can sustain due to the limitation of diffusion.

electrochemical cell—an electrochemical system consisting of an anode and a cathode in metallic contact and immersed in an electrolyte. (The anode and cathode may be different metals or dissimilar areas on the same metal surface.)

electrochemical potential (electrochemical tension)—the partial derivative of the total electrochemical free energy of the system with respect to the number of moles of the constituent in a solution when all other factors are constant. (Analogous to the chemical potential of the constituent except that it includes the electrical as well as the chemical contributions to the free energy.)

electrode potential—the potential of an electrode in an electrolyte as measured against a reference electrode. (The electrode potential does not include any resistance losses in potential in either the solution or external cir-

cuit. It represents the reversible work to move a unit charge from the electrode surface through the solution to the reference electrode.)

electrolysis—production of chemical changes of the electrolyte by the passage of current through an electrochemical cell.

electrolytic cleaning—a process of removing soil, scale, or corrosion products from a metal surface by subjecting it as an electrode to an electric current in an electrolytic bath.

Electromotive Force Series (EMF Series)—a list of elements arranged according to their standard electrode potentials, with "noble" metals such as gold being positive and "active" metals such as zinc being negative.

embrittlement—the severe loss of ductility or toughness or both, of a material, usually a metal or alloy.

equilibrium (reversible) potential—the potential of an electrode in an electrolytic solution when the forward rate of a given reaction is exactly equal to the reverse rate. (The equilibrium potential can only be defined with respect to a specific electrochemical reaction.)

erosion—the progressive loss of material from a solid surface due to mechanical interaction between that surface and a fluid, a multicomponent fluid, or solid particles carried with the fluid.

erosion-corrosion—a conjoint action involving corrosion and erosion in the presence of a moving corrosive fluid, leading to the accelerated loss of material.

exchange current density—the rate of charge transfer per unit area when an electrode reaches dynamic equilibrium (at its reversible potential) in a solution; that is, the rate of anodic charge transfer (oxidation) balances the rate of cathodic charge transfer (reduction).

exfoliation—corrosion that proceeds laterally from the sites of initiation along planes parallel to the surface, generally at grain boundaries, forming corrosion products that force metal away from the body of the material, giving rise to a layered appearance.

external circuit—the wires, connectors, measuring devices, current sources, etc., that are used to bring about or measure the desired electrical conditions within the test cell.

filiform corrosion—corrosion that occurs under some coatings in the form of randomly distributed threadlike filaments.

fretting corrosion—the deterioration at the interface between contacting surfaces as the result of corrosion and slight oscillatory slip between the two surfaces.

galvanic corrosion—accelerated corrosion of a metal because of an electrical contact with a more noble metal or nonmetallic conductor in a corrosive electrolyte.

galvanic couple—a pair of dissimilar conductors, commonly metals, in electrical contact. (See **galvanic corrosion**.)

galvanic current—the electric current that flows between metals or conductive nonmetals in a galvanic couple.

Galvanic Series—a list of metals and alloys arranged according to their relative corrosion potentials in a given environment.

galvanostatic—an experimental technique whereby an electrode is maintained at a constant current in an electrolyte.

grain dropping—the dislodgement and loss of a grain or grains (crystals) from a metal surface as a result of intergranular corrosion.

graphitic corrosion—the deterioration of metallic constituents in gray cast iron, which leaves the graphitic particles intact. (The term "graphitization" is commonly used to identify this form of corrosion but is not recommended because of its use in metallurgy for the decomposition of carbide to graphite.)

hot corrosion—an accelerated corrosion of metal surfaces that results from the combined effect of oxidation and reactions with sulfur compounds and other contaminants, such as chlorides, to form a molten salt on a metal surface which fluxes, destroys, or disrupts the normal protective oxide.

hydrogen blistering—the formation of blisters on or below a metal surface from excessive internal hydrogen pressure. (Hydrogen may be formed during cleaning, plating, corrosion, etc.)

hydrogen embrittlement—hydrogen-induced cracking or severe loss of ductility caused by the presence of hydrogen in the metal.

immunity—a state of resistance to corrosion or anodic dissolution of a metal caused by thermodynamic stability of the metal.

impingement corrosion—a form of erosion-corrosion generally associated with the local

impingement of a high-velocity, flowing fluid against a solid surface.

impressed current—an electric current supplied by a device employing a power source that is external to the electrode system. (An example is d-c current for cathodic protection.)

inhibitor—a chemical substance or combination of substances that, when present in the proper concentration and forms in the environment, prevents or reduces corrosion.

intensiostatic—See **galvanostatic**.

intercrystalline corrosion—See **intergranular corrosion**.

intergranular corrosion—preferential corrosion at or adjacent to the grain boundaries of a metal or alloy.

internal oxidation—the formation of isolated particles of corrosion products beneath the metal surface. (This occurs as the result of preferential oxidation of certain alloy constituents by inward diffusion of oxygen, nitrogen, sulfur, etc.)

knife-line attack—intergranular corrosion of an alloy, usually stabilized stainless steel, along a line adjoining or in contact with a weld after heating into the sensitization temperature range.

local action corrosion—corrosion caused by local corrosion cells on a metal surface.

local corrosion cell—an electrochemical cell created on a metal surface because of a difference in potential between adjacent areas on that surface.

localized corrosion—corrosion at discrete sites, for example, pitting, crevice corrosion, and stress corrosion cracking.

long-line current—current that flows through the earth from an anodic to a cathodic area of a continuous metallic structure. (Usually used only where the areas are separated by considerable distance and where the current results from concentration-cell action.)

Luggin probe or Luggin-Haber capillary—a device used in measuring the potential of an electrode with a significant current density imposed on its surface. (The probe minimizes the IR drop that would otherwise be included in the measurement and without significantly disturbing the current distribution on the specimen.)

metal dusting—accelerated deterioration of metals in carbonaceous gases at elevated temperatures to form a dust-like corrosion product.

metallizing—See **thermal spraying**.

microbial corrosion—corrosion that is affected by the action of microorganisms in the environment.

mixed potential—the potential of a specimen when two or more electrochemical reactions are occurring simultaneously.

noble—the positive (increasingly oxidizing) direction of electrode potential.

noble metal—a metal with a standard electrode potential that is more noble (positive) than that of hydrogen.

open-circuit potential—the potential of an electrode measured with respect to a reference electrode or another electrode when no current flows to or from it.

overvoltage—the change in potential of an electrode from its equilibrium or steady state value when current is applied.

oxidation—loss of electrons by a constituent of a chemical reaction. (Also refers to the corrosion of a metal that is exposed to an oxidizing gas at elevated temperatures.)

parting—the selective corrosion of one or more components of a solid solution alloy.

parting limit—the minimum concentration of a more noble component in an alloy, above which parting does not occur in a specific environment.

passivation—the process in metal corrosion by which metals become passive. (See **passive**.)

passivator—a type of inhibitor which appreciably changes the potential of a metal to a more noble (positive) value.

passive—the state of the metal surface characterized by low corrosion rates in a potential region that is strongly oxidizing for the metal.

passive-active cell—a corrosion cell in which the anode is a metal in the active state and the cathode is the same metal in the passive state.

pitting—corrosion of a metal surface, confined to a point or small area, that takes the form of cavities.

pitting factor—ratio of the depth of the deepest pit resulting from corrosion divided by the average penetration as calculated from weight loss.

polarization—the change from the open-circuit electrode potential as the result of the passage of current.

polarization admittance—the reciprocal of po-

larization resistance (di/dE).

polarization resistance—the slope (dE/di) at the corrosion potential of a potential (E)–current density (i) curve. (It is inversely proportional to the corrosion current density when the polarization resistance technique is applicable.)

potentiodynamic (potentiokinetic)—the technique for varying the potential of an electrode in a continuous manner at a preset rate.

potentiostat—an instrument for automatically maintaining an electrode in an electrolyte at a constant potential or controlled potentials with respect to a suitable reference electrode.

potentiostatic—the technique for maintaining a constant electrode potential.

poultice corrosion—see **deposit corrosion**.

Pourbaix diagram (electrode potential-pH diagram)—a graphical representation showing regions of thermodynamic stability of species in metal-water electrolyte systems.

primary passive potential (passivation potential)—the potential corresponding to the maximum active current density (critical anodic current density) of an electrode that exhibits active-passive corrosion behavior.

protection potential—the most noble potential where pitting and crevice corrosion will not propagate.

redox potential—the potential of a reversible oxidation-reduction electrode measured with respect to a reference electrode, corrected to the hydrogen electrode, in a given electrolyte.

reduction—the gain of electrons by a constituent of a chemical reaction.

rest potential—See **open-circuit potential**.

rust—a corrosion product consisting primarily of hydrated iron oxide. (A term properly applied only to ferrous alloys.)

season cracking—See **stress-corrosion cracking**.

stray current corrosion—the corrosion caused by electric current from a source external to the intended electrical circuit, for example, extraneous current in the earth.

stress-corrosion cracking—a cracking process that requires the simultaneous action of a corrodent and sustained tensile stress. (This excludes corrosion-reduced sections which fail by fast fracture. It also excludes intercrystalline or transcrystalline corrosion which can disintegrate an alloy without either applied or residual stress.)

subsurface corrosion—See **internal oxidation**.

sulfidation—the reaction of a metal or alloy with a sulfur-containing species to produce a sulfur compound that forms on or beneath the surface of the metal or alloy.

Tafel slope—the slope of the straight line portion of a polarization curve, usually occurring at more than 50 mV from the open-circuit potential, when presented in a semilogarithmic plot in terms of volts per logarithmic cycle of current density (commonly referred to as volts per decade).

thermal spraying—a group of processes wherein finely divided metallic or nonmetallic materials are deposited in a molten or semimolten condition to form a coating. (The coating material may be in the form of powder, ceramic rod, wire, or molten materials.)

thermogalvanic corrosion—the corrosive effect resulting from the galvanic cell caused by a thermal gradient across the metal surface.

transpassive region—the region of an anodic polarization curve, noble to and above the passive potential range, in which there is a significant increase in current density (increased metal dissolution) as the potential becomes more positive (noble).

tuberculation—the formation of localized corrosion products that appear on a surface as knoblike prominences (tubercules).

uniform corrosion—corrosion that proceeds at about the same rate over a metal surface.

weld decay—not a preferred term. Integranular corrosion, usually of stainless steels or certain nickel-base alloys, that occurs as the result of sensitization in the heat-affected zone during the welding operation.

working electrode—the test or specimen electrode in an electrochemical cell.

This standard is subject to revision at any time by the responsible technical committee and must be reviewed every five years and if not revised, either reapproved or withdrawn. Your comments are invited either for revision of this standard or for additional standards and should be addressed to ASTM Headquarters. Your comments will receive careful consideration at a meeting of the responsible technical committee, which you may attend. If you feel that your comments have not received a fair hearing you should make your views known to the ASTM Committee on Standards, 1916 Race St., Philadelphia, Pa. 19103.

Designation: G 28 – 85

Standard Test Methods of DETECTING SUSCEPTIBILITY TO INTERGRANULAR ATTACK IN WROUGHT, NICKEL-RICH, CHROMIUM-BEARING ALLOYS[1]

This standard is issued under the fixed designation G 28; the number immediately following the designation indicates the year of original adoption or, in the case of revision, the year of last revision. A number in parentheses indicates the year of last reapproval. A superscript epsilon (ε) indicates an editorial change since the last revision or reapproval.

1. Scope

1.1 These test methods cover two tests as follows:

1.1.1 *Method A*—This method covers the procedures for the boiling ferric sulfate—50 % sulfuric acid test which applies to nine alloys and measures the susceptibility of certain nickel-rich, chromium-bearing alloys to intergranular attack, which may be encountered in certain service environments.

1.1.2 *Method B*—This method covers the procedures for a test in boiling 23 % H_2SO_4 + 1.2 % HCl + 1 % $FeCl_3$ + 1 % $CuCl_2$ that applies to one alloy for measuring the susceptibility to intergranular attack, which may be encountered in certain service environments.

1.2 *This standard may involve hazardous materials, operations, and equipment. This standard does not purport to address all of the safety problems associated with its use. It is the responsibility of whoever uses this standard to consult and establish appropriate safety and health practices and determine the applicability of regulatory limitations prior to use.* (For more specific safety precautionary statements see 5.1.1, 5.1.9, 12.1.1, and 12.1.10.)

2. Applicable Document

2.1 *ASTM Standard:*

A 262 Practices for Detecting Susceptibility to Intergranular Attack in Austenitic Stainless Steels[2]

METHOD A—Ferric Sulfate—50 % Sulfuric Acid Test

3. Significance and Use

3.1 The boiling ferric sulfate-sulfuric acid test may be applied to the following alloys in the wrought condition:

Alloy	Testing Time, h
N10276	24
N06455	24
N06007	120
N06985	120
N08020	120
N00600	24
N06625	120
N08800	120
N08825[4]	120

[4] While the ferric sulfate-sulfuric acid test does detect susceptibility to intergranular attack in Alloy N08825, the boiling 65 % nitric acid test, ASTM Practice A 262, Part C, for detecting susceptibility to intergranular attack in stainless steels is more sensitive.

3.2 Nominal compositions of these alloys are given in Table 1.

3.3 This method may be used to evaluate as-received material and to evaluate the effects of subsequent heat treatments. In the case of nickel-rich, chromium-bearing alloys, the method may be applied only to wrought products. The test is not applicable to cast products.

4. Apparatus (See Fig. 1.)

4.1 *Allihn or Soxhlet Condenser*, 4-bulb,[3] with a 45/50 ground-glass joint, overall length about

[1] These test methods are under the jurisdiction of ASTM Committee G-1 on Corrosion of Metals and is the direct responsibility of Subcommittee G01.05 on Laboratory Corrosion Tests.

Current edition approved April 26, 1985. Published August 1985. Originally published as G 28 – 71. Last previous edition G 28 – 72 (1979)[ε1].

[2] *Annual Book of ASTM Standards*, Vol 03.02.

[3] To avoid frequent chipping of the drip-tip of the condenser during handling, the modified condenser described by Streicher, M. A., and Sweet, A. J., *Corrosion*, Vol 25, 1969, pp. 1, may be used.

330 mm, condensing section about 240 mm.

4.2 *Erlenmeyer Flask*, 1-L, with a 45/50 ground-glass joint. The ground-glass opening shall be 40 mm wide.

4.3 *Glass Cradle* (Fig. 2)—This can be supplied by a glass blowing shop. To pass through the ground-glass joint on the Erlenmeyer flask, the width of the cradle should not exceed 40 mm and the front-to-back distance must be such that the cradle will fit the 40-mm diameter opening. It should have three or four holes to increase circulation of the test solution around the specimen.

NOTE 1—Other equivalent means of specimen support, such as glass hooks or stirrups, may also be used.

4.4 *Boiling Chips*, or some other boiling aids must be used to prevent bumping.

4.5 *Silicone Grease*[4] is recommended for the ground-glass joint.

4.6 *Electrically Heated Hot Plate*, or equivalent to provide heat for continuous boiling of the solution.

4.7 *Analytical Balance*, capable of weighing to the nearest 0.001 g.

5. Test Solution

5.1 Prepare 600 mL of 50 % (49.4 to 50.9 %) solution as follows:

5.1.1 **Caution**—Protect the eyes and use rubber gloves for handling acid. Place the test flask under a hood.

5.1.2 First, measure 400.0 mL of distilled water in a 500-mL graduate and pour into the Erlenmeyer flask.

5.1.3 Then measure 236.0 mL of reagent-grade sulfuric acid (H_2SO_4) of a concentration which must be in the range from 95.0 to 98.0 weight % in a 250-mL graduate. Add the acid slowly to the water in the Erlenmeyer flask to avoid boiling by the heat evolved. Externally cooling the flask with water during the mixing will also reduce overheating.

NOTE 2—Loss of vapor results in concentration of the acid.

5.1.4 Weigh 25 g of reagent grade ferric sulfate (contains about 75 % $Fe_2(SO_4)_3$) and add to the H_2SO_4 solution. A trip balance may be used.

NOTE 3—Ferritic sulfate is a specific additive that establishes and controls the corrosion potential. No substitutions are permitted.

5.1.5 Add boiling aids.

5.1.6 Lubricate the ground glass of the condenser joint with silicone grease.

5.1.7 Cover the flask with the condenser and circulate cooling water.

5.1.8 Boil the solution until all ferritic sulfate is dissolved.

5.1.9 **Caution**—It has been reported that violent boiling resulting in acid spills can occur. It is important to ensure that the concentration of acid does not become more concentrated and that an adequate number of boiling chips (which are resistant to attack by the test solution) are present.[5]

6. Test Specimens

6.1 A specimen having a total surface area of 5 to 20 cm^2 is recommended.

6.2 The intent is to test a specimen representing as nearly as possible the material as used in service. The specimens should be cut to represent the grain flow direction that will see service, for example, specimens should not contain large cross-sectional areas unless it is the intent of the test to evaluate these. Only such surface finishing should be performed as is required to remove foreign material and obtain a standard, uniform finish as specified in 6.4. For very heavy sections, specimens should be machined to represent the appropriate surface while maintaining reasonable specimen size for convenience in testing. Ordinarily, removal of more material than necessary will have little influence on the test results. However, in the special case of surface decarburization or of carburization (the latter is sometimes encountered in tubing when lubricants or binders containing carbonaceous materials are employed), it may be possible by heavy grinding or machining to remove the affected layer completely. Such treatment of test specimens is not permissible, except in tests undertaken to demonstrate such surface effects.

6.3 When specimens are cut by shearing, the deformed material should be removed by machining or grinding prior to testing.

6.4 All surfaces of the specimen, including edges, should be finished using wet No. 80- or day No. 120-grit abrasive paper. If dry abrasive paper is used, polish slowly to avoid overheating. Sand blasting should not be used.

6.5 Residual oxide scale causes galvanic ac-

[4] Stopcock grease has been found satisfactory for this purpose.

[5] Amphoteric alundum granules, Hengar Granules, from the Hengar Co., Philadelphia, PA have been found satisfactory for this purpose.

tion and consequent activation in the test solution. Therefore, the formation of oxide scale in stamped codes must be prevented, and all traces of oxide scale formed during heat treatment must be thoroughly removed.

6.6 The specimen dimensions should be measured including the edges and inner surfaces of any holes and the total exposed area calculated.

6.7 The specimen should then be degreased and dried using suitable nonchlorinated agents such as soap and acetone and then weighed to the nearest 0.001 g.

7. Procedure

7.1 Place the specimen in the glass cradle, remove the condenser, immerse the cradle by means of a hook in the actively boiling solution (Fig. 1), and immediately replace the condenser. A fresh solution should be used for each test.

7.2 Mark the liquid level on the flask with wax crayon to provide a check on vapor loss which would result in concentration of the acid. If there is an appreciable change in the level (a 0.5-cm or more drop), repeat the test with fresh solution and with a fresh specimen or a reground specimen.

7.3 Continue immersion of the specimen for the length of time specified in Section 2, then remove the specimen, rinse in water and acetone, and dry.

7.4 Weigh the specimen and subtract this mass from the original mass.

7.5 No intermediate weighing are necessary, except as noted in 7.7. The tests can be run without interruption. However, if preliminary results are desired, the specimen can be removed at any time for weighing.

7.6 No replacement of acid is necessary during the test periods.

7.7 If the corrosion rate is extraordinarily high in Method A, as evidenced by a change in color (green) of the solution, additional ferric, sulfate must be added during the test. The amount of ferric sulfate that must be added if the total mass loss of all specimens exceeds 2 g, as indicated by an intermediate weight, is 10 g for each 1 g of dissolved alloy. This does not apply to Method B.

7.8 In Method A, several specimens of the same alloy may be tested simultaneously. The number (3 or 4) is limited only by the number of glass cradles that can be fitted into the flask and the consumption of ferric sulfate. Only one sample of Alloy N10276 should be tested in a flask for Method B.

7.9 During testing, there is some deposition of iron oxides on the upper part for the Erlenmeyer flask. This can be readily removed after test completion by boiling a solution of 10 % hydrochloric acid (HCl) in the flask.

8. Calculation and Interpretation of Results

8.1 *Calculation*—Measure the effect of the acid solution on the material by determining the loss of mass of the specimen. Calculate the corrosion rates as follows:

$$\text{Corrosion Rate} = (K \times W)/A \times T \times D)$$

where

K = a constant (see the following paragraph),
T = time of exposure, h, to the nearest 0.01 h,
A = area, cm^2, to the nearest 0.01 cm^2,
W = mass loss, g, to the nearest 0.001 g, and
D = density, g/cm^3 (see Table 2).

Many different units are used to express corrosion rates. Using the above units for T, A, W, and D, the corrosion rate can be calculated in a variety of units with the following appropriate value of K:

Corrosion Rate Units Desired	Constant K in Corrosion Rate Equation (A)
mils per year (mpy)	3.45×10^6
inches per year (ipy)	3.45×10^3
inches per month (ipm)	2.87×10^2
millimeters per year (mm/Y)	8.76×10^4
micrometers per year (μm/y)	8.76×10^7
picometers per second (pm/s)	2.78×10^6
grams per square meter-hour (g/m^2-h)	$1.00 \times 10^4 \times D^B$
milligrams per square decimeter-day (mdd)	$2.40 \times 10^6 \times D^B$
micrograms per square meter-second (μg/m^2-s)	$2.78 \times 10^6 \times D^B$

[A] If desired, these constants may also be used to convert corrosion rates from one set of units to another. To convert a corrosion rate in units X to a rate in units Y, multiply by K_Y/K_X. For example:

$$15 \text{ mpy} = 15 \times [(2.78 \times 10^6)/(3.45 \times 10^6)]\text{pm/s} = 12.1 \text{ pm/s}$$

[B] Density is not needed to calculate the corrosion rate in these units. The density in the constant K cancels out the density in the corrosion rate equation.

8.2 *Interpretation of Results*—The presence of intergranular attack is usually determined by comparing the calculated corrosion rate to that for properly annealed material. Even in the absence of intergranular attack, the rate of general or grain-face corrosion of properly annealed material will vary from one alloy to another. These

differences are demonstrated in Refs. (1-7).[6]

8.3 As an alternative or in addition to calculating a corrosion rate from mass loss data, metallographic examination may be used to evaluate the degree of intergranular attack. However, metallography is of limited use for evaluating the detrimental effects of prior thermal treatment when the grain size is very small or when there is considerable precipitation of deleterious phases within the grains themselves. In these cases, high corrosion rates may be associated with a general roughening of the surface rather than the more typical undermining and dislodging of grains.

9. Precision and Bias

9.1 The precision and bias for this method are discussed in the references for Method A (1-7) and are dependent on the alloy examined by the method.

METHOD B—23 % H_2SO_4 + 1.2 % HCl + 1 % $FeCl_3$ + 1 % $CuCl_2$ Test

10. Significance and Use

10.1 The boiling 23 % H_2SO_4 + 1.2 % HCl + 1 % $FeCl_3$ + 1 % $CuCl_2$ acid mixture test may be applied to the following alloy in the wrought condition:

Alloy	Testing Time, h
N10276	24

10.2 Nominal composition of this alloy is given in Table 1.

10.3 This practice may be used to evaluate as-received material and to evaluate the effects of subsequent heat treatments. In the case of nickel-rich, chromium-bearing alloys, the method may be applied only to wrought products. The test is not applicable to cast products.

11. Apparatus

11.1 See Section 3.

12. Test Solution

12.1 23 % H_2SO_4 + 1.2 % HCl + 1 % $FeCl_3$ + 1 % $CuCl_2$ Acid Mixture Test—Prepare 600 mL of the solution as follows:

12.1.1 **Caution**—Protect the eyes and use rubber gloves for handling acid. Place the test flask under a hood.

12.1.2 First, weigh 10 g of reagent-grade ferric chloride ($FeCl_3$ $6H_2O$) and put into Erlenmeyer flask.

12.1.3 Then weigh 7.2 g of reagent grade cupric chloride ($CuCl_2$ $2H_2O$) and add to Erlenmeyer flask.

12.1.4 Measure 475 mL of distilled water in a 500-mL graduate and pour into the Erlenmeyer flask.

12.1.4 Then measure 90 mL of reagent-grade sulfuric acid (H_2SO_4) of a concentration that must be in the range from 95.0 to 98.0 weight % in a 100-mL graduate. Add the acid slowly to the water in the Erlenmeyer flask to avoid boiling by the heat evolved. Externally cooling the flask with water during the mixing will reduce overheating.

NOTE 4—Loss of vapor results in concentration of the acid.

12.1.5 Measure 18 mL of reagent-grade hydrochloric acid (HCl) of a concentration that must be in the range from 36.5 to 38 weight % in a 25-mL graduate. Add the acid slowly to the solution to avoid over heating and vapor loss.

12.1.6 Add boiling aids.

12.1.7 Lubricate the ground glass of the condenser joint with silicone grease.

12.1.8 Cover the flask with the condenser and circulate cooling water.

12.1.9 Boil the solution until all ferric chloride and cupric chloride are dissolved.

12.1.10 **Caution**—It has been reported that violent boiling resulting in acid spills can occur. It is important to ensure that the concentration of acid does not become more concentrated and that an adequate number of boiling chips (which are resistant to attack by the test solution) are present.[5]

13. Test Specimens

13.1 See Section 5.

14. Procedure

14.1 See Section 6.

15. Calculation and Interpretation of Results

15.1 See Section 7.

16. Precision and Bias

16.1 The precision and bias for this method are discussed in the references of Method B (6, 7).

[6] The boldface numbers refer to the list of references at the end of these test methods.

TABLE 1 Limiting Compositions of Nickel-Rich, Chromium-Bearing Alloys

	Composition, Weight %														
	Nickel	Chromium	Iron	Molybdenum	Manganese, max	Carbon, max	Copper	Silicon, max	Sulfur, max	Aluminum	Titanium	Columbium and Tantalum	Tungsten	Phosphorus, max	Vanadium, max	Cobalt, max
Hastelloy Alloy C	balance	14.5 to 16.5	4.0 to 7.0	15.0 to 17.0	1.0	0.08	...	1.0	0.030	...	...	...	3.0 to 4.5	0.040	0.35	2.5
Hastelloy Alloy C-276	balance	14.5 to 16.5	4.0 to 7.0	15.0 to 17.0	1.0	0.02	...	0.05	0.030	...	...	...	3.0 to 4.5	0.040	0.35	2.5
Hastelloy Alloy G	balance	21.0 to 23.5	18.0 to 21.0	5.5 to 7.50	1.0 to 2.0	0.05	1.50 to 2.50	1.00	0.030	...	...	1.75 to 2.50	1.0 max	0.040	...	2.5
Carpenter Stainless No. 20 Cb-3	32.0 to 38.0	19.0 to 21.0	balance	2.0 to 3.0	2.0	0.07	3.0 to 4.0	1.0	0.035	...	...	8×C to 1.00	...	0.045	...	...
Inconel Alloy 600	72.0[A] min	14.0 to 17.0	6.0 to 10.0	...	1.0	0.15	0.5	0.5	0.015	...	...	...	...	...	...	...
Inconel Alloy 625	balance	20.0 to 23.0	5.0 max	8.0 to 10.0	0.50	0.10	...	0.5	0.015	0.40	0.40	3.15 to 4.15	...	0.015	...	1.0[B] max
Incoloy Alloy 800	30.0 to 35.0	19.0 to 23.0	balance	...	1.5	0.10	0.75	1.0	0.015	0.15 to 0.60	0.15 to 0.60	...	...	...	...	...
Incoloy Alloy 825	38.0 to 46.0	19.5 to 23.5	balance	2.5 to 3.5	1.0	0.05	1.5 to 3.0	0.5	0.03	0.2	0.6 to 1.2	...	...	...	...	...

[A] = cobalt counting as nickel.
[B] = if determined.

TABLE 2 Density

Alloy	Density, g/cm³
N10276	8.92
N06455	8.92
N06007	8.28
N06985	8.28
N08020	8.05
N06600	8.41
N06625	8.44
N08800	8.03
N08825	8.14

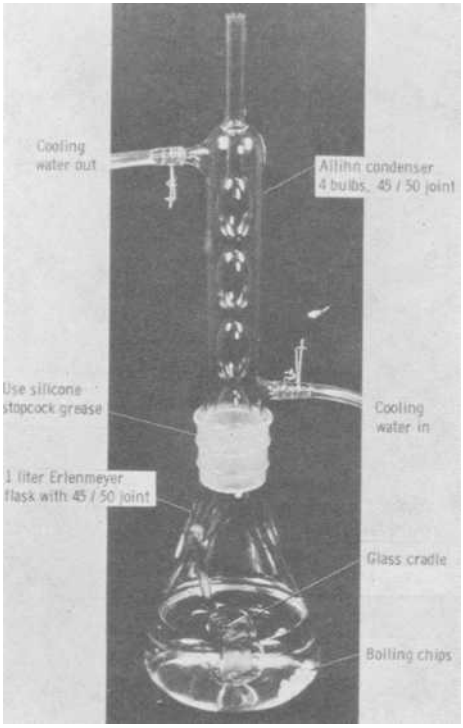


FIG. 1 Apparatus for Ferric Sulfate-Sulfuric Acid Test

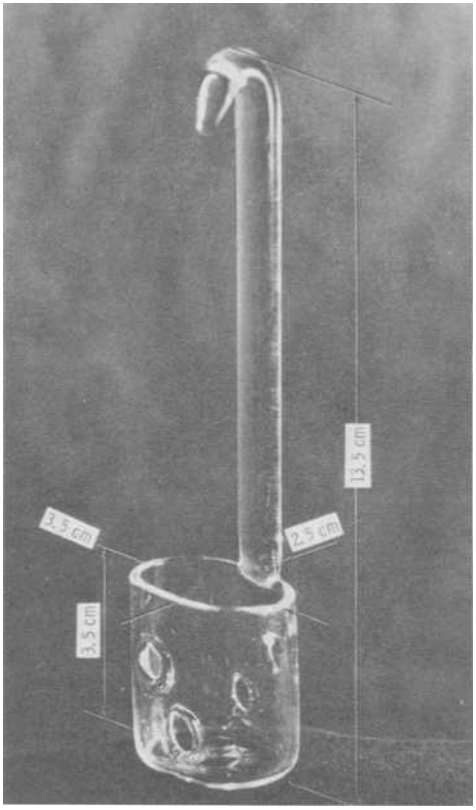


FIG. 2 Glass Cradle

REFERENCES

(1) For original descriptions of the use of the ferric sulfate-sulfuric acid test for nickel-rich, chromium-bearing alloys, see Streicher, M. A., "Relationship of Heat Treatment and Microstructure to Corrosion Resistance in Wrought Ni-Cr-Mo Alloys," *Corrosion*, Vol 19, 1963, pp. 272t–284t.

(2) For application of the ferric sulfate-sulfuric acid test to other nickel-rich, chromium-bearing alloys, see Brown, M. H., "Relationship of Heat Treatment to the Corrosion Resistance of Stainless Alloys," *Corrosion*, Vol 25, 1969, pp. 438–443.

(3) For data on HASTELLOY Alloy C-276, see Leonard, R. B., "Thermal Stability of HASTELLOY Alloy C-276," *Corrosion*, Vol 25, 1969, pp. 222–228.

(4) For data on Carpenter 20CB-3, see Henthorne,

M. and DeBold, T. A., "Intergranular Corrosion Resistance of Carpenter 20CB-3," *Corrosion*, Vol 27, 1971, pp. 255–262.

(5) Streicher, M. A., "Effect of Composition and Structure on Crevice, Intergranular, and Stress Corrosion of Some Wrought Ni-Cr-Mo Alloys," *Corrosion*, Vol 32, 1976, pp. 79–93.

(6) Manning, P. E., "An Improved Intergranular Corrosion Test for HASTELLOY alloy C-276," *ASTM International Symposium or Laboratory Corrosion and Standards*, Bal Harbour, FL, November 14–16, 1983.

(7) ASTM Research Report No. G-1-1002, "Round Robin on New Immersion Test for Detection of Intergranular Corrosion of HASTELLOY alloy C-276."

The American Society for Testing and Materials takes no position respecting the validity of any patent rights asserted in connection with any item mentioned in this standard. Users of this standard are expressly advised that determination of the validity of any such patent rights, and the risk of infringement of such rights, are entirely their own responsibility.

This standard is subject to revision at any time by the responsible technical committee and must be reviewed every five years and if not revised, either reapproved or withdrawn. Your comments are invited either for revision of this standard or for additional standards and should be addressed to ASTM Headquarters. Your comments will receive careful consideration at a meeting of the responsible technical committee, which you may attend. If you feel that your comments have not received a fair hearing you should make your views known to the ASTM Committee on Standards, 1916 Race St., Philadelphia, PA 19103.

Designation: G 31 - 72 (Reapproved 1985)[ε1]

Standard Practice for LABORATORY IMMERSION CORROSION TESTING OF METALS[1]

This standard is issued under the fixed designation G 31; the number immediately following the designation indicates the year of original adoption or, in the case of revision, the year of last revision. A number in parentheses indicates the year of last reapproval. A superscript epsilon (ε) indicates an editorial change since the last revision or reapproval.

[ε1] NOTE—Editorial changes were made throughout in May 1985.

1. Scope

1.1 This practice[2] describes accepted procedures for and factors that influence laboratory immersion corrosion tests, particularly mass loss tests. These factors include specimen preparation, apparatus, test conditions, methods of cleaning specimens, evaluation of results, and calculation and reporting of corrosion rates. This practice also emphasizes the importance of recording all pertinent data and provides a checklist for reporting test data. Other ASTM procedures for laboratory corrosion tests are tabulated in the Appendix.

NOTE 1: **Caution**—In many cases the corrosion product on the reactive metals titanium and zirconium is a hard and tightly bonded oxide that defies removal by chemical or ordinary mechanical means. In many such cases, corrosion rates are established by weight gain rather than weight loss.

1.2 *This standard may involve hazardous materials, operations, and equipment. This standard does not purport to address all of the safety problems associated with its use. It is the responsibility of whoever uses this standard to consult and establish appropriate safety and health practices and determine the applicability of regulatory limitations prior to use.*

2. Applicable Documents

2.1 *ASTM Standards:*

A 262 Practices for Detecting Susceptibility to Intergranular Attack in Stainless Steels[3,4]

E 8 Methods for Tension Testing of Metallic Materials[5]

G 1 Practice for Preparing, Cleaning, and Evaluating Corrosion Test Specimens[4]

G 4 Method for Conducting Corrosion Coupon Tests in Plant Equipment[4]

G 16 Practice for Applying Statistics to Analysis of Corrosion Data[4]

G 46 Recommended Practice for Examination and Evaluation of Pitting Corrosion[4]

3. Significance and Use

3.1 Corrosion testing by its very nature precludes complete standardization. This practice, rather than a standardized procedure, is presented as a guide so that some of the pitfalls of such testing may be avoided.

3.2 Experience has shown that all metals and alloys do not respond alike to the many factors that affect corrosion and that "accelerated" corrosion tests give indicative results only, or may even be entirely misleading. It is impractical to propose an inflexible standard laboratory corrosion testing procedure for general use, except for material qualification tests where standardization is obviously required.

3.3 In designing any corrosion test, consideration must be given to the various factors dis-

[1] This practice is under the jurisdiction of ASTM Committee G-1 on Corrosion of Metals and is the direct responsibility of Subcommittee G01.05 on Laboratory Corrosion Tests.

Current edition approved May 30, 1972. Published July 1972.

[2] This practice is based upon NACE Standard TM-01-69, "Test Method-Laboratory Corrosion Testing of Metals for the Process Industries", with modifications to relate more directly to Practices G 1 and G 31 and Method G 4.

[3] *Annual Book of ASTM Standards*, Vol 01.03.

[4] *Annual Book of ASTM Standards*, Vol 03.02.

[5] *Annual Book of ASTM Standards*, Vol 03.01.

cussed in this practice, because these factors have been found to affect greatly the results obtained.

4. Interferences

4.1 The methods and procedures described herein represent the best current practices for conducting laboratory corrosion tests as developed by corrosion specialists in the process industries. For proper interpretation of the results obtained, the specific influence of certain variables must be considered. These include:

4.1.1 Metal specimens immersed in a specific hot liquid may not corrode at the same rate or in the same manner as in equipment where the metal acts as a heat transfer medium in heating or cooling the liquid. If the influence of heat transfer effects is specifically of interest, specialized procedures (in which the corrosion specimen serves as a heat transfer agent) must be employed (**1**).[6]

4.1.2 In laboratory tests, the velocity of the environment relative to the specimens will normally be determined by convection currents or the effects induced by aeration or boiling or both. If the specific effects of high velocity are to be studied, special techniques must be employed to transfer the environment through tubular specimens or to move it rapidly past the plane face of a corrosion coupon (**2**). Alternatively, the coupon may be rotated through the environment, although it is then difficult to evaluate the velocity quantitatively because of the stirring effects incurred.

4.1.3 The behavior of certain metals and alloys may be profoundly influenced by the presence of dissolved oxygen. If this is a factor to be considered in a specific test, the solution should be completely aerated or deaerated in accordance with 8.7.

4.1.4 In some cases, the rate of corrosion may be governed by other minor constituents in the solution, in which case they will have to be continually or intermittently replenished by changing the solution in the test.

4.1.5 Corrosion products may have undesirable effects on a chemical product. The amount of possible contamination can be estimated from the loss in mass of the specimen, with proper application of the expected relationships among (*1*) the area of corroding surface, (*2*) the mass of the chemical product handled, and (*3*) the duration of contact of a unit of mass of the chemical product with the corroding surface.

4.1.6 Corrosion products from the coupon may influence the corrosion rate of the metal itself or of different metals exposed at the same time. For example, the accumulation of cupric ions in the testing of copper alloys in intermediate strengths of sulfuric acid will accelerate the corrosion of copper alloys, as compared to the rates that would be obtained if the corrosion products were continually removed. Cupric ions may also exhibit a passivating effect upon stainless steel coupons exposed at the same time. In practice, only alloys of the same general type should be exposed in the testing apparatus.

4.1.7 Coupon corrosion testing is predominantly designed to investigate general corrosion. There are a number of other special types of phenomena of which one must be aware in the design and interpretation of corrosion tests.

4.1.7.1 Galvanic corrosion may be investigated by special devices which couple one coupon to another in electrical contact. The behavior of the specimens in this galvanic couple are compared with that of insulated specimens exposed on the same holder and the galvanic effects noted. It should be observed, however, that galvanic corrosion can be greatly affected by the area ratios of the respective metals, the distance between the metals and the resistivity of the electrolyte. The coupling of corrosion coupons then yields only qualitative results, as a particular coupon reflects only the relationship between these two metals at the particular area ratio involved.

4.1.7.2 Crevice corrosion or concentration cell corrosion may occur where the metal surface is partially blocked from the corroding liquid as under a spacer or supporting hook. It is necessary to evaluate this localized corrosion separately from the overall mass loss.

4.1.7.3 Selective corrosion at the grain boundaries (for example, intergranular corrosion of sensitized austenitic stainless steels) will not be readily observable in mass loss measurements unless the attack is severe enough to cause grain dropping, and often requires microscopic examination of the coupons after exposure.

4.1.7.4 Dealloying or "parting" corrosion is a condition in which one constituent is selectively removed from an alloy, as in the dezincification

[6] The boldface numbers in parentheses refer to the list of references at the end of this practice.

of brass or the graphitization of cast iron. Close attention and a more sophisticated evaluation than a simple mass loss measurement is required to detect this phenomenon.

4.1.7.5 Certain metals and alloys are subject to a highly localized type of attack called pitting corrosion. This cannot be evaluated by mass loss alone. The reporting of nonuniform corrosion is discussed below. It should be appreciated that pitting is a statistical phenomenon and that the incidence of pitting may be directly related to the area of metal exposed. For example, a small coupon is not as prone to exhibit pitting as a large one and it is possible to miss the phenomenon altogether in the corrosion testing of certain alloys, such as the AISI Type 300 series stainless steels in chloride contaminated environments.

4.1.7.6 All metals and alloys are subject to stress-corrosion cracking under some circumstances. This cracking occurs under conditions of applied or residual tensile stress, and it may or may not be visible to the unaided eye or upon casual inspection. A metallographic examination may confirm the presence of stress-corrosion cracking. It is imperative to note that this usually occurs with no significant loss in mass of the test coupon, although certain refractory metals are an exception to these observations. Generally, if cracking is observed on the coupon, it can be taken as positive indication of susceptibility, whereas failure to effect this phenomenon simply means that it did not occur under the duration and specific conditions of the test. Separate and special techniques are employed for the specific evaluation of the susceptibility of metals and alloys to stress corrosion cracking (see **Ref. (3)**).

5. Apparatus

5.1 A versatile and convenient apparatus should be used, consisting of a kettle or flask of suitable size (usually 500 to 5000 mL), a reflux condenser with atmospheric seal, a sparger for controlling atmosphere or aeration, a thermowell and temperature-regulating device, a heating device (mantle, hot plate, or bath), and a specimen support system. If agitation is required, the apparatus can be modified to accept a suitable stirring mechanism, such as a magnetic stirrer. A typical resin flask setup for this type test is shown in Fig. 1.

5.2 The suggested components can be modified, simplified, or made more sophisticated to fit the needs of a particular investigation. The suggested apparatus is basic and the apparatus is limited only by the judgment and ingenuity of the investigator.

5.2.1 A glass reaction kettle can be used where the configuration and size of the specimen will permit entry through the narrow kettle neck (for example, 45/50 ground-glass joint). For solutions corrosive to glass, suitable metallic or plastic kettles may be employed.

5.2.2 In some cases a wide-mouth jar with a suitable closure is sufficient when simple immersion tests at ambient temperatures are to be investigated.

5.2.3 Open-beaker tests should not be used because of evaporation and contamination.

5.2.4 In more complex tests, provisions might be needed for continuous flow or replenishment of the corrosive liquid, while simultaneously maintaining a controlled atmosphere.

6. Sampling

6.1 The bulk sampling of products is outside the scope of this practice.

7. Test Specimen

7.1 In laboratory tests, uniform corrosion rates of duplicate specimens are usually within $\pm 10\,\%$ under the same test conditions. Occasional exceptions, in which a large difference is observed, can occur under conditions of borderline passivity of metals or alloys that depend on a passive film for their resistance to corrosion. Therefore, at least duplicate specimens should normally be exposed in each test.

7.2 If the effects of corrosion are to be determined by changes in mechanical properties, untested duplicate specimens should be preserved in a noncorrosive environment at the same temperature as the test environment for comparison with the corroded specimens. The mechanical property commonly used for comparison is the tensile strength. Measurement of percent elongation is a useful index of embrittlement. The procedures for determining these values are shown in detail in Methods E 8.

7.3 The size and shape of specimens will vary with the purpose of the test, nature of the materials, and apparatus used. A large surface-to-mass ratio and a small ratio of edge area to total area are desirable. These ratios can be achieved through the use of square or circular specimens

of minimum thickness. Masking may also be used to achieve the desired area ratios but may cause crevice corrosion problems. Circular specimens should preferably be cut from sheet and not bar stock, to minimize the exposed end grain. Special coupons (for example, sections of welded tubing) may be employed for specific purposes.

7.3.1 A circular specimen of about 38-mm (1.5-in.) diameter is a convenient shape for laboratory corrosion tests. With a thickness of approximately 3 mm (0.125-in.) and an 8-mm (5/16-in.) or 11-mm (7/16-in.) diameter hole for mounting, these specimens will readily pass through a 45/50 ground-glass joint of a distillation kettle. The total surface area of a circular specimen is given by the following equation:

$$A = \pi/2(D^2 - d^2) + t\pi D + t\pi d$$

where:

t = thickness,
D = diameter of the specimen, and
d = diameter of the mounting hole.

7.3.1.2 If the hole is completely covered by the mounting support, the last term ($t\pi d$) in the equation is omitted.

7.3.2 Strip coupons 50 by 25 by 1.6 or 3 mm (2 by 1 by 1/16 or 1/8 in.) may be preferred as corrosion specimens, particularly if interface or liquid line effects are to be studied by the laboratory tests (see Fig. 1), but the evaluation of such specific effects are beyond the scope of this practice.

7.3.3 All specimens should be measured carefully to permit accurate calculation of the exposed areas. A geometric area calculation accurate to ±1 % is usually adequate.

7.4 More uniform results may be expected if a substantial layer of metal is removed from the specimens to eliminate variations in condition of the original metallic surface. This can be done by chemical treatment (pickling), electrolytic removal, or by grinding with a coarse abrasive paper or cloth such as No. 50, using care not to work harden the surface (see 5.7). At least 0.0025 mm (0.0001 in.) or 1.55 to 2.33 mg/cm.^{2} (10 to 15 mg/in.^{2}) should be removed. (If clad alloy specimens are to be used, special attention must be given to ensure that excessive metal is not removed.) After final preparation of the specimen surface, the specimens should be stored in a desiccator until exposure, if they are not used immediately. In special cases (for example, for aluminum and certain copper alloys), a minimum of 24 h storage in a desiccator is recommended. The choice of a specific treatment must be considered on the basis of the alloy to be tested and the reasons for testing. A commercial surface may sometimes yield the most significant results. Too much surface preparation may remove segregated elements, surface contamination, etc., and therefore not be representative.

7.5 Exposure of sheared edges should be avoided unless the purpose of the test is to study effects of the shearing operation. It may be desirable to test a surface representative of the material and metallurgical conditions used in practice.

7.6 The specimen can be stamped with an appropriate identifying mark. If metallic contamination of the stamped area may influence the corrosion behavior, chemical cleaning must be employed to remove any traces of foreign particles from the surface of the coupon (for example, by immersion of stainless steel coupons in dilute nitric acid following stamping with steel dies).

7.6.1 The stamp, besides identifying the specimen, introduces stresses and cold work in the specimen that could be responsible for localized corrosion or stress-corrosion cracking, or both.

7.6.2 Stress-corrosion cracking at the identifying mark is a positive indication of susceptibility to such corrosion. However, the absence of cracking should not be interpreted as indicating resistance (see 4.1.7.6).

7.7 Final surface treatment of the specimens should include finishing with No. 120 abrasive paper or cloth or the equivalent, unless the surface is to be used in the mill finished condition. This resurfacing may cause some surface work hardening, to an extent which will be determined by the vigor of the surfacing operation, but is not ordinarily significant. The surface finish to be encountered in service may be more appropriate for some testing.

7.7.1 Coupons of different alloy compositions should never be ground on the same cloth.

7.7.2 Wet grinding should be used on alloys which work harden quickly, such as the austenitic stainless steels.

7.8 The specimens should be finally degreased by scrubbing with bleach-free scouring powder, followed by thorough rinsing in water and in a suitable solvent (such as acetone, methanol, or a mixture of 50 % methanol and 50 % ether), and air dried. For relatively soft metals (such as aluminum, magnesium, and copper), scrubbing with abrasive powder is not always needed and

can mar the surface of the specimen. Proper ultrasonic procedures are an acceptable alternate. The use of towels for drying may introduce an error through contamination of the specimens with grease or lint.

7.9 The dried specimens should be weighed on an analytical balance to an accuracy of at least ±0.5 mg. If cleaning deposits (for example, scouring powder) remain or lack of complete dryness is suspected, then recleaning and drying is performed until a constant mass is attained.

7.10 The method of specimen preparation should be described when reporting test results, to facilitate interpretation of data by other persons.

7.11 The use of welded specimens is sometimes desirable, because some welds may be cathodic or anodic to the parent metal and may affect the corrosion rate.

7.11.1 The heat-affected zone is also of importance but should be studied separately, because welds on coupons do not faithfully reproduce heat input or size effects of full-size weldments.

7.11.2 Corrosion of a welded coupon is best reported by description and thickness measurements rather than a mils per year rate, because the attack is normally localized and not representative of the entire surface.

7.11.3 A complete discussion of corrosion testing of welded coupons or the effect of heat treatment on the corrosion resistance of a metal is not within the scope of this practice.

8. Test Conditions

8.1 Selection of the conditions for a laboratory corrosion test will be determined by the purpose of the test.

8.1.1 If the test is to be a guide for the selection of a material for a particular purpose, the limits of the controlling factors in service must be determined. These factors include oxygen concentration, temperature, rate of flow, pH value, composition, and other important characteristics of the solution.

8.2 An effort should be made to duplicate all pertinent service conditions in the corrosion test.

8.3 It is important that test conditions be controlled throughout the test in order to ensure reproducible results.

8.4 The spread in corrosion rate values for duplicate specimens in a given test probably should not exceed ±10 % of the average when the attack is uniform.

8.5 *Composition of Solution:*

8.5.1 Test solutions should be prepared accurately from chemicals conforming to the Specifications of the Committee on Analytical Reagents of the American Chemical Society[7] and distilled water, except in those cases where naturally occurring solutions or those taken directly from some plant process are used.

8.5.2 The composition of the test solutions should be controlled to the fullest extent possible and should be described as completely and as accurately as possible when the results are reported.

8.5.2.1 Minor constituents should not be overlooked because they often affect corrosion rates.

8.5.2.2 Chemical content should be reported as percentage by weight of the solutions. Molarity and normality are also helpful in defining the concentration of chemicals in some test solutions.

8.5.3 If problems are suspected, the composition of the test solutions should be checked by analysis at the end of the test to determine the extent of change in composition, such as might result from evaporation or depletion.

8.5.4 Evaporation losses may be controlled by a constant level device or by frequent addition of appropriate solution to maintain the original volume within ±1 %. Preferably, the use of a reflux condenser ordinarily precludes the necessity of adding to the original kettle charge.

8.5.5 In some cases, composition of the test solution may change as a result of catalytic decomposition or by reaction with the test coupons. These changes should be determined if possible. Where required, the exhausted constituents should be added or a fresh solution provided during the course of the test.

8.5.6 When possible, only one type of metal should be exposed in a given test (see 4.1.6).

8.6 *Temperature of Solution:*

8.6.1 Temperature of the corroding solution should be controlled within ±1°C (±1.8°F) and

[7] "Reagent Chemicals. American Chemical Society Specifications." Am. Chemical Soc., Washington, DC. For suggestions on the testing of reagents not listed by the American Chemical Society, see "Reagent Chemicals and Standards," by Joseph Rosin, D. Van Nostrand Co., Inc., New York, NY, and the "United States Pharmacopeia."

must be stated in the report of test results.

8.6.2 If no specific temperature, such as boiling point, is required or if a temperature range is to be investigated, the selected temperatures used in the test, and their respective duration, must be reported.

8.6.3 For tests at ambient temperature, the tests should be conducted at the highest temperature anticipated for stagnant storage in summer months. This temperature may be as high as from 40 to 45°C (104 to 113°F) in some areas. The variation in temperature should be reported also (for example, 40 ± 2°C).

8.7 *Aeration of Solution:*

8.7.1 Unless specified, the solution should not be aerated. Most tests related to process equipment should be run with the natural atmosphere inherent in the process, such as the vapors of the boiling liquid.

8.7.2 If aeration is employed, the specimen should not be located in the direct air stream from the sparger. Extraneous effects can be encountered if the air stream impinges on the specimens.

8.7.3 If exclusion of dissolved oxygen is necessary, specific techniques are required, such as prior heating of the solution and sparging with an inert gas (usually nitrogen). A liquid atmospheric seal is required on the test vessel to prevent further contamination.

8.7.4 If oxygen saturation of the test solution is desired, this can best be achieved by sparging with oxygen. For other degrees of aeration, the solution should be sparaged with air or synthetic mixtures of air or oxygen with an inert gas. Oxygen saturation is a function of the partial pressure of oxygen in the gas.

8.8 *Solution Velocity:*

8.8.1 The effect of velocity is not usually determined in normal laboratory tests, although specific tests have been designed for this purpose.

8.8.2 Tests at the boiling point should be conducted with the minimum possible heat input, and boiling chips should be used to avoid excessive turbulence and bubble impingement.

8.8.3 In tests below the boiling point, thermal convection generally is the only source of liquid velocity.

8.8.4 In test solutions with high viscosity, supplemental controlled stirring with a magnetic stirrer is recommended.

8.9 *Volume of Test Solution:*

8.9.1 The volume of the test solution should be large enough to avoid any appreciable change in its corrosivity during the test, either through exhaustion of corrosive constituents or by accumulation of corrosion products that might affect further corrosion.

8.9.2 Two examples of a minimum "solution volume-to-specimen area" ratio are 20 mL/cm^2 (125 mL/in.^{2}) of specimen surface (Practice A 262), and 40 mL/cm^2 (250 mL/in.^{2}).

8.9.3 When the test objective is to determine the effect of a metal or alloy on the characteristics of the test solution (for example, to determine the effects of metals on dyes), it is desirable to reproduce the ratio of solution volume to exposed metal surface that exists in practice. The actual time of contact of the metal with the solution must also be taken into account. Any necessary distortion of the test conditions must be considered when interpreting the results.

8.10 *Method of Supporting Specimens:*

8.10.1 The supporting device and container should not be affected by or cause contamination of the test solution.

8.10.2 The method of supporting specimens will vary with the apparatus used for conducting the test, but should be designed to insulate the specimens from each other physically and electrically and to insulate the specimens from any metallic container or supporting device used within the apparatus.

8.10.3 Shape and form of the specimen support should assure free contact of the specimen with the corroding solution, the liquid line, or the vapor phase as shown in Fig. 1. If clad alloys are exposed, special procedures will be required to ensure that only the cladding is exposed, unless the purpose is to test the ability of the cladding to protect cut edges in the test solution.

8.10.4 Some common supports are glass or ceramic rods, glass saddles, glass hooks, fluorocarbon plastic strings, and various insulated or coated metallic supports.

8.11 *Duration of Test:*

8.11.1 Although duration of any test will be determined by the nature and purpose of the test, an excellent procedure for evaluating the effect of time on corrosion of the metal and also on the corrosiveness of the environment in laboratory tests has been presented by Wachter and Treseder **(4)**. This technique is called the "planned interval test," and the procedure and evaluation of results

are given in Table 1. Other procedures that require the removal of solid corrosion products between exposure periods will not measure accurately the normal changes of corrosion with time.

8.11.2 Materials that experience severe corrosion generally do not ordinarily need lengthy tests to obtain accurate corrosion rates. However, there are cases where this assumption is not valid. For example, lead exposed to sulfuric acid corrodes at an extremely high rate at first, while building a protective film; then the rates decrease considerably so that further corrosion is negligible. The phenomenon of forming a protective film is observed with many corrosion-resistant materials. Therefore, short tests on such materials would indicate a high corrosion rate and be completely misleading.

8.11.3 Short-time tests also can give misleading results on alloys that form passive films, such as stainless steels. With borderline conditions, a prolonged test may be needed to permit breakdown of the passive film and subsequent more rapid attack. Consequently, tests run for long periods are considerably more realistic than those conducted for short durations. This statement must be qualified by stating that corrosion should not proceed to the point where the original specimen size or the exposed area is drastically reduced or where the metal is perforated.

8.11.4 If anticipated corrosion rates are moderate or low, the following equation gives the suggested test duration:

$$\text{Hours} = 2000/(\text{corrosion rate in mpy})$$

where mpy = mils per year (see 11.2.1 and Note 2 for conversion to other units).

8.11.4.1 *Example*—Where the corrosion rate is 10 mpy, the test should run for at least 200 h.

8.11.4.2 This method of estimating test duration is useful only as an aid in deciding, after a test has been made, whether or not it is desirable to repeat the test for a longer period. The most common testing periods are 48 to 168 h (2 to 7 days).

8.11.5 In some cases, it may be necessary to know the degree of contamination caused by the products of corrosion. This can be accomplished by analysis of the solution after corrosion has occurred. The corrosion rate can be calculated from the concentration of the matrix metal found in the solution and it can be compared to that determined from the mass loss of the specimens. However, some of the corrosion products usually adhere to the specimen as a scale and the corrosion rate calculated from the metal content in the solution is not always correct.

8.12 The design of corrosion testing programs is further discussed in Practice G 16.

9. Methods of Cleaning Specimens after Test

9.1 Before specimens are cleaned, their appearance should be observed and recorded. Location of deposits, variations in types of deposits, or variations in corrosion products are extremely important in evaluating localized corrosion, such as pitting and concentration cell attack.

9.2 Cleaning specimens after the test is a vital step in the corrosion test procedure and if not done properly, can cause misleading results.

9.2.1 Generally, the cleaning procedure should remove all corrosion products from specimens with a minimum removal of sound metal.

9.2.2 Set rules cannot be applied to specimen cleaning, because procedures will vary, depending on the type of metal being cleaned and on the degree of adherence of corrosion products.

9.3 Cleaning methods can be divided into three general categories: mechanical, chemical, and electrolytic.

9.3.1 Mechanical cleaning includes scrubbing, scraping, brushing, mechanical shocking, and ultrasonic procedures. Scrubbing with a bristle brush and mild abrasive is the most popular of these methods. The others are used principally as a supplement to remove heavily encrusted corrosion products before scrubbing. Care should be used to avoid the removal of sound metal.

9.3.2 Chemical cleaning implies the removal of material from the surface of the specimen by dissolution in an appropriate chemical solution. Solvents such as acetone, carbon tetrachloride, and alcohol are used to remove oil, grease, or resin and are usually applied prior to other methods of cleaning. Chemicals are chosen for application to a specific material. Methods for chemical cleaning after testing of specific metals and alloys are described in Practice G 1.

9.3.3 Electrolytic cleaning should be preceded by scrubbing to remove loosely adhering corrosion products. A method of electrolytic cleaning is described in Practice G 1.

9.3.3.1 Precautions must be taken to ensure good electrical contact with the specimen, to avoid contamination of the solution with easily

reducible metal ions, and to ensure that inhibitor decomposition has not occurred.

9.4 Whatever treatment is used to clean specimens after a corrosion test, its effect in removing metal should be determined and the mass loss should be corrected accordingly. A "blank" specimen should be weighed before and after exposure to the cleaning procedure to establish this mass loss (see also Practice G 1). Careful observation is needed to ensure that pitting does not occur during cleaning.

9.4.1 Following removal of all scale, the specimen should be treated as discussed in 5.8.

9.4.2 The description of the cleaning method should be included with the data reported.

10. Interpretation of Results

10.1 After corroded specimens have been cleaned, they should be reweighed with an accuracy corresponding to that of the original weighing. The mass loss during the test period can be used as the principal measure of corrosion.

10.2 After the specimens have been reweighed, they should be examined carefully for the presence of any pits. If there are any pits, the average and maximum depths of pits are determined with a pit gage or a calibrated microscope which can be focused first on the edges and then on the bottoms of the pits. The degree of lateral spreading of pits may also be noted.

10.2.1 Pit depths should be reported in millimeters or thousandths of an inch for the test period and not interpolated or extrapolated to millimeters per year, thousandths of an inch per year, or any other arbitrary period because rarely, if ever, is the rate of initiation or propagation of pits uniform.

10.2.2 The size, shape, and distribution of pits should be noted. A distinction should be made between those occurring underneath the supporting devices (concentration cells) and those on the surfaces that were freely exposed to the test solution (see Recommended Practice G 46).

10.3 If the material being tested is suspected of being subject to dealloying forms of corrosion such as dezincification or to intergranular attack, a cross section of the specimen should be microscopically examined for evidence of such attack.

10.4 The specimen may be subjected to simple bending tests to determine whether any embrittlement attack has occurred.

10.5 It may be desirable to make quantitative mechanical tests, comparing the exposed specimens with uncorroded specimens reserved for the purpose, as described in 7.2.

11. Calculating Corrosion Rates

11.1 Calculating corrosion rates requires several pieces of information and several assumptions:

11.1.1 The use of corrosion rates implies that all mass loss has been due to general corrosion and not to localized corrosion, such as pitting or intergranular corrosion of sensitized areas on welded coupons. Localized corrosion is reported separately.

11.1.2 The use of corrosion rates also implies that the material has not been internally attacked as by dezincification or intergranular corrosion.

11.1.3 Internal attack can be expressed as a corrosion rate if desired. However, the calculations must not be based on weight loss (except in qualification tests such as Practice A 262), which is usually small but on microsections which show depth of attack.

11.2 Assuming that localized or internal corrosion is not present or is recorded separately in the report, the average corrosion rate can be calculated by the following equation:

$$\text{Corrosion rate} = (K \times W)/(A \times T \times D)$$

where:

K = a constant (see below)
T = time of exposure in hours to the nearest 0.01 h,
A = area in cm^2 to the nearest 0.01 cm^2,
W = mass loss in g, to nearest 1 mg (corrected for any loss during cleaning (see 9.4)), and
D = density in g/cm^3, (see Appendix X1 of Practice G 1).

11.2.1 Many different units are used to express corrosion rates. Using the above units for T, A, W, and D, the corrosion rate can be calculated in a variety of units with the following appropriate value of K:

Corrosion Rate Units Desired	Constant (K) in Corrosion Rate Equation
mils per year (mpy)	3.45×10^6
inches per year (ipy)	3.45×10^3
inches per month (ipm)	2.87×10^2
millimetres per year (mm/y)	8.76×10^4
micrometres per year (μm/y)	8.76×10^7
picometres per second (pm/s)	2.78×10^6

Corrosion Rate Units Desired	Constant (K) in Corrosion Rate Equation
grams per square metre per hour (g/$m^2 \cdot h$)	$1.00 \times 10^4 \times D^A$
milligrams per square decimetre per day (mdd)	$2.40 \times 10^6 \times D^A$
micrograms per square metre per second ($\mu g/m^2 \cdot s$)	$2.78 \times 10^6 \times D^A$

[A] Density is not needed to calculate the corrosion rate in these units. The density in the constant K cancels out the density in the corrosion rate equation.

NOTE 2—If desired, these constants may also be used to convert corrosion rates from one set of units to another. To convert a corrosion rate in units X to a rate of units Y, multiply by K_Y/K_X for example:

$$15 \text{ mpy} = 15 \times [(2.78 \times 10^6)/(3.45 \times 10^6)]\text{pm/s} = 12.1 \text{ pm/s}$$

12. Reporting the Data

12.1 The importance of reporting all data as completely as possible cannot be overemphasized.

12.2 Expansion of the testing program in the future or correlating the results with tests of other investigators will be possible only if all pertinent information is properly recorded.

12.3 The following checklist is a recommended guide for reporting all important information and data.

12.3.1 Corrosive media and concentration (any changes during test).

12.3.2 Volume of test solution.

12.3.3 Temperature (maximum, minimum, average).

12.3.4 Aeration (describe conditions or technique).

12.3.5 Agitation (describe conditions or technique).

12.3.6 Type of apparatus used for test.

12.3.7 Duration of each test.

12.3.8 Chemical composition or trade name of metals tested.

12.3.9 Form and metallurgical conditions of specimens.

12.3.10 Exact size, shape, and area of specimens.

12.3.11 Treatment used to prepare specimens for test.

12.3.12 Number of specimens of each material tested, and whether specimens were tested separately or which specimens tested in the same container.

12.3.13 Method used to clean specimens after exposure and the extent of any error expected by this treatment.

12.3.14 Initial and final masses and actual mass losses for each specimen.

12.3.15 Evaluation of attack if other than general, such as crevice corrosion under support rod, pit depth and distribution, and results of microscopical examination or bend tests.

12.3.16 Corrosion rates for each specimen.

12.4 Minor occurrences or deviations from the proposed test program often can have significant effects and should be reported if known.

12.5 Statistics can be a valuable tool for analyzing the results from test programs designed to generate adequate data. Excellent references for the use of statistics in corrosion studies include **Ref. (5)** through **(7)** and in Practice G 16.

REFERENCES

(1) Fisher, A. O. and Whitney, Jr., F. L., "Laboratory Methods for Determining Corrosion Rates Under Heat Flux Conditions," *Corrosion*, Vol 15, No. 5, May 1959, p. 257t.

(2) U.S. Patent 3,228,236, 1969.

(3) "Stress Corrosion Test Environments and Test Durations," *Symposium on Stress Corrosion Testing, ASTM STP 425*, ASTM, 1967.

(4) Wachter, A. and Treseder, R. S., "Corrosion Testing Evaluation of Metals for Process Equipment," *Chemical Engineering Progress*, Vol 43, June 1947, pp. 315–326.

(5) Mickley, H. S., Sherwood, T. K., and Reed, C. E. editors, *Applied Mathematics in Chemical Engineering* 2nd Edition, McGraw-Hill Book Co., New York, NY 1957.

(6) Youden, W. J., *Experimentation and Measurement*, National Science Teachers Assn., Washington, DC, 1962.

(7) Booth, F. F. and Tucker, G. E. G., "Statistical Distribution of Endurance in Electrochemical Stress-Corrosion Tests," *Corrosion*, Vol 21, No. 5, May 1965, pp. 173–177.

(8) Champion, F. A., *Corrosion Testing Procedures*, 2nd Edition, John Wiley & Sons, Inc., New York, NY, 1965.

TABLE 1 Planned Interval Corrosion Test

(Reprinted by permission from *Chemical Engineering Progress*, June 1947.)

Identical specimens all placed in the same corrosive fluid. Imposed conditions of the test kept constant for entire time $t + 1$. Letters, A_1, A_t, A_{t+1}, B, represent corrosion damage experienced by each test specimen. A_2 is calculated by subtracting A_t from A_{t+1}.

Occurrences During Corrosion Test		Criteria
Liquid corrosiveness	unchanged	$A_1 = B$
	decreased	$B < A_1$
	increased	$A_1 < B$
Metal corrodibility	unchanged	$A_2 = B$
	decreased	$A_2 < B$
	increased	$B < A_2$

Combinations of Situations

Liquid corrosiveness	Metal corrodibility	Criteria
1. unchanged	unchanged	$A_1 = A_2 = B$
2. unchanged	decreased	$A_2 < A_1 = B$
3. unchanged	increased	$A_1 = B < A_2$
4. decreased	unchanged	$A_2 = B < A_1$
5. decreased	decreased	$A_2 < B < A_1$
6. decreased	increased	$A_1 > B < A_2$
7. increased	unchanged	$A_1 < A_2 = B$
8. increased	decreased	$A_1 < B > A_2$
9. increased	increased	$A_1 < B < A_2$

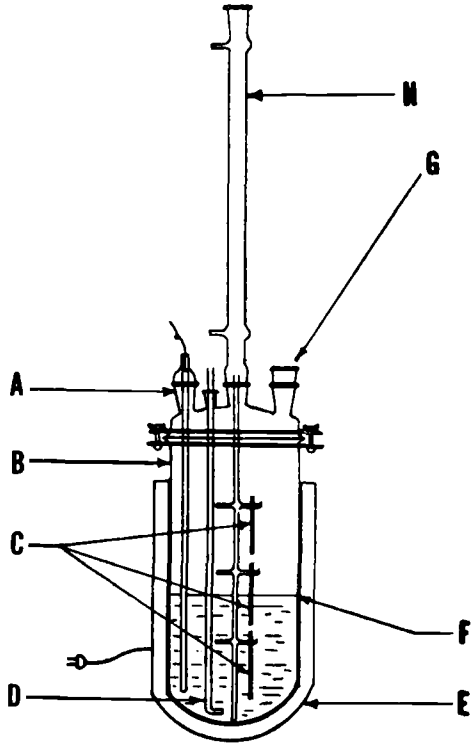
Example: Conditions: Duplicate strips of low-carbon steel, each ¾ by 3 in., immersed in 200 mL of 10 % $AlCl_3$-90 % $SbCl_3$ mixture through which dried HCl gas was slowly bubbled at atmospheric pressure. Temperature 90°C.

	Interval, days	Mass Loss, mg	Penetration, mils	Apparent Corrosion Rate, mpy
A_1	0–1	1080	1.69	620
A_t	0–3	1430	2.24	270
A_{t+1}	0–4	1460	2.29	210
B	3–4	70	0.11	40
A_2	calc. 3–4	30	0.05	18

Example: $A_2 < B < A_1$

$0.05 < 0.11 < 1.69$

Therefore, liquid markedly decreased in corrosiveness during test, and formation of partially protective scale on the steel was indicated.



NOTE—The flask can be used as a versatile and convenient apparatus to conduct simple immersion tests. Configuration of top to flask is such that more sophisticated apparatus can be added as required by the specific test being conducted. *A* = thermowell, *B* = resin flask, *C* = specimens hung on supporting device, *D* = air inlet, *E* = heating mantle, *F* = liquid interface, *G* = opening in flask for additional apparatus that may be required, and *H* = reflux condenser.

FIG. 1 Typical Resin Flask

The American Society for Testing and Materials takes no position respecting the validity of any patent rights asserted in connection with any item mentioned in this standard. Users of this standard are expressly advised that determination of the validity of any such patent rights, and the risk of infringement of such rights, are entirely their own responsibility.

This standard is subject to revision at any time by the responsible technical committee and must be reviewed every five years and if not revised, either reapproved or withdrawn. Your comments are invited either for revision of this standard or for additional standards and should be addressed to ASTM Headquarters. Your comments will receive careful consideration at a meeting of the responsible technical committee, which you may attend. If you feel that your comments have not received a fair hearing you should make your views known to the ASTM Committee on Standards, 1916 Race St., Philadelphia, PA 19103.

Designation: G 34 - 79

Standard Test Method for EXFOLIATION CORROSION SUSCEPTIBILITY IN 2XXX AND 7XXX SERIES ALUMINUM ALLOYS (EXCO TEST)[1]

This standard is issued under the fixed designation G 34; the number immediately following the designation indicates the year of original adoption or, in the case of revision, the year of last revision. A number in parentheses indicates the year of last reapproval. A superscript epsilon (ε) indicates an editorial change since the last revision or reapproval.

This method has been approved for use by agencies of the Department of Defense and for listing in the DoD Index of Specifications and Standards.

1. Scope

1.1 This method describes a procedure for constant immersion exfoliation corrosion (EXCO) testing of high-strength 2XXX and 7XXX series aluminum alloys.

1.2 This method applies only to wrought products such as sheet, plate, extrusions, and forgings.

1.3 This method can be used with any form of specimen or part that can be immersed in the test solution.

2. Applicable Documents

2.1 *ASTM Standards:*

D 1193 Specification for Reagent Water[2]

E 3 Methods of Preparation of Metallographic Specimens[3]

G 15 Definitions of Terms Relating to Corrosion and Corrosion Testing[4]

3. Summary of Method

3.1 This method provides an accelerated exfoliation corrosion test for 2XXX and 7XXX series aluminum alloys that involves the continuous immersion of test materials in a solution containing 4 *M* sodium chloride, 0.5 *M* potassium nitrate, and 0.1 *M* nitric acid at 25 ± 3°C (77 ± 5°F). The susceptibility to exfoliation is determined by visual examination, with performance ratings established by reference to standard photographs.

4. Significance and Use

4.1 Use of this method provides a useful prediction of the exfoliation corrosion behavior of these alloys in various types of outdoor service, especially in marine and industrial environments.[5] The test solution is very corrosive and represents the more severe types of environmental service, excluding, of course, unusual chemicals not likely to be encountered in "natural" environments.

4.2 The exfoliation ratings were arbitrarily chosen to illustrate a wide range in resistance to exfoliation in this test. However, it remains to be determined whether correlations can be established between EXCO test ratings and realistic service conditions for a given alloy. It is an ongoing activity of the Joint Task Group on Exfoliation Corrosion of Aluminum Alloys (Aluminum Association and ASTM G01.05.02.08 Task Group) to maintain outdoor exposure tests for this purpose. For example, it has been reported[6] that samples of Al-Zn-Mg-

---

[1] This method is under the jurisdiction of ASTM Committee G-1 on Corrosion of Metals and is the direct responsibility of Subcommittee G01.05 on Laboratory Corrosion Tests.

Current edition approved April 27, 1979. Published June 1979. Originally published as G 34 - 72. Last previous edition G 34 - 72.

[2] *Annual Book of ASTM Standards*, Vols 02.05, 05.05, 06.03, 09.01, 10.01, 10.02, 10.05, 11.01, and 15.09.

[3] *Annual Book of ASTM Standards*, Vol 03.03.

[4] *Annual Book of ASTM Standards*, Vol 03.02.

[5] Ketcham, S. J., and Jeffrey, P. W., "Exfoliation Corrosion Testing of 7178 and 7075 Aluminum Alloys" (Report of ASTM G01.05 Interlaboratory Testing Program in Cooperation with the Aluminum Association); and Sprowls, D. O., Walsh, J. D., and Shumaker, M. B., "Simplified Exfoliation Testing of Aluminum Alloys," *Localized Corrosion—Cause of Metal Failure, ASTM STP 516*, Am. Soc. Testing Mats., 1972.

[6] Sprowls, D. O., Summerson, T. J., and Loftin, F. E., "Exfoliation Corrosion Testing of 7075 and 7178 Aluminum Alloys—Interim Report on Atmospheric Exposure Tests" (Report of ASTM G01.05.02 Interlaboratory Testing Program in Cooperation with the Aluminum Association); and Lifka, B. W. and Sprowls, D. O., "Relationship of Accelerated Test Methods for Exfoliation Resistance in 7XXX Series Aluminum Alloys With Exposure to a Seacoast Atmosphere," *Corrosion in Natural Environments, ASTM STP 558*, Am. Soc. Testing Mats., 1974.

Cu alloys rated EA in a 48-h EXCO test did not develop more than a slight amount of incipient exfoliation (EA) during a four-year exposure in a seacoast atmosphere, whereas, ED rated materials in most cases developed severe exfoliation within a year in the seacoast atmosphere. It is anticipated that additional comparisons will become available as the outdoor tests are extended.

5. Definitions

5.1 *exfoliation*—corrosion that proceeds laterally from the sites of initiation along planes parallel to the surface, generally at grain boundaries, forming corrosion products that force metal away from the body of the material giving rise to a layered appearance (Definitions G 15).

6. Apparatus

6.1 Any suitable glass, plastic, or similarly inert container can be used to contain the solution and specimens during the period of test. Depending upon the shape and size of the specimens, rods or racks of glass, plastic, or any inert substance shall be used to support the specimen above the bottom of the container. The container should be fitted with a loose-fitting cover to reduce evaporation.

7. Reagents

7.1 *Purity of Reagents*—The test solution shall be prepared with reagent grade sodium chloride (NaCl), potassium nitrate (KNO_3), and nitric acid (HNO_3).

7.2 *Purity of Water*—Distilled or deionized water conforming to Specification D 1193, Type IV, shall be used to prepare the test solution.

7.3 A test solution of the following composition shall be used:

NaCl	(4.0 *M*)
KNO_3	(0.5 *M*)
HNO_3	(0.1 *M*)

Dissolve 234 g of NaCl, 50 g of KNO_3 in water, and add 6.3 ml of concentrated HNO_3 (70 weight %). Dilute to 1 litre. This solution has an apparent pH of 0.4.

7.4 The solution shall be maintained at a temperature of 25 ± 3°C (77 ± 5°F).

8. Sampling

8.1 Sampling procedures are not considered applicable to this standard, as they are often covered by product specifications. It is assumed that the test specimens are removed from representative samples of materials.

9. Test Specimens

9.1 Specimens may be of any practical size or shape. Nevertheless, for the results to be of most significance a specimen size of at least 50 by 100 mm (2 by 4 in.), or the equivalent, is recommended.

9.2 The edges of sawed specimens need not be machined, but specimens obtained by blanking or shearing shall have edges dressed by machining or filling to a depth equal to the thickness of the specimen to remove cold-worked metal.

9.3 Remove the cladding of alclad sheet by machining the test surface; remove or mask the cladding on the back side (non-test surface) also.

9.4 When removing test specimens from extrusions and forgings, take care to avoid specimen locations underneath flanges, ribs, etc., where the grain structure is usually variable.

10. Standardization

10.1 To provide an indication when some inadvertent deviation from the correct test conditions occurs, it is necessary to expose to the test at regular intervals a control specimen of a material with known resistance. This control should exhibit the same degree of exfoliation each time it is included in the test.

10.2 The control may be any material of the alloy type included in the scope of this standard, preferably one with an intermediate degree of susceptibility (Figs. 4 and 5).

11. Procedure

11.1 Degrease the specimens with a suitable solvent.

11.2 Mask the back surfaces of the specimens to minimize corrosion of non-test areas. Protective coatings must have good adherence to avoid crevice corrosion beneath the coating; also, they should not contain leachable ions or protective oils that will influence the corrosion of the test surface.[7]

[7] Coatings that have been satisfactorily used include: No. 35 Vinyl Plastic Electrical Tape or No. 470 Electroplaters Tape made by the Minnesota Mining and Mfg. Co., St. Paul, Minn.

11.3 Use the solution in sufficient quantity to provide a volume-to-metal surface area ratio of 10 to 30 ml/cm^2 (65 to 200 ml/in.^{2}). Include all exposed metal area in the determination of total surface area.

11.4 Use fresh solution at the start of each test. Do not change the solution even though the pH increases during the test. It is normal for the pH to increase from the initial apparent value of 0.4 to about 3 during the first several hours depending upon the amount of corrosion that occurs.

11.5 Immerse the specimens in the solution using rods or racks of inert material to support the specimens above the bottom of the container. Place the test surface upward in a horizontal position to prevent loss of exfoliated metal from the surface of the specimen. Do not concurrently immerse in the same container alloys containing less than 0.25 % copper with those containing greater amounts of copper.

11.6 The following maximum periods of exposure are recommended for testing the alloy types indicated:

2XXX Series	96 h
7XXX Series	48 h

The length of time to develop exfoliation in material of a given alloy and temper may vary with the mill product form, with some materials developing severe exfoliation in much shorter periods than those listed. Therefore, inspect test specimens in place and rate in accordance with Section 12 at periods such as 5, 24, 48, and 72 h, and discontinue the exposure of a specimen when it has developed the most severe exfoliation rating (Fig. 6).

11.7 Rate the performance of test specimens in accordance with Section 12 immediately after discontinuation of the exposure while the specimen is still wet or moist, taking into account all loose products of exfoliation lying on the test specimen or on the bottom of the container.

11.8 Clean exposed test specimens by rinsing in water and soaking in concentrated nitric acid only after the specimens have been inspected and rated.

12. Interpretation of Results

12.1 The following codes and classifications shall be used when reporting the visual rating of corroded specimens:

Classification	Code
No appreciable attack	N
Pitting	P
Exfoliation	EA through ED

12.2 Descriptions of the various classifications, which are illustrated in Figs. 1 through 6,[8] are as follows:

12.2.1 *N*—No appreciable attack: Surface may be discolored or etched, but no evidence of pitting or exfoliation.

12.2.2 *P*—Pitting: Discrete pits, sometimes with a tendency for undermining and slight lifting of metal at the pit edges (Figs. 1a and 2).

12.2.3 *EA through ED*—Exfoliation:

12.2.3.1 Visible separation of the metal into layers manifested in various forms, such as blisters, slivers, flakes, fairly continuous sheets, and sometimes granular particles resulting from disintegration of thin layers, depending upon the grain morphology of the sample. Various degrees of exfoliation with increasing penetration and loss of metal are illustrated in Figs. 3 through 6.

12.2.3.2 The formation of tiny "pit-blisters" or the dislodgement of an extremely thin surface layer of metal after only a few hours of exposure may resemble superficial exfoliation (EA), but can in fact result from undermining pitting. If continued exposure to the recommended periods in 11.6 produces more corrosion but no evidence of advancing delamination, metallographic examination (see Methods E 3) will be required to determine whether the initial effect was truly exfoliation (Fig. 1b) or undermining pitting (Fig. 1a); in the latter case the rating should be P.

12.2.3.3 When exfoliation occurs in isolated sites, rate the attack in the individual sites rather than the relative number of sites.

12.3 The visual ratings are intended to be finite indications of the resistance to exfoliation, and care should be taken when rating a series of test specimens to compare them with the photographs and captions in Figs. 2 through 6 rather than with each other. The final rating of a specimen shall be determined by the poorest classification observed during the exposure.

[8] Enlarged glossy prints of Figs. 1 through 6 are available from ASTM Headquarters. Order PCN 12-700340-22.

13. Report

13.1 The report should contain the following essential information:

13.1.1 Alloy and temper of the material tested,

13.1.2 Mill product, section thickness, and the surface tested, including reference to applicable product specification,

13.1.3 Sampling procedure if other than that specified in referenced product specification,

13.1.4 A rating of the test specimens using the codes and classifications in Section 12, and

13.1.5 Notation of any deviation in test procedure from that set forth in preceding paragraphs.

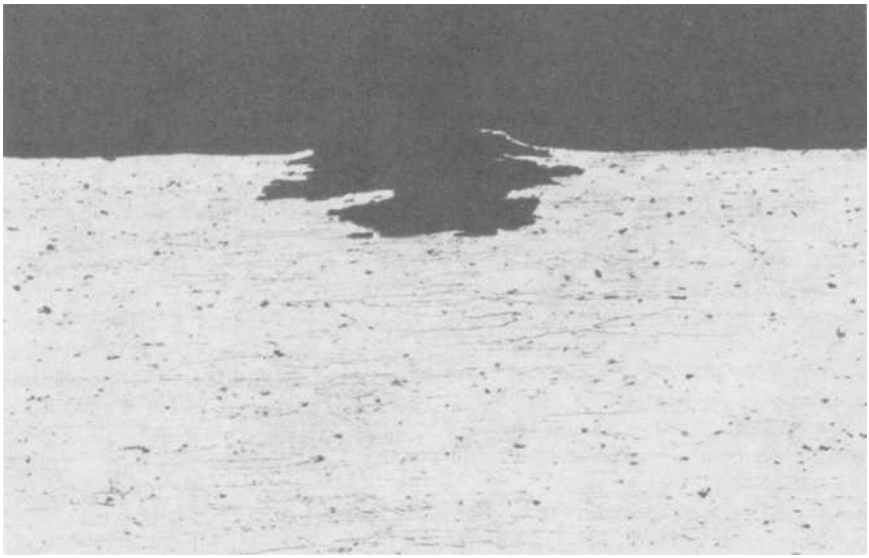
13.2 Other information that may be desirable for certain types of reports includes:

13.2.1 Size, type, and number of replicate specimens; method of edge preparation, and

13.2.2 Volume to surface ratio.

14. Precision and Accuracy

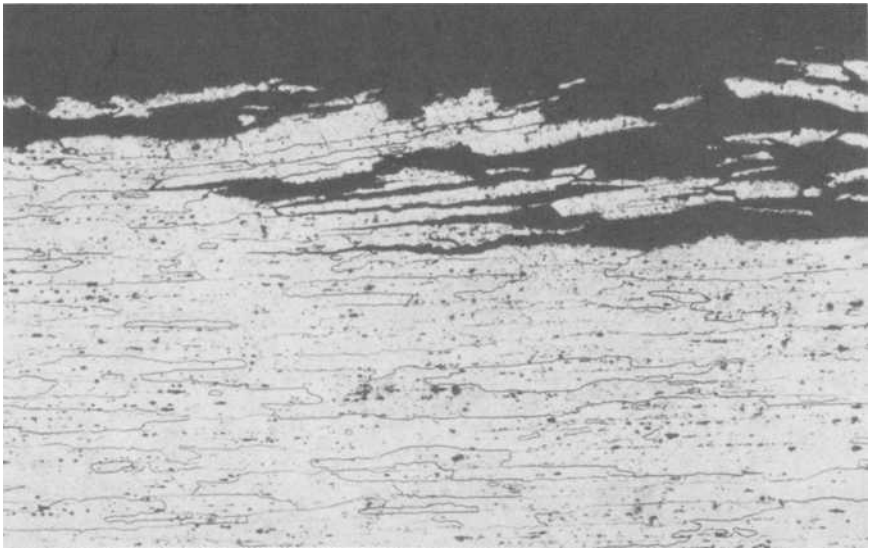
14.1 Exfoliation ratings obtained by the visual interpretation guidelines in Section 12 are, at best, judgments by the inspector. Hence, they are subject to variation among inspectors, but experience has shown that differences greater than one rating letter are rare among trained inspectors.



1a— Undermining pitting that may from the surface give the appearance of incipient exfoliation.

The American Society for Testing and Materials takes no position respecting the validity of any patent rights asserted in connection with any item mentioned in this standard. Users of this standard are expressly advised that determination of the validity of any such patent rights, and the risk of infringement of such rights, are entirely their own responsibility.

This standard is subject to revision at any time by the responsible technical committee and must be reviewed every five years and if not revised, either reapproved or withdrawn. Your comments are invited either for revision of this standard or for additional standards and should be addressed to ASTM Headquarters. Your comments will receive careful consideration at a meeting of the responsible technical committee, which you may attend. If you feel that your comments have not received a fair hearing you should make your views known to the ASTM Committee on Standards, 1916 Race St., Philadelphia, Pa. 19103.



1b— Exfoliation resulting from rapid lateral attack of selective boundaries or strata forming wedges of corrosion product that force layers of metal upward giving rise to a layered appearance.

FIG. 1 Metallographic Sections Illustrating Two Different Types of Attack (Keller's Etch; 100×).

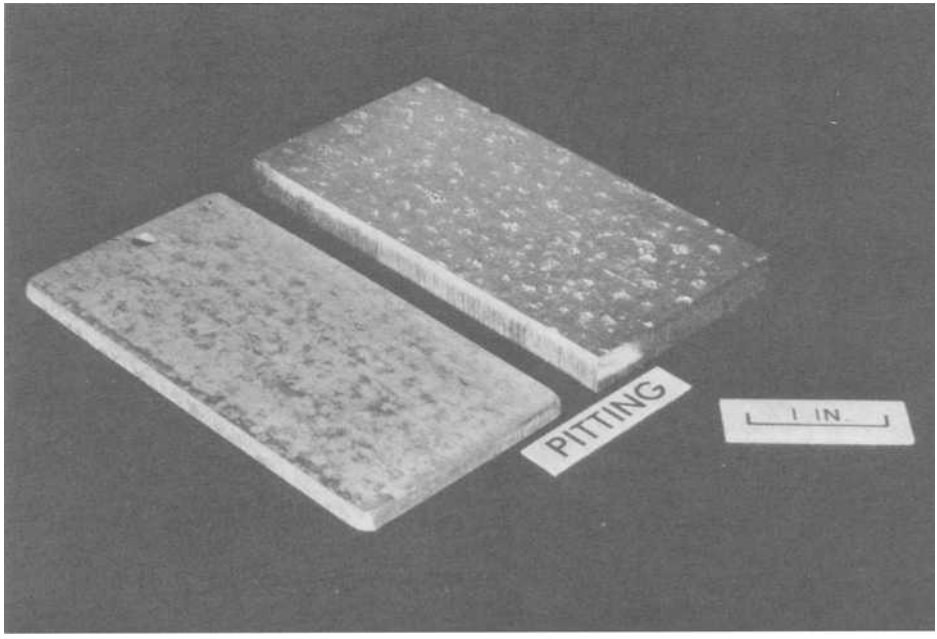
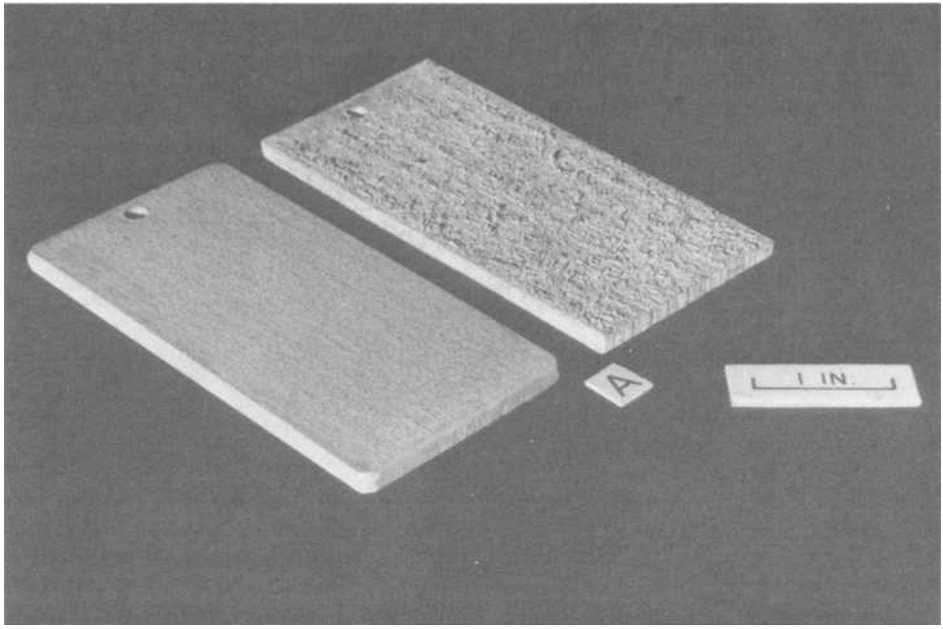
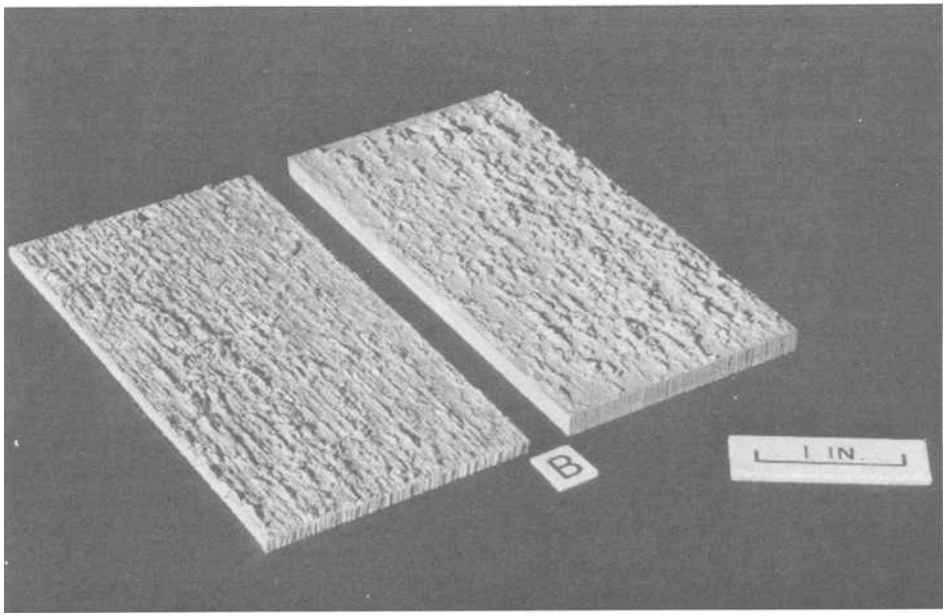


FIG. 2 Examples of Pitting Corrosion.



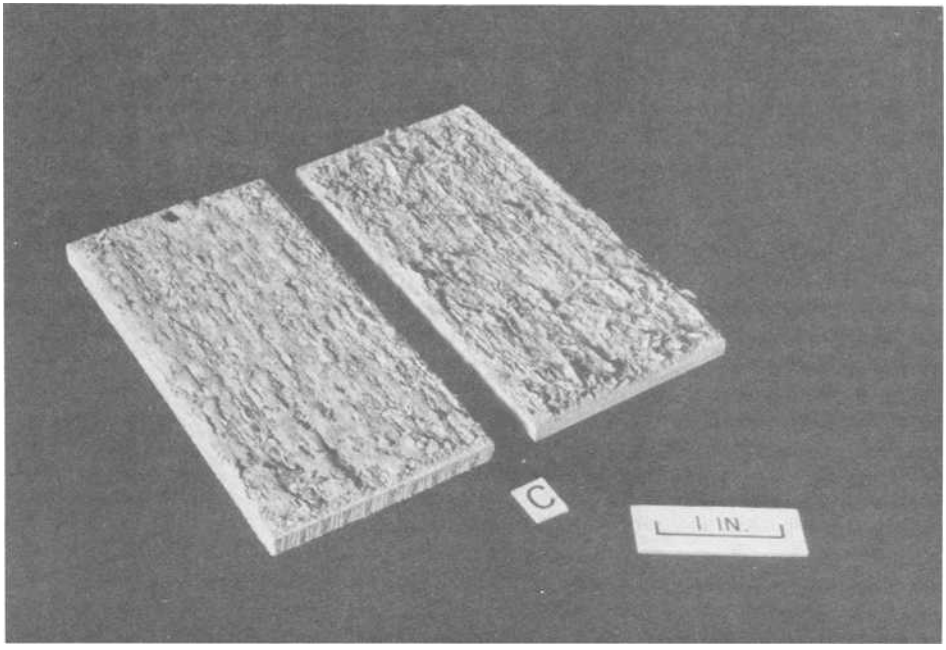
NOTE—The panel on the right illustrates an extreme condition, and a worse appearing panel should be given a less favorable rating.

FIG. 3 Examples of Exfoliation Rating EA (Superficial): Tiny Blisters, Thin Slivers, Flakes or Powder, with only Slight Separation of Metal.



NOTE—The panel on the right illustrates an extreme condition.

FIG. 4 Example of Exfoliation Rating EB (moderate); notable layering and penetration into the metal.



NOTE The panel on the right illustrates an extreme condition.

FIG. 5 Examples of Exfoliation Rating EC (severe): Penetration to a Considerable Depth into the Metal.

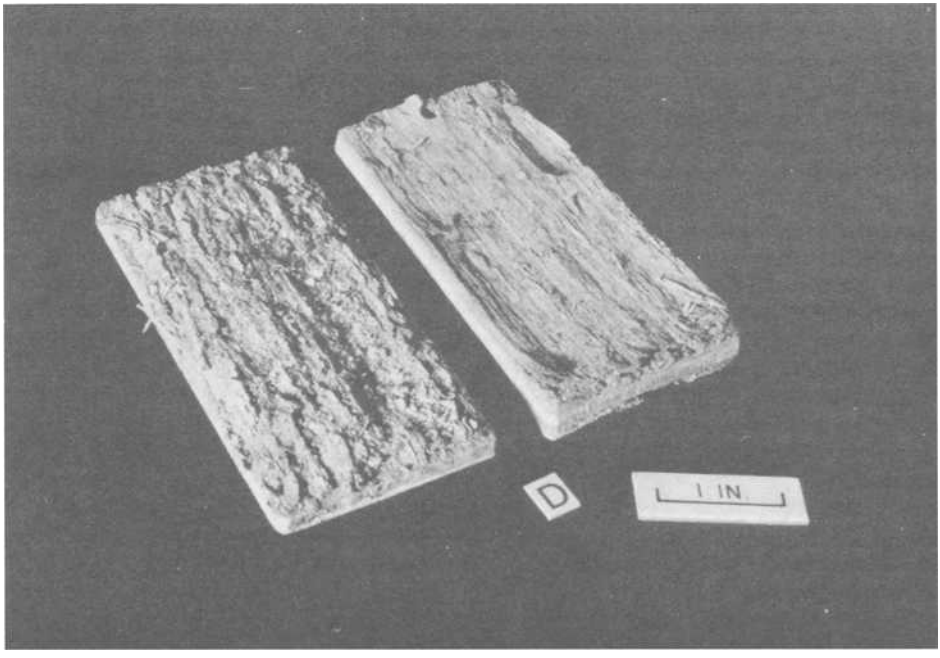


FIG. 6 Examples of Exfoliation rating ED (Very Severe) (similar to EC except for much greater penetration and loss of metal).

Designation: G 46 - 76 (Reapproved 1980)

Standard Recommended Practice for EXAMINATION AND EVALUATION OF PITTING CORROSION[1]

This standard is issued under the fixed designation G 46; the number immediately following the designation indicates the year of original adoption or, in the case of revision, the year of last revision. A number in parentheses indicates the year of last reapproval. A superscript epsilon (ε) indicates an editorial change since the last revision or reapproval.

1. Scope

1.1 This recommended practice is a guide to assist in the selection of procedures that can be used in the identification and examination of pits and in the evaluation of pitting corrosion to determine the extent of its effect.

2. Applicable Documents

2.1 *ASTM Standards:*

E 3 Methods of Preparation of Metallographic Specimens[2]

G 1 Practice for Preparing, Cleaning, and Evaluating Corrosion Test Specimens[3]

G 16 Practice for Applying Statistics to Analysis of Corrosion Data[3]

2.2 *National Association of Corrosion Engineers Standard:*

RP-01-73 Collection and Identification of Corrosion Products[4]

3. Significance

3.1 It is important to be able to determine the extent of pitting, either in a service application where it is necessary to predict the remaining life in a metal structure, or in laboratory test programs that are used to select the most pitting-resistant materials for service.

4. Definition

4.1 *pitting* – the localized corrosion of a metal surface, confined to a point or small area, that takes the form of cavities.

5. Identification and Examination of Pits

5.1 *Visual Inspection* – A visual examination of the corroded metal surface is usually beneficial, and this is done under ordinary light, with or without the use of a low-power magnifying glass, to determine the extent of corrosion and the apparent location of pits. It is often advisable to photograph the corroded surface at this point so that it can be compared with the clean surface after the removal of corrosion products.

5.1.1 If the metal specimen has been exposed to an unknown environment, the composition of the corrosion products may be of value in determining the cause of corrosion. Follow recommended procedures in the removal of particulate corrosion products and reserve them for future identification (see NACE Standard RP-01-73).

5.1.2 To expose the pits fully, use recommended cleaning procedures to remove the corrosion products and avoid solutions that attack the base metal excessively (see Practice G 1). It may be advisable during cleaning to probe the pits with a pointed tool to determine the extent of undercutting or subsurface corrosion (Fig. 1). However, scrubbing with a stiff bristle brush will often enlarge the pit openings sufficiently by removal of corrosion products, or undercut metal to make the pits easier to evaluate.

5.1.3 Examine the cleaned metal surface under ordinary light to determine the approximate size and distribution of pits. Follow this procedure by a more detailed examination through a microscope using low magnification (20×).

5.1.4 Determine the size, shape, and den-

[1] This recommended practice is under the jurisdiction of ASTM Committee G-1 on Corrosion of Metals, and is the direct responsibility of Subcommittee G01.05 on Laboratory Corrosion Tests.

Current edition approved April 9, 1976. Published July 1976.

[2] *Annual Book of ASTM Standards*, Vol 03.03.

[3] *Annual Book of ASTM Standards*, Vol 03.02.

[4] Insert in *Materials Protection and Performance*, Vol 12, June 1973, p. 65.

sity of pits.

5.1.4.1 Pits may have various sizes and shapes. A visual examination of the metal surface may show a round, elongated, or irregular opening, but it seldom provides an accurate indication of corrosion beneath the surface. Thus, it is often necessary to cross section the pit to see its actual shape and to determine its true depth. Several variations in the cross-sectioned shape of pits are shown in Fig. 1.

5.1.4.2 It is a tedious job to determine pit density by counting pits through a microscope eyepiece, but the task can be made easier by the use of a plastic grid. Place the grid, containing 3 to 6-mm squares, on the metal surface. Count and record the number of pits in each square, and move across the grid in a systematic manner until all the surface has been covered. This approach minimizes eyestrain because the eyes can be taken from the field of view without fear of losing the area of interest.

5.1.5 *Metallographic Examination*—Select and cut out a representative portion of the metal surface containing the pits and prepare a metallographic specimen in accordance with the recommended procedures given in Method E 3. Examine microscopically to determine whether there is a relation between pits and inclusions or microstructure, or whether the cavities are true pits or might have resulted from metal dropout caused by intergranular corrosion, dealloying, etc.

5.2 *Nondestructive Inspection*—A number of techniques have been developed to assist in the detection of cracks or cavities in a metal surface without destroying the material **(1)**.[5] These methods are less effective for locating and defining the shape of pits than some of those previously discussed, but they merit consideration because they are often used *in situ*, and thus are more applicable to field applications.

5.2.1 *Radiographic*—Radiation, such as X rays, are passed through the object. The intensity of the emergent rays varies with the thickness of the material. Imperfections may be detected if they cause a change in the absorption of X rays. Detectors or films are used to provide an image of interior imperfections. The metal thickness that can be inspected is dependent on the available energy output. Pores or pits must be as large as 1/2% of the metal thickness to be detected. This technique has only slight application to pitting detection, but it might be a useful means to compare specimens before and after corrosion to determine whether pitting has occurred and whether it is associated with previous porosity. It may also be useful to determine the extent of subsurface and undercutting pitting (Fig. 1).

5.2.2 *Electromagnetic:*

5.2.2.1 Eddy currents can be used to detect defects or irregularities in the structure of electrically conducting materials. When a specimen is exposed to a varying magnetic field, produced by connecting an alternating current to a coil, eddy currents are induced in the specimen, and they in turn produce a magnetic field of their own. Materials with defects will produce a magnetic field that is different from that of a reference material without defects, and an appropriate detection instrument is required to determine these differences.

5.2.2.2 The induction of a magnetic field in ferromagnetic materials is another approach that is used. Discontinuities that are transverse to the direction of the magnetic field cause a leakage field to form above the surface of the part. Ferromagnetic particles are placed on the surface to detect the leakage field and to outline the size and shape of the discontinuities. Rather small imperfections can be detected by this method. However, the method is limited by the required directionality of defects to the magnetic field, by the possible need for demagnetization of the material, and by the limited shape of parts that can be examined.

5.2.3 *Sonics:*

5.2.3.1 In the use of ultrasonics, pulses of sound energy are transmitted through a couplant, such as oil or water, onto the metal surface where waves are generated. The reflected echoes are converted to electrical signals that can be interpreted to show the location of flaws or pits. Both contact and immersion methods are used. The test has good sensitivity and provides instantaneous information about the size and location of flaws. However, reference standards are required

[5] The boldface numbers in parentheses refer to the list of references at the end of this recommended practice.

for comparison, and training is needed to interpret the results properly.

5.2.3.2 An alternative approach is to use acoustic emissions in detecting flaws in metals. Imperfections, such as pits, generate high-frequency emissions under thermal or mechanical stress. The frequency of emission and the number of occurrences per unit time determine the presence of defects.

5.2.4 *Penetrants* – Defects opening to the surface can be detected by the application of a penetrating liquid that subsequently exudes from the surface after the excess penetrant has been removed. Defects are located by spraying the surface with a developer that reacts with a dye in the penetrant, or the penetrant may contain a fluorescent material that is viewed under black light. The size of the defect is shown by the intensity of the color and the rate of bleed-out. This technique provides only an approximation of the depth and size of pits.

5.2.5 None of these nondestructive test methods provide satisfactory detailed information about pitting. They can be used to locate pits and to provide some information about the size of pits, but they generally are not able to detect small pits, and confusion may arise in attempting to differentiate between pits and other surface blemishes. Most of these methods were developed to detect cracks or flaws in metals, but with more refined development they may become more applicable to pitting measurements.

6. Extent of Pitting

6.1 *Weight Loss* – Metal weight loss is not ordinarily recommended for use as a measure of the extent of pitting unless general corrosion is slight and pitting is fairly severe. If uniform corrosion is significant, the contribution of pitting to total metal loss is small, and pitting damage cannot be determined accurately from weight loss. In any case, weight loss can only provide information about total metal loss due to pitting but nothing about depth of penetration. However, weight loss should not be neglected in every case because it may be of value; for example, weight loss along with a visual comparison of pitted surfaces may be adequate to evaluate the pitting resistance of alloys in laboratory tests.

6.2 *Pit Depth Measurement:*

6.2.1 *Metallographic*—Pit depth can be determined by sectioning vertically through a preselected pit, mounting the cross-sectioned pit metallographically, and polishing the surface. The depth of the pit is measured on the flat, polished surface by the use of a microscope with a calibrated eyepiece. The method is very accurate, but it requires good judgment in the selection of the pit and good technique in cutting through the pit. Its limitations are that it is time consuming, the deepest pit may not have been selected, and the pit may not have been sectioned at the deepest point of penetration.

6.2.2 *Machining* **(2, 3):**

6.2.2.1 This method requires a sample that is fairly regular in shape, and it involves the destruction of the specimen. Measure the thickness of the specimen between two areas that have not been affected by general corrosion. Select a portion of the surface on one side of the specimen that is relatively unaffected; then machine the opposite surface where the pits are located on a precision lathe, grinder, or mill until all signs of corrosion have disappeared. (Some difficulty from galling and smearing may be encountered with soft metals, and pits may be obliterated.) Measure the thickness of the specimen between the unaffected surface and subtract from the original thickness to give the maximum depth of pitting. Repeat this procedure on the unmachined surface unless the thickness has been reduced by 50% or more during the machining of the first side.

6.2.2.2 This method is equally suitable for determining the number of pits with specific depths. Count the visible pits; then machine away the surface of the metal in measured stages and count the number of visible pits remaining at each stage. Subtract the number of pits at each stage from the count at the previous stage to obtain the number of pits at each depth of cut.

6.2.3 *Micrometer or Depth Gage:*

6.2.3.1 This method is based on the use of a pointed needle attached to a micrometer or calibrated depth gage to penetrate the pit cavity. Zero the instrument on an unaffected area at the lip of the pit. Insert the needle in the pit until it reaches the base where a new measurement is taken. The distance traveled by the needle is the depth of the pit. It is best to use

constant-tension instruments to minimize metal penetration at the base of the pit. It can be advantageous to use a stereomicroscope in conjunction with this technique so that the pit can be magnified to ensure that the needle point is at the bottom of the pit. The method is limited to pits that have a sufficiently large opening to accommodate the needle without obstruction; this eliminates those pits where undercutting or directional orientation has occurred.

6.2.3.2 In a variation of this method, attach the probe to a spherometer and connect through a microammeter and battery to the specimen **(3, 4).** When the probe touches the bottom of the pit, it completes the electrical circuit, and the probe movement is a measurement of pit depth. This method is limited to very regularly shaped pits because contact with the side of the pit would give a false reading.

6.2.4 *Microscopical*—This method is particularly valuable when pits are too narrow or difficult to penetrate with a probe type of instrument. The method is amenable to use as long as light can be focused on the base of the pit, which would not be possible in the case of example (*e*) in Fig. 1.

6.2.4.1 Use a metallurgical microscope with a magnification range from 50 to 500X and a calibrated fine-focus knob (for example, 1 division = 0.001 mm). If the latter is not available, a dial micrometer can be attached to the microscope in such a way that it will show movement of the stage relative to the microscope body.

6.2.4.2 Locate a single pit on the metal surface and center under the objective lens of the microscope at low magnification (for example, 50X). Increase the objective lens magnification until the pit area covers most of the field under view. Focus the specimen surface at the lip of the pit, using first the coarse and then the fine-focusing knobs of the microscope. Record the initial reading from the fine-focusing knob. Refocus on the bottom of the pit with the fine-focusing knob and record the reading. The difference between the initial and the final readings on the fine-focusing knob is the pit depth.

6.2.4.3 Repeat the steps in 6.2.4.2 to obtain additional measurements or until satisfactory duplication has been obtained. The repeatability of pit depth measurements on a single pit at four magnifications is shown in Annex A1.

6.2.4.4 A variation of the microscopical technique employs the use of an interference microscope. A beam of light is split, and one portion is projected on the specimen and the other on a reference mirror surface. The reflected light from these two surfaces is recombined, and interference fringes are formed that provide a topographical map of the specimen surface. These fringes can be used to measure vertical deviations on the metal surface. However, the method is limited to the shallower pits, that is, less than 25 μm, because the number of fringes increases to the point where they are difficult to count.

7. Evaluation of Pitting

7.1 There are several ways in which pitting can be described, given a quantitative expression to indicate its significance, or used to predict the life of a material. Some of the more commonly used methods are described in this section, although it is often found that no single method is sufficient by itself.

7.2 *Standard Charts* **(3):**

7.2.1 Rate the pits in terms of density, size, and depth on the basis of standard charts, such as those shown in Fig. 2. Columns A and B relate to the extent of pitting at the surface of the metal (that is, Column A is a means for rating the number of sites per unit area and Column B a means for showing the average size of these sites). Column C rates the intensity or average depth of attack. A typical rating might be A-3, B-2, C-3, representing a density of 5×10^4 pits/m^2, an average pit opening of 2.0 mm^2, and an average pit depth of 1.6 mm.

7.2.2 This method offers an effective means of communication between those who are familiar with the charts, and it is a simple means for storing data for comparison with other test results. However, it is tedious and time consuming to measure all pits, and the time is usually not justified because maximum values (for example, pit depths) usually have more significance than average values.

7.3 *Metal Penetration:*

7.3.1 Measure the deepest pits and express metal penetration in terms of the maximum pit depth or the average of the ten deepest

pits, preferably both. This type of measurement is particularly significant when the metal is associated with an enclosure for a gas or liquid, and a hole could lead to a loss of fluid.

7.3.2 Metal penetration can also be expressed in terms of a pitting factor. This is the ratio of the deepest metal penetration to the average metal penetration, determined from weight loss, as shown in the following relationship:

$$\text{Pitting Factor} = \frac{\text{deepest metal penetration}}{\text{average metal penetration}}$$

A pitting factor of one represents uniform corrosion; the larger the number, the greater the depth of penetration. The factor does not apply in those cases where pitting or general corrosion is very small because values of zero or infinity can readily be obtained when dealing with a ratio.

7.4 *Statistical:*

7.4.1 The application of statistics to the analysis of corrosion data is covered in detail in Practice G 16. The subject is discussed briefly in this standard to show that statistics have a bearing on the evaluation of pitting data; more detailed information can be obtained from other publications.

7.4.2 The probability that pits will initiate on a metal surface is dependent on a number of factors, such as the pitting tendency of the metal, the corrosivity of the solution, the specimen area, and the time of exposure. A pitting probability test can be conducted to determine the susceptibility of metals to pitting, but it will not provide information about the rate of propagation, and the results are only applicable to the conditions of exposure. The pitting probability (P) in % after the exposure of a number of specimens to a particular set of conditions can be expressed as follows **(5, 6):**

$$P = \frac{N_p}{N} \times 100$$

where:

N_p = number of specimens that pit, and

N = total number of specimens.

7.4.2 The relationship between pit depth and area or time of exposure may vary with the environment, the metal exposed, and other variables. The relationships cited in 7.4.2.1 and 7.4.2.2 are examples that have been found to apply under certain exposure conditions.

7.4.2.1 The following relationship was found between the maximum pit depth (D) and the area (A) of a pipeline exposed to soil **(7, 8, 9):**

$$D = bA^a$$

where a and $b > 0$, and a and b are constants that were derived from the slope and the y-intercept of a straight line curve obtained when the logarithms of the mean pit depth for successively increasing areas on the pipe were plotted against the logarithms of the corresponding areas. The dependence on area is attributed to the increased chance for the deepest pit to be found when the size of the sample of pits is increased through an increased area of corroded surface.

7.4.2.2 The maximum pit depth (D) of aluminum exposed to various waters was found to vary as the cube root of time (t), as shown in the following relationship **(5, 10):**

$$D = Kt^{1/3}$$

K is a constant that is a function of the composition of the water and alloy. This relationship has been found to apply to several aluminum alloys exposed to different waters.

7.4.3 Extreme value probability statistics **(11, 12)** have been applied successfully to maximum pit depth data to estimate the maximum pit depth of a large area of material on the basis of examination of a small portion of that area **(3, 5, 10).** The procedure is to measure maximum pit depths on several replicate specimens that have pitted, and then arrange the pit depth values in order of increasing rank. A plotting position for each order of ranking is obtained by substituting in the relation, $M/(n+1)$, where M = order of ranking, and n = total number of specimens or values. For example, the plotting position for the second value out of 10 would be $2/(10+1) = 0.1818$. These values are plotted on the ordinate of extreme value probability paper versus their respective maximum pit depths. If a straight line is obtained, it shows that extreme value statistics apply. Extrapolation of the straight line can be used to determine the probability that a specific depth will occur or the number of observations that must be made to find a particular pit depth.

7.5 *Loss in Mechanical Properties* – If pitting is the predominant form of corrosion and the density of pitting is relatively high, the change in a mechanical property may be used advantageously to evaluate the degree of pitting. Typical properties that are considered for this purpose are tensile strength, elongation, fatigue strength, impact resistance, and burst pressure **(13, 14)**.

7.5.1 The precautions that must be taken in the application of these mechanical test procedures are covered in most standard methods, but it must be stressed that it is important to use as nearly replicate specimens as possible for both the exposed and unexposed specimens. Thus, consideration should be given to edge effects, direction of rolling, surface conditions, etc.

7.5.2 Representative specimens of the metal are exposed to the same conditions except for the corrosive environment. The mechanical properties of the exposed and unexposed specimens are measured after the exposure; the difference between the two results is attributed to corrosion.

7.5.3 Some of these methods are more properly suited to the evaluation of other forms of localized corrosion, such as intergranular or stress corrosion, so their limitations must be considered. The often erratic nature of pitting and the location of pits on the specimen can affect results. In some cases the change in mechanical properties due to pitting may be too small to provide meaningful results. Probably one of the most difficult problems is to separate the effects due to pitting from those caused by some other form of corrosion.

8. Report

8.1 The report should include as much detailed information as possible, such as the following:

8.1.1 Metallurgical treatment of the metal, surface preparation, and final surface finish before exposure to test,

8.1.2 Environmental conditions and duration of exposure,

8.1.3 Appearance of the corroded surface before and after cleaning,

8.1.4 Identification of corrosion products,

8.1.5 Characterization of pits to include: size, shape, density, uniformity of distribution, depth (average and maximum), and location of pits with reference to microstructure, face, edge, crevice, etc.,

8.1.6 Change in mechanical properties as the result of corrosion, and the method by which determined, and

8.1.7 Statistical information.

REFERENCES

(1) Mock, J. A., "A Guide to Nondestructive Testing," *Materials Engineering*, MAENB, Vol 69, June 1969, p. 60.

(2) Bengough, G. D. and Wormwell, F., Special Report for Corrosion Committee, *Iron and Steel Institute*, Vol 3, 1935, p. 168.

(3) Champion, F. A., *Corrosion Testing Procedures*, 2nd ed., John Wiley & Sons, New York, N. Y., 1965, p. 205.

(4) Thornhill, R. S., *Journal of the Iron and Steel Institute*, JISIA, Vol 146, 1942, p. 90P.

(5) Pathak, B. R., "Testing in Fresh Waters," *Handbook on Corrosion Testing and Evaluation*, W. H. Ailor, ed., John Wiley & Sons, New York, N.Y., 1971, p. 553.

(6) Aziz, P. M., and Godard, H. P., "Influence of Specimen Area on the Pitting Probability of Aluminum," *Journal of the Electrochemical Society*, JESOA, Vol 102, October 1955, p. 577.

(7) Scott, G. N., "Adjustment of Soil Corrosion Pit Depth Measurements for Size of Sample," *Proceedings of the American Petroleum Institute, Section IV*, PAPPA, Vol 14, 1934, p. 204.

(8) Romanoff, M., *Underground Corrosion*, National Bureau of Standards Circular 579, Washington, D. C.: U.S. Govt. Printing Office, 1957, p. 71.

(9) Denison, I. A., "Soil Exposure Tests," *Corrosion Handbook*, H. H. Uhlig, ed., John Wiley & Sons, New York, N.Y., 1948, p. 1048.

(10) Godard, H. P., "The Corrosion Behavior of Aluminum in Natural Waters," *Canadian Journal of Chemical Engineering*, CJCEA, Vol 38, October 1960, p. 1671.

(11) Gumbel, E. J., *Statistical Theory of Extreme Values and Some Practical Applications*, U. S. Dept. of Commerce Applied Mathematics Series 33, 1954.

(12) Aziz, P. M., "Application of the Statistical Theory of Extreme Values to the Analysis of Maximum Pit Depth Data for Aluminum," *Corrosion*, CORRA, Vol 12, October 1956, p. 495t.

(13) Summerson, T. J., Pryor, M. J., Keir, D. S., and Hogan, R. J., "Pit Depth Measurements as a Means of Evaluating the Corrosion Resistance of Aluminum in Sea Water," *Metals, ASTM STP 196*, Am. Soc. Testing Mats., 1957, p. 157.

(14) Baboian, R., "Corrosion Resistant High-Strength Clad Metal System for Hydraulic Brake Line Tubing," *SAE Preprint No. 740290*, Detroit, Mich., 1972.

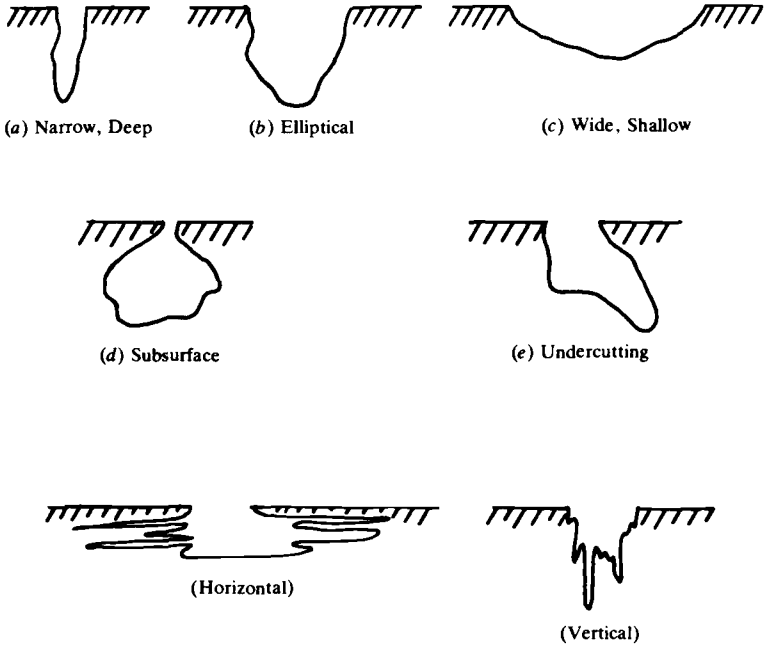


Fig. 1 Variations in the Cross-Sectional Shape of Pits.

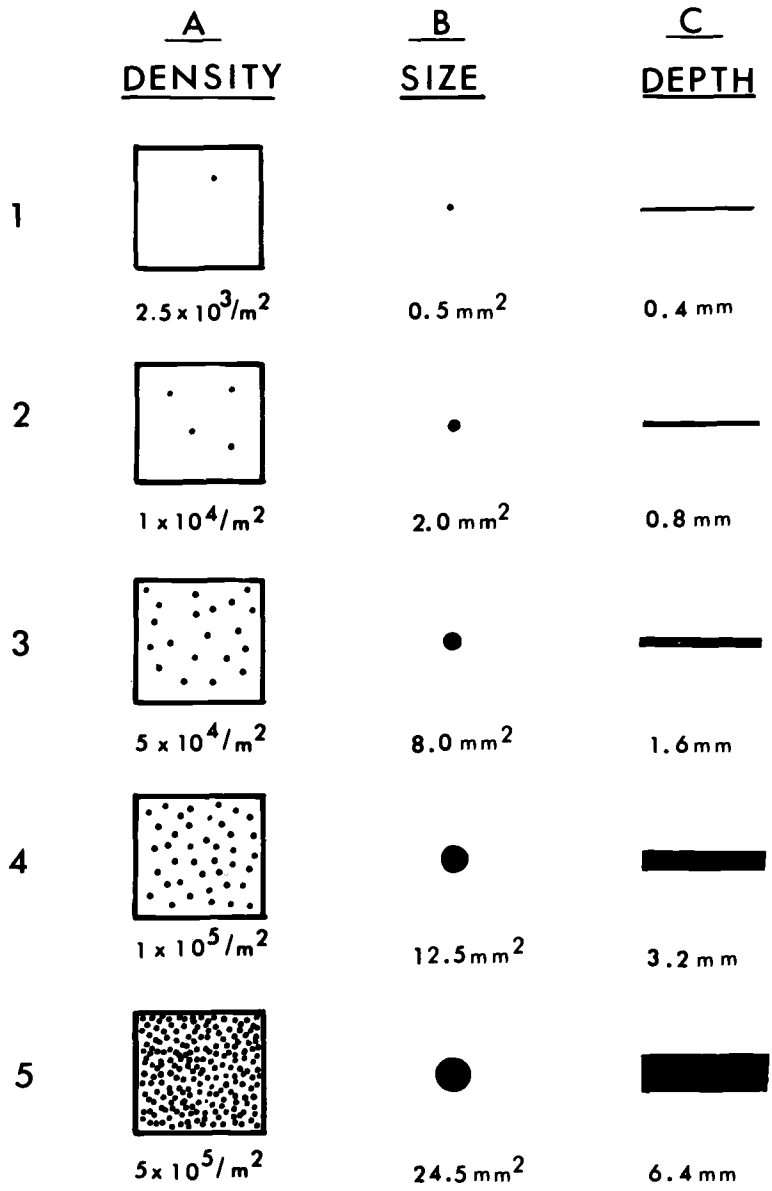


Fig. 2 Standard Rating Charts for Pits.

ANNEX

A1. REPEATABILITY OF MICROSCOPICAL PIT DEPTH MEASUREMENTS

A1.1 Repeatability of pit depth measurements on a single pit at four magnifications is shown in Table A1.

A1.2 The data in Table A1 indicate that as the magnification was increased (that is, from 65 to 370×), the average pit depth that was measured decreased from 0.174 mm to 0.151 mm. Repeatability of measurement improved with magnification,

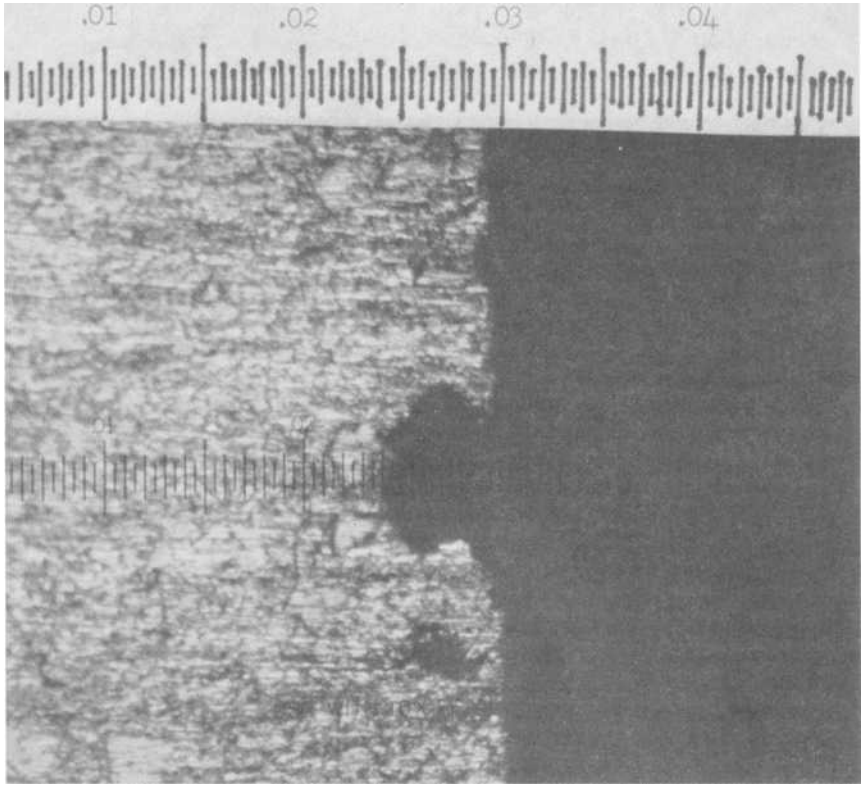
and, as will be shown in A1.3, accuracy also showed marked improvement.

A1.3 The pit used for the measurements in Table A1 was cross sectioned and photographed at 100× through a microscope with a micrometer reticle. As shown in Fig. A1, the depth measured in cross section is 0.152 mm. This result is in excellent agreement with that found under high magnification, and shown in Table A1.

A1.4 Pit depth measurements have been made over the range from 0.04 to 0.34 mm. The only limitation to this method is that associated with the range of movement of the calibrated focusing knob on the microscope.

TABLE A1 Microscopical Pit Depth Measurements

Magnification	Pit Depth, mm
65	0.183
	0.159
	0.179
	0.174 avg
132	0.159
	0.160
	0.155
	0.159
	0.159 avg
200	0.149
	0.157
	0.150
	0.153
	0.152 avg
370	0.151
	0.151
	0.152
	0.151 avg



NOTE—Use with 10× F.F. Objective.

FIG. A1 Cross Section of Pit Used for Depth Measurements in Table A1 (Each Scale Division Equals 0.0005 in. (13 μm)).

The American Society for Testing and Materials takes no position respecting the validity of any patent rights asserted in connection with any item mentioned in this standard. Users of this standard are expressly advised that determination of the validity of any such patent rights, and the risk of infringement of such rights, are entirely their own responsibility.

This standard is subject to revision at any time by the responsible technical committee and must be reviewed every five years and if not revised, either reapproved or withdrawn. Your comments are invited either for revision of this standard or for additional standards and should be addressed to ASTM Headquarters. Your comments will receive careful consideration at a meeting of the responsible technical committee, which you may attend. If you feel that your comments have not received a fair hearing you should make your views known to the ASTM Committee on Standards, 1916 Race St., Philadelphia, Pa. 19103.

Designation: G 48 – 76 (Reapproved 1980)ε1

Standard Test Methods for PITTING AND CREVICE CORROSION RESISTANCE OF STAINLESS STEELS AND RELATED ALLOYS BY THE USE OF FERRIC CHLORIDE SOLUTION[1]

This standard is issued under the fixed designation G 48; the number immediately following the designation indicates the year of original adoption or, in the case of revision, the year of last revision. A number in parentheses indicates the year of last reapproval. A superscript epsilon (ε) indicates an editorial change since the last revision or reapproval.

ε1 NOTE—Editorial changes were made throughout in November 1980.

1. Scope

1.1 These methods cover procedures for the determination of pitting and crevice corrosion resistance of stainless steels and related alloys when exposed to oxidizing chloride environments. Two procedures are described and identified as Methods A and B:

1.1.1 *Method A*—Total immersion ferric chloride test.

1.1.2 *Method B*—Ferric chloride crevice test.

1.2 Method A is designed to determine the relative pitting resistance of stainless steels and nickel-base, chromium-bearing alloys, whereas Method B can be used for determining both the pitting and crevice corrosion resistance of these alloys.

1.3 These tests may be used to determine the effects of alloying additives, heat treatment, and surface finishes on pitting and crevice corrosion resistance.

2. Applicable Document

2.1 *ASTM Standard:*

G 46 Recommended Practice for Examination and Evaluation of Pitting Corrosion[2]

3. Ferric Chloride Test Solution

3.1 Dissolve 100 g of reagent grade ferric chloride, $FeCl_3 \cdot 6H_2O$, in 900 ml of distilled water (about 6% $FeCl_3$ by weight). Filter through glass wool or filter paper to remove insoluble particles.

4. Test Specimens

4.1 A test specimen 25 by 50 mm (1 by 2 in.) is recommended as a standard size, although various shapes and sizes can be tested by this method. All specimens in a test series should have the same dimensions when comparisons are to be made. Unless end-grain pitting is an integral part of the evaluation, the proportion of end-grain surface to specimen surface should be kept small because of the susceptibility of end-grain surfaces to pitting.

NOTE 1—The thickness of the specimen can influence the tightness of the crevice and the test results.

4.2 When specimens are cut by shearing, the deformed material should be removed by machining or grinding prior to testing unless the sheared edges are being evaluated.

4.3 All surfaces of the specimen should be polished to a uniform finish. A 120-grit abrasive paper has been found to provide a satisfactory standard finish. Wet polishing is preferred, but if dry polishing is used, it should be done slowly to avoid overheating. Sharp edges of the specimen should be rounded to avoid cutting rubber band or O-ring.

NOTE 2—While a polished surface is preferred for uniformity, the test may be varied at the discretion of the investigator to evaluate other surface finishes, such as a mill finish.

4.4 Measure the dimensions of the specimen

[1] These methods are under the jurisdiction of ASTM Committee G-1 on Corrosion of Metals, and are the direct responsibility of Subcommittee G01.05 on Laboratory Corrosion Tests.

Current edition approved June 11, 1976. Published August 1976.

[2] *Annual Book of ASTM Standards*, Vol 03.02.

and calculate the total exposed area of interest.

4.5 Clean specimen surfaces with magnesium oxide paste or equivalent, rinse well with water, dip in acetone or methyl alcohol, and air dry.

4.6 Weigh each specimen to the nearest 0.001 g or better and store in a desiccator until ready for use.

5. Method A—Total Immersion Ferric Chloride Test

5.1 *Apparatus:*

5.1.1 *Glass Beakers,* 1000-ml, tall-form, or Erlenmeyer flasks, 1000-ml, wide neck.

5.1.2 *Glass Cradles* (Fig. 1)—The dimensions of the cradle shall be restricted to those that will permit its passage through the test container opening, a diameter of about 40 mm (1.6 in.) in the case of the Erlenmeyer flask.

5.1.3 *Water or Oil Bath,* constant-temperature.

5.2 *Procedure:*

5.2.1 Pour 600 ml of the ferric chloride test solution into the test container. If specimens larger than the standard are used, provide a solution volume of at least 20 ml/cm^2 (125 ml/in.^{2}) of surface area. Transfer the container to a constant-temperature bath and allow to come to the equilibrium temperature of interest. Suitable temperatures for evaluation are 22 ± 2°C and 50 ± 2°C.

5.2.2 Place the specimen in a glass cradle and immerse in the test solution after it has reached the desired temperature. Maintain temperature throughout the test.

5.2.3 Cover the container with a watch glass. A reasonable test period is 72 h, although variations may be used at the discretion of the investigator and depend on the materials being evaluated.

5.2.4 Remove the specimens, rinse with water, and scrub with a nylon bristle brush under running water to remove corrosion products, dip in acetone or methanol, and dry. Ultrasonic cleaning may be used as a substitute method in those cases where it is difficult to remove corrosion products from deep pits.

5.2.5 Weigh each specimen to 0.001 g or better and reserve for examination.

6. Method B—Ferric Chloride Crevice Test[3]

6.1 *Apparatus:*

6.1.1 *Cylindrical TFE-fluorocarbon Blocks,* two for each test specimen. Each block shall be 12.7 mm (0.5 in.) in diameter and 12.7 mm high, with perpendicular grooves 1.6 mm (0.063 in.) wide and 1.6 mm deep cut in the top of each cylinder for retention of the O-rings or rubber bands. Blocks can be machined from bar or rod stock.

6.1.2 *Fluorinated Elastomer*[4] *O-Rings or Rubber Bands* (low sulfur (0.02% max)), two for each test specimen.

NOTE 3—It is good practice to use all O-rings or all rubber bands in a given test program.

6.1.2.1 O-rings shall be 1.75 mm (0.070 in.) in cross section; one ring with an inside diameter of about 20 mm (0.8 in.) and one with an inside diameter of about 30 mm (1.2 in.). Rubber bands should be one No. 12 (38 mm (1.5 in.) long) and one No. 14 (51 mm (2 in.) long).

NOTE 4—Rubber bands or O-rings can be boiled in water prior to use to ensure the removal of water-soluble ingredients that might affect corrosion.

6.1.3 *Test Tube,* 38 mm (1.5 in.) in diameter and 300 mm (11.5 in.) long.

6.1.4 *Rubber Stopper,* No. 8, with center hole for insertion of 6.4-mm (0.25-in.) diameter, 102-mm (4-in.) long glass tube (medicine dropper tube may be conveniently used) to serve as a vent and condenser.

6.1.5 *Water or Oil Bath,* thermostated.

6.2 *Procedure:*

6.2.1 Add 150 ml of ferric chloride solution to each test tube, insert a rubber stopper, and place the tube in a thermostated bath until it comes to the equilibrium temperature of interest. Suitable temperatures for evaluation are 22 ± 2°C and 50 ± 2°C.

6.2.2 Fasten two TFE-fluorocarbon blocks to the test specimen with O-rings or a double loop of each of two rubber bands as shown in Fig. 2. Use plastic gloves to avoid hand contact with metal surfaces during this operation. Use the small O-ring or the No. 12 rubber band for the 25-mm (1-in.) dimension and the large O-ring or the No. 14 rubber band for the 50-mm (2-in.) dimension.

6.2.3 After the test solution has reached the desired temperature, tilt the tube at a 45-deg angle and slide the test specimen to the bottom

[3] Streicher, M. A., "Development of Pitting Resistant Fe-Cr-Mo Alloys," *Corrosion,* SBIIA, Vol 30, No. 77, March 1974.

[4] Viton®, a trademark of DuPont, has been found acceptable.

of the tube, replace the stopper, and return the tube to the bath.

6.2.4 A reasonable test period is 72 h, although variations may be used at the discretion of the investigator and depend on the materials being evaluated. Specimens may be inspected at intervals by decanting the test solution into a clean beaker and sliding the specimen from the tube. Rinse the specimen in water and examine under four O-ring or rubber band crevices and TFE-fluorocarbon blocks. If further exposure is required, return the specimen and solution to the tube without allowing the specimen to dry and replace the tube in the bath.

NOTE 5—The removal of specimens for inspection may affect the rate of corrosion, and caution should be observed when comparing these results with those obtained from constant immersion tests.

6.2.5 After the test has been completed, remove the test specimens, rinse with water, and scrub with a nylon bristle brush under running water to remove corrosion products, dip in acetone or methanol, and dry. Ultrasonic cleaning may be used in those cases where it is difficult to remove corrosion products from deep pits or crevices.

6.2.6 Weigh each specimen to 0.001 g or better and reserve for examination.

7. Examination and Evaluation

7.1 A visual examination (Note 4) and photographic reproduction of specimen surfaces, along with specimen weight losses, are often sufficient to characterize the pitting and crevice resistance of different materials. A more detailed examination will include the measurement of maximum pit depth, average pit depth, pit density, and crevice depth (see Recommended Practice G 46).

NOTE 6—It is often desirable to probe pit sites on the metal surface with a needle to expose subsurface attack.

NOTE 7—A test shall be disregarded if the rubber band or O-ring breaks during exposure.

7.2 Examine planar surfaces for pits under low-power (for example, 20×) magnification. (Disregard end pits unless this is an important phase of test, recognizing that these pits may affect pitting on planar surfaces.)

7.3 Measure the deepest pits with the appropriate technique; for example, needle point micrometer gage or microscope with calibrated fine-focus knob. It may be necessary to probe some pits to ensure exposure of the cavity. Measure a significant number of pits to determine the deepest pit and the average of the ten deepest pits. Do not measure the depth of pits that intersect the edge of the specimen.

7.4 Count the number of pits on the planar surface under low-power magnification (for example, 20×) to determine pit density. A clear plastic grid, divided in centimetres, may be helpful, or the surface can be subdivided by scribing with light lines.

7.5 Determine crevice attack (Method B) under O-rings or rubber bands and TFE-fluorocarbon blocks. Measure the depth of attack (open notch) at O-ring or rubber band contact areas using a microscope with a calibrated eyepiece or other suitable technique. Measure the depth of attack under TFE-fluorocarbon blocks in a manner similar to that used for determining depth of pits.

8. Report

8.1 Record the test procedure used, specimen size and surface preparation, time of test, and temperature.

8.2 Calculate the specimen weight loss and record as grams per square metre.

8.3 Record the maximum pit depth and the average of the ten deepest pits in micrometres and pit density in pits per square metre for both front and back faces of the specimen. Record the maximum pit depth of edges if end grain attack is of interest.

8.4 Record the average depth of crevice attack (Method B) in micrometres under elastic contact at vertical edges and horizontal edges and under blocks at faces.

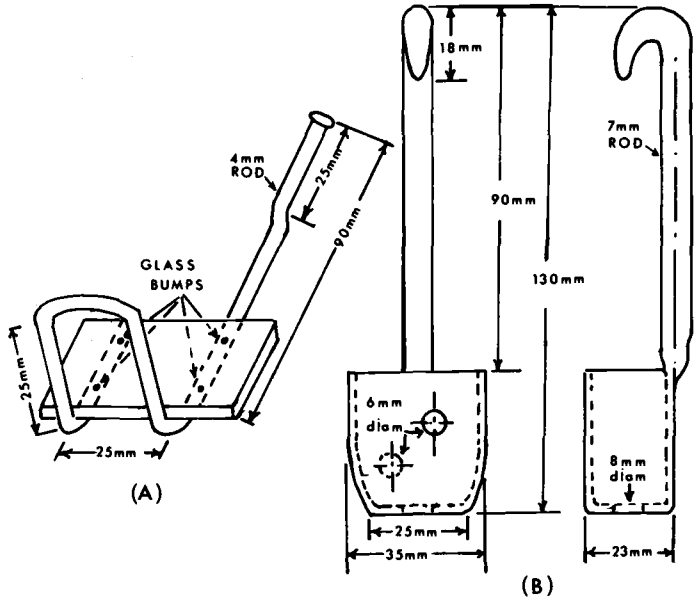
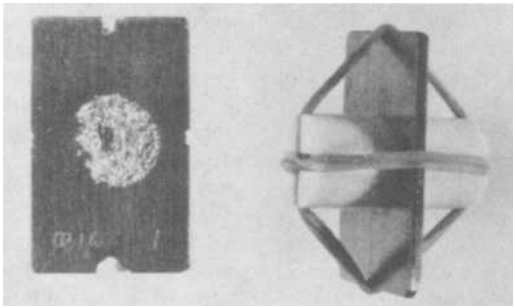


FIG. 1 Examples of Glass Cradles that Can Be Used to Support the Specimen



(a) Specimen After Test with Attack at Four Crevices Under Rubber Bands and Under One Block

(b) Assembled Crevice Test Specimen

FIG. 2 Ferric Chloride Crevice Test Specimen

The American Society for Testing and Materials takes no position respecting the validity of any patent rights asserted in connection with any item mentioned in this standard. Users of this standard are expressly advised that determination of the validity of any such patent rights, and the risk of infringement of such rights, are entirely their own responsibility.

This standard is subject to revision at any time by the responsible technical committee and must be reviewed every five years and if not revised, either reapproved or withdrawn. Your comments are invited either for revision of this standard or for additional standards and should be addressed to ASTM Headquarters. Your comments will receive careful consideration at a meeting of the responsible technical committee, which you may attend. If you feel that your comments have not received a fair hearing you should make your views known to the ASTM Committee on Standards, 1916 Race St., Philadelphia, Pa. 19103.

Designation: G 61 – 78

An American National Standard

Standard Practice for CONDUCTING CYCLIC POTENTIODYNAMIC POLARIZATION MEASUREMENTS FOR LOCALIZED CORROSION[1]

This standard is issued under the fixed designation G 61; the number immediately following the designation indicates the year of original adoption or, in the case of revision, the year of last revision. A number in parentheses indicates the year of last reapproval. A superscript epsilon (ε) indicates an editorial change since the last revision or reapproval.

1. Scope

1.1 This practice gives a suggested procedure for conducting cyclic potentiodynamic polarization measurements to determine susceptibility to localized corrosion (pitting and crevice corrosion). If followed, this practice will provide repeatable cyclic potentiodynamic anodic polarization measurements that will reproduce data determined by others at other times in other laboratories. The procedure is preferably used for iron, nickel, or cobalt-based alloys.

1.2 A standard potentiodynamic polarization plot is included. These reference data are based on the results from five different laboratories that followed the standard procedure, using specific alloys of Type 304 stainless steel and Hastelloy C-276. Curves are included which have been constructed using statistical analysis to indicate the acceptable range of polarization curves.

1.3 Samples of the standard Type 304 stainless steel and the Hastelloy C-276 used in obtaining the standard reference plot are available for those who wish to check their own test procedure and equipment.[2]

2. Applicable Documents

2.1 *ASTM Standards:*

G3 Practice for Conventions Applicable to Electrochemical Measurements in Corrosion Testing[3]

G5 Practice for Standard Reference Method for Making Potentiostatic and Potentiodynamic Anodic Polarization Measurements[3]

3. Apparatus

3.1 The polarization cell should be similar to the one described in Practice G 5. Other polarization cells may be equally suitable.

3.1.1 The cell should have a capacity of about 1 litre and should have suitable necks or seals to permit the introduction of electrodes, gas inlet and outlet tubes, and a thermometer. The Luggin probe-salt bridge separates the bulk solution from the saturated calomel reference electrode. The probe tip should be adjustable so that it can be brought into close proximity with the working electrode.

3.2 *Specimen Holder:*

3.2.1 Specimens should be mounted in a suitable holder designed for flat strip, exposing 1 cm^2 to the test solution (Fig. 1). Such specimen holders have been described in the literature.[4, 5] It is important that the circular TFE-fluorocarbon gasket be drilled and machined flat in order to minimize crevices.

3.3 *Potentiostat* (Note 1)—A potentiostat

---

[1] This practice is under the jurisdiction of ASTM Committee G-1 on Corrosion of Metals, and is the direct responsibility of Subcommittee G01.11 on Electrochemical Measurements in Corrosion Testing.

Current edition approved Dec. 29, 1978. Published April 1979.

[2] These standard samples are available as a set of one of each type from ASTM Headquarters. Order PCN 12-700610-22.

[3] *Annual Book of ASTM Standards*, Vol 03.02.

[4] France, W. D., Jr., *Journal of the Electrochemical Society*, JESOA, Vol 114, 1967, p. 818.

[5] Myers, J. R., Gruewlar, F. G., and Smulczenski, L. A., *Corrosion*, CORRA, Vol 24, 1968, p. 352.

that will maintain an electrode potential within 1 mV of a preset value over a wide range of applied currents should be used. For the type and size of standard specimen supplied, the potentiostat should have a potential range of −1.0 to +1.6 V and an anodic current output range of 1.0 to 10^5 μA. Most commercial potentiostats meet the specific requirements for these types of measurements.

NOTE 1—These instrumental requirements are based upon values typical of the instruments in the five laboratories that have provided the data used in determining the standard polarization plot.

3.4 *Potential-Measuring Instruments* (Note 1)—The potential-measuring circuit should have a high input impedance on the order of 10^{11} to 10^{14} Ω to minimize current drawn from the system during measurements. Instruments should have sufficient sensitivity and accuracy to detect a change in potential of ±1 mV, usually included in commercial potentiostats. An output as a voltage is preferred for recording purposes.

3.5 *Current-Measuring Instruments* (Note 1)—An instrument that is capable of measuring a current accurately to within 1 % of the absolute value over a current range between 1.0 and 10^5 μA should be used. Many commercial units have a built-in instrument with an output as a voltage, which is preferred for recording purposes. For the purpose of the present test a logarithmic output is desirable.

3.6 *Anodic Polarization Circuit*—A scanning potentiostat is used for potentiodynamic measurements. Potential and current are plotted continuously using an *X-Y* recorder and a logarithmic converter (contained in the potentiostat or incorporated into the circuit) for the current. Commercially available units are suitable.

3.7 *Electrodes:*

3.7.1 The standard Type 304 stainless steel and Hastelloy Alloy C-276 should be machined into flat 0.625-in. (14-mm) diameter disks. The chemical composition of these alloys is listed in Table 1.

3.7.2 *Counter Electrodes*—The counter electrodes may be prepared as described in Practice G 5 or may be prepared from high-purity platinum flat stock and wire. A suitable method would be to seal the platinum wire in glass tubing and introduce the platinum electrode assembly through a sliding seal. Counter electrodes should have an area at least twice as large as the test electrode.

3.7.3 *Reference Electrode*[6]—A saturated calomel electrode with a controlled rate of leakage (about 3 μl/h) is recommended. This type of electrode is durable, reliable, and commercially available. Precautions should be taken to ensure that it is maintained in the proper condition. The potential of the calomel electrode should be checked at periodic intervals to ensure the accuracy of the electrode.

4. Standard Experimental Procedure

4.1 *Test Specimen Preparation:*

4.1.1 Wet grind with 240-grit SiC paper, wet polish with 600-grit SiC paper until previous coarse scratches are removed, rinse, and dry.

4.1.2 Prior to assembly of the specimen holder, ultrasonically degrease the specimen for 5 min in detergent and water, rinse thoroughly in distilled water, and dry.

4.1.3 Mount the specimen in the electrode holder. Tighten the assembly until the TFE-fluorocarbon gasket is sufficiently compressed to avoid leakage in the gasket.

4.2 Prepare a 3.56 % (by weight) sodium chloride solution by dissolving 34 g of reagent grade NaCl in 920 ml of distilled water.

4.3 Assemble the electrode holder and place in the polarization cell. Transfer 900 ml of test solution to the polarization cell, ensuring that the specimen remains above the solution level.

4.4 Bring the temperature of the solution of 25 ± 1°C by immersing the test cell in a controlled-temperature water bath or by other convenient means.

4.5 Place the platinum auxiliary electrodes, salt-bridge probe, and other components in the test cell. Fill the salt bridge with test solution and locate the probe tip approximately 1 mm from the working electrode.

NOTE 2—The levels of the solution in the reference and polarization cells should be the same. If this is impossible, a closed solution-wet (not greased) stopcock can be used in the salt bridge to eliminate siphoning.

4.6 Purge the solution sufficiently with an appropriate gas to remove oxygen before specimen immersion (minimum of 1 h).

[6] Ives, D. J., and Janz, G. J., *Reference Electrodes, Theory and Practice*, Academic Press, New York, N.Y., 1961.

4.7 Immerse the specimen for 1 h before initiating polarization. A sliding seal can be used to ensure that an oxygen-free environment is maintained while the specimen is lowered. It is important that all oxygen be removed by purging prior to polarization, otherwise, more noble initial corrosion potential values will be observed.

4.8 Record the platinum potential 50 min after immersion of the specimen. Record the open-circuit specimen potential, that is, the corrosion potential, the instant before beginning polarization.

4.9 *Potential Scan*—Start the potential scan 1 h after specimen immersion, beginning at the corrosion potential (E_{corr}), and scan in the more noble direction at a scan rate of 0.6 V/h (±5 %). Record the current continuously with change in potential on an *X-Y* recorder using semilogarithmic paper.

4.9.1 The onset of localized corrosion is usually marked by a rapid increase of the anodic current at potentials below the oxygen-evolution potential. When the current reaches 5 mA (5×10^3 μA), reverse the scanning direction (toward more active potentials).

4.9.2 Continue the reverse scan until the hysteresis loop closes or until the corrosion potential is reached.

4.10 Plot anodic polarization data on semilogarithmic paper in accordance with Practice G 3 (potential-ordinate, current density-abscissa). A plot of representative polarization curves generated by the practice is shown in Fig. 2.

5. Standard Reference Plot

5.1 A standard polarization plot, based on the potentiodynamic data from five different laboratories, has been prepared. The plot has been separated into the forward (Fig. 3) and reverse (Fig. 4) scans for clarity. These plots show the mean values and a range of ±2 standard deviations.

5.2 These plots were prepared from data obtained by following the standard procedure discussed in this practice.

5.3 A curve obtained by the potentiodynamic technique described above should show good agreement with the standard plots.

6. Reproducibility

6.1 The spread in data obtained from a number of laboratories and used in the preparation of the standard plot (Fig. 3 and 4) demonstrates the reproducibility that is possible when a standard procedure is followed.

6.2 The availability of a standard procedure, standard material, and standard plots should make it easy for an investigator to check his techniques to evaluate susceptibility to localized corrosion. An investigator's data should fall within the range of ±2 standard deviations since this includes 95 % of all data, provided random variations are the only source of error.

7. Evaluation of Results

7.1 In general, localized corrosion can propagate at potentials more noble than that at which the hysteresis loop is completed. In these cases the more noble this potential, the less likely E_{corr} will exceed it, and the less likely that localized corrosion will occur.

7.2 An indication of the susceptibility to initiation of localized corrosion is given by the potential at which the anodic current increases rapidly (see Figs. 2 and 3). The more noble this potential, the less susceptible is the alloy to initiation of localized corrosion.

7.3 The polarization curves shown in Figs. 2, 3, and 4 indicate that initiation and propagation of localized corrosion occurs at potentials below the oxygen-evolution potential in Type 304 stainless steel. The curve for Hastelloy Alloy C-276 is not a result of localized corrosion but of uniform corrosion in the transpassive or oxygen evolution region. Since the corrosion potentials (E_{corr} values) for Hastelloy Alloy C-276 and Type 304 stainless steel are usually similar, these curves indicate that Hastelloy Alloy C-276 is more resistant to initiation and propagation of localized corrosion than Type 304 stainless steel.

TABLE 1 Chemical Composition of Standard Alloys, Weight %

Element	Hastelloy C-276	Type 304 Stainless Steel
Carbon	0.003	0.060
Chromium	15.29	18.46
Cobalt	2.05	...
Columbium	...	0.11
Copper	...	0.17
Iron	5.78	balance
Manganese	0.48	1.43
Molybdenum	16.03	0.17
Nickel	balance	8.74
Phosphorus	0.018	0.029
Silicon	0.05	0.60
Sulfur	0.006	0.014
Vanadium	0.20	...
Tungsten	3.62	...

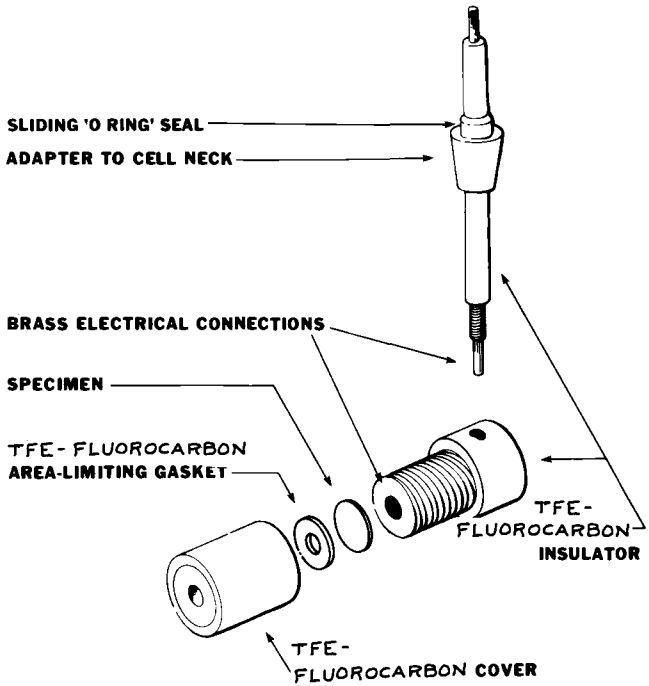


FIG. 1 Schematic Diagram of Specimen Holder.[4,5]

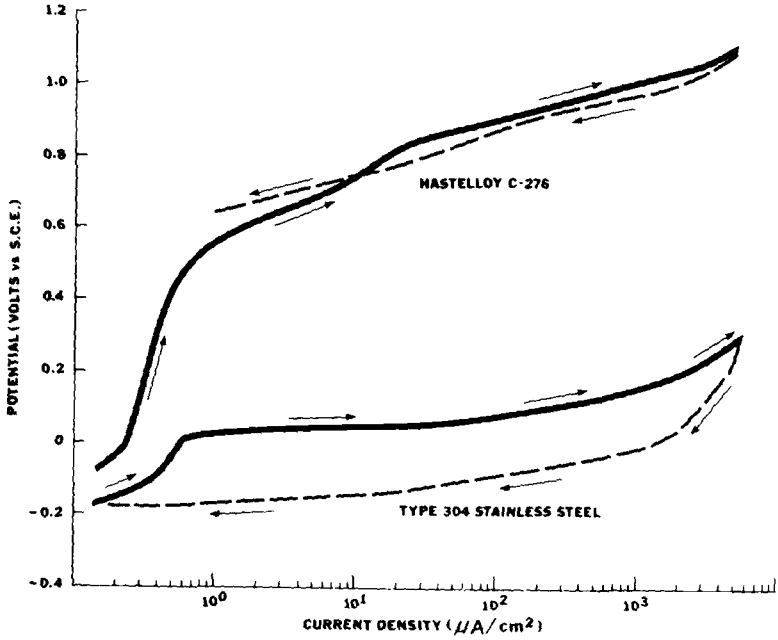


FIG. 2 Representative Cyclic Potentiodynamic Polarization Curves.

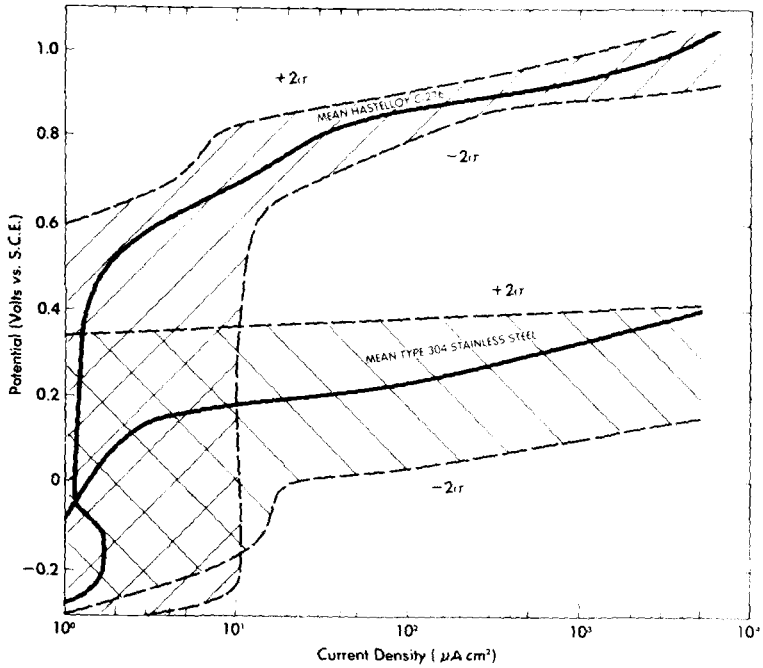


FIG. 3 Standard Potentiodynamic Polarization Plot (Forward Scan).

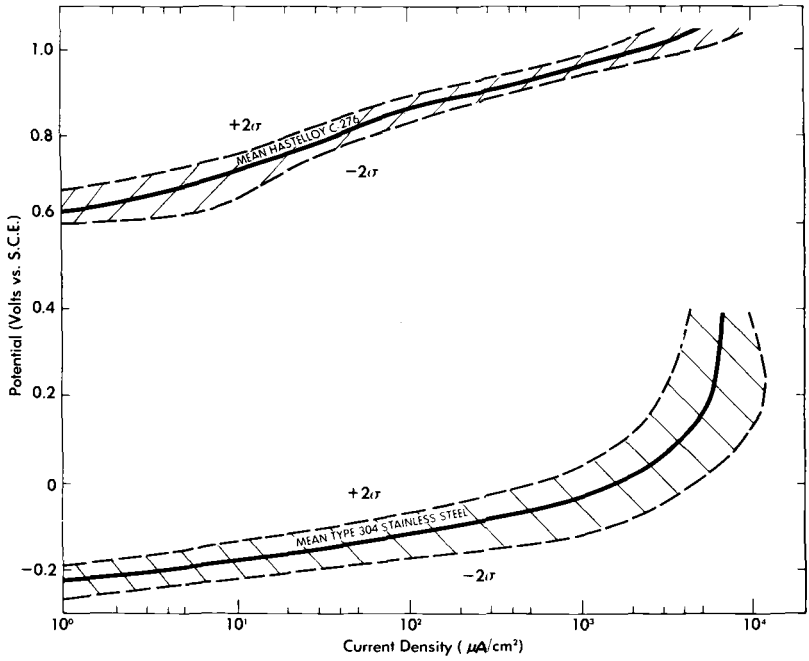


FIG. 4 Standard Potentiodynamic Polarization Plot (Reverse Scan).

The American Society for Testing and Materials takes no position respecting the validity of any patent rights asserted in connection with any item mentioned in this standard. Users of this standard are expressly advised that determination of the validity of any such patent rights, and the risk of infringement of such rights, are entirely their own responsibility.

This standard is subject to revision at any time by the responsible technical committee and must be reviewed every five years and if not revised, either reapproved or withdrawn. Your comments are invited either for revision of this standard or for additional standards and should be addressed to ASTM Headquarters. Your comments will receive careful consideration at a meeting of the responsible technical committee, which you may attend. If you feel that your comments have not received a fair hearing you should make your views known to the ASTM Committee on Standards, 1916 Race St., Philadelphia, Pa. 19103.

Designation: G 71 - 81

Standard Practice for CONDUCTING AND EVALUATING GALVANIC CORROSION TESTS IN ELECTROLYTES[1]

This standard is issued under the fixed designation G 71; the number immediately following the designation indicates the year of original adoption or, in the case of revision, the year of last revision. A number in parentheses indicates the year of last reapproval. A superscript epsilon (ε) indicates an editorial change since the last revision or reapproval.

1. Scope

1.1 This practice is an outline or guide for galvanic corrosion tests to characterize the behavior of two dissimilar metals in electrical contact in an electrolyte under low-flow conditions. It can be adapted to wrought or cast metals and alloys.

1.2 This practice covers the selection of materials, specimen preparation, test environment, method of exposure, and method for evaluating the results to characterize the behavior of galvanic couples in an electrolyte.

NOTE—Additional information on galvanic corrosion testing and examples of the conduct and evaluation of galvanic corrosion tests in electrolytes are given in Refs (**1**)[2] through (7).

2. Applicable Documents

2.1 *ASTM Standards:*

G 1 Practice for Preparing, Cleaning, and Evaluating Corrosion Test Specimens[3]

G 3 Practice for Conventions Applicable to Electrochemical Measurements in Corrosion Testing[3]

G 4 Method for Conducting Corrosion Coupon Tests in Plant Equipment[4]

G 16 Practice for Applying Statistics to Analysis of Corrosion Data[3]

G 31 Practice for Laboratory Immersion Corrosion Testing of Metals[4]

G 46 Recommended Practice for Examination and Evaluation of Pitting Corrosion[3]

3. Significance and Use

3.1 Use of this practice is intended to provide information on the galvanic corrosion of metals in electrical contact in an electrolyte that does not have a flow velocity sufficient to cause erosion-corrosion or cavitation.

3.2 This practice is presented as a guide for conducting galvanic corrosion tests in liquid electrolyte solutions, both in the laboratory and in service environments. Adherence to this practice will aid in avoiding some of the inherent difficulties in such testing.

4. Test Specimens

4.1 *Material*—Test specimens should be manufactured from the same material as those used in the service application being modeled. Minor compositional or processing differences between materials or between different heats can greatly affect the results in some cases.

4.2 *Size and Shape*:

4.2.1 The size and shape of the test specimens are dependent on restrictions imposed by the test location. When determining material behavior in the laboratory, it is advisable to use the largest specimens permissible within the constraints of the test equipment. In general, the ratio of surface area to metal volume should be large in order to favor maximum corrosion loss per weight. Sufficient thickness should be employed, however, to minimize the possibility of perforation of the specimens during the test exposure. When modeling large components, the size of the specimens should be as large as practical. When modeling smaller components, specimen size should be as close as possible to that of the application being modeled. Surface

[1] This practice is under the jurisdiction of ASTM Committee G-1 on Corrosion of Metals and is the direct responsibility of Subcommittee G01.07 on Galvanic Corrosion.

Current edition approved Nov. 27, 1981. Published January 1982.

[2] The boldface numbers in parentheses refer to the list of references appended to the practice.

[3] *Annual Book of ASTM Standards*, Vol 03.02.

[4] *Annual Book of ASTM Standards*, Vols 01.03 and 03.02.

area ratio in the test should be identical to the application being modeled. This ratio is defined as the surface area of one member of the couple divided by the surface area of the other member of the couple. Only the area in contact with the electrolyte (wetted area) is used in this calculation. In low-resistivity electrolytes, maintaining proximity between the materials being coupled may be more important than maintaining the exact area ratio. Also, with some couples, such as copper coupled to aluminum, there may be effects of corrosion products washing from one electrode to another which may have to be considered in determining specimen placement.

4.2.2 Laboratory tests are normally performed on rectangular plates or on cylinders. When modeling service applications, the shapes of the couple members should approximate the shapes in the application. Frequently complex shapes are simplified for testing purposes. The shape of the specimen is more important in electrolytes of low conductivity, where voltage drop in the electrolyte is significant. In highly conductive electrolytes, the shapes of the couple members may therefore deviate somewhat from the shapes in the application.

4.3 *Specimen Preparation*:

4.3.1 The edges of the test specimens should be prepared so as to eliminate all sheared or cold-worked metal except that cold-working introduced by stamping for identification. Shearing will, in some cases, cause considerable attack. Therefore, specimens having sheared edges should not be used. The edges should be finished by machining or polishing. The slight amount of cold working resulting from machining will not introduce any serious error.

4.3.2 Specimens should be cleaned in accordance with Practice G 1, or else the specimen surface condition should be similar to the application being modeled. The metallurgical condition of the specimens should be similar to the application being modeled. In all cases surface contamination, such as dirt, grease, oil, and thick oxides, should be removed prior to weighing and exposure to the test environment.

4.3.3 The specimen identification system must be one that will endure throughout the test period. Edge notches, drilled holes, stamped numbers, and tags are some of the methods used for identification. The identification system must not induce corrosion attack in any way.

4.4 *Number of Specimens*:

4.4.1 The number of galvanic couples to be tested will be determined by whether or not one or more periodic specimen removals are scheduled during the course of the test. As a minimum, duplicate and preferably triplicate specimens should be tested for any given test period to determine the variability in the galvanic corrosion behavior. The effect of the number of replications on the application of the results is set forth in Practice G 16.

4.4.2 Control specimens should also be tested to provide corrosion rates of the individual metals and alloys without coupling for comparisons. These specimens should be of the same alloys, shapes, sizes, and metallurgical conditions as the materials in the couple.

5. Test Environment

5.1 *Laboratory Tests*:

5.1.1 In the laboratory, the test solution should closely approximate the service environment. The amount of test solution used depends on the size of the test specimens. A good rule of thumb is to use 40 cm^3 of test solution for every 1 cm^2 of exposed surface area of both members of the couple. The volume of test solution may be varied to closely approximate the service application.

5.1.2 Galvanic corrosion tests conducted for an extensive period of time may exhaust important constituents of the original solution. Some accumulated corrosion products may act as corrosion accelerators or inhibitors. These variables may greatly change the end results, and replenishment of the solution should be chosen to be representative of the service application. A test system using continuously replenished test electrolytes is often the only solution to this problem.

5.1.3 Periodic measurements of the test environment should be made when the test duration in a fixed volume solution is for periods of several days or longer. These observations may include temperature, pH, O_2, H_2S, CO_2, NH_3, conductivity, and pertinent metal ion content.

5.2 *Field Tests*—Field testing should be performed in an environment similar to the service environment. Periodic measurements of those environmental variables which could vary with

time, such as temperature, dissolved O_2, etc., should be made.

6. Procedure

6.1 *Laboratory Versus Field Testing*:

6.1.1 Galvanic corrosion tests are conducted in the laboratory for several purposes: (*1*) inexpensive screening to reduce expensive field testing, (*2*) study of the effects of environmental variables, and (*3*) study of the corrosion accelerating or protective effects of various anode/cathode surface area ratios.

6.1.2 The materials proven in the laboratory to be the most promising should also be tested in the field, since it is frequently impossible to duplicate the actual service environment in the laboratory.

6.2 *Test Procedure*:

6.2.1 Specimens should be electrically joined before exposure. There are a number of methods for joining the specimens. Laboratory testing generally employs external electrical connection through wires such as to allow current measurement, (see Fig. 1). Field tests frequently employ direct contact physical bonding by threaded rods as in Fig. 2, soldering, brazing, etc. Prime considerations are that the electrical bond to the specimen will not corrode, which could result in decoupling, that the method of joining will not in itself be a galvanic couple or introduce other corrosion mechanisms (crevice, etc.), and that the resistance of the electrical path be small compared to the polarization resistance of the couple materials. Soldering or brazing will prevent the use of mass measurements for calculating corrosion rates. A coating may be applied to the electrical connections to prevent electrolyte access as in Fig. 2, provided the coating does not result in other corrosion phenomena, such as crevice attack, and is sufficiently resistant to the environment.

6.2.2 The physical relationship between the members of each couple should approximate that of the service situation being modeled. This is particularly important in electrolytes with low conductivity, since the effect of *IR* drops will be more noticeable. The specimens may be positioned by the use of nonconductive holders, provided that these do not result in other corrosion phenomena (crevice, etc.). A discussion of the mounting of specimens is included in Method G 4. The supporting device should not be affected by or cause contamination of the test solution.

6.2.3 The coupled assembly is next immersed in the test electrolyte for the period of exposure. Exposure duration should be sufficient to allow prediction of the behavior for the entire service duration. If the service duration is long, corrosion data can be taken as a function of time until a curve can be developed that can be extrapolated to the service duration, provided that steady-state conditions have been reached and that no transient environmental conditions are expected in service to affect this steady state.

6.2.4 Specimen removal should be based on a preplanned removal schedule.

7. Evaluation of Test Specimens

7.1 *Measurements During Exposure*—Data recorded during exposures may include galvanic current measurements and couple and control specimen potentials measured relative to a suitable reference half-cell as recommended in Practice G 3. Current data can then be converted into a theoretical corrosion rate based on Faraday's law.

7.2 *Measurements After Removal*:

7.2.1 After removal, samples of corrosion products may be obtained for chemical and physical analysis. The specimens should then be cleaned of deposits (such as biofouling from fresh or seawater) by scraping or brushing with a wooden scraper or soft bristle brush. Visual observations should be recorded before and after this initial cleaning operation. Color photographs may be taken of each specimen before and after cleaning. Final cleaning of specimens should be in accordance with Practice G 1 after which the specimens should be weighed to determine galvanic corrosion weight loss which can be converted to corrosion as set forth in Practice G 31. Additional recommendations for specimen cleaning may be found in Method G 4 and Practice G 31.

7.2.2 In some cases, mass loss measurements will not be possible or meaningful. For example, soldered assemblies cannot be separated into their components without introducing extra mass due to the remaining solder. In this case, corrosion evaluation of the end product configuration must be based on visual assessments, thickness loss measurements, or on other techniques. Materials suffering localized cor-

rosion such as pitting may be analyzed using Recommended Practice G 46, and those suffering crevice corrosion should have the depth of attack measured and described in detail, with attention to changes at the edges as well as the surfaces. In addition, changes in physical properties such as breaking strength can also be measured. Metallographic examination of specimen cross sections may be necessary to determine parting corrosion depth.

7.2.3 Regardless of the method of assessment, the behavior of the coupled materials should be compared to that of the uncoupled controls. Subtracting control values from values of coupled specimens yields the increase in corrosion due to coupling. A ratio of couple data to the uncoupled data has been used to determine a percentage change in corrosion due to the couple (acceleration factor).

7.2.4 Where replicate couples are exposed, statistical analysis of the data, as set forth in Practice G 16, may be applied to generate confidence intervals for predictive purposes.

8. Report

8.1 The report should include detailed descriptions of the exposed specimens including wetted areas, pertinent data on exposure conditions including the geometry used, the deposits formed, and results of the corrosion evaluation.

8.2 Data for the exposed specimens should include physical dimensions, chemical composition, metallurgical history, surface preparation, and after-exposure cleaning methods.

8.3 Details of exposure conditions should include location, dates, and periods of exposure and description of the environmental conditions prevailing during the exposure period, including electrolyte conductivity.

8.4 The results of the tests may be expressed as corrosion rate in penetration per unit time (for example, millimetres per year) or loss in thickness or mass during the exposure period. Rates for both control (uncoupled) and coupled samples should be reported, with the change in rate due to the coupling reported as either the difference between control and coupled samples or as the coupled rate divided by the control rate (acceleration factor).

8.5 In cases where corrosion is in the form of pitting or crevice corrosion, a pitting factor should be reported in accordance with Recommended Practice G 46. Depths of pitting should be recorded. Pitting factors or depths can then be used to determine the change in corrosion due to coupling.

8.6 If any physical property of the specimens is measured after exposure, the change in that property should be reported and these values can be compared between control and coupled samples in the same manner as corrosion rates or pitting factors.

8.7 Changes in the physical appearance of the specimens during the exposure period should be reported.

REFERENCES

(1) Ailor, W. H., *Handbook on Corrosion Testing and Evaluation,* John Wiley and Sons, Inc., New, York, N.Y., 1971.

(2) Baboian, R., France, W. D., Jr., L. C. Rowe, and J. F. Rynewicz, *Galvanic and Pitting Corrosion – Field and Laboratory Studies, ASTM STP 576,* Philadelphia, Pa., 1976.

(3) Baboian, R., "Galvanic Corrosion," *The Forms of Corrosion – Recognition and Prevention,* Chapter 3, NACE, 1981.

(4) Champion, F. A., *Corrosion Testing Procedures,* John Wiley & Sons, Inc., New York, N.Y., 1952.

(5) Fontana, M. G. and N. D. Greene, *Corrosion Engineering,* McGraw-Hill, New York, N.Y., 1978.

(6) Copson, H. R., and LaQue, F. L. *Corrosion Resistance of Metals and Alloys,* Reinhold Publishing Co., New York, N.Y., 1963.

(7) Uhlig, H. H., *The Corrosion Handbook,* John Wiley & Sons, Inc., New York, N.Y., 1948.

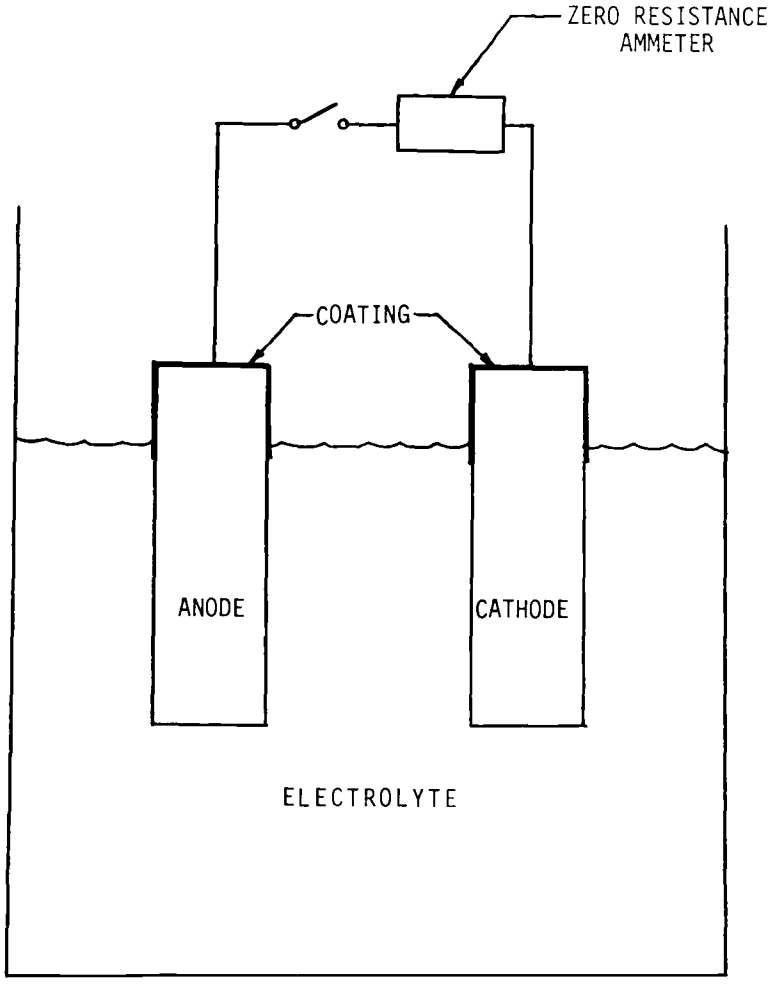
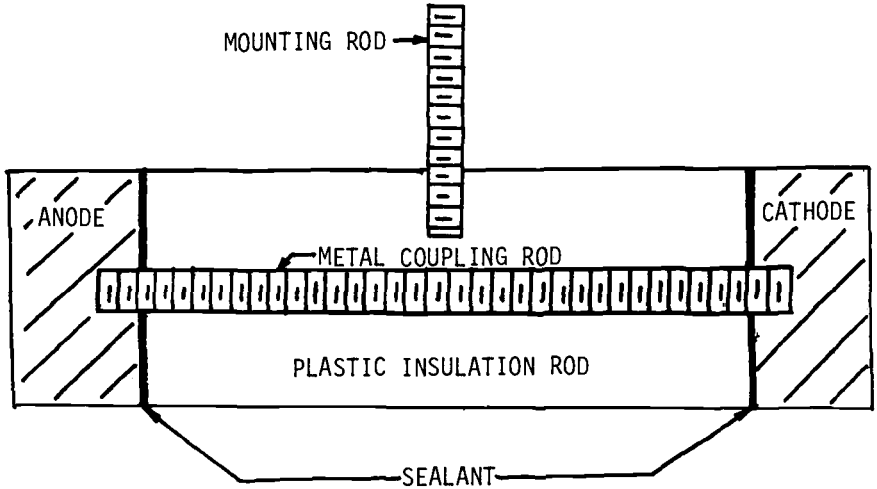


FIG. 1 Laboratory Galvanic Corrosion Test Setup With Facility for Measuring Galvanic Current



NOTE—The length of the plastic insulation rod should approximate the distance between the anode and the cathode of the final product.

FIG. 2 Specimen Configuration for Galvanic Corrosion Tests of Bar Stock Material

The American Society for Testing and Materials takes no position respecting the validity of any patent rights asserted in connection with any item mentioned in this standard. Users of this standard are expressly advised that determination of the validity of any such patent rights, and the risk of infringement of such rights, are entirely their own responsibility.

This standard is subject to revision at any time by the responsible technical committee and must be reviewed every five years and if not revised, either reapproved or withdrawn. Your comments are invited either for revision of this standard or for additional standards and should be addressed to ASTM Headquarters. Your comments will receive careful consideration at a meeting of the responsible technical committee, which you may attend. If you feel that your comments have not received a fair hearing you should make your views known to the ASTM Committee on Standards, 1916 Race St., Philadelphia, Pa. 19103.

Designation: G 85 - 85

Standard Practice for MODIFIED SALT SPRAY (FOG) TESTING[1]

This standard is issued under the fixed designation G 85; the number immediately following the designation indicates the year of original adoption or, in the case of revision, the year of last revision. A number in parentheses indicates the year of last reapproval. A superscript epsilon (ε) indicates an editorial change since the last revision or reapproval.

NOTE—Corrections were made editorially to A2.2.1 and the designation date was changed on Jan. 3, 1985.

1. Scope

1.1 This practice sets forth conditions for four modifications in salt spray (fog) testing for specification purposes. These are in chronological order of their development:

1.1.1 *Annex A1*, acetic acid-salt spray test, continuous Method B 287.

1.1.2 *Annex A2*, cyclic acidified salt spray test.

1.1.3 *Annex A3*, seawater acidified test, cyclic (SWAAT), Method G 43.

1.1.4 *Annex A4*, SO_2 salt spray test, cyclic.

1.2 Suitable apparatus that may be used to obtain these conditions is described in Annex A1 of Method B 117.

1.3 This practice does not prescribe the type of modification, test specimen or exposure periods to be used for a specific product, nor the interpretation to be given to the results.

1.4 *This standard may involve hazardous materials, operations, and equipment. This standard does not purport to address all of the safety problems associated with its use. It is the responsibility of whoever uses this standard to consult and establish appropriate safety and health practices and determine the applicablity of regulatory limitations prior to use.*

2. Applicable Documents

2.1 *ASTM Standards:*

B 117 Method of Salt Spray (Fog) Testing[2]

B 287 Method of Acetic Acid-Salt Spray (Fog) Testing[2]

D 609 Method for Preparation of Steel Panels for Testing Paint, Varnish, Lacquer, and Related Products[3]

D 1141 Specification for Substitute Ocean Water[4]

D 1193 Specification for Reagent Water[5]

D 1654 Method for Evaluation of Painted or Coated Specimens Subjected to Corrosive Environments[3]

E 70 Test Method for pH of Aqueous Solutions with the Glass Electrode[6]

G 43 Method of Acidified Synthetic Sea Water (Fog) Testing[2]

3. Significance and Use

3.1 This practice is applicable to ferrous and nonferrous metals; also organic and inorganic coatings. The variations described herein are useful when a more corrosive environment than the salt fog described in Method B 117 is desired.

4. Apparatus

4.1 *Cabinet:*

4.1.1 The apparatus required for salt spray (fog) testing consists of a fog chamber, a salt solution reservoir, a supply of suitably conditioned compressed air, one or more atomizing nozzles, specimen supports, provision for heating the chamber, and necessary means of control. The size and detailed construction of the cabinet are optional, provided the conditions obtained meet the requirements of this practice. The material of construction shall be such that it will not affect the corrosiveness of the fog. Suitable apparatus that may be used to obtain these conditions is described in Appendix A1 of Method B 117.

4.1.2 Design the cabinet so that drops of so-

[1] This practice is under the jurisdiction of ASTM Committee G-1 on Corrosion of Metals and is the direct responsibility of Subcommittee G01.05 on Laboratory Corrosion Tests.

Current edition approved Jan. 3, 1985. Published August 1985.

[2] *Annual Book of ASTM Standards*, Vols 02.05 and 03.02.

[3] *Annual Book of ASTM Standards*, Vol 06.01.

[4] *Annual Book of ASTM Standards*, Vol 11.02.

[5] *Annual Book of ASTM Standards*, Vol 11.01.

[6] *Annual Book of ASTM Standards*, Vol 15.05.

lution that accumulate on the ceiling or cover of the chamber do not fall on the specimens being tested. Do not return drops of solution that fall from the specimens to the solution reservoir for respraying.

4.1.3 Equip the cabinet with one or more timing devices to provide for intermittent spraying or periodic introduction of a gas, or both.

4.2 *Air Supply:*

4.2.1 Make sure the compressed air supply to the nozzle or nozzles for atomizing the salt solution is free of oil and dirt and maintain the air supply between 69 and 172 kPa (10 and 25 psi).

NOTE 1—The air supply may be freed of oil and dirt by passing it through a water scrubber or at least 610 mm (2 ft) of suitable cleaning material such as asbestos, sheep's wool, or activated alumina.

4.2.2 Temperature in the saturator tower (bubble tower) varies depending on the test method used.

4.3 *Conditions in Salt-Spray Chamber:*

4.3.1 *Temperature*—The temperature in the exposure zone varies with the test method used. For recommended exposure zone temperatures for the various methods see the Annex. Record the temperature within the exposure zone of the closed cabinet at least twice a day at least 7 h apart (except on weekends and holidays, when the salt spray test is not interrupted for exposing, rearranging, or removing test specimens or to check and replenish the solution in the reservoir).

NOTE 2—Suitable methods to record the temperature are a continuous recording device or a thermometer which can be read from outside the closed cabinet. Obtain the recorded temperature with the salt spray chamber closed to avoid a false low reading because of wet-bulb effect when the chamber is open.

4.3.2 *Atomization and Quantity of Fog*—Place at least two clean fog collectors within the exposure zone so that no drops of solution from the test specimens or any other source can be collected. Position the collectors in the proximity of the test specimens, one nearest to any nozzle and the other farthest from all nozzles. Make sure that for each 80 cm^2 of horizontal-collecting area fog accumulates in each collector from 1.0 to 2.0 mL of solution per hour based on an average run of at least 16 h continuous spray.

NOTE 3—Suitable collecting devices are glass funnels with the stems inserted through stoppers into graduated cylinders or crystallizing dishes. Funnels and dishes with a diameter of 100 mm have an area of about 80 cm^2.

4.3.3 Direct or baffle the nozzle or nozzles so that none of the spray can impinge directly on the test specimens.

5. Test Specimens

5.1 Define the type and number of test specimens to be used, as well as the criteria for the evaluation of the test results in the specifications covering the material or product being tested or upon mutual agreement between the purchaser and the seller.

5.2 *Preparation of Test Specimens:*

5.2.1 Clean metallic and metallic-coated specimens. The cleaning method is optional depending on the nature of the surface and the contaminants; however, when using a cleaning method do not include in the contents abrasives other than a paste of pure magnesium oxide nor of solvents which may form corrosive or inhibitive films. The use of nitric acid solution for the chemical cleaning, or passivation, of stainless steel specimens is permissible when agreed upon between the purchaser and the seller. Take care that specimens are not recontaminated after cleaning by excessive or careless handling.

5.2.2 Prepare specimens for evaluation of paints and other organic coatings in accordance with applicable specification(s) for the material(s) being tested, or as agreed upon between the purchaser and supplier. Otherwise, make sure the test specimens consist of steel meeting the requirements of Methods D 609; clean and prepare the specimens for coating in accordance with applicable procedure of Methods D 609.

5.2.4 Whenever it is desired to determine the development of corrosion from an abraded area in the paint or organic coating, make a scratch or scribed line through the coating with a sharp instrument so that the underlying metal is exposed before testing. Use the conditions of making the scratch as defined in Method D 1654, unless otherwise agreed upon between the purchaser and seller.

5.2.5 Protect the cut edges of plated, coated, or duplex materials and areas that contain identification marks or that are in contact with the racks or supports with a suitable coating that is stable under the conditions of the test, such as ceresin wax, unless otherwise specified.

NOTE 4—Should it be desirable to cut test specimens from parts or from preplated, painted, or otherwise coated-steel sheet, protect the cut edges by coating them

with paint, wax, tape, or other effective media so that the development of preferential attack or a galvanic effect between such edges and the adjacent plated or otherwise coated-metal surfaces, is prevented.

6. Salt Solutions

6.1 Make the salt solutions by using either synthetic sea salt in accordance with Specification D 1141 or sodium chloride in accordance with Method B 117. Make-up water shall be distilled or deionized water conforming to Type III reagent water described in Specification D 1193.

6.2 *Synthetic Sea Salt Solution:*

6.2.1 Make the salt solution so that it consists of 42 g of synthetic sea salt in accordance with Specification D 1141 per litre of solution (see Note 5).

6.3 *Sodium Chloride Solution:*

6.3.1 Prepare the salt solution by dissolving 5 ± 1 parts by weight of sodium chloride in 95 parts of distilled water or water containing not more than 200 ppm of total solids (see Note 5). The sodium chloride shall be substantially free of nickel and copper and shall contain on the dry basis not more than 0.1 % of sodium iodide and not more than 0.3 % of total impurities. Some salts contain additives that may act as corrosion inhibitors; careful attention should be given to the chemical content of the salt. Upon agreement between purchaser and seller, analysis may be required and limits established for elements or compounds not specified in the chemical composition given above.

NOTE 5—A solution having a specific gravity of 1.0255 to 1.0400 at 25°C (77°F) will meet the concentration requirement of 6.2.1 and 6.3.1. It is suggested that a daily check be made.

6.4 The pH of the salt solutions will vary depending on the test method used. Before the solution is atomized, free it of suspended solids (see Note 6). Take the pH measurements electrometrically at 25°C (77°F) using a glass electrode with a saturated potassium chloride bridge in accordance with Test Method E 70.

NOTE 6—The freshly prepared salt solution may be filtered or decanted before it is placed in the reservoir, or the end of the tube leading from the solution to the atomizer may be covered with a double layer of cheesecloth or suitable nonmetallic filter cloth to prevent plugging of the nozzle.

7. Procedure

7.1 *Position of Specimens During Test:*

7.1.1 Unless otherwise specified, support or suspend the specimens between 6 and 45° from the vertical, and preferably parallel to the principal direction of horizontal flow of fog through the chamber, based upon the dominant surface being tested. Note that test severity increases as angle from the vertical increases.

7.1.2 Do not allow contact of the specimens between each other, between any metallic material, or between any material capable of acting as a wick.

7.1.3 Place each specimen so as to permit free settling of fog on all specimens. A minimum spacing between specimens of 30 mm is recommended.

7.1.4 Do not permit the salt solution from one specimen to drip on any other specimen.

7.1.5 It is recommended that placement of replicate specimens be randomized to avoid possible bias caused by difference in spray patterns. Individual specimens may also be rotated daily for the same reason.

7.1.6 Suitable materials for the construction or coating of racks and supports are glass, rubber, plastic, or suitably coated wood. Do not use bare metal. Support specimens preferably from the bottom or the side. Slotted wooden, laminated plastic, or inert plastic strips are suitable for the support of flat panels. Suspension from glass hooks or waxed string may be used as long as the specified position of the specimens is obtained, and, if necessary, by means of secondary support at the bottom of the specimens.

7.2 *Continuity of Test:*

7.2.1 Unless otherwise specified, in the specifications covering the material or product being tested, allow the test to be continuous for the duration of the entire test period. Continuous operation implies that the chamber be closed except for the short daily interruptions necessary to inspect, rearrange, or remove test specimens, and to check and replenish the solution in the reservoir. Schedule operations so that these interruptions are held to a minimum.

7.3 *Period of Test:*

7.3.1 Designate the period of test in accordance with the specifications covering the material or product being tested or as mutually agreed upon between the purchaser and the seller. Exposure periods of multiples of 24 h are suggested.

7.4 *Cleaning of Tested Specimens:*

7.4.1 Unless otherwise specified in the specifications covering the material or product being tested, at the end of the test, specimens may be

gently washed or dipped in clean running water no warmer than 38°C (100°F) to remove salt deposits from their surface, and then immediately dried. Dry with a stream of clean, compressed air.

NOTE 7—Drying with compressed air may not be desirable for aluminum specimens to be tested for exfoliation corrosion resistance.

8. Evaluation of Results

8.1 Make a careful and immediate examination for the extent of corrosion of the dry test specimens or for other failure as required by the specifications covering the material or product being tested or by agreement between the purchaser and the seller.

9. Records and Reports

9.1 Record the following information, unless otherwise prescribed in the specifications covering the material or product being tested:

9.1.1 Type of salt and water used in preparing the salt solution,

9.1.2 All readings of temperature within the exposure zone of the chamber,

9.1.3 Weekly records of data obtained from each fog-collecting device including the following:

9.1.3.1 Volume of salt solution collected in millilitres per hour per 80 cm^2,

9.1.3.2 Concentration or specific gravity at 35°C (95°F) of solution collected, (see Note 8), and

9.1.3.3 pH of collected solution.

9.1.4 Type of specimen and its dimensions, or number or description of part,

9.1.5 Method of cleaning specimens before and after testing,

9.1.6 Method of supporting or suspending article in the salt spray chamber,

9.1.7 Description of protection used as required in 5.2.5,

9.1.8 Exposure period,

9.1.9 Interruptions in test, cause and length of time, and

9.1.10 Results of all inspections.

NOTE 8—It is also advisable to record the concentration or specific gravity of any atomized salt solution that has not made contact with the test specimen and that was returned to the reservoir.

ANNEX

Mandatory Information

A1. ACETIC ACID-SALT SPRAY (FOG) TESTING—(METHOD B 287)

A1.1 *Salt Solution:*

A1.1 A sodium chloride solution made in accordance with 6.3.

A1.1.2 Adjust the pH of this solution measured in accordance with Test Method E 70 to range from 3.1 to 3.3 by the addition of acetic acid.

NOTE A1—The initial solution may be adjusted to pH of 3.0 to 3.1 with the expectation that the pH of the collected fog will be within the specified limits. Base the adjustment of the initial pH for make-up solution upon the requirements to maintain the required pH of the collected samples. If less than 0.1 or more than 0.3 % of the glacial acetic acid is required to attain the specified pH, the purity of the water or salt, or both may not be satisfactory.

A1.2 *Conditions in Saturator Tower:*

A1.2.1 Make sure the temperature in the saturator tower (bubble tower) is 47 ± 1°C (117 ± 2°F).

A1.3 *Conditions in the Salt Spray Chamber:*

A1.3.1 *Temperature*—Maintain the exposure zone of the acetic acid-salt spray fog chamber at 35 + 1.1 or −1.7°C (95 + 2 or −3°F).

NOTE A2—This test is particularly applicable to research studies that have the effect of altering parameters of the electroplating process in connection with decorative chromium plating on steel or zinc die-cast base as well as for the evaluation of the quality of the product. This is true because of the normal duration of the test, which may be as brief as 16 h, but normally runs for 144 to 240 h or more giving ample opportunity for observations at practical intervals of the effects of minor parameter changes.

A2. CYCLIC ACIDIFIED SALT FOG TESTING

A2.1 *Salt Solution:*

A2.1 Use a sodium chloride solution made in accordance with 6.3.

A2.1.2 Adjust the pH of this solution to range from

2.8 to 3.0 by the addition of acetic acid.

A2.2 *Conditions in Saturator Tower:*

A2.2.1 Make sure the temperature in the saturator tower (bubble tower) is 57 ± 1°C (135 ± 2°F).

A2.3 *Conditions in Salt-Spray Chamber:*

A2.3.1 *Temperature*—Maintain the temperature in the exposure zone of the salt spray chamber at 49 + 1.1 or −1.7°C (120°F + 2 or −3°F).

A2.3.2 *Humidity*—Although the humidity limits for optimum test conditions have not been determined, operate the salt spray chamber under wet bottom conditions (that is, make sure an inch or so of water is present in the bottom of the box) for most testing. This ensures that the interior of the box does not become dry, a condition that decreases corrosion rate. (The dry bottom is recommended, however, for testing 2000-series aluminum alloys and paint coatings that require a less agressive environment.)[7]

A2.3.3 *Cabinet*—Equip the chamber with a timing device that can be used for the following 6-h repetitive cycles: ¾-h spray; 2-h dry-air purge; and 3¼-h soak at high relative humidity.

A2.3.4 *Purge*—Purging of the fog atmosphere immediately after spraying is the most unique feature of this test. Dry all droplets of water on the specimens and dry the corrosion products so that they are of a white, rather than a damp gray appearance. Perform this by electrically switching the air-flow to by-pass the saturator tower and aspirator nozzle and allowing it to enter directly into the test chamber for 120 min at an angle that sweeps the fog out of the peaked lid of the cabinet. This reduces the relative humidity from 40 to 7 %, depending on the climatic conditions of the ambient air. After purging, the specimens remain in the closed cabinet until the next spray cycle. Since most testing requires a wet bottom, the humidity gradually increases from 65 to 95 % during this period.

A2.3.5 *Atomization and Quantity of Fog*—Collect the fog in a special continuous spray run periodically between test runs. Determine the proper consumption of solution by monitoring solution level in the glass reservoir.

[7] Personal communication, Alcoa Technical Center, New Kensington, PA.

A3. ACIDIFIED SYNTHETIC SEA WATER (FOG) TESTING (METHOD G 43)

A3.1 *Salt Solution:*

A3.1.1 Use a synthetic sea salt solution made in accordance with 6.2 with the addition of 10 mL of glacial acetic acid per litre of solution.

A3.1.2 Adjust the pH of the salt solution between 2.8 and 3.0.

A3.2 *Conditions in Saturator Tower*—Make sure the temperature in the saturator tower (bubble tower) is 47 ± 1°C (117 ± 2°F) if cabinet temperature is 35°C (95°F); and 57 ± 1°C (135 ± 2°F) if cabinet temperature is 49°C (120°F).

A3.3 *Conditions in Salt Spray Chamber:*

A3.3.1 *Temperature*—The temperature in the exposure zone of the salt spray chamber may vary to suit the material being tested.The specifications that cover the material or product being tested define the temperature or the temperature may be mutually agreed upon between the purchaser and the seller. See Note A3 for recommended exposure zone temperatures for some materials.

NOTE A3—This test is particularly applicable to production control of exfoliation-resistant heat treatments for the 2000, 5000, and 7000-series aluminum alloys.[8] It is also applicable to developmental studies of varying heat treatment parameters to determine effect on corrosion behavior. For this purpose, a temperature of 49°C (120°F) is recommended for the exposure zone. For testing organic coatings on various metallic substrates, an exposure zone temperature of 24 to 35°C (75 to 95°F) may be used since temperatures in excess of 35°C frequently result in paint blistering.

A3.3.2 *Humidity*—Although the humidity limits for optimum test conditions have not been determined, results of an interlaboratory testing program indicate that it is necessary to operate under wet bottom conditions (that is, an inch or so of water should always be present in the bottom of the box). This ensures that the interior of the box does not become dry, a condition that will decrease the corrosion rate.

A3.3.3 *Cabinet*—Equip the cabinet with a timing device that can be used for the following cycle: 30-min spray followed by 90-min soak at above 98 % relative humidity.

[8] Ketcham, S. J., and Jeffrey, P. W., "Localized Corrosion-Cause of Metal Failure," *ASTM STP 516*, ASTM, 1973, pp. 273–302.

A4. SALT/SO_2 SPRAY (FOG) TESTING

A4.1 This test consists of spraying salt fog with introduction of SO_2 gas directly into the chamber periodically.

A4.2 *Salt Solution:*

A4.2.1 Define the salt solution by using the specifications covering the material or product being tested or upon mutual agreement between the purchaser and the seller.

A4.2.2 If synthetic sea salt is specified, prepare it in accordance with 6.2.

A4.2.3 If sodium chloride is specified, prepare it in accordance with 6.3.

A4.3 *Conditions in Saturator Tower:*

A4.3.1 Make sure the temperature in the saturator tower (bubble tower) is 47 ± 1°C (117 ± 2°F).

A4.4 *Conditions in the Salt Spray Chamber:*

A4.4.1 *Temperature*—Maintain the exposure zone of the salt spray chamber at 35 + 1.1, −1.7°C (95 + 2, −3°F).

A4.4.2 *SO_2 Gas*—Equipment and materials required for addition of SO_2 to cabinet are as follows:

A4.4.2.1 Cylinder of SO_2 gas.

A4.4.2.2 Flowmeter capable of measuring SO^2 gas flow of 1 $cm^3/min \cdot ft^3$ of cabinet volume (35 $cm^3/min \cdot m^3$); also constructed of materials inert to SO_2 gas.

A4.4.2.3 Timer.

A4.4.2.4 Two-way solenoid valve fabricated of materials inert to SO_2 gas.

A4.4.2.5 Tubing and fittings for SO_2 line of materials inert to SO_2 gas. A schematic of the SO_2 line is shown in Fig. A4.1.

NOTE A4—It is highly desirable to have the SO_2 gas introduced into the chamber in such a way that a uniform dispersion throughout the interior will result. If the cabinet is equipped with a central dispersion tower, holes can be drilled in the poly(methyl methacrylate) (PMMA) baffle at the top of the tower so that the gas comes out of eight uniformly spaced ports. There are undoubtedly other means for accomplishing a uniform dispersion of the gas. However, avoid introducing the gas into the chamber through one or two tubes at the side.

A4.4.3 The pH of the collected solution range from 2.5 to 3.2.

A4.4.4 *Cycle*—Define the cycle to be used by using the specifications covering the material or product being tested or upon mutual agreement between the purchaser and the seller. Examples of some possible cycles are as follows:

A4.4.4.1 Constant spray with introduction of SO_2 gas for 1 h 4 × a day (every 6 h).

A4.4.4.2 ½-h salt spray, ½-h SO_2, 2-h soak.

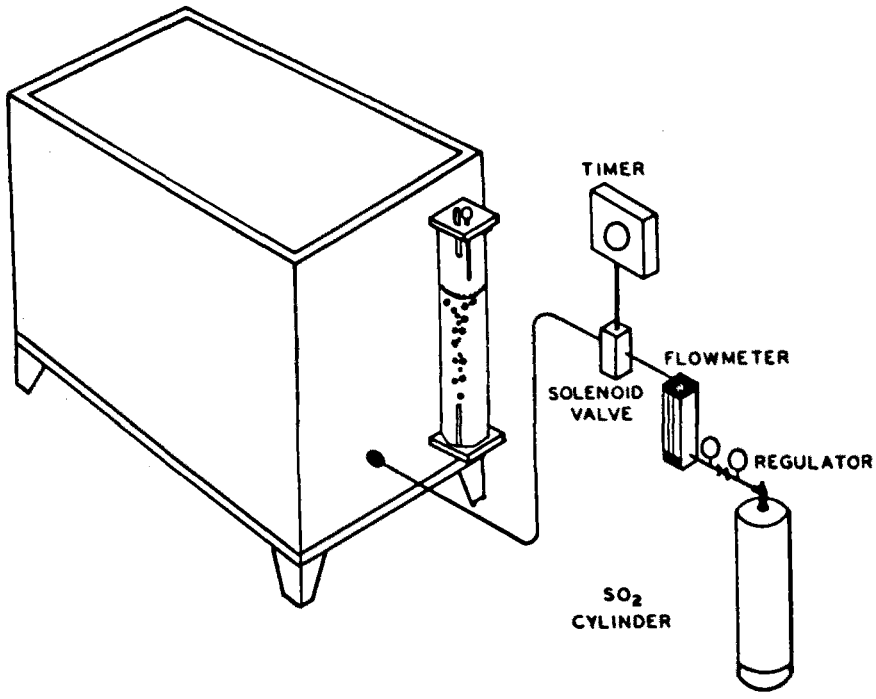


FIG. A4.1 Schematic of SO_2 Line into Salt Fog Cabinet

The American Society for Testing and Materials takes no position respecting the validity of any patent rights asserted in connection with any item mentioned in this standard. Users of this standard are expressly advised that determination of the validity of any such patent rights, and the risk of infringement of such rights, are entirely their own responsibility.

This standard is subject to revision at any time by the responsible technical committee and must be reviewed every five years and if not revised, either reapproved or withdrawn. Your comments are invited either for revision of this standard or for additional standards and should be addressed to ASTM Headquarters. Your comments will receive careful consideration at a meeting of the responsible technical committee, which you may attend. If you feel that your comments have not received a fair hearing you should make your views known to the ASTM Committee on Standards, 1916 Race St., Philadelphia, Pa. 19103.

Designation: G 87 - 84

Standard Practice for CONDUCTING MOIST SO_2 TESTS[1]

This standard is issued under the fixed designation G 87; the number immediately following the designation indicates the year of original adoption or, in the case of revision, the year of last revision. A number in parentheses indicates the year of last reapproval. A superscript epsilon (ε) indicates an editorial change since the last revision or reapproval.

1. Scope

1.1 This practice describes the apparatus and procedure to be used in conducting qualitative assessment tests in accordance with the requirements of material or product specifications by means of specimen exposure to condensed moisture containing sulfur dioxide.

1.2 The exposure conditions may be varied to suit particular requirements and this practice includes provisions for use of different concentrations of sulfur dioxide and for tests either running continuously or in cycles of alternate exposure to the sulfur dioxide containing atmosphere and to the ambient atmosphere.

1.3 The variant of the test to be used, the exposure period required, the type of test specimen, and the criteria of failure are not prescribed by this practice. Such details are provided in appropriate material and product purchase specifications.

1.4 The values stated in SI units are to be regarded as standard. The inch-pound values in parentheses may be approximate.

1.5 *This standard may involve hazardous materials, operations, and equipment. This standard does not purport to address all of the safety problems associated with its use. It is the responsibility of whoever uses this standard to consult and establish appropriate safety and health practices and determine the applicability of regulatory limitations prior to use.* (For specific precautionary statement, see 9.1.1.)

2. Applicable Documents

2.1 *ASTM Standards:*

D 714 Method of Evaluating Degree of Blistering of Paints[2]

D 1193 Specification for Reagent Water[3]

D 1654 Method for Evaluation of Painted or Coated Specimens Subjected to Corrosive Environments[2]

3. Significance and Use

3.1 Moist air containing sulfur dioxide quickly produces easily visible corrosion on many metals in a form resembling that occurring in industrial environments. It is therefore a test medium well suited to detect pores or other sources of weakness in protective coatings and deficiencies in corrosion resistance associated with unsuitable alloy composition or treatments.

3.2 The results obtained in the test should not be regarded as a general guide to the corrosion resistance of the tested materials in all environments where these materials may be used. Performance of different materials in the test should only be taken as a general guide to the relative corrosion resistance of these materials in moist SO_2 service.

4. Apparatus

4.1 The apparatus required for moist SO_2 testing consists of a test chamber having an internal capacity of 300 L (10.6 ft^3), a supply of sulfur dioxide with metering device, specimen supports, provisions for heating the chamber, and necessary means of control. The size and detailed construction of the apparatus are optional, provided the conditions obtained meet the requirements of this method. Suitable apparatus which may be used to obtain these conditions is described in Appendix X1.

---

[1] This practice is under the jurisdiction of ASTM Committee G-1 on Corrosion of Metals and is the direct responsibility of Subcommittee G01.05 on Laboratory Corrosion Tests.

Current edition approved April 27, 1984. Published July 1984.

[2] *Annual Book of ASTM Standards*, Vol 06.01.

[3] *Annual Book of ASTM Standards*, Vol 11.01.

4.2 Drops of condensing moisture which accumulate on the ceiling of the chamber shall not be permitted to fall on the specimens being tested.

5. Sampling

5.1 The specific location of samples in a mill product, the number of samples that should be tested, and other factors concerning sampling, are not within the scope of this practice. These factors should be mutually agreed upon between purchaser and supplier (see 6.1).

6. Test Specimens

6.1 Select the number and type of test specimens, and their shape and dimensions according to the specification covering the product or material being tested or agreed upon between purchaser and supplier.

6.2 The total combined exposed surface area of the material tested at any one time should be substantially the same and unless otherwise agreed upon, it shall be 0.5 ± 0.1 m^2.

6.3 To obtain quantitative corrosion-rate data, only materials with similar reactivities should be included in a test run.

6.4 *Preparation of Test Specimens:*

6.4.1 Suitably clean the specimens before testing. Unless otherwise agreed upon the cleaning method shall be optional depending on the nature of the surface and of likely contamination except that it shall not include the use of abrasives (other than a paste of pure magnesium oxide) or of solvents that are corrosive or that may deposit either corrosion-promoting or protective films. Take care that specimens are not recontaminated by excessive or careless handling after cleaning.

6.4.2 If test specimens are cut from a larger coated article, carry out the cutting in such a way that coating damage is minimized in the area adjacent to the cut. Unless otherwise specified, adequately protect the cut edges by coating them with a suitable medium, stable under the conditions of the test, such as wax or tape. High-quality platers tape or microcrystalline wax are generally suitable.

6.5 *Position of Specimens During Test:*

6.5.1 Place the test specimens in the cabinet so that no part of any specimen is within 20 mm (5 in.) of another or within 100 mm (25 in.) of the walls or the ceiling or within 200 mm (50 in.) of the surface of the water in the base of the chamber.

6.5.2 Arrange the specimens so that moisture which may condense on any of them or their supports will not fall on other specimens placed at lower levels.

6.5.3 Unless otherwise agreed upon, the angle of inclination of test surfaces to the vertical is optional. However, a near vertical orientation (0 to 10° from vertical) is suggested.

7. Reagents

7.1 *Purity of Reagents*—Reagent grade chemicals shall be used in all tests. Unless otherwise indicated, it is intended that all reagents shall conform to the specifications of the Committee on Analytical Reagents of the American Chemical Society, where such specifications are available[4]. Other grades may be used, provided it is first ascertained that the reagent is of sufficiently high purity to permit its use without lessening the accuracy of the determination.

7.2 *Purity of Water*—Unless otherwise indicated, references to water shall be understood to mean reagent water as defined by Type IV of Specification D 1193.

7.3 A commercially available source of bottled SO_2 gas having a minimum purity of 99.9 % (liquid phase) with proper regulator, and means of measuring the volumes of gas required for delivery into test chamber shall be provided.

7.3.1 **Caution**—Suck-back into cylinder may cause explosion. Always use a check valve, vacuum break, or other protective apparatus in any line or piping from cylinder to test chamber to prevent suck-back.

7.4 The volume of gas delivered into test chamber shall be measured by means of either a properly calibrated flowmeter (rotameter type) with metering valve, or in a gas buret using viscous paraffin oil as the pressure controlling fluid.

7.4.1 The volume to be measured may be as small as 0.2 L, and measures should be taken to avoid errors from such as air contained in delivery tubes between flowmeter or gas burette and test chamber.

[4] "Reagent Chemicals, American Chemical Society Specifications," Am. Chemical Soc., Washington, DC. For suggestions on the testing of reagents not listed by the American Chemical Society, see "Reagent Chemicals and Standards," by Joseph Rosin, D. Van Nostrand Co., Inc., New York, NY, and the "United States Pharmacopeia."

8. Conditioning

8.1 Operate a new chamber for at least ten 24-h cycles without introduction of any test material by the procedure applicable to an atmosphere containing an addition of 2 L of sulfur dioxide before it is brought into use for testing. This should reduce any risks of contamination of the atmosphere by vapors from construction materials of chamber.

9. Procedure

9.1 Introduce 2 ± 0.2 L of distilled water into the base of chamber.

9.2 Place the test specimens in position and close the door of the chamber.

9.3 Introduce the volume of sulfur dioxide, required by the governing materials specification, into the chamber through the inlet pipe. Usually this volume will be 0.2, 1, or 2 L.

9.4 Switch on the heater below the chamber, and raise the temperature inside the chamber to 40 ± 3°C (104 ± 5.4°F) in about 1.5 h. Make sure the heating is under control to keep the temperature inside the chamber at 40 ± 3°C (104 ± 5.4°F) for the specified period.

9.5 One test cycle is 24 h and may be either continuous exposure of the specimens or alternate exposure for 8 h followed by drying in the ambient atmosphere inside the chamber for 16 h. For either test cycle, replace the water in the chamber and the sulfur dioxide in the air of the chamber before each 24-h cycle begins.

9.5.1 For a test of continuous exposure in the chamber for 24 h, the replacement of water and sulfur dioxide for a second period of test shall be made with a minimum of disturbance of the test specimens.

9.5.2 For specimens exposed to ambient conditions for part of the test cycle, such conditions shall be an indoor atmosphere with no unusual pollution other than that arising from the test cabinet, a temperature in the range of 20 to 30°C (68 to 86°F), and a relative humidity below 75 %.

9.6 *Duration of Test*—The number of cycles shall be designated by the specification for the material or product being tested or mutually agreed upon by purchaser and seller.

9.7 *Cleaning of Tested Specimens*—At the end of the test period, remove the specimens from the chamber. Before they are examined, allow them to hang freely in a normal indoor atmosphere until any fluid corrosion product dries. Examine with all corrosion product in position and any cleaning carried out depends on the criteria laid down for evaluation of the test result.

10. Evaluation of Results

10.1 Different criteria for evaluation of the results of the test may be applied to meet particular requirements, for example, mass change, change in appearance, alteration revealed by micrographic examination, or change in mechanical properties. Usually the appropriate criteria will be indicated in the specification for the material or product tested. For most routine applications of the test, only the following need to be considered:

10.1.1 Appearance after drying in air,

10.1.2 Appearance after removing superficial corrosion products by washing with water and a soft bristle brush,

10.1.3 The number and distribution of corrosion defects, for example, pits, cracks, blisters, and other defects may conveniently be assessed by methods such as that described in Method D 1654, and Method D 714, and

10.1.4 The number of cycles elapsing before the appearance of the first sign of corrosion.

11. Report

11.1 The report shall indicate the outcome of the test according to the criteria for evaluation of results prescribed for the test. The result obtained for each specimen tested and, when appropriate, the average result for a group of replicate test specimens shall be reported. The report, may, if required, be accompanied by photographic records of the tested specimens.

11.2 The report shall contain information about all test details. This information may vary according to the purposes of the test and to the directions prescribed for it but a general list of the details likely to be required is as follows:

11.2.1 Chemical composition of the material tested,

11.2.2 Dimensions and shape of the test specimen and the nature and area of the surface tested,

11.2.3 Preparation of the test specimen including any cleaning treatment applied and any protection given to edges or other special areas. Known characteristics of any coating with an indication of the surface finish,

11.2.4 Amount of sulfur dioxide introduced per cycle,

11.2.5 Number of test specimens subjected to test representing each material or product,

11.2.6 Method used to clean test specimens after test with, when appropriate, an indication of the loss of mass resulting from the cleaning operation,

11.2.7 Temperature of test,

11.2.8 Duration of test (number of cycles), and

11.2.9 Character of any control test panels placed in the cabinet expressly to check the correctness of the operating conditions and the results obtained with them.

12. Precision and Bias

12.1 The precision and bias of results obtained with this method depend on the type of material or specimen used and cannot be generalized.

APPENDIX

(Nonmandatory Information)

X1. MOIST-SO_2 TEST APPARATUS

X1.1 Location

X1.1.1 The chamber shall be located in an area free of unusual pollution, direct sunlight, and drafts. Temperature should be controlled between 20 to 30°C (68 to 86°F) at a relative humidity below 75 %.

X1.2 Chamber

X1.2.1 Standard SO_2 chambers are available from several suppliers, but certain pertinent details are required before they will function according to this practice and provide consistent control for duplication of results.

X1.2.2 The chamber consists of the basic chamber, nonconducting specimen supports, provisions for heating the chamber, and suitable controls for maintaining the desired temperature.

X1.2.3 The chamber shall have an inlet tube through which gas can be introduced into the chamber located at a point no less than 50 mm above the internal floor, a means by which excess pressure can be relieved located in or near the ceiling and a suitable drain in the floor of the chamber.

X1.2.4 The floor and lower parts of the walls of chamber shall be capable of being heated from an external source and must be able to retain without leakage at least 2.5 L of water containing dissolved sulfur dioxide.

X1.2.5 External means of heating the water placed in the base of chamber, sufficient to maintain the temperature inside the chamber at 40 ± 3°C (104 ± 5.4°F) shall be provided.

X1.2.6 A full-opening door made of transparent material such as glass, acrylic, polycarbonate or suitable plastic material shall be provided and should occupy at least 75 % of the area of the front wall of the chamber.

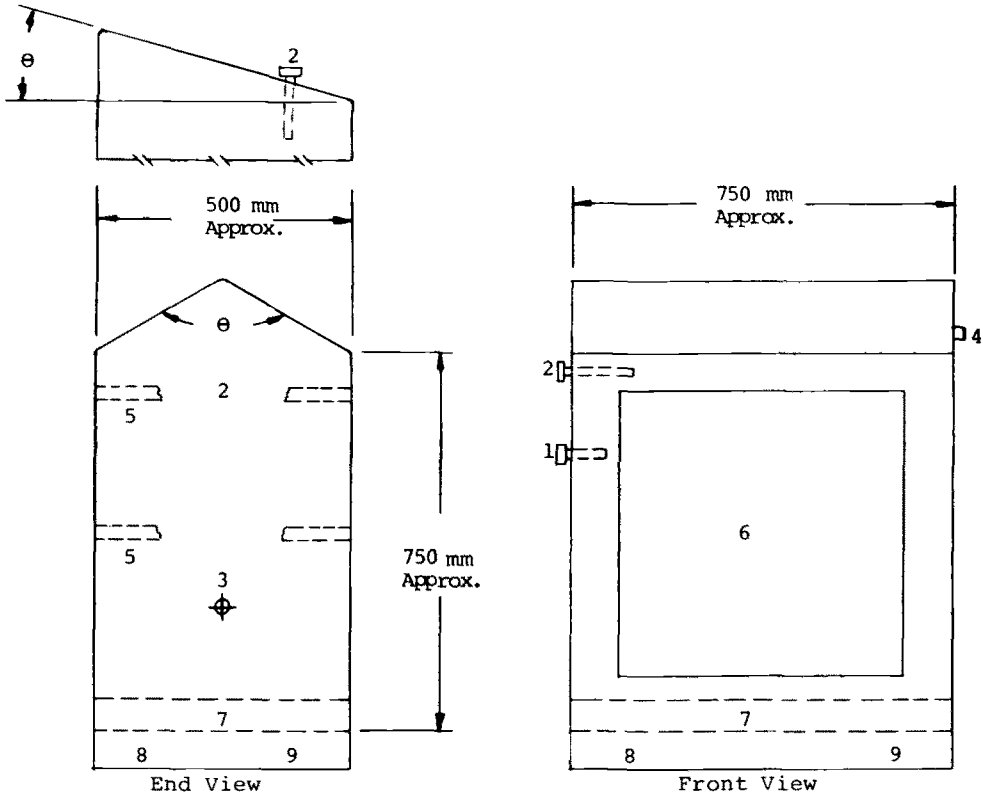
X1.2.7 All materials used in the construction of the chamber must be resistant to the action of moist sulfur dioxide and shall themselves not emit any gases or vapors likely to influence corrosion of test materials. A suitable plastic material, lead or plastic clad steel, or austenitic stainless steel may be used for the basic construction of the chamber and internal fittings.

X1.2.8 Specimen supports shall be of nonconducting material such as glass, plastic, or suitably coated wood or steel. Any material used to suspend the test specimens in the chamber shall be of synthetic fibre or other inert insulating material; metallic materials shall not be used.

X1.2.9 Some variation in the dimensions and shape of the chamber can be tolerated but the total internal area of chamber (including ceiling) should be 300 L (10.6 ft^3). The ceiling must be so shaped that moisture condensing on it shall not fall on specimens being tested. An inclination or slope of the ceiling of at least 12° to the horizontal or installation of an internal baffle suspended from the ceiling at that angle provides a suitable safeguard. Suitable dimensions and shape for the chamber are outlined in Fig. X1.

X1.3 Temperature Controls

X1.3.1 A temperature controlling device with its actuating element shall be placed in the upper part of the chamber. A thermometer capable of being read from outside the cabinet shall also be installed in the upper part of the chamber with its bulb located approximately 250 mm from any side wall.



θ Angle of Ceiling
Inclined Type: 12° Minimum (from horizontal)
Gable Type: 120° Minimum (included angle)

1 Automatic thermostat for controlling heater
2 Thermometer
3 Gas inlet
4 Excessive pressure vent
5 Specimen support
6 Door
7 Internal reservoir
8 Heater
9 Air space or water jacket

FIG. X1 Typical Moist SO_2 Test Chamber

The American Society for Testing and Materials takes no position respecting the validity of any patent rights asserted in connection with any item mentioned in this standard. Users of this standard are expressly advised that determination of the validity of any such patent rights, and the risk of infringement of such rights, are entirely their own responsibility.

This standard is subject to revision at any time by the responsible technical committee and must be reviewed every five years and if not revised, either reapproved or withdrawn. Your comments are invited either for revision of this standard or for additional standards and should be addressed to ASTM Headquarters. Your comments will receive careful consideration at a meeting of the responsible technical committee, which you may attend. If you feel that your comments have not received a fair hearing you should make your views known to the ASTM Committee on Standards, 1916 Race St., Philadelphia, Pa. 19103.

Summary

Summary

The thirty-one (31) papers in this book have been divided into the following three sections: (1) the design and interpretation of laboratory tests, (2) laboratory tests for specific environments, and (3) laboratory tests for specific types of corrosion. Since most papers on laboratory corrosion testing address all three subject areas, the papers have been divided according to their principle emphasis. An Appendix containing the standards most often referred to in the papers is included.

The section on Design and Interpretation of Laboratory Tests begins with a paper by Treseder that discussed the problem of engineer-user acceptance of laboratory corrosion tests. Examples of test methods for evaluating stress corrosion cracking and crevice corrosion were used to illustrate the problem of making engineering decisions based on laboratory tests. The author stressed the need for improved definition of the limits of tests, use of rank ordering, correlation of laboratory data with field experience, and standardization of the tests.

Development of an accelerated corrosion test for materials for naval aircraft was described by Ketcham and Jankowsky. Experiments were conducted with periodic injections of sulfur dioxide gas into a salt fog chamber. Results from these tests correlated well with aircraft carrier exposure for most materials, however, the test gave misleading results for some materials. It was concluded that a single accelerated test could not be used to evaluate all materials for aircraft service and that it is essential to correlate test results with service exposure.

Tipton described the use of computers in corrosion research for data acquisition and processing. In addition to presenting typical hardware and software considerations, the author described uses for computers in corrosion research such as potential, current, potentiodynamic polarization, current distribution, and fatigue crack growth measurements.

The topic of corrosion under heat-transfer conditions was covered by Yau and Webster. Their test loop consisted of heat exchanging tubes that contained wire specimens that were not subject to heat transfer. Their results showed that heat flux does not play an important role in zirconium corrosion.

Accelerated corrosion tests for coatings on steel were addressed in two papers. Warwick and Hampshire described an accelerated test for tinplate and compared it with industrial experience with containers. The accelerated test provided a reliable way of reducing the need for pack testing. Berke and Friel used the

Copyright© 1985 by ASTM International www.astm.org

linear polarization technique as a screening tool for predicting the relative atmospheric corrosion performance of metallic coated steels. Relative corrosion rates determined with this technique were found to be in general agreement with long-term marine and industrial exposures.

Laboratory electrochemical tests were covered in a number of papers. Electrical resistance tests, tafel extrapolation, linear polarization, potentiodynamic polarization, corrosion behavior diagrams, and AC impedance were covered in a review paper by Siebert. Particular attention was given to scan rate effects and the development and interpretation of corrosion behavior diagrams. Hakkarainen described a novel method of determining pit nucleation and repassivation potentials using a multilayered textile tape. The author applied this method to stainless steel plates and welds as well as prestressing steel wire. Galvanostaircase and potentiostaircase polarization techniques were described by Hirozawa. He concluded that the galvanostaircase technique provided more accurate values for the breakdown and protection potentials of aluminum in inhibited solutions and that potentiostaircase polarization gave more accurate values for polarization resistance. The corrosion behavior of polybutadiene coatings on bare and conversion coated steel, commercial conversion coatings on aluminum alloys, and anodized aluminum alloys was investigated by Mansfeld and Kendig using electrochemical impedance measurements. The authors developed models for the impedance behavior of the coating systems and methods for analysis of experimental impedance diagrams in terms of coating and interface properties and their changes during exposure to corrosive environments.

The final paper in this section by Suga described improvements to the apparatus for light and water exposure of nonmetallic materials (ASTM Recommended Practice for Operating Light- and Water-Exposure Apparatus [Fluorescent UV-Condensation Type] for Exposure of Nonmetallic Materials] [G 53]). These improvements resulted in a more uniform, higher level of irradiance of the test specimens.

The section on Laboratory Tests for Specific Environments contains papers on tests developed to evaluate the corrosion performance of materials in a specific environment. In the paper by Nielsen corrosion testing in potable waters was reviewed. The influence of water composition on corrosion and the difficulty of developing a comprehensive test were discussed. The paper also includes a review of corrosion problems with the metals and alloys commonly used for construction of potable water systems. Francis and Mercer found that dissolution of borosilicate glass in water above 60°C lowers the corrosion rate of steel in distilled water. They described a new apparatus to overcome this problem and determined that, above a critical level, oxygen has a passivating effect on steel in potable water while the chloride ion is aggressive.

Bogar and Peterson compared the actual corrosion rates of mild steel in seawater with those obtained using the linear polarization technique. They found good agreement between the rates for up to 60 days however after 120 days the rates differed substantially. They also found that the polarization resistance was semilogarithmically related to the scan rate. Nye et al cathodically polarized

mild steel in once-through and recirculated seawater. The films formed in once-through seawater polarized the cathodic reactions more effectively than those formed in artificial or recirculated natural seawater. The calcareous deposit formed on the mild steel resulted in an 86% reduction of the cathodic current density in once-through seawater at -1.0 V versus the standard calomel electrode (SCE).

A number of papers dealt with corrosion in unique environments. Baboian and Haynes described the development of an environmental wear corrosion test for coinage materials. The behavior of coins in the test mechanistically and visually duplicated the behavior of coins in circulation. Noble steel clad (steel cored) sandwich coins had similar performance to their respective noble monometal coins in the wear tests. A test for the corrosiveness of fibrous insulations was described by Crume. He concluded that the test provided consistent and reproducible results but suffered the limitation that it required subjective visual ranking of the specimens. Rosskopf and Virnelson described a galvanostatic technique for identifying environments that effect the passivity of steel embedded in concrete. Results of test using this technique were correlated with observations of concrete structures. Dial et al described the corrosion induced deformation behavior of brick masonry wall panels. They found that corrosion of embedded steel plates resulted in an expansion behavior of the brick masonry.

Electrochemical methods for evaluating corrosion inhibitors in strong acid systems were evaluated by Dean et al. They found that the correlation between mass loss measurements and electrochemical corrosion rates was poor. The return potential corrosion rate from the reverse scan polarization technique did provide a qualitative measure of pitting tendency that agreed with surface examination. Mack et al described test methods for weight loss, pitting, crevice corrosion, and environmentally assisted cracking in environments containing hydrogen sulfide. A strong emphasis was placed on safety including selection of materials for containment vessels, flow lines, disposal of hydrogen sulfide, and training of personnel.

The section on Laboratory Tests for Specific Types of Corrosion contains papers on tests for crevice corrosion, erosion corrosion, stress corrosion cracking, and intergranular corrosion. Kain and Lee described test techniques utilizing a remote crevice assembly and a compartmentalized cell. These techniques allowed the measurement of corrosion potentials, current data, mass loss, and penetration data while having the advantage that neither required the application of external current. The relative effects of bulk environment chloride level, dissolved oxygen content, and crevice solution pH on crevice initiation and propogation for a number of stainless steels were evaluated with these techniques. Hubbell et al reviewed the four techniques that have been used to determine the protection potential of stainless steels. They compared their results using these techniques with longer term potentiostatically derived protection potentials and concluded that the longer term tests produced more conservative results. Jain et al described an autoclave assembly containing high magnesium nearly saturated brine and equipment for measuring current and potential variations to monitor the progress of crevice corrosion under hydrothermal conditions. The final pH of the crevice

solution and the decoupled potentials of the cathode and anode were used to provide information about the mechanisms of corrosion. Grade −12 titanium was found to be much less susceptible to crevice corrosion than Grade −2 titanium in some of their experiments.

A jet-in-slit test that causes oxide film fracture by impulse force in addition to shear stress was developed by Matsumura et al. The test was used to evaluate erosion corrosion of brass in sodium chloride solution. Comparison of results from this test with those from conventional impingement tests indicated that the jet-in-slit test more closely duplicated erosion corrosion that has been observed in condenser tubes. Treseder and Kachik described five test procedures used to rank materials for resistance to general corrosion, crevice corrosion, and stress corrosion cracking by the chemical process industry. A critical value of a test variable (temperature, concentration, and so forth) was used to rank the corrosion resistance of each alloy.

Three papers dealt with tests for stress corrosion cracking. Whitehead and Baloun used potentiostatic anodic polarization to study pitting resistance of AISI 420 (Unified Numbering System [UNS] 542000) stainless steel in simulated sweet and sour well environments. Total alkalinity and chloride concentration had more influence on pitting resistance than hydrogen sulfide in their tests. Constant applied potential step stress tests showed that pitting was necessary for cracking to occur. Rosborg and Rosengren conducted slow strain rate tests in high purity water using a closed-loop oxygen dosage and electrode potential control system. The electrode potential below which intergranular stress corrosion cracking of AISI 304 (UNS 530400) stainless steel did not occur was −250 mV (standard hydrogen electrode) [SHE] at 200°C. Gálvez et al studied the stress corrosion cracking behavior of prestressing steels using a slow strain rate test in an aqueous solution of calcium hydroxide with small additions of sodium chloride. The slow strain rate technique was superior to constant load tests. Steels failed because of hydrogen embrittlement at potentials more negative than −0.9 V (SCE) while a second regime of cracking was found at potentials more positive than −0.8 V (SCE).

An improved intergranular corrosion test for HASTELLOY ® Alloy C276 was described by Manning. The new test consistently detected undesirable microstructural problems in mill-produced material that were not detected by the ferric sulfate-sulfuric acid ASTM Detecting Susceptibility to Intergranular Attack in Wrouht Nickel-Rich, Chromium-Bearing Alloys (G 28). The former provided a step function increase in corrosion rates on sensitized material while a high and variable uniform corrosion rate in the latter masked the intergranular corrosion rate. Schluter and Chivinsky reported the results of a round-robin study of ASTM Recommended Practices for Detecting Susceptibility to Intergranular Attack in Stainless Steels (A 262). The test data indicated that the reproducibility of Practice C was excellent for any given surface preparation, however, variations in surface preparation were found to have a significant effect on test results.

This STP on laboratory corrosion tests and standards presents comprehensive

and balanced coverage of the subject. In addition to describing new test procedures the authors addressed the limitations of accelerated tests as well as the relevance of many widely used tests. Many of the test procedures were correlated with the actual service environment. The severity of the environments ranged from relatively benign to extremely corrosive. The techniques covered ranged from very basic ones, such as immersion tests, to highly sophisticated ones, such as electrochemical techniques. This book truely defines the state of the art in laboratory corrosion testing.

Gardner S. Haynes and
Robert Baboian

Texas Instruments, Incorporated, Attleboro, MA 02703, symposium cochairmen and coeditors

Author Index

A

Ahn, Tae-Moon, 337–357

B

Baboian, Robert, Editor, 1–2, 260–274, 591–595
Baloun, Calvin H., 400–414
Berke, Neal S., 143–157
Bogar, Frederic D., 197–206
Breen, John E., 285–296

C

Caballero, Luis, 428–436
Carrasquillo, Ramon L., 285–296
Chivinsky, Joseph A., 455–464
Crume, Stephen V., 215–227

D

Dean, Sheldon W., 228–245
Dial, Stephen A., 285–296

E

Elices, Manuel, 428–436

F

Francis, Peter E., 184–196
Friel, John J., 143–158
Furuya, Hiroyuki, 358–372

G

Galvéz, V. Sánchez, 428–436

H

Hakkarainen, Tero, 91–107
Hampshire, W. B., 48–64
Hartt, William H., 207–214
Haynes, Gardener S., Editor, 1–2, 260–274, 591–595
Heidersbach, R. H., 324–337
Hirozawa, Stanley T., 108–121
Hubbell, M., 324–336

J

Jain, Himashu, 337–356
Jankowsky, Edward J., 14–21

K

Kachik, Edward A., 373–399
Kain, Robert M., 299–323
Kendig, Martin W., 122–142
Ketcham, Sara J., 14–21

L

Lee, Thad S., 299–323

M

Mack, Robert D., 246–259
Manning, Paul E., 437–454
Mansfield, Florian, 122–142
Matsumura, Masanobu, 358–372
Mercer, Antony D., 184–196

Copyright© 1985 by ASTM International www.astm.org

N

Nichols, James, 228–245
Nielsen, Kate, 169–183
Nye, Tracy L., 207–214

O

Oka, Yoshinori, 358–372
Okumoto, Satofumi, 358–372

P

Peterson, Miller H., 197–206
Price, C., 324–336

R

Rooskopf, Philip, 275–286
Rosborg, Bo, 415–427
Rosengren, Anders, 415–427

S

Siebert, Oliver W., 65–90
Soo, Peter, 337–357
Smith, Samuel W., 207–215
Steinberg, Beverlee G., 246–259
Suga, Shigeru, 159–168

T

Tipton, David G., 22–35
Treseder, Richard S., 5–13, 373–399

V

Virnelson, R. Craig, 275–284

W

Warwick, Malcolm E., 48–64
Webster, R. Terry, 36–47
Whitehead, Timothy D., 400–414
Wilhelm, S. Mark, 246–259
Woodroof, Robert A., Jr., 228–245

Y

Yau, Te-Lin, 36–47

Subject Index

A

Acid rain, 287
Aeration, 187
Aluminum, 17, 262
  2024, 132
  6061, 132
  7075, 20, 131, 132
Anodized aluminum, 135
ASTM standards
  A 262, 455–464
  B 457, 139
  C 665, 215
  C 764, 216
  D 610, 129
  D 1141, 249
  E 399, 34
  E 647, 34
  G 1, 225, 231, 375
  G 3, 74, 403
  G 5, 255, 328
  G 28, 437, 438, 442, 450, 452
  G 30, 251, 376
  G 31, 67, 78, 250, 375
  G 36, 376
  G 38, 252
  G 39, 252
  G 40, 359
  G 43, 19
  G 46, 375
  G 48, 251, 315, 375
  G 53, 159, 161
  G 59, 198, 233
  G 61, 326, 328, 334
Autoclave, 339, 417

B

Bent beam test, 251
Biofouling, 203
Bode plot, 126–137
Brass, 262
Brazed joints, 177
Brick masonry, 285–296
  cracking, 293
Brine, 341

C

Cabinet tests
  Cyclic, 19
  Humidity tests, 215–227
  Kesternich, 144
  Salt spray, 14, 144
  Sulfur dioxide, 144
  Sulfur dioxide-salt fog, 15
Calcareous deposit, 212
Can corrosion
  Accelerated test, 48–64
  Effects of chromium, 60–61
  Effect of lacquer, 57
  Pack test, 59
  Solder attack, 53
  Storage conditions, 57
Cathodic depolarizer, 49, 71
Cathodic protection, 207–214
Cement
  Calcium chloride content, 277
Clad metal, 260–274
Coatings
  Alodine 600, 131

Coatings (*continued*)
Chromate conversion, 123
Deterioration of, 159
Epoxy/polyurethane, 20
Inorganic, 17
Lacquer, 48
Undermining, 60
Coinage material, 260–274
Soilage properties, 271–274
Computer program, 28
Concrete, 275–284, 429
Sodium thiocyonate content, 283
Copper and copper alloys, 262
614 yellow brass, 360
Correlation
ASCC test, 54
Corrosion ranking, 225
Cyclic sulfur dioxide-salt fog, 21
Electrochemical tests, 144
Environmental wear behavior, 274
FUCA test, 160
Immersion tests, 177
Laboratory tests, 11
Pit ranking, 244
Salt spray tests, 14
Tafel extrapolation, 238
Corrosion behavior diagram, 75–79
Corrosion fatigue, 34, 174
Fatigue crack growth, 34
Creep, 292
Crevice corrosion, 9, 78, 103, 227, 250, 299–323, 324–336, 337–357, 376
Area ratio effects, 318
Critical concentration, 10
Critical temperature, 9
Effect of geometry, 10, 313, 354
Effect of pH, 315, 349
Incubation period, 354
Mathematical model, 300
Multiple crevice assembly, 385, 396
Oxygen concentration effects, 319
Propagation, 303
C-ring test, 251
Cupro-nickel, 262
Current decay curve, 210

D

Data acquisition, 24–35
Dealloying
Solders, 57
Deformation
Corrosion induced, 292
Deicing salts, 275
Dezincification, 176
Double cantilever beams, 251

E

Electrochemical tests, 65–90, 325
Cell design, 339
Compartmentalized cell, 304
Controlled potential, 72, 210, 406, 416, 431
Cyclic potentiodynamic polarization, 77, 95, 110, 228, 328
Electrical resistance, 67
EPR test, 421
Galvanostaircase polarization, 112
Galvanostatic polarization, 254, 276
Impedance, 87, 122–142
Polarization resistance, 71, 113–120, 147, 197–206, 233
Effect of scan rate, 201
Potential measurements, 236, 277, 309, 345
Metallic coated steel, 146–151
Nickel-aluminum bronze, 30
Potential step method, 327
Potentiodynamic polarization, 31, 71, 72, 255
Effect of scan rate, 72, 96
Rapid scan technique, 75
Slow scan technique, 73
Potentiostaircase polarization, 113
Potentiostatic polarization, 254, 401

Tape method, 91–107
Tafel region, 69, 154, 199, 233
Environmental wear test, 260–274
Environments
Aircraft carrier, 17
Erosion corrosion, 175, 358–372
Effect of velocity, 361
Jet test, 360
Shear stress, 363
Exfoliation tests, 19

F

Ferric chloride test, 375
Fluid velocity, 82
Fluorescent UV and condensation test, 159
Fretting corrosion, 262

G

Galvanic corrosion, 7, 50, 147
Area ratio effects, 50
Current distribution, 32
Soldered tin, 57
Tin plated steel, 49
Zero resistance ammeters, 32
Galvanized steel, 147, 172

H

Heat exchanger, 36–47
Galvanic corrosion, 33
Zirconium, 36
Heat exchanger tubes, 359
Current distribution, 33
Heat transfer
Corrosion effects, 36
High temperature
Reference electrode, 417
Humidity test
Cyclic, 261
Hydrogen embrittlement, 251
Hydrogen induced cracking, 7, 254
Hydrogen sulfide, 246
Hydrothermal conditions, 338
Hysteresis, 110, 111, 229, 242, 325

I

Immersion tests, 66, 374
Electrolyte-volume ratio, 51
Inhibitors, 12, 228–245
Insulation, 215–217
Intergranular corrosion, 437–454
Effect of mill condition, 459
Effect of surface preparation, 455
Stress corrosion cracking, 421

L

Localized corrosion, 66
Weld metal attack, 41

M

Masonry, 286
Metal pick-up, 179
Microcomputer, 24–35
Mortar, 275–284
Multiple crevice assembly, 302, 329

N

Nickel and nickel alloys, 262
Hastelloy C, 437–454

P

Pipe
Brass, 176
Copper, 173
Galvanized steel, 172
Pitting, 10, 77, 91–107, 172, 250, 324–336, 444
Effect of pH, 98
Pitting potential, 10, 242, 413
Effect of surface pretreatment, 97
Polarization curves
3003 aluminum, 112
Brass, 113, 367
Copper, 112, 114

Polarization curves (*continued*)
Nickel-aluminum bronze, 32
Stainless steel
18-2 ferritic, 101
Type 304, 96, 97, 100
Type 316, 319
Type 420, 404–412
Steel, 280, 281
Coated, 155–156
N80, 232
Pore water, 280
Potable water, 170
Pourbaix diagrams, 67–68
Precracked specimen, 253
Prestressed steel (see reinforcing steel)

R

Reinforcing steel, 102, 275–284, 286, 428–436
Repassivation potential, 324
Effect of scan rate, 96
Rotating cylinder, 82

S

Seawater, 197–206, 207–214, 304
Fouling, 203
Synthetic, 208, 304
Sensitization, 456
Austenitic stainless steel, 416
Slow strain rate tests, 253, 415–425
Solder attack, 177
Can corrosion, 53
Lead dissolution, 56
Solder joints, 178
Sour gas, 7, 249
Specimen preparation, 231, 342, 455–464
Stainless steel
17-4, 20
18Cr-2Mo, 100, 307
18Cr-4Ni-2Mo, 308
26Cr-1Mo, 308
254 SMO, 308
Type 304, 94, 307, 327, 415, 421, 455
Type 316, 307
Type 317, 308
Type 420, 401
Type 430, 307
Type 904, 306, 317
Steel, 17, 185, 198, 209, 216, 262, 276, 428
A36, 287
N80, 231
1005, 203
1010, 130
Metallic coated, 144
Polybutadiene coated, 125
Pore resistance, 127
Tin plate, 48
Stress corrosion cracking, 6, 84, 251, 376, 415–427, 428
Constant load test, 432
Controlled potential test, 406
Critical stress, 10
Effect of chloride concentration, 407
Effect of hydrogen sulfide, 406
Effect of pH, 407
Intergranular
Critical potential for, 421
Modulus measurements, 85
Polarization tests, 86
Slow strain rate test, 84, 433
Step-stress tension test, 404
U-bend specimens, 251, 392
Stress intensity, 253
Stress-strain curves
Type 304 stainless steel, 423
Sulfide stress cracking, 7, 251, 400–414
Step-stress tension test, 404
Surface preparation, 105, 217, 223
Surface treatment, 128

T

Tensile bars, 251
Tin plate
  Can corrosion, 49
  Passivation treatment, 60–62
Titanium
  Grade 2, 338
  Grade 12, 337

V

Vapor phase corrosion, 44
Velocity effects, 81–83

W

Wear corrosion, 262
Wear tests, 260–274
Weld metal attack, 41, 100, 450

Z

Zirconium, 36
  P60707, 37
  Effect of heat flux, 42
  Weld metal attack, 41

ISBN 0-8031-0443-X